

Medical Radiology

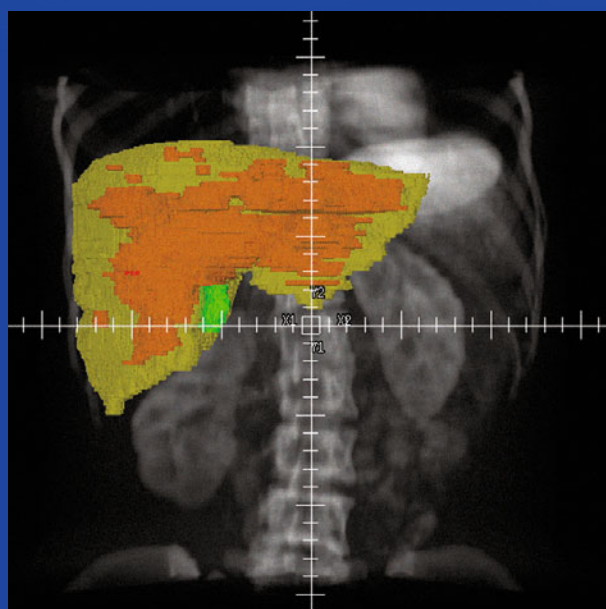
Diagnostic Imaging

M.F. Reiser  
H.-U. Kauczor  
H. Hricak  
M. Knauth

José Ignacio Bilbao  
Maximilian F. Reiser  
*Editors*

# Liver Radioembolization with $^{90}\text{Y}$ Microspheres

*Second Edition*



 Springer

---

# Medical Radiology

## Diagnostic Imaging

### *Series editors*

Maximilian F. Reiser  
Hans-Ulrich Kauczor  
Hedvig Hricak  
Michael Knauth

### *Editorial Board*

Andy Adam, London  
Fred Avni, Brussels  
Richard L. Baron, Chicago  
Carlo Bartolozzi, Pisa  
George S. Bisset, Durham  
A. Mark Davies, Birmingham  
William P. Dillon, San Francisco  
D. David Dershaw, New York  
Sam Sanjiv Gambhir, Stanford  
Nicolas Grenier, Bordeaux  
Gertraud Heinz-Peer, Vienna  
Robert Hermans, Leuven  
Hans-Ulrich Kauczor, Heidelberg  
Theresa McLoud, Boston  
Konstantin Nikolaou, Munich  
Caroline Reinhold, Montreal  
Donald Resnick, San Diego  
Rüdiger Schulz-Wendtland, Erlangen  
Stephen Solomon, New York  
Richard D. White, Columbus

For further volumes:  
<http://www.springer.com/series/4354>

---

José Ignacio Bilbao • Maximilian F. Reiser  
Editors

# Liver Radioembolization with $^{90}\text{Y}$ Microspheres

Second Edition

 Springer

*Editors*

José Ignacio Bilbao  
Departamento de Radiología  
Clínica Universidad de Navarra  
Pamplona  
Spain

Maximilian F. Reiser  
Institut für Klinische Radiologie  
Universitätsklinikum München Klinikum  
Großhadern  
Munich  
Germany

ISSN 0942-5373                      ISSN 2197-4187 (electronic)  
ISBN 978-3-642-36472-3            ISBN 978-3-642-36473-0 (eBook)  
DOI 10.1007/978-3-642-36473-0  
Springer Heidelberg New York Dordrecht London

Library of Congress Control Number: 2014930007

© Springer-Verlag Berlin Heidelberg 2014

This work is subject to copyright. All rights are reserved by the Publisher, whether the whole or part of the material is concerned, specifically the rights of translation, reprinting, reuse of illustrations, recitation, broadcasting, reproduction on microfilms or in any other physical way, and transmission or information storage and retrieval, electronic adaptation, computer software, or by similar or dissimilar methodology now known or hereafter developed. Exempted from this legal reservation are brief excerpts in connection with reviews or scholarly analysis or material supplied specifically for the purpose of being entered and executed on a computer system, for exclusive use by the purchaser of the work. Duplication of this publication or parts thereof is permitted only under the provisions of the Copyright Law of the Publisher's location, in its current version, and permission for use must always be obtained from Springer. Permissions for use may be obtained through RightsLink at the Copyright Clearance Center. Violations are liable to prosecution under the respective Copyright Law.

The use of general descriptive names, registered names, trademarks, service marks, etc. in this publication does not imply, even in the absence of a specific statement, that such names are exempt from the relevant protective laws and regulations and therefore free for general use.

While the advice and information in this book are believed to be true and accurate at the date of publication, neither the authors nor the editors nor the publisher can accept any legal responsibility for any errors or omissions that may be made. The publisher makes no warranty, express or implied, with respect to the material contained herein.

Printed on acid-free paper

Springer is part of Springer Science+Business Media (www.springer.com)



---

## Preface

Primary hepatic tumors, mostly hepatocellular carcinoma (HCC), are the fifth most common cause of cancer-related deaths. Its frequency is progressively increasing worldwide and major investigations are being made in order to improve its dismal prognosis. Similarly, the presence of synchronic or metachronic liver metastases from different tumors (colorectal, neuroendocrine, pancreas, breast, etc.) decreases significantly the probability of survival related with a progressive deterioration in the liver performance. An early detection of the presence of liver tumors (early stages) allows to implement curative therapies, mainly hepatectomy or liver transplantation (for primary tumors), with which 70 % of patients can get a survival of 5 years. However, surgery is suitable in only a minority of them and its selection will depend on the volume and extension of the tumor as well as on the functionality of the remaining liver parenchyma.

For inoperable patients, irrespective of the reason, other therapeutic strategies such as the application of transparietohepatic ablative techniques are actively investigated and, thus, clinically established as effective alternatives, not only to obtain local control of the disease but also to put patients as surgical candidates (downstaging) and then increasing patient's survival. These techniques include radiofrequency, ethanol ablation, microwave ablation, and now, electroporation, and are applicable in both primary and metastatic lesions.

The incorporation, along the past decades, of new drugs for the systemic treatment of metastatic diseases has allowed a dramatic increase in patients' expectations and, for example, in colorectal liver metastases the mean overall survival is four times higher than the obtained with just supportive care (23 mo vs 6 mo). However, if a patient cannot receive surgery his/her life expectancy at 5 years is still as low as 7 %. For this reason, it seems evident that any strategy with which a maximal control of the liver disease can be obtained will have a definitive impact on the survival. Clinical decisions have been oriented toward the combination of drugs with new targeted specific therapies, thus personalizing the strategies to the patients' needs and to combine methods with different, non-summative toxicities that may even multiply their effect. A good example of the latter is the administration of active drugs which are radiosensitizers that may increase the local effect of radiation.

Other possibilities are to increase the local dose by administering the selected agent through the artery that gets the tumor, a branch of the hepatic artery. These trends may be oriented by taking advantage of a unique anatomic characteristic of the liver which is his double blood supply. Since liver neoplasms are mostly (almost exclusive in nodules bigger than 3 mms) supplied by the hepatic artery, any administration from this access may target the tumor and, theoretically, avoid major damage of the healthy, non-tumoral, parenchyma which will be mainly supplied by the portal vein.

The possibility of obtaining an accurate targeting of the liver tumors by an endovascular approach opened in the 1980s a new way to treat patients. Some fundamental investigations have demonstrated that by this approach it is possible to obtain palliation, or to downstage to surgery or, even, to cure by complete ablation, a liver

tumor (mainly HCC). There are many articles, with robust evidence, that have contributed to the allocation of the endovascular procedures in a unique situation within the therapeutic algorithms. This applies mainly for HCC although some liver metastases (i.e., neuroendocrine) have, for years, also been very efficiently treated by this approach.

Focusing on the endovascular treatment of HCC, several articles and reviews have claimed about the great dispersity of procedures that are grouped under the classification of “endovascular treatment.” This may be due to the wide heterogeneity of the underlying disease (different grades of cirrhosis, the presence of hepatitis, etc), some geo-economical issues, and the outstanding creativity of interventional radiologists that push and disperse them, continuously, toward new projects and materials. The consequence is that unfortunately it has been almost impossible, or at least quite difficult, to compare the data obtained from several investigations.

The heterogeneous group of “endovascular procedures” includes bland embolization, chemoembolization and, now, radioembolization. The basic aim of bland embolization is to obtain tumoral necrosis by selectively delivering an occluding material within the afferent arteries thus obtaining ischemia which generates necrosis. Several reports have shown that if the procedure is precisely carried out the tumoral control is very high. Many others have claimed, however, that a “just” bland embolization may, initially, provoke ischemia, but almost immediately, will also trigger the mechanisms of neo-angiogenesis activated by the need of the tumor of new vessels.

This is the reason why in a majority of countries “embolization” has been changed to “chemoembolization,” which means that an active agent (a drug) has been added to the material of embolization. It obviously has increased the heterogeneity of the series making it even more difficult to compare their results.

However, the term “chemoembolization” has introduced a new concept. This concept is that the material for embolization (a fluid as is “Lipiodol” or the particle itself) can be both a carrier and an occluding embolizer. There have been several articles that have shown the advantage of applying occluding particles which deliver drug to the surrounding tissues with marked increases in the local control and in downstaging and final overall survival. Some investigators, however, still claim that the size and amount of the spheres and its intravascular point of delivery, as well as patients’ characteristics, are still too inhomogeneous making it difficult to obtain a final guidance for daily clinical decisions.

The evolving concept is that the particles may just be carriers, avoiding any triggering of neo-angiogenesis and just delivering an active antitumoral agent within the lesion. This initiative has taken profit from the previous knowledge about tumoral characteristics such as anatomy or tumoral hemodynamics and materials for performing the procedure. Nonetheless, it has opened new horizons in terms of delivering new agents to treat tumors. There has always been controversy about the efficacy of chemotherapeutic drugs (as could be for Doxorubicin in HCC) in tumors that have constantly demonstrated its chemoresistance and, for this reason, several groups have, for years, been working on new possibilities for materials that may be delivered locally killing the tumoral cells in different, sometimes, very sophisticated ways. Among them are gene therapy, targeted therapies, hyperthermia, or radiation. The latter is termed as Radioembolization (RE) or, in some places, Selective Internal Radiation Therapy; both terms define the concept of the procedure and the former states that radiation is administered with the aid of an endovascular carrier (embolizer).

The evolving therapeutic strategies raise continuously new challenges. It seems evident that the methodology that needs to be applied for each precise endovascular procedure should/must be different from one another. It is not just the matter of making an angiography and placing selectively a microcatheter and then a bland, or a chemo or a radioembolization can be consecutively performed. Every procedure has its specific requirements. Similarly, the criteria of selection and the methods to evaluate response

may be different. Nowadays, for example, the excellent RECIST classification has been surpassed for some specific treatments such as targeted therapies or endovascular treatments, among them RE.

The term RE refers to the administration of brachytherapy with microspheres embedded with a beta-emitting isotope (Yttrium-90). RE was initially performed in the 1990s and mainly in Australasia; it was later approved in the USA and initiated in Europe in 2003. Currently, many institutions worldwide are using RE, alone or in combination with other treatments, as a fully established modality to treat patients with primary and metastatic liver malignancies. RE has already proven its efficacy in different tumoral indications and seems to be unique in terms of comparison of results. Since the performance of the procedure requires an accurate knowledge of the precise tumoral, and non-tumoral, volume that is going to be treated, since the exact dose that has been administered is precisely detailed, and since the clinical situation must be carefully scrutinized, it is easier to show exactly what is being done to each patient regardless of the institution in which he is being treated. This unique characteristic is offering an easier understanding of its results in different tumoral situations allowing to know the expectancies that can be obtained in many subgroups of patients.

As in many other therapeutic initiatives, the implementation of RE requires some local regulations and a multidisciplinary approach where specialists from different fields (Medical Oncology, Surgery, Hepatology, Nuclear Medicine, Radiology and Radiation Oncology) give their expertise and knowledge with the aim of increasing its accuracy and efficacy and, at the same time, decreasing its possible morbidity. The book has been structured and organized in order to obtain, from experts in such a multidisciplinary approach, an overview of the most important items related to RE. The chapters deal with the selection of the most adequate candidates, their careful evaluation, the work-up needed to administer the microspheres directly to the tumor, and the results obtained in patients affected from primary and a different range of metastatic liver malignancies.

There are, at this moment, a large number of papers that give robust information related to the fundamental aspects of RE. New fresh information will appear in the following years trying to answer to crucial questions that, obligatorily, are continuously appearing about the procedure itself and about its continuous adaptation to the specific needs of each patient and may be of new tumoral locations.

We thought that there is a need, at this moment, to summarize and discuss in a book all matters related with RE. With this book readers will find the basic and advanced information needed not only to be familiar with but also to incorporate RE in their clinical activity.

José Ignacio Bilbao

---

# Contents

<b><sup>90</sup>Y Microspheres: Concepts and Principles</b> . . . . .	1
Andrew S. Kennedy, William A. Dezarn and Patrick McNeillie	
<b>Regulations and Requirements of Hospitals Performing Radioembolization</b> . . . .	11
C. Trumm, R. T. Hoffmann, T. F. Jakobs and M. F. Reiser	
<b>Radiological Evaluation of Patients with Liver Tumors</b> . . . . .	15
Christoph J. Zech and M. F. Reiser	
<b>Vascular Anatomy and Its Implication in Radioembolization</b> . . . . .	27
Ramón Saiz-Mendiguren, Javier Arias, Isabel Vivas and José I. Bilbao	
<b>Radioembolization: Identifying and Managing Anatomic Variants</b> . . . . .	41
Rajesh P. Shah and Daniel Y. Sze	
<b>Dosimetry and Dose Calculation</b> . . . . .	53
Andrew S. Kennedy, William A. Dezarn, Patrick McNeillie and Bruno Sangro	
<b>Nuclear Medicine Procedures for Treatment Evaluation and Administration</b> . . . . .	63
Javier Arbizu, Macarena Rodriguez-Fraile, Josep M. Martí-Climent, Inés Domínguez-Prado and Carmen Vigil	
<b>Radiological Detection and Assessment of Tumor Response</b> . . . . .	77
Tobias F. Jakobs	
<b>Evaluation of the Response by Multimodality Imaging</b> . . . . .	91
Alexander Haug and Gerwin P. Schmidt	
<b>Results in Hepatocellular Carcinoma</b> . . . . .	105
Mercedes Iñárraeraegui and Bruno Sangro	
<b>HCC. Radioembolization Combined with Other Therapeutic Local and Systemic Treatment</b> . . . . .	119
Thomas Helmberger	
<b>Principles for Combining Radioembolisation with Systemic Chemotherapy for Metastatic Colorectal Cancer</b> . . . . .	129
Esme J. Hill, Ashley K. Clift and Ricky A. Sharma	
<b>Results in Liver Metastatic Colorectal Cancer</b> . . . . .	141
Javier Rodríguez, Ana Chopitea, Bruno Sangro and José Ignacio Bilbao	

---

<b>Treatment of Neuroendocrine Tumors with Selective Internal Radiation Therapy</b> . . . . .	151
Douglas M. Coldwell, Martin Vyleta and Mahmood Samman	
<b>Yttrium-90 Microspheres for Other Liver Metastases</b> . . . . .	157
J. Rodriguez, A. Chopitea, B. Sangro and J. I. Bilbao	
<b>Surgical Treatment and Radioembolization</b> . . . . .	167
Patricia Martínez-Ortega, Fernando Pardo and Bruno Sangro	
<b>Complications and Side Effects</b> . . . . .	171
R. T. Hoffmann, Lourdes Diaz-Dorransoro and José I. Bilbao	
<b>Radioembolization-Induced Liver Disease</b> . . . . .	177
Bruno Sangro, Mercedes Iñarrairaegui and Andrew S. Kennedy	
<b>Index</b> . . . . .	187

---

## Contributors

**Javier Arbizu** Department of Nuclear Medicine, Clínica Universidad de Navarra, Pamplona, Spain

**Javier Arias** Department of Radiology, Clínica Universidad de Navarra, Pamplona, Spain

**José Ignacio Bilbao** Department of Radiology, Clínica Universidad de Navarra, Pamplona, Spain; Unit of Interventional Radiology, Clínica Universidad de Navarra, University of Navarra, Pamplona, Spain;

**Ana Chopitea** Unit for the Research and Treatment of Gastrointestinal Malignancies, Department of Medical Oncology, Clínica Universidad de Navarra, University of Navarra, Pamplona, Spain

**Ashley K. Clift** Department of Oncology, Cancer Research UK-Medical Research Council Gray Institute for Radiation Oncology and Biology, University of Oxford, Oxford, UK

**Douglas M. Coldwell** Department of Radiology, University of Louisville, Louisville, KY, USA

**William A. Dezarn** Private Consultant, Siloam, NC, USA

**Lourdes Diaz-Dorronsoro** Department of Radiology, Clínica Universidad de Navarra, Pamplona, Spain; Unit of Interventional Radiology, Clínica Universidad de Navarra, Pamplona, Spain

**Inés Domínguez-Prado** Department of Nuclear Medicine, Clínica Universidad de Navarra, Pamplona, Spain

**Alexander Haug** Department of Nuclear Medicine, University Hospitals Grosshadern, Ludwig-Maximilians-University of Munich, Munich, Germany

**Thomas Helmberger** Institute of Diagnostic and Interventional Radiology, Neuroradiology and Nuclear Medicine, Klinikum Bogenhausen, Munich, Germany

**Esme J. Hill** Department of Oncology, Cancer Research UK-Medical Research Council Gray Institute for Radiation Oncology and Biology, University of Oxford, Oxford, UK; Oncology Department, Churchill Hospital, Oxford University Hospitals NHS Trust, Oxford, UK

**R. T. Hoffmann** Department and Policlinics of Diagnostic Radiology, Universitätsklinikum Carl Gustav Carus, Dresden, Germany; University Hospital Dresden, Dresden, Germany

**Mercedes Iñarrairaegui** Liver Unit, Clínica Universidad de Navarra, Pamplona, Spain; Centro de Investigación Biomedica en Red de Enfermedades Hepáticas y Digestivas (CIBEREHD), Pamplona, Spain

**Tobias F. Jakobs** Department of Diagnostic and Interventional Radiology, Hospital Barmherzige Brüder, Munich, Germany; Department of Radiology, Krankenhaus Barmherzige Brüder, Munich, Germany

**Andrew S. Kennedy** Department of Radiation Oncology, Sarah Cannon Cancer Institute, Nashville, TN, USA; Department of Biomedical Engineering, Department of Mechanical and Aerospace Engineering, North Carolina State University, Raleigh, NC, USA

**Josep M. Martí-Climent** Department of Nuclear Medicine, Clínica Universidad de Navarra, Pamplona, Spain

**Patricia Martínez-Ortega** Clínica Universidad de Navarra, Pamplona, Spain

**Patrick McNeillie** School of Medicine, University of North Carolina, Chapel Hill, NC, USA

**Fernando Pardo** Clínica Universidad de Navarra, Pamplona, Spain

**M. F. Reiser** Klinikum der LMU München, Standort Grosshadern, Institut für Klinische Radiologie, Munich, Germany; Institute of Clinical Radiology, Ludwig Maximilians-University, Munich, Germany

**Javier Rodríguez** Unit for the Research and Treatment of Gastrointestinal Malignancies, Department of Medical Oncology, Clínica Universidad de Navarra, University of Navarra, Pamplona, Spain

**Macarena Rodríguez-Fraile** Department of Nuclear Medicine, Clínica Universidad de Navarra, Pamplona, Spain

**Ramón Saiz-Mendiguren** Department of Radiology, Clínica Universidad de Navarra, Pamplona, Spain

**Mahmood Samman** Department of Radiology, University of Louisville, Louisville, KY, USA

**Bruno Sangro** Clínica Universidad de Navarra, Pamplona, Spain; Centro de Investigación Biomedica en Red de Enfermedades Hepáticas y Digestivas (CIBEREHD), Pamplona, Spain; Liver Unit, Clínica Universidad de Navarra, Pamplona, Spain

**Gerwin P. Schmidt** Radiologie München Zentrum, Munich, Germany

**Rajesh P. Shah** Division of Interventional Radiology, Stanford University Medical Center, Stanford, CA, USA

**Ricky A. Sharma** ; Department of Oncology, Cancer Research UK-Medical Research Council Gray Institute for Radiation Oncology and Biology, University of Oxford, Oxford, UK; Oncology Department, Churchill Hospital, Oxford University Hospitals NHS Trust, Oxford, UK

**Daniel Y. Sze** Division of Interventional Radiology, Stanford University Medical Center, Stanford, CA, USA

**C. Trumm** Institute of Clinical Radiology, Ludwig Maximilians-University, Munich, Germany

**Carmen Vigil** Department of Nuclear Medicine, Clínica Universidad de Navarra, Pamplona, Spain

**Isabel Vivas** Department of Radiology, Clínica Universidad de Navarra, Pamplona, Spain

**Martin Vyleta** Department of Radiology, University of Louisville, Louisville, KY, USA

**Christoph J. Zech** Abteilungsleiter Interventionelle Radiologie, Klinik für Radiologie und Nuklearmedizin, Universitätsspital Basel, Basel, Switzerland



# <sup>90</sup>Y Microspheres: Concepts and Principles

Andrew S. Kennedy, William A. Dezarn, and Patrick McNeillie

## Contents

<b>1</b>	<b>Introduction</b> .....	1
<b>2</b>	<b>Hepatic Intra-Arterial Radioactive Microsphere Brachytherapy Fluid Dynamics</b> .....	2
<b>3</b>	<b>Historical Background of Radioactive Microparticle Therapy for Liver Cancers</b> .....	3
<b>4</b>	<b>Physics of Radiation Therapy</b> .....	3
4.1	Radiation Types.....	3
4.2	Radiation Dose.....	4
4.3	Brachytherapy.....	4
<b>5</b>	<b>Radiobiology</b> .....	5
5.1	Modifiers of Radiation Response.....	5
<b>6</b>	<b>Radiation Effects in the Liver</b> .....	5
<b>7</b>	<b>Rationale for <sup>90</sup>Y Microsphere Therapy</b> .....	6
7.1	Anatomic/Vascular Summary.....	6
7.2	Preclinical Reports of Microsphere Deposition.....	7
<b>8</b>	<b>Human Studies of Microsphere Deposition</b> .....	8
<b>9</b>	<b>Commerically Available<sup>90</sup>Y-Microsphere Productsfor Human Medical Use</b> .....	8
	<b>References</b> .....	8

## Abstract

Effective use of intra-arterial radioactive microsphere therapy for liver malignancies requires understanding of many disciplines. Mastery of radiation physics, radiobiology, vascular anatomy, and modifiers of particle flow all complement the established skill of the physician team delivering <sup>90</sup>Y microspheres in these complex patients. This chapter introduces and explains the key concepts involved from the many disciplines that combined to produce safe, effective, and evolving liver radiotherapy.

## 1 Introduction

Radiotherapy is a cornerstone of anti-cancer therapy, a therapy used in over half of all cancer patient's course of treatment. Although each malignant tumor type has differing sensitivity to radiotherapy, there is not a single solid tumor or hematologic subtype that is not sensitive to therapeutic doses of radiotherapy. The relatively recent evolution of treatment techniques that protect the more radiation-sensitive normal liver parenchyma while still delivering sufficient radiation to malignant cells has dramatically increased the use of liver-directed radiotherapy approaches. These include external beam radiotherapy (stereotactic body radiotherapy, i.e., SBRT), interstitial permanent radioactive seed brachytherapy, and intra-arterial <sup>90</sup>Y microsphere implantation known as radioembolization.

With the development of internal (intra-arterial) brachytherapy, the delivery of tumoricidal doses of radiation to tumors of all origins and in all segments of the liver is a reality. Recent advances in medical oncology (personalized

---

A. S. Kennedy (✉)  
Department of Radiation Oncology,  
Sarah Cannon Cancer Institute,  
3322 West End Avenue, Suite 800, Nashville,  
TN 37203, USA  
e-mail: andrew.kennedy@sarahcannon.com

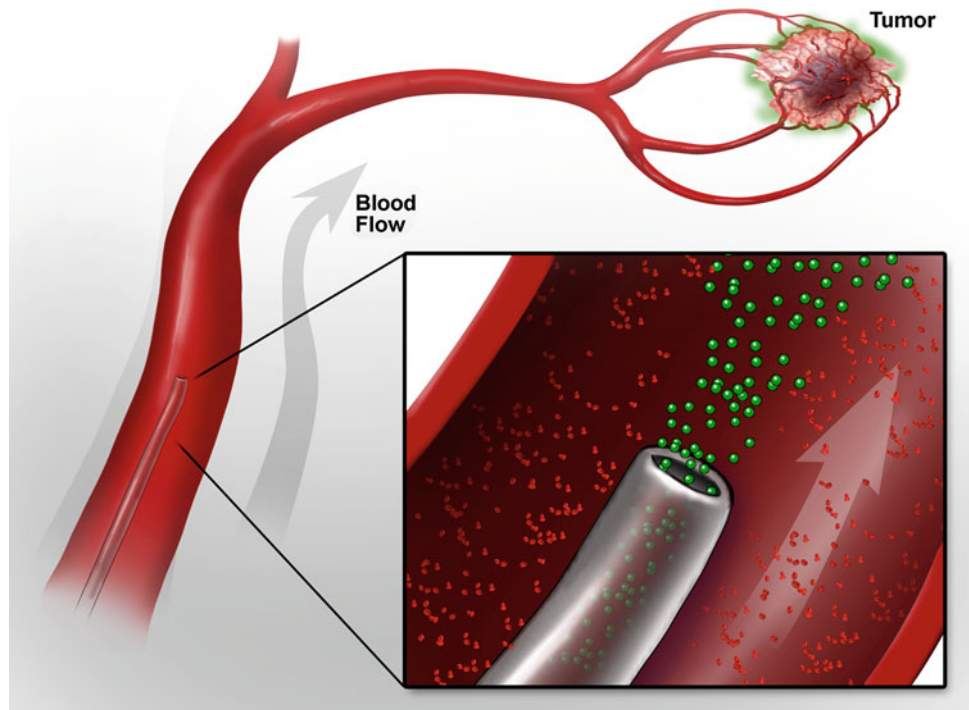
A. S. Kennedy  
Radiation Oncology Research, Sarah Cannon Research Institute,  
3322 West End Avenue, Suite 800, Nashville, TN 37203, USA

A. S. Kennedy  
Department of Biomedical Engineering,  
Department of Mechanical and Aerospace Engineering,  
North Carolina State University,  
Raleigh, NC, USA

W. A. Dezarn  
Private Consultant, Siloam, NC, USA

P. McNeillie  
School of Medicine, University of North Carolina, Chapel Hill,  
NC, USA

**Fig. 1** Illustration of the  $^{90}\text{Y}$  microsphere radioembolization showing microcatheter in the hepatic artery releasing radioactive microspheres in the dominant flow leading to a tumor

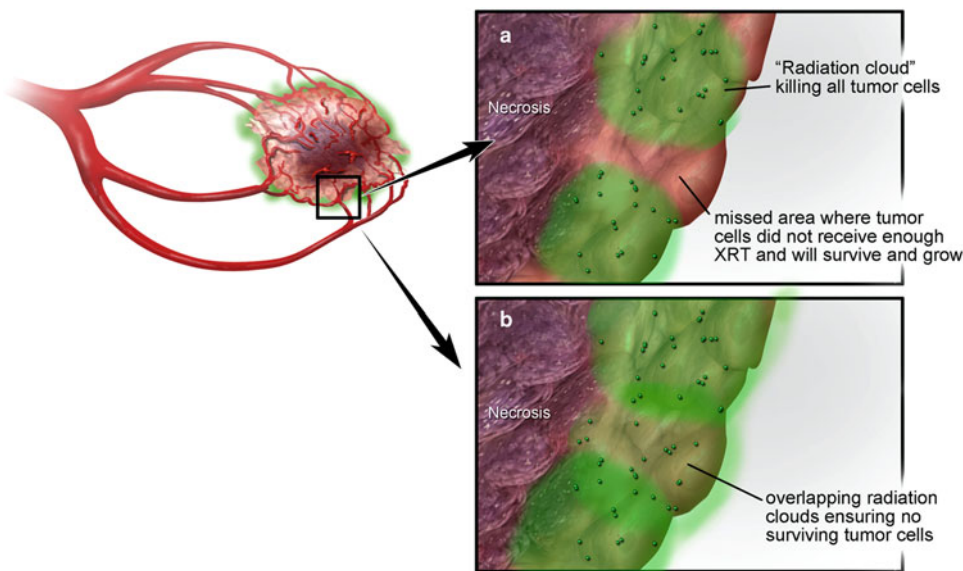


molecular profiling, anti-angiogenic agents, and new systemic chemotherapy agents) have produced improved response rates, disease free survivals, and median survivals for many solid tumors. However, despite clearance of disease elsewhere in the body, the liver is often the site of tumor resistance and ultimately the patient's death. Moreover with increased skill and more sophisticated and specialized catheters, today's interventional radiologists are able to help oncology patients more than ever before. Precise access to the particular artery feeding a chemo-insensitive or unresectable tumor is now a widely available service in most medical centers treating cancer patients. Nuclear medicine equipment and imaging agents have enabled localization of active tumors that are not imaged any other way and detect active tumors amongst those that are already destroyed. Therapeutic radiation has been successful in destroying cancer since the early twentieth century and today is often the difference between life and death for patients with tumors that are no longer sensitive to chemotherapy or for patients that cannot tolerate chemotherapy. Taken as a whole, these data suggest that the question is not 'why use radiation in the liver' rather it is the converse—"why wouldn't you use radiation (microspheres) in the liver?"

## 2 Hepatic Intra-Arterial Radioactive Microsphere Brachytherapy Fluid Dynamics

Surprisingly little research has been published for the hepatic arteries compared to the portal vessels regarding basic data such as velocities, branching patterns, and effects on particle flow, oncotic pressures in terminal arterioles in normal and tumor vessels, and many more important factors. Morgan reported on this aspect as an area in need of further study to optimize radioembolization therapy (Morgan et al. 2011). Kennedy recently investigated the use of computational fluid particle dynamics (CFPD) approaches to model the environment in the liver into which we are attempting to selectively deposit radioactive microspheres (Basciano et al. 2010; Childress et al. 2012; Kennedy et al. 2010; Kleinstreuer et al. 2012; Richards et al. 2012) (Figs. 1, 2). Computer modeling of microsphere deposition in the hepatic arteries was validated in a 4:1 scale 3D printed hepatic arterial system. There were also modest differences in distribution of resin microspheres versus glass microspheres due to the specific gravity of each sphere type.

**Fig. 2** Two possible scenarios depending on multiple factors: **a** incomplete coverage of radioactive fields and **b** intended implantation of adequate numbers of microspheres in sufficiently close proximity to each other



### 3 Historical Background of Radioactive Microparticle Therapy for Liver Cancers

The delivery of radioactive isotopes via vascular-borne microparticles to internal tumors dates back to 1947 when Muller and Rossier infused <sup>63</sup>Zn and <sup>198</sup>Au to treat renal cell metastases to the lungs, previously irradiated for bronchial carcinoma. Radioactive carbon particles that were used were 40–50 μm in diameter and were successfully trapped in bronchial tumors (Muller and Rossier 1947, 1951). Di Matteo reported the most extensive experience using <sup>198</sup>Au particles delivered by intra-arterial injection to treat lung carcinoma, but subsequently abandoned this approach in favor of microsphere therapy (Di Matteo et al. 1962). Although most clinical experience is with <sup>90</sup>Y, a variety of solid tumors have been treated with intra-arterial <sup>32</sup>P particles suspended in solution as the therapeutic isotope (Dogliotti et al. 1966; Caldarola et al. 1965, 1966).

### 4 Physics of Radiation Therapy

#### 4.1 Radiation Types

Radiation energy that causes ionization in the cell is of two types: electromagnetic or particulate. Electromagnetic energy, photons can be produced naturally by decay of radioactive isotopes (gamma rays) or by an electrical device accelerating electrons, which abruptly stop in a target, releasing energy (X-rays). The type of particulate energy most commonly used against malignant cells are electrons

(charge  $-1$ , mass = 0.511 MeV), but others in limited use via external beam accelerators include protons (charge  $+1$ , mass = 2000  $\times$  electrons), alpha particles (helium ions), and neutrons (same mass as proton, no charge). In general terms, alpha particles are effective penetrating only up to 1 mm thick of tissue, beta is effective up to 3 mm, with gamma and neutron radiation passing completely through the body and stopping only in thick walls of concrete. Photons are discrete packets of electromagnetic energy which can cause cell damage via collision with a cell, transferring some of its energy to the cell. The exchange of energy to the cell deflects the path of the photon, with a resulting reduction in its energy. Energy absorbed by the cell can create damage to the DNA/RNA leading to cell death. A photons-only path of travel is linear and cannot be altered in the liver except by collision with tissue, and therein lies the key disadvantage in using photons (external beam radiation) for hepatic tumors. Normal tissues surround metastatic and primary cancers in the liver and are always either above, below, or beside the target tumor and will be in the entrance or exit path of the photon beam. Linear accelerators can produce electron beams, which differ from photon beams, in that electron are particles with mass and charge, and thus have a finite range of tissue penetrance, allowing for treatment of more superficial tumors, while significantly sparing deeper normal tissues. Electron beam therapy may be appropriate in treating a mass in the liver, which is only 1–2 cm deep to the surface. The dose 4 cm below the tumor could be nearly zero if the appropriate energy was chosen, compared to a dose of 80 % of the tumor dose at that depth, if photons were used. Protons can

**Table 1** Radiation dose definitions

Radiation dose delivered	Effect/Result/Value
1 Gray (Gy) SI unit of dose	1 Joule of energy deposited into 1 kg of tissue (absorbed dose)
1 Gy Common Nomenclature	100 cGy, (100 “rads” in older terms)
1 Gy Striking Nucleus	40—DNA double strand breaks (usually lethal to the cell) 1,000—DNA single strand breaks (often lethal to the cell) 4,000—DNA base modifications (possibly lethal to the cell)
1 Gy External Beam Radiation	>300 cGy per min dose rate
1 Gy High Dose Rate Gamma Brachytherapy ( <sup>192</sup> Ir)	>20 cGy per min dose rate (typically 1 cm from source)
1 Gy Low Dose Rate Brachytherapy ( <sup>137</sup> Cs)	~1 cGy per min dose rate at calculated point of interest
1 Gy <sup>90</sup> Y-microspheres	~1 cGy per min inside 1 kg of mass with 1 GBq evenly distributed
1 Gy <sup>90</sup> Y-monoclonal Antibodies	0.01 cGy sec <sup>-1</sup> (systemic therapy for CD20 <sup>+</sup> lymphoma) Delivery method i.e., microsphere versus antibody will not affect dose rate which is GBq/kg

Note HDR ≥12 Gy/hr—definition by AAPM Task Group #59 (TG59)

LDR ~50 cGy/hr—definition by AAPM Task Group #59 (TG59)

Microsphere ~54 cGy kg (GBq hr)<sup>-1</sup> × 1 GBq/1 kg/60 min in h ≅ 1 cGy per min

be used similarly to electrons, but with a much deeper penetration if required (Table 1).

## 4.2 Radiation Dose

Dose of ionizing radiation absorbed by the liver, solid tumor, or other tissues is a cornerstone of clinical trial design. Older reports used the term roentgen (R), which described ionization in air, i.e., exposure of gamma rays. Newer nomenclature uses the SI unit for absorbed dose in tissue (1 Joule/kg = 1 gray (Gy) = 100 rads = 100 cGy (centigray)), as the basic unit of measurement. Conversion of older literature values listed as R is approximately 1 R = 0.01 Gy for gamma. It is less well known how to convert beta radiation doses, which are low dose, constant release radiotherapy, into equivalent external beam doses due to the differences in biologic response due to dose rate, fractionation, and activity (Zeman 2000). Thus brachytherapy doses are recorded as Gy, but these doses are not likely to be equivalent to the same dose Gy given as daily fractionated external beam doses of X-rays. This is an area of active investigation.

## 4.3 Brachytherapy

It was not long after Dr. Wilhelm Conrad Roentgen discovered X-rays in 1895 that the *Lancet* reported its use in January 1896 for medical use (Hall 2000). Shortly after the turn of the century, it was suggested by Alexander Graham Bell that radioactive isotopes be applied directly to tissues, and thus *brachytherapy* was born—from the Greek “*brachy*” meaning “*short range*”. The French

coined the term endocurietherapy, Greek “*endo*”, meaning “*within*”. Radioactive isotopes such as iridium (<sup>192</sup>Ir), cesium (<sup>137</sup>Cs), and iodine (<sup>125</sup>I and <sup>131</sup>I) have been used extensively since the early 1900s as primary therapy, and in addition to external beam radiation as a ‘boost’ to the tumor. Brachytherapy attempts to spare normal regional tissues by delivering a high dose locally in the tumor, and although gamma radiation photons are used mostly, there is relatively low dose at a distance from the tumor of several centimeters. The dose rate of radiation delivery via a brachytherapy isotope (50 cGy/h) is much lower than photons delivered by an accelerator, (500–2,400 Gy/min). Radioactive decay from an isotope that produces electrons (charge -1) is termed “beta decay”. These particles are used in such products as radiolabeled antibodies used in hematologic malignancies, or in higher energies, for bone metastases and thyroid malignancies. Currently, there is significant clinical use of pure beta emitting isotopes (no gamma photons emitted) yttrium and strontium (<sup>90</sup>Y, <sup>90</sup>Sr) in brachytherapy in liver lesions and systemically with antibody carriers (Wiseman and Witzig 2005; Wiseman et al. 2003; Knox et al. 1996; Macklis et al. 1994). An advantage and potential disadvantage of beta sources is that most of the effective radiation is delivered within 2–4 mm of the source, with virtually no radiation dose effect >1 cm away. Because there are no gamma rays, nuclear medicine detectors cannot readily image pure beta sources, making localization of implanted sources problematic. Brachytherapy sources can be implanted via blood infusion, needle applicator, directly applied and sutured into place as a permanent implant, or placed temporarily (minutes–hours) within a catheter that is removed from the body.



## 5 Radiobiology

An understanding of radiation effects in living tissues began at the turn of the century with observations of skin reaction, primarily erythema and breakdown (Hall 2000). Since then clinical experience has produced observations regarding normal and malignant tissue response and repair to ionizing radiation. DNA must be damaged and remain unrepaired or misrepaired to cause loss of reproductive ability or initiate apoptotic death. It has been estimated that in the presence of sufficient oxygen tension (>10 mm Hg) (Hall 2000; Kennedy et al. 1997) any form of radiation (X-rays, gamma rays, charged or uncharged particles) will be absorbed and potentially interact with the DNA. Approximately 75 % of the damage to the DNA is *indirect*, with a photon striking a water molecule (water is 80 % of the cell) within 4 nm of the DNA strand. Kinetic energy from the incident photon is transferred to an orbital electron of the water molecule, ejecting it, now called a secondary electron. Energy transferred to a water molecule forms a free radical, which is highly reactive and breaks bonds of DNA strands nearby. There can also be interaction of the secondary electron directly on the DNA strand causing damage, referred to as *direct* action (Hall 2000).

### 5.1 Modifiers of Radiation Response

The presence of oxygen is the single most important biologic modifier of radiation effect at the cellular level (Zeman 2000; Withers 2002). Oxygen is needed to make radiation damage caused by free radicals “permanent”, however, in a hypoxic state this damage can be repaired. The ratio of radiation dose without oxygen compared to the dose with oxygen which will produce the same biologic effect is termed the “oxygen enhancement ratio” or OER. For X-rays OER is between 2 and 3, i.e., a given X-ray will be 2–3 times as damaging in the presence of oxygen to the cell than it will in a hypoxic milieu (Hall 2000). This has significant implications clinically for microsphere therapy as many patients with liver malignancies are first considered for embolization procedures (TACE and Bland Embolization), which will likely produce a relative hypoxic environment within the tumor mass and reducing the OER. Other factors known to impact radiation effectiveness are widely known as the 4 “R”s: Reoxygenation (OER); *Repair* of radiation damage, *Reassortment* of cells into more or less sensitive portions of the cell cycle (S phase most radioresistant, G2-M most sensitive); *Repopulation* during a course of radiation, which is seen in rapidly dividing tumor populations, however, the continuous low dose of radiation over 14 days delivered by <sup>90</sup>Y can

overcome this possible factor. Repopulation can also become an issue after surgical resection, chemoembolization, cryotherapy, or radiofrequency ablation, where hepatic hypertrophy in the regional normal cells is stimulated. These normal clonogens are more susceptible to radiotherapy damage in this phase, limiting the use of radiation, which may allow for residual malignant cells to repopulate (Lawrence et al. 1995). Repair of radiation damage or “sublethal damage repair” is enhanced in low oxygen environments and with fractionation (multiple radiation doses). The break (24 h typically) between each fraction of external beam radiotherapy provides opportunity to repair DNA strand breaks in normal and malignant cells. Brachytherapy differs in this regard with continuous radiation, without a discrete “fraction” of radiation, but delivers lower dose rate of radiation continually.

## 6 Radiation Effects in the Liver

Acute and late effects of ionizing radiation to the liver have been described in the literature since the early 1960s (Ingold et al. 1965; Ogata et al. 1963). During radiotherapy, acute transient effects are often reflected as elevation of liver transaminases, and depending upon the treated volume, hematologic effects such as neutropenia and coagulopathy can occur. However, permanent effects can be produced, occurring weeks or months after radiation (“late effects”) such as fibrosis, persistent enzyme elevation, ascites, jaundice, and rarely, radiation-induced liver disease (RILD) and fatal veno-occlusive disease (VOD) (Lawrence et al. 1995, 1992; Austin-Seymour et al. 1986; Dawson et al. 2001). RILD is often what is called “radiation hepatitis” and classically was described as occurring within 3 months of initiation of radiation, with rapid weight gain, increase in abdominal girth, liver enlargement, and occasionally, ascites or jaundice, with elevation in serum alkaline phosphatase. The clinical picture resembled Budd-Chiari syndrome, but most patients survived, although some died of this condition without proven tumor progression. It was described that the whole liver could not be treated with radiation above 30–35 Gy in conventional fractionation (1.8–2 Gy/day, 5 days per week) or else RILD or VOD was likely to occur. Interestingly, VOD can also occur without radiotherapy in patients receiving high dose chemotherapy in hematologic malignancies, alkaloids, toxic exposure to urethane, arsphenamine, and long-term oral contraceptives, (Fajardo et al. 2001) as well as patients receiving radiation combined with chemotherapy or radiation alone. The clinical presentation can differ between RILD and chemotherapy plus radiation liver disease, but the common pathological lesion associated with RILD is VOD. The pathologic changes in VOD can affect a fraction of a lobe,



**Fig. 3** **a** Digitally reconstructed radiograph (DRR) produced by a CT scan of a woman prior to receiving  $^{90}\text{Y}$ -microsphere therapy for hepatic metastases originating from breast cancer that had become unresponsive to chemotherapy. The liver (*tan*) gallbladder (*green*) and tumor (*red*) were drawn on axial CT images within the radiation therapy software. The entire CT volume is rendered as a three-dimensional volume, which is viewed from the anterior position. Specific data on the volume of each structure identified can be determined and used in preplanning the activity of microsphere to use

for a given patient. **b** Axial CT image of the same patient prior to therapy. **c** Axial CT image 65 days after liver radiation showing effects of RILD with contraction of the liver, scalloped contour, and large volume ascites. She eventually died of disseminated disease. She had received 3 years of near continuous chemotherapy in addition to internal radiation. This type of long-term scarring of the liver with dysfunction is rare, occurring in only about 1 % of all patients receiving radioembolization

or the entire liver. It is best observed on low power microscopy, which demonstrates severe congestion of the sinusoids in the central portion of the lobules with atrophy of the inner portion of the liver plates (zone 3) (Lawrence et al. 1995; Fajardo et al. 2001). Foci of yellow necrosis may appear in the center of affected areas. If the affected area is large, it can produce shrinkage and a wrinkled granular capsule. The sublobular veins show significant obstruction by fine collagen fibers, which do not form in the larger veins and (suprahepatic and cava) which is a distinction between RILD and Budd–Chiari syndrome (Lawrence et al. 1995; Fajardo et al. 2001). Most livers heal and will display chronic changes after 6 months with little congestion, but distorted lobular architecture with variable distances between central veins and portal areas. These chronic liver changes are typically asymptomatic but are reproducibly seen on liver biopsies as late as 6 years after presentation. Further investigation of the pathogenesis of VOD is difficult as most animals do not develop VOD in response to radiation (Fajardo et al. 2001). Unfortunately, no animal model exists to study VOD. Hahn used radioactive colloid of up to 67,000 cGy of  $^{198}\text{Au}$  in dogs that survived up to 62 days (Hahn et al. 1951). Wollner demonstrated that dogs treated with glass  $^{90}\text{Y}$  microspheres dosed up to 35,480 cGy survived without developing VOD or liver failure. This dosage far exceeds the level of liver radiation humans could tolerate (Wollner et al. 1988). Extensive radiation damage was noted, including necrosis and fibrosis mainly in the central vein regions, and numerous microspheres that had congregated in the gallbladder wall. Long-term survivors retained a multinodular,

firm, and shrunken liver compared to dogs receiving non-radioactive microspheres (Wollner et al. 1988). Similar results were noted by Wollner in dogs with hepatic artery infusion of 5-bromo-2'-deoxyuridine (BUDR) concurrent with delivery of resin or glass  $^{90}\text{Y}$  microspheres (Wollner et al. 1987) (Fig. 3).

## 7 Rationale for $^{90}\text{Y}$ Microsphere Therapy

The unique vascular supply of the liver is well described and understood by radiologists and surgeons, but less well so by other specialists that now are key members of the liver brachytherapy team. A brief review is presented of the scientific evidence confirming microspheres' implantation preferentially in the peripheral zone of hepatic solid tumors, thus sparing the normal adjacent tissue.

### 7.1 Anatomic/Vascular Summary

The portal venous system supplies 80 % or more of the blood supply to normal liver (Breedis and Young 1954). The hepatic artery, with branches to the gallbladder, duodenum, and stomach, provides up to 20 % of the required blood supply to the normal liver. However, in the presence of tumor growth in the liver, the hepatic artery is the main supply of blood, from 80 to 100 %. Tumor vessel growth is many times more concentrated in the periphery of the tumor compared to the tumor center and normal liver, minimally 3:1 up to 20:1 and are abnormal (Lien and Ackerman 1970).

**Fig. 4** **a** Hematoxylin and eosin stained human liver section with microspheres in a typical cluster at the periphery of the lobule (original magnification 100x). **b** Inset is a close-up of the microspheres (diameter 32 μm) in relation to the nearby red blood cells with an 8 μm diameter

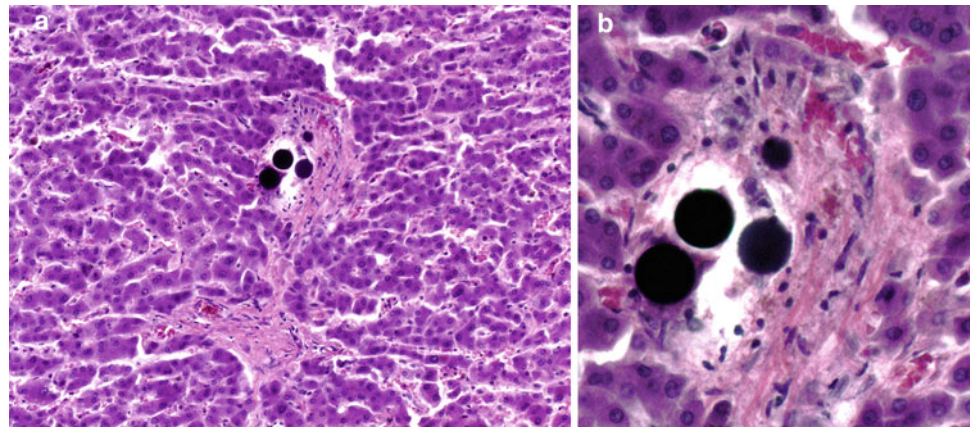


**Table 2** Properties of resin and glass <sup>90</sup>Y microspheres (Kennedy and Salem 2003; Kennedy et al. 2004)

Parameter	Resin	Glass
Trade name	SIR-spheres <sup>a</sup>	Theraspheres <sup>b</sup>
Manufacturer	Sirtex medical, Lane Cove, Australia	MDS nordion, Kanata, Canada
Diameter	20–60 microns <sup>a</sup>	20–30 microns <sup>b</sup>
Specific gravity	1.6 g/dl	3.6 g/dl
Activity per Particle	50 Bq	2500 Bq
Number of microspheres/3 GBq	40–80 million	1.2 million
Typical number delivered/patient	12–18 million	1.0–8.1 million
Material	Resin with bound yttrium	Glass with yttrium in matrix

<sup>a</sup> Sir-spheres<sup>®</sup>, Package Insert, Sirtex Medical, Inc., Lane Cove, Australia

<sup>b</sup> Therasphere<sup>®</sup>, Package Insert, MDS Nordion, Kanata, Canada

These data have been shown to be reliable in a number of trials (Lien and Ackerman 1970; Ackerman et al. 1970; Meade et al. 1987).

## 7.2 Preclinical Reports of Microsphere Deposition

Breedis and Young performed a series of animal studies with numerous species including rat, frog, rabbit and mouse, and 13 human livers which contained metastatic solid tumors. It was demonstrated that 80–100 % of the blood supply to tumors comes from the hepatic artery (Breedis and Young 1954). Comparable results were obtained by Ackerman et al. (1970) and Lien and Ackerman (1970) using a carcinosarcoma liver metastases rat system. Two treatment methods were employed: either <sup>131</sup>I-tagged human serum albumin (RISA) or resin microspheres with <sup>90</sup>Y (where diameters ranged between 55 and 86 μm). Infusions via the hepatic artery were compared to those of the portal vein in regard to uptake in the tumors versus the

normal liver tissue. Results showed that tumors larger than 30 mg received 75 % of their blood supply from the hepatic artery, with an estimated tumor-to-normal tissue ratio of 3:1. Vessel diameter, a key determinate regarding any microparticle penetration into the growth area of tumors, was studied by Lien using silicone rubber casts of tumor vessels. These casts confirmed vessels formed a ring around the periphery of the tumor in a plexus, with arterial diameters ranging between 25 and 75 μm, or about up to three times the diameter of nonmalignant arterial diameter (Lien and Ackerman 1970). Meade used rat livers to test for an optimal microsphere diameter. Using radioactive microspheres of 15, 32.5, and 50 μm, the coefficient of variance between tumor and normal vessels in adenocarcinoma masses in the liver favored the 32.5 μm microspheres, with the 50 μm having the worst variance (Meade et al. 1987). Pillai used 27 μm diameter microspheres in rabbits growing hepatic tumors from VX2 immortalized cells. The infusion of 15–30 million spheres showed 6–10 times as many microspheres in the periphery of the tumors compared with the normal liver ( $p < 0.008$ ) (Pillai et al. 1991).





**Fig. 5** (Left) A treatment vial containing a typical dose of glass microspheres ( $\sim 5$  GBq at time of delivery to the patient), which appear as a small amount of white material seen at the bottom of the vial. (Right) A shipping container of resin microspheres ( $\sim 3$  GBq) as delivered to the medical facility. An average dose is often less than 50 % of the volume of microspheres in this container, roughly 15 million microspheres. Resin microspheres appear tan colored and are transferred to a smaller treatment vial for delivery to the patient

## 8 Human Studies of Microsphere Deposition

Clinical experience with  $^{90}\text{Y}$  microspheres dates back to the early 1960s (Ariel 1965; Ariel and Pack 1967; Ariel and Padula 1982; Blanchard et al. 1964, 1965; Grady 1979) with significant interest in this approach developing in the US since 2000 (Kennedy et al. 2001a, b, 2002a, b, c; Kennedy and Salem 2003; Murthy et al. 2002a, b, c; Van Echo et al. 2001; Coldwell et al. 2001; Salem et al. 2002; Sarfaraz et al. 2001; Carr et al. 2002a, b). The study of microspheres in the livers of humans after treatment for both metastatic colon and primary hepatoma have been published from a review of biopsy (Fox et al. 1991) of the left lobe (Campbell et al. 2000) and four entire livers (Kennedy et al. 2004). The key findings were in agreement regarding preferential implantation of microspheres in the periphery of tumors, sparing of the normal liver, and the heterogeneous, nonrandom clustering of microspheres numbering 5–25 microspheres (Fig. 4).

## 9 Commercially Available $^{90}\text{Y}$ -Microsphere Products for Human Medical Use

Although they differ in significant ways, the two available microspheres have been shown to be equally effective thus far in a variety of solid tumor types. Understanding the unique features of each sphere may allow clinicians to exploit certain aspects for particular tumor types (Table 2) (Fig. 5).

## References

- Ackerman NB, Lien WM, Kondi ES, Silverman NA (1970) The blood supply of experimental liver metastases I: the distribution of hepatic artery and portal vein blood to “small” and “large” tumors. *Surgery* 66(6):1067–1072
- Ariel IM (1965) Treatment of inoperable primary pancreatic and liver cancer by the intra-arterial administration of radioactive isotopes (Y90 radiating microspheres). *Ann Surg* 162:267–278
- Ariel IM, Pack GT (1967) Treatment of inoperable cancer of the liver by intra-arterial radioactive isotopes and chemotherapy. *Cancer* 20(5):793–804
- Ariel IM, Padula G (1982) Treatment of asymptomatic metastatic cancer to the liver from primary colon and rectal cancer by the intraarterial administration of chemotherapy and radioactive isotopes. *J Surg Oncol* 20(3):151–156
- Austin-Seymour MM, Chen GT, Castro JR (1986) Dose volume histogram analysis of liver radiation tolerance. *J Radiat Oncol Biol Phys* 12:31–35
- Basciano CA, Kleinstreuer C, Kennedy AS, Dezarn WA, Childress E (2010) Computer modeling of controlled microsphere release and targeting in a representative hepatic artery system. *Ann Biomed Eng* 38(5):1862–1879
- Blanchard RJ, Grotenhuis I, LaFave JW (1964) Treatment of experimental tumors: utilization of radioactive microspheres. *Arch Surg* 89:406
- Blanchard RJ, LaFave JW, Kim YS (1965) Treatment of patients with advanced cancer using Y-90 microspheres. *Cancer* 18:375
- Breedis C, Young G (1954) The blood supply of neoplasms in the liver. *Am J Pathol* 30:969–984
- Caldarola L, Rosa U, Badellino F (1965) Preparation of  $^{32}\text{P}$  labelled resin microspheres for radiation treatment of tumors by intraarterial injection. *Panminerva Med* 7:102
- Caldarola L, Badellino F, Del Fante FM (1966) L'impiego del  $^{32}\text{P}$  nel trattamento chirurgico dei tumori maligni oro-maxillo-faciali. *Minerva Stomatol* 15:471
- Campbell AM, Bailey IH, Burton MA (2000) Analysis of the distribution of intra-arterial microspheres in human liver following hepatic yttrium-90 microsphere therapy. *Phys Med Biol* 45:1023–1033
- Carr B, Salem R, Sheetz M et al (2002a) Hepatic arterial yttrium labeled glass microspheres (TheraSphere) as treatment for unresectable HCC in 36 patients. *Proceedings of ASCO*
- Carr B, Torok F, Sheetz M et al (2002b) A novel and safe therapy for advanced-stage hepatocellular carcinoma (HCC): hepatic arterial  $^{90}\text{Y}$  yttrium-labeled glass microspheres (TheraSphere). *Int J Cancer Supplement* 13:459
- Childress EM, Kleinstreuer C, Kennedy AS (2012) A new catheter for tumor-targeting with radioactive microspheres in representative



- hepatic artery systems—part II: solid tumor-targeting in a patient-inspired hepatic artery system. *J Biomech Eng* 134(5):051005
- Coldwell D, Kennedy AS, Van Echo DA, et al (2001) Feasibility of treatment of hepatic tumors utilizing embolization with yttrium-90 glass microspheres. *J Vasc Interv Radiol* 12(S1): S113
- Dawson LA, Ten Haken RK, Lawrence TS (2001) Partial irradiation of the liver. *Semin Radiat Oncol* 11(3):240–246
- Di Matteo G, Gennarelli L, Lenti R (1962) Una nuova metodica per la fissazione elettiva dell' Au198 adsorbio su carbonio in terriori lobari e sublobari. *Gazz Intern Med Chir* 67:1875
- Dogliotti AM, Caldarella L, Badellino F (1966) Endoarterial regional injection of radioisotopes in the treatment of malignant tumours. *IJARI* 17:51
- Fajardo LF, Berthrong M, Anderson RE (2001) Chapter 15: liver. *Radiation Pathology*, 1st edn. Oxford University Press, New York pp 249–257
- Fox RA, Klemp PF, Egan G, Mina LL, Burton MA, Gray BN (1991) Dose distribution following selective internal radiation therapy. *Int J Radiat Oncol Biol Phys* 21(2):463–467
- Grady ED (1979) Internal radiation therapy of hepatic cancer. *Dis Colon Rectum* 22(6):371–375
- Hahn PF, Jackson MA, Goldie H (1951) Liver cirrhosis with ascites, induced in dogs by chronic massive hepatic irradiation with radioactive colloidal gold. *Science* 114:303–305
- Hall E (2000) *Radiobiology for the Radiologist*, 5th edn. Lippincott, Williams & Wilkins, Philadelphia pp 5–16, 80–87
- Ingold J, Reed G, Kaplan H (1965) Radiation hepatitis. *Am J Roentgenol* 93:200–208
- Kennedy AS, Salem R (2003) Comparison of two 90Yttrium microsphere agents for hepatic artery brachytherapy. In: *Proceedings of the 14th international congress on anti-cancer treatment*, vol 1, p 156
- Kennedy AS, Raleigh JA, Varia MA (1997) Proliferation and hypoxia in human squamous cell carcinoma of the cervix: first report of combined immunohistochemical assays. *Int J Radiat Oncol Biol Phys* 37(4):897–905
- Kennedy AS, Murthy R, Sarfaraz M, Yu C, Line BR, Ma L, et al (2001a) Outpatient hepatic artery brachytherapy for primary and secondary hepatic malignancies. *Radiology* 221P(Suppl):468
- Kennedy AS, Murthy R, Van Echo DA (2001b) Preliminary results of outpatient hepatic artery brachytherapy for colorectal hepatic metastases. *Eu J Cancer* 37(Suppl 6):289
- Kennedy AS, Murthy R, Kwok Y, et al (2002a) Hepatic Artery Brachytherapy for Unresectable Hepatocellular Carcinoma: An Outpatient Treatment Approach. In: *Proceedings of the 12th international congress on anti-cancer treatment* vol 1, pp 198–199
- Kennedy AS, Van Echo DA, Murthy R (2002b) Hepatic artery brachytherapy for neuroendocrine carcinoma. *Regul Pept* 108(1):32
- Kennedy AS, Van Echo DA, Murthy R (2002c) Colorectal (CRC) liver metastases and hepatocellular carcinoma (HCC) treated with outpatient hepatic artery brachytherapy, therasphere: imaging response and toxicity. *Int J Cancer* S13:226–227
- Kennedy AS, Coldwell D, Nutting C, Tucker G, Van Echo DA (eds) (2004a) 90Y-microspheres in the treatment of colorectal metastases: USA experience. In: *Proceedings of the 15th international congress on anti-cancer treatment*, T.C.O, Paris, France 10 Feb 2004
- Kennedy AS, Nutting C, Coldwell D, Gaiser J, Drachenberg C (2004b) Pathologic response and microdosimetry of 90Y microspheres in man: review of four explanted whole livers. *Int J Radiat Oncol Biol Phys* 60(5):1552–1563
- Kennedy AS, Kleinstreuer C, Basciano CA, Dezarn WA (2010) Computer modeling of yttrium-90-microsphere transport in the hepatic arterial tree to improve clinical outcomes. *Int J Radiat Oncol Biol Phys* 76(2):631–637
- Kleinstreuer C, Basciano CA, Childress EM, Kennedy AS (2012) A new catheter for tumor targeting with radioactive microspheres in representative hepatic artery systems. Part I: impact of catheter presence on local blood flow and microsphere delivery. *J Biomech Eng* 134(5):051004
- Knox SJ, Goris ML, Trisler K, Negrin R, Davis T, Liles TM, et al (1996) Yttrium-90-labeled anti-CD20 monoclonal antibody therapy of recurrent B-cell lymphoma. *Clin Cancer Res* 2(3):457–470. PubMed PMID: 9816191. eng
- Lawrence TS, Ten Haken RK, Kessler ML, Robertson JM, Lyman JT, Lavigne ML et al (1992) The use of 3-D dose volume analysis to predict radiation hepatitis. *Int J Radiat Oncol Biol Phys* 23(4):781–788
- Lawrence TS, Robertson JM, Anscher MS, Jirtle RL, Ensminger WD, Fajardo LF (1995) Hepatic toxicity resulting from cancer treatment. *Int J Radiat Oncol Biol Phys* 31(5):1237–1248
- Lien WM, Ackerman NB (1970) The blood supply of experimental liver metastases II: A microcirculatory study of the normal and tumor vessels of the liver with the use of perfused silicone rubber. *Surgery* 68(2):334–340
- Macklis RM, Beresford BA, Humm JL (1994) Radiobiologic studies of low-dose-rate 90Y-lymphoma therapy. *Cancer* 73(3 Suppl): 966–973. PubMed PMID: 8306286. eng
- Meade VM, Burton MA, Gray BN, Self GW (1987) Distribution of different sized microspheres in experimental hepatic tumours. *Eur J Cancer Clin Oncol* 23(1):37–41
- Morgan B, Kennedy AS, Lewington V, Jones B, Sharma RA (2011) Intra-arterial brachytherapy of hepatic malignancies: watch the flow. *Nat Rev Clin oncol* 8(2):115–120
- Muller JH, Rossier PH (1947) Treatment of cancer of the lungs by artificial radioactivity. *Experientia* 3:75
- Muller JH, Rossier PH (1951) A new method for the treatment of cancer of the lungs by means of artificial radioactivity (Zn63 and Au198). *Acta Radiol* 35:449–468
- Murthy R, Line BR, Kennedy AS et al (2002a) Clinical utility of Brehmstrahlung scan (BRM-Scan) after TheraSphere (TS). *J Vasc Interv Radiol* 13(2):S2
- Murthy R, Kennedy AS, Tucker G et al (2002b) Outpatient trans arterial hepatic 'low dose rate' (TAH-LDR) brachytherapy for unresectable hepatocellular carcinoma. *Proceedings of American Association for Cancer Research*, vol 43, p 485
- Murthy R, Kennedy AS, Coldwell D (2002c) Technical aspects of TheraSphere (TS) infusion. *J Vasc Interv Radiol* 13(2):S2
- Ogata K, Hizawa K, Yoshida M (1963) Hepatic injury following irradiation: a morphologic study. *Tukushima J Exp Med* 9:240–251
- Pillai KM, McKeever PE, Knutsen CA, Terrio PA, Prieskorn DM, Ensminger W (1991) Microscopic analysis of arterial microsphere distribution in rabbit liver and hepatic VX2 tumor. *Sel Cancer Ther* 7(2):39–48
- Richards AL, Kleinstreuer C, Kennedy AS, Childress E, Buckner GD (2012) Experimental microsphere targeting in a representative hepatic artery system. *IEEE Trans Bio-Med Eng* 59(1):198–204
- Salem R, Thurston KG, Carr B (2002) Yttrium-90 microspheres: Radiation therapy for unresectable liver cancer. *J Vasc Interv Radiol* 13:S223–S229
- Sarfaraz M, Kennedy AS, Cao ZJ, Li A, Yu C (2001) Radiation dose distribution in patients treated with Y-90 Microspheres for non-resectable hepatic tumors. *Int J Rad Biol Phys* 51(3 S1):32–33
- Van Echo DA, Kennedy AS, Coldwell D (2001) TheraSphere (TS) at 143 Gy median dose for mixed hepatic cancers; feasibility and toxicities. *Amer Soc Clin Oncol* 260a:1038
- Wiseman GA, Witzig TE (2005) Yttrium-90 (90Y) ibritumomab tiuxetan (Zevalin) induces long-term durable responses in patients with relapsed or refractory B-Cell non-Hodgkin's lymphoma.

- Cancer Biother Radiopharm 20(2):185–188. PubMed PMID: 15869453. eng
- Wiseman GA, Leigh BR, Erwin WD, Sparks RB, Podoloff DA, Schilder RJ, et al (2003) Radiation dosimetry results from a Phase II trial of ibritumomab tiuxetan (Zevalin) radioimmunotherapy for patients with non-Hodgkin's lymphoma and mild thrombocytopenia. *Cancer Biother Radiopharm* 18(2):165–178. PubMed PMID: 12804042. eng
- Withers HR (2002) Gastrointestinal cancer: radiation oncology. In: Kelsen DP, Daly JM, Levin B, Kern SE, Tepper JE (eds) *Gastrointestinal oncology: principles and practice*, 1st edn. Lippincott Williams & Wilkins, Philadelphia, pp 83–96
- Wollner IS, Knutsen CA, Ullrich KA, Chrisp CE, Juni JE, Andrews JC et al (1987) Effects of hepatic arterial yttrium-90 microsphere administration alone and combined with regional bromodeoxyuridine infusion in dogs. *Cancer Res* 47:3285–3290
- Wollner I, Knutsen C, Smith P, Prieskorn D, Chrisp C, Andrews J et al (1988) Effects of hepatic arterial yttrium 90 glass microspheres in dogs. *Cancer* 61(7):1336–1344
- Zeman E (2000) *Biologic Basis of Radiation Oncology*. In: Gunderson L, Tepper J (eds) *Clinical radiation oncology*, 1st edn. Churchill Livingstone, Philadelphia, pp 1–41

---

# Regulations and Requirements of Hospitals Performing Radioembolization

C. Trumm, R. T. Hoffmann, T. F. Jakobs, and M. F. Reiser

## Contents

<b>1</b>	<b>Introduction</b> .....	11
1.1	Multidisciplinary Approach.....	11
1.2	Radioembolization Team .....	11
<b>2</b>	<b>Legal Regulations of Hospitals Performing Radioembolization</b> .....	12
2.1	Legal Regulations .....	12
<b>3</b>	<b>Infrastructural Requirements of Hospitals Performing Radioembolization</b> .....	13
3.1	Appropriate Facilities .....	13
3.2	Training of Interventional Radiologist .....	13
3.3	Diagnostic Imaging Equipment.....	13
3.4	Radiation Safety Issues .....	13
	<b>References</b> .....	14

---

## Abstract

Centers performing SIRT should ideally be characterized by a multidisciplinary approach to the design, delivery, and reappraisal of primary or metastatic liver cancer treatment, or by referral from a multidisciplinary team familiar with the procedure (Table 1) (Kennedy et al. 2007; Wang et al. 2010). Moreover, the likely interactions between SIRT and any prior, concurrent or planned biological, chemotherapeutic, local or loco-regional ablative, surgical, external beam radiation treatment, or radiosurgery should be extensively discussed within a multidisciplinary tumor board

---

## 1 Introduction

### 1.1 Multidisciplinary Approach

Centers performing SIRT should ideally be characterized by a multidisciplinary approach to the design, delivery, and reappraisal of primary or metastatic liver cancer treatment, or by referral from a multidisciplinary team familiar with the procedure (Table 1) (Kennedy et al. 2007; Wang et al. 2010). Moreover, the likely interactions between SIRT and any prior, concurrent or planned biological, chemotherapeutic, local or loco-regional ablative, surgical, external beam radiation treatment, or radiosurgery should be extensively discussed within a multidisciplinary tumor board.

### 1.2 Radioembolization Team

According to the recommendations by the radioembolization brachytherapy oncology consortium (REBOC) (Kennedy et al. 2007), the team performing radioembolization should include individuals with sufficient expertise to:

---

C. Trumm (✉) · M. F. Reiser  
Institute of Clinical Radiology, Ludwig Maximilians-University,  
Munich, Germany  
e-mail: christoph.trumm@med.lmu.de

R. T. Hoffmann  
Department and Polyclinics of Diagnostic Radiology,  
Universitätsklinikum Carl Gustav Carus, Dresden, Germany

T. F. Jakobs  
Department of Radiology, Krankenhaus Barmherzige Brüder,  
Munich, Germany

**Table 1** Mandatory and desirable facilities and personnel for centers performing  $^{90}\text{Y}$  radioembolization (according to Dezar [2008](#); Kennedy et al. [2007](#); Wang et al. [2010](#))

<i>Mandatory</i>
Multidisciplinary team approach to reviewing liver cancer patients, including an interventional radiologist and at least three of
Hepatic surgeon
Medical oncologist
Radiation oncologist
Nuclear medicine physician
Pain physician or anesthetist
Gastroenterologist/hepatologist
Medical physicist/radiation safety officer
Dedicated oncology nursing staff
Established radiation safety, spill, contamination and disposal protocols
Triple phase CT, DSA, and gamma camera $^{99\text{m}}\text{Tc}$ MAA equipment
<i>Desirable</i>
Admitting and clinic rights for radiologists
On-site consultant medical physicist
Magnetic resonance imaging (MRI)
Single photon emission computed tomography (SPECT)
Positron emission tomography (PET)
Hybrid Imaging including PET-CT and PET-MRI

- Care for the overall medical treatment of the cancer patient
- Perform vascular catheterization
- Perform and interpret radiologic scans
- Assume the responsibility for the delivery of the  $^{90}\text{Y}$  microspheres and be the authorized user
- Monitor radiation safety.

While the interventional radiologist is particularly responsible for the assessment and delivery of the  $^{99\text{m}}\text{Tc}$  MAA angiography and radioembolization procedure, further care for the treated patients is usually assumed by the referring clinician or another designated member of the multidisciplinary team (Dezar [2008](#)).

Before SIRT, the technical complexity, the potential outcomes and complications of the diagnostic workup ( $^{99\text{m}}\text{Tc}$  MAA angiography) and the radioembolization procedure should be extensively explained to each patient in a dedicated counselling interview.

Furthermore, during this first clinical appointment the suitability and physical fitness of the patient should be evaluated. Referral for SIRT should never imply an obligation to treat the patient. At least 24 h prior to both the diagnostic  $^{99\text{m}}\text{Tc}$  MAA angiography and the radioembolization procedure, patients' written consent should be documented. After SIRT, each case should be reviewed again by the multidisciplinary team in order to inform the team

**Table 2** Hospital requirements for initiating a SIRT program

Country	$^{90}\text{Y}$ Licence	Specific authority to use radioisotopes in the angiography suite
Germany	x	x
France	x	x
UK	x	x
Belgium	x	x
The Netherlands	x	x
Italy	x	x
Spain	x	–
Switzerland	x	x
Austria	x	x
Sweden	x	–
Norway	x	x
Denmark	x	x
Finland	x	–
Portugal	x	–
Poland	x	–
Slovenia	x	–
Ireland	x	x
Scotland	x	x
Greece	x	x
Turkey	x	–

members with respect to subsequent treatment decisions. Moreover, at discharge the patient should receive recommendations and information on further hydration and nutrition, peri-procedural medication, radiation safety instructions, the next necessary follow-up visits, and contact details in case of post-procedural side-effects.

## 2 Legal Regulations of Hospitals Performing Radioembolization

### 2.1 Legal Regulations

In most countries hospitals have to apply for a  $^{90}\text{Y}$  license with the appropriate authorities or professional bodies before initiating a SIRT program (Table 2). This license refers to the permission to store and dispose of  $^{90}\text{Y}$  in the hospital. In case  $^{90}\text{Y}$  isotopes are already used for other therapeutic purposes (e.g.,  $^{90}\text{Y}$  radiosynoviorthesis) in the hospital, the  $^{90}\text{Y}$  license—if defined according to quantity—should be increased in addition to the amount of  $^{90}\text{Y}$  currently used in the department (e.g., 8-10 GBq daily, 15-20 GBq monthly).

Beside the  $^{90}\text{Y}$  license, a permission for particular users to administer radioisotopes within the radiology department

has to be separately requested from a specific authority (Table 2).

In the United States,  $^{90}\text{Y}$  therapy is regulated by the Nuclear Regulatory Commission under the code of federal register (CFR) 10, part 35.1000, as a brachytherapy device (i.e., not a drug) used for permanent brachytherapy implantation therapy (Kennedy et al. 2007). The use of  $^{90}\text{Y}$  microspheres is only permitted under the supervision of an authorized user, who must fulfill the training and experience requirements for manual brachytherapy, as well as the specific vendor training in handling of the microspheres and the delivery system. For U.S. institutions performing brachytherapy under a broadscope license, the physician must be authorized by the institutional radionuclide committee. According to Kennedy et al. (2007), interventional radiologists, nuclear medicine physicians and radiation oncologists are sufficiently trained, certified and involved within  $^{90}\text{Y}$  treatment programs to use  $^{90}\text{Y}$  microspheres. In this context, they would either have to fulfill the training and experience requirements set in CFR 10, part 35.390 (for unsealed sources) or 35.490 (for manual brachytherapy), as well as the specific vendor training.

### 3 Infrastructural Requirements of Hospitals Performing Radioembolization

#### 3.1 Appropriate Facilities

Radioembolization is a complex and technically demanding procedure. However, emerging centers commonly underestimate the expertise required to safely perform treatments with  $^{90}\text{Y}$  microspheres (Wang et al. 2010). First and foremost, a multidisciplinary treatment protocol should be well established before the treatment of the first patient. This includes the structured interaction between diagnostic imaging, nuclear medicine, radiation safety, the multidisciplinary care team, oncology nursing staff, discharge and follow-up procedures, and hospital administration—even if not all of these resources are available at the same site.

#### 3.2 Training of Interventional Radiologist

In addition to absolving the mandatory training by the company delivering the  $^{90}\text{Y}$  microspheres, radiologists planning to perform SIRT should initially be instructed at a centre of excellence by a clinical mentor experienced in the procedure, and familiar with the guidelines published by the responsible professional institutions and societies (i.e., Society of Interventional Radiology, Cardiovascular and Interventional Society of Europe) (Dezarn 2008; Murthy

et al. 2005). As soon as the interventional radiologist is sufficiently instructed and practically trained to perform radioembolization at his own institution, he or she should conduct a series of treatments in order to absolve a learning curve experience of his/her own, and optimize the interaction with the local infrastructural resources.

#### 3.3 Diagnostic Imaging Equipment

Although the availability of imaging technology and expertise varies between institutions, the minimal diagnostic workup for SIRT candidates involves the following imaging studies:

- a recent multiphase CT of the liver (performed within 4–6 weeks of angiographic workup)
- digital subtraction angiography (DSA)
- gamma camera  $^{99\text{m}}\text{Tc}$  macro-aggregated albumin ( $^{99\text{m}}\text{Tc}$  MAA) scanning.

Additional diagnostic information may be provided in selected institutions where the following modalities or imaging techniques are available:

- CT hepatic angiography with intra-arterial contrast-delivery (e.g., cone beam CT)
- Magnetic resonance imaging (MRI)
- Single photon emission computed tomography (SPECT)
- Positron emission tomography (PET)
- Hybrid Imaging including PET-CT and PET-MRI.

#### 3.4 Radiation Safety Issues

In centers performing radioembolization, according to Kennedy et al. (2007) the following radiation precaution guidelines should be followed:

##### 3.4.1 Angiography Suite

- In order to avoid microspheres becoming lodged in crevices from which they are difficult to remove, the floor of the angiography suite should be characterized by a closed surface.
- The angiography suite area underneath the delivery system and the staff involved in dose administration should be draped and plastic covers placed over pedals as a precautionary measure in case of contamination.

##### 3.4.2 Delivery Catheter and Other Devices

- The delivery catheter should be considered radioactive and disposed of with respect to radiation precautions. All other potentially contaminated material (e.g., exit tubing from the dose vial, three-way-valve, etc.) should also be considered radioactive and disposed of equivalently after catheter removal.

- Though not being considered ‘hot’, tubing and syringes to deliver and flush the catheter sheath should be checked for radioactivity before routine disposal.

### 3.4.3 Staff

- Pregnant staff and/or pregnant family members should be excluded from the procedural or post-procedural care of  $^{90}\text{Y}$  patients.
- Infusion personnel must remain behind the delivery system containing the dose. Anyone assisting should remain clear of the tubing connected to the catheters.
- The administering staff should wear double gloves, double shoe covering and protective eye-wear.
- All personnel within the angiography suite must have their shoe covers checked for radiation at the end of the procedure and before leaving the suite. The suite must be checked at the end of the procedure after all contaminated waste and the patient have been removed from the room to rule out any radiation contamination.

### 3.4.4 Patient

- Because  $^{90}\text{Y}$  resin microspheres may have trace amounts of free  $^{90}\text{Y}$  on their surface, which can be excreted in the urine in the first 24 h, patients are advised to wash their hands after voiding. In contrast,  $^{90}\text{Y}$  glass microspheres are not known to have free  $^{90}\text{Y}$  in trace amounts in the treatment vial, and therefore no specific precautions are

required for handling the urine of patients treated with  $^{90}\text{Y}$  glass microspheres.

- At discharge, the patient should be given a letter confirming that they have received radiation internally. In addition, a wristband indicating the isotope given, the date of delivery, and a contact number for questions may be advantageous.

---

## References

- Dezarn WA (2008) Quality assurance issues for therapeutic application of radioactive microspheres. *Int J Radiat Oncol Biol Phys* 71(1 Suppl):S147–S151
- Kennedy A, Nag S, Salem R, Murthy R, McEwan AJ, Nutting C, Benson A 3rd, Espat J, Bilbao JJ, Sharma RA, Thomas JP, Coldwell D (2007) Recommendations for radioembolization of hepatic malignancies using yttrium-90 microsphere brachytherapy: a consensus panel report from the radioembolization brachytherapy oncology consortium. *Int J Radiat Oncol Biol Phys* 68(1):13–23
- Murthy R, Nunez R, Szklaruk J, Erwin W, Madoff DC, Gupta S, Ahrar K, Wallace MJ, Cohen A, Coldwell DM, Kennedy AS, Hicks ME (2005) Yttrium-90 microsphere therapy for hepatic malignancy: devices, indications, technical considerations, and potential complications. *Radiographics* 25(Suppl 1):S41–S55
- Wang SC, Bester L, Burnes JP, Clouston JE, Hugh TJ, Little AF, Padbury RT, Price D (2010) Clinical care and technical recommendations for  $^{90}\text{Y}$  microsphere treatment of liver cancer. *J Med Imaging Radiat Oncol* 54(3):178–187



---

# Radiological Evaluation of Patients with Liver Tumors

Christoph J. Zech and Maximilian F. Reiser

## Contents

<b>1</b>	<b>Introduction</b> .....	15
<b>2</b>	<b>Modalities for the Radiological Evaluation of Patients with Liver Tumors</b> .....	16
2.1	Ultrasound.....	16
2.2	Computed Tomography.....	16
2.3	Magnetic Resonance Imaging.....	20
2.4	Angiography .....	23
<b>3</b>	<b>Summary and Conclusion</b> .....	24
	<b>References</b> .....	25

---

## Abstract

For a successful radioembolization, a proper planning of the procedure is necessary—ensuring that the indication for the treatment is correct and helping to deliver the therapy substance to the right places in the liver finally. One cornerstone for such a treatment plan is the radiological evaluation of patients scheduled for radioembolization. The aim of imaging has to be an accurate assessment of number, size, and localization of malignant liver lesions. Moreover, benign differential diagnoses of different liver lesions have to be considered. Depending on the logistics within the hospital and the clinical background, several modalities can be selected for imaging patients with liver tumors. These imaging modalities will be described in this chapter and their respective advantages and limitations will be analyzed.

---

## 1 Introduction

The radiological evaluation of patients with liver tumors is an important and highly relevant field of diagnostic imaging due to the large number of patients with liver disease (e.g., the increasing number of patients with viral hepatitis) or with at least potential involvement of the liver (e.g., patients with extrahepatic malignancies as colonic carcinoma). The aim of imaging has to be an accurate assessment of number, size, and localization of malignant liver lesions. Moreover, various benign liver lesions have to be differentiated from malignant lesions, since these benign entities seldom need treatment. For malignant lesions the therapeutic decisions usually depend strongly on the extent of liver involvement—a limited number of lesions can be surgically resected or treated with local ablative therapies, whereas multifocal lesions require a different approach including systemic chemotherapy and various treatment options including selective internal radiation therapy.

---

C. J. Zech (✉)

Abteilungsleiter Interventionelle Radiologie, Klinik für Radiologie und Nuklearmedizin, Universitätsspital Basel, Petersgraben 4, CH-4031, Basel, Switzerland  
e-mail: Christoph.Zech@usb.ch

M. F. Reiser

Klinikum der LMU München, Standort Grosshadern, Institut für Klinische Radiologie, Munich, Germany

Depending on the logistics within the hospital and the clinical background, several modalities can be selected for imaging patients with liver tumors. These imaging modalities will be described in this chapter and their respective advantages and limitations will be analyzed.

## 2 Modalities for the Radiological Evaluation of Patients with Liver Tumors

### 2.1 Ultrasound

Ultrasound can be still regarded as a first-line imaging modality used in patients with known or suspected liver tumors. Gross anatomical abnormalities and lesions can be detected and further examinations planned. The main advantage of this widespread technology is the easy and fast access. One limitation is that the diagnostic value of a Sonographic examination depends strongly on the skill and experience of the examiner. Moreover, in patients with liver cirrhosis or with extensive bowel gas superimposition, the visualization of the liver may be reduced. With gray-scale B-mode ultrasound detection rates of 58–70 % for liver tumors can be achieved depending on the patient selection (Harvey and Albrecht 2001; Bartolozzi et al. 1996). In comparison with conventional B-mode ultrasound, new techniques, such as “tissue harmonic imaging”, in which the echoes are recorded with doubled frequency, allow for a better delineation and detection of focal liver lesions (Tanaka et al. 2000). Other new techniques include 3D-scanning, speckle reduction imaging, and cross beam-techniques. The gray-scale ultrasound is highly useful in the differential diagnosis of the most common benign lesions, namely simple cysts and hemangiomas.

In addition to B-mode sonography flow-dependent techniques like color-coded duplex sonography or power-Doppler sonography can be employed in liver imaging. Although these techniques are used in most cases to obtain information about the hepatic vasculature, it has been described that they also provide additional information in the characterization of focal liver lesions based on their perfusion patterns (Reinhold et al. 1995).

Contrast-enhanced ultrasound is now an established part in the work-up of focal liver lesions (Fig. 1). There have been publications that showed an increased detection rate for focal liver lesions from 63 % for B-mode ultrasound to 91 % for combined B-mode and contrast-enhanced ultrasound (Albrecht et al. 2001). Especially with regard to lesion characterization, contrast-enhanced ultrasound enables to improve lesion type diagnosis significantly. In a trial with 63 patients, correct lesion characterization was increased from 65 to 92 % by using contrast-enhanced

sonography. The contrast agents for ultrasound consist of microbubbles with a diameter from 2 to 6  $\mu\text{m}$  (Quaia 2007). They are composed of a shell of biocompatible materials, including proteins, lipids or biopolymers, and a filling gas. First generation contrast agents almost completely vanished from the market. Approved agents of the second generation ultrasound contrast agents are Optison<sup>®</sup> (GE Healthcare, Princeton, US) or SonoVue<sup>®</sup> (Bracco Imaging, Milano, Italy). However, among these second generation contrast agents only SonoVue<sup>®</sup> is approved for liver imaging. Together with CT and with liver-specific MRI contrast-enhanced sonography in daily practice represents a modality that allows for the confident assessment of lesion vascularity and increases the detection of focal liver disease. Nowadays, the technique is also widely accessible.

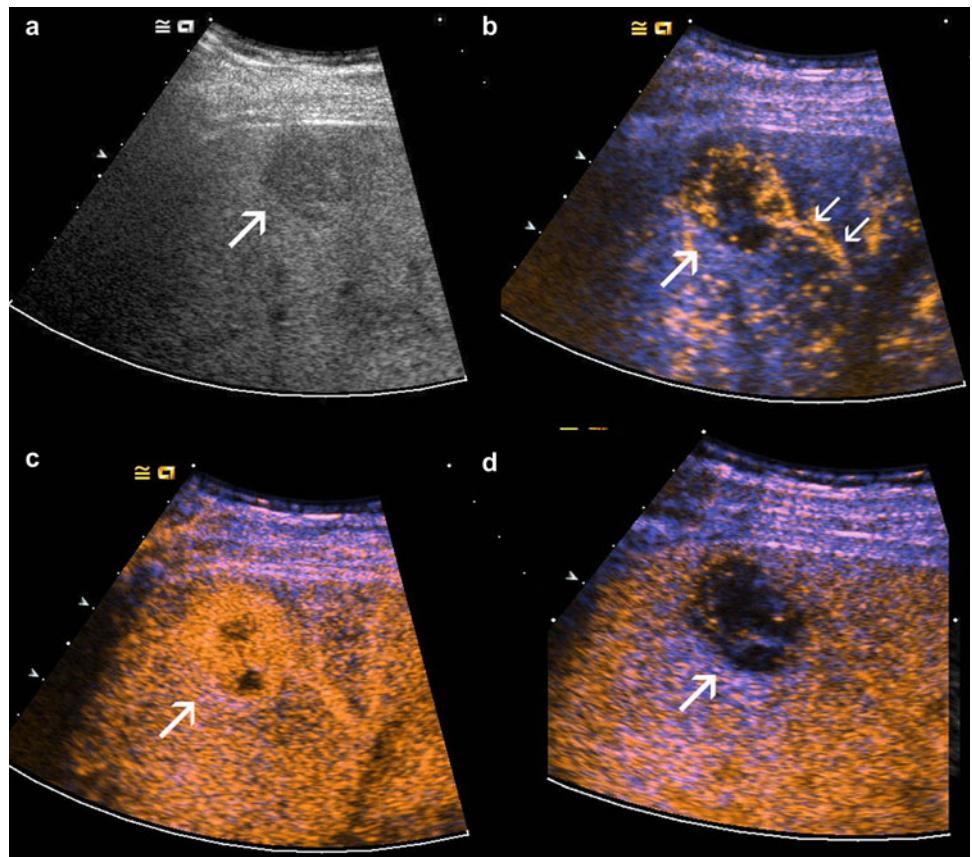
### 2.2 Computed Tomography

Computed Tomography (CT) has developed dramatically with the introduction of the multi-detector technology and with newly explored features like dual energy CT. Especially the abdomen, where motion artifacts due to respiratory motion and bowel peristalsis are disturbing, takes great advantage from these techniques. While scanners with 64 or more detector rows are still most common in large community or university hospitals, scanners with 2–16 slices are widely available even in private practice or in small hospitals. With the introduction of multi-detector CT (MDCT) bi- or even tri-phasic examinations of the liver can be combined into a thoraco-abdominal CT examination without compromises with regard to spatial or temporal resolution. The acquisition of the liver with a 64-slice scanner for example only requires a few seconds despite a submillimeter collimation. Even patients with a compromised general state of health are able to tolerate these breath-hold times. However, even on single slice spiral CT scanners adequate image quality of the liver can be obtained. However, combination with thoraco-abdominal examinations is not possible without compromise in temporal and spatial resolution.

Recently developed PET/CT—scanners, which combine the advantages of PET (functional imaging with high sensitivity), with the advantages of CT (morphological imaging with high spatial resolution) within one examination and nearly perfect image co-registration are with regard to imaging in oncological patients a real contribution. The value of PET-CT for pretreatment evaluation of patients or for response evaluation will be discussed in “Nuclear Medicine Procedures for Treatment Evaluation” and “Radiological Detection and Assessment of Tumor Response” respectively.



**Fig. 1** Hypervascular liver metastasis (*arrows*) from an esophageal carcinoma depicted with B-mode gray-scale ultrasound (**a**) and contrast-enhanced ultrasound 16 s (**b**), 23 s (**c**), and 3 min 40 s (**d**) after injection of 2.5 ml SonoVue® (Bracco Imaging, Milano, Italy) and 10 ml NaCl-flushing. *Note* the increased conspicuity of the lesion especially in the delayed phase (**d**) as compared to plain B-mode ultrasound. The dynamic study shows the feeding vessel (*small arrows*) with an early peripheral enhancement (**b**) and ongoing complete enhancement of the lesion with two small necrotic spots (**c**), which are spared from enhancement. In the delayed phase (**d**) strong wash-out has taken place, being typical for liver metastases



Adequate examination technique is critical for sensitive detection and specific characterization of focal liver lesions. A bi-phasic examination of the liver with a late-arterial and a porto-venous phase can be regarded as standard today. For specific indications like the follow-up of hepatocellular carcinoma (HCC) after transarterial chemoembolization (TACE) or for the depiction of the arterial vessels prior to angiography an early arterial phase scan, which can be post-processed into a CT-angiography, is helpful (Fig. 2). The value of delayed scans (e.g., 5 min after contrast agent injection) is controversial in the literature; mainly centers with a focus on imaging in liver cirrhosis consider the use of late phase images as necessary whereas other authors see no added value for it (Hwang et al. 1997; Schima et al. 2006).

With the short acquisition times of MDCT, contrast agent timing has become critical, since the optimal enhancement phase has to be included within a very short acquisition window. Therefore, the use of modern contrast agent power injectors and bolus timing are mandatory (Schima et al. 2005). For bolus timing automatic bolus triggering is recommended which is available from all CT vendors. Non-ionic iodine-based contrast agents with a concentration of 300–400 mg iodine/ml have become standard. Depending on the iodine concentration fast flow rates up to 5 or 6 ml/second are recommended (Schima

et al. 2005). The dosing of the contrast agent should be related to the body-weight with 1.5–2 ml per kg body-weight (for a concentration of 300 mg iodine/ml) (Baron 1994). Whereas the enhancement in the arterial phases can be optimized with help of high-concentration (370–400 mg iodine/ml) contrast agents, the enhancement in the porto-venous phase is not dependent on the iodine delivery per time but rather on the total amount of iodine (Brink 2003). With dual-head power injectors a saline-chaser of 30–50 ml can be injected directly after contrast agent injection allowing for a somewhat reduced contrast agent dose despite optimal contrast enhancement in the arterial phase (Schoellnast et al. 2003).

For focal liver lesions, detection rates of biphasic spiral CT typically ranging from roughly 60 to 75 %, and differentiation of benign and malignant lesions in around 70 % have been reported in literature (Kondo et al. 1999; Semelka et al. 1999; Reimer et al. 2000; Bartolozzi et al. 2004; Oudkerk et al. 2002). CT (even with recent MDCT technology) has shown to be inferior with regard to lesion detection (and lesion characterization) in trials which compared it directly to Gadolinium-enhanced MRI (Semelka et al. 2001) or liver-specific MRI (Reimer et al. 2000; Bartolozzi et al. 2004; Oudkerk et al. 2002). This was especially seen in the subgroup of lesions smaller than 1 cm

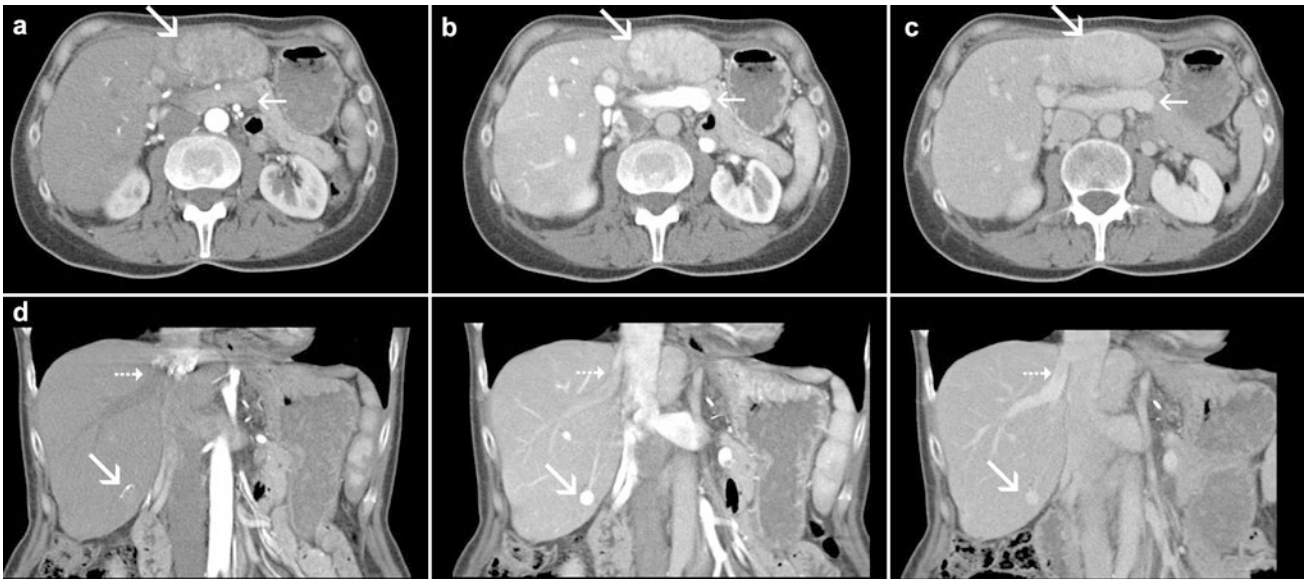


**Fig. 2** Axial and coronal sections in the early arterial phase (*left*), late-arterial phase (*middle*), and porto-venous phase (*right*) in a female patient suffering from a hepatocellular carcinoma (HCC) under treatment with transarterial chemoembolization (TACE). In the early arterial phase only the liver arteries are properly enhanced, the portal vein and also the liver parenchyma are not yet opacified. The two HCC nodules in segment 2/3 and segment 6 (*marked by large arrows*) are also both not properly demarcated. The early arterial phase is, therefore, not suitable for detection of hypervascular tumors; it is rather a CT angiographic phase and can be omitted in most cases. The most important phase for detection of hypervascular tumors is the late-

arterial phase (also called arterial-dominant phase or phase of porto-venous inflow). In this phase there is already enhancement in the portal vein (*small arrow in the upper row*) and in the liver parenchyma. The liver veins are not yet opacified in this phase (*small arrow in the lower row*). Most hypervascular tumors reach their highest attenuation in this phase. In the porto-venous phase enhancement of the liver parenchyma is highest, the vascular enhancement in the portal-venous system and in the hepatic vein is similar. Hypervascular tumors show decreased attenuation compared to the late-arterial phase, depending on the degree of wash-out they can be still hyperdense (as in this case), isodense (see Fig. 4), or even hypodense

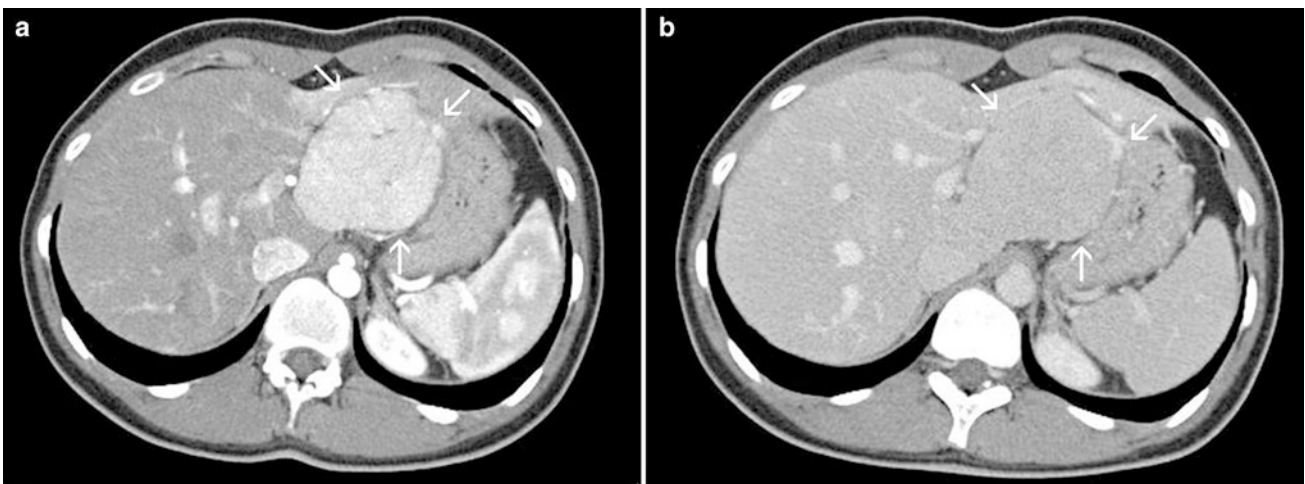


**Fig. 3** Focal nodular hyperplasia of the liver in a young female patient in the late-arterial (**a**) and porto-venous phase (**b**). *Note* the strong, homogenous enhancement of the lesion in the arterial phase with a spot of hypodensity in the central parts, representing the central

scar. The adjacent liver parenchyma is rather compressed than infiltrated by the lesion. Together with additional features like the wash-out to isointensity and the lobulated, well-defined margin the diagnosis of a FNH can be made with confidence in this case

in diameter. This limitation is presumably due to the limited contrast resolution of CT which is not compensated by the excellent geometric spatial resolution.

Benign solid liver lesions, such as Focal Nodular Hyperplasia (FNH) or liver cell adenoma can be detected in CT by the characteristic tumor blush to be seen in the late-

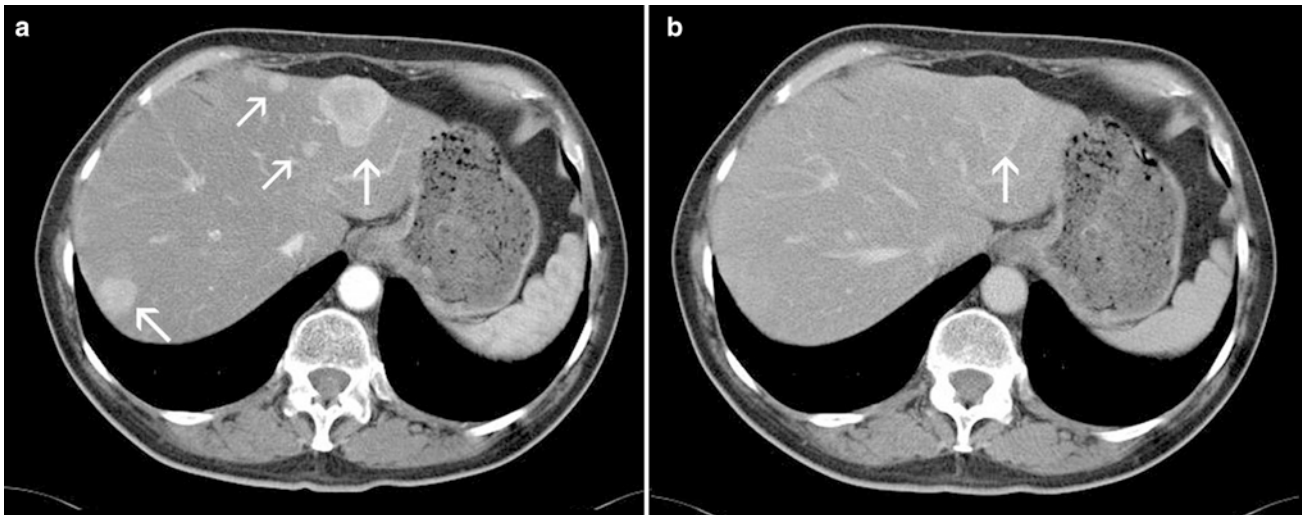


**Fig. 4** MDCT in the late-arterial **a** and porto-venous phase **b** in a male patient suffering from a neuro-endocrine carcinoma with liver metastases (arrows). Note the strong wash-out of the metastases to nearly isointensity, so that even the larger lesions can retrospectively

not be properly detected in the porto-venous phase in contrast to the excellent conspicuity of the lesions in the arterial phase. This example strikingly demonstrates the importance of a correctly timed late-arterial phase

arterial phase (Grazioli et al. 2001; Carlson et al. 2000). In addition to the contrast agent behavior, morphological features like the central scar recognizable in FNHs or fatty or regressive changes and hemorrhage in adenomas contribute to establish the correct diagnosis (Fig. 3). Further criteria can be delineated with help of MRI; these criteria will be described in Sect. 2.3.

According to the literature liver metastases are detected with spiral CT with a sensitivity ranging from 58 to 85 % (Lencioni et al. 1998; Ward et al. 1999; Valls et al. 2001). Data from single-row spiral CT and MDCT show that the optimal reconstructed slice thickness for reading CT examinations of the liver on transversal sections is in the range of 2.5–5 mm (Weg et al. 1998; Haider et al. 2002). Since a reconstructed slice thickness of 2.5 mm is difficult to obtain without motion artifacts on single-row scanners, the use of MDCT can be regarded as helpful and advantageous per se. As mentioned above, modern scanners allow for submillimeter collimations, so that slices with <1 mm can be obtained without problems. Our own experience and the data from the literature, however, showed that such thin slices are not superior in the detection of liver metastases. On the contrary, the large number of slices to be reviewed and the strong increase in image noise are rather disadvantageous (Haider et al. 2002; Kawata et al. 2002).

Depending on the primary tumor, liver metastases can present with different morphological and enhancement characteristics, which mainly correspond to the consistency (cystic, mucinous, solid) and the vascularity (hypovascular or hypervascular). Some primary tumors usually have hypervascular liver metastases. These include thyroid carcinoma, carcinoid tumors, neuro-endocrine tumors, and

renal cell carcinoma (Danet et al. 2003). Metastases from pancreatic carcinoma, breast carcinoma, and colonic carcinoma may sometimes also be hypervascular (Danet et al. 2003). In liver metastases from a cancer of unknown primary (CUP) hypervascular lesions can be seen occasionally. The hypervascular nature of these lesions can be best appreciated in the late-arterial phase of the liver. The pronounced vascularity leads to a fast wash-out of the contrast agent in later phases, which underlines the need for a proper timing of the late-arterial phase as described above (Fig. 4). Hypovascular metastases appear hypodense in both arterial and portal-venous phases. One should be aware of the fact that this classification reflects only the degree of lesion enhancement compared to the normal liver parenchyma in the arterial and portal-venous phases. It is known that even hypovascular lesions have a considerable amount of vascularization (which is a basic presumption for the Radio-embolization treatment of hypovascular metastases) and show contrast uptake, but to a lesser degree compared with the surrounding liver parenchyma (Danet et al. 2003).

Imaging of the cirrhotic liver is a challenging task for every modality. The detection rates of HCC reported in the literature are highly variable. One trial with a very stringent methodology showed a sensitivity of 61 %, a specificity of 66 %, and a negative predictive value of 30 % for the detection of HCC (Burrel et al. 2003). A subgroup analysis in this trial revealed a strong influence of the lesion size. While lesions >2 cm were detected in 100 %, lesions smaller than 1 cm were only detected in 10 % (Burrel et al. 2003). Another trial with a 4-row MDCT demonstrated an overall sensitivity of 73 % for lesion detection, with also markedly reduced detection rates (33 %) for lesions smaller



than 1 cm (Kawata et al. 2002). Since CT can only depict the vascularity of lesions, it is difficult to distinguish between simple regenerative nodules, high-grade dysplastic nodules, and early HCC in the cirrhotic liver (Burrel et al. 2003). The advantages of MRI in this respect are the possibility of tissue characterization based on different contrast weightings of the pulse sequences (T1, T2) and the availability of liver-specific contrast agents (see Sect. 2.3).

In emergency cases, such as acute hemorrhage within the liver (e.g., in a pre-existing tumor or after liver biopsy), acute vascular occlusion, or inflammatory lesions as abscesses, MDCT is the modality of choice, since it is broadly available, allows for very fast scanning and is based on well-established examination techniques. Following surgical and interventional procedures, MDCT allows for reliable diagnosis of complications, such as hematomas, abscesses, or biliomas (Romano et al. 2005) which can be treated percutaneously with CT-guidance, if required. In the follow-up after transarterial chemoembolization (TACE), the accumulation of Lipiodol is readily visualized with CT, even on non-contrast scans without contrast enhancement, contributing to predict the success of the therapy (Guan et al. 2004; Takayasu et al. 2000).

### 2.3 Magnetic Resonance Imaging

Magnetic resonance imaging (MRI) is used since the early 1990s as a standard procedure in abdominal and liver imaging. Since then various technical developments have taken place, which helped to further increase the diagnostic value of the method and to further improve image quality. Important milestones toward a fast and robust utilization of MRI in abdominal imaging have been the development of gradient-echo (GRE) sequences, single-shot techniques, and phased-array coils. However, only recently MRI has reached a quality, in which respiratory or motion artifacts are negligible and spatial resolution is considered sufficient. Among various other factors the development of 3D sequences, respiratory triggering, and parallel imaging strategies were important milestones toward robust high quality liver imaging with MRI (Zech et al. 2004a). The introduction of high-field systems might allow an additional improvement in spatial resolution and image quality.

The evolution of 3D sequences has been of special value for applications requiring a very high spatial resolution and dedicated post-processing as for example MR angiography. Dynamic studies after bolus injection of contrast agents with T1-weighted (w) 3D gradient-echo sequences are also very useful in liver imaging (Lee et al. 2000). The inherent higher SNR of 3D sequences as compared to 2D sequences allows increasing spatial resolution in 3D sequences without substantial loss in SNR in comparison to an equivalent 2D

sequence (Rofsky et al. 1999). Therefore, with this sequence type the whole liver can be covered within an acceptable breath-hold time of 15–20 s with a slice thickness down to 2 mm. In contrast to MDCT image quality of these thin slice examinations is not degraded by increased image noise, which represents a major limitation in MDCT with less than 3 mm reconstructed slice thicknesses (see Sect. 2.2). Artifacts from respiratory motion are an important problem, which results in degradation of image quality in MR examinations of the liver. In T2-w sequences the introduction of T2-w FSE and single-shot sequences in the 1990s have made breath-hold examinations of the liver feasible in more or less acceptable image quality. *Respiratory triggering* for T2-w sequences have also been explored for the compensation of breathing artifacts (Katayama et al. 2001; Augui et al. 2002; Zech et al. 2004b). According to Katayama et al. one advantage of respiratory triggering is a better T2 contrast with superior signal-to-noise ratio of the liver parenchyma and improved liver-to-lesion contrast in comparison to breath-hold T2-w FSE and single-shot sequences. Our own results (Zech et al. 2004b) also indicate that respiratory triggering is superior over breath-hold strategies, being one cornerstone for minimized artifacts in T2-w sequences (Fig. 5). The balance between spatial resolution, signal-to-noise ratio (SNR), and acquisition time is crucial for liver MRI. *Parallel imaging* as a universal tool for accelerated acquisition is therefore of high interest for liver imaging. The positive effect of reduced acquisition times with parallel imaging can be utilized both in T1-w and T2-w sequences without a loss in image quality (McKenzie et al. 2004; Zech et al. 2004b). With the use of parallel imaging techniques in single-shot sequences, as for example HASTE or EPI—sequences for diffusion-weighted imaging, the decreased number of phase-encoding steps enables shortened echo trains leading to an improved definition of edges and reduced blurring.

With modern scanner generations and the above mentioned applications, MRI provides a high and quite robust image quality in imaging of the liver. This high image quality is a prerequisite to make use of the inherent advantages of MRI over CT, which are on the one hand the high soft tissue contrast, on the other hand the ability to discriminate different tissue compounds (e.g., fat, mucin, blood, water, but also hepatocytes, bile ducts) based on different signal behavior in T1- and T2-weighted (w) sequences and also based on tissue-specific MR contrast agents.

Extracellular Gadolinium-based contrast agents are still highly important in liver imaging. However, there are also tissue-specific contrast agents available, which allow for an increased detection rate and more specific characterization of focal and diffuse liver diseases. Liver-specific contrast agents can be basically divided into two groups: On the one

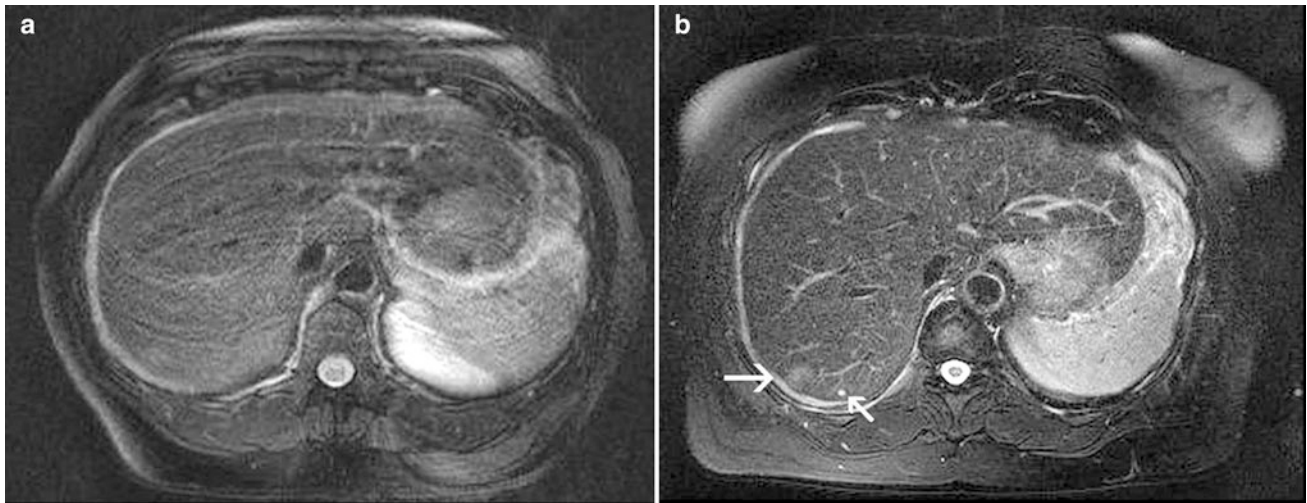


**Fig. 5** T2w fast spin echo sequence in breath-hold technique **a** and with respiratory triggering **b** in a female patient suffering from breast cancer, in whom liver metastases had to be ruled out. Although the patient has been in a good general state of health, she was not able to hold her breath properly, which resulted in severe breathing artifacts in the breath-hold T2-w fast spin echo sequence with fat saturation.

These artifacts also obscure the focal liver lesion in segment 7. In the corresponding slice of the respiratory-triggered T2-w fast spin echo sequence the focal lesion with slight hyperintensity (*arrow*), suspicious of a metastasis, is clearly depicted. *Note* also the tiny liver cyst adjacent to the metastasis (*small arrow*). Both sequences are acquired with parallel imaging (acceleration factor  $R = 2$ )

hand there are iron-oxide particles (SPIO = Superparamagnetic Particles of Iron Oxide), which are targeted to the reticulo-endothelium-system (RES), specifically to the so-called Kupffer cells. These agents cause a signal decrease in T2/T2\* weighted sequences by inducing local inhomogeneities of the magnetic field. On the other hand there is the group of hepato-biliary contrast agents, which are targeted directly to the hepatocytes and are excreted via the bile. These agents cause signal increase in T1-weighted sequences by shortening of the T1 relaxation time.

The basic principle behind SPIO is the fact, that there are usually no Kupffer cells in malignant liver tumors, whereas normal liver parenchyma and solid benign liver lesions contain variable amounts of Kupffer cells (Namkung et al. 2007). Therefore, in the liver-specific phase high contrast is achieved between malignant liver lesions and normal liver parenchyma. Due to the signal loss in normal liver parenchyma the malignant lesions are highlighted as hyperintense lesions in T2\*w and T2w sequences compared to the dark liver parenchyma. In most countries SPIO agents are currently not available on the market.

The basic principle of hepato-biliary contrast agents is the specific uptake directly into the hepatocytes. Since all these agents shorten the T1-relaxation times, they cause a signal increase in normal liver parenchyma and in solid benign lesions, whereas malignant lesions like metastases lack specific uptake of hepato-biliary contrast agents. Thus malignant lesions contrast as hypointense lesions against the bright liver parenchyma. In Europe the manganese-based agent mangafodipir trisodium (Teslascan<sup>®</sup>, Amersham Health, Nydalen, Norway), and the gadolinium-based

agents gadobenate-dimeglumine (MultiHance<sup>®</sup>, Bracco, Milano, Italy) and gadoxetic-acid (Primovist<sup>®</sup>, Bayer, Berlin, Germany) are approved. Mangafodipir has the drawback that it has to be administered as a short infusion and not as a bolus; therefore, dynamic studies are not possible with mangafodipir. However, the liver specificity is high and the high uptake in normal liver parenchyma enables imaging of e.g., metastases with high contrast to the surrounding liver parenchyma. Gadobenate-dimeglumine and gadoxetic-acid are allowed to be injected as a bolus. With both of these contrast agents early dynamic examinations can be performed, allowing to differentiate lesions with regard to their vascularity into hyper- or hypovascular lesions (Petersein et al. 2000; Huppertz et al. 2005). Due to the lower liver specificity of gadobenate-dimeglumine the imaging time-point of the liver-specific phase starts about 40 min after injection, whereas gadoxetic acid allows for imaging 20 min after injection, with implications mainly on the work-flow of the MR department.

Following injection of unspecific extracellular gadolinium-based contrast agents, solid benign liver tumors (e.g., FNH, adenoma) exhibit a blush-like hypervascularization with fast wash-out to isointensity in MRI which parallels the pattern in contrast-enhanced CT. While central scars are characteristic for FNH, fatty changes, or hemorrhage are typical findings in adenoma. Due to the superior soft tissue contrast of MRI, these morphological details are more often detected with MRI than with CT. Enhancement characteristics with administration of liver-specific contrast agents also greatly contribute to specific characterization of these entities. With hepatobiliary contrast agents such as

gadobenate-dimeglumine (MultiHance<sup>®</sup>) and gadoxetic acid (Primovist<sup>®</sup>), hypervascularity as well as the presence of hepatocytes in FNH can be assessed (Grazioli et al. 2012; Huppertz et al. 2005; Zech et al. 2008a). Adenoma, on the other hand, usually does not show uptake of hepato-biliary contrast agents and, therefore, can be differentiated from FNH (Grazioli et al. 2012). The challenge in adenomas is nowadays rather the differentiation between adenoma on the one hand and hypervascular metastases or HCC-lesions in non-cirrhotic liver on the other hand. Moreover, by now it is known that adenoma is not a uniform entity and that based on immunohistopathology subtypes can be differentiated which may have a different risk profile (Grazioli et al. 2012).

Imaging of liver metastases typically represents a very common indication for MRI of the liver. On unenhanced MR images, the signal intensity of liver metastases is typically low in T1w GRE images and moderately high in T2w sequences. Due to the relatively high contrast between metastases and unaffected liver parenchyma in unenhanced T1-w GRE images, many metastases are detected already with this sequence. T2-w images do not contribute merely to lesion detection, but also to lesion characterization. Solid benign lesions are frequently almost isointense to normal liver tissue on unenhanced T2-w images whereas cysts and hemangiomas are markedly hyperintense. With gadolinium-enhanced MRI hypo- and hypervascular metastases can be differentiated (Sect. 2.2). In contrast to hemangiomas with their “cotton-wool” enhancement and the centripetal fill-in, hypervascular metastases tend to show a rather homogenous enhancement with indistinct margins. Diffusion-weighted MRI proved to be a valuable tool especially to differentiate metastases from small hemangioma or cysts (Taouli et al. 2003).

For the detection of liver metastases with MRI, sensitivities ranging from 54 to 81 % were reported in the literature (Del Frate et al. 2002; Matsuo et al. 2001). In a direct comparative trial gadolinium-enhanced MRI was superior to biphasic spiral CT with regard to lesion detection and lesion characterization and the superior diagnostic value of MRI had substantial impact on the treatment of the patients (Semelka et al. 2001). Liver-specific contrast agents result in a significant increase in the detection rate and namely in the rate of true-positive lesions in patients with suspected metastases. Diffusion-weighted MRI is nowadays an established part of a modern liver MRI protocol. Its superiority for lesion detection over other plain sequences has been shown in several publications (Zech et al. 2008b). Together with hepatobiliary contrast agents, very high and confident lesion detection rates can be achieved (Löwenthal et al. 2011).

The detection rates for liver metastases with hepatobiliary contrast agents range between 70 and 90 %

(Bartolozzi et al. 2004; Huppertz et al. 2004; Bluemke et al. 2005). Despite the value of the early arterial phase for lesion characterization in identifying signs of hypervascularity, hepato-biliary phase images are also crucial for lesion detection, especially in hypervascular metastases. Hypervascular lesions can sometimes only be detected faintly in the arterial phase of dynamic standard gadolinium chelates, whereas hepatobiliary phase images after administration of liver-specific contrast agents enable a confident detection regardless of the contrast agent timing (Kettritz et al. 1996; Ward et al. 2000; Youk et al. 2004). The combined reading of early dynamic phase images (obtained with standard gadolinium-chelates) and delayed phase images obtained from liver-specific agents yielded the highest detection rate (Kettritz et al. 1996; Ward et al. 2000; Youk et al. 2004). With Primovist<sup>®</sup> and MultiHance<sup>®</sup> both an early dynamic phase and a liver-specific phase can be acquired within in one examination after one single injection of contrast agent (Fig. 6). Nowadays, these contrast agents are regarded to be the best noninvasive choice for detection of liver metastases, especially if additional diffusion-weighted sequences are acquired (Löwenthal et al. 2011).

The evaluation of the cirrhotic liver is a challenging task for every imaging modality and this holds also true for MRI. Gadolinium-enhanced MRI with T1w 3D-GRE sequences, allowing for thin slices, enables detection of HCC nodules with 76 % sensitivity, 75 % specificity, and a negative predictive value of 50 % (Burrel et al. 2003). The typical enhancement pattern of HCC with Gadolinium-based MR contrast agents is hypervascularity in the arterial phase and wash-out in the portovenous phase. In the latest version of the practice guidelines issued by the AASLD (American Association for the Study of Liver Diseases) in 2010/2011, a liver tumor larger than 1 cm can be diagnosed as a HCC without the need of a biopsy, if it exhibits that typical pattern in MDCT or MRI (Bruix and Sherman 2011). MRI is, however, superior to spiral CT in the detection of HCC (sensitivity 76 % MRI vs. 61 % CT) (Burrel et al. 2003). In other trials ultrasound, biphasic spiral CT and MRI were compared and again MRI proved to be superior to the other modalities in the detection of HCC (Rode et al. 2001; de Ledinghen et al. 2002; Stoker et al. 2002; Kang et al. 2003). Since CT can only depict the vascularity of lesions, it is difficult to distinguish between simple regenerative nodules, high-grade dysplastic nodules, and early HCC in the cirrhotic liver (Burrel et al. 2003). The advantages of MRI in this respect are the possibility of tissue characterization based on different contrast weightings of the pulse sequences (T1, T2, DWI) and the availability of liver-specific contrast agents.

As mentioned before the two available hepatobiliary contrast agents Primovist<sup>®</sup> and MultiHance<sup>®</sup> help to detect



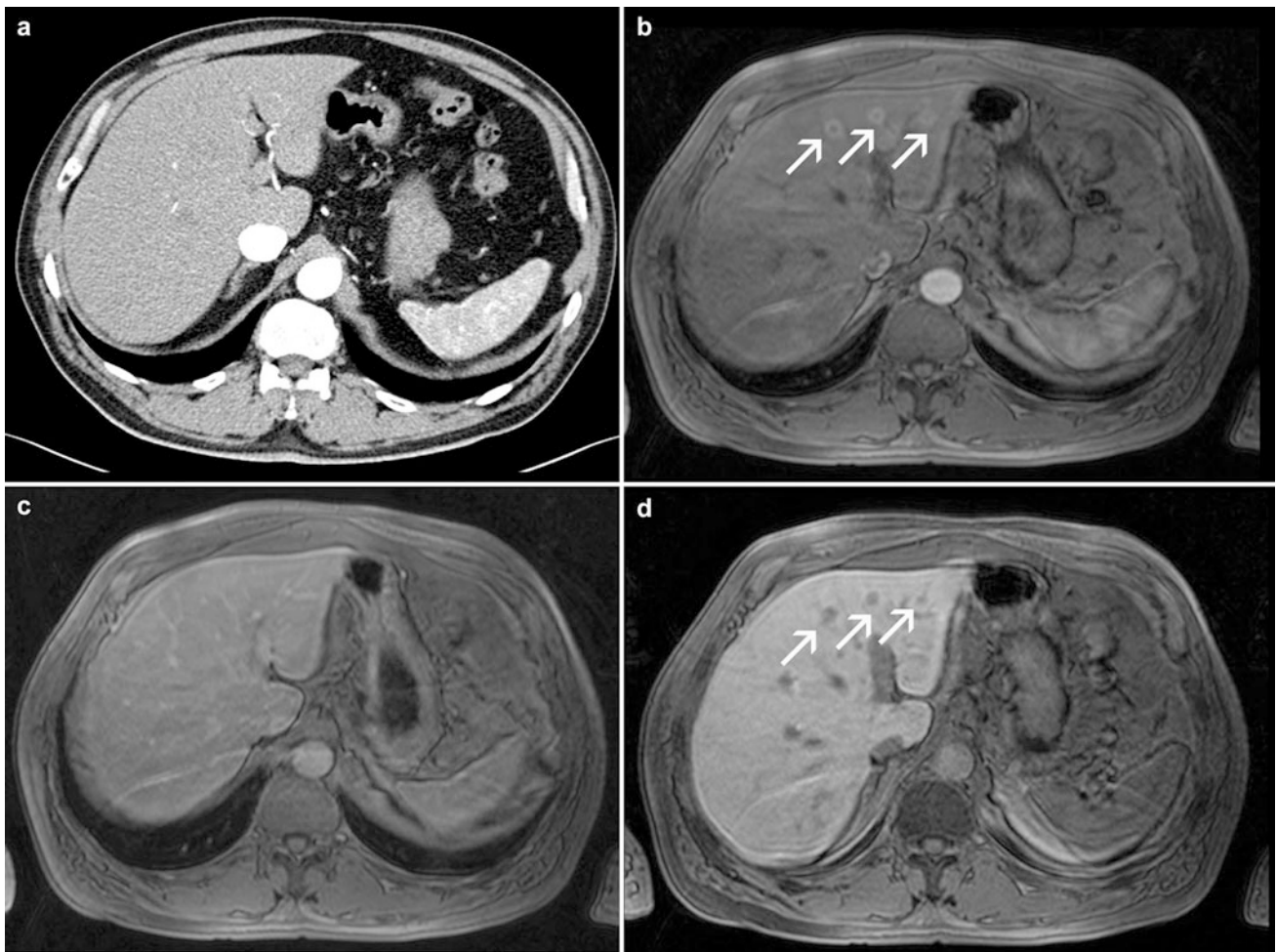


**Fig. 6** MDCT in the arterial phase (a) and MRI with the hepatobiliary contrast agent Gd-EOB-DTPA in the arterial phase (b) portovenous phase (c) and liver-specific phase 20 min after injection (d) each examined with a T1w 3D GRE sequence with fat saturation in a patient with a neuroendocrine tumor and liver metastases. The hypervascular metastases were not detected with MDCT. In the arterial phase after Gd-EOB-DTPA injection hyperintense lesions are

demarcated. The hypervascular metastases show a wash-out to isointensity in the portovenous phase. With Gd-EOB-DTPA liver-specific phase imaging can be performed in addition to the early dynamic phase. *Note* the signal increase in the normal liver parenchyma is (d) caused by the physiological Gd-EOB-DTPA uptake whereas the suspected liver metastases are demarcated as areas spared from specific Gd-EOB-DTPA uptake

and characterize HCC nodules. Usually HCC does not show liver-specific uptake and depicts as hypointense lesions in the liver. However, for both agents uptake with depiction as hyperintense lesions in malignant HCCs in the liver-specific phase has been demonstrated, but usually the frequency of this finding is low (<5%) and confined to well-differentiated HCC (Choi et al. 2011; Kim et al. 2008). Generally, the presence of typical changes of the vascular supply will help to correctly characterize these lesions. Up to now no exact thresholds for the uptake of regenerative nodules, dysplastic nodules, and HCC have been defined. However, the potential value of showing impaired biliary uptake for the evaluation of nodules in the cirrhotic liver has been appreciated by several authors (Kanematsu et al. 2008; Bartolozzi et al. 2007). In this respect it has been pointed out that hepatobiliary MRI helps to detect hepatic nodules

“at risk” for transformation into well-differentiated HCC (e.g., high-grade dysplastic nodules) prior to neo-vascularization and prior to development of overt HCC (Bartolozzi et al. 2007). That implicated that in the future, e.g., nodules with features of a high-grade dysplasia at pre-contrast MRI (T1w hyperintense, T2w iso- or hyperintense) and with hypointense depiction in hepatobiliary phase images might be considered as HCC from a certain size on even with missing neo-vascularization—helping to overcome the diagnostic gap which exists in hypovascular HCC (Golfieri et al. 2007).

## 2.4 Angiography

Pure diagnostic angiography has nowadays a limited role and is restricted to special indications, since it has been

broadly replaced by cross-sectional imaging modalities. The basic principle of angiography for the diagnostic evaluation of liver tumors has been the strong vascularity of some tumors (e.g., HCC), so that pathological tumor vessels and a tumor blush is visible on angiographic images. Since the sensitivity and specificity for lesion detection with this projectional modality is confined to larger tumors, it does not play a role in diagnostic imaging any longer. However, angiography has redefined its value in radiology and has become a tool for the delivery of therapeutic agents to the liver, e.g., in radioembolization, which is the main topic of this monograph. Moreover, new technical developments enable the use of flat panel detectors in angiography systems with an adequate spatial resolution. Together with modern C-arms with a high degree of mobility and fast rotations, transversal sections can be acquired during an angiographic examination with the so-called Dyna-CT (Siemens Medical Solutions, Erlangen, Germany), which can contribute to a more precise evaluation of the vascular supply of liver lesions and anatomic variants (Fig. 7). The role of angiography for the evaluation of vascular variants prior to the radioembolization will be addressed in “Radioembolization: Identifying and Managing Anatomic Variants”.

### 3 Summary and Conclusion

Even if the difference between the diagnostic value of CT and MRI has become smaller due to ongoing improvements in CT, MRI with liver-specific contrast agents has to be considered the modality of choice for dedicated liver examinations. MRI has an excellent contrast resolution which allows for sensitive detection of intrahepatic lesions. 3D dynamic Gadolinium—chelate-enhanced scans allow for the assessment of vascularity and perfusion. Hepatocyte-specific contrast agents and new techniques like diffusion-weighted imaging further enhance sensitivity and specificity. Moreover, the lack of radiation exposure can be regarded as an issue of increasing importance. MDCT on the other hand, enables to combine dedicated liver examinations with a whole-body staging (or thoracic and abdominal) to provide information of the hepatic and extrahepatic tumor burden within one examination.

For dedicated examinations of unclear, potentially benign liver lesions and for hepatic staging prior to liver surgery, MRI can be recommended as the method of choice. In case a CT scan has already been performed (e.g., a staging CT scan of the thorax and abdomen) MRI should not be omitted, if the intrahepatic findings have direct influence on the further treatment. MDCT is suitable for all emergency situations, since it allows for easy patient access and is associated with very short acquisition times, so that

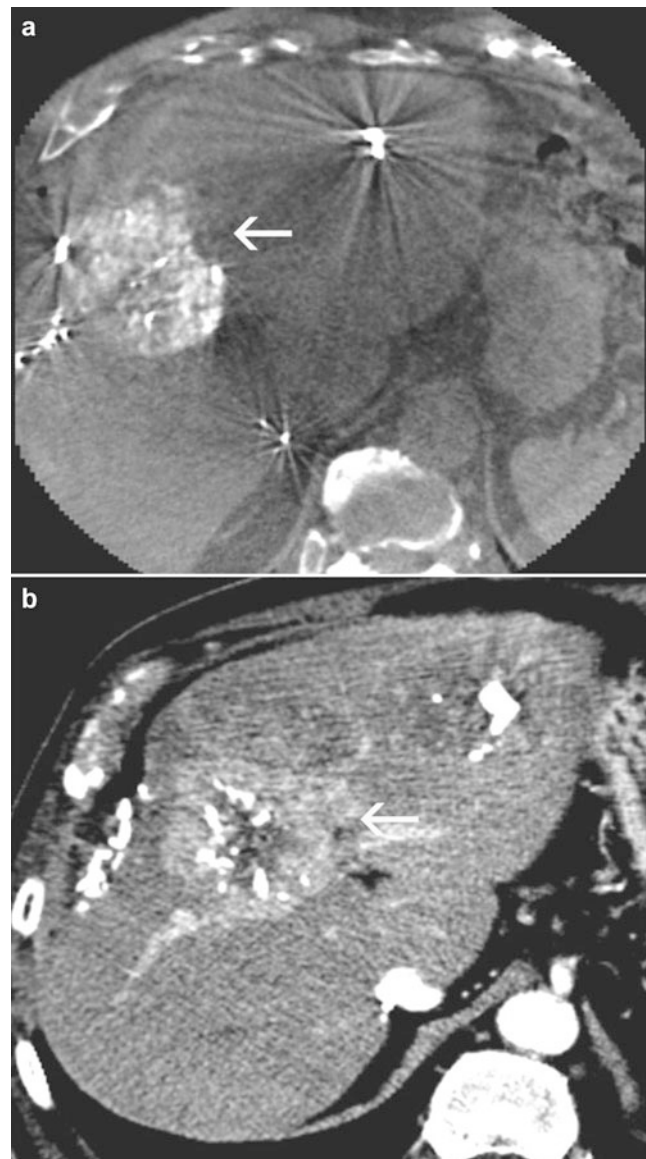


**Fig. 7** Male patient suffering from a multifocal hepatocellular carcinoma (HCC), treated with repeated sessions of transarterial chemoembolization (TACE). Dyna-CT (Siemens Medical Solutions, Erlangen, Germany) image started together with injection of 10 ml iodinated contrast agent via a super-selective catheter system placed in the right hepatic artery compared with a corresponding MDCT section in the arterial phase after i.v. injection of 120 ml iodinated contrast agent. Note the excellent, direct depiction of arterial blood supply of the HCC nodule in liver segment 5/8 (arrow). The artifacts in the left and right liver lobe are caused by spots of Lipiodol in already treated HCC nodules after earlier transarterial chemoembolization

not cooperative or clinically unstable patients can be easily examined.

Sonography will still be the first imaging modality to be used in patients with liver tumors. Lesions being unclear in B-mode ultrasound can often be characterized with confidence with help of contrast-enhanced ultrasound. However, sonography can not replace MDCT and MRI in the pre-



interventional or pre-operative work-up of patients with liver tumors. Pure diagnostic angiography is obsolete; however, angiographic delivery of drugs (e.g., radioembolization or transarterial chemoembolization) and dedicated pre-interventional vascular assessment have revived the utilization of angiography.

## References

- Albrecht T, Hoffmann CW, Schmitz SA et al (2001) Phase-inversion sonography during the liver-specific late phase of contrast enhancement: improved detection of liver metastases. *AJR Am J Roentgenol* 176:1191–1198
- Augui J, Vignaux O, Argaud C et al (2002) Liver: T2-weighted MR imaging with breath-hold fast-recovery optimized fast spin-echo compared with breath-hold half-Fourier and non-breath-hold respiratory-triggered fast spin-echo pulse sequences. *Radiology* 223:853–859
- Baron RL (1994) Understanding and optimizing use of contrast material for CT of the liver. *AJR Am J Roentgenol* 163:323–331
- Bartolozzi C, Lencioni R, Caramella D, Palla A, Bassi AM, Di Candio G (1996) Small hepatocellular carcinoma. Detection with US, CT, MR imaging, DSA, and Lipiodol-CT. *Acta Radiol* 37:69–74
- Bartolozzi C, Donati F, Cioni D et al (2004) Detection of colorectal liver metastases: a prospective multicenter trial comparing unenhanced MRI, MnDPDP-enhanced MRI, and spiral CT. *Eur Radiol* 14:14–20
- Bartolozzi C, Crocetti L, Lencioni R, Cioni D, Della Pina C, Campani D (2007) Biliary and reticuloendothelial impairment in hepatocarcinogenesis: the diagnostic role of tissue-specific MR contrast media. *Eur Radiol* 17:2519–2530
- Bluemke DA, Sahani D, Amendola M et al (2005) Efficacy and safety of MR imaging with liver-specific contrast agent: US multicenter phase III study. *Radiology* 237:89–98
- Brink JA (2003) Contrast optimization and scan timing for single and multidetector-row computed tomography. *Eur J Radiol [Suppl 1]* 27:3–8
- Bruix J, Sherman M (2011) Management of hepatocellular carcinoma: an update. *Hepatology* 53:1020–1022
- Burrell M, Llovet JM, Ayuso C et al (2003) MRI angiography is superior to helical CT for detection of HCC prior to liver transplantation: an explant correlation. *Hepatology* 38:1034–1042
- Carlson SK, Johnson CD, Bender CE, Welch TJ (2000) CT of focal nodular hyperplasia of the liver. *AJR Am J Roentgenol* 174:705–712
- Choi JY, Kim MJ, Park YN et al (2011) Gadoxetate disodium-enhanced hepatobiliary phase MRI of hepatocellular carcinoma: correlation with histological characteristics. *AJR Am J Roentgenol* 197:399–405
- Danet IM, Semelka RC, Leonardou P et al (2003) Spectrum of MRI appearances of untreated metastases of the liver. *AJR Am J Roentgenol* 181:809–817
- de Ledinghen V, Laharie D, Lecesne R et al (2002) Detection of nodules in liver cirrhosis: spiral computed tomography or magnetic resonance imaging? A prospective study of 88 nodules in 34 patients. *Eur J Gastroenterol Hepatol* 14:159–165
- Del Frate C, Bazzocchi M, Mortele KJ et al (2002) Detection of liver metastases: comparison of gadobenate dimeglumine-enhanced and ferumoxides-enhanced MR imaging examinations. *Radiology* 225:766–772
- Golfieri R, Coppola F, Fusco F et al (2007) Malignant progression of a small HCC nodule: hypovascular ‘early HCC’ converted to hypervascular ‘small HCC’ within 6 months. *Dig Liver Dis* 39:883–890
- Grazioli L, Federle MP, Brancatelli G, Ichikawa T, Olivetti L, Blachar A (2001) Hepatic adenomas: imaging and pathologic findings. *RadioGraphics* 21:877–894
- Grazioli L, Bondioni MP, Haradome H et al (2012) Hepatocellular adenoma and focal nodular hyperplasia: value of gadoxetic acid-enhanced MR imaging in differential diagnosis. *Radiology* 262:520–529
- Guan YS, Zheng XH, Zhou XP et al (2004) Multidetector CT in evaluating blood supply of hepatocellular carcinoma after transcatheter arterial chemoembolization. *World J Gastroenterol* 10:2127–2129
- Haider MA, Amitai MM, Rappaport DC et al (2002) Multi-detector row helical CT in preoperative assessment of small (< or = 1.5 cm) liver metastases: is thinner collimation better? *Radiology* 225:137–142
- Harvey CJ, Albrecht T (2001) Ultrasound of focal liver lesions. *Eur Radiol* 11:1578–1593
- Huppertz A, Balzer T, Blakeborough A et al (2004) Improved detection of focal liver lesions at MR imaging: multicenter comparison of gadoxetic acid-enhanced MR images with intraoperative findings. *Radiology* 230:266–275
- Huppertz A, Haraida S, Kraus A, Zech CJ et al (2005) Enhancement of focal liver lesions at gadoxetic acid-enhanced MR imaging: correlation with histopathologic findings and spiral CT—initial observations. *Radiology* 234:468–478
- Hwang GJ, Kim M-J, Yoo HS, Lee JT (1997) Nodular hepatocellular carcinoma: detection with arterial-, portal- and delayed-phase images at spiral CT. *Radiology* 202:383–388
- Kanematsu M, Kondo H, Goshima S, Tsuge Y, Watanabe H (2008) Magnetic resonance imaging of hepatocellular carcinoma. *Oncology* 75(Suppl 1):65–71
- Kang BK, Lim JH, Kim SH et al (2003) Preoperative depiction of hepatocellular carcinoma: ferumoxides-enhanced MR imaging versus triple-phase helical CT. *Radiology* 226:79–85
- Katayama M, Masui T, Kobayashi S et al (2001) Fat-suppressed T2-weighted MRI of the liver: comparison of respiratory-triggered fast spin-echo, breath-hold single-shot fast spin-echo, and breath-hold fast-recovery fast spin-echo sequences. *J Magn Reson Imaging* 14:439–449
- Kawata S, Murakami T, Kim T et al (2002) Multidetector CT: diagnostic impact of slice thickness on detection of hypervascular hepatocellular carcinoma. *AJR Am J Roentgenol* 179:61–66
- Kettritz U, Schlund JF, Wilbur K, Eisenberg LB, Semelka RC (1996) Comparison of gadolinium chelates with manganese-DPDP for liver lesion detection and characterization: preliminary results. *Magn Reson Imaging* 14:1185–1190
- Kim JI, Lee JM, Choi JY et al (2008) The value of gadobenate dimeglumine-enhanced delayed phase MR imaging for characterization of hepatocellular nodules in the cirrhotic liver. *Invest Radiol* 43:202–210
- Kondo H, Kanematsu M, Hashi H et al (1999) Preoperative detection of malignant hepatic tumors: comparison of combined methods of MR imaging with combined methods of CT. *AJR Am J Roentgenol* 174:947–954
- Lee VS, Lavelle MT, Rofsky NM et al (2000) Hepatic MR imaging with a dynamic contrast-enhanced isotropic volumetric interpolated breath-hold examination: feasibility, reproducibility, and technical quality. *Radiology* 215:365–372
- Lencioni R, Donati F, Cioni D, Paolicchi A, Cicorelli A, Bartolozzi C (1998) Detection of colorectal liver metastases: prospective comparison of unenhanced and ferumoxides-enhanced magnetic resonance imaging at 1.5 T, dual-phase spiral CT, and spiral CT during arterial portography. *MAGMA* 7:76–87

- Löwenthal D, Zeile M, Lim WY et al (2011) Detection and characterisation of focal liver lesions in colorectal carcinoma patients: comparison of diffusion-weighted and Gd-EOB-DTPA enhanced MR imaging. *Eur Radiol* 21:832–840
- Matsuo M, Kanematsu M, Itoh K et al (2001) Detection of malignant hepatic tumors: comparison of gadolinium-and ferumoxide-enhanced MR imaging. *AJR Am J Roentgenol* 177:637–643
- McKenzie CA, Lim D, Ransil BJ et al (2004) Shortening MR image acquisition time for volumetric interpolated breath-hold examination with a recently developed parallel imaging reconstruction technique: clinical feasibility. *Radiology* 230:589–594
- Namkung S, Zech CJ, Helmberger T, Reiser MF, Schönberg SO (2007) Superparamagnetic iron oxide (SPIO)-enhanced liver MR imaging with ferucarbotran: efficacy for characterization of focal liver lesions. *J Magn Reson Imaging* 25:755–765
- Oudkerk M, Torres CG, Song B et al (2002) Characterization of liver lesions with mangafodipir trisodium-enhanced MR imaging: multicenter study comparing MR and dual-phase spiral CT. *Radiology* 223:517–524
- Petersein J, Spinazzi A, Giovagnoni A et al (2000) Focal liver lesions: evaluation of the efficacy of gadobenate dimeglumine in MR imaging—a multicenter phase III clinical study. *Radiology* 215:727–736
- Quaia E (2007) Microbubble ultrasound contrast agents: an update. *Eur Radiol* 17:1995–2008
- Reimer P, Jähnke N, Fiebich M et al (2000) Hepatic lesion detection and characterization: value of nonenhanced MR imaging, superparamagnetic iron oxide-enhanced MR imaging, and spiral CT—ROC analysis. *Radiology* 217:152–158
- Reinhold C, Hammers L, Taylor CR, Quedens-Case CL, Holland CK, Taylor KJ (1995) Characterization of focal hepatic lesions with duplex sonography: findings in 198 patients. *AJR Am J Roentgenol* 164:1131–1135
- Rode A, Bancel B, Douek P et al (2001) Small nodule detection in cirrhotic livers: evaluation with US, spiral CT, and MRI and correlation with pathologic examination of explanted liver. *J Comput Assist Tomogr* 25:327–336
- Rofsky NM, Lee VS, Laub G et al (1999) Abdominal MR imaging with a volumetric interpolated breath-hold examination. *Radiology* 212:876–884
- Romano S, Tortora G, Scaglione M et al (2005) MDCT imaging of post interventional liver: a pictorial essay. *Eur J Radiol* 53:425–432
- Schima W, Kulinna C, Ba-Ssalamah A, Grunberger T (2005) Multidetector computed tomography of the liver. *Radiologe* 45:15–23
- Schima W, Hammerstingl R, Catalano C et al (2006) Quadruple-phase MDCT of the liver in patients with suspected hepatocellular carcinoma: effect of contrast material flow rate. *AJR Am J Roentgenol* 186:1571–1579
- Schoellnast H, Tillich M, Deutschmann HA et al (2003) Abdominal multidetector row computed tomography. Reduction of cost and contrast material dose using saline flush. *J Comput Assist Tomogr* 27:847–853
- Semelka RC, Cance WG, Marcos HB, Mauro MA (1999) Liver metastases: comparison of current MR techniques and spiral CT during arterial portography for detection in 20 surgically staged cases. *Radiology* 213:86–91
- Semelka RC, Martin DR, Balci C, Lance T (2001) Focal liver lesions: comparison of dual-phase CT and multisequence multiplanar MR imaging including dynamic gadolinium enhancement. *J Magn Reson Imaging* 13:397–401
- Stoker J, Romijn MG, de Man RA et al (2002) Prospective comparative study of spiral computer tomography and magnetic resonance imaging for detection of hepatocellular carcinoma. *Gut* 51:105–107
- Takayasu K, Arii S, Matsuo N et al (2000) Comparison of CT findings with resected specimens after chemoembolization with iodized oil for hepatocellular carcinoma. *AJR Am J Roentgenol* 175:699–704
- Tanaka S, Oshikawa O, Sasaki T, Ioka T, Tsukuma H (2000) Evaluation of tissue harmonic imaging for the diagnosis of focal liver lesions. *Ultrasound Med Biol* 26:183–187
- Taouli B, Vilgrain V, Dumont E, Daire JL, Fan B, Menu Y (2003) Evaluation of liver diffusion isotropy and characterization of focal hepatic lesions with two single-shot echo-planar MR imaging sequences: prospective study in 66 patients. *Radiology* 226:71–78
- Valls C, Andia E, Sanchez A et al (2001) Hepatic metastases from colorectal cancer: preoperative detection and assessment of resectability with helical CT. *Radiology* 218:55–60
- Ward J, Naik KS, Guthrie JA, Wilson D, Robinson PJ (1999) Hepatic lesion detection: comparison of MR imaging after the administration of superparamagnetic iron oxide with dual-phase CT by using alternative-free response receiver operating characteristic analysis. *Radiology* 210:459–466
- Ward J, Guthrie JA, Scott DJ et al (2000) Hepatocellular carcinoma in the cirrhotic liver: double-contrast MR imaging for diagnosis. *Radiology* 216:154–162
- Weg N, Scheer MR, Gabor MP (1998) Liver lesions: improved detection with dual-detector-array CT and routine 2.5 mm thin collimation. *Radiology* 209:417–426
- Youk JH, Lee JM, Kim CS (2004) MRI for detection of hepatocellular carcinoma: comparison of mangafodipir trisodium and gadopentetate dimeglumine contrast agents. *AJR Am J Roentgenol* 183:1049–1054
- Zech CJ, Schoenberg SO, Herrmann KA et al (2004a) Modern visualization of the liver with MRT. Current trends and future perspectives. *Radiologe* 44:1160–1169
- Zech CJ, Herrmann KA, Huber A et al (2004b) High-resolution MR-imaging of the liver with T2-weighted sequences using integrated parallel imaging: comparison of prospective motion correction and respiratory triggering. *J Magn Reson Imaging* 20:443–450
- Zech CJ, Grazioli L, Breuer J, Reiser MF, Schoenberg SO (2008a) Diagnostic performance and description of morphological features of focal nodular hyperplasia in Gd-EOB-DTPA-enhanced liver magnetic resonance imaging: results of a multicenter trial. *Invest Radiol* 43:504–511
- Zech CJ, Herrmann KA, Dietrich O, Horger W, Reiser MF, Schoenberg SO (2008b) Black-blood diffusion-weighted EPI acquisition of the liver with parallel imaging: comparison with a standard T2-weighted sequence for detection of focal liver lesions. *Invest Radiol* 2008(43):261–266

# Vascular Anatomy and Its Implication in Radioembolization

Ramón Saiz-Mendiguren, Javier Arias, Isabel Vivas, and José I. Bilbao

## Contents

<b>1</b>	<b>Introduction</b> .....	28
<b>2</b>	<b>Liver Arterial Anatomy</b> .....	28
2.1	Classical Description.....	28
2.2	Terminology.....	28
2.3	Michels' Classification of Anatomical Variants.....	29
2.4	Other Anatomical Variants.....	30
<b>3</b>	<b>Extrahepatic Vessels Originating from the Hepatic Vasculature</b> .....	30
3.1	Vessels Originating from the CHA and Proper Hepatic Artery.....	30
3.2	Vessels Originating from the LHA.....	32
3.3	Vessels Originating from the RHA.....	38
<b>4</b>	<b>Hepatic Vessels Originating from the Extrahepatic Vasculature</b> .....	38
	<b>References</b> .....	39

## Abstract

The anatomy of the mesenteric system and the hepatic arterial bed has a high degree of variation. The celiac trunk trifurcates into the left gastric, splenic, and common hepatic arteries. The common hepatic artery divides into the gastroduodenal artery and proper hepatic artery. This itself bifurcates into a right and left branch to supply each of the lobes of the liver. Quite often the hepatic artery has an incomplete set of branches because one or the other of its usual branches arises from a source other than the proper hepatic artery from the celiac trunk. Such a vessel, if from an outside source, is spoken of as 'aberrant' (a variation). Aberrant hepatic arteries are of two types, replacing and accessory. An aberrant hepatic artery refers to a branch that does not arise from its usual source (i.e. proper hepatic artery from the celiac trunk). This type of artery may be a substitute for the usual hepatic artery that is absent, in which case it is referred to as an aberrant 'replaced' hepatic artery. In other cases there may be an additional artery to the one normally present, hence the term aberrant 'accessory' artery. In 1953, Michels published his classical study of hepatic arterial anatomy, which detailed the results following the dissection of 200 cadavers. He defined 10 anatomical variations of the hepatic artery. Later on in 1966, Michels proposed an internationally recognized classification of these hepatic abnormalities, which was later, modified by Hiatt in 1994. When performing a radioembolization procedure, it is of utmost importance to identify and isolate any vessel which may supply blood to organs other than the liver as this may result in non-target  $^{90}\text{Y}$  administration. Many hepatic vessels originating from non-hepatic sources and extrahepatic collateral pathways to the liver may be established in various conditions such as following surgical ligation of the hepatic artery or arterial injury induced by repeated endovascular treatments.

R. Saiz-Mendiguren · J. Arias · I. Vivas · J. I. Bilbao (✉)  
Department of Radiology, University Hospital of Navarra,  
Pamplona, Spain  
e-mail: jibilbao@unav.es

## 1 Introduction

It is well known by liver surgeons and interventional radiologists that the anatomy of the mesenteric system and the hepatic arterial bed has a high degree of variation. In order to perform any kind of therapeutic transarterial procedure in the liver in a safe and efficient manner, it is essential to be acquainted with the hepatic arterial anatomy. This is particularly true when performing intraarterial brachytherapy as infusion of radioactive microspheres (radioembolization) in unrecognized collateral vessels may result in gastrointestinal ulceration, pancreatitis, cholecystitis, skin necrosis, and other non-target radiation complications (Liu et al. 2005). Despite the advances in vascular imaging techniques (CT angiography and MR angiography), at present there is no substitute for conventional digital subtraction angiography (DSA) as many of the small vessels are beyond the resolution capabilities of CTA and MRA and, furthermore, DSA not only provides anatomical information, but also and equally important, will allow to assess the flow characteristics. Nevertheless, CTA and MRA are capable of providing useful information prior to DSA workup (Fig. 1).

## 2 Liver Arterial Anatomy

### 2.1 Classical Description

In the classical description of the arterial anatomy, the celiac trunk trifurcates into the left gastric, splenic, and common hepatic arteries. The common hepatic artery divides into the gastroduodenal artery and proper hepatic artery. This itself bifurcates into a right and left branch to supply each of the lobes of the liver. From this point onward, the arterial branching pattern follows the segmental anatomy of this organ and hence the right hepatic artery further divides into the right anterior and posterior hepatic arteries, while the left hepatic artery divides into branches supplying segment II and segment III. The arterial supply to segment IV may occur from one or more branches arising from the right, left, or proper hepatic artery. However, this classical description of the hepatic arterial anatomy occurs in only 55–65 % of the population. Any hepatic arterial anatomy that differs from what has been so far described is considered to represent an anatomical variation.

### 2.2 Terminology

Quite often, the hepatic artery has an incomplete set of branches because one or the other of its usual branches arises from a source other than the proper hepatic artery



**Fig. 1** CT angiogram showing an independent origin from the abdominal aorta of the common hepatic artery, the left gastric artery, and the splenic artery. This information is useful prior to performing a DSA study



**Fig. 2** Aberrant replaced right hepatic artery coming of the superior mesenteric artery (*arrow*) and aberrant accessory left hepatic artery (*arrowhead*) coming of the left gastric artery



from the celiac trunk. Such a vessel if from an outside source is spoken of as ‘aberrant’ (a variation). Aberrant hepatic arteries are of two types, replacing and accessory (Fig. 2). An aberrant hepatic artery refers to a branch that does not arise from its usual source (i.e., proper hepatic artery from the celiac trunk). This type of artery may be a substitute for the usual hepatic artery that is absent, in which case it is referred to as an aberrant ‘replaced’ hepatic artery. In other cases, there may be an additional artery to the one normally present; hence, the term aberrant ‘accessory’ artery.

### 2.3 Michels’ Classification of Anatomical Variants

The first published description of aberrant hepatic arteries is attributed to Haller in 1756. The data necessary for the study of such variations may be obtained from direct observation of large autopsies, surgical series, or from radiological studies, initially by conventional angiography including DSA or more recently from CT or MR angiography.

In 1953, Michels published his classical study of hepatic arterial anatomy, which detailed the results following the dissection of 200 cadavers (Michels 1953).

He defined 10 anatomical variations of the hepatic artery (Table 1). Later on in 1966, Michels proposed an internationally recognized classification of these hepatic abnormalities, which was later, modified by Hiatt in 1994 (Hiatt et al. 1994).

In the conventional anatomy defined as type I according to Michels’ classification (Fig. 3), the main hepatic artery originates from celiac trunk, gives off the gastroduodenal artery and the proper hepatic artery, the proper hepatic artery continues as the right hepatic artery after giving off the left hepatic artery and then the right hepatic artery splits into its anterior and posterior branches. The left hepatic artery splits into branches that feed segments II and III. Segment IV is fed by the branch or branches originating from the right, left, or the proper hepatic artery. The left hepatic artery originating from the left gastric artery (replaced left hepatic artery) is defined as type II (Fig. 4), the right hepatic artery stemming from the superior mesenteric artery (replaced right hepatic artery) as type III (Fig. 5), and coexistence of both situations is defined as type IV. The left lobe is also fed by the accessory left hepatic artery originating from the left gastric artery in type V variation, and the right lobe is also fed by accessory right hepatic artery originating from the superior mesenteric artery in type VI variation. Both the left and right accessory

**Table 1** Relevant anatomic variants described by Michels

Type I	Standard (55 %)
Type II	Replaced LHA (10 %)
Type III	Replaced RHA (11 %)
Type IV	Replaced RHA and LHA (1 %)
Type V	Accessory LHA from LGA (8 %)
Type VI	Accessory RHA from SMA (7 %)
Type VII	Accessory RHA and LHA (1 %)
Type VIII	Accessory RHA and LHA and replaced RHA or LHA (2 %)
Type IX	CHA replaced to SMA (4.5 %)
Type X	CHA replaced to LGA (0.5 %)

*LHA* left hepatic artery, *RHA* right hepatic artery, *LGA* left gastric artery, *SMA* superior mesenteric artery, *CHA* common hepatic artery

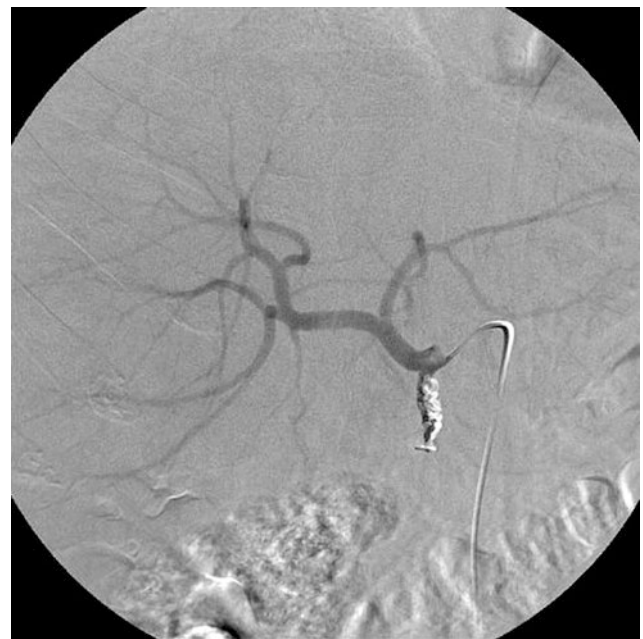


**Fig. 3** Conventional anatomy defined as type I according to Michels’ classification. The main hepatic artery originates from celiac trunk, gives off the gastroduodenal artery (which has been embolized with coils) and the proper hepatic artery, this later continues as the right hepatic artery after giving off the left hepatic artery and then the right hepatic artery splits into its anterior and posterior branches. The left hepatic artery feeds segments II and III. Segment IV is fed by the branch or branches originating from the right, left, or the proper hepatic artery

artery exist in type VII; the replaced right hepatic artery and the accessory left hepatic artery or the accessory right hepatic artery and the replaced left hepatic artery coexist in type VIII. The hepatic trunk originates from the superior mesenteric artery in type IX and from the left gastric artery in type X.

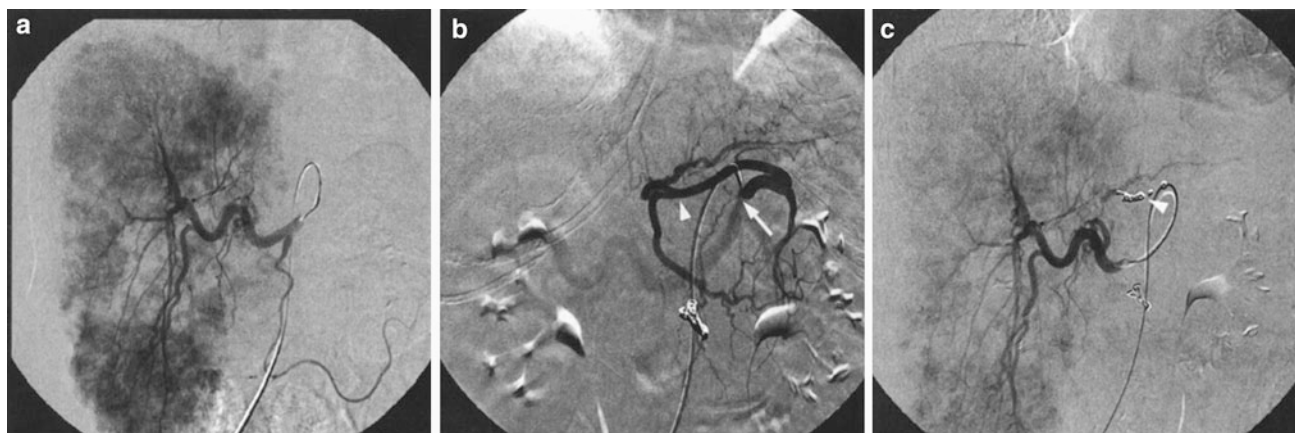


**Fig. 4** **a** Absence of opacification of the left lobe of the liver following injection of contrast in the common hepatic artery . **b** Injection in the left gastric artery (*arrow*) shows filling of a replaced left hepatic artery (*arrowheads*) (type II in Michels' classification).

**c** Following coil embolization of the origin of the left hepatic artery from the left gastric artery (*arrowhead*) there is immediate opacification of the whole liver from the common hepatic artery allowing for whole liver treatment from a single injection site

## 2.4 Other Anatomical Variants

The reported prevalence of anomalies not included in Michels' system varies from 1.8 (Koops et al. 2004) to 16.6 % (Coskun et al. 2005). The knowledge of these aberrant vessels can be useful in radioembolization, in order to recognize liver parenchyma supplied these arteries and if necessary embolize them before treatment.

Additional clinically relevant anatomical variants are summarized in Table 2 (Figs. 6, 7, and 8).

## 3 Extrahepatic Vessels Originating from the Hepatic Vasculature

When performing a radioembolization procedure it is of utmost importance to identify and isolate any vessel which may supply blood to other organs than the liver as this may result in non-target <sup>90</sup>Y administration. This is one of the most serious complications, particularly when it happens to affect the GI tract, as it will invariably lead to severe gastritis and possibly even ulceration (Carretero et al. 2007).

Small, previously unseen vessels can become more prominent after embolization of the gastroduodenal and right gastric arteries. If this redistribution phenomenon is not recognized at the time of treatment, complications may ensue (Lewandowski et al. 2007) (Fig. 9).

### 3.1 Vessels Originating from the CHA and Proper Hepatic Artery

#### 3.1.1 Gastroduodenal Artery and Pancreaticoduodenal Arcade

The GDA is usually not only the largest extrahepatic vessel but also one that is almost constantly present,

having many possible origins, the common hepatic artery (92.3 %) being the most common. Together with the pancreaticoduodenal arcade it supplies blood to the duodenum, pancreas, and stomach and forms an important part of the anastomotic system between the celiac axis and the superior mesenteric artery, having the potential to become important collaterals in cases of celiac stenosis, providing a potential route for redirection of flow (Liu et al. 2005; Song et al. 2002) (Fig. 10). Because of this it is of utmost importance to carry out a proper angiographic assessment and consider prophylactic occlusion of this vessel prior to radioembolization in order to avoid pancreatitis or duodenal ulceration and perforation (Carr et al. 1997).

The pancreaticoduodenal arcade provides an extensive collateral vascular network to the head of the pancreas, uncinate process, and duodenal bulb with a complex anatomical disposition and anastomotic channels with named arteries such as the dorsal pancreatic artery, the supraduodenal artery, and the retroduodenal artery (Hentati et al. 1999; Bertelli et al. 1995, 1996a, b, 1997, 1998).

The retroduodenal artery (Michels 1951) or posterior pancreaticoduodenal arcade arises as the first branch of the gastroduodenal artery crossing anterior to the supraduodenal portion of the common bile duct, and then behind the intrapancreatic portion of the common duct to form an arterial arcade on the posterior surface of the head of the pancreas with numerous branches to the duodenum (Figs. 11 and 12). This artery gives rise to multiple arteriolar branches that contribute the blood supply to the common hepatic duct (Arias Fernández et al. 2011). It has been reported that the inflow of the retroportal artery in the right hepatic lobe may result in a poor distribution of the radioembolization microspheres, whereas its selective embolization resulted in an improvement of the microspheres

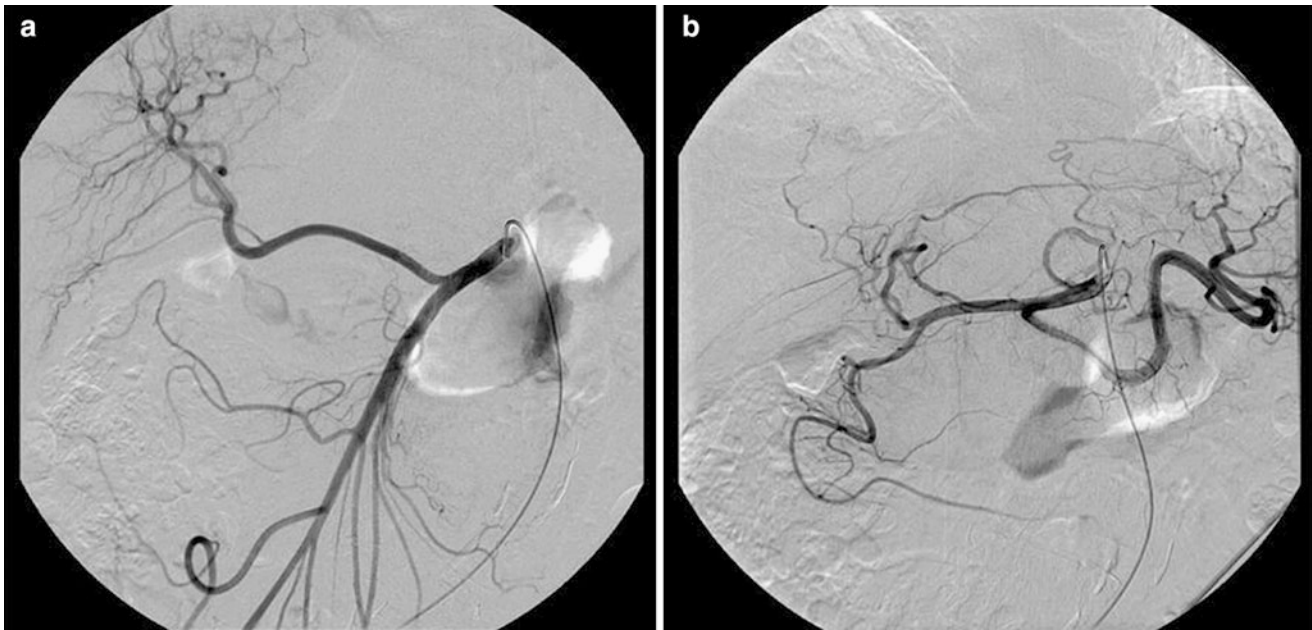


**Fig. 5** Type III anatomic variant according to Michels' classification. Replaced right hepatic artery originating from the superior mesenteric artery

**Table 2** Relevant anatomic variants not described by Michels

CHA from aorta
LHA from LGA + RHA from CHA
CHA from aorta + aberrant LHA from LGA + aberrant RHA from SMA
LHA from CHA + RHA from GDA
CHA from CT + aberrant LHA from LGA + aberrant RHA from aorta
Celiac mesenteric trunk + LHA from LGA
RHA from GDA
LHA from CHA + RHA from SMA
RHA from CT

*CHA* common hepatic artery, *LHA* left hepatic artery, *LGA* left gastric artery, *RHA* right hepatic artery, *SMA* superior mesenteric artery, *GDA* gastroduodenal artery, *CT* celiac trunk

distribution (Yamagami et al. 2005). Its catheterization may be easier from the SMA (Arias Fernández et al. 2011).

The dorsal pancreatic artery is the first major pancreatic branch, usually coming off the splenic artery, although many variations have been described (right hepatic artery, SMA, and celiac artery) (Arias Fernández et al. 2011). After supplying the dorsal surface of the neck of the pancreas, it divides into a left branch, the transverse pancreatic, and into a right branch (branches), which unites with the gastroduodenal or the superior pancreaticoduodenal (Michels 1951).

The transverse pancreatic artery is one of the major arteries of the pancreas and generally the major left branch



**Fig. 6** Another rare variant not described by Michels, consisting in a segmental right hepatic artery (*arrowhead*) originating from the gastroduodenal artery (*arrow*)

of the dorsal pancreatic. It courses along the inferior surface of the pancreas to unite with the a. pancreatica magna (branch of the splenic artery) (Michels 1951).

The supraduodenal artery (of Wilkie) (Michels 1951) is a small artery that supplies blood to the anterior and posterior surfaces and upper portion of the duodenum and pylorus, and communicates with the pancreaticoduodenal arcade, as well as right gastric branches. It is reported to be present in



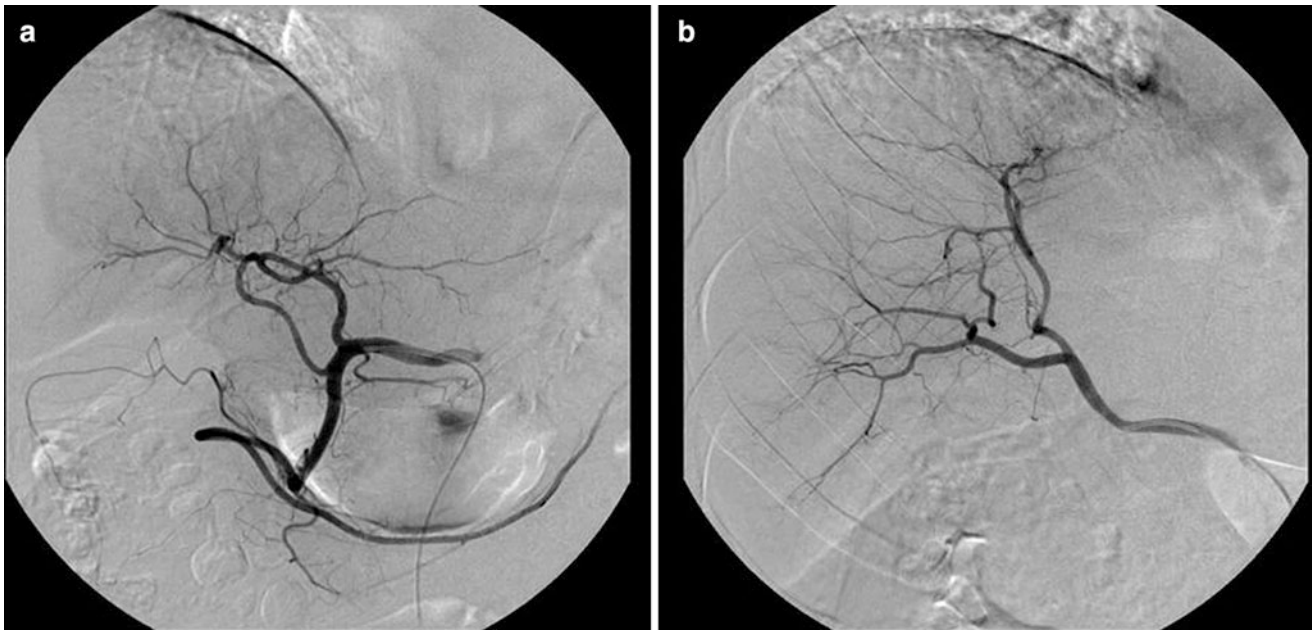


**Fig. 7** Anatomical variant not included in Michel's system. **a** Aberrant accessory left hepatic artery arising from the gastroduodenal artery and **b** aberrant replaced right hepatic artery arising from the superior mesenteric artery



**Fig. 8** A rare anatomical variant consisting in the origin of the right hepatic artery (*arrow*) from the common hepatic artery

93 % of patients, with a high degree of variation in its origin, the most frequent being the gastroduodenal artery (27 %), followed by the common hepatic artery (20 %), left hepatic artery (20 %), right hepatic artery (13 %), and cystic arteries (10 %). Duplication of the artery has been described in 2–3 % of cases (Van Damme and Bonte 1990; Bianchi and Albanese 1989).

### 3.1.2 Arteries of the Peribiliary Plexus

Also known as “communicating arcades” (Arias Fernández et al. 2011). It is a vascular network distributed around the intra- and extrahepatic bile ducts (Kan and Madoff 2008). The peribiliary plexus connects the hepatic arteries with the portal venous system through the bile duct walls (Uchikawa et al. 2011). Cirrhotic patients typically have an increased peribiliary plexus that supplies the biliary tract (Arias Fernández et al. 2011). Communicating arcades function as a collateral pathway in cases of segmental arterial or portal occlusion allowing the revascularization of hepatic segmental territories (Fig. 13) (Arias Fernández et al. 2011; Uchikawa et al. 2011).

## 3.2 Vessels Originating from the LHA

### 3.2.1 Right Gastric Artery

The right gastric artery should be actively searched during the angiographic work-up as it may sometimes prove quite inconspicuous (Figs. 14). It may arise from any site from the hepatic artery, although most frequently arises from the left hepatic artery, anastomosing with the left gastric artery via an arterial arcade (Van Damme and Bonte 1990). This anatomical disposition may be useful in those cases where antegrade catheterization and occlusion of the right gastric artery cannot be performed allowing access to it from the left gastric artery (Yamagami et al. 2002; Cosin et al. 2007). Although a minor contributor to the



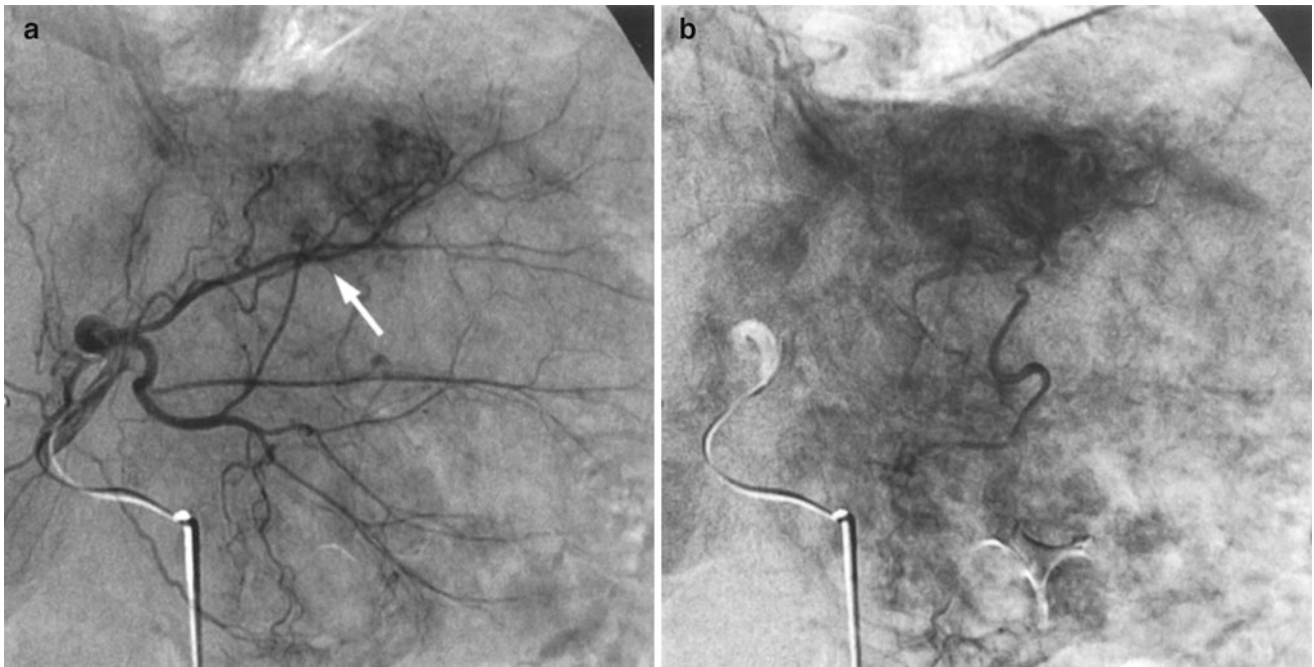


**Fig. 9** **a** Small, yet important, accessory gastric artery (*arrow*) coming off segment III hepatic artery only seen after superselective catheterization. **b** Existence of venous gastric stain confirms the presence of the artery

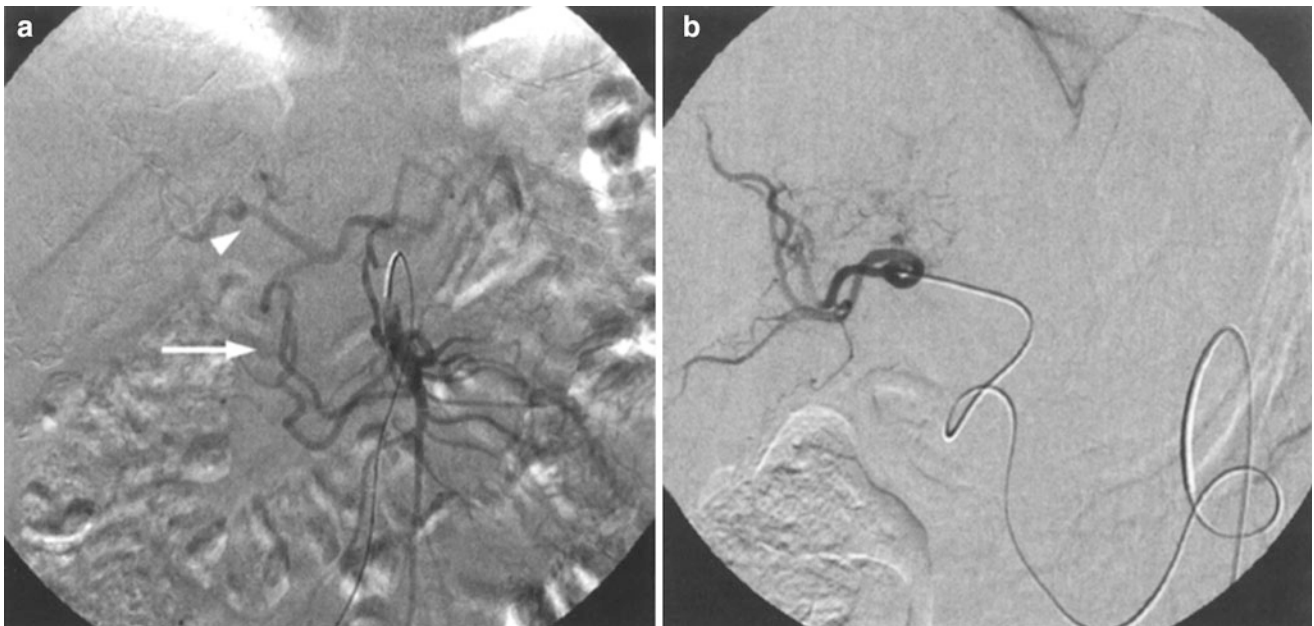


**Fig. 10** Patient with a stenosis of the celiac trunk. **a** Superior mesenteric angiography demonstrates reversed flow through the pancreaticoduodenal arcade (*arrow*) with opacification of the hepatic

artery (*arrowhead*). **b** Tumor was treated after selective catheterization of the right hepatic artery through the collateral network

blood supply of the stomach, the right gastric artery plays an important role in radioembolization procedures as passage of spheres through it may result in gastric necrosis, ulceration, and eventually perforation (Inaba

et al. 2001). The decision to perform prophylactic embolization will depend largely on the origin of the right gastric artery and the probability of non-target embolization (Liu et al. 2005).

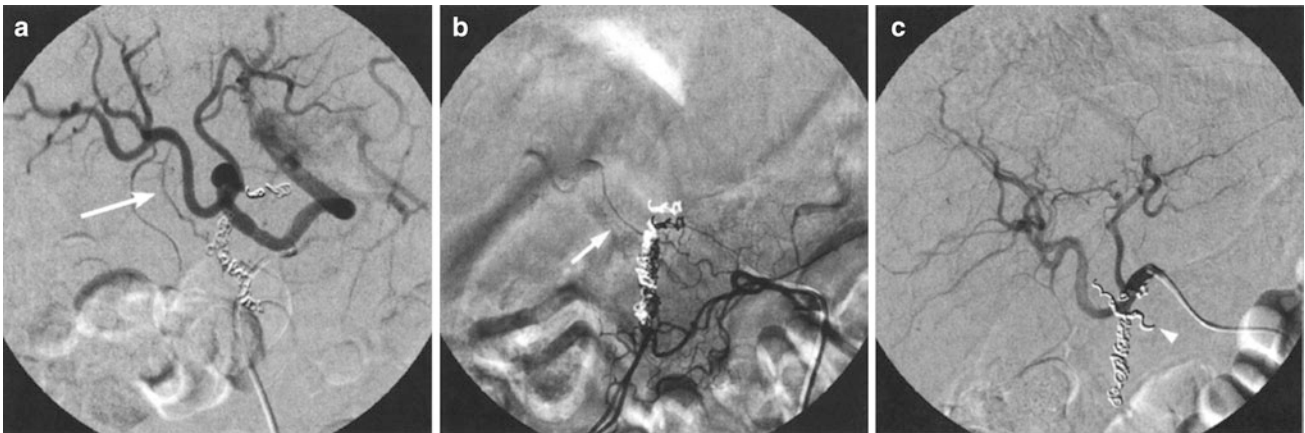


**Fig. 11** Angiography performed after coiling of the gastroduodenal and right gastric arteries. **a** An oblique view shows the presence of an extrahepatic artery (*arrow*) that arises from the right hepatic artery.

**b** Selective catheterization of the retroduodenal artery (*arrow*) which originates in the inferior pancreaticoduodenal arcade. **c** Angiography performed after occlusion of the retroduodenal artery (*arrowhead*)

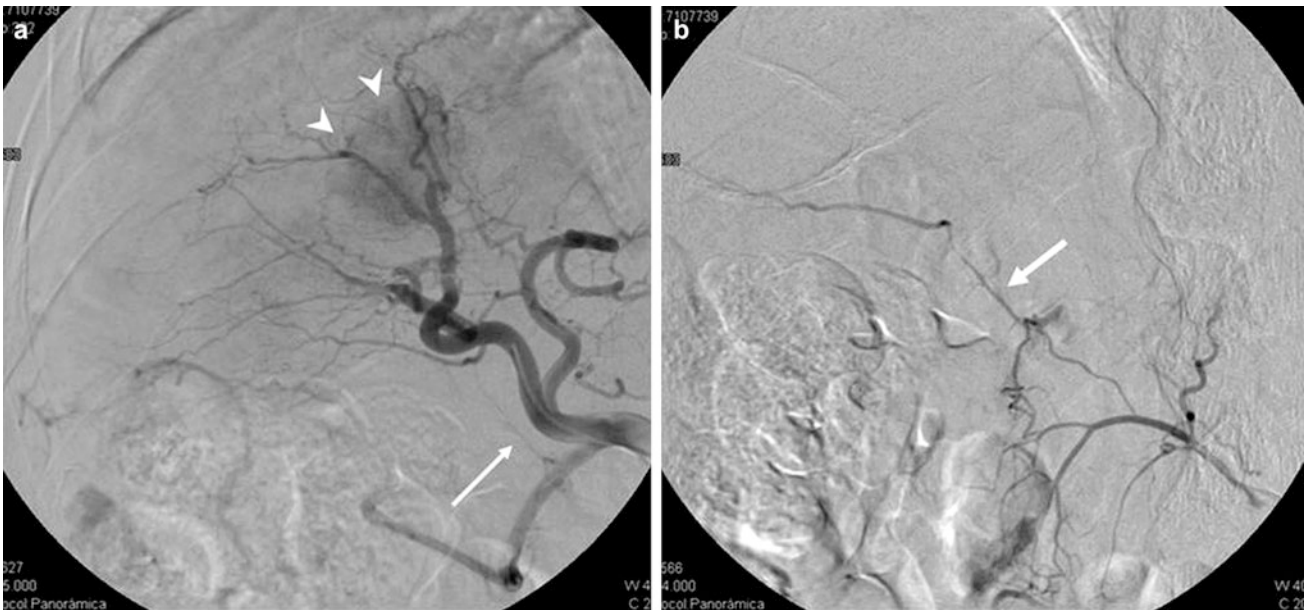


**Fig. 12 a** Hepatocellular carcinoma in the right lobe (*arrowheads*). Arteriography from the CHA. Opacification of the retroportal artery (*arrow*). **b** Contrast injection from the SMA. Retrograde filling of the

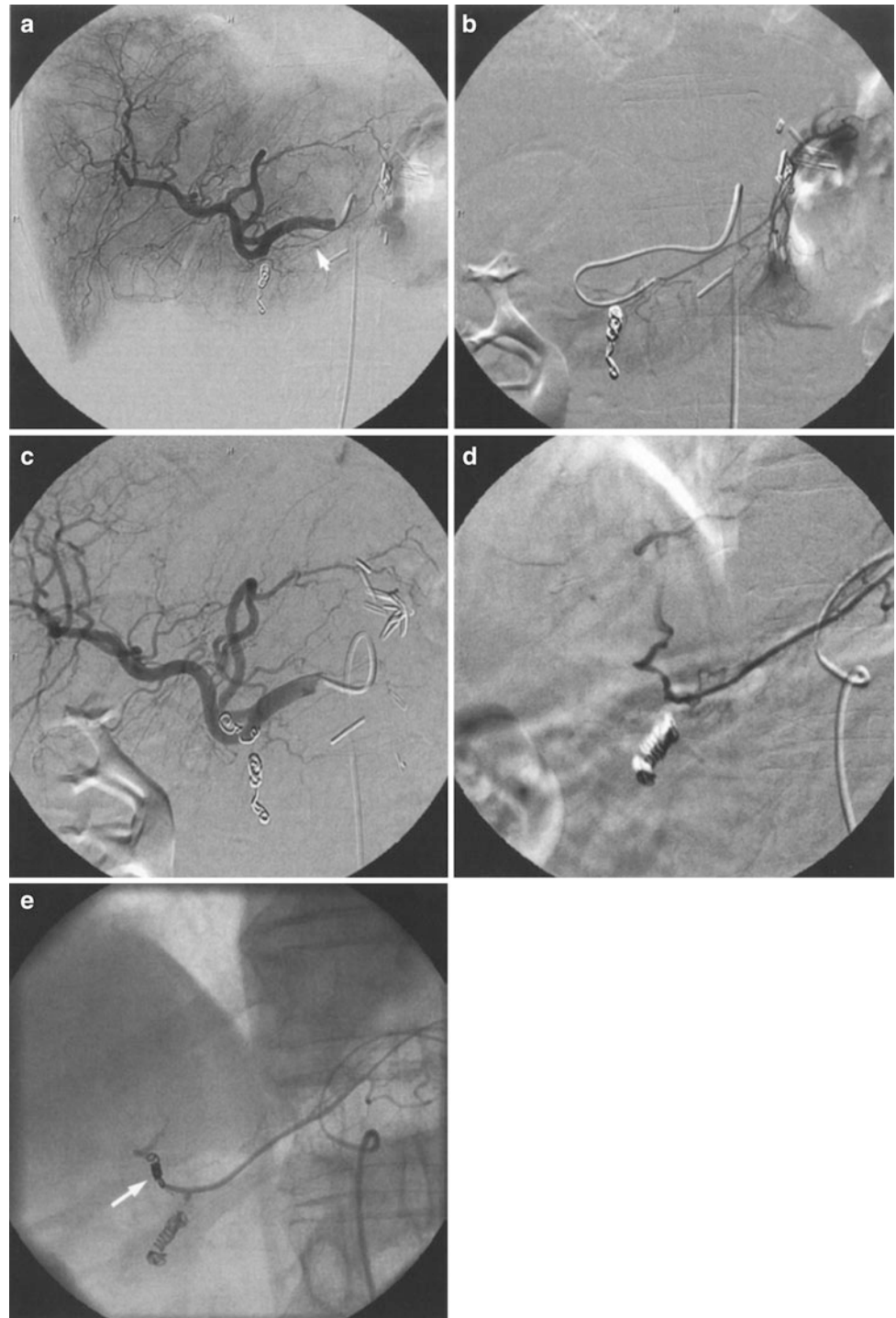
retroportal artery (*arrow*) with contrast passing into the branch of segment VI (with permission from: Arias Fernández et al. 2011)



**Fig. 13** Liver metastases. **a** Angiography performed from the CHA. Segment II branch is not detected (*star*). **b** Selective catheterization of the accessory left hepatic artery that arises from the LGA. Angiogram shows a large caliber collateral vessel that reaches the right lobe

(*arrow*). **c** Coil occlusion of the accessory LHA. Recanalization via the collaterals of segment II branch (*arrow*) (with permission from: Arias Fernández et al. 2011)

**Fig. 14** **a** Right gastric artery (*arrowhead*) arising from the left hepatic artery. **b** Selective antegrade catheterization of the right gastric artery. **c** Hepatic angiography performed after coiling of the right gastric and gastroduodenal arteries. **d** When access to the right gastric artery in an antegrade fashion is not possible, it may be catheterized in a retrograde fashion from the left gastric artery and **e** subsequently coiled (*arrow*)



### 3.2.2 Falciform Artery

The falciform artery was first described by Albrecht Von Haller in 1753. It arises as a terminal branch of the middle or left hepatic artery and runs within the falciform ligament together with the umbilical vein (Williams et al. 1985; Baba et al. 2000). It may be visualized in approximately 2–25 % of hepatic angiograms, this figure rising to 67 % on

postmortem dissection of the falciform ligament (Williams et al. 1985; Kim et al. 1999; Gibo et al. 2001). It follows a characteristic course running in an oblique plane, from the left intersegmental fissure to the anterior abdominal wall, not to be confused with the cystic or omental arteries (Fig. 15). When present, it may provide anastomoses with the vasculature from the anterior abdominal wall, namely



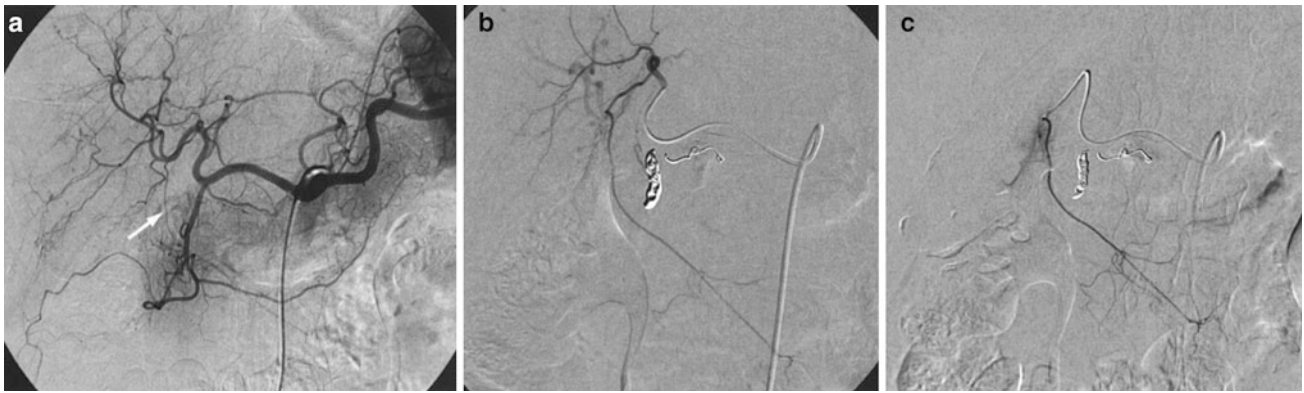


**Fig. 15** **a** Inconspicuous falciform artery (*arrow*) arising from a branch of the left hepatic artery. **b** Selective catheterization of the left hepatic artery confirms the presence of a falciform artery which is

subsequently entered with a microcatheter (**c**) in order to coil it, thus preventing non-target radioembolization

**Fig. 16** Liver metastases. **a** Common origin of the LHA and RGA (*arrow*). A branch that does not correspond to any of the left segmental arteries arises from the PHA/RHA (*arrowheads*). **b** Opacification of the gastric coronary vein in the venous phase (*arrow*) implies that the catheterized arterial branch is an accessory left gastric artery (with permission from: Arias Fernández et al. 2011)

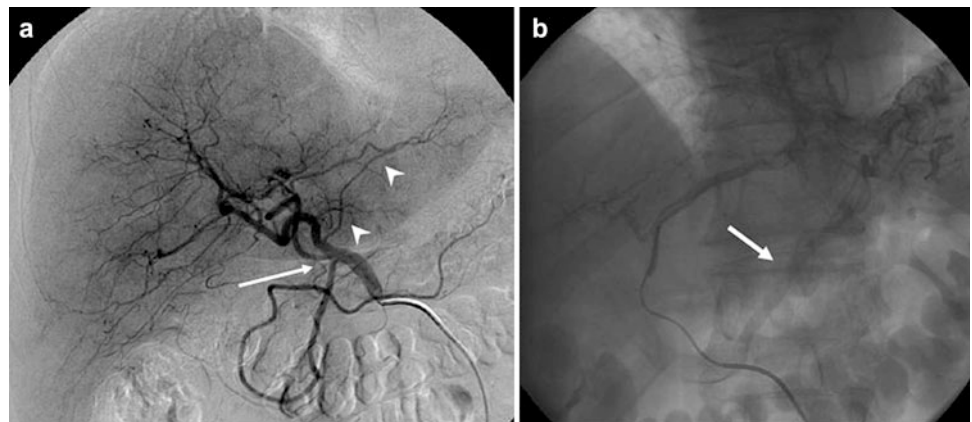


**Fig. 17** Liver metastases. Previous cholecystectomy, stenosis of the RHA. The angiogram shows a branch arising from the LHA that reaches the left subphrenic area (*arrow*) (with permission from: Arias Fernández et al. 2011)

the terminal vessels of the internal mammary and superior epigastric arteries (Michels 1953). Failure to identify and prophylactically occlude this vessel may result in delivery of 90Y particles to the anterior abdominal wall, which may result in adverse events in the form of severe abdominal pain, skin necrosis, and rash (Gibo et al. 2001; Ueno et al. 1995).

### 3.2.3 Accessory Left Gastric Artery

It has been published that the accessory left gastric artery is present in up to 21 % of the population (Song et al. 2006). It can originate from the proper hepatic artery, the arteries of the hepatic segments II or III and connects with the esophagus and gastric fundus (Song et al. 2010). It is best visualized during the venous phase of the left hepatic angiogram (Fig. 16) (Arias Fernández et al. 2011). If detected, this artery must be embolized before radioembolization in order to prevent adverse effects such as necrosis, ulceration, or even gastric perforation.

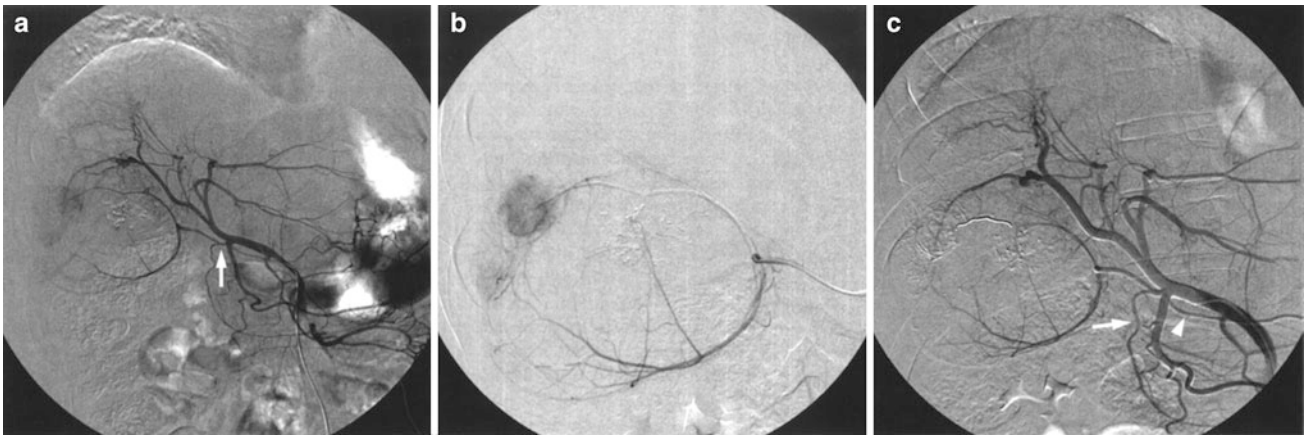


**Fig. 18** **a** Uncommon origin of the cystic artery (*arrow*) from the gastroduodenal artery. **b** The cystic artery provides parasitic supply to the tumor, best seen on superselective catheterization. **c** Following coil embolization of the parasitic branch there is redistribution of flow and

radioembolization may be carried out from the hepatic artery. This case shows a rather infrequent trunk, which consists in a common origin of the cystic artery, the right gastric artery (*arrowhead*), and the supraduodenal artery (*arrow*) from the top of the gastroduodenal artery

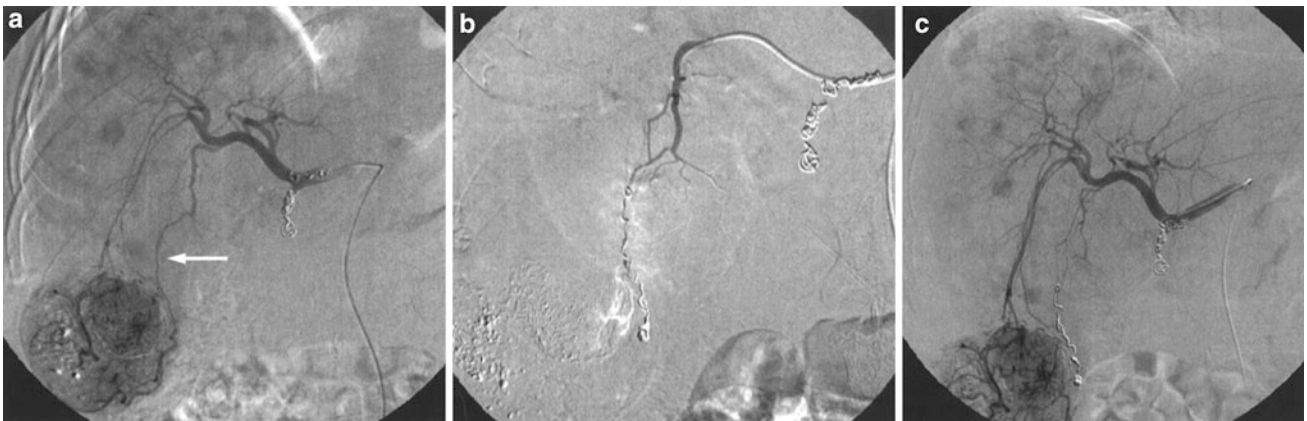


**Fig. 19** **a** Marked parasitic supply to the tumor from the cystic artery (*arrow*). **b** In order to diminish the probability of non-target deposition of microspheres within the gallbladder, coil embolization of the

parasitic branch is carried out. **c** The subsequent angiogram shows flow redistribution with complete opacification of the tumor bed which has now been disconnected from the cystic artery

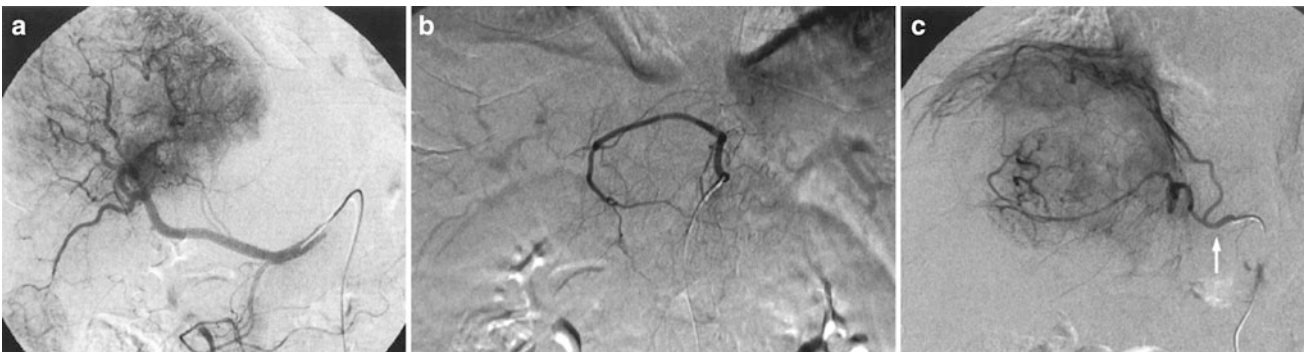


**Fig. 20** **a** Common hepatic angiogram showing a tumor located close to the dome of the liver. Note absence of left hepatic artery. **b** Angiogram carried out from the left gastric artery confirms the presence of an accessory replaced left hepatic artery which does not

seem to contribute to the tumor blood supply. **c** Given the large size of the tumor and its location, a right phrenic artery (*arrow*) selective injection is performed confirming the presence of extrahepatic blood supply



### 3.2.4 Accessory Left Phrenic Artery

The left phrenic artery usually arises from the celiac trunk or abdominal aorta, if its origin is not identified arising from these arteries it is necessary to review the left gastric artery or left hepatic artery. This artery rarely arises from left hepatic artery (Fig. 17), with a reported incidence from 0 (Piao et al. 1998) to 2 % (Song et al. 2006). Even though no radioembolization related complications have been described, if this artery is present it is advisable to embolize it prior to treatment (Arias Fernández et al. 2011).

## 3.3 Vessels Originating from the RHA

### 3.3.1 Cystic Artery

The typical origin of this vessel is the right hepatic artery in as many as 95 % of patients (Ottery et al. 1986), but it may also come up from the left hepatic artery (7 %), common hepatic artery (3 %), replaced or accessory right hepatic arteries (18 %), as well as the gastroduodenal artery (1 %), or superior mesenteric artery (Daseler et al. 1947; Mlakar et al. 2003; Molmenti et al. 2003; Sarkar and Roy 2000). There is a 2–15 % incidence of double cystic artery (Daseler et al. 1947; Loukas et al. 2006) (Fig. 18).

The gallbladder blood supply comes not only from the cystic artery, but also from perforators to the body of the gallbladder from the hepatic parenchyma and the GDA. This is important from a practical viewpoint as, if the cystic artery is small, then this alternative route of blood supply to the gallbladder may be assumed to be present and prophylactic occlusion may be considered when avoiding microsphere flow into the cystic artery becomes impossible.

In contrast, the cystic artery may be a source of parasitic supply for tumors located near the gallbladder fossa and, although infrequently, for tumors located in the right lobe or medial segment of the liver when the hepatic artery is attenuated (Wagnetz et al. 2010) (Fig. 19).

Occlusion of the cystic artery may lead to cholecystitis or gallbladder infarction (Takayasu et al. 1985; Miyayama et al. 2006).

## 4 Hepatic Vessels Originating from the Extrahepatic Vasculature

Although this is not the topic of this chapter, it is important to highlight that there are many hepatic vessels originating from non-hepatic sources.

Extrahepatic collateral pathways to the liver may be established in various conditions such as following surgical ligation of the hepatic artery or arterial injury induced by repeated endovascular treatments. Adhesion between the liver and other organs exaggerates the degree of

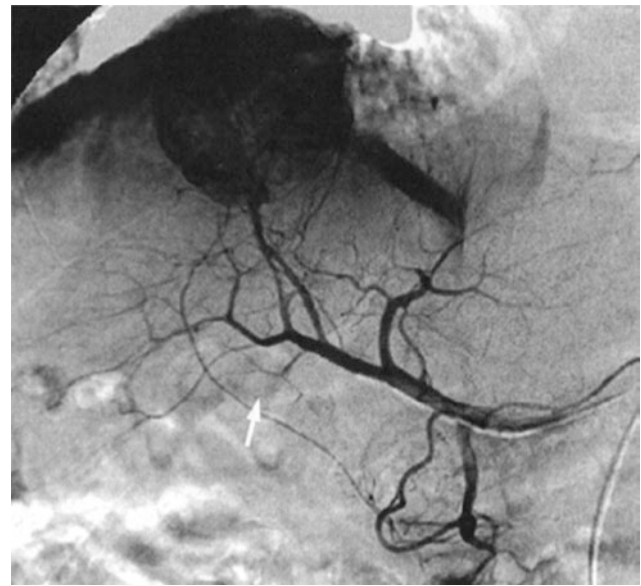


**Fig. 21** Parasitic blood supply to a hepatocellular carcinoma from an omental artery (arrow)

extrahepatic collaterals. An extrahepatic blood supply to HCC or parasitization may also develop even when the hepatic arterial supply remains intact, particularly when there is extracapsular invasion and extension. For transcatheter management of HCC to be effective, these collaterals should be adequately recognized as they may feed an important bulk of tumor which may not undergo treatment otherwise. In fact, it has been proposed that tumoral size is the most important predictive factor for the recruitment of extrahepatic supply (Chung et al. 2006). Miyayama et al. (2006) found this event in at least 25 % of the 386 angiographic procedures performed in 181 patients. In this study, the incidences of collateral blood supply to HCC were 83 % from the right inferior phrenic artery (Fig. 20), 13 % from the omental artery (Fig. 21), 12 % from the right renal capsular artery and left inferior phrenic artery, 8 % from the right internal mammary artery and right intercostal arteries, and 7 % from the right inferior adrenal artery.

Miyayama et al. also reported on the close relationship between the tumor location within the liver and the likely origin of the parasitic arteries. Tumors located at the posterior surface of the right lobe and near the diaphragm were likely to be fed by the right inferior phrenic artery, right intercostal arteries, and lumbar arteries. Blood supply from the right internal mammary artery could be seen when the tumor was located close to the diaphragm or anterior chest wall. Tumors located near the right renal fossa were likely to receive supply from the right renal capsular artery and right middle and inferior adrenal arteries. Tumors located at the anterior surface of the right lobe of the liver or at the lower edge of the medial segment of the liver could be fed

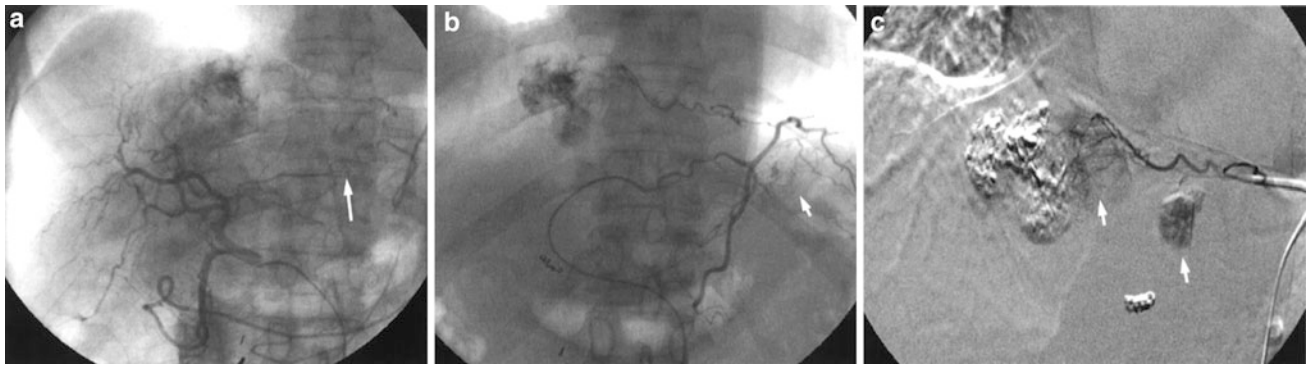


**Fig. 22** **a** Relapse of a hepatocellular carcinoma fed mainly by branches of the right hepatic artery. A common trunk (*arrow*) between the left hepatic artery and the left phrenic artery is also seen.

**b** Selective catheterization of the mentioned common trunk also shows gastric branches (*arrowhead*). **c** Superselective catheterization demonstrates tumor uptake (*arrowheads*) from this artery

by the omental artery or colic artery. Tumors in the left lobe of the liver could be supplied by the right gastric artery, left gastric artery, or even the left inferior phrenic artery (Fig. 22). Finally, tumors located in the caudate lobe tended to be fed by the right inferior phrenic artery, right renal capsular artery, and gastric artery.

Chemoembolization of the inferior phrenic artery has been associated with right subcostal pain, upper quadrant tenderness, and basal atelectasis (Chung et al. 1998) whereas gastrointestinal tract ulceration and/or perforation have been reported after gastric, omental, and colic branch artery embolization (Carretero et al. 2007; Sueyoshi et al. 2010).

If internal mammary, intercostal, or lumbar artery is embolized, cutaneous complications may appear (Sueyoshi et al. 2010). Severe complications such as spinal infarction can appear after proximal occlusion of the intercostal artery (Cheng et al. 2010).

## References

- Arias Fernández J, Martín Martín B, Pinheiro da Silva N et al (2011) Extrahepatic vessels depending on the hepatic artery. Identification and management. *Radiologia* 53(1):18–26
- Baba Y, Miyazono N, Ueno K et al (2000) Hepatic falciform artery. Angiographic findings in 25 patients. *Acta Radiol* 41:329–333
- Bertelli E, Di Gregorio F, Bertelli L, Mosca S (1995) The arterial blood supply of the pancreas: a review. I. The superior pancreaticoduodenal and the anterior superior pancreaticoduodenal arteries. An anatomical and radiological study. *Surg Radiol Anat* 17:97–106, 1–3
- Bertelli E, Di Gregorio F, Bertelli L, Civeli L, Mosca S (1996a) The arterial blood supply of the pancreas: a review. II. The posterior superior pancreaticoduodenal artery. An anatomical and radiological study. *Surg Radiol Anat* 18:1–9
- Bertelli E, Di Gregorio F, Bertelli L, Civeli L, Mosca S (1996b) The arterial blood supply of the pancreas: a review. III. The inferior pancreaticoduodenal artery. An anatomical review and a radiological study. *Surg Radiol Anat* 18:67–74
- Bertelli E, Di Gregorio F, Bertelli L, Orazioli D, Bastianini A (1997) The arterial blood supply of the pancreas: a review. IV. The anterior inferior and posterior pancreaticoduodenal aa., and minor sources of blood supply for the head of the pancreas. An anatomical review and radiologic study. *Surg Radiol Anat* 19:203–212
- Bertelli E, Di Gregorio F, Mosca S, Bastianini A (1998) The arterial blood supply of the pancreas: a review. V. The dorsal pancreatic artery. An anatomical review and a radiologic study. *Surg Radiol Anat* 20:445–452
- Bianchi HF, Albanese EF (1989) The supraduodenal artery. *Surg Radiol Anat* 11:37–40
- Carr BI, Zajko A, Bron K, Orons P, Sammon J, Baron R (1997) Phase II study of Spherex (degradable starch microspheres) injected into the hepatic artery in conjunction with doxorubicin and cisplatin in the treatment of advanced stage hepatocellular carcinoma: interim analysis. *Semin Oncol* 24(2 Suppl 6):S6:97–S6:99
- Carretero C, Munoz-Navas M, Betes M et al (2007) Gastroduodenal injury after radioembolization of hepatic tumors. *Am J Gastroenterol* 102:1216–1220
- Cheng LF, Ma KF, Fan WC et al (2010) Hepatocellular carcinoma with extrahepatic collateral arterial supply. *J Med Imaging Radiat Oncol* 54(1):26–34
- Chung JW, Park JH, Han JK, Choi BI, Kim TK, Han MC (1998) Transcatheter oily chemoembolization of the inferior phrenic artery in hepatocellular carcinoma: the safety and potential therapeutic role. *J Vasc Interv Radiol* 9:495–500
- Chung JW, Kim HC, Yoon JH et al (2006) Transcatheter arterial chemoembolization of hepatocellular carcinoma: prevalence and causative factors of extrahepatic collateral arteries in 479 patients. *Korean J Radiol* 7:257–266
- Cosin O, Bilbao JI, Alvarez S, de Luis E, Alonso A, Martinez-Cuesta A (2007) Right gastric artery embolization prior to treatment with yttrium-90 microspheres. *Cardiovasc Intervent Radiol* 30:98–103
- Coskun M, Kayahan EM, Özbek O et al (2005) Imaging of hepatic arterial anatomy for depicting vascular variations in living related liver transplant donor candidates with multidetector computed tomography: comparison with conventional angiography. *Transplant Proc* 37:1070–1073
- Daseler EH, Anson BJ, Hambley WC, Riemann AF (1947) The cystic artery and constituents of the hepatic pedicle: a study of 500 specimens. *Surg Gynecol Obstet* 85:47–63
- Gibo M, Hasuo K, Inoue A, Miura N, Murata S (2001) Hepatic falciform artery: angiographic observations and significance. *Abdom Imaging* 26:515–519

- Hentati N, Fournier HD, Papon X, Aube C, Vialle R, Mercier P (1999) Arterial supply of the duodenal bulb: an anatomoclinical study. *Surg Radiol Anat* 21:159–164
- Hiatt JR, Gabbay J, Busuttill RW (1994) Surgical anatomy of the hepatic arteries in 1000 cases. *Ann Surg* 220:50–52
- Inaba Y, Arai Y, Matsueda K, Takeuchi Y, Aramaki T (2001) Right gastric artery embolization to prevent acute gastric mucosal lesions in patients undergoing repeat hepatic arterial infusion chemotherapy. *J Vasc Interv Radiol* 12:957–963
- Kan Z, Madoff DC (2008) Liver anatomy: microcirculation of the liver. *Semin Intervent Radiol* 25(2):77–85
- Kim DE, Yoon HK, Ko GY, Kwon JS, Song HY, Sung KB (1999) Hepatic falciform artery: is prophylactic embolization needed before short term hepatic arterial chemoinfusion? *Am J Roentgenol* 172:1597–1599
- Koops A, Wojciechowski B, Broering DC et al (2004) Anatomic variations of the hepatic arteries in 604 selective celiac and superior mesenteric angiographies. *Surg Radiol Anat* 26:239–244
- Lewandowski RJ, Sato KT, Atassi B et al (2007) Radioembolization with 90Y microspheres: angiographic and technical considerations. *Cardiovasc Intervent Radiol* 30:571–592
- Liu DM, Salem R, Bui JT et al (2005) Angiographic considerations in patients undergoing liver directed therapy. *J Vasc Interv Radiol* 16:911–935
- Loukas M, Ferguson A, Louis RG Jr, Colborn GL (2006) Multiple variations of the hepatobiliary vasculature including double cystic arteries, accessory left hepatic artery and hepatosplenic trunk: a case report. *Surg Radiol Anat* 28:525–528
- Michels NA (1951) The hepatic, cystic and retroduodenal arteries and their relations to the biliary ducts with samples of the entire celiacal blood supply. *Ann Surg* 133:503–524
- Michels NA (1953) Collateral arterial pathways to the liver after ligation of the hepatic artery and removal of the celiac axis. *Cancer* 6:708–724
- Miyayama S, Matsui O, Taki K et al (2006) Extrahepatic blood supply to hepatocellular carcinoma: angiographic demonstration and transcatheter arterial chemoembolization. *Cardiovasc Intervent Radiol* 29:39–48
- Mlakar B, Gadzijev EM, Ravnik D, Hribernik M (2003) Anatomical variations of the cystic artery. *Eur J Morphol* 41:31–34
- Molmenti EP, Pinto PA, Klein J, Klein AS (2003) Normal and variant arterial supply of the liver and gallbladder. *Pediatr Transplant* 7:80–82
- Ottery FD, Scupham RK, Weese JL (1986) Chemical cholecystitis after intrahepatic chemotherapy. The case for prophylactic cholecystectomy during pump placement. *Dis Colon Rectum* 29:187–190
- Piao DX, Ohtsuka A, Murakami T (1998) Typology of abdominal arteries, with special reference to inferior phrenic arteries and their esophageal branches. *Acta Med Okayama* 52(189–196):6
- Sarkar AK, Roy TS (2000) Anatomy of the cystic artery arising from the gastroduodenal artery and its choledochal branch—a case report. *J Anat* 197(Pt 3):503–506
- Song SY, Chung JW, Kwon JW et al (2002) Collateral pathways in patients with celiac axis stenosis: angiographic-spiral CT correlation. *Radiographics* 22:881–893
- Song SY, Chung JW, Lim HG et al (2006) Nonhepatic arteries originating from the hepatic arteries: angiographic analysis in 250 patients. *J Vasc Interv Radiol* 17:461–469
- Song SY, Chung JW, Yin YH et al (2010) Celiac axis and common hepatic artery variations in 5002 patients: systematic analysis with spiral CT and DSA. *Radiology* 255(1):278–288
- Sueyoshi E, Hayashida T, Sakamoto I et al (2010) Vascular complications of hepatic artery after transcatheter arterial chemoembolization in patients with hepatocellular carcinoma. *Am J Roentgenol* 195(1):245–251
- Takayasu K, Moriyama N, Muramatsu Y et al (1985) Gallbladder infarction after hepatic artery embolization. *Am J Roentgenol* 144(1):135–138
- Uchikawa Y, Kitamura H, Miyagawa S (2011) Portal blood flow via the peribiliary vascular plexus demonstrated by contrast enhanced ultrasonography with Sonazoid. *J Hepatobiliary Pancreat Sci* 18(4):615–620
- Ueno K, Miyazono N, Inoue H, Miyake S, Nishida H, Nakajo M (1995) Embolization of the hepatic falciform artery to prevent supraumbilical skin rash during transcatheter arterial chemoembolization for hepatocellular carcinoma. *Cardiovasc Intervent Radiol* 18:183–185
- Van Damme JP, Bonte J (1990) Vascular anatomy in abdominal surgery. Thième, New York
- Wagnetz U, Jaskolka J, Yang P et al (2010) Acute ischemic cholecystitis after transarterial chemoembolization of hepatocellular carcinoma: incidence and clinical outcome. *J Comput Assist Tomogr* 34(3):348–353
- Williams DM, Cho KJ, Ensminger WD, Ziessman HA, Gyves JW (1985) Hepatic falciform artery: anatomy, angiographic appearance, and clinical significance. *Radiology* 156:339–340
- Yamagami T, Nakamura T, Iida S, Kato T, Nishimura T (2002) Embolization of the right gastric artery before hepatic arterial infusion chemotherapy to prevent gastric mucosal lesions: approach through the hepatic artery versus the left gastric artery. *Am J Roentgenol* 179:1605–1610
- Yamagami T, Kato T, Tanaka O et al (2005) Influence of hepatopetal flow of the retroportal artery on efficiency of repeated hepatic arterial infusion chemotherapy. *J Vasc Interv Radiol* 16(10):1391–1395



---

# Radioembolization: Identifying and Managing Anatomic Variants

Rajesh P. Shah and Daniel Y. Sze

## Contents

<b>1</b>	<b>Normal, Variant, and Parasitized Extrahepatic Arterial Supply to the Liver</b> .....	41
<b>2</b>	<b>Redistribution and Consolidation of Hepatic Arterial Flow</b> .....	44
2.1	Redistribution.....	44
2.2	Consolidation .....	45
<b>3</b>	<b>Extrahepatic Arterial Anatomy: Identification and Treatment</b> .....	48
<b>4</b>	<b>Conclusion</b> .....	51
	<b>References</b> .....	51

---

## Abstract

Radioembolization treatment carries the risk of non-target embolization as well as of incomplete treatment. The distribution of microspheres reflects the arterial vascular territory subtended by the injected arteries. Thus, it is important to recognize anatomic variants in hepatic arterial anatomy. These variants include congenital accessory and replaced arteries supplying portions of the liver and the tumors within, as well as parasitized non-hepatic arteries recruited to supply arterial blood to intrahepatic tumors. Several different strategies allow more safe and complete radioembolization preparation and treatment in the presence of these variants. Consolidation or redistribution of flow may be performed to simplify or to increase the safety of microsphere administration. Likewise, parasitized extrahepatic vessels may be embolized to restore intrahepatic flow to tumors, thus, limiting risk for non-target embolization and increasing completeness of treatment. Both scenarios require close attention to tumor blood supply and recognition of arterial variants.

---

## 1 Normal, Variant, and Parasitized Extrahepatic Arterial Supply to the Liver

Standard hepatic arterial anatomy and its variants were described by Michels based on his study of 200 cadavers (Michels 1966). He defined ten configurations of hepatic arterial variants. Of these, the most common was a trifurcation of the celiac artery into the splenic, left gastric artery (LGA), and common hepatic arteries (CHA). The CHA bifurcated into the proper hepatic (PHA) and gastroduodenal arteries (GDA). The PHA in turn bifurcated into a right hepatic artery (RHA) and left hepatic artery (LHA). A segment IV artery that arose off the RHA was termed a

---

R. P. Shah (✉)  
Division of Interventional Radiology,  
300 Pasteur Drive H3630,  
Stanford University Medical Center,  
Stanford, CA 94305, USA  
e-mail: rajshah@stanford.edu

D. Y. Sze  
Division of Interventional Radiology,  
Stanford University Medical Center,  
Stanford, CA, USA

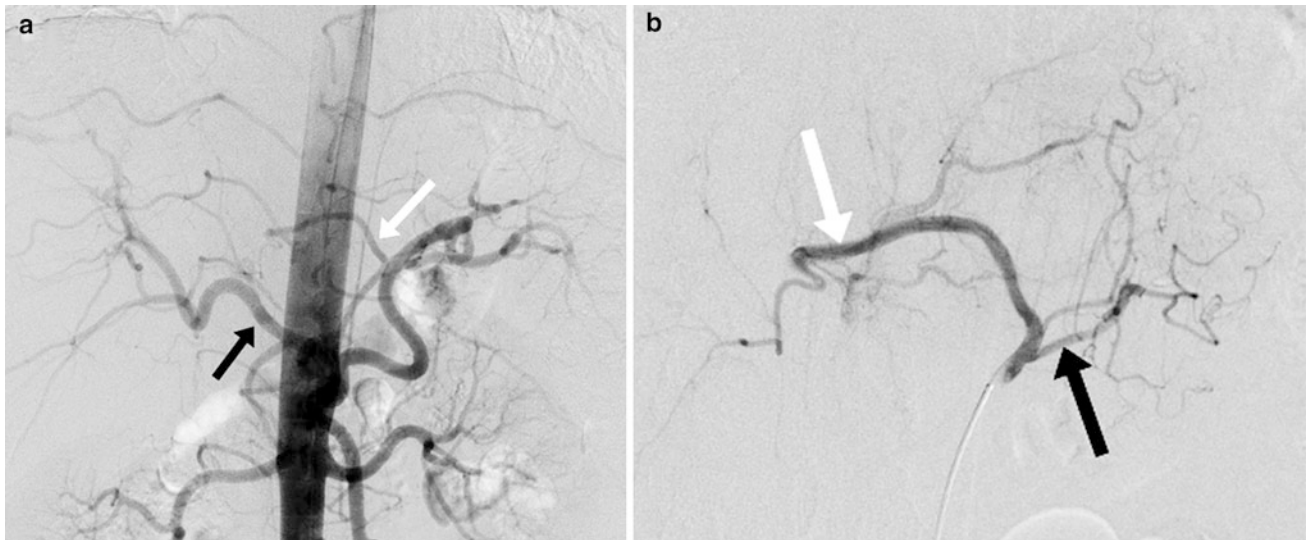


**Fig. 1** 53-year-old male with small bowel adenocarcinoma metastatic to the liver undergoing radioembolization preparatory angiogram. **a** Aortogram showed a replaced left hepatic artery (*white arrow*) arising off the left gastric. Note the lack of any arteries feeding the left hepatic lobe arising from the proper hepatic artery (*black arrow*),

**b** Selective angiogram of the gastrohepatic trunk confirmed the replaced left hepatic artery (*white arrow*) sharing a common origin as the left gastric artery (*black arrow*). This represents a Michels Type II configuration of hepatic arterial anatomy and is the most common variant

**Table 1** Michels classification of variant hepatic arterial anatomy

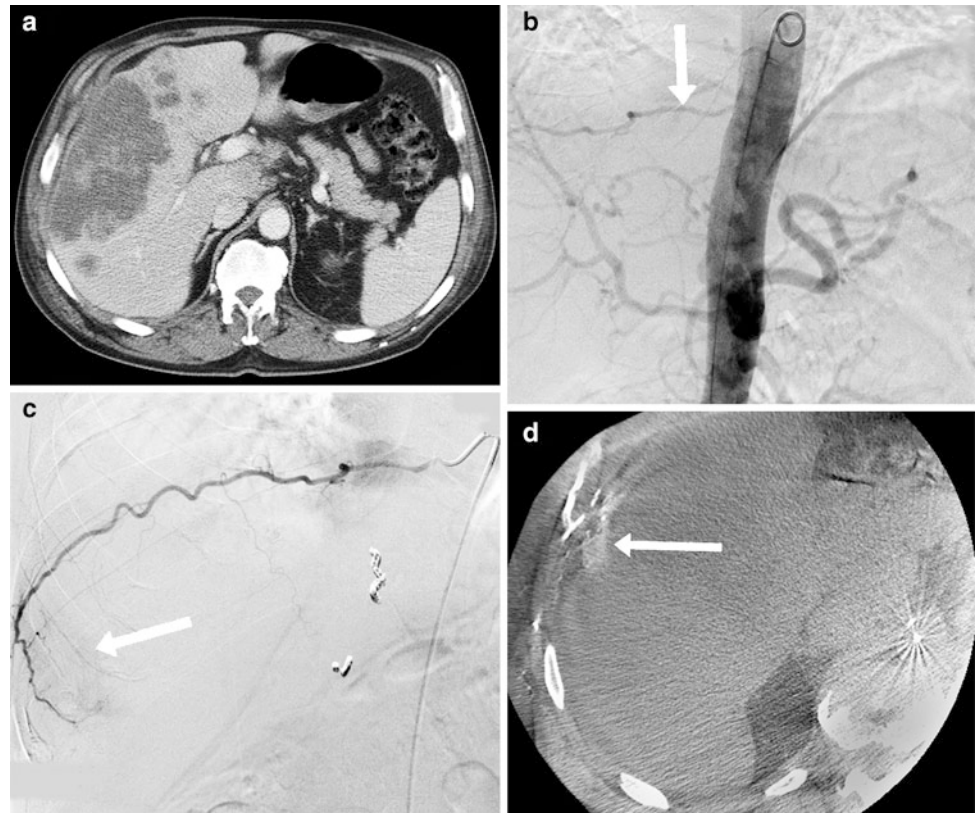
Michels type	Description	Incidence <sup>a</sup> (%)
I	Standard anatomy with right hepatic, middle hepatic, and left hepatic arising from the celiac axis	55
II	Replaced left hepatic from left gastric artery	11
III	Replaced right hepatic from superior mesenteric artery	10
IV	Replaced right hepatic from superior mesenteric artery; replaced left hepatic from the left gastric artery; middle hepatic from celiac artery	1
V	Accessory left hepatic from left gastric artery	8
VI	Accessory right hepatic from superior mesenteric artery	7
VII	Accessory right hepatic from superior mesenteric artery; accessory left hepatic from left gastric artery	1
VIII	Combination of replaced right hepatic with accessory left hepatic OR accessory right hepatic with replaced left hepatic	2
IX	Common hepatic from superior mesenteric artery	2.5
X	Common hepatic from the left gastric artery	<1

<sup>a</sup> Denotes incidence in Michels' study of 200 cadavers

middle hepatic artery, or segment IV could originate from the LHA. Although this configuration was called “standard” or “normal,” it was only found in 55 % of subjects. Other common variants included a replaced left hepatic artery (rLHA) arising from the left gastric artery seen in 11 % of patients (Fig. 1), a replaced right hepatic artery (rRHA) arising from the superior mesenteric artery (SMA) seen in 10 % of patients, and an accessory left hepatic artery (aLHA) arising from the LGA seen in 8 % of patients. Table 1 shows a complete list of anatomic variants according to the Michels classifications.

A study evaluating 600 patients that had undergone angiography showed a similar distribution of patients with variant hepatic arterial anatomy (Covey et al. 2002). Standard anatomy was seen in 61.3 % of patients. The most common variant was an aLHA arising from the LGA in 10.7 % of patients, and an rRHA from the SMA in 8.7 % of patients. In addition, several other variants were present that were not mentioned in Michels' study, including an origin of the CHA directly from the aorta, and a “double hepatic” artery where one or both of the left and right hepatic arteries arose directly from the aorta or from the celiac artery. These

**Fig. 2** 63-year-old male with cholangiocarcinoma undergoing radioembolization preparatory angiogram. **a** Pre-procedure CT scan showed a large tumor along the anterolateral margin of the right lobe of the liver, **b** Aortogram showed a hypertrophied right T9 intercostal artery (*white arrow*), **c** Selective angiography of T9 showed tumor blush (*white arrow*), **d** CACT on selective injection of the right T9 intercostal artery confirmed tumor enhancement (*white arrow*). To deliver radioactive microspheres to this territory, the parasitized intercostal artery was pre-emptively bland embolized with large particles to re-establish intrahepatic perfusion from the hepatic artery



two studies demonstrate the wide variability that can occur with variant hepatic arterial anatomy.

The perihilar plexus includes arteries that provide a communicating arcade between the right and left hepatic arteries (Tohma et al. 2005). This arcade connects the segment IV branch or the main LHA with the main or anterior trunk of the RHA. Intrahepatic communications between segments also exist, and provide collateral flow when branch hepatic arteries are occluded or compromised. These interlobar and intersegmental communicating branches were described several decades ago during studies of patients after hepatic arterial ligation for trauma or tumor treatment. Proximal interruption of any major hepatic artery, such as the RHA or LHA, results in near immediate filling via cross collaterals of the occluded branch (Charnsangavej et al. 1982; Mays and Wheeler 1974). This property was successfully exploited over 30 years ago in consolidation of flow for intra-arterial chemotherapy (Chuang and Wallace 1980). Familiarity with and evaluation of these arcades are important in expanding options concerning catheter placement for radioembolization.

Michels also recognized the importance of extrahepatic blood supply to the liver. He categorized 16 different routes, apart from the hepatic arterial variants, from which blood could supply parts of the liver (Michels 1966). The extrahepatic branches described included inferior phrenic,

internal mammary, and intercostal arteries (Fig. 2). Other studies have shown that tumors near the surface of the liver are more likely to recruit extrahepatic blood supply, which become particularly evident when there has been compromise of normal intrahepatic arteries, for instance, from intra-arterial therapies (Seki et al. 1998). Parasitized extrahepatic arteries frequently supply tumors at the bare area of the liver, even prior to any treatment, and are a cause of recurrence after chemoembolization of intrahepatic supplying branches (Miyayama et al. 2010). Therefore, these potential routes require close attention and appropriate recognition in the evaluation of radioembolization patients, since unmanaged they can lead to incomplete treatment and recurrence after treatment.

Special attention should be paid to several suspect vessels that are the most common parasitized extrahepatic arterial sources of tumor supply, which can be found in about 18 % of untreated patients. The most common is the right inferior phrenic artery, which one study found to be the supply in almost half of all patients where an extrahepatic source was found (Chung et al. 2006). The same study found that greater omental arteries were the extrahepatic source in 15.6 % of cases, with cystic, adrenal, and intercostal arteries accounting for 5.4–8.8 % each. Much less frequent were left and right gastric, right and left internal mammary, renal or renal capsular, superior mesenteric, left inferior phrenic, and pancreaticoduodenal arteries.



**Fig. 3** 74-year-old male with rectal cancer metastatic to the liver undergoing radioembolization preparatory angiogram. **a** Pre-procedure CT scan showed bilobar metastases including in segment 4 (*white arrow*), **b** Aortogram showed a replaced right hepatic artery (*white arrow*), accessory left hepatic artery (*black arrow*), and a segment 4 artery arising off the proper hepatic artery (*white arrowhead*),

**c** Selective angiography of the celiac artery confirmed the accessory left hepatic artery (*white arrow*), **d** Common hepatic arteriogram better demonstrated the segment 4 artery arising off the proper hepatic artery (*white arrow*). In this instance, embolization of the segment 4 artery could be performed to consolidate flow to the replaced right and left hepatic arteries in order to reduce the number of treatment sites

For optimum treatment—complete treatment of all intrahepatic tumors and avoidance of intra and extrahepatic non-target embolization—hepatic arterial variants, and parasitized extrahepatic vessels need to be addressed during planning of radioembolization.

## 2 Redistribution and Consolidation of Hepatic Arterial Flow

### 2.1 Redistribution

Intrahepatic collateral vessels can supply arterial flow to tumors across segments or lobes. Selective embolization of intrahepatic branches to redistribute intrahepatic flow patterns to the tumors has been shown to be effective and safe (Karunanithy et al. 2011; Bilbao et al. 2010). During evaluation of intrahepatic arterial tumor supply, multiple feeding vessels may be identified, often in close proximity to hepatico-enteric or hepatico-splanchnic vessels. Although, pre-emptive coil embolization of the hepatico-

enteric vessels imparts a high degree of safety, some vessels may be too small or angulated to allow this skeletonization. Embolizing one or more intrahepatic feeding branches can reduce the number of sites of administration of radioactive microspheres, and can facilitate administration distal to recognized hepatico-enteric vessels. For instance, a disadvantageous segment IV artery with small ductal artery branches can be coil embolized so that arterial supply to that segment is taken over by branches of the LHA or RHA or both (Fig. 3). Alternatively, coil embolization of a segment VIII artery supplying the lateral edge of a left lobe tumor can reduce treatment to only the LHA, sparing the remainder of the right lobe.

In a study of 24 patients, 11 of whom had Michels Type I anatomy, single photon emission computed tomography (SPECT) combined with computed tomography (CT) performed after administration of technetium macroaggregated albumin ( $^{99m}\text{Tc}$ -MAA) showed uptake in the redistributed areas in all 11 Michels Type I patients (Bilbao et al. 2010). Branches embolized include segment IV, segment VIII, and LHA. In a separate study, 11 patients underwent



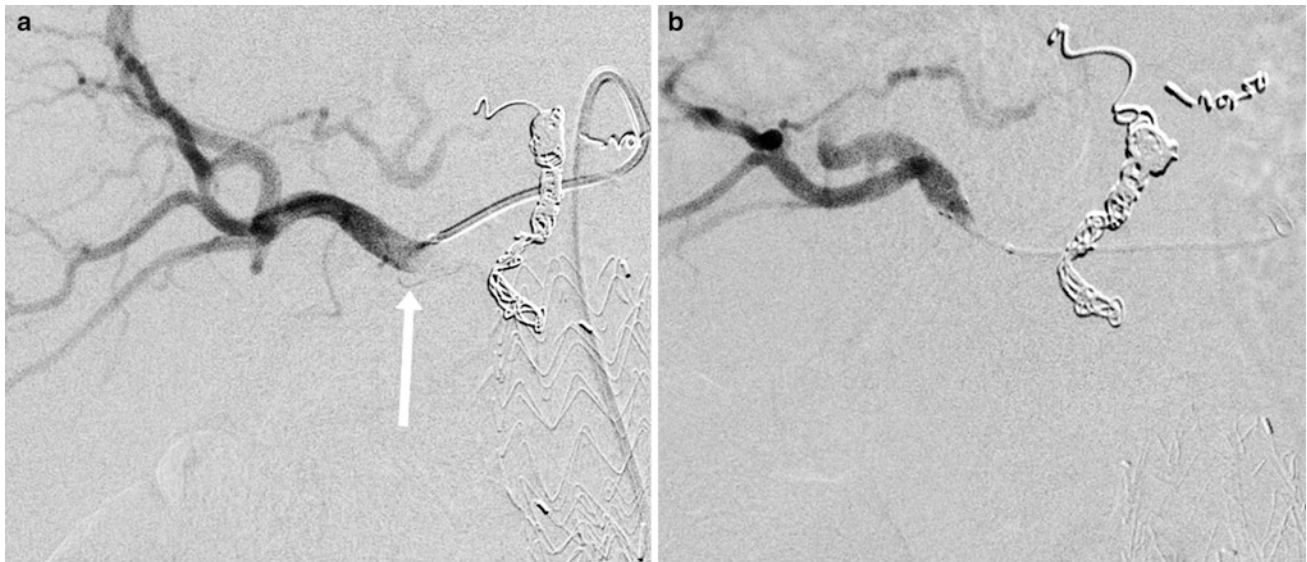


**Fig. 4** 69-year-old male with colorectal cancer metastatic to the liver undergoing radioembolization treatment. **a** Angiography of a replaced right hepatic artery arising from the SMA revealed small proximal branches supplying duodenum (*white arrow*), **b** Because of the multiplicity, small sizes, and acute angulations, the arteries could not

be coil embolized and a reflux protection device (Surefire Medical Inc., Westminster, CO) was used to reduce the risk of radioembolic bead delivery to the bowel. A great deal of biological variability is found in the enteric branching patterns of replaced and accessory right hepatic arteries

embolization of the anterior division RHA, RHA, segment IV, or LHA to redistribute flow for administration of radioactive microspheres (Karunanithy et al. 2011). Post-treatment PET showed a statistically significant decrease in standardized uptake values (SUV). These studies demonstrate that embolization of intrahepatic branches from either the left lobe or right lobe can successfully redistribute flow to simplify and increase the safety of treatment. It is important to note that both studies performed embolization with coils only. More distal embolization using particles would lodge in the tumor at the arteriolar level (Lee et al. 2008). This could theoretically prevent radioactive microspheres from reaching the tumor.

## 2.2 Consolidation

A similar technique for management of variant hepatic arteries can be used. The goal of consolidation is to create a simpler and safer arterial anatomy for the administration of radioactive microspheres. Since many variant hepatic arteries arise off of branches that also supply the gastrointestinal tract, non-target radioembolization is an increased risk (Riaz et al. 2009). For instance, administration in the rLHA or aLHA originating from the LGA can result in reflux into esophageal and gastric branches just proximal to the course of the variant artery in the fissure of the ligamentum venosum. Likewise, the rRHA or aRHA frequently gives off small branches to the duodenum, and arises from the main SMA, which supplies nearly the entire bowel

(Fig. 4). One early study on radioembolization safety consolidated variant hepatic arteries with resultant reconstitution of flow by intrahepatic collaterals and is important because it demonstrated that consolidation is able to limit toxicity, although treatment efficacy was not fully assessed (Andrews et al. 1994). Consolidation by coil embolization of variant or redundant arteries provides a way to achieve distribution of microspheres to the targeted tumors while minimizing non-target deposition complication risk to the patient.

In evaluating for any evidence of variant anatomy, all prior cross-sectional imaging, either contrast enhanced computed tomography (CT) or magnetic resonance (MR) imaging, should be closely studied. Thin-section arterial phase breath-held imaging is the most useful, if available, and coronal and sagittal reformatted images may help to confirm existence, origin, and course of variant vessels. Identified anatomic variants should be compared to the intrahepatic tumor distribution to predict dominant arterial supply to the targeted regions. Scrutiny of cross-sectional imaging will guide and possibly even expedite the preparatory angiography prior to radioembolization treatment.

During preparatory phase angiography, abdominal aortography is performed with injection of contrast medium at up to 15 cc/sec for 30 cc with the flush catheter at the level of mid to lower thorax (T7–T9) to identify variant hepatic and parasitized extrahepatic arteries, including those too small to be detected by CT or MRI, and to establish a baseline for future comparison. Next, all arteries of interest including normal and variant and parasitized vessels should

**Fig. 5** 65-year-old male with hepatocellular carcinoma undergoing radioembolization preparatory angiogram. **a** Pre-procedure coronal reconstruction of venous phase CT scan showed a large tumor abutting the dome of the liver (*white arrow*), **b** CACT on injection of the common hepatic artery after skeletonization showed an area of unenhanced liver (*white arrow*) at the dome, **c** Selective angiography of the right internal mammary artery confirmed supply of a small portion of the tumor at the dome (*white arrow*), fed by a pericardiophrenic branch, **d** CACT of the right internal mammary artery showed enhancement of the previously unenhanced liver (*white arrow*). Because of the area of unenhanced liver, a search was made for extrahepatic arterial supply and the right internal mammary artery was identified as the parasitized vessel. This branch was bland embolized to re-establish intrahepatic perfusion to this area



undergo catheter selection and selective digital subtraction angiography (DSA). When available, C-arm cone beam CT (CACT) should also be performed for volumetric definition of subtended arterial territory. If no variant or parasitized arteries are identified, DSA and CACT should be performed while injecting contrast medium into the PHA or CHA. If any territories and especially if any tumors within the liver do not enhance, the search for additional arterial inflow should be renewed (Fig. 5). Selective catheterization and injection of the mesenteric vessels are performed as needed to confirm anatomy of the SMA, CHA, PHA, GDA, LHA, and RHA. Because of the high incidence of hepatofugal branches arising from the LHA, including the RGA, accessory LGA, left inferior phrenic artery, and falciform artery, some authors recommend power-injected angiography of each LHA (Lewandowski et al. 2007).

Once the anatomy is defined, skeletonization of the hepatic artery (elimination of hepatico-enteric or hepatico-splanchnic anastomoses) has become the standard of care (Lewandowski et al. 2007). In some cases, skeletonization of variant arteries may prove to be the safest and most effective option. For instance, coil embolization of gastroesophageal branches of an LGA may allow for safe administration into an rLHA when the other hepatic arterial inflow routes are even higher in risk. In other cases, high risk variant hepatic arteries may undergo coil embolization

to consolidate the hepatic artery inflow into simpler or safer anatomy (Fig. 6). CACT and DSA should be performed through selective injection of the variant hepatic arteries to identify the hepatic territory and any tumors supplied. The variant hepatic artery may be embolized with 0.018'' or 0.035'' coils, or with a vascular plug if large enough in size (Fig. 7). Because of the pre-existing communicating arcades, the remaining hepatic arterial inflow routes will assume the arterial supply to the tumors. In cases, where there is doubt regarding the adequacy of the communicating arcades, for instance in the post-resection or post-ablation liver, a test balloon-occlusion can be performed from an additional arterial access site.

In certain cases, the variant hepatic artery provides the dominant supply to the tumor(s). Coil embolization of the variant artery may introduce too much uncertainty and dependence on intrahepatic arcades for adequate delivery of microspheres to the tumors. In these situations, the conventional hepatic artery may be embolized instead. The intrahepatic arcades are arterial and thus without valves, so flow may course in either direction. As a result, the supply is consolidated to the variant hepatic artery, and administration of radioactive microspheres only needs to be performed here. The safety of this approach depends on being able to skeletonize the variant artery adequately.



**Fig. 6** 62-year-old male with colonic adenocarcinoma metastatic to the liver undergoing radioembolization preparatory angiogram. **a** Pre-procedure CT scan showed large tumor burden in both the right and left lobe, **b** Angiography demonstrated a replaced left hepatic artery off the left gastric artery (*white arrow*), which was coil embolized (*black arrow*), **c** Selective angiography of the common hepatic artery prior to left hepatic embolization showed a segment 4 branch and right hepatic without a left hepatic artery, **d** Angiogram of the common hepatic artery after embolization of the replaced left hepatic showed filling of the left lobe through intrahepatic anastomoses with the segment 4 branch. This simplified treatment and increased patient safety by eliminating an additional treatment from the replaced left hepatic

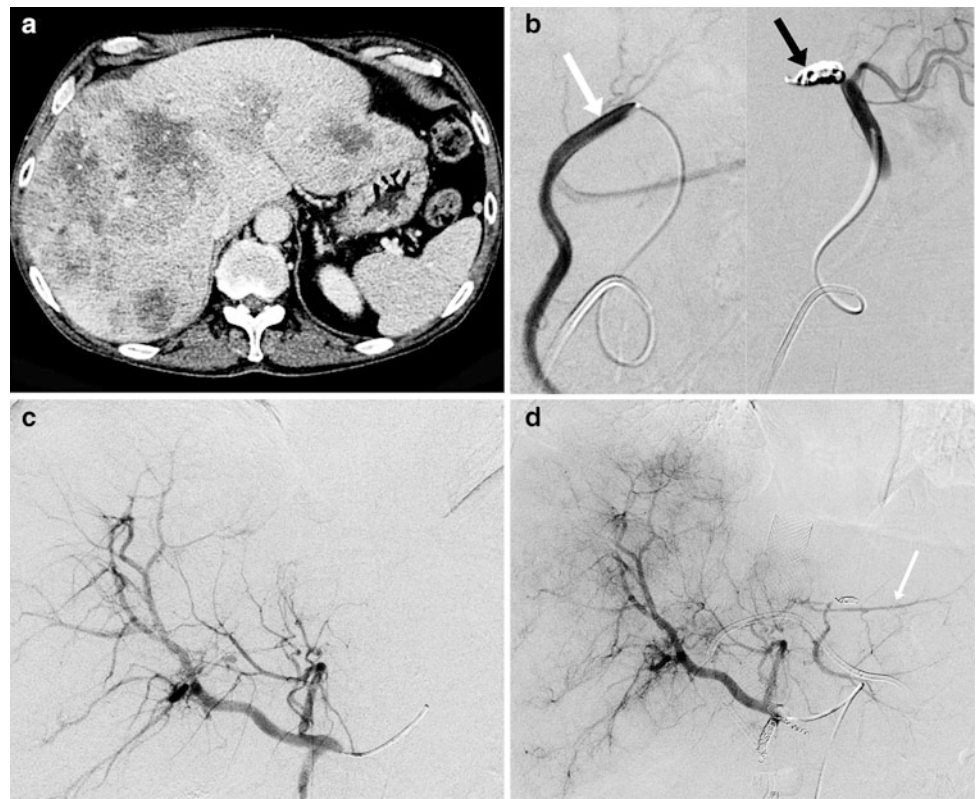
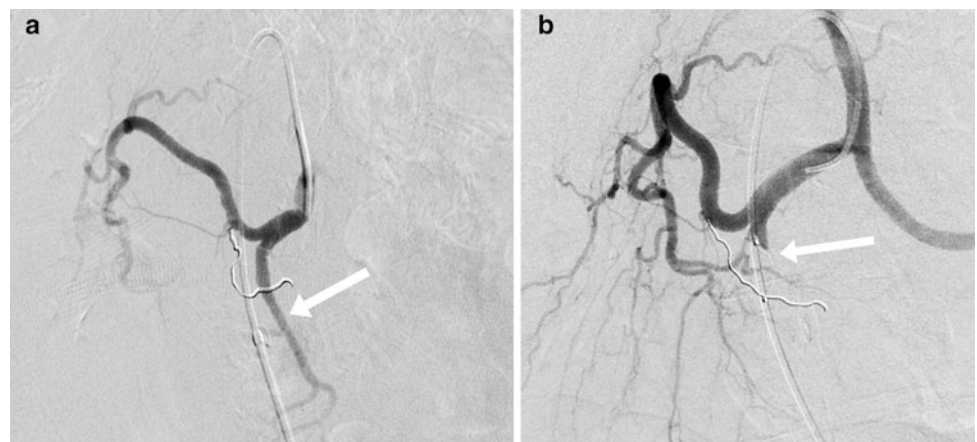


**Fig. 7** 72-year-old female with metastatic oropharyngeal squamous cell cancer to the liver undergoing radioembolization preparatory angiogram. **a** Common hepatic artery angiogram after coil embolization of the RGA showed a patent gastroduodenal artery requiring embolization for treatment of the left lobe (*white arrow*). This patient had a replaced right hepatic artery, **b** Embolization of the GDA was performed using an Amplatzer 4 (St. Jude Medical, St. Paul, MN) vascular plug (*white arrow*)

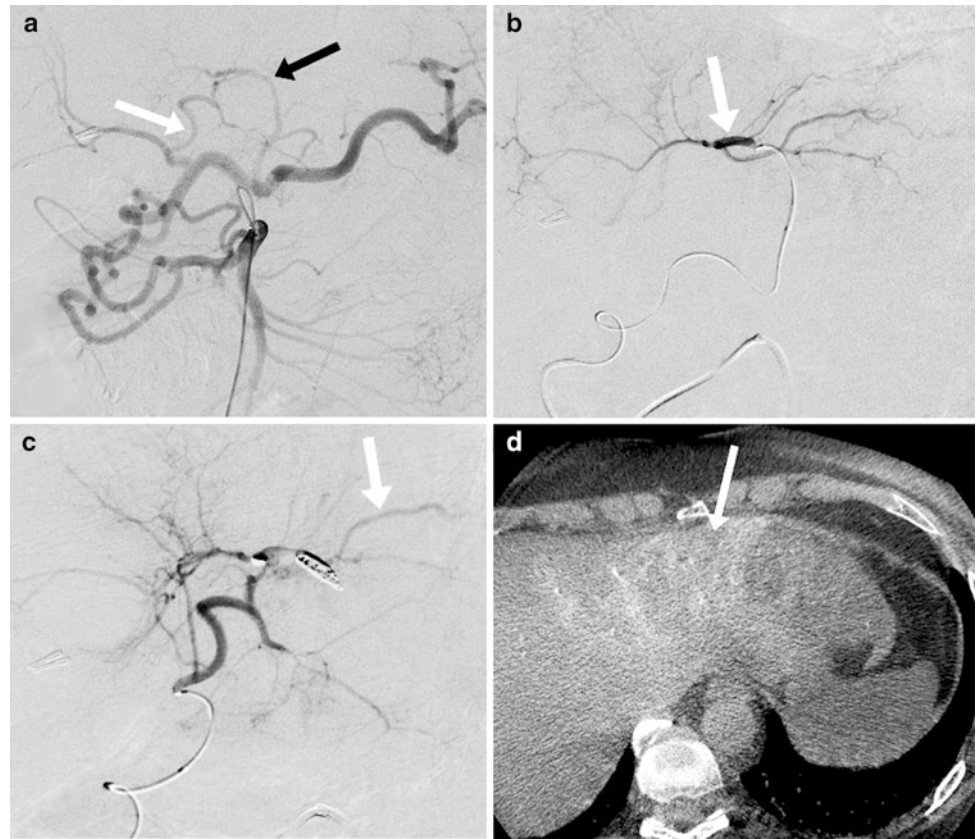


Once consolidative embolization is completed, repeated DSA and CACT should be performed with injection of contrast medium at the planned site of microsphere administration to confirm arterial perfusion of territories previously supplied by the embolized branches (Fig. 8). Discordance can sometimes be observed with slower or weaker contrast enhancement because collateral channels may need time to mature, and such observations should be factored into scheduling of subsequent microsphere administration (Abdelmaksoud et al. 2011). Contrast medium molecules are approximately 4–5 orders of magnitude

smaller than radioactive microspheres, so the ability of contrast medium to traverse intrahepatic collateral networks does not guarantee the ready passage of microspheres. As another confirmatory test,  $^{99m}\text{Tc}$ -MAA ranging in size from 10 to 100 microns is injected at the intended site of microsphere administration and SPECT is performed to model future intrahepatic distribution of microspheres, as well as to calculate the lung shunt fraction according to previously described methods (Lewandowski et al. 2007).

Immediately prior to administration of microspheres, DSA and CACT should be repeated to confirm complete

**Fig. 8** 55-year-old female with gallbladder adenocarcinoma metastatic to the liver undergoing radioembolization preparatory angiogram. **a** Superior mesenteric artery angiogram showed cross-filling of the celiac artery with a left hepatic artery supplying segment 3 (*white arrow*) and an accessory left hepatic artery from the left gastric artery supplying segment 2 (*black arrow*). The patient had a celiac artery occlusion, **b** Accessory left hepatic artery angiogram showed segment 2 and segment 4a supply (*white arrow*), **c** After coil embolization of the aLHA, angiogram through the left hepatic artery showed reconstitution of the segment 2 and 4a branches (*white arrow*), **d** CACT performed on injection of the left hepatic after embolization of the aLHA showed enhancement of all of segments 2 and 4a



perfusion of targeted territories and tumors after redistribution or consolidation. Tumors and regions that do not have adequate perfusion from the intended site of administration may be eligible for additional consolidative embolization. However, redistributive and consolidative embolizations are not reversible.

Consolidation is not indicated in all patients with variant hepatic arterial anatomy. Redistribution and consolidation should only be performed if coil embolization of branch hepatic arteries results in fewer sites of administration, improves the selectivity or completeness of treatment, and/or reduces the risk of non-target radioactive microsphere administration. This most commonly involves patients with diffuse and multifocal disease, which typically requires treatment of the whole liver. The alternative is placement of multiple microcatheters, but this can be time consuming, requires setup of multiple vials, may increase the risk of spill or misadministration, increases radioactive waste, and may increase the complication risk to the patient. In the largest published series, only 59 % of patients with variant hepatic arterial anatomy were expected to benefit, and thus underwent consolidation (Abdelmaksoud et al. 2011). For instance, patients that did not require consolidation had segments supplied by variant anatomy free of tumor or had a solitary tumor fed by a single variant hepatic artery. The same study showed a 95.5 % success rate of adequate

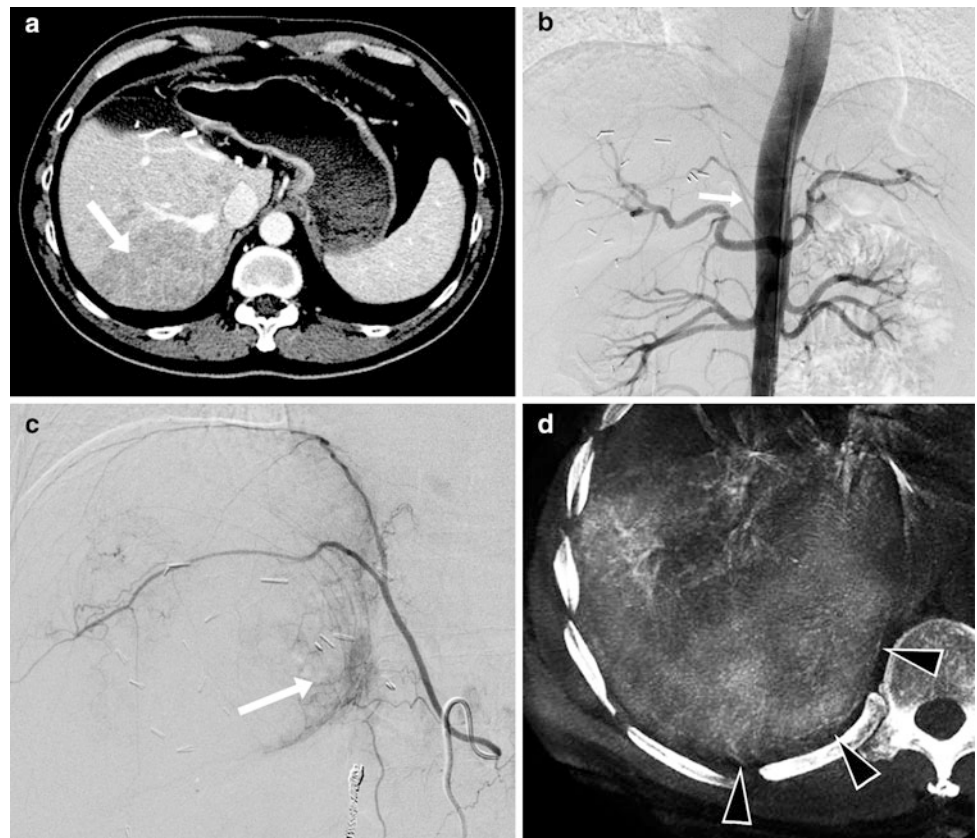
delivery of microspheres to consolidated regions previously supplied by variant arteries in patients who responded to radioembolization.

### 3 Extrahepatic Arterial Anatomy: Identification and Treatment

Parasitized extrahepatic arteries can be found in approximately 17 % of all patients undergoing initial chemoembolization (Chung et al. 2006) and 17 % of patients undergoing radioembolization (Abdelmaksoud et al. 2011). With both of these treatment options, failure to address parasitized extrahepatic vessels results in under treatment of tumors and residual disease (Kim et al. 2005). There is copious literature describing safe and effective chemoembolization delivered through parasitized extrahepatic arteries (Chung et al. 1998; Kim et al. 2007; Miyayama et al. 2001; Park et al. 2003), but the safety of administration of radioactive microspheres in these vessels has not been shown and in many cases would be expected to carry a very high risk. These vessels, though, can be addressed in a similar manner as with variant arteries, relying on intrahepatic collateral channels to assume hepatic arterial supply to tumors.



**Fig. 9** 46-year-old male with hepatocellular carcinoma undergoing radioembolization preparatory angiogram. **a** Pre-procedure CT showed a large mass in the posterior right hepatic lobe involving the bare area of the liver, **b** Aortogram showed a hypertrophied right inferior phrenic artery (*white arrow*), **c** Selective angiography of the right inferior phrenic artery showed tumor blush (*white arrow*), **d** CACT performed on injection of the common hepatic artery after large particle embolization of the right inferior phrenic artery showed enhancement of the entirety of the tumor (*black arrowheads*)



Parasitized extrahepatic arteries should be carefully screened on all diagnostic cross-sectional CT or MR imaging. Factors that should raise suspicion include tumor size over 5 cm, (Chung et al. 2006) tumors in contact with the bare area of the liver, (Miyayama et al. 2010) right border of the liver, or inferior border of the liver, and superficial tumors (Fig. 9) (Seki et al. 1998). Other risk factors include any prior therapies that may compromise the normal hepatic architecture, including surgical ligation of the hepatic artery, (Charnsangavej et al. 1982; Koehler et al. 1975) chemoembolization, (Chung et al. 2006) and prior hepatic arterial infusion pump placement (Seki et al. 1998). Again, thin-section arterial phase breath-held images yield the most useful information.

Angiography is again initiated with abdominal aortography with flush injection of the mid to lower thoracic aorta to identify any hypertrophied extrahepatic vessels which could supply tumor. The flush catheter is positioned cranially to opacify the intercostal arteries from T8 to T11, the most commonly affected levels. For tumors located anteriorly in the left lobe, additional thoracic angiography may need to be performed to interrogate the internal mammary arteries. In equivocal cases, DSA and CACT may be performed with injection of contrast medium into the CHA or PHA to search

for areas of the liver that do not enhance and are thus suspicious for supply from parasitized extrahepatic vessels.

If parasitized extrahepatic arteries are identified, they may be embolized using larger particles, generally the largest that can pass through the catheter or microcatheter being used. This may be as small as 300–500  $\mu\text{m}$  spherical embolics or as large as a slurry of 2 mm gelatin sponge cubes. In general, the largest particles that can fit through the catheter should be used to achieve the goal of elimination of parasitized supply while still allowing the tumor capillary bed to fill via intrahepatic collateral channels. Occlusion of parasitized vessels at the capillary level by smaller particles might have some therapeutic effect from ischemia, but would prevent distribution of radioactive microspheres to these areas, which would be expected to yield a superior outcome. Once stasis is achieved with large particles, coil embolization may be performed for more permanence if desired. Early in our experience, we observed that coil embolization alone of the parasitized vessels is not sufficient to effect intrahepatic flow redistribution, since recruitment of additional parasitized extrahepatic arteries frequently occurred (Abdelmaksoud et al. 2011). For instance, coil embolization of a parasitized intercostal artery usually resulted in immediate recruitment

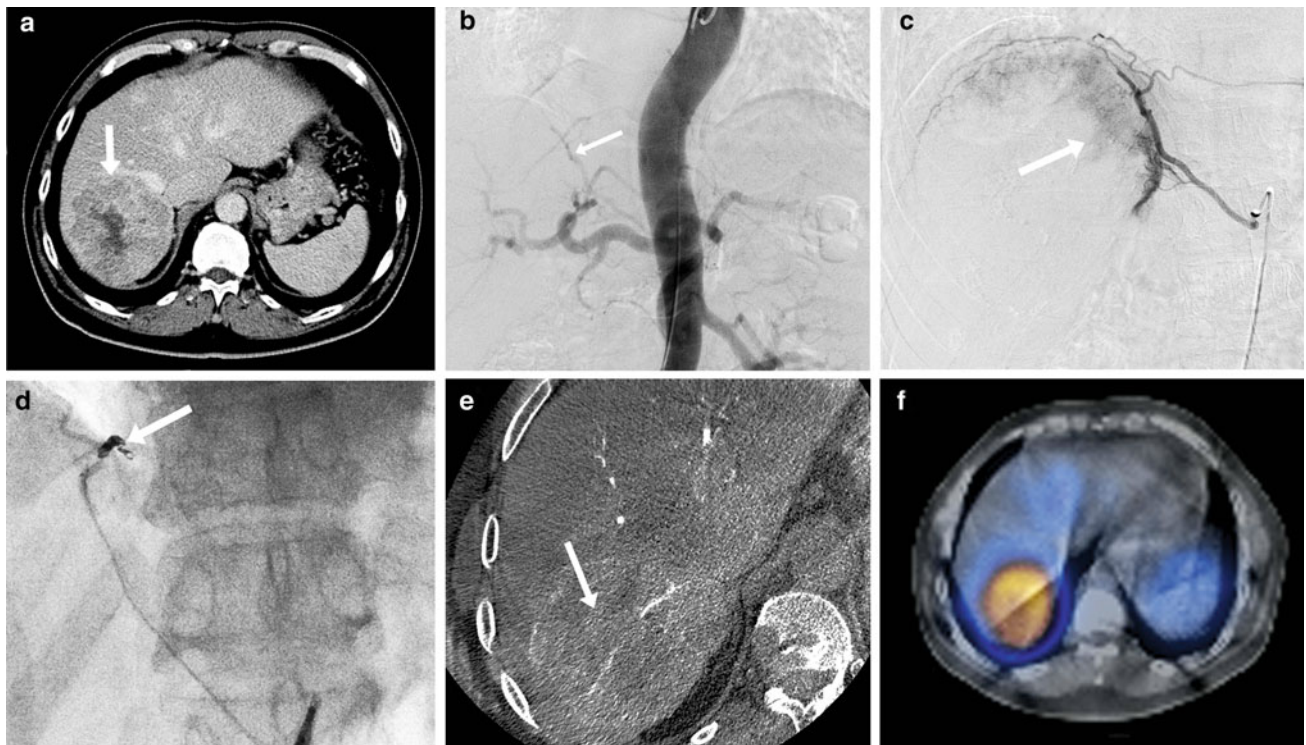


**Fig. 10** 57-year-old male with pancreatic neuroendocrine tumor metastatic to the liver undergoing radioembolization preparatory angiogram. **a** Pre-procedure CT scan showed a large metastasis in posterior right lobe of the liver (*white arrow*), **b** Aortogram showed a hypertrophied right inferior phrenic artery (*white arrow*), **c** Selective angiography of the right inferior phrenic artery showed tumor blush

and the left inferior phrenic artery (*white arrow*), **d** The left inferior phrenic artery was coil embolized (*white arrow*) to allow particle occlusion of the parasitized right inferior phrenic artery, **e** CACT on injection of the common hepatic artery showed enhancement of the entire tumor (*white arrow*), **f** Fused  $^{99m}\text{Tc}$ -MAA SPECT/CT confirms complete tumor coverage

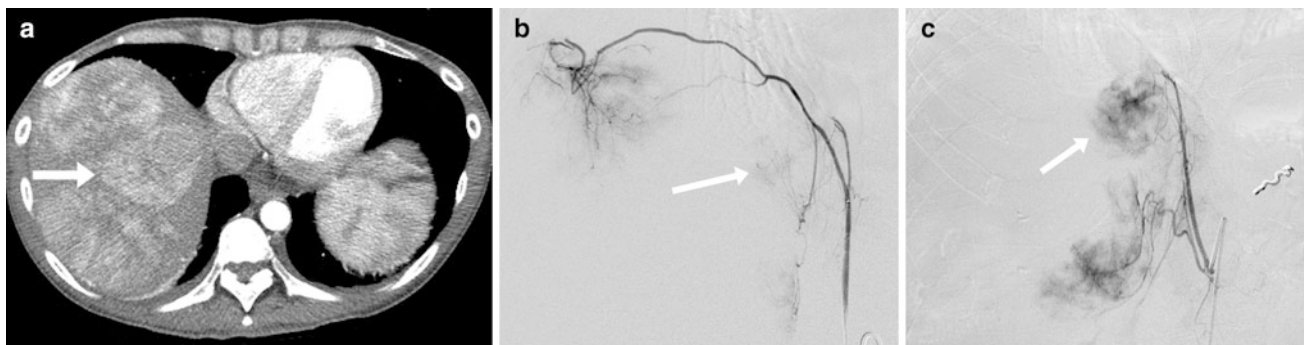


**Fig. 11** 39-year-old male with metastatic neuroendocrine tumor to the liver undergoing radioembolization. **a** Pre-procedure CT showed several large masses in the right hepatic lobe (*white arrow*), **b** Selective angiography of the right inferior phrenic artery showed tumor blush (*white arrow*). The patient underwent large particle embolization of

the right inferior phrenic artery to stasis and subsequent radioembolization of the left lobe, **c** The patient returned 1 month later for treatment of the right lobe and had new parasitized branches off the right inferior phrenic artery to the bare area (*white arrow*), although the dome area of parasitization remained occluded

of the intercostal arteries immediately adjacent, rather than recruitment of intrahepatic collateral supply.

If numerous side branches of a trunk are parasitized, the parent vessel distal to the origin of the parasitized branches can be coil embolized first. The side branches can then be embolized with particles without concern for non-target embolization and ischemia in the distal parent vessel

(Fig. 10). Once near stasis is achieved, the parent vessel may be coil embolized proximally as well. For instance, if numerous small pancreaticoduodenal arteries are parasitized, including some too small to select with a microcatheter, the right gastroepiploic artery may be first coil embolized. The pancreaticoduodenal arteries can then be embolized with particles from the proximal GDA, without

significant risk of non-target embolization of the stomach. Coil embolization alone of the GDA without particle embolization could result in additional recruitment of parasitized flow via the supraduodenal and inferior pancreaticoduodenal arteries.

Upon particle embolization of the parasitized vessel, repeated DSA and CACT should be performed on the CHA or PHA to confirm that intrahepatic reperfusion of the tumor has occurred. Similar to simulation after redistributive or consolidative embolization, scintigraphy and SPECT after  $^{99m}\text{Tc}$ -MAA injection should be performed for additional confirmation of intrahepatic reperfusion (Fig. 10).

Since tumors that have previously parasitized extrahepatic blood flow are likely to be at persistent, increased tendency to recruit additional vessels, repeat abdominal aortography should be performed to assess for development of new parasitized extrahepatic arteries at the time of radioactive microsphere administration (Fig. 11). In addition, contrast enhanced DSA and CACT with injection of contrast medium at the intended site of microsphere administration should be performed to confirm complete tumor coverage via an intrahepatic route. When additional parasitized extrahepatic vessels are found, they can be managed in the same way as during the preparatory angiogram.

As with chemoembolization, failure to address parasitized extrahepatic vessels can result in under treatment of tumors, but unlike chemoembolization, administration of radioactive microspheres into the intercostal, phrenic, internal mammary, omental, pancreaticoduodenal, adrenal, and colic arteries could be expected to cause substantial toxicity (Kim et al. 2005). Pre-emptive embolization of these parasitized vessels to re-establish intrahepatic supply is an effective alternative. 94.1 % of patients with parasitized extrahepatic arteries who were treated by particle and coil embolization to redistribute intrahepatic flow and had evaluable disease on imaging follow-up showed uniform partial response or stable disease. The tumors previously supplied by parasitized extrahepatic vessels responded equivalently to those supplied by native hepatic arteries, suggesting that the intrahepatic collateral vessels were capable of carrying microspheres to the targeted tumors. No patients showed evidence of non-target radioembolization (Abdelmaksoud et al. 2011).

## 4 Conclusion

Variant hepatic arterial anatomy and parasitized extrahepatic arteries can provide challenges for adequate treatment of intrahepatic tumors by radioembolization. Application of redistribution and consolidation techniques to simplify and to increase safety of treatment can be an effective way to

manage these situations. Coil embolization of accessory vessels and particle embolization of parasitized extrahepatic arteries can be employed to redistribute tumor perfusion to be solely from easy to treat intrahepatic branches. Use of these strategies can help to maximize complete radioactive microsphere distribution to the entirety of the tumors, and to minimize the risk of accidental extrahepatic deposition.

## References

- Abdelmaksoud MHK, Louie JD, Kothary N et al (2011) Consolidation of hepatic arterial inflow by embolization of variant hepatic arteries in preparation for yttrium-90 radioembolization. *J Vasc Interv Radiol* 22(10):1364–1372
- Abdelmaksoud MHK, Louie JD, Kothary N et al (2011) Embolization of parasitized extrahepatic arteries to reestablish intrahepatic arterial supply to tumors before yttrium-90 radioembolization. *J Vasc Interv Radiol* 22(10):1355–1362
- Andrews JC, Walker SC, Ackermann RJ, Cotton LA, Ensminger WD, Shapiro B (1994) Hepatic radioembolization with y-90 containing glass microspheres-preliminary-results and clinical follow-up. *J Nucl Med* 35(10):1637–1644
- Bilbao JI, Garrastachu P, Herraiz MJ et al (2010) Safety and efficacy assessment of flow redistribution by occlusion of intrahepatic vessels prior to radioembolization in the treatment of liver tumors. *Cardiovasc Interv Radiol* 33(3):523–531
- Charnsangavej C, Chuang VP, Wallace S, Soo CS, Bowers T (1982) Angiographic classification of hepatic arterial collaterals. *Radiology* 144(3):485–494
- Chuang VP, Wallace S (1980) Hepatic arterial redistribution for intra-arterial infusion of hepatic neoplasms. *Radiology* 135(2):295–299
- Chung JW, Park JH, Han JK, Choi BI, Kim TK, Han MC (1998) Transcatheter oily chemoembolization of the inferior phrenic artery in hepatocellular carcinoma: the safety and potential therapeutic role. *J Vasc Interv Radiol* 9(3):495–500
- Chung JW, Kim HC, Yoon JH et al (2006) Transcatheter arterial chemoembolization of hepatocellular carcinoma: prevalence and causative factors of extrahepatic collateral arteries in 479 patients. *Korean J Radiol* 7(4):257–266
- Covey AM, Brody LA, Maluccio MA, Getrajdman GI, Brown KT (2002) Variant hepatic arterial anatomy revisited: digital subtraction angiography performed in 600 patients. *Radiology* 224(2):542–547
- Karunanithy N, Gordon F, Hodolic M et al (2011) Embolization of hepatic arterial branches to simplify hepatic blood flow before yttrium 90 radioembolization: a useful technique in the presence of challenging anatomy. *Cardiovasc Interv Radiol* 34(2):287–294
- Kim HC, Chung JW, Lee W, Jae HJ, Park JH (2005) Recognizing extrahepatic collateral vessels that supply hepatocellular carcinoma to avoid complications of transcatheter arterial chemoembolization. *Radiographics* 25:S25–S40
- Kim HC, Chung JW, Choi SH, et al (2007) Hepatocellular carcinoma with internal mammary artery supply: feasibility and efficacy of transarterial chemoembolization and factors affecting patient prognosis. *J Vasc Interv Radiol* 18(5):611–619 (quiz 620)
- Koehler RE, Korobkin M, Lewis F (1975) Arteriographic demonstration of collateral arterial supply to liver after hepatic-artery ligation. *Radiology* 117(1):49–54
- Lee KH, Liapi E, Vossen JA et al (2008) Distribution of iron oxide-containing embosphere particles after transcatheter arterial embolization in an animal model of liver cancer: evaluation with MR



- imaging and implication for therapy. *J Vasc Interv Radiol* 19(10):1490–1496
- Lewandowski RJ, Sato KT, Atassi B et al (2007) Radioembolization with <sup>90</sup>Y microspheres: angiographic and technical considerations. *Cardiovasc Interv Radiol* 30(4):571–592
- Mays ET, Wheeler CS (1974) Demonstration of collateral arterial flow after interruption of hepatic arteries in man. *N Engl J Med* 290(18):993–996
- Michels NA (1966) Newer anatomy of liver and its variant blood supply and collateral circulation. *Am J Surg* 112(3):337–347
- Miyayama S, Matsui O, Akakura Y et al (2001) Hepatocellular carcinoma with blood supply from omental branches: treatment with transcatheter arterial embolization. *J Vasc Interv Radiol* 12(11):1285–1290
- Miyayama S, Yamashiro M, Okuda M et al (2010) The march of extrahepatic collaterals: analysis of blood supply to hepatocellular carcinoma located in the bare area of the liver after chemoembolization. *Cardiovasc Interv Radiol* 33(3):513–522
- Park SI, Yun Lee D, Yoon Won J, Tae Lee J (2003) Extrahepatic collateral supply of hepatocellular carcinoma by the intercostal arteries. *J Vasc Interv Radiol* 14(4):461–468
- Riaz A, Lewandowski RJ, Kulik LM, et al (2009) Complications following radioembolization with yttrium-90 microspheres: a comprehensive literature review. *J Vasc Interv Radiol* 20(9):1121–1130 (quiz 1131)
- Seki H, Kimura M, Yoshimura N, Yamamoto S, Ozaki T, Sakai K (1998) Development of extrahepatic arterial blood supply to the liver during hepatic arterial infusion chemotherapy. *Eur Radiol* 8(9):1613–1618
- Tohma T, Cho A, Okazumi S et al (2005) Communicating arcade between the right and left hepatic arteries: evaluation with CT and angiography during temporary balloon occlusion of the right or left hepatic artery. *Radiology* 237(1):361–365

---

# Dosimetry and Dose Calculation

Andrew S. Kennedy, William A. Dezarn, Patrick McNeillie,  
and Bruno Sangro

## Contents

<b>1</b>	<b>Introduction</b> .....	53
<b>2</b>	<b>Liver Tolerance to Ionizing Radiation</b> .....	54
<b>3</b>	<b>Human Microsphere Dose Studies</b> .....	54
<b>4</b>	<b>Selection of <sup>90</sup>Y Activity</b> .....	55
4.1	Therapeutic Isotope .....	55
4.2	Glass Microspheres.....	55
4.3	Resin Microspheres .....	56
4.4	Empiric Method.....	57
4.5	Body Surface Area Method .....	57
4.6	Partition Method.....	58
<b>5</b>	<b>Selection of <sup>90</sup>Y Activity in Resin Microsphere Therapy</b> .....	58
<b>6</b>	<b>Conclusions</b> .....	59
	<b>References</b> .....	59

---

## Abstract

The selection of the optimal activity of <sup>90</sup>Y for implantation for an individual patient requires understanding of the strengths and potential weaknesses of various calculation methods. Details of each methods origin and derivation are presented with inclusion of the most recent consensus recommendations on which approach is best used for primary and metastatic malignancies of the liver.

---

A. S. Kennedy (✉)  
Radiation Oncology, Sarah Cannon,  
Radiation Oncology Research, Sarah Cannon Research Institute,  
3322 West End Avenue, Suite 800, Nashville,  
TN 37203, USA  
e-mail: andrew.kennedy@sarahcannon.com

A. S. Kennedy  
Department of Biomedical Engineering,  
Department of Mechanical and Aerospace Engineering,  
North Carolina State University, Raleigh, NC, USA

W. A. Dezarn  
Siloam, NC, USA

P. McNeillie  
University of North Carolina, Chapel Hill, NC, USA

P. McNeillie  
School of Medicine, Chapel Hill, NC, USA

B. Sangro  
Liver Unit, Clinica Universidad de Navarra, Pamplona, Spain

B. Sangro  
Universidad de Navarra, Pamplona, Spain

B. Sangro  
Centro de Investigacion Biomedica en Red de Enfermedades,  
Hepaticas y Digestivas (CIBEREHD), Pamplona, Spain

---

## 1 Introduction

Two components relate to the topic of *dosimetry* in microsphere therapy. *Dose* (Gy) is specifically defined as that energy absorbed in tissue; and *activity* (GBq) of Yttrium-90 (<sup>90</sup>Y) is the amount of isotope delivered to the target organ. Classically, dosimetry is a Radiation Oncology term for the estimation of the absorbed dose expressed in units of Gy of radiation in tissue that will be or has been delivered. For microsphere treatment, it is more appropriate to describe an *activity* of radiation that will be implanted into the liver tumors, as there is not yet a proven way of preplan or post-plan confirmation of the absorbed dose in the target tissue. In other brachytherapy sites, seeds measuring several millimeters in size can be readily identified on CT scan or plain film and the resultant absorbed dose in the tissue calculated by hand or software solution. Microsphere implantation is a hybrid of interstitial brachytherapy and radioactive liquid therapy which at the present time is more accurately characterized by Nuclear Medicine conventions (Medical Internal Radiation Dose (MIRD) Committee of the Society of Nuclear Medicine (Toohey et al. 2000) MIRD

(Gulec et al. 2006a; Stabin 2006; Stabin and Konijnenberg 2000; Stabin and Siegel 2003) and Partition Model (Sarfaraz et al. 2003, 2004) than current or historical brachytherapy dose calculation methods (Patterson Parker, Point Source, and Volume Implant Rules).

The selection of an activity of ( $^{90}\text{Y}$ ) to deliver into the liver is a critical but imperfect task that requires experience and knowledge of many factors. Paramount among these factors is an understanding of liver health and reserve. This is difficult to know and is often unknown as the long-term effects of newer chemotherapy agents (oxaliplatin, irinotecan, gemcitabine, etc.) on the liver parenchyma are not yet documented and in the short term have caused liver fibrosis and cirrhosis. Unfortunately no single laboratory test is a valid measure of liver health. Surrogates include non-specific liver enzymes, transaminases and bilirubin levels. The liver's complex and varied functions are a challenge for treatment teams as they attempt to assess the risk of acute and permanent liver injury and determine the suitability of an individual patient for microsphere therapy. Clinical experience in non-radioactive arterial-based particle therapy has established patient selection criteria that protect against treatment of livers where serious and sometimes fatal liver dysfunction is likely to result. Although these guidelines are a helpful starting point for radioembolization, they represent in some ways, a more stringent standard based on the particle size, flow pattern, deposition properties and effect on hepatic neovascularization compared to what we now know can be the case for the much smaller radioactive microspheres. In short, patients that are not candidates for either transarterial chemoembolization (TACE) or bland embolization (TAE) but *are* able to safely receive radioembolization can enjoy excellent outcomes. Moreover it is essential that radioembolization research teams continue the development of clinically proven guidelines for radiation activity and patient selection. This section will discuss the selection of  $^{90}\text{Y}$  activity and what is known about microsphere dosimetry at the level of the hepatic lobule where microspheres become permanently embedded.

---

## 2 Liver Tolerance to Ionizing Radiation

Nearly all the experimental and clinical data to date has been using external beam radiation. Furthermore, animal models are not good surrogates for human hepatic radiation response. Whole liver radiation by external beam causes radiation induced liver disease (RILD) in 5–10 % of patients (Dawson 2005; Dawson and Lawrence 2004; Dawson and Ten Haken 2005). RILD is a clinical syndrome of anicteric hepatomegaly, ascites, and elevated liver enzymes (especially alkaline phosphatase) which occurs usually from 2 weeks up to 90 days post radiation delivery

and can lead to permanent, progressive and/or fatal liver dysfunction (Fajardo et al. 2001; Fajardo and Colby 1980).

Studies of external beam radiotherapy liver effects date back to the 1920s (Bolliger and Inglis 1933; Doub et al. 1925, 1927; Warren 1928). Brachytherapy in the lung and liver also has a significant history of investigation (Kennedy et al. 2004a). Preclinical studies utilized a variety of animal models, and various infusion methods (vein, heart, aorta, hepatic artery, and portal vein) with and without liver tumors to study microsphere deposition in normal and tumor tissues. Common observations in animals and humans confirmed arterial delivery of microspheres causes them to embed in the periphery of the tumor in highly non-uniform (but not random) patterns with nearly all located within a few millimeters of tumor nodules. Groups or clusters of a few microspheres up to several dozen spheres were identified per cluster (Pillai et al. 1991). Attempts were made to quantify the radiation dose delivered in the early 1960s with dog and rabbit systems which crudely measured the location and intensity of microspheres from sectioning of the liver for autoradiography (Ya et al. 1961; Kim et al. 1962; Chamberlain et al. 1983). Geiger-Mueller survey meters or scintillation crystal probes recorded the location of Bremsstrahlung gamma ray production in the liver (Grady et al. 1963), or tiny Teflon coated lithium fluoride phosphor discs (Blanchard et al. 1964). Gray reported on a review of liver tissues from resin microsphere-treated patients via biopsies taken 7–9 months post treatment. Serum biochemical data and microscopic review of core biopsies from normal liver tissue confirmed minimal detectable effects from microsphere therapy (Gray et al. 1990).

---

## 3 Human Microsphere Dose Studies

Human liver tissue analyses to calculate absorbed dose in Gy have been done. Patients that received resin microspheres during laparotomy provided an opportunity to measure portions of the liver and tumors directly from small biopsies with a specialized 3-channel liquid scintillation  $\beta$ -radiation detection probe, which also detected gamma rays. After infusion of 49–118 million microspheres (diameter 17 or 32  $\mu\text{m}$ ), (Burton et al. 1989a, b, 1990) Burton estimated that the normal liver received 9.0–75 Gy, and tumor 34–1,474 Gy, as calculated by Tumor:Normal ratios of 0.4:1 to 45:1 (Burton et al. 1989b). Fox et al. (1991) studied the left lobe of a patient with metastatic colon cancer which was resected after having previously received resin microspheres. Predicted isodose curves by microspheres, which could be seen on pathologic sectioning, were produced similar to standard brachytherapy reports. Tumor received 75 Gy, and the normal liver received an estimated 30 Gy. It was also shown that for analysis of pathology sections for dosimetry calculations,

sampling of tissues at 500  $\mu\text{m}$  intervals was as accurate as smaller intervals (Fox et al. 1991). Campbell et al. (2000, 2001) also used tissues from a lobe of liver containing colon cancer metastases in a single patient previously treated with resin microspheres to study microsphere distribution radiation absorbed. Samples of four regions were taken; normal liver, the interface of tumor with normal liver, the surface of the tumor and the center of the tumor. The patient studied had previously received 3.2 GBq ( $60 \times 10^6$  microspheres) delivered with systemic Angiotensin II which constricts normal hepatic arteries but not tumor arteries. A residual 8 cm tumor nodule was resected and analyzed. Cluster analysis showed most sphere groupings were  $<1200 \mu\text{m}$  apart, and contained fewer than 15 individual spheres/grouping. The tumor center and normal liver contained a similar number of spheres, but the periphery of the tumor contained a 50–70 times higher concentration of spheres than the other areas (Campbell et al. 2000, 2001). This area was about 6 mm wide around tumors. The average doses found in portions of the tumor periphery were 200–600 Gy, with minimums of 70–190 Gy. Only 1 % of the normal liver absorbed a dose of 30 Gy or higher (Campbell et al. 2001).

Kennedy studied four whole livers from patients previously treated with microspheres. Two patients with hepatocellular carcinoma had received glass microspheres prior to lifesaving cadaveric transplantation. Also, two patients with metastatic colon cancer that had received resin microspheres were examined (Kennedy et al. 2004a). The distribution of microspheres was almost exclusively in the periphery of tumor nodules, and was similar for both microsphere types. Microscopic three dimensional radiation dose calculations using Monte Carlo method were performed on a tumor nodule implanted with glass microspheres. The 100 Gy isodose volume encompassed a 2  $\text{cm}^3$  tumor volume, with significant areas receiving 1000–3000 Gy (Kennedy et al. 2004b).

## 4 Selection of $^{90}\text{Y}$ Activity

### 4.1 Therapeutic Isotope

Yttrium-90 ( $^{90}\text{Y}$ ) is a pure-beta emitter that decays to stable zirconium-90 with an average energy of 0.9267 MeV via a half-life of 2.6684 days (64.04 h). It is produced by neutron bombardment of  $^{89}\text{Y}$  in a commercial nuclear reactor, which yields  $^{90}\text{Y}$  beta radiation having a tissue penetration of 2.5 mm and a maximum range of 1.1 cm. One GBq (27 mCi) of  $^{90}\text{Y}$  delivers a total dose of 49.38 Gy/kg in tissue. Commercially available radioactive microspheres include a glass<sup>1</sup> and

resin<sup>2</sup> microspheres in which  $^{90}\text{Y}$  is permanently embedded within its structure. No significant amount of  $^{90}\text{Y}$  leaches from the microsphere within the patient.

### 4.2 Glass Microspheres

The recommended approach to selecting an activity for these high-activity microspheres (2500 Bq/sphere initially, down to 350 Bq/sphere when used in many cases) is to use the MIRD convention and adjust downward according to the calculated shunt of particles to the lung. Microspheres are delivered in preset activities based on the day of calibration, ranging from 3 to 20 GBq, depending upon user request. The target dose of glass microspheres is 100–150 Gy predicted absorbed dose per the MIRD formulation, which assumes uniform distribution of microspheres in the treatment volume. The appropriate volume and mass (whole liver or single lobe) are determined using the CT or MR images, assuming a conversion factor of 1.03  $\text{g}/\text{cm}^3$ .

The amount of radioactivity required to deliver the dose to the selected liver target (whole liver or single lobe) is calculated using the following formula:

(1)

**Activity Required (GBq)**

$$= \frac{[\text{Desired Dose (Gy)}][\text{Mass of Selected Liver Target (kg)}]}{50[1 - F]}$$

Calculation of the liver absorbed dose is in Gy delivered after injection:

(2)

$$\text{Liver Dose (Gy)} = \frac{50 [\text{Injected Activity (GBq)}][1 - F]}{\text{Mass of Selected Liver Target (kg)}}$$

where  $F$  is the fraction of injected activity deposited into the lungs as measured by Tc-99 MAA. In these equations for glass microspheres  $F = 0.61$  when GBq is used, (representing the upper limit of activity that can safely be delivered to the lungs in a single glass microsphere administration) to estimate the fraction of dose that could be deposited into the lungs.

Many factors are taken into consideration when determining the activity to use for an individual patient. The formulae above have been clinically verified in more than 2,000 patients over the past 10 years. However, there are limitations in using the MIRD convention. It is not the case that microspheres are uniformly deposited in the treatment volume; in fact from the preclinical and human clinical data

<sup>1</sup> TheraSphere<sup>®</sup>—MDS Nordion, Inc., Ontario, Canada.

<sup>2</sup> SIR-Spheres<sup>®</sup>—SIRTex Medical Limited, Sydney, Australia.

it is very much the opposite. However, the MIRD formulae do enable microspheres to develop confidence in the range of activity that is suggested by these conventions, and must use their experience, skill and collaborative medical expertise to choose the most appropriate activity for a particular patient.

### 4.3 Resin Microspheres

Because resin microspheres carry less activity (50–80 Bq/sphere on average when delivered to patient) compared to glass microspheres, many more are used to deliver an adequate dose tumor. The typical patient receives about 15–20 million spheres for a 1.5–2 GBq activity distributed in both lobes of the liver. This can cause temporary embolic side effects (pain, fever, nausea), which are similar but far less intense than is seen in TACE post embolic symptoms. However, not all hepatic vascular beds can accept the number of microspheres desired from the pre treatment planning formulae, and thus the delivery of microspheres discontinued prior to completely emptying the volume of microspheres planned. It is not the desire or intent to perform an embolic treatment, rather it is a brachytherapy procedure and therefore it is recommended that the delivery of microspheres not cause stasis and/or reflux. Optimal implantation of microspheres is for the tumor-only to have spheres, and the normal adjacent liver free of radiation. Once stasis has occurred however, the normal liver arteries have also been filled with microspheres and the selectivity and therapeutic benefit to brachytherapy is lost. If the whole lobe or segment is receiving the same dose of radiation (tumor and normal liver) than external beam radiation could have been used instead. Also, many patients are selected for microsphere therapy specifically because an embolic treatment was not felt to be safe or in their best interests.

The manufacturer's User's Manual<sup>3</sup> suggests three methods of estimating the activity to use for resin microsphere treatment: (I) Body Surface Area method (*BSA*), (II) Empiric method, and (III) Partition method (Ho et al. 1996, 1997) (Eq. 3), appears in the manual as Eq. 3. The manufacturer's recommendation for the use of Eq. 3 did not appear to be intended for diffuse tumors; however the guidelines regarding the appropriateness of this equation are unclear. Therefore, we tested its application for all tumor types.

To better understand the following activity calculations (Toohey et al. 2000; Gulec et al. 2006a; Stabin 2006; Stabin and Konijnenberg 2000), a brief review is shown of the schema developed by the Medical Internal Radiation Dose

(MIRD) Committee of the Society of Nuclear Medicine (Toohey et al. 2000).

In this formalism the dose rate,  $\dot{D}$  can be written as (1)

$$\dot{D} = k \frac{A}{m} \langle E \rangle$$

where  $k$  is a constant to yield the dose rate in desired units,  $A$  is the source activity,  $m$  is the mass of tissue that the radiation is absorbed within, and  $\langle E \rangle$  is the average energy emitted per nuclear transition. Since we are dealing with a source undergoing nuclear decay, the activity of the source is not constant in time. Also the source is permanently implanted in the patient with no biologic excretion. Thus the activity as a function of time is described by the radioactive decay equation.

(2)

$$A(t) = A_0 e^{-\ln(2)t/T}$$

where  $A_0$  is the calibrated activity,  $t$  is the time from calibration, and  $T$  is the half-life of the radioactive source. The absorbed dose, calculated by integrating over all time, is then given by the following

(3)

$$D = \frac{k \langle E \rangle A_0}{m} \int_0^{\infty} e^{-\ln(2)t/T} dt = k \frac{A_0}{m} \langle E \rangle \frac{T}{\ln(2)}$$

From the published  $^{90}\text{Y}$  decay data, the average energy released in the  $\beta^-$  decay of  $^{90}\text{Y}$  is  $0.9267 \text{ MeV (Bq s)}^{-1}$ , assuming that all of the energy of the  $\beta^-$  decay is absorbed in tissue. Using the half-life  $T = 64.04 \text{ h}$ , the total radiation absorbed dose after the complete  $\beta^-$  decay of  $^{90}\text{Y}$  is given by

$$D[\text{Gy}] = 49.38 \frac{A_0[\text{GBq}]}{m[\text{kg}]}$$

The difference between the 49.38 constant given here and the 49670 constant given below is explained by taking the mass in kg instead of g and current values for the average energy released in the decay process.

#### I. Body Surface Area Method Calculation (Eqs. 1–5)

1.

$$\text{BSA}[\text{m}^2] = 0.20247 \times (\text{height}[\text{m}])^{0.725} \times (\text{weight}[\text{kg}])^{0.425}$$

2.

$$A[\text{GBq}] = (\text{BSA} - 0.2) + \frac{\text{vol of tumor}}{\text{vol of tumor} + \text{vol of liver}}$$

<sup>3</sup> Sirtex User's Manual issued March 2002, pp. 38–42.



3.

$$A[\text{GBq}]_{\text{resin}} = \frac{D_{\text{liver}}((T : N \times M_{\text{tumor}}) + M_{\text{liver}})}{49670(1 - L/100)}$$

- $D_{\text{liver}}$  Nominal dose (Gy) to the liver
- $T:N$  Tumor to normal ratio was calculated (see below)
- $L$  Shunt fraction (%) of microspheres from liver to lung based on macro agglutinated albumin (MAA) nuclear medicine scan
- $M_{\text{liver}}$  Total mass of liver (g) from CT volume
- $M_{\text{tumor}}$  Total mass of tumor (g) from CT volume
- 49670 Absorbed dose conversion constant from infinite decay
- $V_T$  cc from CT scan
- $V_L$  cc from CT scan

4.

$$T : N = (A_{\text{tumor}}/M_{\text{tumor}})/(A_{\text{liver}}/M_{\text{liver}})$$

- $A_{\text{tumor}}$  Activity in tumor from MAA scan
- $A_{\text{liver}}$  Activity in liver from MAA scan
- $M_{\text{liver}}$  Mass in g of normal liver (excluding tumor) from CT scan
- $M_{\text{tumor}}$  Mass in g of tumor in liver (excluding normal liver tissue) from CT scan

5.

$$L[\text{Lung Shunt \%}] = \frac{\text{ROI}_{\text{Lung Counts}} \times 100}{\text{ROI}_{\text{Lung Counts}} + \text{ROI}_{\text{Liver Counts}}}$$

### II. Empiric Method Calculation

Tumor  $\leq 25\%$  of the total mass of the liver by CT scan = use 2 GBq whole liver delivery

Tumor  $> 25\%$  but  $< 50\%$  of liver mass by CT scan = use 2.5 GBq whole liver delivery

Tumor  $> 50\%$  of liver mass by CT scan = 3 GBq for whole liver delivery

### III. Partition Method Calculation—“Eq. 3”

$$\begin{aligned} &\text{Tissue Radiation Dose [Gy] liver} \\ &= \frac{49670 \times \text{Total } ^{90}\text{Y activity in liver [GBq]}}{\text{Mass of liver [g]}} \end{aligned}$$

## 4.4 Empiric Method

The first method developed for resin microspheres was clinically derived with the added data of intraoperative activity calculations (Burton et al. 1989a, b, 1990; Gray et al. 1989). There are important details regarding the differences in these patients and those now treated worldwide

with resin microspheres. First, patients were previously untreated by chemotherapy or early in a course of standard 5-fluorouracil and leucovorin. Typical patients with breast, colorectal and primary cancers of the liver now have had often received multiagent chemotherapy reducing overall and liver-specific tolerance to additional anticancer therapies. Second, the volume treated included both lobes at the same time. This is not much different than current treatment approaches, which try to treat all of the tumors in each lobe with placement of microcatheters in more than one position or at the bifurcation of the right and left hepatic arteries. However, if less than the whole liver is the intent of treatment, this must be accounted for with a proportional reduction in the calculated activity planned for delivery. Third, concurrent infusion of the vasoactive agent Angiotensin II shifted microsphere deposition away from normal liver and toward irregular tumor-related neovascular arteries (Gray et al. 1989, 1990, 1992; Burton et al. 1985, 1988, 1989a, b; Van Hazel et al. 2004). Although this is potentially a useful pharmacologic strategy for broad adoption, this agent is currently only available in limited circumstances in Japan (Wu et al. 1996; Anderson et al. 1991, 1992; Goldberg et al. 1987, 1988, 1991; Archer and Gray 1989). Fourth, older resin microspheres held less activity per sphere, and therefore up to 120 million spheres were used per treatment.

It is a common finding now that if the Empiric Method is used that up to 50 % of treatments will be incomplete, i.e. not all of the microspheres can be implanted due to vascular stasis (Gulec et al. 2006b; Kennedy et al. 2006a, b). This issue is important not only from radiation safety and clean up standpoint, but also bears careful attention in the procedure not to try and deliver all the microspheres. This is not to suggest that the Empiric Method is not useful, as it can delineate the upper limit of safety in the conditions listed above in which it was developed. However in most modern-day patients, a more consistent and accurate calculation approach is the Body Surface Area method. The majority of patients will have aggregate tumor volumes between 5 and 23 %. Obviously in this wide range, individual patients cannot be optimally treated with a single activity recommendation i.e. 2 GBq.

## 4.5 Body Surface Area Method

Van Hazel first instituted this modification during clinical trials where radiation hepatitis appeared in patients with smaller liver volumes (Van Hazel et al. 2004). Unfortunately there has not been a subsequent publication showing the rationale, validity or correlation between BSA, liver volume, tumor volume, and radiation hepatitis. It can represent a significant decrease in activity (small patient, small

liver) compared to the Empiric approach, and at other times, it calls for a modest increase in activity (small patient, large liver) compared to the Empiric Method. It has been demonstrated that the Empiric and BSA methods usually overestimate the activity that can be delivered to a patient (Kennedy et al. 2006a, b).

#### 4.6 Partition Method

There are special situations in which a discrete lesion in the liver can be identified and the total volume of the three compartments; liver, tumor and lung, are accurately known. Using the Partition method, absorbed dose can be very accurately determined. This approach has been validated by Ho et al. (1996, 1997a, b) in a series of important papers based on human patients treated with resin microspheres. Sarfaraz concluded that using state of the art computerized radiation dose planning compared favorably to the Partition method in selected patients receiving glass microspheres (Sarfaraz et al. 2001, 2003, 2004). However, when the Partition method is misapplied and used in patients with diffuse disease it will recommend activities that would be life-threatening if delivered as shown by Kennedy et al. (2006a, b).

### 5 Selection of $^{90}\text{Y}$ Activity in Resin Microsphere Therapy

Guidance for resin microsphere activity calculations is more numerous than for glass microspheres. Several publications have specifically addressed the recommended approach to resin microspheres for metastatic and hepatocellular cancers in regards to minimizing the risk of radiation-induced liver damage (Gil-Alzugaray et al. 2013a, b; Lau et al. 2012; Kennedy et al. 2009). Specific to the risks and prognostic factors for radiation induced liver disease (RILD) Gil-Alzugaray reported on a single institution experience of 260 consecutive patients with primary and metastatic tumors treated with resin microspheres (Gil-Alzugaray et al. 2013a, b). The early experience in that group was to use BSA method and Partition approaches for both cirrhotic and noncirrhotic patients. They noted prognostic factors associated with a higher incidence of radioembolization-induced liver disease (REILD)—a term coined by this group—which is similar to RILD, except with elevated bilirubin very similar to chemoradiotherapy-induced liver disease (Sangro et al. 2008). A total of 75 patients were treated via standard BSA calculation with a 22.7 % incidence of any REILD, most were limited and transient, but 13.2 % were severe and 5.3 % fatal. With adjustments in their protocol, which included a 10–20 % reduction in activity delivered,

the next 185 patients experienced far fewer ( $p = 0.0001$ ) REILD events: 5.4 % mild, 2.2 % severe, and 0.5 % fatal. In addition to a reduction in activity, they treated all patients with ursodeoxycholic acid and methyl-prednisolone for 2 months after radiation. Independent prognostic factors for REILD in non-cirrhotic patients were use of full BSA calculated activity of  $^{90}\text{Y}$  and chemotherapy following radiation. Independent factors associated with REILD for cirrhotic patients were small liver volume ( $<1.5\text{L}$ ), elevated total bilirubin ( $>1.2\text{ mg/dL}$ ) at time of radiation, and a selective approach versus whole liver. Cirrhosis patients more likely to develop REILD were those with small livers (total volume  $<1.5\text{ L}$ ), an abnormal bilirubin at baseline ( $>1.2\text{ mg/dL}$ ), hypersplenism (platelets  $<100/\text{pL}$ ), treated in a whole-liver fashion, not receiving steroids or ursodeoxycholic acid, or treated by the standard protocol. In the corresponding multivariate model, only the presence of a small liver, an abnormal bilirubin, and treatment in a whole-liver fashion were independently associated to the development of REILD. This occurs even though treatment was more intense when delivered in a selective rather than in a whole-liver fashion (average activity relative to target volume: 1.79 GBq/L versus 0.92 GBq/L,  $p = 0.002$ ) (Gil-Alzugaray et al. 2013a, b).

The threshold activity from these data for REILD is suggested to be 0.8 GBq/L liver (Gil-Alzugaray et al. 2013a, b). The response rate and outcomes of patients in the most recent cohort with an activity reduction was exactly the same as the initial group with higher  $^{90}\text{Y}$  delivered (Gil-Alzugaray et al. 2013a, b).

Lau was joined by a multidisciplinary group of experts in radioembolization and reported a consensus guide for patient selection and  $^{90}\text{Y}$  activity planning (Lau et al. 2012). The group produced a pathway which is supported by the latest published and at that time, unpublished experiences in radioembolization across all tumor types. It recommended the BSA method as most appropriate for multiple, indiscrete tumors, and the partition model, with a target tumor dose of 120 Gy, for discrete lesions with clearly definable regions of interest, predominately hepatocellular carcinomas. Additional modifications were recommended to decrease either the volume of liver treated, or the amount of activity delivered, or both variables based on several criteria (Lau et al. 2012). Kennedy previously had reported on a cohort of 515 patients, 680 treatments, of both metastatic and primary liver cancers, in collaboration with 16 institutions (Kennedy et al. 2009). An extensive list of clinical, physical, and dosimetric factors were examined statistically regarding prognostic factors for RILD/REILD. A predictive model was not achieved, but ten factors were independently associated with RILD, all related in some way to either the volume of normal liver treated, prior liver treatments, and magnitude of radiation delivered. For resin microspheres

empiric method of calculation was associated ( $p < 0.0001$ ) with RILD but BSA method was not (Kennedy et al. 2009). Kennedy reported on a 548 patient cohort of metastatic colorectal cancer patients who received resin microspheres after three lines of chemotherapy and biologic agents. The incidence of any RILD/REILD was 0.5 % using the BSA method, which is in close agreement with other reports (Kennedy et al. 2013). This type of approach is of intense interest and research efforts in radiation oncology and nuclear medicine, with a number of future-looking publications by leaders in various specialties (Pan et al. 2010; Jaffray et al. 2010; Bentzen et al. 2010).

Attempts continue to enhance our understanding of radiation dose absorption in the tumor and liver by using software tools, pretreatment MAA and SPECT CT data (Kao et al. 2012; Kennedy et al. 2011). Thus far patient-specific 3D image based radiation dose estimates of  $^{90}\text{Y}$  prior to radiation implantation has not been validated in a larger group of patients, only retrospective data exists. Kao used MAA SPECT/CT partition modeling (MIRD estimates) successfully in describing the potential of this approach in 10 patients with hepatocellular carcinoma. (Kao et al. 2012) Kennedy used non-MIRD, 3D patient CT and SPECT MAA data via a Monte Carlo dose algorithm, first in a phantom, then retrospectively in 50 consecutive patients. The dose volume histograms (DVHs) of each patient were correlated with response and toxicity. The clinical data was consistent with the DVHs curves showing significant sparing of normal liver during high-dose coverage of tumors. The preservation of spatial data is very important in this approach and is the main difference in MIRD-based dose methods (Kennedy et al. 2011). With the discovery of PET-Bremsstrahlung SPECT data there is the possibility of at least performing accurate post- $^{90}\text{Y}$  implant dose estimation, but certainly the goal is to improve our pre-treatment radiation planning.

## 6 Conclusions

Resin  $^{90}\text{Y}$  microsphere activity selection continues to be challenging however clinical data are enhancing our ability to safely treat all eligible patients. Optimal activity of microspheres for an individual patient is a complex endeavor involving multiple modalities and physician specialists. There is not yet a software solution to accurately predict or model  $^{90}\text{Y}$  absorbed dose in normal liver and tumor. Like much of medicine in general, and oncology in particular, clinical experience, provides the “art” of activity selection, while a strong understanding of radiation, liver tolerance and vascular anatomy is the science that makes for effective use of microsphere brachytherapy. For glass microspheres, the current MIRD-based activity calculation

appears safe and reproducible regarding toxicity and outcomes. Resin microspheres should be planned using BSA and/or Partition Method as recommended in consensus reports.

## References

- Anderson JH, Angerson WJ, Willmott N, Kerr DJ, McArdle CS, Cooke TG (1991) Regional delivery of microspheres to liver metastases: the effects of particle size and concentration on intrahepatic distribution. *Br J Cancer* 64:1031–1034
- Anderson JH, Angerson WJ, Willmott N, Kerr DJ, McArdle CS, Cooke TG (1992) Is there a relationship between regional microsphere distribution and hepatic arterial blood flow? *Br J Cancer* 66:287–289
- Archer SG, Gray BN (1989) Vascularization of small liver metastases. *Br J Surg* 76(6):545–548
- Bentzen SM, Constine LS, Deasy JO, Eisbruch A, Jackson A, Marks LB et al (2010) Quantitative Analyses of Normal Tissue Effects in the Clinic (QUANTEC): an introduction to the scientific issues. *Int J Radiat Oncol Biol Phys* 76(3 Suppl):S3–S9
- Blanchard RJ, Grotenhuis I, LaFave JW (1964) Treatment of experimental tumors: utilization of radioactive microspheres. *Arch Surg* 89:406
- Bolliger A, Inglis K (1933) Experimental liver disease produced by X-ray irradiation of the exposed organ. *J Pathol* 36:19–30
- Burton MA, Gray BN, Self GW, Heggie JC, Townsend PS (1985) Manipulation of experimental rat and rabbit liver tumor blood flow with angiotensin II. *Cancer Res* 45(11 Pt 1):5390–5393
- Burton MA, Gray BN, Coletti A (1988) Effect of angiotensin II on blood flow in the transplanted sheep squamous cell carcinoma. *Eur J Cancer Clin Oncol* 24(8):1373–1376
- Burton MA, Gray BN, Jones C, Coletti A (1989a) Intraoperative dosimetry of  $^{90}\text{Y}$  in liver tissue. *Int J Rad Appl Instrum B* 16(5):495–498
- Burton MA, Gray BN, Klemp PF, Kelleher DK, Hardy N (1989b) Selective internal radiation therapy: distribution of radiation in the liver. *Eur J Cancer Clin Oncol* 25(10):1487–1491
- Burton MA, Gray BN, Kelleher DK, Klemp PF (1990) Selective internal radiation therapy: validation of intraoperative dosimetry. *Radiology* 175(1):253–255
- Campbell AM, Bailey IH, Burton MA (2000) Analysis of the distribution of intra-arterial microspheres in human liver following hepatic yttrium-90 microsphere therapy. *Phys Med Biol* 45:1023–1033
- Campbell AM, Bailey IH, Burton MA (2001) Tumor dosimetry in human liver following hepatic yttrium-90 microsphere therapy. *Phys Med Biol* 46:487–498
- Chamberlain MN, Gray BN, Heggie JC, Chmiel RL, Bennett RC (1983) Hepatic metastases—a physiological approach to treatment. *Br J Surg* 70(10):596–598
- Dawson LA (2005) Hepatic arterial yttrium 90 microspheres: another treatment option for hepatocellular carcinoma. *J Vasc Interv Radiol* 16(2 Pt 1):161–164
- Dawson LA, Lawrence TS (2004) The role of radiotherapy in the treatment of liver metastases. *Cancer J* 10(2):139–144
- Dawson LA, Ten Haken RK (2005) Partial volume tolerance of the liver to radiation. *Semin Radiat Oncol* 15(4):279–283
- Doub HP, Bolliger A, Hartman FW (1925) Radiation sickness in dog. *Am J Roentgenol* 13:54
- Doub HP, Hartman FW, Bolliger A (1927) X-rays in the canine liver. *Radiology* 8:142

- Fajardo LF, Colby TV (1980) Pathogenesis of veno-occlusive liver disease after radiation. *Arch Pathol Lab Med* 104:584–588
- Fajardo LF, Berthrong M, Anderson RE (2001) *Liver. Radiation Pathology*, 1st edn. Oxford University Press, New York, pp 249–257
- Fox RA, Klemp PF, Egan G, Mina LL, Burton MA, Gray BN (1991) Dose distribution following selective internal radiation therapy. *Int J Radiat Oncol Biol Phys* 21(2):463–467
- Gil-Alzugaray B, Chopitea A, Inarrairaegui M, Bilbao JI, Rodriguez-Fraile M, Rodriguez J et al (2013a) Prognostic factors and prevention of radioembolization-induced liver disease. *Hepatology* 57(3):1078–1087 (Epub) 2012/12/120
- Gil-Alzugaray B, Chopitea A, Inarrairaegui M, Bilbao JI, Rodriguez-Fraile M, Rodriguez J et al (2013b) Correction. *Hepatology* 1 (Epub 6 May 2013)
- Goldberg JA, Bradnam MS, Kerr DJ, McKillop JH, Bessent RG, McArdle CS et al (1987) Single photon emission computed tomographic studies (SPECT) of hepatic arterial perfusion scintigraphy (HAPS) in patients with colorectal liver metastases: improved tumour targeting by microspheres with angiotensin II. *Nucl Med Commun* 8(12):1025–1032
- Goldberg JA, Kerr DJ, Willmott N, McKillop JH, McArdle CS (1988) Pharmacokinetics and pharmacodynamics of locoregional 5 fluorouracil (5FU) in advanced colorectal liver metastases. *Br J Cancer* 57(2):186–189
- Goldberg JA, Murray T, Kerr DJ, Willmott N, Bessent RG, McKillop JH et al (1991) The use of angiotensin II as a potential method of targeting cytotoxic microspheres in patients with intrahepatic tumour. *Br J Cancer* 63(2):308–310
- Grady ED, Sale WT, Rollins LC (1963) Localization of radioactivity by intravascular injection of large radioactive particles. *Ann Surg* 157(1):97–114
- Gray BN, Burton MA, Kelleher DK, Anderson J, Klemp P (1989) Selective internal radiation (SIR) therapy for treatment of liver metastases: measurement of response rate. *J Surg Oncol* 42(3):192–196
- Gray BN, Burton MA, Kelleher D, Klemp P, Matz L (1990) Tolerance of the liver to the effects of Yttrium-90 radiation. *Int J Radiat Oncol Biol Phys* 18(3):619–623
- Gray BN, Anderson JE, Burton MA, van Hazel G, Codde J, Morgan C et al (1992) Regression of liver metastases following treatment with yttrium-90 microspheres. *Aust N Z J Surg* 62(2):105–110
- Gulec SA, Mesoloras G, Stabin M (2006a) Dosimetric techniques in 90Y-microsphere therapy of liver cancer: the MIRD equations for dose calculations. *J Nucl Med* 47(7):1209–1211
- Gulec SA, Mesoloras G, Dezarn WA, McNeillie P, Kennedy AS (2006b) Safety and efficacy evaluation of Y-90 microsphere treatment using medical internal radiation dosimetry (MIRD) in patients with liver malignancies. *J Nucl Med* 47:493P
- Ho S, Lau WY, Leung TW, Chan M, Ngar YK, Johnson PJ et al (1996) Partition model for estimating radiation doses from yttrium-90 microspheres in treating hepatic tumours. *Eur J Nucl Med* 23(8):947–952
- Ho S, Lau WY, Leung TW, Chan M, Johnson PJ, Li AK (1997a) Clinical evaluation of the partition model for estimating radiation doses from yttrium-90 microspheres in the treatment of hepatic cancer. *Eur J Nucl Med* 24(3):293–298
- Ho S, Lau WY, Leung TW, Chan M, Chan KW, Lee WY et al (1997b) Tumour-to-normal uptake ratio of 90Y microspheres in hepatic cancer assessed with 99Tcm macroaggregated albumin. *Br J Radiol* 70(836):823–828
- Jaffray DA, Lindsay PE, Brock KK, Deasy JO, Tome WA (2010) Accurate accumulation of dose for improved understanding of radiation effects in normal tissue. *Int J Radiat Oncol Biol Phys* 76(3 Suppl):S135–S139
- Kao YH, Hock Tan AE, Burgmans MC, Irani FG, Khoo LS, Gong Lo RH et al (2012) Image-guided personalized predictive dosimetry by artery-specific SPECT/CT partition modeling for safe and effective 90Y radioembolization. *J Nucl Med* 53(4):559–566
- Kennedy AS, Nutting C, Coldwell D, Gaiser J, Drachenberg C (2004a) Pathologic response and microdosimetry of 90Y microspheres in man: Review of four explanted whole livers. *Int J Radiat Oncol Biol Phys* 60(5):1552–1563
- Kennedy AS, Coldwell D, Nutting C, Tucker G, Van Echo DA (eds) (2004b) 90Y-microspheres in the treatment of colorectal metastases: USA experience. In: Fifteenth international congress on anti-cancer treatment, Feb 10 2004. T.C.O., Paris
- Kennedy AS, Dezarn WA, McNeillie P, Overton C, England M, Sailer SL (2006a) Fractionation, dose selection, and response of hepatic metastases of neuroendocrine tumors after 90 Y—microsphere brachytherapy. *Brachytherapy* 5:103–104
- Kennedy AS, Dezarn WA, McNeillie P, Overton C, England M, Sailer SL (2006b) Dose selection of resin 90Y-microspheres for liver brachytherapy: a single center review. *Brachytherapy* 5:104
- Kennedy AS, McNeillie P, Dezarn WA, Nutting C, Sangro B, Wertman D et al (2009) Treatment parameters and outcome in 680 treatments of internal radiation with resin 90Y-microspheres for unresectable hepatic tumors. *Int J Radiat Oncol Biol Phys* 74(5):1494–1500
- Kennedy AS, Dezarn WA, Weiss A (2011) Patient specific 3D image-based radiation dose estimates for 90Y microsphere hepatic radioembolization in metastatic tumors. *J Nucl Med Radiat Ther* 2(111):1–8
- Kennedy AS, Ball D, Cohen SJ, Cohn M, Coldwell D, Drooz A et al (2013) Safety and efficacy of resin 90Y-microspheres in 548 patients with colorectal liver metastases progressing on systemic chemotherapy. *J Clin Oncol* 31(4 suppl):264
- Kim YS, LaFave JW, MacLean LD (1962) The use of radiating microspheres in the treatment of experimental and human malignancy. *Surgery* 52:220
- Lau WY, Kennedy AS, Kim YH, Lai HK, Lee RC, Leung TW et al (2012) Patient selection and activity planning guide for selective internal radiotherapy with yttrium-90 resin microspheres. *Int J Radiat Oncol Biol Phys* 82(1):401–407
- Pan CC, Kavanagh BD, Dawson LA, Li XA, Das SK, Miften M et al (2010) Radiation-associated liver injury. *Int J Radiat Oncol Biol Phys* 76(3 Suppl):S94–S100
- Pillai KM, McKeever PE, Knutsen CA, Terrio PA, Prieskorn DM, Ensminger W (1991) Microscopic analysis of arterial microsphere distribution in rabbit liver and hepatic VX2 tumor. *Select Cancer Ther* 7(2):39–48
- Sangro B, Gil-Alzugaray B, Rodriguez J, Sola I, Martinez-Cuesta A, Viudez A et al (2008) Liver disease induced by radioembolization of liver tumors: description and possible risk factors. *Cancer* 112(7):1538–1546
- Sarfaraz M, Kennedy AS, Cao ZJ, Li A, Yu C (2001) Radiation dose distribution in patients treated with Y-90 Microspheres for non-resectable hepatic tumors. *Int J Rad Biol Phys* 51(3 S1):32–33
- Sarfaraz M, Kennedy AS, Cao ZJ, Sackett GD, Yu CX, Lodge MA, Murthy R, Line BR, Van Echo DA (2003) Physical aspects of yttrium-90 microsphere therapy for nonresectable hepatic tumors. *Med Phys* 30(2):199–203
- Sarfaraz M, Kennedy AS, Lodge MA, Li XA, Wu X, Yu CX (2004) Radiation absorbed dose distribution in a patient treated with yttrium-90 microspheres for hepatocellular carcinoma. *Med Phys* 31(9):2449–2453
- Stabin M (2006) Nuclear medicine dosimetry. *Phys Med Biol* 51(13):R187–R202
- Stabin MG, Konijnenberg MW (2000) Re-evaluation of absorbed fractions for photons and electrons in spheres of various sizes. *J Nucl Med* 41(1):149–160



- Stabin MG, Siegel JA (2003) Physical models and dose factors for use in internal dose assessment. *Health Phys* 85(3):294–310
- Toohey RE, Stabin MG, Watson EE (2000) The AAPM/RSNA physics tutorial for residents: internal radiation dosimetry: principles and applications. *Radiographics* 20(2):533–546 (quiz 1–2)
- Van Hazel G, Blackwell A, Anderson J, Price D, Moroz P, Bower G, Cardaci J, Gray B (2004) Randomised Phase II trial of SIR-spheres plus fluorouracil/leucovorin chemotherapy versus fluorouracil/leucovorin chemotherapy alone in advanced colorectal cancer. *J Surg Oncol* 88(2):78–85
- Warren LS (1928) Physiological effects of X-rays. *Physiol Rev* 8:114
- Wu Y, Cahill PA, Sitzmann JV (1996) Decreased angiotensin II receptors mediate decreased vascular response in hepatocellular cancer. *Ann Surg* 223(2):225–231
- Ya PM, Guzman T, Loken MK, Perry JF (1961) Isotope localization with tagged microspheres. *Surgery* 49(5):644–650

# Nuclear Medicine Procedures for Treatment Evaluation and Administration

Javier Arbizu, Macarena Rodriguez-Fraile, Josep M Martí-Climent, Inés Domínguez-Prado, and Carmen Vigil

## Contents

<b>1</b>	<b>Introduction</b> .....	64
<b>2</b>	<b>Patient Selection and Therapy Planning: Nuclear Medicine Procedures</b> .....	64
2.1	Technical Issues.....	64
2.2	Calculation of Hepatopulmonary Shunting.....	65
2.3	Extrahepatic Vessels: Unnoticed Collateral Vessels.....	67
2.4	Effective Tumour Targeting and Liver Target Volume.....	67
2.5	Conditioning Factors.....	69
<b>3</b>	<b>Treatment Administration and Monitorisation</b> .....	70
3.1	Dose Preparation.....	70
3.2	Treatment Administration.....	71
3.3	Early Post-treatment monitorisation.....	71
<b>4</b>	<b>Future Directions</b> .....	72
4.1	Positron-Emitting Radionuclide-Labelled Microspheres for Pre-treatment Assessment.....	72
4.2	Combined Positron-Emitting Radionuclides and <sup>90</sup> Y-Labelled Microspheres for Post-treatment Monitorization.....	73
	<b>References</b> .....	73

## Abstract

The <sup>90</sup>Yttrium radioembolisation (RE) procedure requires the collaboration of a multidisciplinary team that includes hepatologists, oncologists, interventional radiologists and nuclear medicine specialists working together in close collaboration. To avoid toxicity to the patient, a thorough angiographic evaluation is performed to identify extrahepatic vessels that may feed the tumours (to guarantee efficacy). To mimic the microsphere application during the treatment, angiographic evaluation is accomplished with <sup>99m</sup>Tc-MAA injection into the vessel of interest, followed by imaging. Both procedures combined are essential to plan the RE therapy, and to detect and eventually occlude every collateral vessel arising from a hepatic artery that may carry microspheres to the gastrointestinal tract or other extrahepatic organs. Moreover, this approach permits the calculation of hepatopulmonary shunting, and tumour and liver tissue targeting. With this information taken together, the treatment is designed and activity is calculated to maximise the dose of radiation delivered to liver tumours while safely preserving the non-tumoural parenchyma.

## Abbreviations

RE	Radioembolisation
<sup>90</sup> Y RE	<sup>90</sup> Yttrium-loaded microspheres radioembolisation
GI	Gastrointestinal
<sup>99m</sup> Tc-MAA	<sup>99m</sup> Tc-MAA-labelled macroaggregated albumin
SPECT	Single photon emission computed tomography imaging
SPECT/CT	Single photon emission computed tomography imaging combined with X-ray computer tomography
PET	Positron emission tomography

J. Arbizu (✉) · M. Rodriguez-Fraile · J. M. Martí-Climent · I. Domínguez-Prado · C. Vigil  
Department of Nuclear Medicine, Clinica Universidad De Navarra, Avenida de Pío XII, 36, 31008 Pamplona, Spain  
e-mail: jarbizu@unav.es

PET/CT	Positron emission tomography combined with X-ray computer tomography
MRI	Magnetic resonance imaging
Bq	Becquerel; unit of radioactivity
OS-EM	Ordered subsets expectation maximisation iterative reconstruction
ROI	Region of interest
LS	Hepatopulmonary or lung shunting
Gy	Grey; units of radiation dose
MIRD	Medical internal radiation dosimetry
T/N	Tumour targeting or tumour-to-non-tumour ratio
5-FU	5 Fluorouracil
BS	Bremsstrahlung

## 1 Introduction

Radioembolisation (RE) using intra-arterially injected  $^{90}\text{Y}$ trium-loaded microspheres ( $^{90}\text{Y}$  RE) to treat liver tumours has an excellent tolerability; however, the radiation delivered by the isotope results in both benefits and side effects for the patient. The main complications of  $^{90}\text{Y}$  RE result from an excessive irradiation of non-target tissues, including the liver. In this regard, it should be borne in mind that absolute and relative contraindications for  $^{90}\text{Y}$  RE are related to excessive lung radiation due to leakage via hepatopulmonary shunts, the presence of  $^{90}\text{Y}$ -loaded microspheres in the gastrointestinal (GI) tract, and the radiation of non-tumoural liver parenchyma, which increases the risk of liver failure. Regarding these contraindications, the main role of nuclear medicine procedures is to contribute to the multidisciplinary approach to assess, from a clinical standpoint, the patient suitability for  $^{90}\text{Y}$  RE and to determine the activity to be administered during the treatment.

An angiographic evaluation is performed some weeks prior to RE, which involves a simulation of the actual treatment carried out using  $^{99\text{m}}\text{Tc}$ -labelled macroaggregated albumin ( $^{99\text{m}}\text{Tc}$ -MAA) particles that are of similar size to that of the  $^{90}\text{Y}$ -microspheres.  $^{99\text{m}}\text{Tc}$ -MAA allows for planar scintigraphy, single photon emission computed tomography imaging (SPECT) alone or combined with X-ray computed tomography scanners (SPECT/CT). This procedure can be used to measure hepatopulmonary shunting, and to detect unnoticed collateral vessels arising from a hepatic artery that may carry microspheres into the GI tract or other extrahepatic organs. The procedure can also be used to anticipate the tumour and normal liver tissue targeting. Additionally, images performed a few hours after the treatment using planar scintigraphy, SPECT or positron

emission tomography (PET), are useful in evaluating the likely  $^{90}\text{Y}$  microsphere distribution.

Recent advances in nuclear medicine equipment development (multimodal SPECT/CT or PET/CT scanners and software packages) may enable the distribution of  $^{99\text{m}}\text{Tc}$ -MAA or  $^{90}\text{Y}$ -microspheres for a given patient to be combined with anatomic information [from CT or magnetic resonance imaging (MRI)] to yield diagnostic data for that particular patient.

## 2 Patient Selection and Therapy Planning: Nuclear Medicine Procedures

### 2.1 Technical Issues

#### 2.1.1 Simulation Procedure Using $^{99\text{m}}\text{Tc}$ -MAA: Pearls and Pitfalls

Unlike other forms of brachytherapy, an accurate dosimetry cannot be predicted for  $^{90}\text{Y}$  RE. A simulation of the actual treatment is performed 1–2 weeks prior to  $^{90}\text{Y}$  RE with  $^{99\text{m}}\text{Tc}$ -MAA particles that are of comparable size to the microspheres. During the diagnostic angiography procedure, 111–185 MBq of  $^{99\text{m}}\text{Tc}$ -MAA are injected into the selected vessel to estimate the  $^{90}\text{Y}$  microsphere distribution prior to treatment. However, the capacity of  $^{99\text{m}}\text{Tc}$ -MAA to mimic the microsphere distribution is a matter of controversy. Some authors have shown that the therapeutic response might not be predicted accurately if it is based exclusively on  $^{99\text{m}}\text{Tc}$ -MAA particle distribution (Knesaurek et al. 2010; Haug et al. 2011). This is probably because the broad range of radiolabelled  $^{99\text{m}}\text{Tc}$ -MAA particle sizes ( $\phi$ : 10–100  $\mu\text{m}$ ) may result in an altered distribution kinetics compared to that obtained with  $^{90}\text{Y}$ -microspheres (SIR-Spheres<sup>TM</sup>: average  $\phi$ : 32.5  $\mu\text{m}$ , range 20–60  $\mu\text{m}$ ; Thera-Spheres<sup>TM</sup>: average  $\phi$ : 25  $\mu\text{m}$ , range 20–30  $\mu\text{m}$ ). Furthermore, the number of MAA and microsphere particles injected for a typical procedure is significantly different (on average,  $0.5 \times 10^6$  MAA particles vs. more than  $22 \times 10^6$   $^{90}\text{Y}$ -microspheres) (Van de Wiele et al. 2012). Despite these limitations, many authors have shown that the MAA tumour-to-normal perfusion ratio serves not only as a good response predictor (Flamen et al. 2008; Kao et al. 2012), but it also enables the accurate determination of uptake via pulmonary (Jha et al. 2012; Leung et al. 1994) and GI shunts (Lenoir et al. 2012). Moreover, the use of tumour dosimetry based on  $^{99\text{m}}\text{Tc}$ -MAA SPECT/CT data may also facilitate therapy planning and estimation of the amount of activity to be administered (Garin et al. 2012). Therefore,  $^{99\text{m}}\text{Tc}$ -MAA scans can be used as a sham procedure to predict  $^{90}\text{Y}$  microsphere distribution during actual treatment.

Degradation of  $^{99m}\text{Tc}$ -MAA can occur during the procedure, leading to free  $^{99m}\text{Tc}$  in the circulation; this is physiologically trapped and secreted by the thyroid, stomach and GI tract, which may result in an overestimation or misinterpretation of hepatopulmonary and GI shunting in the  $^{99m}\text{Tc}$ -MAA images. To avoid this accumulation, it is suggested that  $^{99m}\text{Tc}$ -MAA labelling should be performed shortly before the injection, and that the interval between the injection and scanning be kept as brief as possible (Lambert et al. 2010). In this respect, it is important to note that oral administration of 600 mg sodium perchlorate, 30 min before  $^{99m}\text{Tc}$ -MAA injection, prevents the “non-specific” uptake of  $^{99m}\text{Tc}$  into the thyroid and stomach, thereby avoiding equivocal findings in the gastroduodenal region (Ahmadzadehfar et al. 2010; Sabet et al. 2011).

### 2.1.2 Imaging Acquisition and Processing

Within 2 h of the  $^{99m}\text{Tc}$ -MAA administration, the scintigraphic image is obtained with a gamma camera positioned anteriorly and posteriorly to the patient. Planar images of the thorax and abdomen are acquired for 10 min for each projection in a  $128 \times 128$  matrix. Total counts are calculated inside regions of interest (ROIs) outlined over each lung and the entire liver on the anterior and posterior views for hepatopulmonary shunt calculations (see Sect. 2.2).

Additionally, a SPECT or SPECT/CT scan of the abdomen is obtained. The SPECT detectors usually have an axial field of view that covers the entire abdomen. The scan consists of a single SPECT acquisition (e.g. dual detectors;  $180^\circ$  rotation; 60 projections per detector, 10 s per projection;  $128 \times 128$  matrix) followed by a low-dose CT scan during shallow free breathing by the patient. SPECT/CT images are usually reconstructed with ordered subsets expectation maximisation (OS-EM) iterative reconstruction, accompanied by distance-dependent resolution compensation with corrections for attenuation (CT-based, using reconstructed CT images) and scatter (with dual energy window acquisition). Several circular ROIs of a fixed diameter could be outlined over the SPECT images, and placed over the tumour lesions and normal liver tissue for targeting calculation purposes (see Sect. 2.4).

### 2.1.3 Advantages of SPECT and SPECT/CT

Although most reports focus on planar  $^{99m}\text{Tc}$ -MAA scintigraphy to identify pulmonary shunts, full 3D acquisition SPECT or SPECT/CT are increasingly being integrated to detect extrahepatic shunts.

SPECT images allow a precise identification of extrahepatic shunts and enable evaluation of the arterial perfusion of each tumoural lesion without overlap. Besides, SPECT constitutes the basis for image fusion with other pre- and post-therapeutic tomographic images (SPECT, PET, CT or MRI). The current availability of new

multimodal SPECT/CT devices with advanced reconstruction parameters permits shorter acquisition times and provides accurate attenuation correction and image co-registration.

Apart from intrinsic hardware differences between devices, a primary cause for poor quality SPECT images is the attenuation of photons. Gamma photons emitted by radionuclides in the liver must cross different abdominal structures to be finally detected by the gamma camera. SPECT/CT facilitates attenuation correction using an X-ray-based patient-specific attenuation map that can be obtained rapidly and with higher accuracy than maps generated with external radionuclide sources. Other benefits of using CT for attenuation correction include reduced noise, no influence of the gamma photons on CT data and no need to replace transmission sources (Even-Sapir et al. 2009).

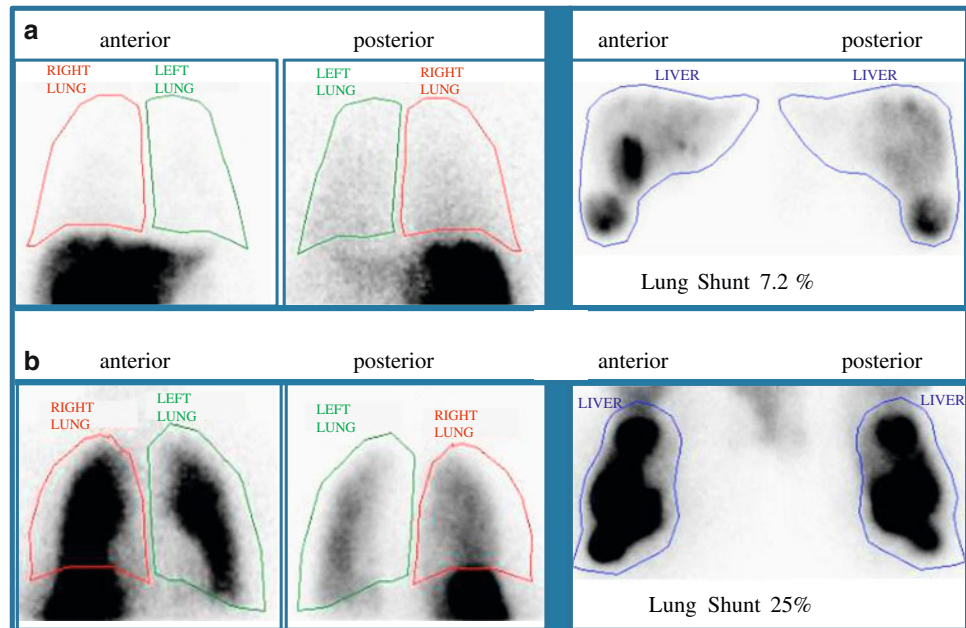
The usefulness of SPECT/CT on the identification of extrahepatic uptake sites has been recently revealed by a number of studies, notably in cases where no arterial shunts had been detected by angiography (Ahmadzadehfar et al. 2010; Lenoir et al. 2012). In addition, the analysis of SPECT with CT and/or MRI fused images is an essential aspect for better defining the  $^{99m}\text{Tc}$ -MAA distribution pattern related to the anatomic location of the tumours and, consequently, for better predicting the selectivity of the radioactive microsphere distribution within the tumours. For this purpose, and following suitable attenuation correction, SPECT/CT offers some advantages over planar or SPECT images. First, this approach increases focus intensity on the attenuated data, especially in the more centrally localised foci, with improved sensitivity as a consequence. Second, it allows an accurate localisation of tumour lesions and non-tumoural liver tissue, thus enabling an improved calculation of the microsphere activity to be delivered. Moreover, SPECT/CT-based dosimetry is superior to that of planar scintigraphy because it reduces overlapping radiotracer activity, it allows the evaluation of heterogeneous radiotracer uptake, and it detects activity in small lesions. Phantom studies have shown that  $^{99m}\text{Tc}$ -MAA SPECT/CT volume measurements are accurate and reproducible, and that SPECT alone (visual delimitation of the tumour volume based on the hot spot) is acceptable for the measurement of large volumes (<10 % error for volumes greater than 473 ml), but inaccurate for the measurement of small volumes (Garin et al. 2011).

## 2.2 Calculation of Hepatopulmonary Shunting

A specific feature of the neoplastic vasculature within tumours is the formation of intratumoural arteriovenous anastomoses or shunts. Interestingly, a high hepatopulmonary



**Fig. 1** Hepatopulmonary shunt calculation using the values obtained from  $^{99m}\text{Tc}$ -MAA planar scintigraphy for two different cases (**a** and **b**). ROIs are drawn in anterior and posterior planar images covering both lungs and the liver area to be treated



shunting is most frequently observed among patients with hepatocellular carcinoma or metastatic disease with a large tumour burden (Leung et al. 1995).

In the presence of detectable hepatopulmonary or lung shunting (LS), a proportion of the microspheres would bypass the hepatic capillaries and end up in the pulmonary capillary mesh. Because lung tissue is sensitive to radiation, the administration of  $^{90}\text{Y}$ -microspheres in the presence of a sizable shunt increases the risk of clinically significant radiation pneumonitis. Radiation pneumonitis is an inflammatory reaction that resembles pneumonia symptoms, including dry cough, progressive dyspnea and restrictive ventilatory defects, resulting in a deterioration of lung function, and even death in a worst case scenario.

Accordingly, the measurement of LS is essential to ensure the safety of the procedure and also to calculate the radiation dose that will reach the lungs. The procedure is performed at the same time as the diagnostic angiogram by injecting  $^{99m}\text{Tc}$ -MAA through the catheter placed in the feeding arteries (see Sect. 2.1.1).

Using a gamma camera, the amount of  $^{99m}\text{Tc}$ -MAA in the lungs can be quantified and compared to the injected dose in the liver, allowing for calculation of LS (Fig. 1).

The percentage of LS can be determined from the total counts within ROIs over both lungs and the liver, using the geometrical mean of anterior and posterior thoracic and abdominal planar images.

$$\text{Lung shunt \%} = \frac{\text{ROI Lung counts} \times 100}{\text{ROI Lung counts} + \text{ROI Liver counts}}$$

A good correlation exists between the calculation of LS using  $^{99m}\text{Tc}$ -MAA scintigraphy and the LS calculated using

$^{90}\text{Y}$  microsphere images [mean LS with  $^{99m}\text{Tc}$  MAA:  $4.77 \pm 2.81$ , mean LS after treatment:  $4.52 \pm 2.5$  %; coefficient of correlation ( $r$ ) 0.96], which confirms the ability of  $^{99m}\text{Tc}$ -MAA to predict the LS of  $^{90}\text{Y}$ -microspheres during RE (Jha et al. 2012).

Only recently, the use of SPECT/CT for LS calculation has been proposed to circumvent the limitations of planar images to accurately delineate liver and lung tissues (Yu et al. 2013). Moreover, as planar images lack the 3-D tissue densities required for an adequate attenuation correction of lung and liver tissues, LS calculations based on the use of such images could be overestimated.

The radiation dose (Gy) to the lungs can be predicted by the  $^{99m}\text{Tc}$ -MAA shunt fraction and the injected activity of the  $^{90}\text{Y}$ -microspheres according to the following equation (Leung et al. 1994).

$$\begin{aligned} &\text{Cumulative absorbed lung radiation dose} \\ &= 50 \times \left( \sum_{i=1}^n A_i \times LS_i / 100 \right) / \text{Lung mass} \end{aligned}$$

where:

$A_i$	activity infused (GBq)
$LS_i$	lung shunt fraction during infusion
$N$	number of infusions,
Lung mass	assumed to be 1 kg.

Previous pre-clinical and clinical studies with  $^{90}\text{Y}$ -microspheres demonstrated that the highest tolerable dose to the lungs is 30 Gy for a single injection (Leung et al. 1995; Yorke et al. 2005). In cases where several treatments are administered, the lung dose of radiation is the cumulative

absorbed lung radiation dose from all treatments and should not exceed 50 Gy. Depending on the LS value, it might also be necessary to reduce the total administered activity to the liver, or even to contraindicate the use of  $^{90}\text{Y}$  RE.

### 2.3 Extrahepatic Vessels: Unnoticed Collateral Vessels

To perform any therapeutic transarterial procedure in the liver in a safe and efficient manner, it is essential to be acquainted with the hepatic arterial anatomy (Covey et al. 2002). This is particularly important when  $^{90}\text{Y}$ -microspheres could be inadvertently deposited in excessive amounts in organs other than the liver, such as the stomach, duodenum, gall bladder, pancreas, mesentery and, to a lesser degree, vascular structures. Serious complications that include GI ulceration, bleeding, gastritis, duodenitis, cholecystitis, pancreatitis, radiation dermatitis and pneumonitis, could occur (Leong et al. 2009; Riaz et al. 2009).

Evaluation of the extrahepatic uptake of  $^{99\text{m}}\text{Tc}$ -MAA using planar scintigraphy analysis can be challenging at times, leading to the misinterpretation of possible extrahepatic side effects. The location of several organs within a relatively small region in the upper abdomen demands the analysis of tomographic images. SPECT and CT or MRI fused images can be employed for the detection of the extrahepatic location of  $^{99\text{m}}\text{Tc}$ -MAA and, thus, detection of the potentially dangerous misplacement of the radiospheres.

As was discussed above, SPECT with integrated low-dose CT increases the sensitivity and specificity of  $^{99\text{m}}\text{Tc}$ -MAA SPECT when detecting extrahepatic arterial shunting. Planar  $^{99\text{m}}\text{Tc}$ -MAA scintigraphy, non-attenuation-corrected SPECT, and SPECT/CT have been reviewed retrospectively for extrahepatic  $^{99\text{m}}\text{Tc}$ -MAA deposition in ninety diagnostic hepatic angiograms obtained from 76 patients with different types of cancer (Ahmadzadehfar et al. 2010). The sensitivity for detecting extrahepatic shunting with planar imaging, SPECT, and SPECT/CT was 32, 41 and 100 %, respectively, while specificity was 98, 98 and 93, respectively. Moreover, therapy planning was changed according to the results of planar imaging, SPECT, and SPECT/CT in 7.8, 8.9 and 29 % of patients, respectively (Ahmadzadehfar et al. 2010). These results have been confirmed recently, suggesting the superiority of SPECT/CT over planar imaging for the identification of digestive, extrahepatic  $^{99\text{m}}\text{Tc}$ -MAA uptake sites, including the gall bladder, which were found in more than one-third of cases (Lenoir et al. 2012).

Accordingly,  $^{99\text{m}}\text{Tc}$ -MAA SPECT/CT should now form part of the clinical assessment prior to RE in order to better identify the risk of digestive shunts. In cases of GI uptake on  $^{99\text{m}}\text{Tc}$ -MAA SPECT/CT, a repeated angiographic

assessment is mandatory as the source of gastroduodenal flow can frequently be identified and corrected. However, the described series (Lenoir et al. 2012) revealed a high frequency of vascular uptake at the level of portal vein thrombosis, hepatic artery, falciform artery or coil embolisation sites, without any consequences for the therapeutic management of patients. Experts must recognise these uptake sites as possible sources of error (Fig. 2).

### 2.4 Effective Tumour Targeting and Liver Target Volume

RE with  $^{90}\text{Y}$ -microspheres is based on delivering a high dose of internal radiation to the tumour while maintaining a safe dose of radiation to sensitive tissues such as the lung and non-tumoural liver. The radiation dose is therefore non-homogeneous, and the precise dose received will vary within the tumour and normal liver parenchyma. For the calculation of the activity that allows the highest dose in the tumour while sparing normal liver tissue, some models have been proposed. One of these is the partition model. This model, which is based on medical internal radiation dosimetry (MIRD), partitions the lungs, tumour and non-tumoural liver into separate compartments for radiation dose modelling.

Assuming that LS and the relative distribution of  $^{99\text{m}}\text{Tc}$ -MAA in the tumoural and non-tumoural liver compartments (tumour targeting or tumour-to-non-tumour ratio, T/N) are similar to that of  $^{90}\text{Y}$ -microspheres during subsequent treatment, the activity of  $^{90}\text{Y}$ -microspheres to be administered can be estimated using the percentage of LS and T/N determined from the  $^{99\text{m}}\text{Tc}$ -MAA images (Ho et al. 1996).

T/N can be determined from the following equation:

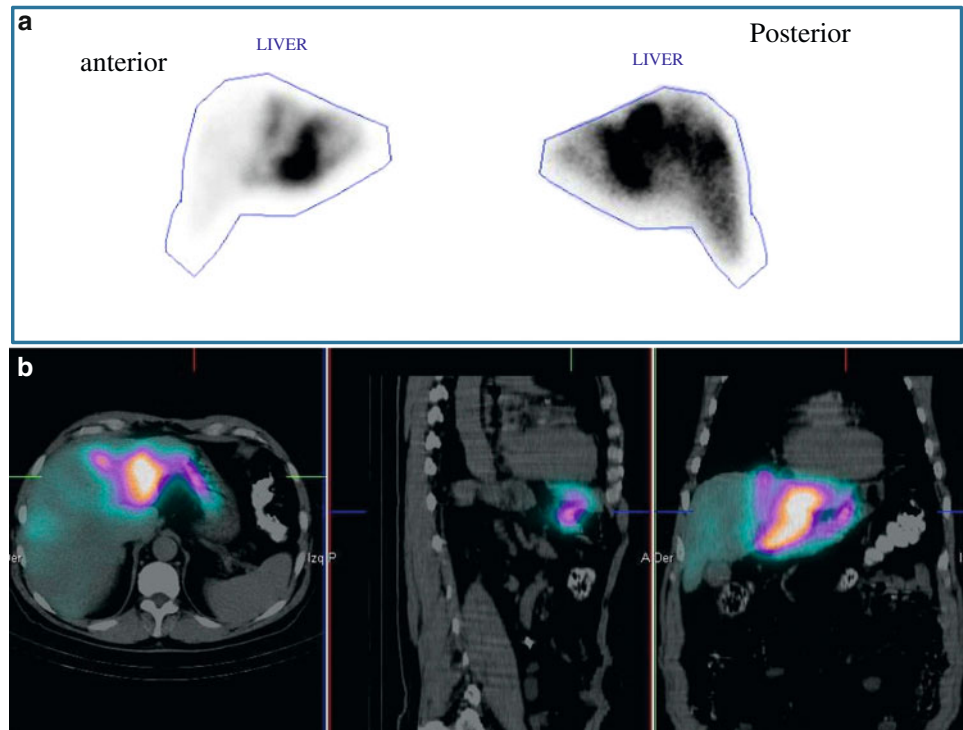
$$T/N = \frac{(A_{\text{tumour}}/M_{\text{tumour}})}{(A_{\text{liver}}/M_{\text{liver}})}$$

where:

$A_{\text{Tumour}}$	activity in the tumour determined from $^{99\text{m}}\text{Tc}$ -MAA images
$M_{\text{Tumour}}$	mass of tumour in the liver
$A_{\text{Liver}}$	activity in the normal liver determined from $^{99\text{m}}\text{Tc}$ -MAA images
$M_{\text{Liver}}$	mass of the normal liver (excluding tumour).

Although no standardised technique has been defined, several methods have been described for the calculation of SPECT/CT-based T/N ratios (Campbell et al. 2009; Flamen et al. 2008; Gulec et al. 2007; Kao et al. 2012). However, European Association Nuclear Medicine procedure guidelines for the treatment of liver cancer with intra-arterial radioactive compounds specify that the T/N ratio cannot be

**Fig. 2**  $^{99m}\text{Tc}$ -MAA planar scintigraphy (a), and SPECT/CT (b) in a patient with liver metastases from colorectal cancer. Unsuspected extrahepatic visceral shunting in the planar scintigraphy is clearly shown in the fused SPECT/CT images (gastric accumulation)



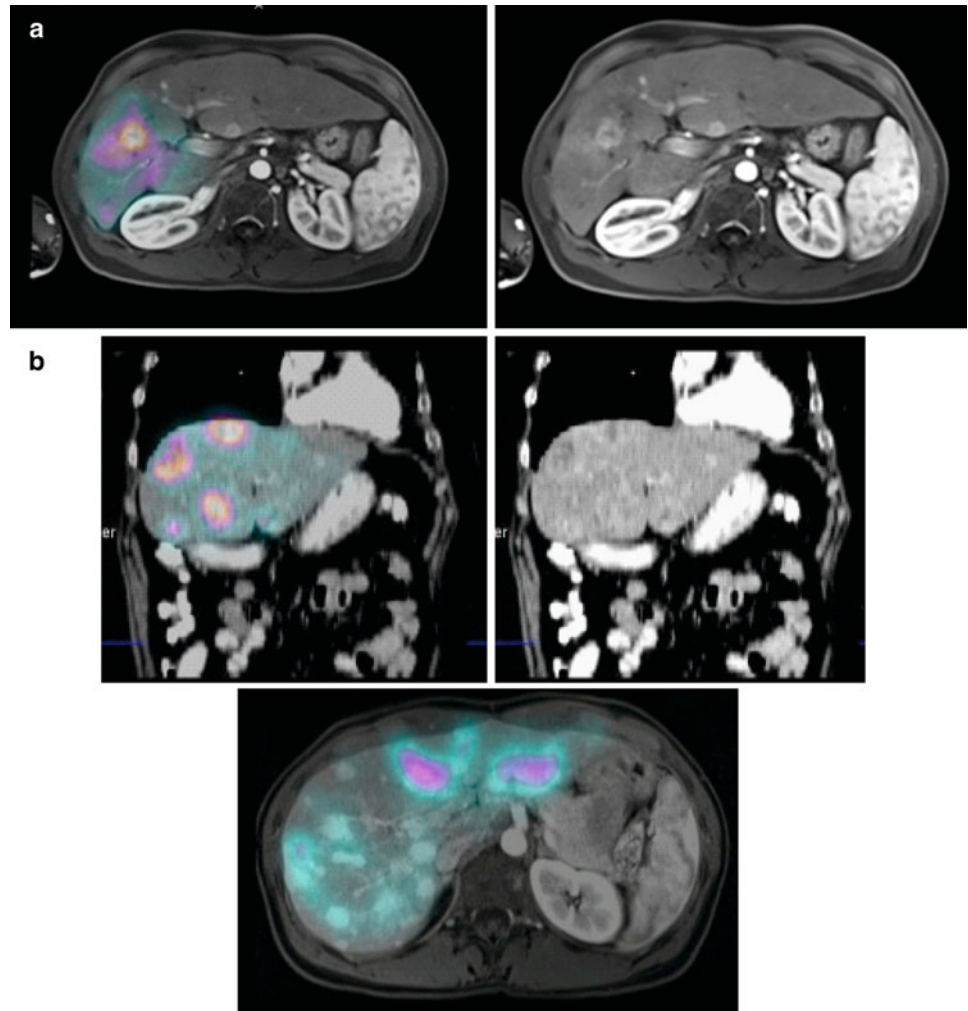
accurately determined unless an attenuation-corrected SPECT scan is used (Giammarile et al. 2011). According to our experience, we calculate the T/N ratio by obtaining the activities of ten identical ROIs drawn on the attenuation-corrected SPECT images obtained by means of SPECT/CT. Five ROIs are of relevant tumour lesions and another five involve relevant non-tumoural areas of the liver. As the number and size are the same for tumoural and non-tumoural tissue, the ratio between the sum of image counts represents an estimation of the T/N ratio. If the tumour is poorly delineated with the CT images obtained from the SPECT/CT acquisition, coregistered SPECT and diagnostic contrast-enhanced CT or MRI fused images should be obtained (Fig. 3).

According to Lau et al. (1994), the tumour targeting (T/N ratio) predicted by the  $^{99m}\text{Tc}$ -MAA images showed good correlation with the T/N of radiation doses measured with a calibrated beta-probe during open surgery and also with the T/N determined from the liquid scintillation counting of biopsies taken after infusion of the microspheres (Lau et al. 1994). Consequently, we could hypothesise that tumours with high  $^{99m}\text{Tc}$ -MAA uptake receive a high dose of  $^{90}\text{Y}$ -microspheres and, therefore, may respond correspondingly better than tumours demonstrating a low uptake of  $^{99m}\text{Tc}$ -MAA. However, this hypothesis has not been entirely corroborated. Some authors have not found a significant correlation between tumour  $^{99m}\text{Tc}$ -MAA uptake and tumour response (Hamami et al. 2009). In this regard, we studied 138 target lesions from a group consisting of 17

hepatocellular carcinoma, 14 colorectal cancer and seven neuroendocrine metastasis patients treated with  $^{90}\text{Y}$  RE (Rodríguez-Fraile et al. 2008). The response to RE was based on CT or MRI changes in the maximal diameter observed in each target lesion at 3 and 6 months after RE. In agreement with the previous studies, we did not find any significant correlation between the tumour size changes during the follow-up and the  $^{99m}\text{Tc}$ -MAA SPECT T/N ratio for each target lesion. In contrast, other authors have shown that the T/N ratio predicts the tumoural response and even the survival (Dancey et al. 2000; Flamen et al. 2008). Using a T/N ratio threshold of unity, Flamen et al. showed that positive and negative predictive values for tumour response prediction were 71 % (17/24) and 87 % (13/15), respectively (Flamen et al. 2008) (Fig. 4).

The liver volume that shows an increased uptake after selective injection of  $^{99m}\text{Tc}$ -MAA into the hepatic artery reflects the vascularised volume to be treated with  $^{90}\text{Y}$ -microspheres. For this reason, an important goal of the  $^{99m}\text{Tc}$ -MAA hepatic perfusion study is to identify the liver volume fed by a selective arterial branch (liver target volume). The calculation of this volume is critical because it directly affects the radiation-absorbed dose estimation. This is especially relevant when planning for selective (lobar) or superselective (segmental or subsegmental)  $^{90}\text{Y}$  RE, and in patients with complex anatomical liver vascularisation.  $^{99m}\text{Tc}$ -MAA SPECT/CT vascularised volume measurement is a more functional and reliable method than current volume calculations made using anatomical images based on

**Fig. 3** Effective tumour targeting between structural lesions (MR or CT) and  $^{99m}\text{Tc}$ -SPECT/CT distribution in a case of hepatocellular carcinoma (a), and liver metastases from colorectal cancer (b)



CT or MRI data. Moreover, an unexpectedly large volume of target liver, slightly or non-vascularised, was revealed for some patients in the  $^{99m}\text{Tc}$ -MAA SPECT/CT images (Garin et al. 2011). This is probably due to the existence of microvascular communications between different anatomic segments, most likely via intratumoural arterioportal shunts with low arterial blood flow that went unnoticed on angiography but were identified with  $^{99m}\text{Tc}$ -MAA SPECT/CT. The existence of an unexpected non-vascularised liver target volume requires the site for delivering  $^{90}\text{Y}$ -microspheres to be redefined.

## 2.5 Conditioning Factors

Some factors can affect the vascular flow of liver tumours and may need to be taken into account when performing the pre-treatment assessment of candidate patients for  $^{90}\text{Y}$  RE. Consequently, these factors can also affect the  $^{99m}\text{Tc}$ -MAA scintigraphy distribution, and should be considered during the evaluation of nuclear medicine procedures.

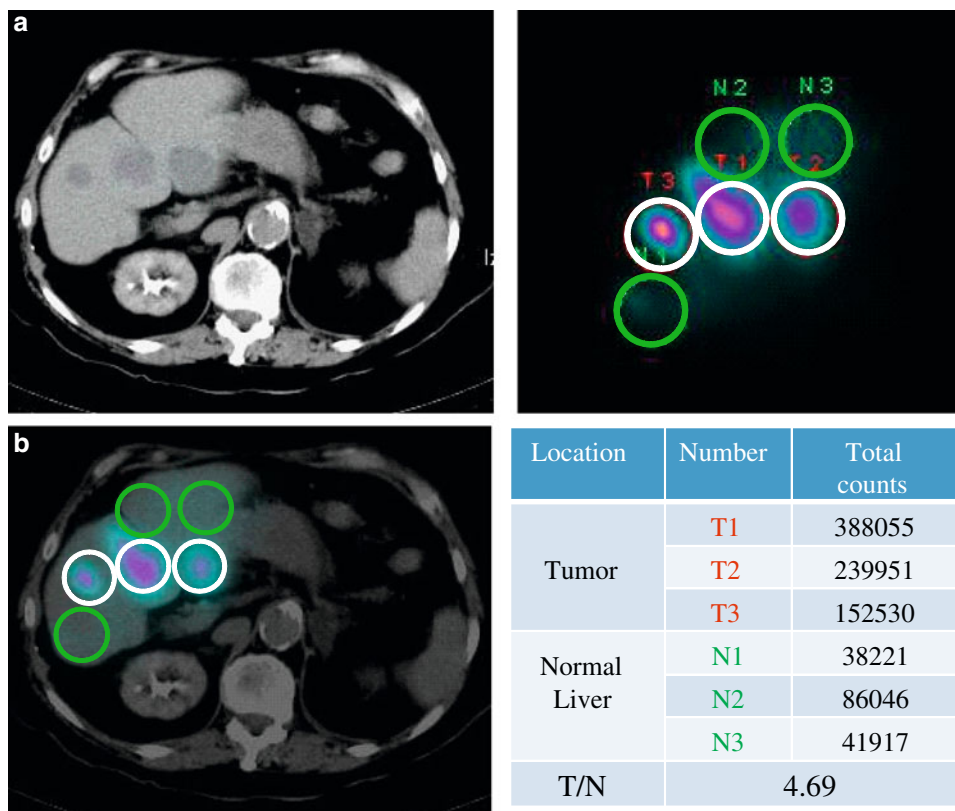
### 2.5.1 Prior Treatments

Previously administered treatments are not an excluding factor for hepatic  $^{90}\text{Y}$  RE, the only exceptions being prior liver external-beam radiotherapy, and patients with tumour recurrence after liver transplantation (Kennedy et al. 2012).

Exposure to systemic treatments often compromises the hepatic vascular flow, its morphology and neogenesis in the neoplastic tissue and even in the normal parenchyma. All these changes might affect pre-treatment  $^{99m}\text{Tc}$ -MAA scintigraphy and, therefore, the biodistribution of  $^{90}\text{Y}$ -microspheres. In this respect, it is important to note that irinotecan and oxaliplatin can produce sinusoidal obstruction syndrome, and that gemcitabine and 5-FU might increase the risk of liver toxicity. Because of the increased risk of radiation-induced liver disease, concomitant chemotherapy with capecitabine should be discontinued at least for 2 months prior to  $^{90}\text{Y}$  RE and must not be prescribed at any time after treatment (Giammarile et al. 2011; Lau et al. 2012; Murthy et al. 2005). Nevertheless, it remains unclear if these drugs represent a contraindication to RE.



**Fig. 4**  $^{99m}\text{Tc}$ -MAA SPECT/CT carried out for T/N calculation during the evaluation work-up of a patient with liver metastases from a neuroendocrine tumour. *White circles* are located over the liver tumour lesions, and *green circles* of the same size over the normal liver tissue are shown in the attenuation-corrected SPECT images. Total counts for each region and the calculated TN value are shown in the table



Special attention should be paid to anti-angiogenic therapy (bevacizumab, sorafenib). In our experience, patients treated with anti-angiogenic therapeutic drugs show a limited uptake of  $^{99m}\text{Tc}$ -MAA and poor tumour targeting and, consequently, a very low T/N ratio, which is probably related to the hypoxic conditions created by this therapy. It has been recommended that these drugs be discontinued for at least 8 weeks before evaluation work-up (Ahmadzadehfar et al. 2012).

### 2.5.2 Vascular Flow Redistribution

The term ‘vascular redistribution’ defines any endovascular technique performed to proximally occlude a major hepatic arterial trunk (lobar or segmental) and thereby allow the perfusion of its distal branches by intrahepatic collaterals. In some cases, the liver lobe has two or more afferent vessels originating from different abdominal trunks (replaced or aberrant arteries), while in others, two or more segmental vessels originate from the right and left hepatic arteries (i.e. segment IV vascularisation). For such cases, the flow redistribution during the pre-treatment angiography, by means of modification to the arterial hemodynamics as well as isolation of the main injection point(s) (one or two), permits to safely administer the  $^{90}\text{Y}$ -microspheres to the whole tumoural volume (Bilbao et al. 2010).

To confirm the safety and efficacy of vascular redistribution,  $^{99m}\text{Tc}$ -MAA SPECT/CT images must show a

homogeneous accumulation of MAA over the entire tumoural territory (Kennedy et al. 2009).

## 3 Treatment Administration and Monitorisation

$^{90}\text{Y}$  RE implies the manipulation of radioactive material to ensure the accurate administration of the previously calculated activity of  $^{90}\text{Y}$  for each individual. Additionally, the facility in which treatment is administered must be appropriately staffed, be fitted with radiation safety equipment as well as procedures available for waste handling and disposal, and for handling contamination. Personnel must also be able to monitor for accidental contamination and to control its spread. Trained medical staff with supporting physicist and nursing staff should undertake the administration of  $^{90}\text{Y}$ -microspheres. Planar scintigraphy, SPECT or PET acquisition, performed a few hours after the administration, is useful to locate the activity (Giammarile et al. 2011).

### 3.1 Dose Preparation

Commercially available  $^{90}\text{Y}$ -microspheres (SIR-Spheres<sup>TM</sup>, Theraspheres<sup>TM</sup>) are 20–40  $\mu\text{m}$  ( $\phi$ ) particles that emit

$\beta$ -radiation. SIR-Spheres<sup>TM</sup> are provided in vials with an activity of 3 GBq, while Theraspheres<sup>TM</sup> are supplied in 6 different activities: 3, 5, 7, 10, 15 and 20 GBq. Consequently, it is necessary to remove the desired activity of <sup>90</sup>Y-microspheres from the shipping container and place in the treatment vial for use.

The activity of <sup>90</sup>Y-microspheres must be determined by measurement using an appropriate dose calibrator, such as an ion chamber, on arrival or at the time of dose preparation. It is important to note that the dose calibrator is unable to detect  $\beta$ -particles, but can measure the radiation that results from the interaction of  $\beta$ -particles with atomic nuclei in the object, which is defined as bremsstrahlung (BS) radiation. Nevertheless, the ion chamber should be calibrated to measure <sup>90</sup>Y, for which the calibration factor is calculated from a standard <sup>90</sup>Y source.

The delivery vial contains the activity of <sup>90</sup>Y-microspheres in 5 ml (SIR-Spheres<sup>TM</sup>) or 0.6 ml (Theraspheres<sup>TM</sup>) of water. Once the received activity has been measured, a simple ratio between the prescribed activity and the known activity per volume can be used to calculate the volume of solution to be drawn up.

Activity measurements should be conducted using fully suspended microspheres to avoid inconsistencies associated with self-shielding due to geometry changes.

### 3.2 Treatment Administration

The administration of <sup>90</sup>Y-microspheres is performed through a catheter placed in the arterial hepatic vasculature, for which this procedure must be carried out in the interventional radiology catheterisation laboratory. Additionally, a delivery system that allows the administration to be carried out in a step by step manner is necessary to avoid an early full embolisation of vasculature that restricts the total infusion of the estimated dose. The administration equipment set (SIR-Sphere<sup>TM</sup> and TheraSphere<sup>TM</sup>) consists of a methacrylate shield, the dose vial and inlet and outlet tubing with needles or a plunger assembly. A 5-ml syringe is used to infuse saline solution (Theraspheres<sup>TM</sup>) or sterile water for injection (SIR-Spheres<sup>TM</sup>) through the system. When the catheter is positioned at the treatment site and the nuclear physician verifies the integrity of the delivery system, the catheter is connected to the outlet tubing. Usually, slow and deliberate hand-injection of the <sup>90</sup>Y-microspheres through the catheter system is adequate. Care should be taken not to allow too vigorous an injection rate, because this may result in leaks at points of potential weakness (e.g. septum, tubing connections). The infusion may be done with alternating injections of sterile water/saline solution and contrast medium, thereby allowing specific monitoring with the use of fluoroscopy to ensure that stasis is not

reached. This approach also enables one to confirm that the flow of microspheres closely mimics that observed in the angiographic work-up. Flushing should be continued until optimal delivery of the microspheres is achieved.

The remaining microspheres may be expelled from the vial and tubing by pressurising the system with a column of air; this will result in a slow expulsion of the final 1–2 % of <sup>90</sup>Y-microspheres.

During the administration, two different radiation detectors should be available in the room. A survey metre with a thin window Geiger-Müller detector is necessary for detecting possible radioactive contamination of medical personnel or of fixed equipment in the room, along with the location of waste material. A portable ionisation chamber should be available to measure the BS radiation dose from the patient.

When a full dose cannot be administered (usually due to vascular stasis), it is recommended that the undelivered activity be measured. An approximation to the actual administered dose could be calculated by multiplying the prepared activity by a correction factor obtained from the dose rates measured around the delivery box before and after the treatment.

$$\text{Administered Activity} = \text{Prepared Activity} \\ (1 - \text{dose rate after}/\text{dose rate before})$$

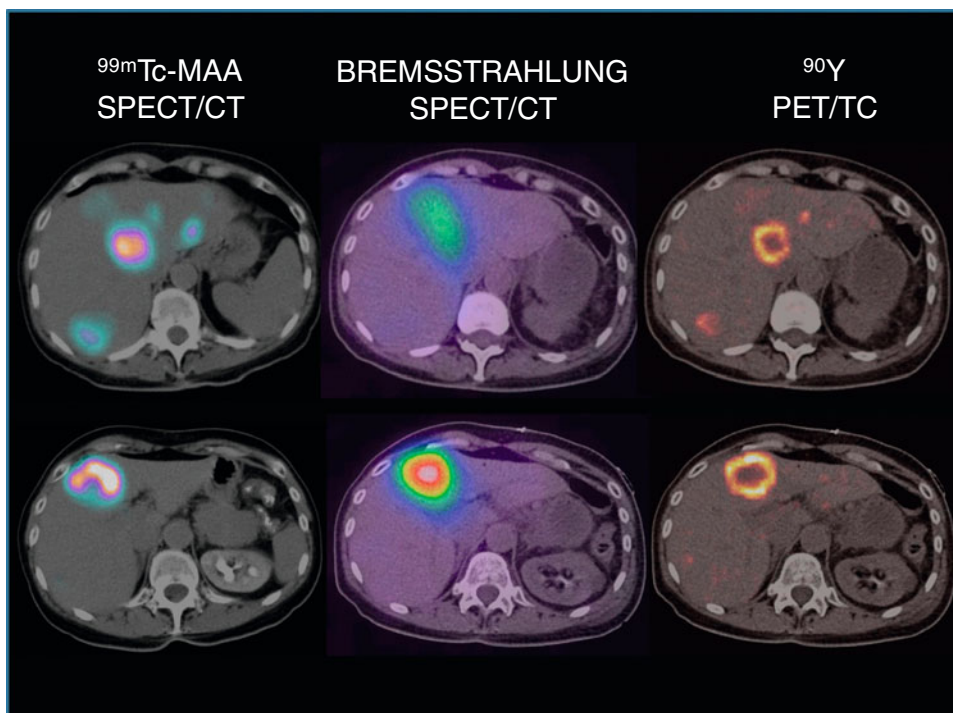
The final activity delivered to the patient must be recorded and used for dosimetric purposes.

### 3.3 Early Post-treatment monitorisation

A precise evaluation of microsphere deposition after treatment is critical for two main reasons: first, to exclude non-targeted microsphere deposition, and second to evaluate the radiation-absorbed dose delivered to the tumour. The infusion of <sup>90</sup>Y-microspheres to unintended areas, such as the GI tract, could cause severe complications (Carretero et al. 2007; Kennedy et al. 2007; Salem and Thurston 2006). The identification of GI accumulation during the first hours after treatment allows the prompt initiation of proton pump inhibitors and the performance of a diagnostic gastroendoscopy as early as possible in order to avoid a potentially fatal ulcer.

Although LS calculated by <sup>99m</sup>Tc-MAA scan prior to treatment seems to predict the LS calculated using <sup>90</sup>Y-microspheres (Jha et al. 2012), dosimetry based on <sup>99m</sup>Tc-MAA images can provide inaccurate results due to differences between MAA and microsphere distributions as mentioned above. Therefore, to calculate a precise patient-specific dosimetry, high-quality imaging of the <sup>90</sup>Y microsphere distribution is essential (Fig. 5).

**Fig. 5** Correlation between pre-treatment distribution of  $^{99m}\text{Tc}$ -MAA SPECT/CT (left column), and post-treatment bremsstrahlung SPECT/CT (central column) and  $^{90}\text{Y}$  PET/CT (right column) images in a patient with hepatocellular carcinoma. In this case, a better correlation is obtained between  $^{99m}\text{Tc}$ -MAA SPECT/CT and  $^{90}\text{Y}$  PET/CT, than with bremsstrahlung SPECT/CT



At present, the biodistribution of  $^{90}\text{Y}$ -microspheres is generally assessed through BS scan images within 24 h of the treatment. Although BS planar, SPECT or SPECT/CT images are routinely performed, BS SPECT/CT provides the best-quality image (Ahmadzadehfar et al. 2011). Using the gastroduodenoscopy as a reference standard to evaluate GI microsphere deposition, the sensitivity, specificity, positive and negative predictive values and the accuracy of BS SPECT and SPECT/CT in the prediction of GI ulcers were 13, 88, 8, 92 and 82 %, and 87, 100, 100, 99 and 99 %, respectively.

Despite the ability of BS images to facilitate the determination of  $^{90}\text{Y}$  microsphere deposition and patient dosimetry (Fabbri et al. 2009), the BS continuous energy spectrum is associated with low resolution and poor quality imaging. Moreover, the nature of its energy spectrum compromises the accurate quantification of microsphere distribution, especially in small lesions. Although some methods have been developed for optimising BS SPECT images (Rong et al. 2012a, b), it is reasonable to assume that the higher the image resolution, the better the accuracy of microsphere distribution will be. In this respect, the PET scan offers images of better spatial resolution.

Although  $^{90}\text{Y}$  was discovered to have a low electron-positron pair emission (0.003 %) in 1955 (Ford 1955), it was not until 2009 when this pair production was used to assess the  $^{90}\text{Y}$  distribution by PET (Lhommel et al. 2009). Since then, several authors have demonstrated the increase of image resolution using PET that allows a better localization of microsphere deposition, that might even go

unnoticed on BS SPECT (Gupta et al. 2012; Kao et al. 2011, 2012). This better resolution provided by PET imaging increases one's confidence in the evaluation of intra- and extrahepatic  $^{90}\text{Y}$  microsphere location. Moreover, these high-resolution images may allow an easy assessment of the absorbed dose delivered in  $^{90}\text{Y}$  RE (D'Arienzo et al. 2012; Lhommel et al. 2010). Although it was shown that routine PET scanners can produce good-quality  $^{90}\text{Y}$  images, further studies are needed to determine which reconstruction methods and acquisition parameters should be used (van Elmbt et al. 2011).

## 4 Future Directions

### 4.1 Positron-Emitting Radionuclide-Labelled Microspheres for Pre-treatment Assessment

A new resin-based microsphere with a rapid, efficient and simple radiolabelling process using  $^{18}\text{F}$  has been developed to serve as a surrogate for the treatment microsphere in a rabbit model (Selwyn et al. 2007). However, a major drawback for its clinical application is the microembolisation generated by these nonabsorbable particles. To prevent this, other types of particles with specific characteristics (size in the range of  $^{90}\text{Y}$ -microspheres, resorbable, prevent damage to the vascular endothelium, non-aggregated, etc.), such as serum albumin microspheres, could be used and labelled with pure positron-emitting radionuclides (Maziere et al. 1986).

It has been recently reported that  $^{18}\text{F}$ -MAA could be an ideal PET imaging surrogate for  $^{99\text{m}}\text{Tc}$ -MAA for clinical PET applications (Wu et al. 2012). In this pre-clinical study, an excellent correlation between  $^{18}\text{F}$ -MAA and  $^{99\text{m}}\text{Tc}$ -MAA has been demonstrated in their distribution within the tumour, liver and lungs, as well as in the tumour-to-liver and tumour-to-lung ratios. Therefore, PET imaging using  $^{18}\text{F}$ -MAA would allow a more accurate methodology for  $^{90}\text{Y}$ -RE dosimetry.

#### 4.2 Combined Positron-Emitting Radionuclides and $^{90}\text{Y}$ -Labelled Microspheres for Post-treatment Monitorization

An accurate evaluation of the actual post-implantation distribution of  $^{90}\text{Y}$ -microspheres is difficult to achieve due to the physical characteristics of  $^{90}\text{Y}$ . BS image quality is poor and the promising  $^{90}\text{Y}$ -PET image depends on the tomograph characteristics (spatial resolution, scintillation crystals, and advanced reconstruction techniques such as time-of-flight) (van Elmbt et al. 2011).

To determine the possible correlation between microsphere location and clinical outcome, an accurate biodistribution assessment should be performed after treatment. An attempt to improve the visualisation of post-implanted microspheres has been developed by injecting  $^{99\text{m}}\text{Tc}$ -MAA and  $^{90}\text{Y}$ -microspheres simultaneously in patients who underwent RE (Bagni et al. 2012).  $^{99\text{m}}\text{Tc}$ -MAA SPECT and a  $^{90}\text{Y}$ -PET were performed after treatment and compared with the pre-treatment FDG-PET (used as reference). The results showed that the  $^{90}\text{Y}$ -PET images were more accurate than  $^{99\text{m}}\text{Tc}$ -MAA SPECT imaging.

Despite these findings,  $^{90}\text{Y}$ -PET images can be improved by using a pure positron emitter radionuclide such as  $^{68}\text{Ga}$  or  $^{18}\text{F}$ . In a pre-clinical study performed at our institution, decayed  $^{90}\text{Y}$ -microspheres were radiolabelled with  $^{18}\text{F}$ . A dose of double-radiolabelled  $^{18}\text{F}/^{90}\text{Y}$ -microspheres was injected intravenously in rats, and a microPET acquisition was performed. In our experience, the radiolabelled  $^{18}\text{F}$ -microspheres permitted higher quality PET images to be obtained after adding a small quantity of these to the  $^{90}\text{Y}$ -microspheres, thus increasing the sensitivity and reflecting their actual distribution (Sánchez-Martínez et al. 2012).

$^{90}\text{Y}$  RE dosimetric techniques should enable improved accuracy in different areas like delineation of arterial territory target volumes, microparticle simulation and biodistribution assessment, and predictive radiation dose-response modelling. The future development of positron-labelled microspheres instead of  $^{99\text{m}}\text{Tc}$ -MAA could improve the accuracy of LS calculations and the simulation of liver microsphere biodistribution. It could also improve

predictive radiation modelling by voxel- or Monte-Carlo-based techniques (Gulec et al. 2010).

$^{90}\text{Y}$  RE will also benefit from a wealth of developmental work stemming from radiobiological models based on external-beam radiation therapy (e.g. linear quadratic model and normal tissue complication probability model). Moreover, radiation-planning techniques (e.g. dose-volume histogram) can be meaningfully translated into radionuclide dosimetry models (e.g. MIRD) and vice versa. Application of the concept of biologically effective dose to  $^{90}\text{Y}$  RE dosimetry might help achieve this aim (Cremonesi et al. 2008).

#### References

- Ahmadzadehfar H, Sabet A, Biermann K, Muckle M, Brockmann H, Kuhl C, Wilhelm K, Biersack HJ, Ezziddin S (2010) The significance of  $^{99\text{m}}\text{Tc}$ -MAA SPECT/CT liver perfusion imaging in treatment planning for  $^{90}\text{Y}$ -microsphere selective internal radiation treatment. *J Nucl Med* 51(8):1206–1212
- Ahmadzadehfar H, Muckle M, Sabet A, Wilhelm K, Kuhl C, Biermann K, Haslerud T, Biersack HJ, Ezziddin S (2011) The significance of bremsstrahlung SPECT/CT after yttrium-90 radioembolization treatment in the prediction of extrahepatic side effects. *Eur J Nucl Med Mol Imaging* 39:309–315
- Ahmadzadehfar H, Sabet A, Meyer C, Habibi E, Biersack HJ, Ezziddin S (2012) The importance of  $^{99\text{m}}\text{Tc}$ -MAA SPECT/CT for therapy planning of radioembolization in a patient treated with bevacizumab. *Clin Nucl Med* 37(11):1129–1130
- Bagni O, D'Arienzo M, Chiamida P, Chiacchiararelli L, Cannas P, D'Agostini A, Cianni R, Salvatori R, Scopinaro F (2012)  $^{90}\text{Y}$ -PET for the assessment of microsphere biodistribution after selective internal radiotherapy. *Nucl Med Commun* 33(2):198–204
- Bilbao JI, Garrastachu P, Herráiz MJ, Rodríguez M, Inarraiaegui M, Rodríguez J, Hernández C, de la Cuesta AM, Arbizu J, Sangro B (2010) Safety and efficacy assessment of flow redistribution by occlusion of intrahepatic vessels prior to radioembolization in the treatment of liver tumors. *Cardiovasc Interv Radiol* 33(3):523–531
- Campbell JM, Wong CO, Muzik O, Marples B, Joiner M, Burmeister J (2009) Early dose response to yttrium-90 microsphere treatment of metastatic liver cancer by a patient-specific method using single photon emission computed tomography and positron emission tomography. *Int J Radiat Oncol Biol Phys* 74(1):313–320
- Carretero C, Munoz-Navas M, Betes M, Angos R, Subtil JC, Fernandez-Urien I, De la Riva S, Sola J, Bilbao JI, de Luis E (2007) Gastroduodenal injury after radioembolization of hepatic tumors. *Am J Gastroenterol* 102(6):1216–1220
- Covey AM, Brody LA, Maluccio MA, Getrajdman GI, Brown KT (2002) Variant hepatic arterial anatomy revisited: digital subtraction angiography performed in 600 patients. *Radiology* 224(2):542–547
- Cremonesi M, Ferrari M, Bartolomei M, Orsi F, Bonomo G, Aricò D, Mallia A, De Cicco C, Pedroli G, Paganelli G (2008) Radioembolisation with  $^{90}\text{Y}$ -microspheres: dosimetric and radiobiological investigation for multi-cycle treatment. *Eur J Nucl Med Mol Imaging* 35(11):2088–2096
- D'Arienzo M, Chiamida P, Chiacchiararelli L, Coniglio A, Cianni R, Salvatori R, Ruzza A, Scopinaro F, Bagni O (2012)  $^{90}\text{Y}$  PET-based dosimetry after selective internal radiotherapy treatments. *Nucl Med Commun* 33(6):633–640



- Dancey JE, Shepherd FA, Paul K, Sniderman KW, Houle S, Gabrys J, Hendler AL, Goin JE (2000) Treatment of nonresectable hepatocellular carcinoma with intrahepatic  $^{90}\text{Y}$ -microspheres. *J Nucl Med* 41(10):1673–1681
- Even-Sapir E, Keidar Z, Bar-Shalom R (2009) Hybrid imaging (SPECT/CT and PET/CT)—improving the diagnostic accuracy of functional/metabolic and anatomic imaging. *Sem Nucl Med* 39:264–275
- Fabbri C, Sarti G, Cremonesi M, Ferrari M, Dia AD, Agostini M, Botta F, Paganelli G (2009) Quantitative analysis of  $^{90}\text{Y}$  bremsstrahlung SPECT-CT images for application to 3D patient-specific dosimetry. *Cancer Biother Radiopharm* 24(1):145–154
- Flamen P, Vanderlinden B, Delatte P, Ghanem G, Ameye L, Van Den Eynde M, Hendlitz A (2008) Multimodality imaging can predict the metabolic response of unresectable colorectal liver metastases to radioembolization therapy with yttrium-90 labeled resin microspheres. *Phys Med Biol* 53(22):6591–6603
- Ford KW (1955) Predicted 0+ level in  $^{40}\text{Zr}^{90}$ . *Phys Rev* 98:1516–1517
- Garin E, Lenoir L, Rolland Y, Edeline J, Mesbah H, Laffont S, Poree P, Clement B, Raoul JL, Boucher E (2012) Dosimetry based on  $^{99\text{m}}\text{Tc}$ -macroaggregated albumin SPECT/CT accurately predicts tumor response and survival in hepatocellular carcinoma patients treated with  $^{90}\text{Y}$ -loaded glass microspheres: preliminary results. *J Nucl Med* 53(2):255–263
- Garin E, Rolland Y, Lenoir L, Pracht M, Mesbah H, Poree P, Laffont S, Clement B, Raoul JL, Boucher E (2011) Utility of quantitative  $^{99\text{m}}\text{Tc}$ -MAA SPECT/CT for yttrium-labelled microsphere treatment planning: calculating vascularized hepatic volume and dosimetric approach. *Int J Mol Imaging*. doi:10.1155/2011/398051
- Giammarile F, Bodei L, Chiesa C, Flux G, Forrer F, Kraeber-Bodere F, Brans B, Lambert B, Konijnenberg M, Borson-Chazot F et al (2011) EANM procedure guideline for the treatment of liver cancer and liver metastases with intra-arterial radioactive compounds. *Eur J Nucl Med Mol Imaging* 38(7):1393–1406
- Gulec SA, Mesoloras G, Dezarn WA, McNeillie P, Kennedy AS (2007) Safety and efficacy of  $^{90}\text{Y}$ -microsphere treatment in patients with primary and metastatic liver cancer: the tumor selectivity of the treatment as a function of tumor to liver flow ratio. *J Transl Med* 5:15
- Gulec S, Szejnberg M, Siegel J (2010) Hepatic structural dosimetry in  $^{90}\text{Y}$  microsphere treatment: a monte carlo modeling approach based on lobular microanatomy. *J Nucl Med* 51:301–310
- Gupta A, Gill A, Shrikanth S, Srinivas S (2012) Nontargeted  $^{90}\text{Y}$ -microsphere radioembolization to duodenum visualized on  $^{90}\text{Y}$ -PET/CT and bremsstrahlung SPECT/CT. *Clin Nucl Med* 37:98–99
- Hamami ME, Poepfel TD, Müller S, Heusner T, Bockisch A, Hilgard P, Antoch G (2009) SPECT/CT with  $^{99\text{m}}\text{Tc}$ -MAA in radioembolization with  $^{90}\text{Y}$  microspheres in patients with hepatocellular cancer. *J Nucl Med* 50:688–692
- Haug AR, Heinemann V, Bruns CJ, Hoffmann R, Jakobs T, Bartenstein P, Hacker M (2011)  $^{18}\text{F}$ -FDG PET independently predicts survival in patients with cholangiocellular carcinoma treated with  $^{90}\text{Y}$  microspheres. *Eur J Nucl Med Mol Imaging* 38:1037–1045
- Ho S, Lau W, Leung T, Chan M, Ngar Y, Johnson P, Li A (1996) Partition model for estimating radiation doses from yttrium-90 microspheres in treating hepatic tumours. *Eur J Nucl Med Mol Imaging* 23:947–952
- Jha AK, Zade AA, Rangarajan V, Purandare N, Shah SA, Agrawal A, Kulkarni SS, Shetty N (2012) Comparative analysis of hepatopulmonary shunt obtained from pretherapy  $^{99\text{m}}\text{Tc}$  MAA scintigraphy and post-therapy  $^{90}\text{Y}$  bremsstrahlung imaging in  $^{90}\text{Y}$  microsphere therapy. *Nucl Med Commun* 33:486–490
- Kao YH, Tan EH, Ng CE, Goh SW (2011) Yttrium-90 time-of-flight PET/CT is superior to bremsstrahlung SPECT/CT for post-radioembolization imaging of microsphere biodistribution. *Clin Nucl Med* 36(12):186–187
- Kao YH, Tan AEH, Burgmans MC, Irani FG, Khoo LS, Lo RHG, Tay KH, Tan BS, Chow PKH, Ng DCE (2012) Image-guided personalized predictive dosimetry by artery-specific SPECT/CT partition modeling for safe and effective  $^{90}\text{Y}$  radioembolization. *J Nucl Med* 53(4):559–566
- Kennedy A, Nag S, Salem R, Murthy R, McEwan AJ, Nutting C, Benson A, Espat J, Bilbao JI, Sharma RA (2007) Recommendations for radioembolization of hepatic malignancies using yttrium-90 microsphere brachytherapy: a consensus panel report from the radioembolization brachytherapy oncology consortium. *Int J Radiat Oncol Biol Phys* 68(1):13–23
- Kennedy AS, McNeillie P, Dezarn WA, Nutting C, Sangro B, Wertman D, Garafalo M, Liu D, Coldwell D, Savin M et al (2009) Treatment parameters and outcome in 680 treatments of internal radiation with resin  $^{90}\text{Y}$ -microspheres for unresectable hepatic tumors. *Int J Radiat Oncol Biol Phys* 74(5):1494–1500
- Kennedy A, Coldwell D, Sangro B, Wasan H, Salem R (2012) Radioembolization for the treatment of liver tumors: general principles. *Am J Clin Oncol* 35(1):91–99
- Knesaurek K, Machac J, Muzinic M, DaCosta M, Zhang Z, Heiba S (2010) Quantitative comparison of yttrium-90 ( $^{90}\text{Y}$ )-microspheres and technetium-99 m ( $^{99\text{m}}\text{Tc}$ )-macroaggregated albumin SPECT images for planning  $^{90}\text{Y}$  therapy of liver cancer. *Technol Cancer Res Treat* 9(3):253–262
- Lambert B, Mertens J, Sturm EJ, Stienaers S, Defreyne L, D'Asseler Y (2010)  $^{99\text{m}}\text{Tc}$ -labelled macroaggregated albumin (MAA) scintigraphy for planning treatment with  $^{90}\text{Y}$  microspheres. *Eur J Nucl Med Mol Imaging* 37(12):2328–2333
- Lau W, Leung T, Ho S, Chan M, Leung N, Lin J, Metreweli C, Li A (1994) Diagnostic pharmaco-scintigraphy with hepatic intraarterial technetium-99m macroaggregated albumin in the determination of tumour to non-tumour uptake ratio in hepatocellular carcinoma. *Br J Radiol* 67(794):136–139
- Lau WY, Kennedy AS, Kim YH, Lai HK, Lee RC, Leung TW, Liu CS, Salem R, Sangro B, Shuter B et al (2012) Patient selection and activity planning guide for selective internal radiotherapy with yttrium-90 resin microspheres. *Int J Radiat Oncol Biol Phys* 82(1):401–407
- Lenoir L, Edeline J, Rolland Y, Pracht M, Raoul JL, Ardisson V, Bourguet P, Clement B, Boucher E, Garin E (2012) Usefulness and pitfalls of MAA SPECT/CT in identifying digestive extrahepatic uptake when planning liver radioembolization. *Eur J Nucl Med Mol Imaging* 39(5):872–880
- Leong QM, Lai HK, Lo RG, Teo TK, Goh A, Chow PK (2009) Radiation dermatitis following radioembolization for hepatocellular carcinoma: a case for prophylactic embolization of a patent falciiform artery. *J Vasc Interv Radiol* 20(6):833–836
- Leung WT, Lau WY, Ho SK, Chan M, Leung NW, Lin J, Metreweli C, Johnson PJ, Li AK (1994) Measuring lung shunting in hepatocellular carcinoma with intrahepatic-arterial technetium-99m macroaggregated albumin. *J Nucl Med* 35(1):70–73
- Leung TW, Lau WY, Ho SK, Ward SC, Chow JH, Chan MS, Metreweli C, Johnson PJ, Li AK (1995) Radiation pneumonitis after selective internal radiation treatment with intraarterial  $^{90}\text{Y}$ -microspheres for inoperable hepatic tumors. *Int J Radiat Oncol Biol Phys* 33(4):919–924
- Lhommel R, Goffette P, Van den Eynde M, Jamar F, Pauwels S, Bilbao JI, Walrand S (2009) Yttrium-90 TOF PET scan demonstrates high-resolution biodistribution after liver SIRT. *Eur J Nucl Med Mol Imaging* 36(10):1696

- Lhommel R, van Elmbt L, Goffette P, Van den Eynde M, Jamar F, Pauwels S, Walrand S (2010) Feasibility of  $^{90}\text{Y}$  TOF PET-based dosimetry in liver metastasis therapy using SIR-spheres. *Eur J Nucl Med Mol Imaging* 37(9):1654–1662
- Maziere B, Loc'h C, Steinling M, Comar D (1986) Stable labelling of serum albumin microspheres with gallium-68. *Int J Radiat Appl Instrum Part A Appl Radiat Isot* 37(4):360–361
- Murthy R, Nunez R, Szklaruk J, Erwin W, Madoff DC, Gupta S, Ahrar K, Wallace MJ, Cohen A, Coldwell DM (2005) Yttrium-90 microsphere therapy for hepatic malignancy: devices, indications, technical considerations, and potential complications. *Radiographics* 25(Suppl 1):S41–S55
- Riaz A, Lewandowski RJ, Kulik LM, Mulcahy MF, Sato KT, Ryu RK, Omary RA, Salem R (2009) Complications following radioembolization with yttrium-90 microspheres: a comprehensive literature review. *J Vasc Interv Radiol* 20(9):1121–1130
- Rodríguez-Fraile M, Arbizu J, Iñárraegui M, Martí-Climent J, Quincoces G, Garrastachu P, Domínguez I, Peñuelas I, Sangro B, Richter J (2008) Evaluation of  $^{99\text{m}}\text{Tc}$ -MAA SPECT as a biomarker of liver tumor response to radioembolization with  $^{90}\text{-yttrium}$ . *Eur J Nucl Med Mol Imaging* 35(Suppl 2):S278
- Rong X, Du Y, Frey EC (2012a) A method for energy window optimization for quantitative tasks that includes the effects of model-mismatch on bias: application to  $^{90}\text{Y}$  bremsstrahlung SPECT imaging. *Phys Med Biol* 57:3711–3725
- Rong X, Du Y, Ljungberg M, Rault E, Vandenberghe S, Frey EC (2012b) Development and evaluation of an improved quantitative  $^{90}\text{Y}$  bremsstrahlung SPECT method. *Med Phys* 39:2346–2358
- Sabet A, Ahmadzadehfard H, Muckle M, Haslerud T, Wilhelm K, Biersack HJ, Ezziddin S (2011) Significance of oral administration of sodium perchlorate in planning liver-directed radioembolization. *J Nucl Med* 52:1063–1067
- Salem R, Thurston KG (2006) Radioembolization with  $^{90}\text{yttrium}$  microspheres: a state-of-the-art brachytherapy treatment for primary and secondary liver malignancies: Part 1: Technical and methodologic considerations. *J Vasc Interv Radiol* 17:1251–1278
- Sánchez-Martínez M, Colantes M, Rodríguez-Fraile M, Domínguez-Prado I, Vidal A, Iñárraegui M, Bilbao J, Sangro B, Peñuelas I (2012) Fluorine-18 radiolabelling of SIR-spheres as biodistribution surrogate of radiospheres treatment: in vivo micro-PET and in vitro stability studies. *Eur J Nucl Med Mol Imaging* 39 (Suppl 2):S-168
- Selwyn R, Avila-Rodríguez M, Converse A, Hampel J, Jaskowiak C, McDermott J, Warner T, Nickles R, Thomadsen B (2007)  $^{18}\text{F}$ -labeled resin microspheres as surrogates for  $^{90}\text{Y}$  resin microspheres used in the treatment of hepatic tumors: a radiolabeling and PET validation study. *Phys Med Biol* 52:7397–7408
- Van de Wiele C, Maes A, Brugman E, D'Asseler Y, De Spiegeleer B, Mees G, Stellamans K (2012) SIRT of liver metastases: physiological and pathophysiological considerations. *Eur J Nucl Med Mol Imaging* 39:1646–1655
- van Elmbt L, Vandenberghe S, Walrand S, Pauwels S, Jamar F (2011) Comparison of yttrium-90 quantitative imaging by TOF and non-TOF PET in a phantom of liver selective internal radiotherapy. *Phys Med Biol* 56:6759–6777
- Wu SY, Kuo JW, Chang TK, Liu RS, Lee RC, Wang SJ, Lin WJ, Wang HE (2012) Preclinical characterization of  $^{18}\text{F}$ -MAA, a novel PET surrogate of  $^{99\text{m}}\text{Tc}$ -MAA. *Nucl Med Biol* 39:1026–1033
- Yorke ED, Jackson A, Rosenzweig KE, Braban L, Leibel SA, Ling CC (2005) Correlation of dosimetric factors and radiation pneumonitis for non-small-cell lung cancer patients in a recently completed dose escalation study. *Int J Radiat Oncol Biol Phys* 63:672–682
- Yu N, Srinivas SM, Difilippo FP, Shrikanthan S, Levitin A, McLennan G, Spain J, Xia P, Wilkinson A (2013) Lung dose calculation with SPECT/CT for  $^{90}\text{Y}$  yttrium radioembolization of liver cancer. *Int J Radiat Oncol Biol Phys* 85:834–839

---

# Radiological Detection and Assessment of Tumor Response

Tobias F. Jakobs

## Contents

<b>1</b>	<b>Introduction</b> .....	77
<b>2</b>	<b>Methods of Assessment</b> .....	78
2.1	WHO and RECIST 1.1 .....	78
2.2	EASL criteria and mRECIST (for Hepatocellular Carcinoma).....	79
2.3	Alternative Measurements.....	81
<b>3</b>	<b>Imaging</b> .....	81
3.1	Dual-Modality Positron Emission Tomography/Computed Tomography.....	82
3.2	Whole-Body Magnetic Resonance Imaging.....	82
<b>4</b>	<b>Discussion</b> .....	83
4.1	Detection of Liver Metastases .....	83
4.2	Follow-up of Recurrent Metastatic Disease .....	85
4.3	PET or PET-CT .....	85
4.4	What does MRI add? .....	86
<b>5</b>	<b>Outlook</b> .....	87
<b>6</b>	<b>Conclusion</b> .....	88
	<b>References</b> .....	88

---

## 1 Introduction

The liver is the most common site of metastatic spread in malignancies. In autopsy studies, the incidence of hepatic metastases is up to 100 % dependent on the primary tumor. Even if this fact represents the final status of a malignancy, about half of all patients dying from a malignant disease will have apparent hepatic metastases. The risk of developing hepatic metastases varies widely among different types of primary malignancy.

In the case of predominant metastatic spread to the liver, the long-term survival is mostly determined by the extent of this particular tumor manifestation.

Presently, numerous palliative hepatic-directed therapies are available for the treatment of nonresectable liver tumors, including conformal radiation therapy, Yttrium-90 microsphere embolization, hepatic arterial infusion chemotherapy, isolated hepatic chemoperfusion, transarterial chemoembolization, radiofrequency- or microwave-ablation, irreversible electroporation, percutaneous brachytherapy, and combinations of these treatments.

Therefore, reliable tumor assessment with high diagnostic accuracy is a fundamental precondition for selecting the appropriate therapy and is indispensable for assessing patient's response to treatment. Consequently, applied diagnostic methods should be as sensitive and specific as possible. An effective treatment of hepatic tumors is crucial for improved survival outcome. So far, a complete evaluation of tumor spread in patients with advanced cancer requires various imaging procedures, such as computed tomography (CT), magnetic resonance imaging (MRI), ultrasound, radiography, radiographic skeletal survey, and bone scintigraphy. This approach is time-consuming, inconvenient for the patient, and expensive and can miss lesions outside the fields of study.

Recently, whole-body (WB) imaging modalities like dual-modality positron emission tomography (PET)/CT and WB MRI have been introduced and offer a complete head-to-toe coverage of the patient in a single examination with

---

T. F. Jakobs (✉)  
Department of Diagnostic and Interventional Radiology,  
Hospital Barmherzige Brüder,  
Romanstr. 93, 80639 Munich, Germany  
e-mail: tobias.jakobs@barmherzige-muenchen.de

**Table 1** Summary of the most widely used criteria for the assessment of tumor response

Category	RECIST	RECIST 1.1	mRECIST	WHO	EASL
CR (complete response)	Disappearance of all target lesions (up to five measurable liver lesions)	Disappearance of all target lesions (up to two measurable liver lesions)	Disappearance of any intra tumoral arterial enhancement in all target lesions (up to two measurable liver lesions)	Complete disappearance of all target lesions	Disappearance of any intratumoral enhancement in all lesions
PR (partial response)	30 % decrease in the sum of the greatest diameter of target lesions	At least 30 % decrease in the sum of the greatest unidimensional diameters of target lesions, compared to baseline	At least a 30 % decrease in the sum of unidimensional diameters of viable (arterially enhancing) target lesion, compared to baseline	At least 50 % decrease in tumor size	At least 50 % decrease in the sum of the product of bidimensional diameters of viable (arterially enhancing) target lesions
SD (stable disease)	Meets neither PR nor PD criteria	Meets neither PR nor PD criteria	Meets neither PR nor PD criteria	Meets neither PR nor PD criteria	Meets neither PR nor PD criteria
PD (progressive disease)	20 % increase in the sum of the greatest diameter of target lesions	An increase of at least 20 % in the sum of the diameters of target lesions, compared to baseline	An increase of at least 20 % in the sum of the diameters of viable (enhancing) target lesions, compared to baseline	>25 % increase of at least 1 lesion or a new lesion	An increase of at least 25 % in the sum of the diameters of viable (enhancing) target lesions

an accurate and sensitive detection of tumor spread (Antoch et al. 2003; Pfannenbergl et al. 2007; Schmidt et al. 2005).

## 2 Methods of Assessment

The response evaluation criteria in solid tumors (RECIST) (Therasse et al. 2000), the new RECIST (RECIST 1.1) (Eisenhauer et al. 2009), the world health organisation (WHO) method (Miller et al. 1981) as well as the European association for the study of the liver (EASL) (Bruix et al. 2001) and the modified RECIST (mRECIST) (Lencioni and Llovet 2010; Llovet et al. 2008) criteria define standard measurement methods for converting visual image observations into a quantitative and statistically tractable framework for measuring tumor size response to therapy. Although the WHO method was first developed for radiography and CT, it was modified in the RECIST publication to make measurement practices procedurally more consistent across multiple trials and accommodate improvements in CT and MRI technology. Both methods offer simple approaches to determining anatomic size and time-evolving lesion-changes during treatment as an indicator of response. Each method uses a pragmatically simplistic technique dependent on observer judgment of lesion boundaries. WHO defines its tumor measurement by summing a group of individual masses, each lesion of which is assessed by the cross product of its greatest diameter and largest perpendicular diameter. RECIST was designed to be sufficiently

aligned with WHO practices such that no major discrepancy would occur in the concept of partial response (PR) between the old and new guidelines. Recently, a revised version of the RECIST guidelines (RECIST 1.1) has been published (Eisenhauer et al. 2009). Major changes compared to the former RECIST criteria include: the number of lesions to be assessed—the number of lesions required to assess tumor burden for response determination has been reduced from a maximum of 10 to 5 total (and from five to two per organ, maximum). Furthermore, the assessment of pathological lymph nodes has been incorporated once the short axis exceeds 15 mm in diameter. Disease progression has been clarified regarding several aspects: in addition to the former definition of progression in target disease of 20 % increase in sum, a 5 mm absolute increase is now required as well to guard against overcalling progressive disease (PD) when the total sum is small. Additionally, a section focussing on the interpretation of [18F]-fluoro-2-deoxy-D-glucose (FDG)-PET imaging assessment has been included. Table 1 provides a clearly understandable overview defining response classification according to RECIST, RECIST 1.1, mRECIST, WHO, and EASL criteria (Table 1).

### 2.1 WHO and RECIST 1.1

Once target lesions (up to five per organ, WHO; up to 2 per organ, RECIST 1.1) are measured using either single linear summation (RECIST 1.1) or the bilinear product approach



WHO, the results are subsequently assigned to response-defined categories of complete response (CR), PR, stable disease (SD), and PD. By somewhat arbitrary decision making, mRECIST defined PR as a more than 30 % linear decrease of the linear sums of the target lesions (thus, by extrapolation, implying a 65 % volumetric decrease) and PD as a more than 20 % increase (implying a 73 % volumetric increase) with at least a 5 mm increase of lesions size. This contrasted with WHO criteria, in which those boundaries are set volumetrically at 65 and 40 %, respectively.

### 2.1.1 Advantages of WHO and RECIST

As a simply implemented procedure, RECIST has both its advocates and critics. Publications both supportive and critical can be cited in the scientific literature (James et al. 1999; Mazumdar et al. 2004; Park et al. 2003). RECIST and WHO have their devotees as easily understood methods that allow simple ruler analysis of printed films as well as workstation use of electronic calipers to produce comprehensible results. Clinical imaging usually provides relative or mostly secondary trial end points, so mRECIST and WHO criteria provide pragmatically adequate tools that satisfy a noncritical role relative to other data and clinical outcome that take primacy. They are accommodating of a variety of imaging acquisition circumstances and place minimal added demand on routine clinical practices. In sum, they have been perceived as simple tools adequate to imaging's supportive role. To date, few widely available alternatives exist that are as easily executed or of provably greater benefit to justify further expense, time demands, or operational complexity (Tran et al. 2004).

### 2.1.2 Disadvantages of WHO and RECIST

As RECIST was framed in the context of individual slices, the research community is currently reexploring the obvious gaps in both RECIST and WHO criteria, which admittedly were constrained by the limits of earlier technology. To list the most obvious shortcomings, neither linear- nor bilinear-based methods address intratumor heterogeneity and its change over time, as it might occur after tumor-targeted therapy (e.g., Yttrium-90 microsphere embolization, radiofrequency ablation, etc.), nor do they reflect appropriate measures for tumor metabolism (Fig. 1). They do not incorporate multislice integrated understanding, register information about time-sequence change of shape or morphologic complexity, or address statistical uncertainties arising from low-intensity lesion edges. The techniques do not provide methodological distinctions between tumors of inherently high contrast compared with their surrounding tissue (e.g. lung), nor do they prescribe specific approaches to the use of contrast materials usually needed to enhance intra-abdominal soft tissue findings (Kamel and Bluemke 2002). Most importantly, little attention was paid to

acknowledge in the guidelines the inconsistencies inherent in the expert observer. The reader makes his/her measurements unassisted by anything other than the most rudimentary form of image processing technology (often simply the use of electronic calipers on a workstation display). Neither RECIST nor WHO provide especially rigorous guidance on the subject of observer variability aside from recommending review panels and independent observers. Disagreement among observers has been noted to be as high as 15–40 % in these contexts and may not be ideally remedied by consensus (Belton et al. 2003). Besides providing only nominal guidance on slice thickness, RECIST does not address at any length image acquisition components that inevitably result in significant lesion contrast differences within and between studies, such as lack of uniformity of machine settings for kVp (peak kilovolts) and mAs (milli-ampere seconds) in CT, and pulse sequences in MRI. As a simply adoptable, widely applicable method, posing no impediment to accrual from a wide range of CT and MRI sites, RECIST has served a useful historic purpose in grouping image data into the rough four-group response classifications (CR, PR, SD, and PD). But since diameter measurements are best determined on smoothly shaped, distinct tumor boundaries, an ideal circumstance encountered infrequently, measurement variability inherent in such judgments is not adequately reflected in the recorded data. Tumors with irregular or diffuse boundaries pose the most significant challenge to data extraction and are highly observer dependent. Indeed, tumor boundary distinctiveness varies on a disease- or organ-specific basis. Observer recognition of boundaries may be further complicated by necrosis-caused internal heterogeneity that permeates the tumor or expresses itself asymmetrically on the lesion edge. Especially in the liver, tumor boundary sharpness in both CT and MRI may be enhanced by injection of contrast agents. But contrast agent pharmacokinetics are variable, and image acquisition routines are often compromised because they are usually prescribed by time from contrast administration, rather than the more definitive, but harder to obtain, contrast arrival time within specific organs.

## 2.2 EASL criteria and mRECIST (for Hepatocellular Carcinoma)

Evaluation of response to treatment is a key aspect in cancer therapy. RECIST or WHO criteria are used in most oncology trials, but those criteria evaluate only uni or bidimensional tumor measurements and disregard the extent of necrosis, which is the target of all effective locoregional therapies, e.g., radioembolization. Therefore, the EASL guidelines recommended that assessment of tumor response should incorporate the reduction in viable tumor burden

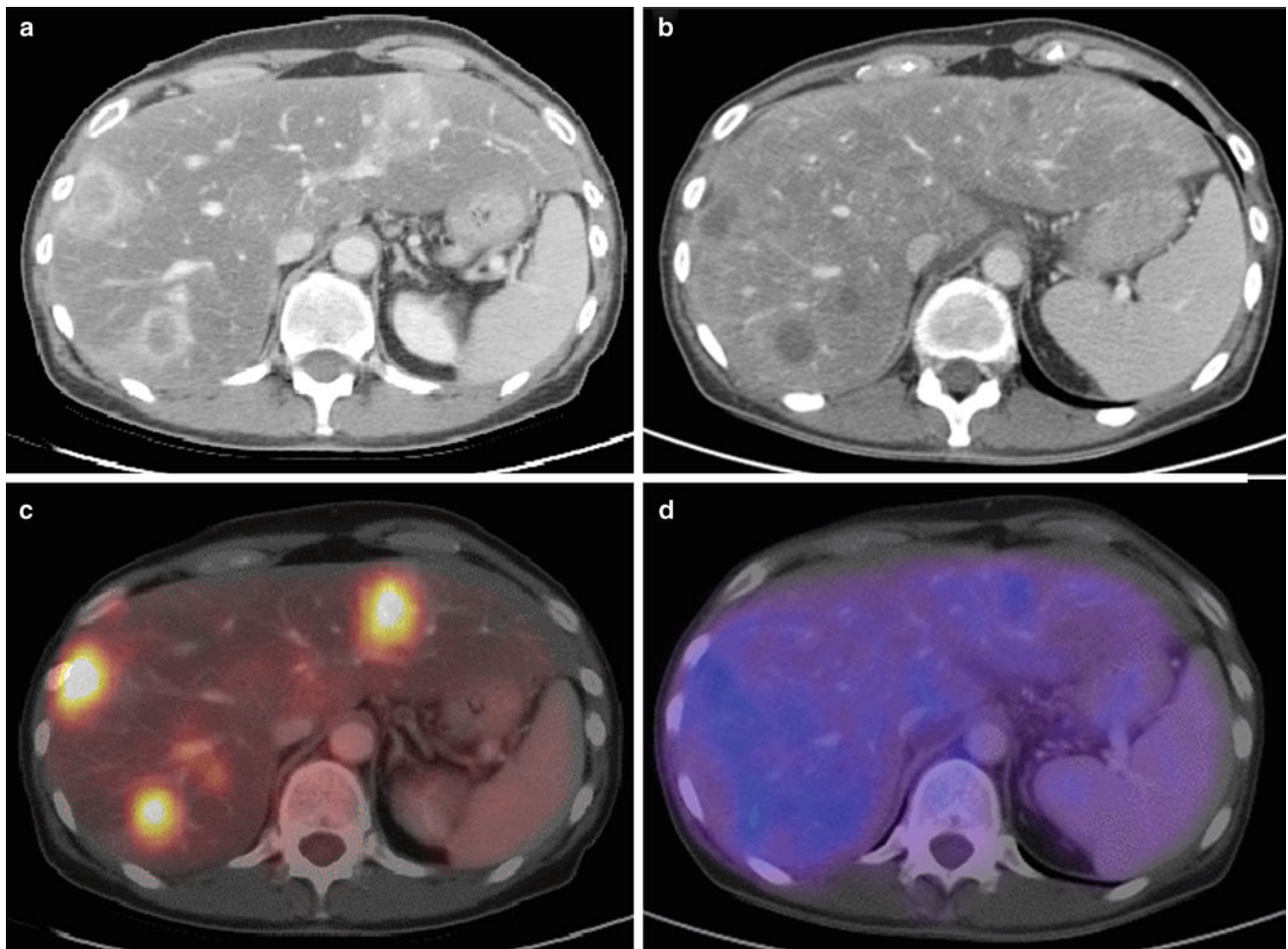


**Fig. 1** 47-year-old female patient with hepatic metastases from pancreatic cancer. Contrast-enhanced CT (a) shows multiple liver lesions with rim enhancement. The corresponding fused PET-CT image (c) demonstrates high FDG-uptake due to increased tumor metabolism. The CT scan 4 months after radioembolization (b) delineates

hypovascular tumor lesions without significant change concerning their size. According to RECIST, this displays the response category “stable disease”. The fused PET-CT image (d) proves that there is no increased tumor metabolism in the area of the former metastases, therefore indicating that this result represents a “complete remission”

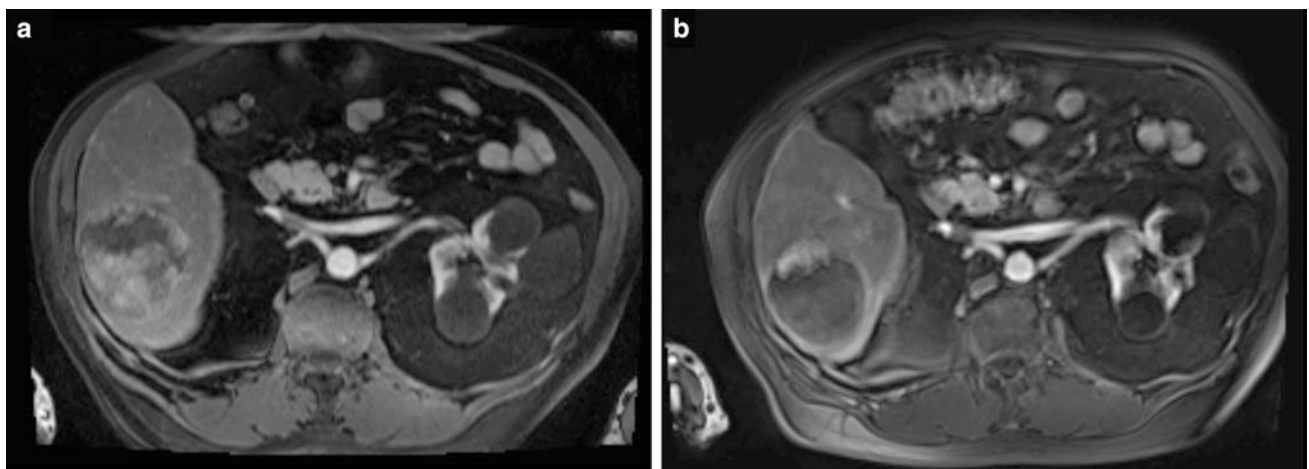


**Fig. 2** 78-year-old male patient with liver cirrhosis and a single HCC. Contrast-enhanced arterial phase MRI (a) shows a large (8 cm) hypervascular HCC before transarterial, loco regional treatment. Follow-up MRI (arterial phase) 6 weeks after treatment shows no significant shrinkage of the lesion but complete devascularization

(b) According to the RECIST, RECIST 1.1, and WHO criteria this would be characterized as “stable disease”, however, employing mRECIST or EASL criteria this would be reported as “partial response” since little nodular rim enhancement is noted

(Therasse et al. 2000; Eisenhauer et al. 2009; Bruix et al. 2001; Forner et al. 2009).

In EASL criteria, quantifying the amount of enhancing (and hence viable) tissue, CR is defined as the absence of any enhancing tissue (Fig. 2); PR is defined as  $\geq 50\%$  decrease in amount of enhancing tissue. SD is defined as  $< 50\%$  decrease in amount of enhancing tissue (Bruix et al. 2001). According to this also the mRECIST criteria (mRECIST) take the arterial enhancement of tumoral tissue before and after (locoregional) treatment into account. CR is defined as complete disappearance of any intratumoral arterial enhancement in all target lesions, PR as at least 30% decrease in the sum of the diameters of the viable (enhancement in arterial phase imaging) target lesions, PD as at least 20% increase in the sum of the diameters of viable (enhancing) target lesions, and SD are any cases that do not qualify for either PR or PD. Recent publications indicate that these enhancement models more accurately help to predict long-term survival in hepatocellular carcinoma (HCC) patients treated by transarterial means (Shim et al. 2012).

### 2.3 Alternative Measurements

Technological advances in tomographic scanners, both CT and MRI, have been unrelenting. In the span of less than a decade, CT scanners have advanced from single-detector arrays that scanned body segments in more than a minute (thus nearly always subject to motion artifacts), to present-day instruments with two simultaneous X-ray sources, 128 detector arrays, submillimeter voxel resolution, and motion-resistant body-segment acquisition speed of less than 10 s. These have been matched by post-processing display improvements that provide real-time visualization from any arbitrary (multiplanar) view. Image processing based on voxel intensity neighborhoods is sufficiently commonplace that near immediate three-dimensional (3D) display of selected organs or the entire body are an expected part of conventional image reconstruction routines. In reality though, the advantages of tomography that offers submillimeter, isovolumetric imaging has yet to be fully absorbed into routine diagnostic practice, not to mention exploited for its potential to enhance the measurement processes in cancer patient's follow-up. Most clinical trial tomographic imaging is still conducted at slice thicknesses of 5 or 7 mm in the intuitive conviction that those parameters are sufficient for the task required and for the convenience of the observer, who does not wish to be burdened by a vast number of images.

The availability of potentially more accurate and reproducible tumor volume data could motivate a re-examination of the foundations of the established categories of CR, PR, SD, and PD. RECIST, as it does not specify WB imaging at

the time of each evaluation which may register conclusions that fail to account for nonimaged parts of the body. Assignment to CR, PR, etc. in following an abdominal malignancy could be misleading if there is not apparent presence of nonimaged metastases in lung or brain when those body regions were not prescribed in the protocol. Imaging techniques that are WB oriented, like PET, combined PET-CT, and WB MRI, thus have advantages from this perspective. RECIST addresses this possibility by acknowledging that events that can occur in the nonmeasurable targets, such as the growth of nonmeasurable lesions or the appearance of new lesions despite unchanged size of target lesions. In these circumstances, RECIST mandates a classification shift from SD to PD. But these body regions must first be imaged in order to trigger those rules. Image processing algorithms, mathematically and globally operating in true 3D data space, as exemplified by techniques known as autocontouring, region growing, nearest neighbor, annealing, gradient following, water shed, and statistical modeling, have been effective in a variety of scientific fields. They hold sufficient promise to deserve an opportunity to contribute to oncology. It is evident from image processing's operational sphere that it is powered by mathematical approaches far exceeding the innate comprehension capacity of human observers. These sophisticated tools have already made key contributions to advances in medical image reconstruction and are the cornerstone of the remarkable anatomic detail we usually take for granted in our clinical environment.

Efforts to develop reproducible methods for measuring volumes of infiltrative tumors that lack clear margins, already recognized as a serious problem for linear and two-dimensional area measurement. Pathologic or histologic validation is unlikely to be clinically practicable. Given that ultimate validation is difficult, the mere task of generating a convincing test, whether precise or statistical, to compare alternative algorithms poses a challenge. In the past it has been convenient to accept expert consensus, despite the obvious flaw of relying on human opinion as a gold standard.

Promising recent developments for validation might be inferred from data derived from coregistration of MRI and CT images or PET-CT, which permit 3D anatomic CT to be combined with simultaneous tumor metabolic activity from the PET in fused, spatially registered images. This might be a first step in a path toward more rigorous validation.

---

## 3 Imaging

In heavily pretreated patients with known malignancy, possible further therapeutic strategies depend on the stage of disease, liver involvement, and whether multiple organ systems have been affected. In the past, patients had to undergo a variety of different diagnostic procedures to

achieve a comprehensive staging or screening, including imaging studies such as ultrasonography, CT, MRI, PET, and X-ray examinations. The combination of these procedures is often time-consuming and inconvenient for the patient. Thus, a single imaging examination providing information of different organ systems (ideally of the entire body) would be of great interest.

Due to the mentioned limitations of conventional tomographic imaging (CT and MRI) in assessing the tumor response after tumor-targeted therapy like Yttrium-90 radioembolization, some studies have suggested that PET or PET-CT represent valuable tools in assessing tumor response (Selzner et al. 2004; Wong et al. 2002, 2004, 2005). As described before, anatomic imaging by CT or MRI is more or less insensitive in correctly determining tumor response by simply measuring the change in diameters because of the presence of central necrosis, edema, cystic changes, and hemorrhage. Given the lack of reliability of tumor markers (where applicable) in the presence of extrahepatic tumor manifestation, PET appears to be an excellent adjunct to define response after regional treatment of liver metastases (Barker et al. 2005).

### 3.1 Dual-Modality Positron Emission Tomography/Computed Tomography

Whole-body PET using FDG is an imaging modality enabling detection of cancerous disease by tracing increased accumulation of FDG in tumor tissue. The introduction of combined PET-CT scanners has made a new modality available for WB imaging, combining the functional data of PET with the detailed anatomical information of CT imaging in a single examination (Beyer et al. 2000).

[18F]-fluoro-2-deoxy-D-glucose-PET provides a functional metabolic map of glucose uptake in the WB. FDG is a glucose analogue that is labeled with the positron emitting radioisotope fluorine-18 that is produced by a cyclotron. The resulting radiopharmaceutical agent F-18 FDG is taken up by metabolically active tumor cells using facilitated transport similar to that used by glucose. The rate of uptake of FDG by tumor cells is proportional to their metabolic activity. Since FDG is a radiopharmaceutical analog of glucose, it also undergoes phosphorylation to form FDG-6-phosphate like glucose. However, unlike glucose, it does not undergo further metabolism, thereby becoming “trapped” in metabolically active cells (Kapoor et al. 2004). In general, PET is limited by poor anatomic detail, and therefore, anatomical correlation with some other form of imaging, such as CT, is desirable for differentiating normal from abnormal radiotracer uptake and accurate lesion localization.

First study results indicate, that a fusion of both modalities (PET and CT) improves diagnostic accuracy as

well as lesion localization and report promising results for the staging of different oncological diseases compared to PET and CT alone (Lardinois et al. 2003; Pelosi et al. 2004). The total standard uptake value (SUV) of the entire axial slices of the liver as well as of the individual lesion correlated well with the laboratory and tomographic imaging results (Wong et al. 2004). However, PET-CT in some cases holds a risk of diagnostic misinterpretation, e.g., due to increased FDG-uptake in muscle or fat tissue, reduced spatial resolution or incorrect lesion localization caused by an inadequate fusion of the PET and CT data due to breathing artifacts. Furthermore, some tumor entities show no or only infrequent FDG-uptake (e.g., HCC), which suggests that FDG-PET-CT does neither represent the imaging modality of choice for detection nor response assessment in these tumor entities.

#### 3.1.1 Proposal for a PET-CT Scan Protocol

Before performing the PET-CT scan patients have to be fasting for at least 6 h to keep blood sugar levels below 120 mg/dl. After an intravenous injection of Furosemide and Butylscopolamine, the application of approximately 370 MBq FDG is followed. Sixty minutes after the tracer application, a low dose-CT scan is performed from the skull base to the proximal femur for attenuation correction. Using a 3D-mode (144 × 144 Matrix), the emission scans are then conducted with 3 min per bed position (FOV 10 cm). For a WB examination an average of 12 positions is needed. After the emission scan, patients have a diagnostic spiral-CT scan (40 mAs, 120 kV, collimation 2 × 5 mm, pitch 1,5; using e.g., a two-detector row PET-CT system) covering thorax, abdomen, and pelvis with 120 ml of nonionic iodinated i.v.-contrast agent in the venous phase (70–80 s delay). Multiplanar reconstructions are performed on the diagnostic CT data set. Using the emission data, a reconstruction of the PET data with and without attenuation correction (Ramla-3D) and a reorientation in axial, sagittal, and coronal direction is followed. Finally, with the use of dedicated software the PET and CT data are fused.

### 3.2 Whole-Body Magnetic Resonance Imaging

#### 3.2.1 Technical Requirements

Whole-body MRI has not been used in routine clinical care either because of extensively long examination times when diagnostic-quality sequences are employed, or because of inferior quality when fast sequences are utilized. To overcome these problems, different strategies have been explored. One approach has been the implementation of a sliding table platform that enables data acquisition of different anatomical regions in rapid succession (Barkhausen



et al. 2001). Signal reception can be accomplished using posteriorly-located spine coils (integrated in the patient table) and an anteriorly positioned torso phased-array coil, which remains fixed to the stationary patient table in the isocenter of the magnet. Hence, data acquisition can be performed with the same stationary coil set. A rolling table platform has been successfully employed for the detection of bone metastases, parenchymal metastases including hepatic, cerebral, and lung metastases (Lauenstein et al. 2004). Other technological advances provide MRI systems with multiple input channels, which allow the simultaneous use of specialized surface coils (Schlemmer et al. 2005). A combination of coils, for example, a head coil with two or more phased-array body coils, can be employed simultaneously. Thus, high resolution images of multiple regions of the body can be acquired without the need of coil repositioning. Automatic table motion can acquire a total scan range of over 200 cm in the z-axis. Beyond the technical improvements in system hardware, concurrent developments have been made in MRI sequence protocols and imaging techniques. An important innovation is the use of fat-suppressed 3D gradient echo (GRE) sequences with nearly isotropic resolution, which has been developed for imaging of parenchymal organs (Lee et al. 2000; Rofsky et al. 1999). These 3D data sets can be acquired within a single breath-hold and provide excellent image quality. Furthermore, 3D data also offers the advantage of multiplanar reconstructions. In conjunction with rapid table motion, these T1-weighted (T1w) sequences permit dynamic imaging of various parenchymal organs after a single intravenous injection of paramagnetic contrast agents. Further improvement of WB-MRI is achieved by using parallel acquisition techniques (PAT). These techniques allow data acquisition with either increased spatial resolution or shorter acquisition time, or a combination of both (Griswold et al. 2002; Kramer et al. 2005). Combining a high number of surface coil elements and receiver channels now enables PAT imaging in all three spatial directions. In principal, the image reconstruction can be facilitated by two different algorithms: either by calculation of the missing k-space lines before Fourier transformation (SMASH or GRAPPA) or by later fusion of the generated incomplete images (SENSE) (Griswold et al. 2002; Pruessmann et al. 1999). Thus, the combined effect of hardware and sequence advances has allowed WB-MRI to be performed more rapidly while maintaining diagnostic image quality.

### 3.2.2 MRI Sequences for Whole-Body Imaging

Examination protocols should be tailored to specific clinical circumstances. However, all WB protocols should include gadolinium-enhanced T1w 3D GRE sequences of all different organ systems, and especially the liver for evaluation of the efficacy of regional tumor therapy. WB-MRI using

only unenhanced imaging would substantially shorten examination times, but diagnostic accuracy would be substantially reduced. After contrast administration, data collection should be started in the abdomen with an arterial, portal venous, and late venous contrast phase of the liver. With this type of protocol, high sensitivity and specificity for focal liver lesions can be achieved. Moreover, antitumoral effects after liver-directed, minimal invasive therapies can be assessed. As compared to PET/CT, WB-MRI has a higher sensitivity in the detection of liver metastases and primary liver tumors. WB-MRI is also definitely superior in the detection of skeletal and brain metastases. In the assessment of lymph node involvement, on the other hand, PET/CT is most accurate.

### 3.2.3 Proposal for a Whole-Body MR Scan Protocol

First, coronal short tau inversion recovery (STIR) -sequences at 5 levels: (head, neck, pelvis, thighs, and lower leg) as well as thorax/abdomen in breath-hold technique with prospective 2D navigation correction of the inspiration phase [prospective acquisition correction (PACE)] are acquired. Using PAT, image acquisition can be completed within an acceptable time with a  $1.8 \times 1.3$  mm in-plane resolution. Additionally, the lung is examined in axial orientation with STIR- and HASTE-sequences. After a navigator-triggered “free-breathing” T2w-fat saturated-SE scan of the liver the five body levels are examined with T1w-SE-sequences, followed by T1w- and STIR imaging of the spine in sagittal orientation. After application of gadolinium-based contrast medium (and saline flushing), axial dynamic (arterial, portal venous, and late venous phase) liver scans are performed, as well as axial T1w- and T2w-imaging of the brain. The last examination step consists of a fat-saturated T1w-GRE-sequence of the whole abdomen in axial orientation. Table 2 provides an overview of the proposed scan protocol. A PAT-factor of 3 is used for the coronal T1w-/STIR WB imaging apart from the lower leg. A PAT-factor of 2 is used for axial imaging of brain, lung, and abdomen, as well as for the sagittal scans of the spine and for the coronal scans of the lower leg.

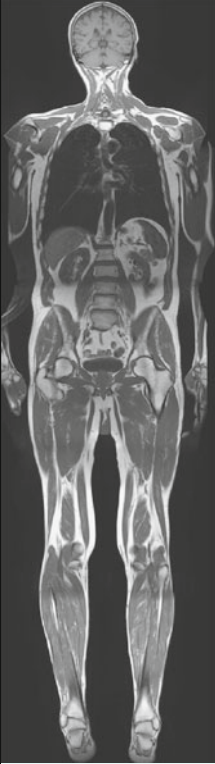
---

## 4 Discussion

### 4.1 Detection of Liver Metastases

Imaging plays a major role in detecting and follow-up of metastatic disease in the liver, which strongly influences the treatment strategy. Contrast-enhanced CT has been reported as the most sensitive test for the detection of hepatic metastases. However, it has a considerable rate of false-positive findings, lowering the positive predictive value

**Table 2** Overview of a proposed scan protocol applied to a whole-body magnetic resonance scanner with 32-receiver channels. Total scan time approximately 55 min

Localization		Whole Body MRI protocol						
	STIR cor		T1 cor				T1 +cor T2 ax skull	
	STIR cor	HASTE/STIR cor + ax lung	T1 cor	T1+STIR upper spine		T1 fs ax + cor abdomen		
	STIR cor	T2 liver	T1 cor	T1+STIR lower spine	3D-VIBE upper abdomen			
	STIR cor		T1 cor					
	STIR cor		T1 cor					
0 min.	→	→	→	→	→	→		→ 55 min.

(Nelson et al. 1989; Soyer et al. 1992). False-positive results from FDG-PET in the liver are rare and occur primarily in hepatic abscesses. Delbeke et al. reported a lower sensitivity (91 vs 97 %) but higher specificity (95 vs 50 %) for FDG-PET resulting in a superior overall diagnostic accuracy compared to contrast-enhanced CT (Delbeke et al. 1997). In the study of Topal et al., PET was shown to be capable of detecting liver metastases with 99 % sensitivity (Topal et al. 2001). Several studies have compared the accuracy of FDG-PET and CT in the detection of hepatic metastases (Arulampalam et al. 2004; Bohm et al. 2004; Ogunbiyi et al. 1997). Overall, FDG-PET was more accurate than CT. Ogunbiyi et al. reported high sensitivity (95 %) and specificity (100 %) of FDG-PET for detecting liver metastases. In their study, the sensitivity and specificity of CT were 74 and 85 %, respectively (Ogunbiyi et al. 1997). In a meta-analysis, Kinkel et al. compared ultrasonography, CT, MRI, and FDG-PET in the detection of hepatic metastases from colorectal, gastric, and esophageal cancer (Kinkel et al. 2002). In this study, the sensitivity of the modalities with

specificity higher than 85 % was 55 % for ultrasonography, 72 % for CT, 76 % for MRI, and 90 % for FDG-PET.

Nevertheless, controversy still remains over the role of FDG-PET in the detection and follow-up of liver tumors. In several articles comparing PET and CT, there were potential sources of bias that could benefit PET over CT including the interval between CT and PET, unequal skill in test performance, variations in CT technology, and bias in test interpretation. Recently, Truant et al. reported equivalent sensitivities for FDG-PET and CT for the detection of colorectal liver metastases (76 %) (Truant et al. 2005). Concerning the comparison with MRI, Yang et al. found no significant difference in the detection of liver metastases with gadolinium chelate-enhanced liver MRI and FDG-PET (Yang et al. 2003). In the study of Bohm et al. comparing FDG-PET with other cross-sectional anatomical imaging techniques, FDG-PET performed better than sonography and CT. However, gadolinium chelate-enhanced MRI had comparable results. In this study, the sensitivity and positive predictive value of PET for hepatic lesions from colorectal

cancer were 94 and 99 %, respectively, compared with 86 and 100 % for abdominal sonography; 88 and 98 % for CT; and 91 and 100 % for MRI (Bohm et al. 2004). Sahani et al. compared mangafodipir trisodium-enhanced liver MRI and FDG-PET for the detection of hepatic metastases from the adenocarcinoma of the colon and pancreas and found accuracies of 97.1 % for MRI and 85.3 % for FDG-PET (Sahani et al. 2005). However, apart from its high sensitivity in the detection of hepatic metastatic lesions, FDG-PET provides a survey of the WB for metastatic disease. Sahani et al. reported that FDG-PET identified extrahepatic disease in 9 of the 34 patients involved in their study. In the study of Arulampalam et al. FDG-PET had an overall sensitivity of 100 % and an overall specificity of 91 % for intra- and extrahepatic metastatic disease. The overall sensitivity and specificity of CT were 47 % and 91 %, respectively (Arulampalam et al. 2004). FDG-PET might be not far superior to CT or MRI in the detection of hepatic metastases, but it surely adds to the decision making power of the oncologist and interventional radiologist and may impact on the management of many patients due to its high sensitivity for intrahepatic and extrahepatic metastatic disease.

#### 4.2 Follow-up of Recurrent Metastatic Disease

The measurement of tumor markers (where applicable) may be used to monitor recurrence, with a sensitivity of 59 % and a specificity of 84 % (Delbeke and Martin 2004). In addition to its low sensitivity, tumor markers do not allow to localize recurrent lesions. CT has been the established imaging modality to demonstrate recurrent hepatic metastases or tumor progression after regional therapy. However, CT is unable to detect hepatic lesions in up to 7 % of patients and underestimates the number of lobes involved in up to 33 % of patients (Delbeke and Martin 2004). Selzner et al. compared CT and FDG-PET in 76 patients evaluated for liver resection for metastatic colorectal cancer (Selzner et al. 2004). CT and FDG-PET provided comparable findings for the detection of intrahepatic metastases with a sensitivity of 95 and 91 %, respectively. However, the specificity of FDG-PET (100 %) was significantly superior to that of CT (50 %) in establishing the diagnosis of intrahepatic recurrences in patients with prior treatment. Selzner et al. reported that in half of the patients with local recurrences in the liver, CT provided no or inconclusive information; whereas all recurrent metastases exhibited positive FDG-uptake in their study. In fact, this finding is not surprising because it is well known that differentiation of postoperative or postinterventional changes after regional

tumor therapy and tumor recurrence based on morphologic findings alone is difficult (Selzner et al. 2004). Since PET has the ability to give information about the metabolic activity of a particular tissue, it has great potential to predict response to systemic chemotherapy or regional therapy much earlier than with morphological imaging methods which require evidence of morphological changes that may take some weeks (Tutt et al. 2004).

Apart from systemic chemotherapy, hepatic metastases can also be treated with regional therapy. Various procedures such as selective chemoembolization, radiofrequency ablation, cryoablation, alcohol ablation, and Yttrium-90 microsphere therapy have been investigated. Vitola et al. and Torizuka et al. showed that FDG-uptake decreases in responding lesions after chemoembolization and the presence of residual uptake in some lesions can help in guiding further therapy (Torizuka et al. 1994; Vitola et al. 1996). Langenhoff et al. have prospectively monitored 23 patients with liver metastases following radiofrequency ablation and cryoablation. Three weeks following therapy, 51 of 56 (91 %) metastases became FDG negative, and no recurrence was detected during the follow-up period of 16 months (Langenhoff et al. 2002). Wong et al. compared PET, CT, or MRI and serum levels of CEA to monitor the therapeutic response of hepatic metastases to Yttrium-90 microsphere brachytherapy. They found significant differences between PET, CT, and MRI; and the changes in FDG-uptake correlated better with the serum levels of CEA (Wong et al. 2004).

#### 4.3 PET or PET-CT

PET and PET-CT have changed the management of patients with liver malignancies as a result of their enhanced ability to detect recurrent or metastatic lesions compared with CT alone (Meta et al. 2001; Rohren et al. 2002). Despite its limitations, PET has also proved to be more accurate than CT in detecting recurrent liver metastases (Fernandez et al. 2004; Valk et al. 1999). The inability to provide detailed anatomic information is, however, an important limitation of PET imaging. It is impossible, for example, to assess the proximity of liver lesions to important anatomical structures such as vena cava, portal vein, or biliary duct (Kinkel et al. 2002). Thus, it is frequently necessary that PET imaging be complemented by other studies such as CT or MRI (Ruers et al. 2002). PET-CT is an integrated imaging modality that combines CT (anatomical information) and PET (functional information). Compared to PET alone, PET/CT greatly improves confidence concerning lesion location (Cohade

et al. 2003). In a study comparing PET alone with PET-CT, the number of lesions with uncertain location was reduced by 55 % (from 42 to 19). Moreover, the number of equivocal and probable lesion characterization was reduced by 50 % (from 50 to 25). Confidence in lesion localization and characterization are linked with each other, as better localization of a lesion probably also improves the accuracy of its characterization as benign or malignant, leading to fewer equivocal lesions and fewer lesions that are considered probably benign or probably malignant.

#### 4.4 What does MRI add?

Initial studies describing WB-MRI focused on the detection of osseous metastases in patients with primary malignancies that had a high likelihood to spread to the skeletal system (Eustace et al. 1997; Steinborn et al. 1999). Bone scintigraphy served as the reference standard in these studies. Dedicated MRI had been found to be more accurate in the detection of bone metastases compared to scintigraphy. In the detection of skeletal metastases, distinct regional advantages and disadvantages were observed for both skeletal scintigraphy and WB-MRI. Scintigraphy proved more sensitive in the assessment of metastases to the ribs, scapula, and skull. However, scintigraphy has some substantial limitations, including exposure to ionizing radiation, difficulty in differentiating degenerative disease, and healing fractures from metastases. MRI has a unique detection rate for osseous metastases in the spine and the pelvis and was found to be definitely superior to skeletal scintigraphy.

To justify the higher costs of WB-MRI, the range of diagnostic capabilities must be broad. Imaging must be performed to detect not only osseous metastases, but also metastases in all other organ systems and tumor recurrences after regional therapy. This may be accomplished with T1w 3D-GRE with nearly isotropic resolution and gadolinium enhancement (Lee et al. 2000; Rofsky et al. 1999). Data are acquired within breath-hold periods, rendering image quality consistent. Good correlation with standard staging examinations including CT was observed. Dynamic imaging of the liver was accurate in the detection and characterization of hepatic mass lesions (Semelka et al. 2001). Other abdominal organs, including the pancreas, adrenal glands, and kidneys were imaged by MRI with a high level of diagnostic accuracy (Low et al. 2000). Lauenstein et al. detected all cerebral and osseous metastases shown by the reference examinations. Image quality of the lungs proved to be slightly inferior to CT scanning. All pulmonary metastases except a single small lesion were correctly detected (Lauenstein et al. 2002). These results were confirmed by other authors indicating that lesions larger than 5 mm in size can be adequately depicted with MRI (Vogt et al. 2004). A follow-up

study which enrolled a larger patient cohort (Lauenstein et al. 2004), comprising 51 patients with known malignant tumors, which all have the propensity to metastasize to different organ systems including brain, lungs, liver, lymph nodes, and bones. Reference staging was based on CT, dedicated MRI, and nuclear scintigraphy. In addition to gadolinium-enhanced T1w 3D GRE of the entire body, supplemental imaging of the thorax and abdomen was acquired with fat-suppressed T2-weighted (T2w) single-shot echo-train spin-echo. All 43 patients who were proven to have metastatic disease were found to have metastases on WB-MRI. However, the reference examinations revealed metastatic disease in 42 patients only. In one patient with a single hepatic metastasis, which was proved by histology, only WB-MRI was able to depict this lesion. There were distinct differences in the sensitivity of metastases detection depending on the anatomical region. More liver metastases were shown on MRI than on CT. WB-MRI did not reveal some lung lesions detected by CT. The addition of T2w sequences to a protocol employing only gadolinium-enhanced 3D-GRE images may improve the diagnostic information in lung involvement.

In another study comprising 98 patients, WB-MRI was compared to dual-modality FDG-PET-CT in patients with a variety of malignancies (Antoch et al. 2003). Both modalities showed high accuracy using TNM staging (77 % PET-CT vs 54 % with WB-MRI). The extent of primary tumors and lymph nodes metastases was more reliably staged with PET-CT, while WB MRI was more sensitive and specific in the detection of hepatic and skeletal lesions. PET-CT performed particularly well in staging patients with primary lung cancer, which was the largest group in this study, reflecting the well-established utility of PET/CT in patients with lung cancer.

The recent hardware developments of multiple phased-array surface coils and receiver channels combined with parallel imaging offer considerable reduction in data acquisition times, thereby permitting acquisition of a variety of sequences while maintaining acceptable study times.

Using these new techniques, the data published by Schmidt et al. revealed distinctly better results and indicate that the tumor stage can be as reliably assessed with WB-MRI as with PET-CT (Schmidt et al. 2005). Both modalities showed high accuracy in TNM staging (96 % PET-CT vs 91 % with WB-MRI). PET-CT achieved a diagnostic sensitivity and specificity of 82 % for the detection of distant metastases, whereas WB-MRI showed a sensitivity of 96 % and a specificity of 82 %. WB-MRI proved more reliable in the detection of skeletal and liver metastases by revealing 76 compared with 50 bone manifestations in PET-CT and 71 versus 62 liver manifestations, respectively (Fig. 3). The cutoff value for lesion detection in the liver was lower in MRI compared to PET-CT (3 vs



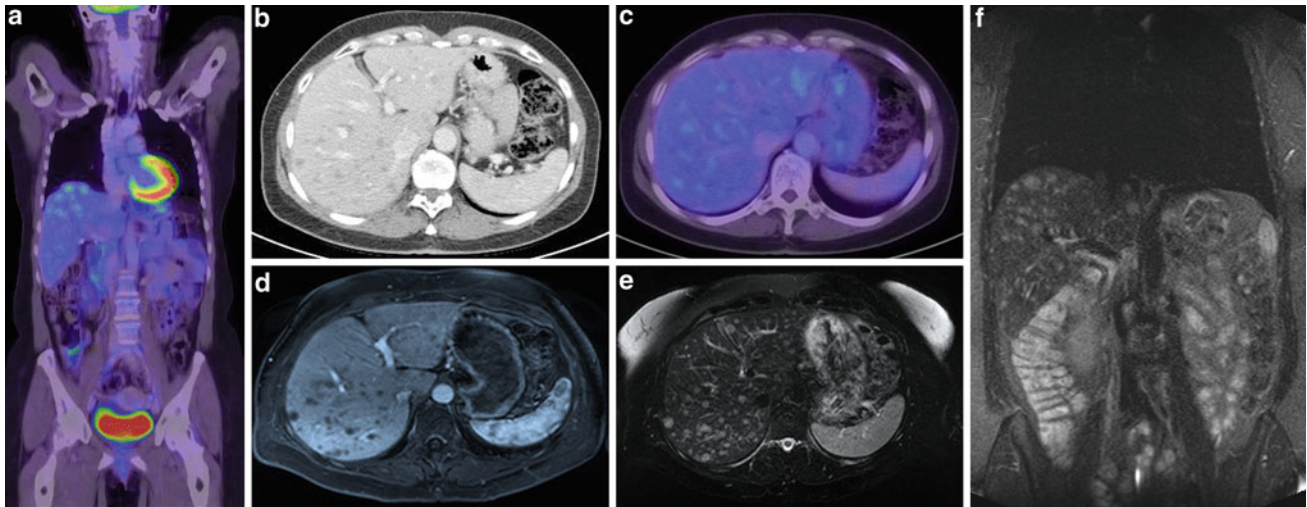


**Fig. 3** 55-year-old female patient with hepatic metastases from breast cancer. The coronal (a) and axial (c) view of the fused PET-CT demonstrate only very few liver lesions with a high FDG-uptake. The contrast-enhanced CT image (b) delineates some more hypodense liver lesions, which are apparently too small for the detection of an increased tumor metabolism. However, the T1w 3D-GRE with nearly

isotropic resolution and gadolinium enhancement (d), as well as the T2w fat saturated Turbo spin-echo image (e) and the coronal STIR image (f) detect more metastases than PET-CT. Therefore, MRT with dedicated sequences is superior to PET-CT in the detection of smaller liver metastases. Especially in PET-negative tumors, this is of special interest

5 mm, respectively). PET-CT enabled the detection of more lung metastases and was also more accurate in the detection of soft tissue metastases. The option of implementing a dynamic MRI scan with PAT acceleration including contrast-enhanced imaging, obviously contributed to a high detection rate and accurate evaluation of liver tumors (Schmidt et al. 2005).

Schlemmer et al. analyzed the diagnostic performance of a multichannel WB-MRI scanner with the use of PAT in 71 patients with oncological diseases in comparison to conventional CT imaging (Schlemmer et al. 2005). The protocol employed in this study was based on coronal STIR- and axial pre- and post-contrast T1w imaging of the WB. WB-MRI showed promising performance for the detection of distant metastatic disease by revealing more metastases to the brain, abdominal organs, bone marrow, and soft tissue in 17 % of the patients. In six patients, therapy was modified according to these findings.

The presence of cerebral metastases, knowledge of which is crucial for patient management and prognosis, is usually not assessable in FDG-PET-CT due to the normal high FDG-uptake in the cerebrum when a WB protocol is used. Cerebral pathologies are imaged with high resolution in WB-MRI which is a clear advantage of this modality, especially in tumors that frequently spread to the brain, like breast carcinoma or bronchial carcinoma. In summary, WB-MRI using T2w and contrast-enhanced T1w imaging includes all properties needed for detection of metastases: it

is fast, provides high-quality MR data, and allows reliable detection of metastatic disease in various organ systems.

## 5 Outlook

Early detection of the response of HCC to Yttrium-90 microsphere radioembolization may be important to permit repeat radioembolization or to alter treatment strategies. Water-mobility measurements with use of diffusion weighted MRI appear useful for noninvasive interrogation of microstructural tissue properties. Findings of diffusion weighted MRI may serve as an early biomarker of HCC response and represents a promising technique for noninvasive assessment of tumor response after radioembolization (Deng et al. 2006a, b). Recent studies indicate HCC tumor response assessed with diffusion weighted imaging at 1 month preceded anatomic size changes at 3 months after radioembolization. Therefore, diffusion weighted imaging may assist in early determination of the response or failure of Yttrium-90 embolization for HCC (Duke et al. 2010; Rhee et al. 2008). Potentially, a so called “MRI-diffusion-PETgraphy” described by Takahara et al. may facilitate diagnosis of metastatic lymph node disease with the use of STIR-EPI-diffusion sequences. The authors demonstrated pathological lymph nodes at high resolution and adequate fat suppression as a promising application in WB-MRI (Takahara et al. 2004).

## 6 Conclusion

Today, PET has an important role in the management of patients with liver metastases from various primaries. It provides functional information that can be used to detect hepatic metastases, to predict their response to therapy, and to follow-up them effectively. PET-CT has the unique advantage of combining functional and anatomic imaging in an integrated scanner and allows for a comprehensive evaluation of patients with liver metastases.

Both, WB-MRI and PET-CT are promising modalities for diagnostics in the oncological patient and seem suitable for accurate tumor staging and may replace extensive and costly multimodality diagnostics. Both modalities have particular diagnostic strengths and weaknesses: while PET-CT is superior in lymph node detection and assessment of tumor viability after regional therapy, high resolution MRI with the use of PAT represent a promising alternative. Especially in the staging of tumors with known poor FDG-uptake, like renal cell carcinoma or HCC, and of tumors with frequent metastatic spread to the bone, liver, or CNS (e.g. breast cancer), WB-MRI, probably in combination with diffusion weighted imaging of the liver, may represent attractive alternatives to PET-CT.

## References

- Antoch G et al (2003) Whole-body dual-modality PET/CT and whole-body MRI for tumor staging in oncology. *JAMA* 290(24):3199–3206
- Arulampalam TH et al (2004) FDG-PET for the pre-operative evaluation of colorectal liver metastases. *Eur J Surg Oncol* 30(3):286–291
- Barker DW et al (2005) Evaluation of liver metastases after radiofrequency ablation: utility of 18F-FDG PET and PET/CT. *AJR Am J Roentgenol* 184(4):1096–1102
- Barkhausen J et al (2001) Whole-body MR imaging in 30 seconds with real-time true FISP and a continuously rolling table platform: feasibility study. *Radiology* 220(1):252–256
- Belton AL et al (2003) Tumour size measurement in an oncology clinical trial: comparison between off-site and on-site measurements. *Clin Radiol* 58(4):311–314
- Beyer T et al (2000) A combined PET/CT scanner for clinical oncology. *J Nucl Med* 41(8):1369–1379
- Bohm B et al (2004) Impact of positron emission tomography on strategy in liver resection for primary and secondary liver tumors. *J Cancer Res Clin Oncol* 130(5):266–272
- Bruix J et al (2001) Clinical management of hepatocellular carcinoma. Conclusions of the Barcelona-2000 EASL conference. European association for the study of the liver. *J Hepatol* 35(3):421–430
- Cohade C et al (2003) Direct comparison of (18) F-FDG PET and PET/CT in patients with colorectal carcinoma. *J Nucl Med* 44(11):1797–1803
- Delbeke D, Martin WH (2004) PET and PET-CT for evaluation of colorectal carcinoma. *Semin Nucl Med* 34(3):209–223
- Delbeke D et al (1997) Staging recurrent metastatic colorectal carcinoma with PET. *J Nucl Med* 38(8):1196–1201
- Deng J et al (2006a) Diffusion-weighted MR imaging for determination of hepatocellular carcinoma response to yttrium-90 radioembolization. *J Vasc Interv Radiol* 17(7):1195–1200
- Deng J et al (2006b) In vivo diffusion-weighted imaging of liver tumor necrosis in the VX2 rabbit model at 1.5 Tesla. *Invest Radiol* 41(4):410–414
- Duke E et al (2010) Agreement between competing imaging measures of response of hepatocellular carcinoma to yttrium-90 radioembolization. *J Vasc Interv Radiol* 21(4):515–521
- Eisenhauer EA et al (2009) New response evaluation criteria in solid tumours: revised RECIST guideline (version 1.1). *Eur J Cancer* 45(2):228–247
- Eustace S et al (1997) A comparison of whole-body turboSTIR MR imaging and planar 99mTc-methylene diphosphonate scintigraphy in the examination of patients with suspected skeletal metastases. *AJR Am J Roentgenol* 169(6):1655–1661
- Fernandez FG et al (2004) Five-year survival after resection of hepatic metastases from colorectal cancer in patients screened by positron emission tomography with F-18 fluorodeoxyglucose (FDG-PET). *Ann Surg* 240(3):438–447
- Forner A et al (2009) Evaluation of tumor response after locoregional therapies in hepatocellular carcinoma: are response evaluation criteria in solid tumors reliable? *Cancer* 115(3):616–623
- Griswold MA et al (2002) Generalized autocalibrating partially parallel acquisitions (GRAPPA). *Magn Reson Med* 47(6):1202–1210
- James K et al (1999) Measuring response in solid tumors: unidimensional versus bidimensional measurement. *J Natl Cancer Inst* 91(6):523–528
- Kamel IR, Bluemke DA (2002) Magnetic resonance imaging of the liver: assessing response to treatment. *Top Magn Reson Imaging* 13(3):191–200
- Kapoor V, McCook BM, Torok FS (2004) An introduction to PET-CT imaging. *Radiographics* 24(2):523–543
- Kinkel K et al (2002) Detection of hepatic metastases from cancers of the gastrointestinal tract by using noninvasive imaging methods (US, CT, MR imaging, PET): a meta-analysis. *Radiology* 224(3):748–756
- Kramer H et al (2005) Cardiovascular screening with parallel imaging techniques and a whole-body MR imager. *Radiology* 236(1):300–310
- Langenhoff BS et al (2002) Efficacy of fluorine-18-deoxyglucose positron emission tomography in detecting tumor recurrence after local ablative therapy for liver metastases: a prospective study. *J Clin Oncol* 20(22):4453–4458
- Lardinois D et al (2003) Staging of non-small-cell lung cancer with integrated positron-emission tomography and computed tomography. *N Engl J Med* 348(25):2500–2507
- Lauenstein TC et al (2002) Three-dimensional volumetric interpolated breath-hold MR imaging for whole-body tumor staging in less than 15 minutes: a feasibility study. *AJR Am J Roentgenol* 179(2):445–449
- Lauenstein TC et al (2004) Whole-body MR imaging: evaluation of patients for metastases. *Radiology* 233(1):139–148
- Lee VS et al (2000) Hepatic MR imaging with a dynamic contrast-enhanced isotropic volumetric interpolated breath-hold examination: feasibility, reproducibility, and technical quality. *Radiology* 215(2):365–372
- Lencioni R, Llovet JM (2010) Modified RECIST (mRECIST) assessment for hepatocellular carcinoma. *Semin Liver Dis* 30(1):52–60
- Llovet JM et al (2008) Design and endpoints of clinical trials in hepatocellular carcinoma. *J Natl Cancer Inst* 100(10):698–711

- Low RN et al (2000) Extrahepatic abdominal imaging in patients with malignancy: comparison of MR imaging and helical CT in 164 patients. *J Magn Reson Imaging* 12(2):269–277
- Mazumdar M, Smith A, Schwartz LH (2004) A statistical simulation study finds discordance between WHO criteria and RECIST guideline. *J Clin Epidemiol* 57(4):358–365
- Meta J et al (2001) Impact of 18F-FDG PET on managing patients with colorectal cancer: the referring physician's perspective. *J Nucl Med* 42(4):586–590
- Miller AB et al (1981) Reporting results of cancer treatment. *Cancer* 47(1):207–214
- Nelson RC et al (1989) Hepatic tumors: comparison of CT during arterial portography, delayed CT, and MR imaging for preoperative evaluation. *Radiology* 172(1):27–34
- Ogunbiyi OA et al (1997) Detection of recurrent and metastatic colorectal cancer: comparison of positron emission tomography and computed tomography. *Ann Surg Oncol* 4(8):613–620
- Park JO et al (2003) Measuring response in solid tumors: comparison of RECIST and WHO response criteria. *Jpn J Clin Oncol* 33(10):533–537
- Pelosi E et al (2004) Value of integrated PET/CT for lesion localisation in cancer patients: a comparative study. *Eur J Nucl Med Mol Imaging* 31(7):932–939
- Pfannenbergh C et al (2007) Prospective comparison of (18)F-fluorodeoxyglucose positron emission tomography/computed tomography and whole-body magnetic resonance imaging in staging of advanced malignant melanoma. *Eur J Cancer* 43(3):557–564
- Pruessmann KP et al (1999) SENSE: sensitivity encoding for fast MRI. *Magn Reson Med* 42(5):952–962
- Rhee TK et al (2008) Tumor response after yttrium-90 radioembolization for hepatocellular carcinoma: comparison of diffusion-weighted functional MR imaging with anatomic MR imaging. *J Vasc Interv Radiol* 19(8):1180–1186
- Rofsky NM et al (1999) Abdominal MR imaging with a volumetric interpolated breath-hold examination. *Radiology* 212(3):876–884
- Rohren EM et al (2002) The role of F-18 FDG positron emission tomography in preoperative assessment of the liver in patients being considered for curative resection of hepatic metastases from colorectal cancer. *Clin Nucl Med* 27(8):550–555
- Ruers TJ et al (2002) Value of positron emission tomography with [F-18] fluorodeoxyglucose in patients with colorectal liver metastases: a prospective study. *J Clin Oncol* 20(2):388–395
- Sahani DV et al (2005) Detection of liver metastases from adenocarcinoma of the colon and pancreas: comparison of mangafodipir trisodium-enhanced liver MRI and whole-body FDG PET. *AJR Am J Roentgenol* 185(1):239–246
- Schlemmer HP et al (2005) Fast whole-body assessment of metastatic disease using a novel magnetic resonance imaging system: initial experiences. *Invest Radiol* 40(2):64–71
- Schmidt GP et al (2005) High-resolution whole-body magnetic resonance image tumor staging with the use of parallel imaging versus dual-modality positron emission tomography-computed tomography: experience on a 32-channel system. *Invest Radiol* 40(12):743–753
- Selzner M et al (2004) Does the novel PET/CT imaging modality impact on the treatment of patients with metastatic colorectal cancer of the liver? *Ann Surg* 240(6):1027–1034
- Semelka RC et al (2001) Focal liver lesions: comparison of dual-phase CT and multisequence multiplanar MR imaging including dynamic gadolinium enhancement. *J Magn Reson Imaging* 13(3):397–401
- Shim JH et al (2012) Which response criteria best help predict survival of patients with hepatocellular carcinoma following chemoembolization? A validation study of old and new models. *Radiology* 262(2):708–718
- Soyer P et al (1992) Detection of liver metastases from colorectal cancer: comparison of intraoperative US and CT during arterial portography. *Radiology* 183(2):541–544
- Steinborn MM et al (1999) Whole-body bone marrow MRI in patients with metastatic disease to the skeletal system. *J Comput Assist Tomogr* 23(1):123–129
- Takahara T et al (2004) Diffusion weighted whole body imaging with background body signal suppression (DWIBS): technical improvement using free breathing, STIR and high resolution 3D display. *Radiat Med* 22(4):275–282
- Therasse P et al (2000) New guidelines to evaluate the response to treatment in solid tumors. European organization for research and treatment of cancer, National Cancer Institute of the United States, National Cancer Institute of Canada. *J Natl Cancer Inst* 92(3):205–216
- Topal B et al (2001) Clinical value of whole-body emission tomography in potentially curable colorectal liver metastases. *Eur J Surg Oncol* 27(2):175–179
- Torizuka T et al (1994) Value of fluorine-18-FDG-PET to monitor hepatocellular carcinoma after interventional therapy. *J Nucl Med* 35(12):1965–1969
- Tran LN et al (2004) Comparison of treatment response classifications between unidimensional, bidimensional, and volumetric measurements of metastatic lung lesions on chest computed tomography. *Acad Radiol* 11(12):1355–1360
- Truant S et al (2005) Prospective evaluation of the impact of [18F] fluoro-2-deoxy-D-glucose positron emission tomography of resectable colorectal liver metastases. *Br J Surg* 92(3):362–369
- Tutt AN et al (2004) The role of positron emission tomography in the management of colorectal cancer. *Colorectal Dis* 6(1):2–9
- Valk PE et al (1999) Whole-body PET imaging with [18F] fluorodeoxyglucose in management of recurrent colorectal cancer. *Arch Surg* 134(5):503–511
- Vitola JV et al (1996) Positron emission tomography with F-18-fluorodeoxyglucose to evaluate the results of hepatic chemoembolization. *Cancer* 78(10):2216–2222
- Vogt FM et al (2004) HASTE MRI versus chest radiography in the detection of pulmonary nodules: comparison with MDCT. *AJR Am J Roentgenol* 183(1):71–78
- Wong CY et al (2002) Evaluating 90Y-glass microsphere treatment response of unresectable colorectal liver metastases by [18F] FDG PET: a comparison with CT or MRI. *Eur J Nucl Med Mol Imaging* 29(6):815–820
- Wong CY et al (2004) Metabolic response after intraarterial 90Y-glass microsphere treatment for colorectal liver metastases: comparison of quantitative and visual analyses by 18F-FDG PET. *J Nucl Med* 45(11):1892–1897
- Wong CY et al (2005) Reduction of metastatic load to liver after intraarterial hepatic yttrium-90 radioembolization as evaluated by [18F] fluorodeoxyglucose positron emission tomographic imaging. *J Vasc Interv Radiol* 16(8):1101–1106
- Yang M et al (2003) Comparison of MR and PET imaging for the evaluation of liver metastases. *J Magn Reson Imaging* 17(3):343–349

---

# Evaluation of the Response by Multimodality Imaging

Alexander Haug and Gerwin P. Schmidt

## Contents

<b>1</b>	<b>Introduction</b> .....	91
<b>2</b>	<b>Established Tumor Response Criteria</b> .....	92
2.1	Response Evaluation Criteria in Solid Tumors (RECIST) ..	92
2.2	Revised RECIST 1.1 .....	92
<b>3</b>	<b>Multimodal Imaging for Evaluation of Therapy Response</b> .....	93
3.1	Ultrasound.....	93
3.2	Magnetic Resonance Imaging .....	96
3.3	Multislice Computed Tomography .....	97
<b>4</b>	<b>Whole-Body Imaging</b> .....	97
4.1	PET and PET-CT .....	98
4.2	Whole-Body MRI .....	98
	<b>References</b> .....	101

---

## Abstract

Radioembolization of primary and secondary liver tumors has emerged as valuable treatment option. CT and especially MRI are very helpful in delineating the tumors and estimating the liver involvement and are still considered as standard in oncologic imaging. Diffusion-weighted MRI has shown promising results in very early treatment assessment in a recent study. However, traditional therapy monitoring using RECIST or WHO criteria may be hampered by the specific changes of tumors treated with radioembolization. Multi-modal imaging, especially in the case of whole-body imaging, may overcome these drawbacks and provide more precise prognostic stratification due to the additional metabolic information. Recent studies indicate an advantage of FDG PET/CT in therapy monitoring of radioembolization, in particular in cholangiocellular carcinoma, breast cancer and colorectal cancer. Further on, whole-body MRI has shown to be useful in pre-therapeutic triage of patients and the diagnosis of extra-hepatic metastases.

---

## 1 Introduction

Primary and secondary liver tumors are common malignancies and are being treated more aggressively nowadays than decades ago. Although resection of solitary liver metastases can result in long-term survival, only 10–20 % of patients with liver metastases are amenable surgical candidates (Schlitt et al. 2008).

Microsphere and particle technologies for the selective transport of tumoricidal agents or radiation represent a new generation of therapeutics in interventional oncology. The intrahepatic application of radioactive microspheres via the hepatic artery allows for locoregional therapy of diffuse or multifocal liver tumors, such as hepatocellular carcinoma or

---

A. Haug (✉)  
Department of Nuclear Medicine,  
University Hospitals Grosshadern,  
Ludwig-Maximilians-University of Munich,  
Marchioninstr 15, 81377 Munich, Germany  
e-mail: alexander.haug@med.lmu.de

G. P. Schmidt  
Radiologie München Zentrum, Sonnenstr. 17,  
80331 Munich, Germany



secondary liver metastases (especially from colorectal and breast cancer), for which to date systemic therapy was the only remaining option (Clark et al. 2005; Kennedy et al. 2006; Jakobs et al. 2008a, b). Current standard is radio-embolization with 90-yttrium glass or resin microspheres. Although it is not considered as a cure, it has been shown to improve quality of life and prolong survival (Khodjibekova et al. 2007; Jakobs et al. 2007). The demands of agent administration and clinical follow-up require reliable and accurate assessment of tumor burden within an experienced interdisciplinary team. To determine patient's progress, it is important to determine both local intrahepatic tumor control and to assess the development of potential extrahepatic metastatic manifestations. Therefore, applied diagnostic methods should be as sensitive and specific as possible.

For the staging and restaging of tumor patients with hepatic involvement, various imaging procedures are employed, including ultrasound, computed tomography (CT), magnetic resonance imaging (MRI), and nuclear medicine procedures, such as skeletal scintigraphy and positron emission tomography (PET). However, multimodal approaches are potentially time consuming, costly, and inconvenient for the patient and may miss out lesions located outside of the imaging field of the study.

Thus, whole-body imaging strategies are increasingly preferred over multimodality algorithms for a rapid assessment of total tumor burden. Especially, the advent of combined PET-CT imaging with the use of fluorodeoxyglucose (FDG) as an "allround" tracer has expanded diagnostic options in oncologic imaging by adding functional information of a PET exam to the detailed anatomical data of multislice-CT (MS-CT) within a single examination. It has been reported that PET-CT has markedly increased malignant lesion localization and diagnostic sensitivity for various tumor entities (Pelosi et al. 2004; Cohade et al. 2003). Alternatively, whole-body MRI (WB-MRI) has been introduced for staging as well as for surveillance of various neoplastic diseases. The good soft tissue contrast in bone marrow or parenchymal organs and its high spatial resolution make MRI a useful application, especially for imaging of metastases from tumors that frequently metastasize to the liver, bone, and brain, such as breast cancer or colorectal cancer (Antoch et al. 2003; Schmidt et al. 2008, 2009).

The following chapter presents the different available imaging methods for tumor monitoring and describes their individual advantages and limitations.

## 2 Established Tumor Response Criteria

Assessment of the change in tumor burden is an important feature of the clinical evaluation of cancer therapy. Both tumor shrinkage (objective response) and time to the

development of disease progression are important endpoints in cancer clinical trials. However, both of these tumor endpoints are useful only if based on widely accepted and readily applied standard criteria reflecting anatomical tumor burden. In 1981 the World Health Organisation (WHO) first published tumor response criteria, which introduced the concept of an overall assessment of tumor burden by summing the products of bidimensional lesion measurements. Accordingly, response to therapy was defined by evaluation of morphologic changes from baseline while on treatment (Miller et al. 1981). This approach was then modified and standardized in 2000 by the RECIST committee (see Table 1). Key features of the original RECIST include definitions of minimum size of measurable lesions, instructions on how many lesions to follow and the use of unidimensional, rather than bidimensional measures for overall evaluation of tumor burden (Therasse et al. 2000). This procedure has been widely adopted by academic institutions, cooperative groups, and industry for trials where the primary endpoints are objective response or progression.

### 2.1 Response Evaluation Criteria in Solid Tumors (RECIST)

Measurable lesions are defined as lesions of 20 mm minimum size in nonspiral CT and 10 mm size in spiral CT data sets. These are attributed to target lesions (up to five per organ) which constitute total tumor burden in their linear summation. All nonmeasurable lesions are assigned to nontarget lesions and also documented. Bone metastases are regarded as nonmeasurable lesions in RECIST. Results are subsequently assigned to response-defined categories of complete response (CR), partial response (PR), stable disease (SD), and progressive disease (PD). PR is defined as more than 30 % decrease in the linear sum of target lesions (corresponding to an extrapolated 65 % decrease in volume, Fig. 2) and PD as more than 20 % increase (approximately 73 % volumetric increase). RECIST has become broadly accepted in clinical practice, by research groups and industry as an easy-to-execute, time-efficient, standardized procedure to assess tumor response to individual therapy (Park et al. 2003). RECIST place minimal added demand on clinical routine practice and at the same time provides comprehensible results and clearly defined target values.

However, there are some inherent methodological drawbacks, which have to be taken into account. First, neither linear or bidimensional measurements adequately address tumor heterogeneity and morphologic changes under therapy. Second, therapy response criteria based on morphology alone do not reflect metabolic changes within tumor tissue. Furthermore, reader-dependent inconsistencies

**Table 1** Overview on WHO- and RECIST criteria

Best response	WHO change in the sum of <i>products</i>	RECIST change in sums <i>longest diameters</i>
CR (complete response)	Disappearance of all target lesions	Disappearance of all target lesions
PR (partial response)	50 % decrease	30 % decrease
SD (stable disease)	Small changes that do not meet above criteria	Small changes that do not meet above criteria
PD (progressive disease)	25 % increase	20 % increase

in data interpretation may occur by the unattended use of rudimentary image-processing or measurement tools (e.g., the use of manually adjusted electronic calipers) with reported disagreements between readers ranging between 15 and 40 % (Belton et al. 2003). Also, measurement recommendations mainly assume sharply defined, high-contrast target lesions which are not necessarily routinely present. Therefore major variance can be expected in ill-defined, asymmetric, or diffuse tumor lesions. Finally, RECIST does not provide specific technical guidelines concerning examination settings in CT image acquisition (e.g., milli-ampere second/mAS, peak kilovolts/kVp) or pulse sequence-specific properties in MRI, which can have substantial influence on image quality and signal behavior.

## 2.2 Revised RECIST 1.1

RECIST has been used and validated since 2000 in multiple prospective trials. Based on this large experience with RECIST, these criteria have been revised (called RECIST 1.1) in 2009 (Eisenhauer et al. 2009). Mainly the assessment of the tumor response has been simplified by reducing the number of target lesions from ten to five and from five to two per organ, maximum. Further on, lymph nodes with size of their short axis above 15 mm are considered as pathological and assessable as target lesions. The short axis measurement should be included in the sum of lesions for response assessment. Shrinkage of pathologically lymph nodes below 10 mm is considered as CR in RECIST 1.1. The response as assessed with RECIST 1.1 has not to be confirmed in randomized trials any more. Also the definition of PD has changed. In addition to the previous criteria in RECIST, in particular a increase of <20 % in the sum of diameters, an absolute 5 mm increase is now required. Further on, “unequivocal progression” of nontarget lesions is in RECIST 1.1 defined more precisely: the increase in size of nontarget lesions has to be representative of overall disease and must not be based on a single lesion. In contrast to RECIST the revised RECIST 1.1 give detailed specifications for standard anatomical radiological imaging.

## 3 Multimodal Imaging for Evaluation of Therapy Response

The principal role of imaging procedures after RE one hand is to display metastatic burden of the liver to assess local response. Therefore, size, number, and localization of lesions need to be accurately displayed and discriminated from potential benign liver lesions. On the other hand it is important to reliably assess potential tumor progression through presence of extrahepatic tumor manifestations, such as lymph node, lung, bone, abdominal, or cerebral metastases. For this purpose a variety of imaging procedures are available, either based on a stepwise, multimodal imaging approach or, alternatively, as integrated, total body imaging techniques.

### 3.1 Ultrasound

Due to its broad availability and cost-effectiveness, ultrasound is regarded as a first-line imaging modality used in patients with known or suspected liver tumors. One of the major advantages of ultrasound is the “dynamic” nature of the technique allowing spontaneous analysis of suspected lesions in any spatial orientation and providing additional information through assessment of lesion mobility, echogenicity, and even elasticity. The B-mode gray scale display is highly useful for the differentiation of malignant lesions from common benign foci, such as benign cysts or haemangiomas. Reported sensitivities for the detection of malignant liver lesions range between 58 and 70 % for B-mode gray scale scanning and can potentially be further enhanced by technical innovations such as “tissue harmonic imaging” (THI), 3D-scanning and cross beam techniques (Bartolozzi et al. 1996; Harvey and Albrecht 2001). Especially, THI allows for enhanced display and lesion delineation by recording echoes with double frequency (Tanaka et al. 2000). Also, color-coded duplex and power Doppler imaging can provide additional information to further categorize focal liver lesions based on their perfusion characteristics. Furthermore, accompanying pathologies of liver

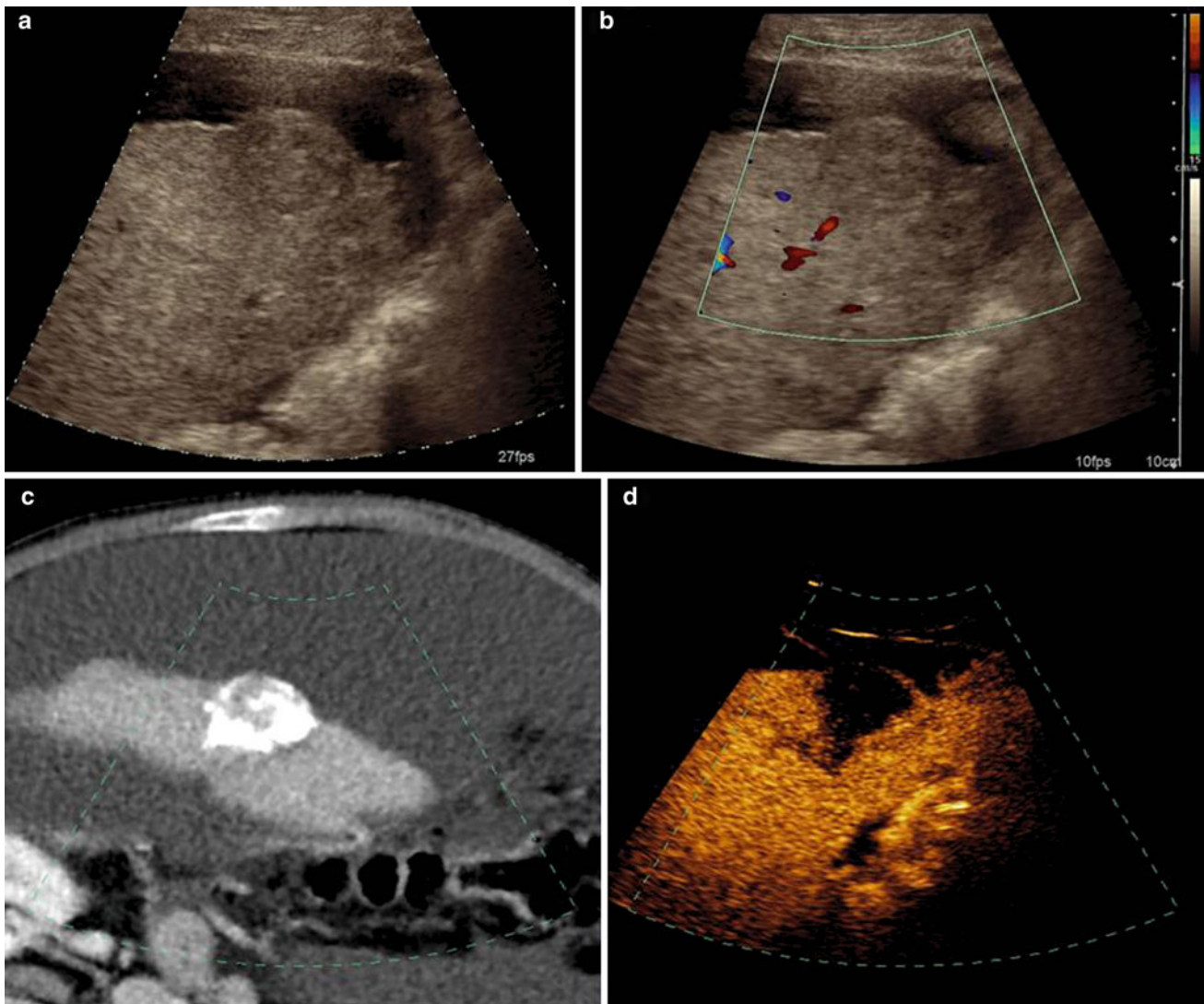


**Fig. 1** Patient with focal liver metastasis under RE therapy. **a**, **b** Unenhanced ultrasound examination in B-mode and Doppler-mode shows a 3.5 cm large hypo- to isointense solid liver mass with capsular bulging consistent with metastasis. Postembolization CT shows

accumulation of toxic agent within the target lesion. **d** Corresponding contrast-enhanced ultrasound indicates therapeutic success by showing hypovascularization of the embolized metastasis. (Courtesy of PD Dr. h.c. Dirk Clevert, Department of Radiology, LMU Munich)

vasculature (e.g., portal vein thrombosis, arterial stenosis) can be assessed (Reinhold et al. 1995). Yet, it has to be taken into account that an important limitation of ultrasound examinations is the examiner-dependent variability of imaging results, conditional to the experience, and skills of the operator. Furthermore, image quality may be impaired by several physical influences, such as present ascites or liver cirrhosis.

The introduction of contrast-enhanced ultrasound (CEUS) with the use of microbubbles with a diameter of 2–6  $\mu\text{m}$  has significantly expanded the diagnostic potential of sonography (Fig. 1) (Quaia 2007). As a major advantage CEUS allows the real-time assessment of focal liver lesion perfusion during low transmit power insonation and it is not limited by motion and blooming artifacts encountered in

color- and power Doppler ultrasound. Microbubbles are comprised of biocompatible materials, including proteins, lipids, and a filling gas, for example nitrogen (Levovist, Bayer Schering Pharma, Berlin, Germany). Microbubbles work by resonating in a US beam, rapidly contracting and expanding in resonance to the pressure changes of the sound wave. If the transmitted acoustic pressure is weak, microbubbles are vibrating symmetrically and there is a conventional linear response, but, if the transmitted acoustic pressure is strong, microbubbles are vibrating asymmetrically, and there is a harmonic nonlinear response. Further developments of micro bubble properties have led to high-molecular weight and low solubility gases with an increased vapor concentration inside the bubbles relative to surrounding tissue and increased stability in the peripheral



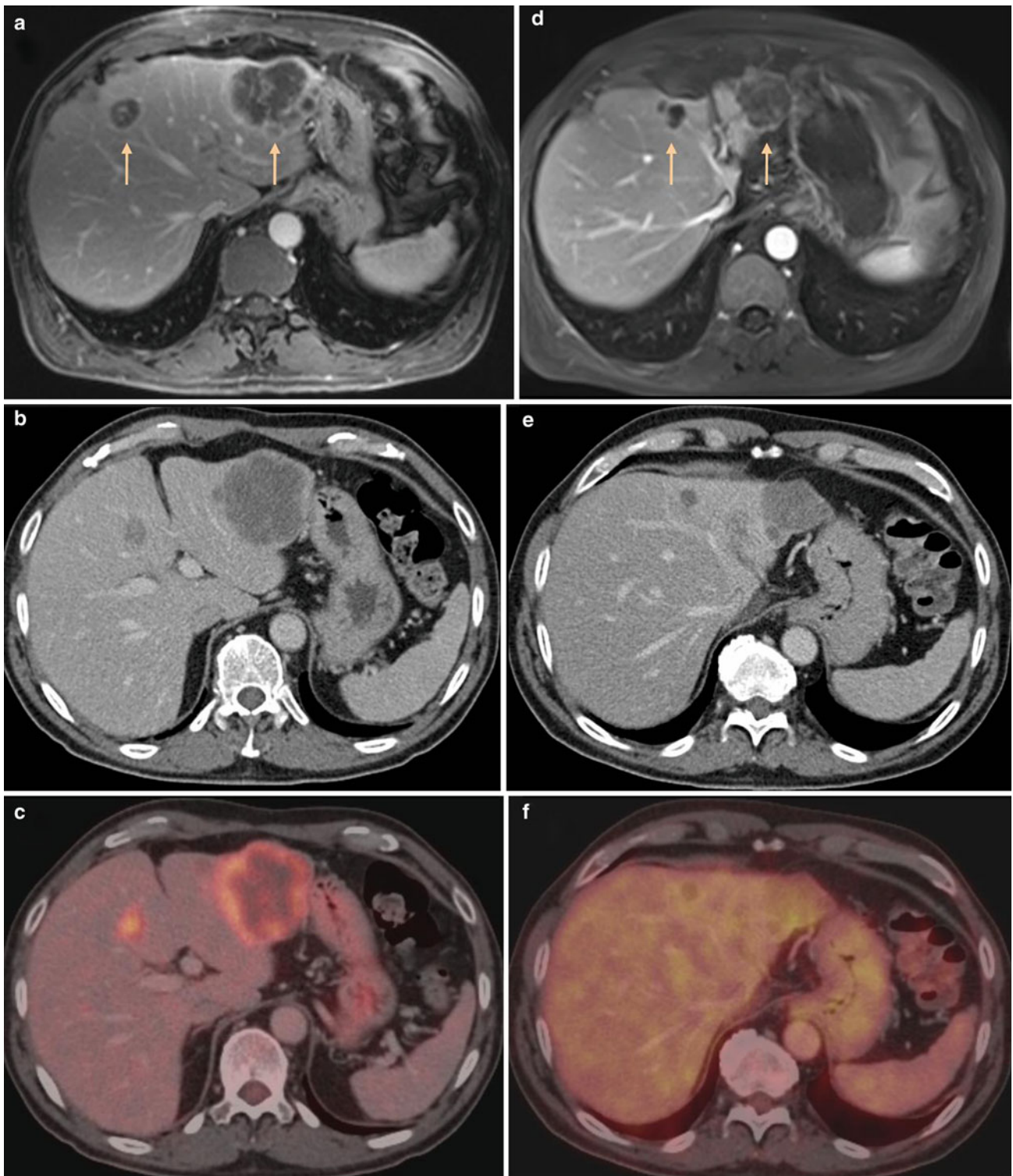


**Fig. 2** Patient with cancer of the sigmoid under RE therapy. **a** Contrast-enhanced 3D-GRE-MRI shows multifocal liver metastases with a large tumor in liver segment 2 and another lesion in segment 4A. Both lesions show marked peripheral enhancement of contrast agent. **b**, **c** Corresponding FDG-PET-CT confirms the lesions with an increased

peripheral tracer uptake (SUVmax 10,0). **d** Follow-up MRI 3 months after RE shows necrotic transformation of the lesions with significant reduction in size (>30 %, PR) and reduced contrast enhancement. **e**, **f** Response is confirmed by PET-CT showing no pathologic tracer uptake above physiological background tracer accumulation



circulation (Quaia 2007). The two approved agents of these second generation particles are Optison (GE Healthcare, Princeton, US) and SonoVue (Bracco Imaging, Milan, Italy). CEUS shows a high level of concordance with CT and MR imaging in depicting the contrast enhancement pattern of focal liver lesions during the arterial phase. Concordance in the portal venous phase is generally lower, reflecting the tendency of CT and MR contrast agents, unlike microbubbles, to diffuse into the tumoral interstitium in cases in which CEUS shows a washout (Burns and Wilson 2007). First trials have indicated an increase of liver lesion conspicuity by the use of contrast agents from 63 % for b-mode imaging alone to 91 % for combined B-mode/contrast-enhanced ultrasound (Albrecht et al. 2001). Especially, lesion characterization is ameliorated from 65 % to 92 % by the use of CEUS, as it has been reported in a different study (Reinhold et al. 1995). Yet, current data has shown, that detection rate is still restricted for liver lesions smaller than 2.5 cm and that lesions smaller than 1 cm cannot reliably be characterized (Rettenbacher et al. 2005). Furthermore, a major limitation of CEUS in comparison to multiphase CT- and MR imaging is the fact that only one liver tumor can be scanned at a time as the transducer has to be kept still during the examination and further micro bubble injections are often necessary to characterize additional liver tumors. Also, the technique requires specific training of the examiner and therefore at present is considered an important add-on rather than a substitute to established cross-section imaging. CEUS may especially provide an added diagnostic value in those incidental focal liver lesions in which contrast-enhanced CT or MR imaging are not conclusive, especially on single-phase scans or scans performed by an incorrect delay time.

### 3.2 Magnetic Resonance Imaging

MRI has been a useful modality in abdominal imaging for more than two decades and various technical improvements in sequence design and contrast media application have been made to enhance its diagnostic accuracy. Especially the development of fast gradient echo- or single-shot sequences, 3D acquisition techniques, and respiratory triggering have markedly ameliorated image quality and significantly decreased motion and respiratory artifacts. Furthermore, the development of parallel image acquisition acceleration techniques (PAT) as well as the introduction of high-field scanners has led to an additional gain in image quality (Zech et al. 2004). An inherent advantage of MRI over CT certainly is its high contrast of liver parenchyma and at the same time its ability to discriminate different tissue properties, such as fat, blood, water, and even cellular

components such as hepatocytes, Kupffer cells or bile ducts based on its T1- and T2-weighted signal behavior and its reaction to tissue-specific contrast agents.

Extracellular gadolinium-based contrast agents still play a major role in liver MR imaging for the assessment of liver pathologies, especially for the detection and monitoring of malignant liver lesions. The reported sensitivities for lesion detection are ranging between 54 and 81 % (del Frate et al. 2002; Matsuo et al. 2001). In direct comparison, gadolinium-enhanced MRI has been reported superior to biphasic spiral CT regarding both lesion detection and characterization with a fundamental impact on patient management (Semelka et al. 2001). In the context of response assessment, dynamic contrast-enhanced multiphase MRI enables to depict hypervascularity and alterations in tumor perfusion following radioembolization (Fig. 2). Yet, at this time there is no clear evidence that this modality is more effective or more accurate than conventional triphasic CT for this purpose (Ibrahim et al. 2009; Atassi et al. 2008).

Liver-specific contrast agents enable a significant increase in the detection rate of suspected liver metastases. These agents are divided into two basic groups: on one hand there are iron oxide particles (SPIO, superparamagnetic particles of iron oxide), targeted to the reticulo-endothelial system (especially Kupffer cells). On the other hand there are hepatobiliary contrast agents, directed to the hepatocytes and subsequently excreted with the bile.

The basic principle of SPIO is based on the fact that there are usually no Kupffer cells in malignant liver lesions. SPIO-based agents, like Resovist (Bayer Schering Pharma, Berlin, Germany), cause a homogeneous signal decrease in healthy liver parenchyma in T2/T2\*-weighted sequences by inducing local inhomogeneities of the magnetic field, consequently leading to a positive, hyperintense contrast of the malignant focus. Although SPIO-based agents are not suitable to evaluate the perfusion and vascularity of focal liver lesions they nevertheless can contribute to lesion characterization. With SPIO-based contrast agents sensitivity ranges between 83 and 97 %, as reported in literature (del Frate et al. 2002; Lencioni et al. 1998). Several studies have confirmed the superior performance of SPIO-based liver MRI compared to biphasic spiral CT (Atassi et al. 2008; Reimer et al. 2000; Namkung et al. 2007).

Hepatobiliary contrast agents work through a direct uptake into the hepatocytes and subsequently cause a signal increase of normal liver parenchyma in T1-weighted sequences by shortening the T1-relaxation time. In contrast, malignant lesions appear hypointense against the hyperintense physiological background. Of this agent group, Gadolinium-based substances such as Primovist (Bayer Schering Pharma, Berlin, Germany) and Multihance (Bracco, Milan, Italy) have been developed. Their important advantage is that they can be administered as a bolus, and

therefore both an early dynamic phase and a liver-specific phase can be acquired within one scan after one single injection, which represents a substantial advantage over SPIO's. The sensitivity for the detection of liver metastases with hepatobiliary contrast agents ranges between 70 and 90 % (Bartolozzi et al. 2004; Bluemke et al. 2005). Especially, the combined analysis of early dynamic phase images and delayed phase images obtained from liver-specific agents yielded the highest detection rate (Kettritz et al. 1996). Furthermore, there are reports that the use of hepatobiliary contrast agents may also lead to a higher sensitivity for the depiction of liver metastases under current therapy, compared to contrast-enhanced CT (Beziat et al. 2004).

Findings of diffusion-weighted MRI (DWI) may potentially serve as an early biomarker, in analogy to information on metabolic changes derived in PET, and represents a promising technique for noninvasive assessment of tumor response after radioembolization (Deng et al. 2006). Studies with both transarterial chemoembolization (TACE) and Y90 radioembolization have shown that DW-MRI may represent a sensitive tool in the early follow-up period to assess therapy response. By evaluating neoplastic tissue water mobility, DW-MRI has been reported to detect tumor response within 42 days of radioembolization, being able to differentiate neoplastic tissue from reactive edema (Atassi et al. 2008; Reimer et al. 2000). Another recent study has described a reproducible, significant decrease of ADC values in responding liver lesions after RE in as early as 2 days following treatment in comparison to nonresponders (Dudeck et al. 2010). Early detection of such alterations in tumor microstructure therefore suggests a sentinel role for DW-MRI in selected patients (Kalva et al. 2008).

### 3.3 Multislice Computed Tomography

CT has developed dramatically in the last decade. Scanners with 64 or more rows enable high spatial and temporal resolution imaging, which allows the integration of bi or triphasic examinations of the liver with a thoracic scan. The short acquisition time of multidetector CT scanners in combination with their reliable high resolution allowing whole-body assessment make them the backbone of oncologic therapy assessment. Of course the imaging technique has to be adapted to the underlying tumor entity, but in most cases a late-arterial and a portal venous phase abdominal CT can be regarded as standard. In selected cases such as hepatocellular carcinomas, hepatic metastases of neuroendocrine tumors or the mapping of the arterial vessels for planning of transarterial therapies an early arterial phase can be included. Therapy monitoring based on CT has shown to be predictive for survival in various tumors and treatments (Eisenhauer et al. 2009).

Several studies have proven its predictive value in patients treated with  $^{90}\text{Y}$ -microspheres as well. Jakobs et al. have analyzed the response rates and survival in 41 patients with colorectal cancer liver metastases treated with radioembolization. Their results indicate that therapy response based on CT is correlated with a significantly improved survival of patients (Jakobs et al. 2008b). The same seems to be true for patients with breast cancer liver metastases. Women with a PR had a survival of 23.6 months as compared to 5.7 months in women not responding to the treatment (Jakobs et al. 2008b). Also in neuroendocrine tumor liver metastases response as assessed on CT scanning is able to predict survival of patients after radioembolization (Saxena et al. 2010). However, some pitfalls for response assessment have to be considered. After radioembolization hepatic perfusion is often inhomogeneous making exact tumor delineation sometimes difficult. Further on, in primary liver tumors such as cholangio-cellular carcinomas and in particular in hepatocellular carcinomas response assessment solely based on size may not accurately reflect the prognosis of the patients after locoregional treatment. There is evidence that in these cases response assessment based on enhancement modes such as the EASL criteria more accurately helps to predict long-term survival (Shim et al. 2012).

---

## 4 Whole-Body Imaging

Whole-body PET using [ $^{18}\text{F}$ ]-fluoro-2-deoxy-D-glucose (FDG) is an imaging modality that can detect cancerous disease by tracing increased FDG uptake in tumor lesions. The introduction of combined PET-CT scanners has made a new modality available for whole-body imaging which combines the functional data of PET with the anatomical information of CT scanners in a single examination. Various study results indicate, that a fusion of both modalities improves diagnostic accuracy as well as lesion localization and report promising results for the staging of various oncologic diseases compared to PET and CT alone (Pelosi et al. 2004; Cohade et al. 2003; Lardinois et al. 2003).

MRI with its lack of ionizing radiation, high soft tissue contrast, and spatial resolution is a useful application for tumor detection and staging of malignancies. In recent years, whole-body MRI (WB-MRI) has fundamentally changed diagnostic concepts for oncologic imaging as an alternative to standard multimodality imaging strategies and is now increasingly applied in clinical routine for integrated imaging of various neoplasms. However, the crucial problem for implementing WB-MRI in the past has been to integrate substantially different requirements in hardware setup, contrast media application, slice positioning, and sequence design into one single comprehensive scan.

Significant improvements in hardware, from pioneering approaches using a rolling platform system mounted on top of a conventional MRI scanner to the essential introduction of multireceiver channel scanners with automated free table movement, have cleared the way for clinically feasible and efficient total body imaging concepts (Barkhausen et al. 2001; Schmidt et al. 2005). Furthermore, important innovations in sequence design and image acquisition, such as parallel acquisition techniques (PAT), have helped to significantly reduce overall examination times without compromising spatial resolution and have increased patient comfort and acceptance. Now, a dedicated assessment of various organ systems by sequences with adequate soft tissue contrast, image orientation, spatial resolution, and contrast media dynamics can be combined with whole-body anatomic coverage.

Especially in the field of oncologic imaging various useful applications have emerged for an integrated diagnostic approach to cancer as a systemic disease, indicating its use as a radiation-free alternative to competing modalities such as multislice-CT (MS-CT) or FDG-PET-CT (Clark et al. 2005; Schlemmer et al. 2005).

#### 4.1 PET and PET-CT

PET using  $^{18}\text{F}$ -fluoro-2-deoxy-glucose (FDG) enables imaging of tumor metabolism. FDG as a glucose analogue is taken up via the glucose transporters located on the cell surface. As the glucose consumption is increased in most cancer cells, FDG uptake is increased as well. After phosphorylation FDG does not undergo further metabolism and cannot be transported outside the cell again, and therefore is trapped inside.

PET/CT using FDG enables the combination of anatomic and functional information and thereby overcomes the limitations of the separate imaging modalities. The technical developments in the recent years have shortened the examination time dramatically. With PET/CT scanners of the newest generation the examination time of a typical whole-body scan is as short as 15 min. Mainly due to this shortening of the scan time, PET/CT scanning can be offered the majority of oncologic patients.

The current standard of monitoring tumor response is measuring tumor shrinkage on CT. Despite several revisions and refinements in recent years CT-based response assessment still has fundamental limitations. Because of difficulties in delineating tumor tissue from secondary changes in the surrounding tissue the inter-observer variability in tumor size measurements is still high (Erasmus et al. 2003). Further on, anatomic imaging has drawbacks in differentiating residual viable tumor tissue from treatment-induced scarring. This may even be more important in

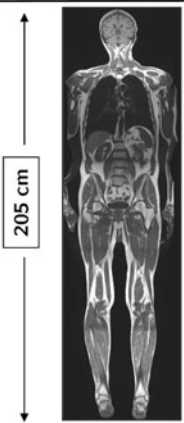
locoregional therapies of liver tumors, because these tumors often show an increasing necrosis without any significant change of size (Miller et al. 2007). In many studies the potential of metabolic imaging in the assessment of therapy response has been shown. Consistently, these studies proved the higher accuracy of FDG PET to differentiate viable tumor from treatment-induced necrosis. Further on, a decline in the metabolic activity of the tumor usually precedes the decline in size indicating therapy response, offering the opportunity of early prediction of patient outcome (Wahl et al. 2009). It has also been shown for different cancer entities that FDG PET response is predictive for survival after therapy (Weber 2009). Therefore, FDG PET/CT seems to be well suited for therapy monitoring of patients after radioembolization. Consequently, more patients show response to hepatic radioembolization on FDG PET as on CT. In a study including 44 women with hepatic metastases from breast cancer response after radioembolization was compared on CT and FDG PET. While on CT 47 % of the women showed a PR, FDG PET indicated therapy response in 95 % (Coldwell et al. 2007). Similar results have been presented in hepatic metastases from colorectal cancer. Up to 95 % of patients had a response on FDG PET (Gulec et al. 2012). Also, the course of the tumor marker CEA is correlation significantly with the metabolic response, but not with the anatomical based response in these patients, indication superiority of FDG PET to CT (Wong et al. 2002). However, none of these studies showed the prognostic value of the metabolic response for the survival of the patients.

Up to now only two studies have proven a predictive value of FDG PET/CT for survival after  $^{90}\text{Y}$ -radioembolization. In an initial study 26 patients with cholangio-cellular carcinoma treated with  $^{90}\text{Y}$ -radioembolization were included. 22 % showed a PR, 65 % a SD and only 13 % further PD 3 months after treatment. However, response based on tumor shrinkage was not significantly associated with overall survival of these patients. On the other side, metabolic response assessment significantly predicted survival (Haug et al. 2011). Similar results have been shown in women with hepatic metastases from breast cancer treated with  $^{90}\text{Y}$ -radioembolization. Again, metabolic responders had a significantly longer survival (65 weeks) than nonresponders (43 weeks), while tumor shrinkage was not significantly predictive (Haug et al. 2012).

#### 4.2 Whole-Body MRI

The technical challenge of oncologic WB-MRI applications is to cover possible routes of locoregional and hematogenous tumor spread with a high standard of image quality (comparable to a dedicated MRI exam) in all anatomic

**Fig. 3** Oncologic whole-body MRI examination protocol with the use of a matrix coil system at 1.5 or 3 T

FOV		Whole body-MRI protocol					
 205 cm	STIR cor		T1 TSE cor			T1+con ax brain	
	STIR cor	HASTE/STIR ax lung	T1 TSE cor	T1+STIR sag spine			T1 GRE fs +con ax abdomen
	STIR cor	T2 TSE ax liver	T1 TSE cor	T1+STIR sag spine	3D-VIBE +con ax lung	3D-VIBE +con ax liver	
	STIR cor		T1 TSE cor				
	STIR cor		T1 TSE cor				
		time → 65 min. @ 1.5 Tesla / 52 min. @ 3 Tesla					

regions within a reasonable total scan time. Therefore, an ideal WB-MRI concept for tumor imaging purposes should include various sequence types and tissue contrasts, as well as different contrast media dynamics within a multiplanar imaging approach to guarantee high diagnostic sensitivity and specificity of the examination.

Initial whole-body imaging approaches on conventional scanners required at least one patient and coil repositioning process, which substantially increased examination time far beyond one hour. First improvements in hardware consisted of a rolling platform system mounted on top of the table of a conventional MRI scanner which for the first time allowed large FOV scanning without restrictions along the z-axis. Despite promising initial results for whole-body tumor staging within markedly reduced scan times, significant compromises in spatial resolution had to be taken in account caused by using the body coil in the head/neck region or on peripheral body parts (Lauenstein et al. 2002).

With the introduction of multichannel MR scanners, using a system of multiple phased-array coils covering the body like a matrix, WB-MRI from head to feet without compromises in spatial resolution became possible (Schmidt et al. 2005). Especially, the combination of free table movement with parallel imaging acquisition techniques (PAT) applicable in all three spatial orientations have resulted in substantially shorter room time. Further evident advantages of PAT is further image enhancement by choosing multiple averaging or the possibility to apply shorter breath holds for abdominal and lung imaging, which represents an important aspect for oncologic WB-MRI often performed on multimorbid patients in impaired physical condition (Griswold et al. 2002).

Recently, approved clinical WB-MRI scanners with a field strength of 3 T have become commercially available. This has opened the way for a migration of multiorgan- and

whole-body protocols to higher field strength. The gain of SNR can be used to reduce the overall examination time, especially for the acquisition of T2-weighted imaging at a constant image resolution (Schmidt et al. 2005). Alternatively, image resolution can be further enhanced to potentially gain higher sensitivity. Potential SAR limitations, often encountered when TSE-sequences are applied for large FOV imaging under high-field conditions, have successfully been addressed by the implementation of hyper-echoes and variable flip angle techniques, keeping SAR levels within a tolerable range (Busse 2004).

Finally, a promising technical innovation was the introduction of MRI data acquisition during continuous movement of the table, similar to the examination technique in CT (Kruger et al. 2002; Weckbach et al. 2010). In contrast to CT, MRI faces the challenge that in most sequences it is not possible to acquire a complete measurement slice with every movement of the table. This means that the raw data have to be buffered prior to complete acquisition of the slice, with the table moving during acquisition of image data. Moreover, the specific acquisition and adjustment parameters now have to be altered and adapted during table movement. Nevertheless, this method possesses enormous potential. Extensive anatomical regions can be swiftly acquired in a seamless series of images in markedly reduced imaging time, thus making redundant the conventional incremental imaging of individual parts of the body.

A state-of-the-art tumor protocol may imply T1-weighted-TSE- and STIR-imaging for the assessment of musculoskeletal pathologies and fast high-resolution imaging of the lung (e.g., HASTE) for detailed assessment of lung parenchyma. Additionally, contrast-enhanced studies of the brain, abdomen, and pelvis, including dynamic contrast media application (e.g., 3D-VIBE) in the upper abdomen are indispensable for an accurate assessment of parenchymal



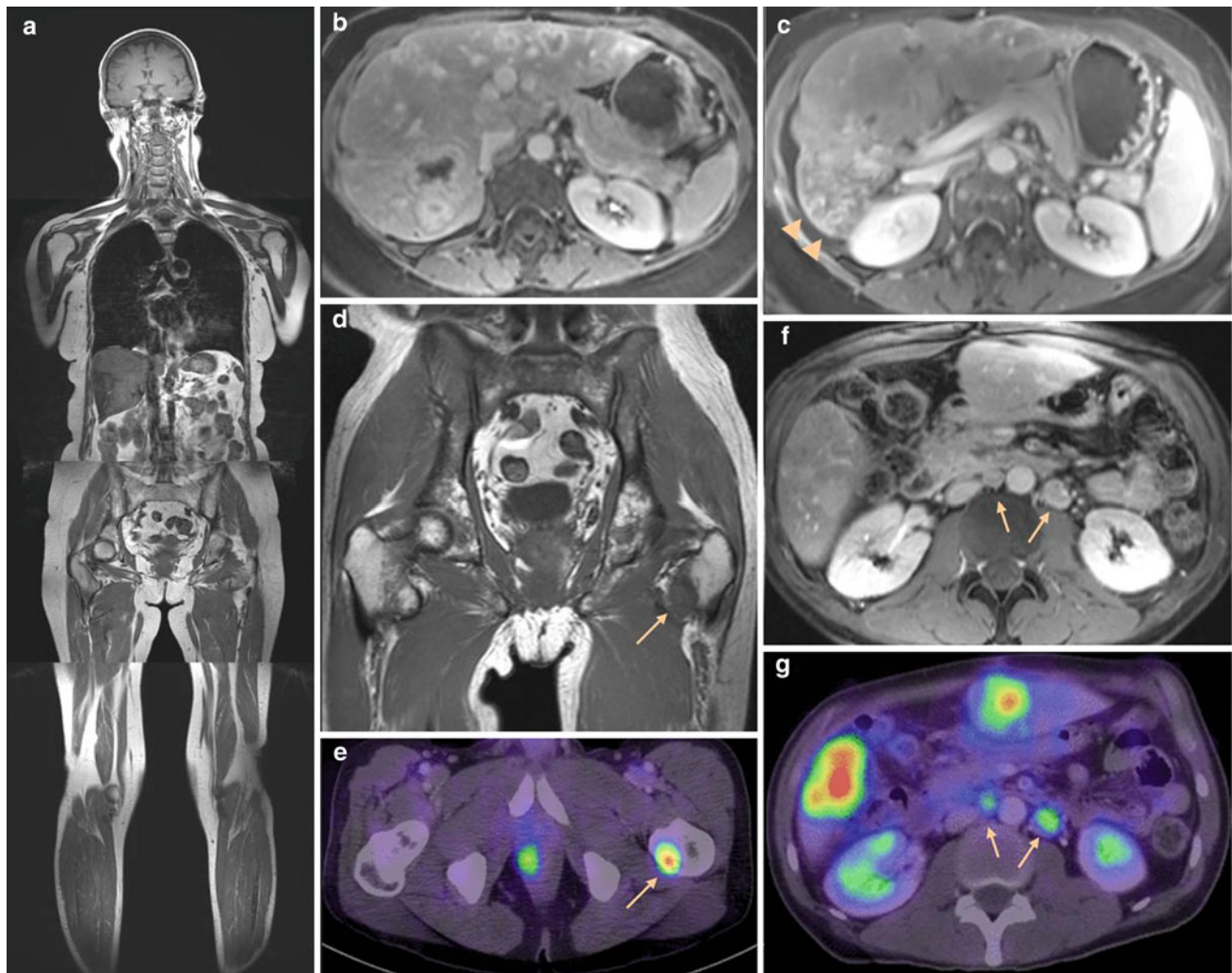


**Fig. 4** **a** T1-weighted whole-body MRI of a 46-year-old patient with breast cancer before RE therapy. **b** 3D-GRE imaging postcontrast indicates multifocal liver metastases. **c** Post-RE these metastases showed clear morphological regression (>50 %, PR), arrowheads indicate post-radiogenic fibrosis of the right liver lobe. **d**, **e** Yet, WB-

MRI follow-up 4 months later shows a new T1-w hypointense bone lesion in the left minor trochanter with a marked FDGF-uptake in the PET-CT correlation, consistent with bone metastasis (*arrow*). **f**, **g** Furthermore, patient showed new abdominal lymph node metastases, overall indicating disease progression (*arrows*)

lesions. An example of an “allround” whole-body tumor protocol with sequence parameters at 1.5 or 3 T is presented in Fig. 3. The described protocol naturally can only be a representative example of an integrated WB-MRI concept and obviously a sensible WB-MRI concept has to be individually adapted to the clinical problem and nature of the examined pathology. It certainly remains difficult to integrate complex dedicated coil setups for imaging of frequent tumor entities like breast or prostate cancer into a clinically feasible whole-body protocol. In this setting, the aspect of tailoring specific protocols to certain tumor types or to a certain risk profile of the patient to further increase both sensitivity and feasibility is a possible approach for the development of WB-MRI concepts in the coming future.

Due to its excellent contrast in soft tissue and parenchymal organs, especially in the brain, bone marrow, and

liver, the main advantage of WB-MRI certainly lies within the detection of distant metastatic disease. Reported diagnostic accuracies for M-staging compared to FDG-PET-CT as a competing whole-body staging strategy range between 82 and 94 % for PET-CT and 92 and 93 % for WB-MRI (Schmidt et al. 2008, 2009). WB-MRI has shown superiority to PET-CT in the detection of liver and bone metastases. Especially, the implementation of a dynamic 3D-VIBE (volume interpolated breath-hold examination, Fig. 3) and high resolution T1-w-TSE-/STIR-imaging allow a reliable diagnosis of pathologies to a cut-off size of 3 mm, which can be invisible in PET-CT, mainly due to low soft tissue contrast and limitations in PET data resolution (Schmidt et al. 2007, 2009). Advantages of PET-CT over WB-MRI have been found for the detection of lung metastases, with a sensitivity of 89 % for PET-CT

compared to 82 % for WB-MRI (Schmidt et al. 2009). The excellent lung tissue contrast inherent to CT and the lower susceptibility to motion artefacts facilitates the detection of lung pathologies. Yet, study results indicate that the implementation of fast single-shot turbo spin echo sequences (HASTE) and contrast-enhanced 3D-VIBE have significantly improved the performance of WB-MRI for the detection of lung pathologies (Frericks et al. 2008). WB-MRI with its total body coverage compared to a standard MS-CT or PET-CT protocol (which usually ranges from the skull base to the pelvis) potentially reveals additional findings of therapeutic and prognostic importance. Detection of previously unknown metastases to the brain and extremities in up to 17 % of cases have been reported (Schmidt et al. 2008, 2012). Especially, the finding of cerebral metastases is of decisive importance for patient survival and planning of therapy. Cerebral and skull metastases are particularly difficult to identify in PET-CT, because of a high physiological tracer uptake in normal brain tissue. In a study performed by Schlemmer et al. WB-MRI for the detection of distant metastases compared to MS-CT as the standard staging method, a change of therapy based on WB-MRI findings alone was reported in six of 63 patients (10 %) (Schlemmer et al. 2005). Another study introducing WB-MRI for staging of advanced malignant melanoma revealed cerebral metastases in 15 of 64 patients examined in pretherapeutic setting, leading to a consecutive change of management (Pffannenberg et al. 2007).

In a recently published study WB-MRI was first introduced as a staging concept within the setting of radioembolization therapy. A total of 135 patients with multifocal hepatic metastases were triaged for RE therapy with whole-body imaging using both FDG-PET-CT and WB-MRI. Both modalities showed high sensitivity for the diagnosis of extrahepatic tumor manifestations and in combination showed a reliable specificity (Fig. 4). In 87 % extrahepatic metastases were detected by both modalities concordantly, in 7 % diagnosis was solely provided by PET-CT, in 6 % by WB-MRI alone. The patient-based sensitivity for detection of extrahepatic disease was 96 % for PET-CT and 93 % for WB-MRI. False-positive diagnoses of extrahepatic disease leading to exclusion from RE therapy were made only in 2 % of patients. Overall, specificity for inclusion of RE therapy by combining both modalities was 99 % (Schmidt et al. 2012).

WB-MRI has great potential as application within tumor surveillance in previously cured cancer patients or for monitoring of a neoplastic disease. WB-MRI can be especially useful in common tumors with a high probability of organ metastases into the brain, liver, bone, or soft tissue, like breast cancer, colorectal cancer, or melanoma (Schmidt et al. 2008; Squillaci et al. 2008). WB-MRI has been successfully introduced on 1.5 T as well as 3 T scanners for the

detection of tumor recurrence in breast cancer patients with suspicion of tumor recurrence (e.g., clinical symptoms, elevated tumor markers). In this high-risk population of 33 patients a 61 % prevalence of recurrent disease was found. WB-MRI showed a persuasive overall diagnostic accuracy (91 %) for lesion-by-lesion detection of tumor recurrence (Fig. 4). Sensitivity was 93 % and specificity 86 %, respectively. Yet, in one patient a false-positive local recurrence was reported (Lauenstein et al. 2002). Recently, the diagnostic potential of WB-MRI at 1.5 or 3 T and FDG-PET-CT for restaging of patients with colorectal cancer was analyzed in a population of 24 patients (Schmidt et al. 2009). Both modalities concordantly revealed 2 local recurrent tumors, WB-MRI proved useful for the detection of organ metastases with a diagnostic accuracy of 86 % compared to 87 % in FDG-PET-CT.

## References

- Albrecht T, Hoffmann CW, Schmitz SA et al (2001) Phase-inversion sonography during the liver-specific late phase of contrast enhancement: improved detection of liver metastases. *AJR Am J Roentgenol* 176:1191–1198
- Antoch G, Vogt FM, Freudenberg LS et al (2003) Whole-body dual-modality PET/CT and whole-body MRI for tumor staging in oncology. *JAMA* 290:3199–3206
- Atassi B, Bangash AK, Bahrani A et al (2008) Multimodality imaging following 90Y radioembolization: a comprehensive review and pictorial essay. *Radiographics* 28:81–99
- Barkhausen J, Quick HH, Lauenstein T et al (2001) Whole-body MR imaging in 30 seconds with real-time true FISP and a continuously rolling table platform: feasibility study. *Radiology* 220:252–256
- Bartolozzi C, Lencioni R, Caramella D et al (1996) Small hepatocellular carcinoma. Detection with US, CT, MR imaging, DSA, and Lipiodol-CT. *Acta Radiol* 37:69–74
- Bartolozzi C, Donati F, Cioni D et al (2004) Detection of colorectal liver metastases: a prospective multicenter trial comparing unenhanced MRI, MnDPDP-enhanced MRI, and spiral CT. *Eur Radiol* 14:14–20
- Belton AL, Saini S, Liebermann K et al (2003) Tumour size measurement in an oncology clinical trial: comparison between off-site and on-site measurements. *Clin Radiol* 58:311–314
- Beziat C, Pilleul F, Yzebe D et al (2004) Detection of liver metastases in colorectal cancer on chemotherapy. Comparative study between MRI with teslascan and computed tomography with intravenous contrast media. *J Radiol* 85:307–311
- Bluemke DA, Sahani D, Amendola M et al (2005) Efficacy and safety of MR imaging with liver-specific contrast agent: U.S. multicenter phase III study. *Radiology* 237:89–98
- Burns PN, Wilson SR (2007) Focal liver masses: enhancement patterns on contrast-enhanced images—concordance of US scans with CT scans and MR images. *Radiology* 242:162–174
- Busse RF (2004) Reduced RF power without blurring: correcting for modulation of refocusing flip angle in FSE sequences. *Magn Reson Med* 51:1031–1037
- Clark HP, Carson WF, Kavanagh PV et al (2005) Staging and current treatment of hepatocellular carcinoma. *Radiographics* 25(Suppl 1): S3–S23

- Cohade C, Osman M, Leal J et al (2003) Direct comparison of  $^{18}\text{F}$ -FDG PET and PET/CT in patients with colorectal carcinoma. *J Nucl Med* 44:1797–1803
- Coldwell DM, Kennedy AS, Nutting CW (2007) Use of yttrium-90 microspheres in the treatment of unresectable hepatic metastases from breast cancer. *Int J Radiat Oncol Biol Phys* 69:800–804
- del Frate C, Bazzocchi M, Morteke KJ et al (2002) Detection of liver metastases: comparison of gadobenate dimeglumine-enhanced and ferumoxides-enhanced MR imaging examinations. *Radiology* 225:766–772
- Deng J, Miller FH, Rhee TK et al (2006) Diffusion-weighted MR imaging for determination of hepatocellular carcinoma response to yttrium-90 radioembolization. *J Vasc Interv Radiol* 17:1195–1200
- Dudeck O, Zeile M, Wybranski C et al (2010) Early prediction of anticancer effects with diffusion-weighted MR imaging in patients with colorectal liver metastases following selective internal radiotherapy. *Eur Radiol* 20:2699–2706
- Eisenhauer EA, Therasse P, Bogaerts J et al (2009) New response evaluation criteria in solid tumours: revised RECIST guideline (version 1.1). *Eur J Cancer* 45:228–247
- Erasmus JJ, Gladish GW, Broemeling L et al (2003) Interobserver and intraobserver variability in measurement of non-small-cell carcinoma lung lesions: implications for assessment of tumor response. *J Clin Oncol* 21:2574–2582
- Frericks BB, Meyer BC, Martus P et al (2008) MRI of the thorax during whole-body MRI: evaluation of different MR sequences and comparison to thoracic multidetector computed tomography (MDCT). *J Magn Reson Imaging* 27:538–545
- Griswold MA, Jakob PM, Heidemann RM et al (2002) Generalized autocalibrating partially parallel acquisitions (GRAPPA). *Magn Reson Med* 47:1202–1210
- Gulec SA, Pennington K, Wheeler J, et al (2012) Yttrium-90 microsphere-selective internal radiation therapy with chemotherapy (Chemo-SIRT) for colorectal cancer liver metastases: an in vivo double-arm-controlled phase II trial. *Am J Clin Oncol*
- Harvey CJ, Albrecht T (2001) Ultrasound of focal liver lesions. *Eur Radiol* 11:1578–1593
- Haug AR, Heinemann V, Bruns CJ, et al (2011)  $^{18}\text{F}$ -FDG PET independently predicts survival in patients with cholangiocellular carcinoma treated with 90Y microspheres. *Eur J Nucl Med Mol Imaging* 38:1037–1045
- Ibrahim SM, Nikolaidis P, Miller FH et al (2009) Radiologic findings following Y90 radioembolization for primary liver malignancies. *Abdom Imaging* 34:566–581
- Jakobs TF, Hoffmann RT, Poepperl G et al (2007) Mid-term results in otherwise treatment refractory primary or secondary liver confined tumours treated with selective internal radiation therapy (SIRT) using (90)Yttrium resin-microspheres. *Eur Radiol* 17:1320–1330
- Jakobs TF, Hoffmann RT, Fischer T et al (2008a) Radioembolization in patients with hepatic metastases from breast cancer. *J Vasc Interv Radiol* 19:683–690
- Jakobs TF, Hoffmann RT, Dehm K et al (2008b) Hepatic yttrium-90 radioembolization of chemotherapy-refractory colorectal cancer liver metastases. *J Vasc Interv Radiol* 19:1187–1195
- Kalva SP, Thabet A, Wicky S (2008) Recent advances in transarterial therapy of primary and secondary liver malignancies. *Radiographics* 28:101–117
- Kennedy AS, Coldwell D, Nutting C et al (2006) Resin 90Y-microsphere brachytherapy for unresectable colorectal liver metastases: modern USA experience. *Int J Radiat Oncol Biol Phys* 65:412–425
- Kettritz U, Schlund JF, Wilbur K et al (1996) Comparison of gadolinium chelates with manganese-DPDP for liver lesion detection and characterization: preliminary results. *Magn Reson Imaging* 14:1185–1190
- Khodjibekova M, Szyszko T, Khan S et al (2007) Selective internal radiation therapy with Yttrium-90 for unresectable liver tumours. *Rev Recent Clin Trials* 2:212–216
- Kruger DG, Riederer SJ, Grimm RC et al (2002) Continuously moving table data acquisition method for long FOV contrast-enhanced MRA and whole-body MRI. *Magn Reson Med* 47:224–231
- Lardinois D, Weder W, Hany TF et al (2003) Staging of non-small-cell lung cancer with integrated positron-emission tomography and computed tomography. *N Engl J Med* 348:2500–2507
- Lauenstein TC, Goehde SC, Herborn CU et al (2002) Three-dimensional volumetric interpolated breath-hold MR imaging for whole-body tumor staging in less than 15 minutes: a feasibility study. *AJR Am J Roentgenol* 179:445–449
- Lencioni R, Donati F, Cioni D et al (1998) Detection of colorectal liver metastases: prospective comparison of unenhanced and ferumoxides-enhanced magnetic resonance imaging at 1.5 T, dual-phase spiral CT, and spiral CT during arterial portography. *MAGMA* 7:76–87
- Matsuo M, Kanematsu M, Itoh K et al (2001) Detection of malignant hepatic tumors: comparison of gadolinium-and ferumoxide-enhanced MR imaging. *AJR Am J Roentgenol* 177:637–643
- Miller AB, Hoogstraten B, Staquet M et al (1981) Reporting results of cancer treatment. *Cancer* 47:207–214
- Miller FH, Kepcke AL, Reddy D et al (2007) Response of liver metastases after treatment with yttrium-90 microspheres: role of size, necrosis, and PET. *AJR Am J Roentgenol* 188:776–783
- Namkung S, Zech CJ, Helmberger T et al (2007) Superparamagnetic iron oxide (SPIO)-enhanced liver MRI with ferucarbotran: efficacy for characterization of focal liver lesions. *J Magn Reson Imaging* 25:755–765
- Park JO, Lee SI, Song SY et al (2003) Measuring response in solid tumors: comparison of RECIST and WHO response criteria. *Jpn J Clin Oncol* 33:533–537
- Pelosi E, Messa C, Sironi S et al (2004) Value of integrated PET/CT for lesion localisation in cancer patients: a comparative study. *Eur J Nucl Med Mol Imaging* 31:932–939
- Pfannenbergh C, Aschoff P, Schanz S et al (2007) Prospective comparison of  $^{18}\text{F}$ -fluorodeoxyglucose positron emission tomography/computed tomography and whole-body magnetic resonance imaging in staging of advanced malignant melanoma. *Eur J Cancer* 43:557–564
- Quaia E (2007) Microbubble ultrasound contrast agents: an update. *Eur Radiol* 17:1995–2008
- Reimer P, Jahnke N, Fiebich M et al (2000) Hepatic lesion detection and characterization: value of nonenhanced MR imaging, superparamagnetic iron oxide-enhanced MR imaging, and spiral CT-ROC analysis. *Radiology* 217:152–158
- Reinhold C, Hammers L, Taylor CR et al (1995) Characterization of focal hepatic lesions with duplex sonography: findings in 198 patients. *AJR Am J Roentgenol* 164:1131–1135
- Rettenbacher THA, Hoflehner A, zur Nedden D (2005) Very small focal liver lesions appearing uncharacteristic at conventional US: does it make sense to investigate with contrast-enhanced US in attempt to further characterize the lesions? *Eur Radiol* 15:159–160
- Saxena A, Chua TC, Bester L, et al (2010) Factors predicting response and survival after yttrium-90 radioembolization of unresectable neuroendocrine tumor liver metastases: a critical appraisal of 48 cases. *Ann Surg* 251:910-916
- Schlemmer HP, Schafer J, Pfannenbergh C et al (2005) Fast whole-body assessment of metastatic disease using a novel magnetic resonance imaging system: initial experiences. *Invest Radiol* 40:64–71

- Schlitt HJ, Arnold D, Knoefel WT et al (2008) Surgical and perioperative therapy of liver metastases. *Onkologie* 31(Suppl 5):9–13
- Schmidt GP, Baur-Melnyk A, Herzog P et al (2005) High-resolution whole-body magnetic resonance image tumor staging with the use of parallel imaging versus dual-modality positron emission tomography-computed tomography: experience on a 32-channel system. *Invest Radiol* 40:743–753
- Schmidt GP, Wintersperger B, Graser A et al (2007) High-resolution whole-body magnetic resonance imaging applications at 1.5 and 3 Tesla: a comparative study. *Invest Radiol* 42:449–459
- Schmidt GP, Baur-Melnyk A, Haug A et al (2008) Comprehensive imaging of tumor recurrence in breast cancer patients using whole-body MRI at 1.5 and 3 T compared to FDG-PET-CT. *Eur J Radiol* 65:47–58
- Schmidt GP, Baur-Melnyk A, Haug A et al (2009) Whole-Body MRI at 1.5 and 3 T compared with FDG-PET-CT for the detection of tumour recurrence in patients with colorectal cancer. *Eur Radiol* 19:1366–1378
- Schmidt GP, Paprottka P, Jakobs TF et al (2012) FDG-PET-CT and whole-body MRI for triage in patients planned for radioembolisation therapy. *Eur J Radiol* 81:e269–e276
- Semelka RC, Martin DR, Balci C et al (2001) Focal liver lesions: comparison of dual-phase CT and multisequence multiplanar MR imaging including dynamic gadolinium enhancement. *J Magn Reson Imaging* 13:397–401
- Shim JH, Lee HC, Kim SO, et al (2012) Which response criteria best help predict survival of patients with hepatocellular carcinoma following chemoembolization? A validation study of old and new models. *Radiology* 262:708–718
- Squillaci E, Manenti G, Mancino S et al (2008) Staging of colon cancer: whole-body MRI vs. whole-body PET-CT—initial clinical experience. *Abdom Imaging* 33:676–688
- Tanaka S, Oshikawa O, Sasaki T et al (2000) Evaluation of tissue harmonic imaging for the diagnosis of focal liver lesions. *Ultrasound Med Biol* 26:183–187
- Therasse P, Arbuck SG, Eisenhauer EA et al (2000) New guidelines to evaluate the response to treatment in solid tumors. European Organization for Research and Treatment of Cancer, National Cancer Institute of the United States, National Cancer Institute of Canada. *J Natl Cancer Inst* 92:205–216
- Wahl RL, Jacene H, Kasamon Y et al (2009) From RECIST to PERCIST: evolving considerations for PET response criteria in solid tumors. *J Nucl Med* 50(Suppl 1):122S–150S
- Weber WA (2009) Assessing tumor response to therapy. *J Nucl Med* 50(Suppl 1):1S–10S
- Weckbach S, Michaely HJ, Stemmer A et al (2010) Comparison of a new whole-body continuous-table-movement protocol versus a standard whole-body MR protocol for the assessment of multiple myeloma. *Eur Radiol* 20:2907–2916
- Wong CY, Salem R, Raman S et al (2002) Evaluating 90Y-glass microsphere treatment response of unresectable colorectal liver metastases by [<sup>18</sup>F]FDG PET: a comparison with CT or MRI. *Eur J Nucl Med Mol Imaging* 29:815–820
- Haug AR, Tiega Donfack BP, Trumm C, et al. (2012) <sup>18</sup>F-FDG PET/CT predicts survival after radioembolization of hepatic metastases from breast cancer. *J Nucl Med* 53:371–377
- Zech CJ, Schoenberg SO, Herrmann KA et al (2004) Modern visualization of the liver with MRT. Current trends and future perspectives. *Radiologe* 44:1160–1169



---

# Results in Hepatocellular Carcinoma

Mercedes Iñárraigui and Bruno Sangro

## Contents

<b>1</b>	<b>Introduction</b> .....	106
<b>2</b>	<b>Effect of Radioembolization in the Tumor</b> .....	106
2.1	Tumor Response by Imaging.....	106
2.2	Tumor Response by Biomarkers.....	109
<b>3</b>	<b>Effect of Radioembolization in the Liver</b> .....	109
3.1	Liver Toxicity.....	109
3.2	Liver Atrophy and Radiation Segmentectomy and Lobectomy.....	110
<b>4</b>	<b>Results in Hepatocellular Carcinoma</b> .....	110
4.1	Early Stage.....	111
4.2	Intermediate Stage.....	112
4.3	Advanced Stage.....	113
<b>5</b>	<b>Future Directions</b> .....	114
<b>6</b>	<b>Conclusion</b> .....	115
	<b>References</b> .....	115

---

## Abstract

In the last years, new locoregional and systemic therapies have been developed for the management of hepatocellular carcinoma. Among the novel therapeutic procedures, yttrium-90 radioembolization has produced encouraging results across the whole spectrum of HCC, from early to advanced stages. All the evidence that support the use of radioembolization in HCC is based on retrospective series or non-controlled prospective studies. However, reliable data can be obtained from the literature, particularly since the recent publication of large series accounting for nearly 700 patients. Radioembolization achieves intense tumor response in targeted lesions and produces average disease control rates above 80 %. This effect supports its use for the treatment of early tumors with a curative intent, as a bridge to liver transplantation, and for unresectable HCC who exceed the transplant criteria or are not suitable for liver resection, with a downstaging intention. When compared to the standard of care for the intermediate and advanced stages (transarterial embolization and sorafenib), radioembolization consistently provides similar survival rates. It can be considered as a treatment option for those patients who are not considered good candidates for or have failed to transarterial embolization. It can also be a true alternative to sorafenib for the treatment of advanced tumors without extrahepatic metastases. The toxicity profile of radioembolization is favorable. Rarely, complications may result from irradiation of nontarget tissues including the liver and liver toxicity is the most challenging adverse event in HCC patients arising in a cirrhotic liver.

---

M. Iñárraigui (✉) · B. Sangro  
Liver Unit, Clínica Universidad de Navarra,  
Avda. Pio XII 36, 31008 Pamplona, Spain  
e-mail: minarra@unav.es

M. Iñárraigui · B. Sangro  
Centro de Investigación Biomedica en Red de Enfermedades  
Hepáticas y Digestivas (CIBEREHD), Pamplona, Spain

## 1 Introduction

Hepatocellular carcinoma (HCC) is the sixth most common cancer in the world and the third most common cause of cancer related mortality (Bosch et al. 2004). Cirrhotic patients of various etiologies and patients infected by viral hepatitis are at special risk of developing HCC, and this underlying liver disease impacts both on therapeutic decision and survival (European Association For The Study Of The Liver; European Organisation For Research And Treatment Of Cancer 2012). Over the last two decades, the treatment of HCC has undergone considerable changes with the development of new locoregional and systemic therapies (and a broadening of the indication for liver surgery and liver transplantation). Among the novel therapeutic procedures, yttrium-90 (90Y) radioembolization (90Y-RE) has produced encouraging results across the whole spectrum of HCC, from early to advanced stages (Lau et al. 1994; Geschwind et al. 2004; Salem et al. 2005, 2010; Sangro et al. 2006, 2011; Kulik et al. 2006, 2008; Lewandowsky et al. 2009; Iñarrairaegui et al. 2010a, b; Hilgard et al. 2010; Mazzaferro et al. 2013).

90Y-RE is a form of brachytherapy in which intraarterially injected microspheres loaded with 90Y (a pure beta emitter with a 2.6-day half-life and an average 2.5-mm tissue penetration) serve as sources for internal radiation purposes. As with other intra-arterial therapies, this technique is based on the preferential arterial blood supply of hepatic tumors, while the majority of non-tumoral liver is supplied primarily by the portal vein. However, the non-tumoral liver absorbs a certain dose of radiation, which intensity and distribution cannot be accurately predicted. Unlike the other main intra-arterial treatment (transarterial chemoembolization—TACE), the effects of 90Y-RE, both beneficial (antitumor effect) and deleterious (liver toxicity including radioembolization-induced liver disease) are derived from the radiation delivered by the isotope and not from the ischemic effect of vessel obstruction. To avoid the complications that may result from harmful irradiation of tissues other than the tumor, patients can only be considered for 90Y-RE provided the degree of arterio-venous shunting to the lung is limited, there is no possibility that microspheres may reach the gastrointestinal tract, and the liver has had no prior exposure to external irradiation (Kennedy et al. 2007).

All the evidence that supports the use of 90Y-RE in HCC is based on non-controlled retrospective or prospective series, and no controlled trials comparing 90Y-RE with other therapies at various disease stages have been published. Nevertheless, in the last years, liver 90Y-RE has become an emerging and expanding tool in the complex algorithm of HCC management and we have more

information delivered from different large series that can be analyzed to provide sound data on the results of 90Y-RE in HCC (Salem et al. 2010; Hilgard et al. 2010; Sangro et al. 2011; Mazzaferro et al. 2013).

---

## 2 Effect of Radioembolization in the Tumor

External-beam radiotherapy was historically considered ineffective for the treatment of unresectable HCC because the doses of radiation necessary to cure HCC far exceeded the tolerance of the entire liver to radiation. The risk of potentially fatal radiation-induced liver disease, observed when whole-liver radiation doses exceeded 30 Gy over 3 weeks, resulted in the near abandonment of radiation therapy as a treatment modality for HCC (Lawrence et al. 1995). However, HCC is a radiosensitive tumor, and several studies have shown the effect of local radiotherapy on HCC, both in terms of tumor response and overall survival (Robertson et al. 1997; Mc Ginn et al. 1998; Dawson et al. 2000; Ben-Josef et al. 2005; Mornex et al. 2006). A variety of techniques have been developed to overcome the liver tolerance issue and deliver radiation therapy to liver cancers while sparing non-tumoral liver from radiation including 3-dimensional conformal RT, stereotactic body RT, proton beam RT, and interstitial brachytherapy. 90Y-RE is another procedure that provides high doses of radiation to liver tumors by the preferential distribution of 90Y loaded microspheres inside the tumor vessels.

### 2.1 Tumor Response by Imaging

The effect of 90Y-RE in targeted tumoral tissue has been reported consistently in the different series, from those consisting of bulky and more advanced tumors (Dancey et al. 2000; Carr et al. 2004; Salem et al. 2005), to those in which earlier tumors were treated (Lewandowski et al. 2009; Riaz et al. 2009). As described in Table 1, response rates varied between 11 and 70 % according to WHO or RECIST criteria. This wide variation in response rates may reflect differences in the time of evaluation or in treatment intensity. Tumor shrinkage after 90Y-RE may take months to occur, with a median time to response of around 6 months according to WHO criteria (Salem et al. 2010), and time of evaluation differs in the published series. This tumor response achieved with 90Y-RE may remain stable for a long time, as shown in Fig. 1. Additionally, as with other intravascular devices or targeted therapies, size response may not capture all the antitumor effect, although its correlation with a benefit in survival has been provided

**Table 1** Tumor response, according to radiologic parameters and biomarkers

Author, year	Radiological tumor response						Biomarkers tumor response		
	N, type of microspheres	Size <sup>1</sup>		Size + Necrosis <sup>2</sup>		TTP	N <sup>a</sup>	(% pt)	AFP reduction
		ORR (CR + PR)	DCR (CR + PR + SD)	ORR (CR + PR)	DCR (CR + PR + SD)				
Lau et al. 1998	71, resin	27 %					46	89	>50 %
							22		Normalization
Dancey et al. 2000	22, glass	20 %	75 %			10.2 m			
Carr et al. 2004	65, glass	38 %							
Salem et al. 2005	43, glass	47 %		79 %					
Sangro et al. 2006	24, resin	24 % $\Psi$	100 % $\Psi$						
Kulik et al. 2006	35, glass	50 %							
Riaz et al. 2009	35, glass	45 %	92 %	57 %	89 %	5.9 m	55	70	>50 %
								77	>20 %
								41	>90 %
								17	Normalization
Gaba et al. 2009	20, glass	55 %	100 %	90 %	100 %		6	50	>50 %
		70 % $\Psi$	100 % $\Psi$					50	Normalization
Lewandosky et al. 2009	43, glass	61 %	98	86 %	100 %				
Iñarrairaegui et al. 2010b	50, resin	12 % $\Psi$	94 % $\Psi$				29	31	>50 %
Salem et al. 2010	291, glass	42 %		57 %		7.9 m			
Carr et al. 2010	99, glass	33 %	76 %						
Kooby et al. 2010	42, resin	11 % $\Psi$	52 % $\Psi$				21	24	>30 %
Hilgard et al. 2010	76, glass	15 %	94 %	40 %	93 %	10 m			
		16 % $\Psi$	90 % $\Psi$	41 % $\Psi$ m	89 % $\Psi$ m				
Iñarrairaegui et al. 2010a	25, resin		67 % $\Psi$						
Salem et al. 2011	123, glass	49 %		72 %		13.3 m			
Lance et al. 2011	38, resin and glass						26	46	>30 %
Mazzaferro et al. 2013	52, glass	40 %	75 %	40 %	79 %	11 m		68	>50 %

ORR overall response rate. CR complete response. PR partial response. SD stable disease. DCR disease control rate. TTP Time to progression. AFP Alpha-fetoprotein

<sup>1</sup> According to WHO criteria, unless otherwise specified.  $\Psi$  RECIST criteria

<sup>2</sup> According to EASL criteria, unless otherwise specified.  $\Psi$ m modified RECIST criteria

<sup>a</sup> Patients with elevated basal levels, according to different cut-off values: Lau et al. 1998 >100 ng/ml; Riaz et al. 2009 >200 ng/ml; Gaba et al. 2009 >200 ng/ml; Iñarrairaegui et al. 2010b, >40 ng/ml; Kooby et al. 2010 >400 ng/ml; Lance et al. 2011 >400 ng/ml

in a large series of patients. The Chicago group analyzed patients separately according to Child-Pugh score and BCLC stage and reported a significantly prolonged survival in patients that were considered responders according to WHO criteria (Salem et al. 2010). However, other small

series have not found a correlation between size response and survival (Iñarrairaegui et al. 2010b). Other imaging characteristics such as arterial contrast enhancement may also be evaluated after 90Y-RE. By using mixed (size and vascular enhancement) response criteria such as those

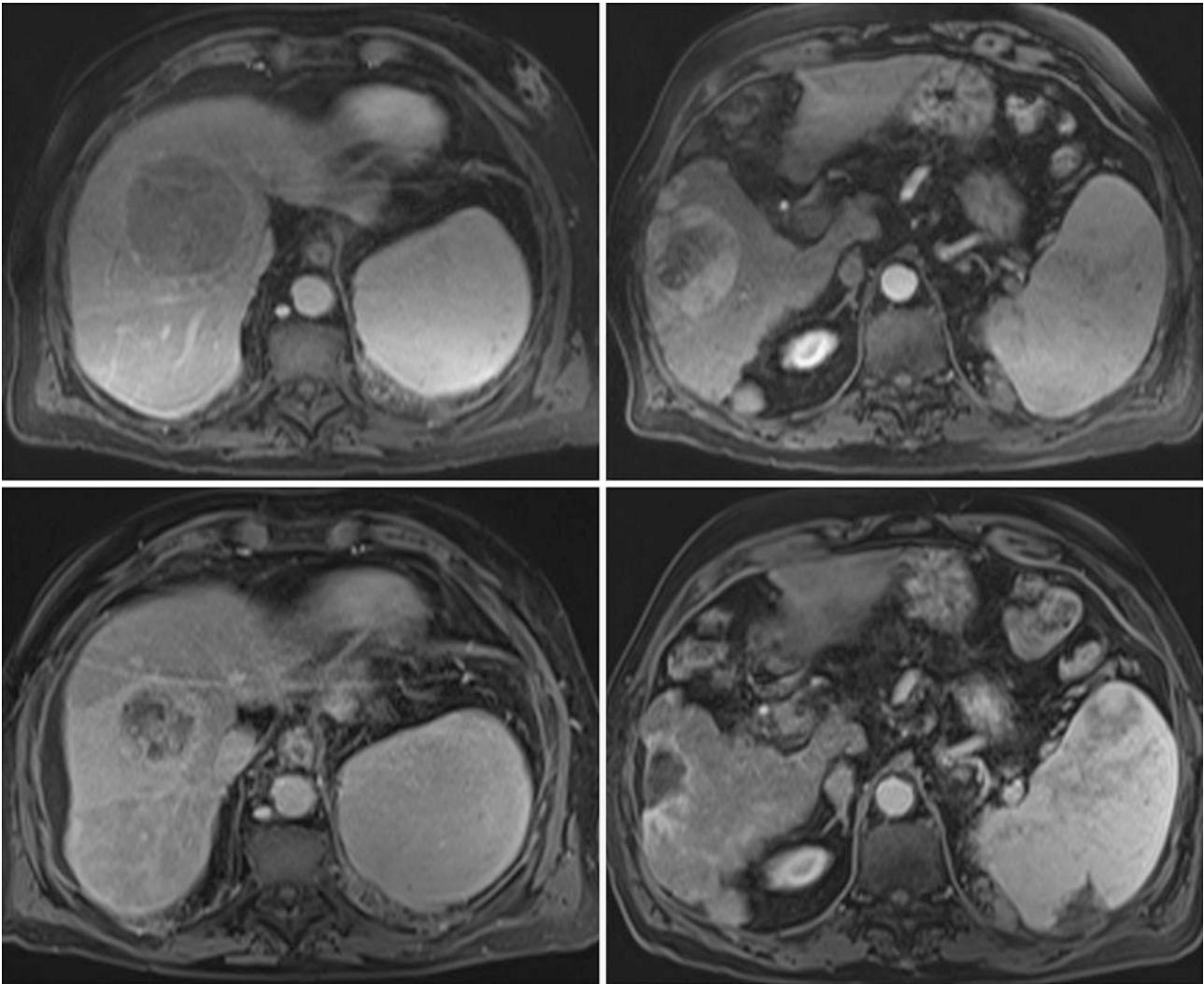


**Fig. 1** A cirrhotic patient with two HCC nodules of 6.8 cm in segment VIII (*arterial phase MRI, top left*) and 9.8 cm in segment VI (*arterial phase MRI, top right*). After 90Y-RE from right hepatic artery, prolonged response was achieved and 18 months after treatment, lesion in segment VIII was reduced in size and showed a

heterogeneous contrast enhancement (*arterial phase MRI, bottom left*) while lesion in segment VI was reduced in size, showed no arterial enhancement and caused a retraction of the liver surface (*arterial phase MRI, bottom right*)

proposed by the European Association for the Study of the Liver (EASL) (Bruix and Sherman 2011), tumor response rates are higher and vary between 40 and 90 %, with a disease control rate in targeted lesions of 80–100 %. Time to response taking into account vascular enhancement occurs earlier, around 2 months from the time of 90Y-RE (Salem et al. 2010). Tumor responders according to EASL criteria have also a significantly prolonged overall survival when compared to nonresponders (Memon et al. 2011).

Among patients with small tumors treated selectively, radiological findings have been found to correlate with pathologic necrosis in a retrospective series of 35 patients treated prior to transplantation. Complete pathologic necrosis was seen in 100 and 93 % of the lesions that showed complete response by EASL criteria or a thin rim of

peripheral contrast enhancement, respectively (Riaz et al. 2009). Evaluation of tumor response may be more complicated in patients with multinodular or diffuse tumors or portal vein thrombosis. Interestingly, a simplified method has been reported that awaits validation in additional series of patients. Among 245 patients treated by locoregional therapies including TACE and 90Y-RE, the response in the so-called “primary index lesion” (the dominant-treated lesion, irrespective of multifocality) by WHO, RECIST, or EASL criteria correlated with improved time to progression and survival (Riaz et al. 2010a).

### 2.1.1 Dose–Response Relationship

The actual dose of radiation absorbed by tumor tissue cannot be calculated after 90Y-RE. It depends on the



activity administered, which can be measured, but also on different parameters that cannot be determined, from the exact positioning of the catheter to the evolving arterial hemodynamics over the injection period or the vessel density inside the different tumors of the same patient. All these factors provide differences in the biodistribution of microspheres and in the absorbed doses of radiation in different areas of the treated tissue. In practice, dosimetry is based on a simulation with macroaggregated albumin labeled with technetium 99 ( $^{99m}\text{Tc}$ -MAA). It is performed in order to calculate lung shunting from a planar scintigraphy, and may be used to estimate the average dose that will be delivered to the non-tumoral liver and to the tumor from planar or SPECT images, calculating the tumor/non-tumor ratio. Although the ability of  $^{99m}\text{Tc}$ -MAA images to predict Y90 activity distribution and dosimetry is far from ideal, the majority of series that explore retrospectively the dosimetry based on  $^{99m}\text{Tc}$ -MAA images have shown a dose–response relationship. Lau et al. (1994) first reported that an objective response by combined WHO and alpha-fetoprotein criteria occurred in higher proportion (7/8) of patients in which every tumor absorbed more than 120 Gy when compared to those (1/8) in which at least one tumor received an estimated absorbed dose of less than 120 Gy. Survival was also better in the former group (median survival: 55.9 vs. 26.2 weeks). More recently, in a study of 36 patients treated with 90Y-RE, a higher estimated dose delivered to the tumor was associated with the appearance of radiological response according to EASL criteria and with overall survival, and a threshold for tumor absorbed dose of 205 Gy enabled response prediction with a high accuracy (Garin et al. 2012). Finally, in a dosimetric analysis of 65 tumor lesions, EASL response correlated with the dose absorbed by target lesions (Spearman's  $r = 0.60$ , 95 % CI: 0.41–0.74,  $p < 0.001$ ). Lesions lacking objective response received a median dose of 275 Gy, while responding tumors were found to absorb a median of 490 Gy. An efficacy threshold of 500 Gy significantly predicted the observed objective response and limited to 20 % the rate of nonresponders (AUC = 0.78) (Mazzaferro et al. 2013). Nevertheless, it should be emphasized that a consistent cut-off value that ensures a tumor response has not been reported, and that no prospective study has confirmed these observations. All these data support the current search for innovative treatment planning based on tumor/non-tumor dosimetry methods applied to  $^{99m}\text{Tc}$ -MAA SPECT as pretreatment prediction of efficacy.

## 2.2 Tumor Response by Biomarkers

It has been recently proposed that changes in levels of alpha-fetoprotein after locoregional therapy can be

considered a good method for assessing tumor response and survival, as well as an early objective screening tool for progression by imaging (Sherman 2010). Alpha-fetoprotein response has also been explored after 90Y-RE, as it is described in Table 1. With different cut-off values for elevated alpha-fetoprotein (40 and 400 ng/ml), alpha-fetoprotein response defined as more than 50 % decrease from baseline was observed in 30–89 % of patients (Lau et al. 1998; Gaba et al. 2009; Riaz et al. 2009; Iñarrairaegui et al. 2010b; Mazzaferro et al. 2013). Time to alpha-fetoprotein response was 2.7 months (CI 95 % 2.3–4 months) and alpha-fetoprotein response correlated with overall survival ( $p < 0.001$ ) (Riaz et al. 2009).

## 3 Effect of Radioembolization in the Liver

The predominantly arterial vascularization of liver tumors provides the basis for the aim of delivering tumoricidal doses of radiation to liver tumors while sparing the non-tumoral tissue. However, in 90Y-RE the non-tumoral liver tissue also absorbs a certain dose of radiation. The effects that this radiation produces in the liver are largely unknown but may translate into a variety of changes in liver function tests, morphological changes such as liver atrophy, and clinical syndromes including radioembolization-induced liver disease (REILD) that is covered in another chapter of this book.

### 3.1 Liver Toxicity

The potential to induce significant liver toxicity is the main drawback of 90Y-RE in cirrhotic patients, because of their reduced functional reserve and regenerative ability. Cirrhosis may influence the development of liver toxicity because the usual distribution of microspheres can be profoundly altered by changes in the microvascular pattern and the presence of anatomical arterio-portal and arterio-venous shunts. These alterations may modify the radiation dose absorbed by the non-tumoral liver and affect treatment tolerance. The functional reserve of a cirrhotic liver is reduced, and this contributes to an increased risk of liver failure after any liver insults as radiation (Furuse et al. 2005). From a theoretical point of view, besides a direct liver cell injury radiation could compromise liver blood flow by a radiation-mediated blood vessel damage. This may result in a higher risk of clinically relevant liver toxicity after 90Y-RE in comparison with non-cirrhotic livers. A dose–response relation has been reported also for liver toxicity. HCC patients with liver toxicity were exposed to significantly higher absorbed doses in the non-tumoral liver (median: 49.9 vs. 27.4 Gy  $p < 0.02$ ) (Sangro et al.

2006). Again, the lack of an adequate dosimetry and the heterogeneous distribution of the microspheres throughout the liver parenchyma may explain the lack of a consistent cut-off point. However, toxicity is extremely rare when patients receive an average of 40 Gy to the non-tumoral liver in a 2-compartment model (Gil-Alzugaray et al. 2012). An expert agreement is that the dose absorbed by the non-tumoral liver tissue should be kept below 50 Gy for all patients and maybe below 40 Gy for patients with an impaired non-tumoral liver (Lau et al. 2012).

REILD can be the most severe liver complication after 90Y-RE. It was initially described in non-cirrhotic patients as jaundice and ascites appearing 1–2 months after RE in the absence of tumor progression or bile duct occlusion (Sangro et al. 2008). More recently, we have analyzed its incidence and predisposing factors in 260 patients (both cirrhotic and non-cirrhotic). In the same cohort, we have evaluated the effect that some modifications in the treatment protocol (changes in treatment design, activity calculation and routine use of ursodeoxycolic acid, and low dose steroids) had on its incidence. In cirrhotic patients, REILD occurred in 9.3 % of patients when using the current modified protocol. REILD was more likely to occur in those patients with small liver volumes (<1.5 L), hypersplenism (platelets <100/pL) or abnormal bilirubin, and in those treated in a selective fashion (Gil-Alzugaray et al. 2012). The actual incidence of this complication in cirrhotics and non-cirrhotics patients is difficult to establish because most published series report on changes in individual laboratory values along different periods of time, from 30 days to the entire follow-up period.

### 3.2 Liver Atrophy and Radiation Segmentectomy and Lobectomy

Liver atrophy may occur in patients treated with 90Y-RE (Jakobs et al. 2008) and has been associated with an increase in bilirubin (Nosher et al. 2011). Although this remains an important issue in cirrhotic patients, no long-term complications derived from portal hypertension have been reported in the literature so far. When a single lobe is targeted (and usually receives a more intense treatment), liver atrophy affects the treated lobe and is associated with a contralateral increase in lobar volume (lobar atrophy–hypertrophy complex formation), in what has been termed “radiation lobectomy” (Gaba et al. 2009; Fernandez-Ross et al. 2013). It has been recently described in patients with unresectable HCC that this hypertrophy along with tumor response in the treated area may allow some patients to receive surgical treatment with a curative intent and prolonged survival (Iñarrairaegui et al. 2012).

Further on, radiation segmentectomy is an approach by which high-dose radiation is delivered to two or fewer hepatic segments, resulting in eradication of the tumor (Riaz et al. 2011). By limiting this high dose of radiation to segmental hepatic anatomy, patients are theoretically able to tolerate these radiation doses with much less risk of developing the potentially fatal complications of liver irradiation. The radiated sector usually develops a process of atrophy and over time, the entire segment can even disappear in cross-sectional images. This technique requires comprehensive and careful hepatic angiography prior to treatment, and can be applied to those tumors in which ablation and resection are contraindicated because of location, co-morbidities, or insufficient liver reserve.

## 4 Results in Hepatocellular Carcinoma

Having described the effects of 90Y-RE in the tumor and the liver, we will review in the next pages the available evidence supporting the role of 90Y-RE in the different stages of HCC using the Barcelona Clinic Liver Cancer (BCLC) classification, that has been endorsed by the two main Western Hepatology societies, EASL (European Association For The Study Of The Liver; European Organisation For Research And Treatment Of Cancer 2012) and the American Association for the Study of Liver Diseases (AASLD) (Bruix and Sherman 2011). All the evidence comes from retrospective series or non-controlled prospective studies (Lau et al. 1994; Geschwind et al. 2004; Salem et al. 2005, 2006; Lewandowski et al. 2009; Kulik et al. 2006, 2008; Iñarrairaegui et al. 2010a, b), without any randomized controlled trials comparing 90Y-RE with other available therapies. However, in the last 3 years four large series have provided valuable information in the different stages of HCC, and may allow to put the outcomes in the perspective of other treatments, mainly in terms of survival (Salem et al. 2010; Hilgard et al. 2010; Sangro et al. 2011; Mazzaferro et al. 2013) (Table 2). Besides, some of these series provide with data on toxicity (Table 3) and on surrogate endpoints that are likely to predict clinical benefit, as objective tumor response rates and time to progression. Despite this growing body of evidence and due to the lack of randomized controlled trials, 90Y-RE is not recommended in the proposed algorithms of treatment in the above mentioned EASL and AASLD guidelines (European Association For The Study Of The Liver; European Organisation For Research And Treatment Of Cancer 2012; Bruix and Sherman 2011). However, its use is considered in others guidelines, as the European Society for Medical Oncology (ESMO) (Jelic et al. 2010) and the National Comprehensive Cancer Network (NCCN) (Benson et al.

**Table 2** Median survival after radioembolization of HCC patients according to tumor stage

Author, year	N	Median survival (months)	95 % confidence interval
<b>BCLC A</b>			
Salem et al. 2010	48	26.9	17.0–30.2
Sangro et al. 2011	52	24.4	18.6–38.1
<b>BCLC B</b>			
Salem et al. 2010	83	17.2	13.5–29.6
Hilgard et al. 2010	51	16.4	12.1–∞
Sangro et al. 2011	87	16.9	12.8–22.8
Mazzaferro et al. 2013	17	18	12–38
<b>BCLC C</b>			
Salem et al. no EHD 2010	107	7.3	6.5–10.1
Salem et al. EHD 2010	45	5.4	2.7–7.5
Sangro et al. 2011	183	10.0	7.7–10.9
Mazzaferro et al. 2013	35	13.	9–17

EHD-extrahepatic disease

**Table 3** Non-liver related clinical toxicity among HCC patients treated by 90Y-RE

Author, year	Salem et al. 2010	Sangro et al. 2011	Hilgard et al. 2010	Mazzaferro et al. 2013 <sup>a</sup>
N	<i>N</i> = 291	<i>N</i> = 325	<i>N</i> = 108	<i>N</i> = 52
Clinical toxicities	Any time after 90Y-RE	3 months after 90Y-RE	Any time after 90Y-RE	3 months after 90Y-RE
Fatigue (%)	57	54	61	2
Nausea/vomiting (%)	20	32	Nr	6
Abdominal pain (%)	23	27	56	4
Fever (%)	3	12	Nr	4
Neumonitis (%)	0	0	0	0
GI ulcerations (%)	0	3	0	0

<sup>a</sup> Only grade 3–4 clinical toxicities are reported GI Gastrointestinal

2009) and has been a matter of debate and editorials in one of the most notable journal of the specialty lately (Kulik 2010; Bolondi and Piscaglia 2013).

#### 4.1 Early Stage

First reports in the literature mainly applied 90Y-RE for the treatment of unresectable advanced HCC. In the last years, as its use has been extended, some series have reported the outcomes of 90Y-RE in early tumors. 90Y-RE can induce complete necrosis in targeted lesions, as has been suggested by the analyses of 35 explanted livers from patients treated with 90Y-RE as a bridge or after successful downstaging to liver transplantation. Nearly 90 % of the tumors up to 3 cm in size and two-thirds of those between 3 and 5 cm had a complete pathologic necrosis (Riaz et al. 2009). These rates compare favorably with those obtained after radiofrequency ablation (Lencioni et al. 2003; Lin et al. 2004; Shiina et al.

2005; Lin et al. 2005; Brunello et al. 2008) and TACE (Riaz et al. 2010a; Golfieri et al. 2011). Nevertheless, these results warrant further validation before 90Y-RE is recommended as a treatment of early tumors with a curative intent in patients with liver surgery contraindication.

In terms of survival, recent series describing outcomes according to tumor stage have reported a consistent median overall survival of around 26 months (Salem et al. 2010, 2011; Sangro et al. 2011) in patients at early stages (inoperable BCLC A) after 90Y-RE. This survival is in between the wide range of median survival reported with TACE/TAE in large series of BCLC A patients, from 16.8 to 45.4 months in (Wang et al. 2008; Chen et al. 2009; Ho et al. 2009; Lewandowski et al. 2010; Hsu et al. 2011; Salem et al. 2011; Burrell et al. 2012). Median time to progression in this early stage has been described as long as 25.1 months (95 % IC 8–27 months), longer than the observed with TACE in a retrospective well-balanced comparative study between both techniques (TACE and

90Y-RE) (Salem et al. 2011), and this may provide a rationale for its use as a bridge to liver transplantation in an attempt to avoid dropping from the waiting list (Heckman et al. 2008).

## 4.2 Intermediate Stage

Intermediate HCC stage (BCLC B) comprises a very heterogeneous group of patients, including asymptomatic patients with multinodular unresectable tumors whose liver function is not severely compromised. In this stage, TACE has become the standard of care, based on the results of two randomized controlled trials (Llovet et al. 2002; Lo et al. 2002) and two retrospective meta-analyses (Camma et al. 2002; Marelli et al. 2007) showing that TACE or TAE improves survival in unresectable HCC patients when compared to best supportive care. The population recruited in these positive trials, nevertheless, includes a substantial proportion of patients in the early stage (single tumors), and most patients in the intermediate stage had single-lobe involvement that could be selectively embolized. However, the intermediate HCC stage (BCLC B) incorporates heterogeneous tumor burdens and liver function stages (Child-Pugh A or B) resulting in a wide interval of expected survival after TACE, from 15 to 43 months (Wang et al. 2008; Chen et al. 2009; Ho et al. 2009; Salem et al. 2011; Burrel et al. 2012). The outcomes of alternative treatments in this group of patients should be analyzed regarding this heterogeneous population. 90Y-RE has been applied for the treatment of patients in the whole spectrum of the BCLC B stage, although most series include patients with preserved liver function (Child-Pugh  $\leq$ B7). The Chicago group reported a median survival of 17.2 months (CI 95 % 13.5–29.6) in the group of 83 BCLC B patients, with a median time to progression of 13.3 months (CI 95 % 4.4–18.1) (Salem et al. 2010). The same authors have reported the compared outcomes of patients treated exclusively by TACE or 90Y-RE in their institution that lacked portal vein thrombosis or extrahepatic disease (Salem et al. 2011). This series included mainly patients with intermediate (53 %) or early (35 %) tumors treated in the same period (2001–2010), in which treatment allocation was decided by a multidisciplinary team. When patients in the intermediate stage were evaluated separately, an identical survival in the intermediate stage was observed after either treatment (15.5 vs. 17.2 months), and the hazard ratio for death in the 90Y-RE cohort was 0.86 ( $p = 0.579$ ) in the multivariate analysis. Although both groups experienced fatigue, nausea, and anorexia, TACE patients were more likely to experience abdominal pain ( $p < 0.001$ ) and exhibited significantly higher hepatic transaminases elevation ( $p = 0.004$ ). Another recent retrospective series that

compared efficacy and safety between 90Y-RE and TACE in the different stages of the BCLC classification, observed a similar overall survival between both therapies in BCLC B patients (16.8 vs. 13 months,  $p$  ns) (Moreno-Luna et al. 2012). Overall, the frequency of any side effect was not different between both groups, although the 90Y-RE group included more patients in the intermediate stage (BCLC B) and the TACE group included more patients in the early stage (BCLC A). Fatigue was significantly more common in patients treated with 90Y-RE, and fever was more common in TACE group patients. There were no significant differences regarding liver tests between both treatments. Two additional centers have describe the outcomes of 51 and 17 BCLC B patients treated with glass microspheres (Hilgard et al. 2010; Mazzaferro et al. 2013), showing a median overall survival of 16.4 months (95 % CI 12.1–a) and 18 months (95 % CI 12–38), respectively. In one of these series, disease control rate was 79 % according to EASL criteria and time to progression was 13 months (95 % CI 6–nc) (Mazzaferro et al. 2013).

Not all patients with intermediate stage HCC are considered good candidates for TACE. Poor candidates are usually those with bulky disease confined to the liver that still have a normal performance status and usually have a single large nodule or more than 5 nodules affecting both lobes (Raoul et al. 2011). Other subgroup of intermediate stage patients are those who have failed TACE but remains in the intermediate stage. For those patients, treatment options are sorafenib or 90Y-RE. The European Network on Radioembolization using 90Y (ENRY) series has analyzed separately the results of 90Y-RE in this individual subgroups of patients, and an encouraging median survival of 15.4 months has been reported for BCLC B patients with bilobar disease or more than 5 nodules ( $n = 32$ ), and 11.4 months in BCLC B patients failing TACE/TAE ( $n = 62$ ) (Sangro et al. 2011). Comparatively, in a subset analysis of the pivotal SHARP trial that showed the superiority of the oral agent sorafenib versus placebo in the advanced stage, median survival was 14.5 months for BCLC B patients not suitable for or refractory to locoregional therapies treated with sorafenib, and 11.9 months for patients with prior TACE (Bruix et al. 2012).

90Y-RE can also be considered for those patients who are ideal candidates to TACE, with median overall survival of 22.8 (95 % CI 13.6–36.0) for patients with 1–5 nodules and 23.2 months (95 % CI 13.6–not reached) for tumors affecting a single lobe (Sangro et al. 2011). In these patients, TACE can achieve also prolonged survival, as has been shown in a recent study from the Barcelona group, where a very selective cohort of BCLC B patients ( $n = 63$ ) treated with TACE using drug eluting beads achieved an overall survival of 42.8 months (95 % CI 27.6–58) (Burrel et al. 2012). In this subgroup of intermediate stage patients



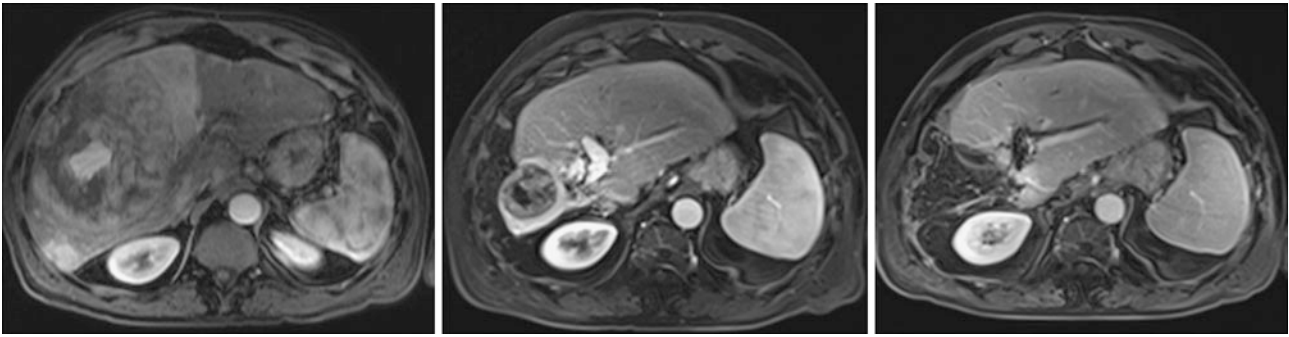


**Fig. 2** A 14-cm right-lobe lesion on a cirrhotic liver (*portal venous phase MRI, left*) was treated by 90Y-RE three times. A 1 year after the third 90Y-RE session, an intense response with contralateral lobe hypertrophy was achieved (*portal venous phase MRI, center*), and the patient underwent a right hepatectomy 28 months after the first

radioembolization (*portal venous phase MRI, right*). About 10 months after surgery, he developed tumor progression (one small nodule in the remnant liver and lung metastases). The patient died 15 months after liver resection from a myocardial infarction

that are optimal candidates for TACE, the additional advantages of 90Y-RE need to be proved.

Last, but not least, in the heterogeneous group of intermediate HCC, another subgroup of patients who could benefit from RE are those in whom downstaging strategies can be applied. In patients with unresectable HCC who exceed the transplant criteria or are not suitable for liver resection, 90Y-RE could be used as a downstaging therapy, to reduce the tumor burden within acceptable limits for liver transplantation, to render non-operable patients operable, or to simplify surgery. As we explained before, tumor response and contralateral lobe hypertrophy as a result of the injection of a high 90Y activity in a lobar hepatic artery, may both contribute to allow resectability (Gaba et al. 2009), as shown in Fig. 2. A few case reports and cohort studies of downstaging after 90Y-RE have been published (Lau et al. 1998; Kulik et al. 2006; Lewandowski et al. 2009; Iñarrairegui et al. 2012). In the largest series, out of 35 patients at United Network for Organ Sharing (UNOS) T3 stage treated by 90Y-RE, 23 (66 %) achieved a T2 stage during follow-up, where resection, RFA, or transplant could be indicated. Eight patients (23 %) preferred close observation rather than RFA or transplantation and the 1- and 3-year survival rates were 84 and 27 %, respectively (Kulik et al. 2006). Compared with TACE, downstaging from UNOS T3 to T2 stage was achieved more frequently with 90Y-RE (58 % vs. 31 %  $p = 0.023$ ) and overall survival favored 90Y-RE (when patients were censored at the time of RFA or transplantation: 35.7 vs. 18.7 months for TACE,  $p = 0.18$ ; when they were not censored: 41.6 vs. 19.2 months,  $p = 0.008$ , respectively) (Lewandowski et al. 2009). Our group has similarly analyzed the rate of downstaging in patients at UNOS T3 stage treated with a palliative intent. Overall, 29 % of 21 UNOS T3 stage patients were downstaged and underwent surgical resection or liver transplantation. The 3-year survival rate was 75 %, which is comparable with the survival in patients with early stage

disease who are treated radically at the time of diagnosis (Iñarrairegui et al. 2012).

### 4.3 Advanced Stage

The three main features of the advanced stage disease (BCLC C stage) are deterioration in performance status, the presence of extrahepatic disease, and/or portal vein invasion in a patient with at least partially preserved liver function. Each of these three features worsens the prognosis of patients regardless of treatment modality. For these patients the recommended treatment is sorafenib, which results in median survival between 6.5 and 9.7 months (Cheng et al. 2009; Bruix et al. 2012). 90Y-RE can offer a similar median survival benefit in the range of 6–13 months (Salem et al. 2010; Sangro et al. 2011; Mazzaferro et al. 2013) with a good safety profile.

90Y-RE has no macroembolic effect (Sato et al. 2006, Bilbao et al. 2009) and can be successfully applied to patients with portal vein thrombosis as shown in Fig. 3. Safety is an issue in these patients, and 90Y-RE has a good safety profile that is comparable in patients with or without portal vein thrombosis (Table 4). In the first and larger series published from the group of Chicago, patients with cirrhosis and portal vein thrombosis involving the main trunk had a higher incidence of adverse events (a non-statistically significant increment in bilirubin levels, and an significant increase in ascites) (Kulik et al. 2008). The ENRY series analyzed main clinical adverse events and liver toxicity in the different BCLC stages, and observed similar liver toxicity across the stages A through C (Sangro et al. 2011). Only fatigue was reported most commonly in the advanced stage (61.2 %) compared with those with intermediate or early stage disease, which is not surprising since fatigue is usually associated with altered performance status. Finally, no significant differences in toxicity were

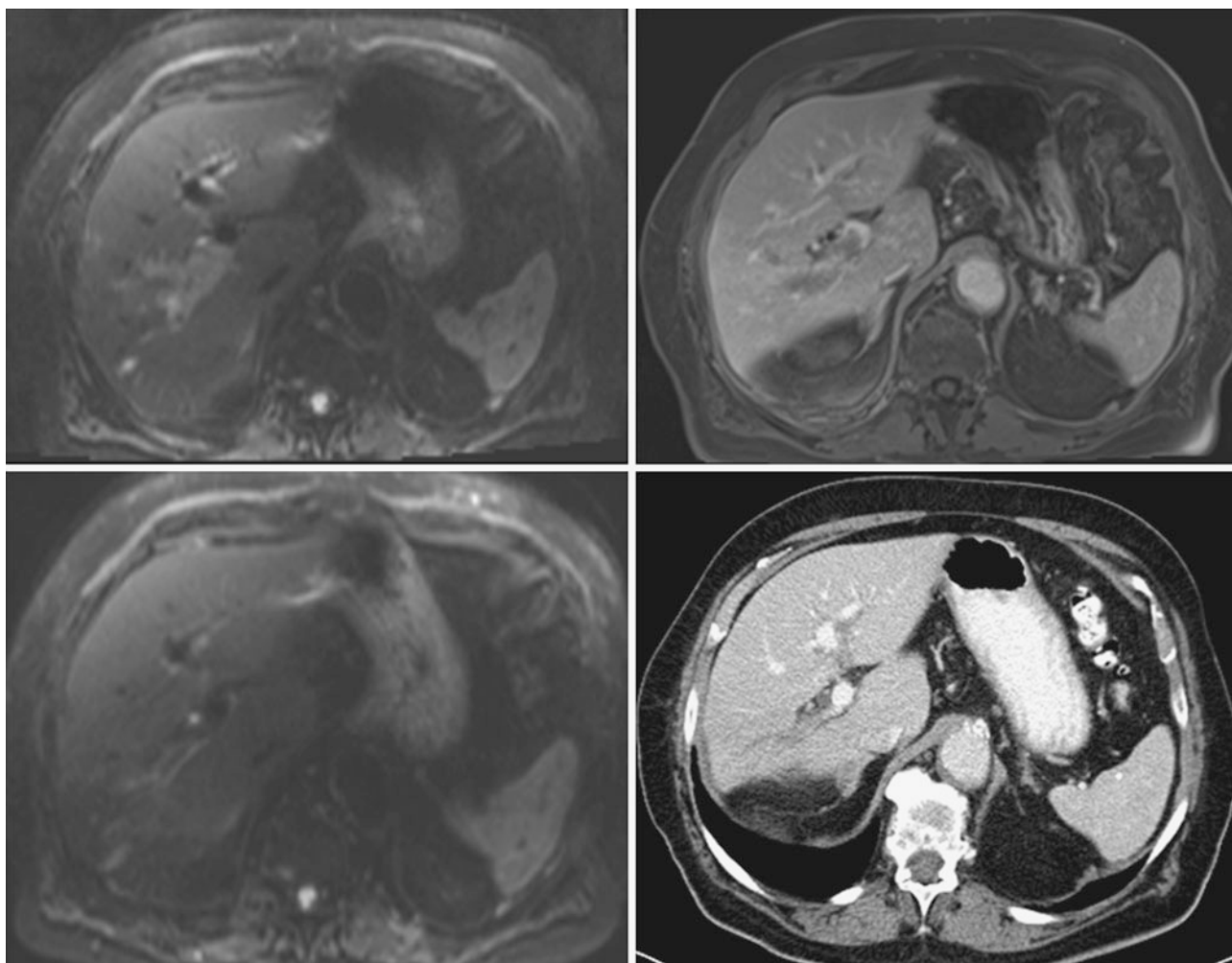


**Fig. 3** A cirrhotic patient with an HCC with portal vein invasion of the right branch and main trunk (*diffusion-weighted MRI, top left and portal venous phase, top right*). About 4 months after 90Y-RE from

right hepatic artery, an objective response in the tumoral thrombus was observed (*diffusion-weighted MRI, bottom left*) that persists 12 months after treatment (*CT portal venous phase, bottom right image*)

registered when patients with and without portal vein thrombosis were compared in the Milan phase 2 trial (Mazzaferro et al. 2013). However, one must take into account that the extent of portal vein thrombosis also matters. When thrombosis affects the main trunk, survival is more disappointing and ranges between 3.2 and 8 months (Kulik et al. 2008; Woodall et al. 2009; Mazzaferro et al. 2013), while survival extends to 10–14 months in patients with only branch thrombosis (Kulik et al. 2008; Iñarrairaegui et al. 2010a; Mazzaferro et al. 2013).

Metastases are not the direct cause of death in the majority of HCC patients and a locoregional treatment may thus be considered when a small metastatic burden involves non-vital organs such as bone, adrenal glands, or lymph nodes. Nevertheless, extrahepatic disease is an indicator of disease aggressiveness (Uchino et al. 2011) and median survival in metastatic patients treated with 90Y-RE is poor,

ranging between 5.4 and 7.4 months (Salem et al. 2010; Sangro et al. 2011).

## 5 Future Directions

With the absence of randomized controlled trials, the limitations of comparing retrospective studies, and the need for higher level of evidence, several international, randomized, phase 2 and 3 studies are now being hold, mostly in the advanced setting, but also in the early and intermediate stage. A prospective randomized trial is currently studying the role of sorafenib as an adjunct to 90Y-RE in the treatment of HCC patients in the waiting list for liver transplantation (NCT00846131). PREMIERE trial is a US large randomized trial comparing 90Y-RE with TACE for patients with unresectable HCC and a preserved liver

**Table 4** Liver toxicity in patients with and without portal vein thrombosis treated by 90Y-RE

Author, year	Sangro et al. 2011 <sup>a</sup>		Kulik et al. 2008 <sup>ψ</sup>			Mazzaferro et al. 2013 <sup>a</sup>	
Liver toxicities	3 months after 90Y-RE		6 months after 90Y-RE			3 months after 90Y-RE	
	BCLC B	BCLC C	No PVT	Branch PVT	Main PVT	No PVT	PVT
Bilirubin (%)	6.6	6	35	42	64	11.8	14.3
Albumin (%)	3.2	0	nr	nr	nr	11.7	11.4
Ascites (%)	Nr	Nr	15	5	55	17.6	2.9
INR (%)	0	1.9	nr	nr	nr	nr	Nr
ALT (%)	3	3.8	nr	nr	nr	nr	Nr
Encephalopathy (%)	nr	Nr	4	5	0	Nr	nr

<sup>a</sup> Only grade 3–4 clinical toxicities are reported, according to CTCAE v 3.0

<sup>ψ</sup> Any grade of liver toxicity according to SWOG criteria

PVT portal vein thrombosis

function (NCT00956930) with response rate at 6 months and time to progression being the main endpoints. Also in the intermediate stage, the results of the completed small SIRTACE trial (NTC00867750) primarily designed to compare quality of life after RE or TACE in patients with unresectable HCC await publication. SORAMIC (NTC 01126645) and STOP-HCC (NTC 01556490) trials investigate the role of 90Y-RE when added to sorafenib (primary endpoint: survival), in non-resectable HCC patients and the second one only in the setting of patients with HCC-associated portal vein thrombosis. Finally, two head to head comparisons of sorafenib versus 90Y-RE with survival as the primary endpoint are now ongoing (SIRveNIB – NTC 01135056-, SARAH–NTC 01482442) and YES-p trial (NTC pending).

## 6 Conclusion

Evidence supporting the usefulness of 90Y-RE in the treatment of HCC patients comes from non-controlled series. However, its use has been widely extended in the last years due to its capacity to induce objective tumor responses and disease control, together with a good safety profile. Most information comes from patients with advanced HCC, not suitable for other locoregional therapies or who have failed to TACE. In recent years, however, encouraging experience has been reported in the treatment of HCC patients at earlier stages, including those in which downstaging is likely to be beneficial or those with early tumors that for any reason could not be ablated surgically or percutaneously. There is a group of patients for which the benefit of being treated with 90Y-RE is unlikely or needs to be further substantiated. This group includes patients with diffuse bulky disease involving more than 50 % of liver volume, and patients with a tumoral thrombosis of the main portal trunk and a poor liver functional reserve. The risk of

complications in cirrhotic patients remains an important issue in the treatment of HCC. Since 90Y-RE can induce REILD and liver atrophy, careful patient selection, and conservative treatment design and activity calculation are mandatory to avoid such complications.

## References

- Ben-Josef E, Normolle D, Ensminger WD et al (2005) Phase II trial of highdose conformal radiation therapy with concurrent hepatic artery floxuridine for unresectable intrahepatic malignancies. *J Clin Oncol* 23:8739–8747
- Benson AB, Abrams TA, Ben-Josef E (2009) NCCN clinical practice guidelines in oncology: hepatobiliary cancers. *J Natl Compr Canc Netw* 7:350–391
- Bilbao JI, de Martino A, de Luis E et al (2009) Biocompatibility, inflammatory response, and recanalization characteristics of nonradioactive resin microspheres: histological findings. *Cardiovasc Intervent Radiol* 32:727–736
- Bolondi L, Piscaglia F (2013) Yttrium 90 radioembolization: the horizon is changing for patients with intermediate and advanced hepatocellular carcinoma *Hepatology*. doi:10.1002/hep.26154
- Bosch FX, Ribes J, Diaz M et al (2004) Primary liver cancer: worldwide incidence and trends. *Gastroenterology* 127:S5–S16
- Bruix J, Sherman M (2011) Management of hepatocellular carcinoma: an update. *Hepatology* 53:1020–1022
- Bruix J, Raoul JL, Sherman M et al (2012) Efficacy and safety of sorafenib in patients with advanced hepatocellular carcinoma: subanalyses of a phase III trial. *J Hepatol* 57:821–829
- Brunello F, Veltri A, Carucci P et al (2008) Radiofrequency ablation versus ethanol injection for early hepatocellular carcinoma: a randomized controlled trial. *Scand J Gastroenterol* 43:727–735
- Burrel M, Reig M, Forner A (2012) Survival of patients with hepatocellular carcinoma treated by transarterial chemoembolisation (TACE) using drug eluting beads. Implications for clinical practice and trial design. *J Hepatol* 56:1330–1335
- Cammà C, Schepis F, Orlando A et al (2002) Transarterial chemoembolization for unresectable hepatocellular carcinoma: meta-analysis of randomized controlled trials. *Radiology* 224:47–54
- Carr BI (2004) Hepatic arterial 90Yttrium glass microspheres (Therasphere) for unresectable hepatocellular carcinoma: interim safety and survival data on 65 patients. *Liver Transpl* 10:S107–S110

- Carr BI, Kondragunta V, Buch SC et al (2010) Therapeutic equivalence in survival for hepatic arterial chemoembolization and yttrium-90 microsphere treatments in unresectable hepatocellular carcinoma: a two-cohort study. *Cancer* 116:1305–1314
- Chen CH, Hu FC, Huang GT et al (2009) Applicability of staging systems for patients with hepatocellular carcinoma is dependent on treatment method analysis of 2010 Taiwanese patients. *Eur J Cancer* 45:1630–1639
- Cheng AL, Kang YK, Chen Z et al (2009) Efficacy and safety of sorafenib in patients in the Asia-Pacific region with advanced hepatocellular carcinoma: a phase III randomized, double-blind, placebo-controlled trial. *Lancet Oncol* 10:25–34
- Dancey JE, Shepherd FA, Paul K et al (2000) Treatment of nonresectable hepatocellular carcinoma with intrahepatic <sup>90</sup>Y-microspheres. *J Nucl Med* 41:1673–1681
- Dawson LA, McGinn CJ, Normolle D et al (2000) Escalated focal liver radiation and concurrent hepatic artery fluorodeoxyuridine for unresectable intrahepatic malignancies. *J Clin Oncol* 18:2210–2218
- European Association For The Study Of The Liver; European Organisation For Research And Treatment Of Cancer (2012) EASL-EORTC clinical practice guidelines: management of hepatocellular carcinoma. *J Hepatol* 56:908–943
- Fernandez-Ros N, Silva N, Bilbao JI et al (2013) Partial liver volume radioembolization induces hypertrophy in the spared lobe without inducing major signs of portal hypertension. *HPB* doi: 10.1111/hpb.12095
- Furuse J, Ishii H, Nagase M et al (2005) Adverse hepatic events caused by radiotherapy for advanced hepatocellular carcinoma. *J Gastroenterol Hepatol* 20:1512–1518
- Gaba RC, Lewandowski RJ, Kulik LM et al (2009) Radiation lobectomy: preliminary findings of hepatic volumetric response to lobar yttrium-90 radioembolization. *Ann Surg Oncol* 16:1587–1596
- Garin E, Lenoir L, Rolland Y et al (2012) Dosimetry based on <sup>99m</sup>Tc-Macroaggregated albumin SPECT/CT accurately predicts tumor response and survival in hepatocellular carcinoma patients treated with <sup>90</sup>Y-loaded glass microspheres: preliminary results. *J Nucl Med* 53:255–263
- Geschwind JF, Salem R, Carr BI et al (2004) Yttrium-90 microspheres for the treatment of hepatocellular carcinoma. *Gastroenterology* 127(Suppl 1):S194–S205
- Gil-Alzugaray B, Chopitea A, Iñarrairaegui M et al (2012) Prognostic factors and prevention of radioembolization-induced liver disease. *Hepatology*. doi: 10.1002/hep.26191
- Golfieri R, Cappelli A, Cucchetti A et al (2011) Efficacy of selective transarterial chemoembolization in inducing tumor necrosis in small (<5 cm) hepatocellular carcinomas. *Hepatology* 53:1580–1589
- Heckman JT, Devera MB, Marsh JW et al (2008) Bridging locoregional therapy for hepatocellular carcinoma prior to liver transplantation. *Ann Surg Oncol* 15:3169–3177
- Hilgard P, Hamami M, Fouly AE et al (2010) Radioembolization with yttrium-90 glass microspheres in hepatocellular carcinoma: European experience on safety and long-term survival. *Hepatology* 52:1741–1749
- Ho MC, Huang GT, Tsang YM et al (2009) Liver resection improves survival of patients with multiple hepatocellular carcinomas. *Ann Surg Oncol* 16:848–855
- Hsu KF, Chu CH, Chan DC et al (2011) Superselective transarterial chemoembolization vs hepatic resection for resectable early-stage hepatocellular carcinoma in patients with Child-Pugh class a liver function. *Eur J Radiol* 81:466–471
- Iñarrairaegui M, Thurston KG, Bilbao JI et al (2010a) Radioembolization with use of yttrium-90 resin microspheres in patients with hepatocellular carcinoma and portal vein thrombosis. *J Vasc Interv Radiol* 21:1205–1212
- Iñarrairaegui M, Martínez-Cuesta A, Rodríguez M et al (2010b) Analysis of prognostic factors after yttrium-90 radioembolization of advanced hepatocellular carcinoma. *Int J Radiat Oncol Biol Phys* 77:1441–1448
- Iñarrairaegui M, Pardo F, Bilbao JI (2012) Response to radioembolization with yttrium-90 resin microspheres may allow surgical treatment with curative intent and prolonged survival in previously unresectable hepatocellular carcinoma. *Eur J Surg Oncol* 38:594–601
- Jakobs TF, Saleem S, Atassi B et al (2008) Fibrosis, portal hypertension, and hepatic volume changes induced by intra-arterial radiotherapy with <sup>90</sup>yttrium microspheres. *Dig Dis Sci* 53:2556–2563
- Jelic S, Sotiropoulos GC; ESMO Guidelines Working Group (2010) Hepatocellular carcinoma: ESMO clinical practice guidelines for diagnosis, treatment and follow-up. *Ann Oncol* 21(suppl 5):59–64
- Kennedy A, Nag S, Salem R et al (2007) Recommendations for radioembolization of hepatic malignancies using yttrium-90 microsphere brachytherapy: a consensus panel report from the radioembolization brachytherapy oncology consortium. *Int J Radiat Oncol Biol Phys* 68:13–23
- Kooby DA, Egnatashvili V, Srinivasan S et al (2010) Comparison of yttrium-90 radioembolization and transcatheter arterial chemoembolization for the treatment of unresectable hepatocellular carcinoma. *J Vasc Interv Radiol* 21:224–230
- Kulik LM, Atassi B, van Holsbeeck L et al (2006) Yttrium-90 microspheres (TheraSphere) treatment of unresectable hepatocellular carcinoma: downstaging to resection, RFA and bridge to transplantation. *J Surg Oncol* 94:572–586
- Kulik LM, Carr BI, Mulcahy MF et al (2008) Safety and efficacy of <sup>90</sup>Y radiotherapy for hepatocellular carcinoma with and without portal vein thrombosis. *Hepatology* 47:71–81
- Kulik L (2010) Is radioembolization ready for the barcelona clinic liver cancer staging system? *Hepatology* 52:1528–1530
- Lance C, Mc Lennan G, Obuchowski N et al (2011) Comparative analysis of the safety and efficacy of transcatheter arterial chemoembolization and yttrium-90 radioembolization in patients with unresectable hepatocellular carcinoma. *J Vasc Interv Radiol* 22:1697–1705
- Lau W, Leung W, Ho S, Leung NW et al (1994) Treatment of hepatocellular carcinoma with intra-hepatic arterial yttrium-90 microspheres: a phase I and II study. *Br J Cancer* 70:994–999
- Lau W, Ho S, Leung T et al (1998) Selective internal radiation therapy for nonresectable hepatocellular carcinoma with intraarterial infusion of <sup>90</sup>yttrium microspheres. *Int J Radiat Oncol Biol Phys* 40:583–592
- Lau W-Y, Kennedy AS, Kim YH et al (2012) Patient selection and activity planning guide for selective internal radiotherapy with yttrium-90 resin microspheres. *Int J Radiat Oncol Biol Phys* 82:401–407
- Lawrence TS, Robertson JM, Anscher MS et al (1995) Hepatic toxicity resulting from cancer treatment. *Int J Radiat Oncol Biol Phys* 31:1237–1248
- Lencioni RA, Allgaier HP, Cioni D et al (2003) Small hepatocellular carcinoma in cirrhosis: randomized comparison of radio-frequency thermal ablation versus percutaneous ethanol injection. *Radiology* 228:235–240
- Lewandowski RJ, Kulik LM, Riaz A et al (2009) A comparative analysis of transarterial downstaging for hepatocellular carcinoma: chemoembolization versus radioembolization. *Am J Transplant* 9:1920–1928
- Lewandowski RJ, Mulcahy MF, Kulik LM et al (2010) Chemoembolization for hepatocellular carcinoma: comprehensive imaging



- and survival analysis in a 172-patient cohort. *Radiology* 255:955–965
- Lin SM, Lin CJ, Lin CC et al (2004) Radiofrequency ablation improves prognosis compared with ethanol injection for hepatocellular carcinoma  $\leq 4$  cm. *Gastroenterology* 127:1714–1723
- Lin SM, Lin CJ, Lin CC et al (2005) Randomized controlled trial comparing percutaneous radiofrequency thermal ablation, percutaneous ethanol injection, and percutaneous acetic acid injection to treat hepatocellular carcinoma of 3 cm or less. *Gut* 54:1151–1156
- Llovet JM, Real MI, Montaña X et al (2002) Arterial embolisation or chemoembolisation versus symptomatic treatment in patients with unresectable hepatocellular carcinoma: a randomized controlled trial. *Lancet* 359:1734–1739
- Lo CM, Ngan H, Tso WK et al (2002) Randomized controlled trial of transarterial lipiodol chemoembolization for unresectable hepatocellular carcinoma. *Hepatology* 35:1164–1171
- Marelli L, Stigliano R, Triantos C et al (2007) Transarterial therapy for hepatocellular carcinoma: which technique is more effective? A systematic review of cohort and randomized studies. *Cardiovasc Intervent Radiol* 30:6–25
- Mazzaferro V, Sposito C, Bhoori S et al (2013) Yttrium-90 radioembolization for intermediate-advanced hepatocarcinoma: a phase II study. *Hepatology*. doi:10.1002/hep.26014
- McGinn CJ, Ten Haken RK, Ensminger WD et al (1998) Treatment of intrahepatic cancers with radiation doses based on a normal tissue complication probability model. *J Clin Oncol* 16:2246–2252
- Memon K, Kulik L, Lewandowski J et al (2011) Radiographic response to locoregional therapy in hepatocellular carcinoma predicts patient survival times. *Gastroenterology* 141:526–535
- Moreno-Luna LE, Yang JD, Sanchez W et al (2012) Efficacy and Safety of transarterial radioembolization versus chemoembolization in patients with hepatocellular carcinoma. *Cardiovasc Intervent Radiol* 24 (epub ahead of print)
- Mornex F, Girard N, Beziat C et al (2006) Feasibility and efficacy of high-dose three-dimensional-conformal radiotherapy in cirrhotic patients with small-size hepatocellular carcinoma non-eligible for curative therapies—mature results of the French phase II RTF-1 trial. *Int J Radiat Oncol Biol Phys* 66:1152–1158
- Nosher J, Ohman-Strickland PA, Jabbour S et al (2011) Changes in liver and spleen volumes and liver function after radioembolization with yttrium-90 resin microspheres. *Vasc Interv Radiol* 22:1706–1713
- Raoul JL, Sangro B, Forner A et al (2011) Evolving strategies for the management of intermediate-stage hepatocellular carcinoma: available evidence and expert opinion on the use of transarterial chemoembolization. *Cancer Treat Rev* 37:212–220
- Riaz A, Kulik L, Lewandowski RJ et al (2009) Radiologic-pathologic correlation of hepatocellular carcinoma treated with internal radiation using yttrium-90 microspheres. *Hepatology* 49:1185–1193
- Riaz A, Miller F, Kulik L et al (2010a) Imaging response in the primary index lesion and clinical outcomes following transarterial locoregional therapy for hepatocellular carcinoma. *JAMA* 303:1062–1069
- Riaz A, Lewandowski RJ, Kulik L et al (2010b) Radiologic-pathologic correlation of hepatocellular carcinoma treated with chemoembolization. *Cardiovasc Intervent Radiol* 33:1143–1152
- Riaz A, Gates VL, Atassi B et al (2011) Radiation segmentectomy: a novel approach to increase safety and efficacy of radioembolization. *Int J Radiat Oncol Biol Phys* 79:163–171
- Robertson JM, McGinn CJ, Walker S et al (1997) A phase I trial of hepatic arterial bromodeoxyuridine and conformal radiation therapy for patients with primary hepatobiliary cancers or colorectal liver metastases. *Int J Radiat Oncol Biol Phys* 39:1087–1092
- Salem R, Lewandowski RJ, Atassi B et al (2005) Treatment of unresectable hepatocellular carcinoma with use of 90Y microspheres (TheraSphere): safety, tumor response, and survival. *J Vasc Interv Radiol* 16:1627–1639
- Salem R, Lewandowski RJ, Mulcahy MF et al (2010) Radioembolization for hepatocellular carcinoma using Yttrium-90 microspheres: a comprehensive report of long-term outcomes. *Gastroenterology* 138:52–64
- Salem R, Lewandowski RJ, Kulik L et al (2011) Radioembolization results in longer time-to-progression and reduced toxicity compared with chemoembolization in patients with hepatocellular carcinoma. *Gastroenterology* 140:497–507
- Sangro B, Bilbao JI, Boan J et al (2006) Radioembolization using 90Y-resin microspheres for patients with advanced hepatocellular carcinoma. *Int J Radiat Oncol Biol Phys* 66:792–780
- Sangro B, Gil-Alzugaray B, Rodriguez J et al (2008) Liver disease induced by radioembolization of liver tumors. *Cancer* 112:1538–1546
- Sangro B, Carpanese L, Cianni R (2011) On behalf of the European network on radioembolization with Yttrium-90 resin microspheres (ENRY). Survival after Yttrium-90 resin microsphere radioembolization of hepatocellular carcinoma across Barcelona clinic liver cancer stages: a European evaluation. *Hepatology* 54:868–878
- Sato K, Lewandowski RJ, Bui JT et al (2006) Treatment of unresectable primary and metastatic liver cancer with yttrium-90 microspheres (TheraSphere): assessment of hepatic arterial embolization. *Cardiovasc Intervent Radiol* 29:522–529
- Sherman M (2010) The resurrection of alpha-fetoprotein. *Hepatology* 52:939–940
- Shiina S, Teratani T, Obi S et al (2005) A randomized controlled trial of radiofrequency ablation with ethanol injection for small hepatocellular carcinoma. *Gastroenterology* 129:122–130
- Uchino K, Tateishi R, Shiina S et al (2011) Hepatocellular carcinoma with extrahepatic metastasis: clinical features and prognostic factors. *Cancer* 117:4475–4483
- Wang JH, Chang chien CS, Hu TH et al (2008) The efficacy of treatment schedules according to Barcelona clinic liver cancer staging for hepatocellular carcinoma—survival analysis of 3892 patients. *Eur J Cancer* 44:1000–1006
- Woodall CE, Scoggins CR, Ellis SF et al (2009) Is selective internal radioembolization safe and effective for patients with inoperable hepatocellular carcinoma and venous thrombosis? *J Am Coll Surg* 208:375–382

# HCC. Radioembolization Combined with Other Therapeutic Local and Systemic Treatment

Thomas Helmberger

## Contents

1	Introduction.....	120
2	RE Before Resection or Transplantation.....	120
3	RE as Alternative When Other Ablative Treatments Cannot Be Applied.....	122
4	Radioembolization in Combination with Systemic Therapies.....	123
5	Conclusion.....	125
	References.....	125

## Abstract

Only in early stages of HCC resection, local ablative therapy, and transplantation are offering a chance of cure, whereas only a minority of patient will amenable for such a therapy. The majority of patients are presenting an intermediate or even advanced tumor stages where the therapeutic options are limited to transarterial and systemic molecular therapies. Radio embolization may augment the therapeutic armamentarium particularly in patients just not meeting the criteria for resection, percutaneous ablation or transplantation by downsizing/downgrading or in progressed disease where transarterial chemotherapy is contraindicated. Recent results of radio embolization in these settings and future directions will be discussed.

## Abbreviations

AASLD	American Association for the Study of Liver Diseases
BCLC	Barcelona-Clinic Liver Cancer
BSC	Best supportive care
C-B	Child-Pugh
CR	Complete response
EASL	European Association for the Study of the Liver
ECOG	Eastern Cooperative Oncology Group
ENRY	European Network on Radioembolization with Yttrium-90 Resin Microspheres
EORTC	European Organization for Research and Treatment of Cancer
ESMO	European Society for Medical Oncology
Gd-EOB-DTPA	Gadoxetic acid (Promovist <sup>®</sup> , Bayer, Germany)
LTx	Liver transplantation
NCCN	National Comprehensive Cancer Network

T. Helmberger (✉)  
Institute of Diagnostic and Interventional Radiology,  
Neuroradiology and Nuclear Medicine, Klinikum Bogenhausen,  
Englschalkinger Str. 77, 81925 Munich, Germany  
e-mail: thomas.helmberger@klinikum-muenchen.de

NCI	National Cancer Institute
PR	Partial response
PVT	Portal-vein thrombosis
RE	Radio-embolization
Rx	Resection
SD	Stable disease
SHARP	Sorafenib HCC Assessment Randomized Protocol
TACE	Transarterial chemo-embolization
TAE	Transarterial embolization
TTP	Time to progression
UNOS	United Network for Organ Sharing
VT	Venous thrombosis

## 1 Introduction

As discussed in the previous chapters hepatocellular carcinoma (HCC) is one of the most common abdominal malignancies worldwide. Its prognosis is determined by the tumor stage and the overall hepatic functional status given by the—in most cases present—underlying liver disease. Assessing the tumor stage incorporates the evaluation of the tumor size, number of tumor nodules, and further expansive tumor growth as portal-vein invasion and extrahepatic metastases. Adding the grades of cirrhosis with its related compromised hepatic function and patients performance status allows for a practical classification of the several disease stages and treatment recommendation as provided by Barcelona-Clinic Liver Cancer (BCLC) group. In this classification, the very-early and early tumor stages (0 and A) are defined by a limited tumor load and a preserved liver function offering curative therapeutic options by local ablation, resection, and liver transplantation (EASL-EO-RTC clinical practice guidelines: management of hepatocellular carcinoma 2012). However, only 30–40 % of the patients might be eligible for such a treatment. The vast majority of about 60 % of patients will present an intermediate (B) or advanced stage (C) with multinodular disease or already macrovascular tumor invasion and extrahepatic spread. These patients are considered as unresectable, in consequence the overall prognosis is poor. Up to now, the main treatment component in these patients is transarterial chemoembolization (TACE ± particles incl. drug eluting particles) or transarterial embolization (TAE), whereas only TACE has provided sufficient evidence for improved survival. Nevertheless, in patients with extensive tumor burden, vascular invasion, and/or impaired liver function with and without reduced performance status TACE is often not applicable anymore (Burrel et al. 2012).

On the other hand, the application of Thyrosine multikinase inhibitors (e.g., Sorafenib (Nexavar®), Bayer AG, Wuppertal, Germany) is the only systemic therapy in advanced stages that has shown some survival benefits but is often hampered by significant adverse events limiting the therapeutic regimen (Llovet et al. 2008).

Already 20 years ago two RTCs applying Iodine-131 Lipiodol embolization in patients with advanced HCC were able to show response rates similar to TACE and even improved survival in advanced tumor stages (Raoul et al. 2010). Nevertheless, this technique did not win broad recognition mainly due to practicability and radiation protection issues. In contrast, the evidence for Yttrium-90 radioembolization (RE) in the treatment of intermediate and advanced stages was rising in recent years. Small retrospective and non-RTCs over the last ten years had indicated that RE might be a valuable adjunct or substitute to the more or less established loco-regional (e.g., TACE, TAE) and systemic (i.e., Thyrosine kinase inhibitors) therapies. Moreover, very recent large US and EU multicenter studies confirmed the significant impact of RE in intermediate and advanced stages, whereas median survival rates of 16–20 months could be achieved—particularly in cases which basically were not eligible anymore for the “established” therapies (Hilgard et al. 2010; Salem et al. 2010, 2011; Sangro et al. 2011).

In consequence, RE seems to expand the therapeutic armamentarium in patients with primarily nonresectable/ablatable HCC that may rise several options for the use of RE.

Thus, some thoughts should be given to the concept of combining RE with other therapies.

- RE before resection or transplantation;
- RE as alternative when other ablative treatments cannot be applied;
- RE in combination with systemic therapies.

## 2 RE Before Resection or Transplantation

Local hepatic tumor resection and transplantation are the accepted surgical therapies in suitable patients according to the BCLC Stage 0 and A. However, only a small proportion of patients will qualify for such a therapy primarily due to tumor size and number, anatomical conditions, or limited hepatic remnant after potential surgery. In these non-surgical candidates local ablative therapies as local thermal ablation, selective and superselective transarterial chemoembolization, etc., have been applied successfully, diminishing the tumor size or even devitalizing tumors effectively. In consequence, applying these therapies leads to the concept of neo-adjuvant treatment simplifying surgery or keeping patients on the transplant waiting list by decreasing tumor progression and improving the long-term

**Table 1** Summary of studies on RE in intermediate and advanced stage as sole therapy (no other treatment applicable) or in comparison to TACE

Author	Pat. #	Therapy	Response (PR, CR, SD)	Survival	Comment
(D'Avola et al. 2009)	35	35 RE (resin)		16 m 8 m	Comparison to not-in-study- included control group
(Woodall et al. 2009)	52	20 RE (glass; no VT) 15 RE (glass; VT) 17 no RE, BSC		13.9 m 2.7 m 5.2 m	
(Hilgard et al. 2010)	108	159 RE (glass)	93 %	16.4 m	European survey TTP 10 m
(Strigari et al. 2010)	73	RE (resin)	55 % (RECIST) 74 % (EASL)	Not reported	
(Salem et al. 2010)	291	526 RE (glass)	42 % (WHO) 57 % (EASL)	17.2 m (C-P A) 7.7 m (C-P B)	Longitudinal cohort study. Survival in patients with PVT 5.6 m
(Sangro et al. 2011)	325	RE (resin)	Not reported	24.4 m (BCLC A) 16.9 m (BCLC B) 10.0 m (BCLC C)	European Network on Radioembolization with Yttrium-90 Resin Microspheres (ENRY): 1.-line treatment or progression after Rx or other treatment
(Carr et al. 2010)	691 99	TACE (with particles) RE (glass)	89 % 77 %	8.5 m 11.5 m	Considering selection bias no difference
(Salem et al. 2011)	122 123	TACE RE (glass)	49 % 36 %	17.4 m 20.5 m	TTP 8.4 vs. 13.3 m; no difference but less toxicities in RE
(Kooby et al. 2010)	44 27	TACE RE	64 % 67 %	6 m 6 m	Retrospective long-term analysis
(Lewandowski et al. 2009)	43 43	TACE RE (glass)	PR 37 % PR 61 %	18.7 m 35.7 m	Downstaging UNOS T3 to T2 31 vs 58 %; event-free survival 7.1 vs 17.7 m; no difference in TTP
(Kulik et al. 2006)	35	15 (RE glass) 19 (RE + Rx/RFA, LTx)	23 (T3 to T2: Rx, RFA) 8 (LTx)	66 m	Primarily only UNOS T3 patients (previous TACE only in 2)
(Inarrairaegui et al. 2012)	21	15 RE (resin) 6 (RE + LTx)		22 m >41.5 m	Primarily only UNOS T3 patients (previous TACE only in 5)

TACE transarterial chemoembolization, RE Radioembolization, PR partial response, CR complete response, SD stable disease, UNOS United Network for Organ Sharing, TTP time to progression, PVT portal-vein thrombosis, LTx liver transplantation, Rx resection, C-B Child-Pugh

results together with downstaging—even enabling resection or transplantation (Chapman et al. 2008; Di Sandro et al. 2012; Otto et al. 2006; Toso et al. 2010). This concept is

already substantiated by several studies reviewed by Gordon-Weeks et al. reporting on 720 patients who were transplanted outside the Milan criteria after downstaging



and who were presenting comparable survival rates in comparison to patients transplanted within the Milan criteria (Garden 2011; Gordon-Weeks et al. 2011).

In mostly mixed patient groups (early, advanced, and intermediate stage) RE could prove to be effective at least as TACE reducing the size of the target lesions (Lewandowski et al. 2009; Riaz et al. 2009; Salem et al. 2010, 2011; Sangro et al. 2006) and additionally, inducing hypertrophy of the non-target hepatic parenchyma (Ahmadzadehfar et al. 2013; Gaba et al. 2009; Jakobs et al. 2008). Taking these two effects into account, RE could be a potential valuable tool for downstaging as initially proven in several recent studies.

In 35 patients with unresectable HCC (UNOS (United Network for Organ Sharing) T3) undergoing selective RE, the Northwestern Memorial Hospital group, Chicago, IL, USA could achieve a downstaging in 23/35 to RFA or resection and in 8/35 to liver transplantation resulting up to now in a median survival of the patients of 800 days (Kulik et al. 2006).

Ibrahim et al. (2012) reported on 8 patients (UNOS 3 T2, 4 T3, 1 T4a; 3 BCLC A, 4 BCLC B, 1 BCLC C) undergoing RE for unresectable HCC within the caudate lobe. 4/8 patients showed a complete response according to WHO (1) and EASL (3) criteria, the other 4 patients were downstaged from T3 to T2 enabling liver transplantation in 3 of them.

Inarrairaegui et al. (2012) presented a group of 21 patients with UNOS T3 stage that had progression after TACE were not eligible for TACE and treated by RE. 6/21 were downstaged followed by liver transplantation in 2, resection in 3, and radiofrequency ablation and subsequent resection in 1. This group of 6 patients presented a significantly superior survival (48 months) in comparison to 15 not additionally treated patients (22 months) (Table 1).

So far, based on the yet limited but very promising data basis on effective downstaging after RE a recent international consensus conference for recommendations in liver transplantation in HCC stated that “*newer strategies such as a combination of TACE with RFA and use of 90yttrium radioembolization or targeted therapies, have shown some benefits in preliminary studies*” and therefore, “*based on current absence of evidence, no recommendation can be made on bridging therapy in patients with UNOS T1 ( $\leq 2$  cm) HCC*”, but “*in patients with UNOS T2 (one nodule 2–5 cm or three or fewer nodules each  $\leq 3$  cm) HCC (Milan criteria) and a likely waiting time of longer than 6 months, locoregional therapy may be appropriate;... no recommendation can be made for preferring one type of locoregional therapy to others*” (Clavien et al. 2012). In consequence, a paradigm change on transplant concepts might happen in terms of keeping patients on a transplant waiting list and allowing for downstaging even if they are

not eligible for listing any more due to progressive disease (Clavien et al. 2012). Further studies have to prove the potential benefit of such concepts.

Independently from the displayed options for downsizing and downgrading making a tumor resection, transplantation or local thermal or chemical ablation possible, there are situations where the remnant liver is too small in terms of functional reserve hindering any type of resection. However, there is already some evidence that lobar or segmental-selective RE may lead to ipsilateral-/segmental hepatic parenchymal hypotrophy and contra-lobar hypertrophy allowing subsequent surgery. In several case (Gulec et al. 2009; Seidensticker et al. 2012), reports and small studies including various types of tumors incl. HCC a volume increase between 21.2 % (Jakobs et al. 2008) and 35 % (Yoon et al. 2012) of the non-treated liver lobe after RE was described. Therefore, RE could become an important component in a multimodality treatment concept with curative intention—like preoperative portal-vein embolization, however, with an additional primary therapeutic impact on the targeted tumor (Anaya et al. 2008; Denys et al. 2012; Garden 2011).

### 3 RE as Alternative When Other Ablative Treatments Cannot Be Applied

Unfortunately, there are still a substantial number of patients who might be primarily not amenable for a local ablative treatment or will present significant progress after such a therapy. Therefore, high hopes were pinned on sorafenib as systemic therapy in such cases which were fulfilled to some degree as the SHARP trial—a randomized controlled study comparing sorafenib to placebo—could show (Bruix et al. 2012). However, performing RE as a first-line therapy in patients similar to the patients included in the SHARP trial D’Avola et al. could gain an ample superior survival rate of 16 months in comparison to 8 months in a matched control group without RE (D’Avola et al. 2009). Despite the limitations of this study, the results with survival rates ranging from 9 to 16 months could be paralleled by several other studies and also by the study of the European Network on Radioembolization with Yttrium-90 Resin Microspheres (ENRY) as a subgroup analysis could show (Dancey et al. 2000; Hilgard et al. 2010; Lau et al. 1998; Sangro et al. 2011; Woodall et al. 2009).

Macro-vascular occlusion of the portal vein or its branches is considered as a dismal prognostic factor. It is in general an indicator for a progressed disease possibly associated with extensive intrahepatic tumor growth, extrahepatic spread and progressive functional impairment, and, therefore, often considered as a contraindication for

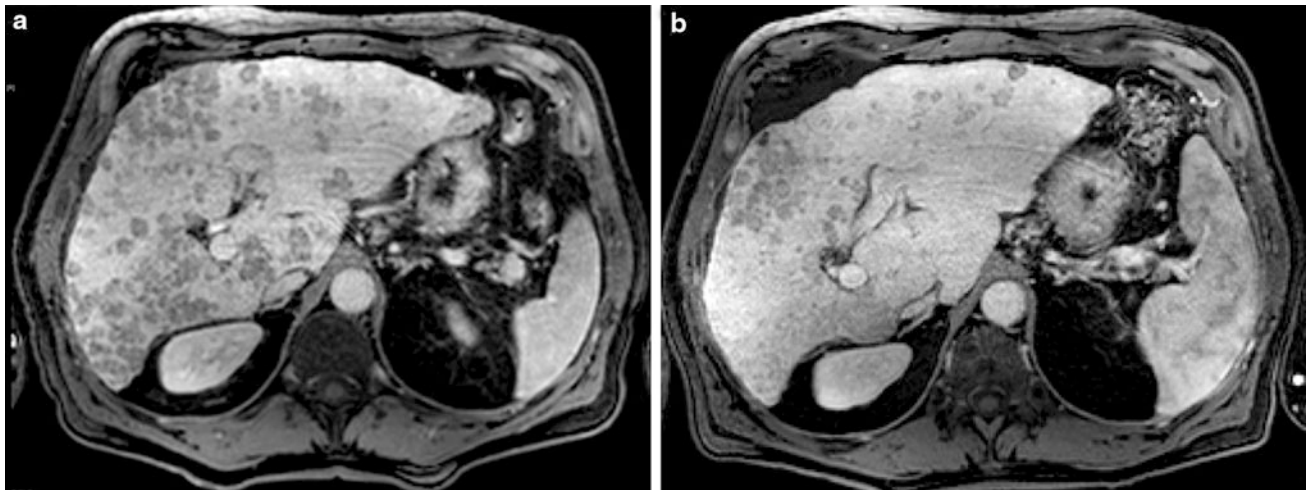


**Fig. 1** A 62-year-old patient with Child-Pugh A cirrhosis and multifocal HCC, intermediate Stage. **a** T1- MRI 20 min post Gd-EOB: bilobar, multinodular HCC. **b** 11 months post RE—2.2 GBq,

synchronous bilobar application—significant reduction of tumor load, patent liver function, ECOG 0, no new tumor activity

TACE (Bruix and Sherman 2011). In consequence, many patients with portal-vein occlusion—often without differentiation between tumor thrombus and tumor ingrowth or central and peripheral branch thrombosis—are often excluded from a targeted therapy. Nevertheless, during recent years, the evidence is growing TACE with advanced technique can be performed successfully and may improve the patients survival (Luo et al. 2011). For example, in 125 patients with main portal-vein invasion, Chung et al. (2011) could demonstrate a significant superior survival in the TACE treated group (83 patients, 7.4 months median survival) in comparison to the supportive care group (42 patients, 2.6 months median survival) {Chung, 2011 #190, Vogl et al. 2011; Wu et al. 2011; Yoo et al. 2011; Yoshidome et al. 2011}. Moreover, this results can be reproduced by RE as presented in recent studies achieving median survival rates up to 17 months (Carr et al. 2010; Denys et al. 2012; Inarrairaegui et al. 2010; Mazzaferro et al. 2012; Memon et al. 2012; Woodall et al. 2009; Yoon et al. 2012; Zhang et al. 2009).

In consequence due to the excellent safety profile and an improved survival time in patients with poor prognosis RE and selective TACE might get the favorable therapy over systemic therapy in advanced and very advanced patients. Though to date, prospective studies comparing both treatment modalities in a randomized setting are lacking (Fig. 1. A 62-year-old patient with Child-Pugh A cirrhosis and multifocal HCC, intermediate Stage. (a) T1- MRI 20 min post Gd-EOB: bilobar, multinodular HCC. (b) 11 months post RE—2.2 GBq, synchronous bilobar application—significant reduction of tumor load, patent liver function, ECOG 0, no new tumor activity).

#### 4 Radioembolization in Combination with Systemic Therapies

As discussed above, there is significantly growing study evidence establishing the place of RE within the therapeutic concepts for the different stages accepting RE as valuable component, e.g., in downsizing and downgrading of early HCC. Based on this results, the role of RE may expand to tumor stages where primarily no local therapy is employable due to anatomical (for local therapy unfavorable tumor location, e.g., within the dome or center of the liver, close vicinity to biliary or vascular structures) and/or functional restrictions (e.g., limited hepatic functional reserve). Moreover, most of the HCC patients will present in an intermediate or advanced stage where local ablation, resection or transplantation is not a therapeutic option in clinical reality. Unfortunately, in these patients no effective “classic oncological” therapy in terms of chemotherapy exists, actually all typical anti-cancer drugs failed in HCC.

Over the past 10–15 years, the insight into molecular carcinogenesis expanded dramatically. In many tumors a huge variety of molecular pathways responsible for malignant growth could be identified and used to develop targeted drugs (e.g., based on antibodies or specific cellular transporter inhibitors). In contrast to the many other gastrointestinal tumors, in HCC much more genetic alterations and variations in signaling pathways are involved creating a complex, multistep process of carcinogenesis resulting in the known molecular (and clinical) heterogeneity of HCC (Worns et al. 2009). Therefore, special attention turned on molecular targeted therapy in HCC since sorafenib among a variety of

**Table 2** Recent phase I to III trials on RE and Sorafenib and RE and TACE (adopted from <http://www.clinicaltrials.gov/>)

Study	Phase	Status	Purpose
<i>NCT00846131</i> : A Single-Center Proof of Concept Pilot Study to Evaluate the Safety, Efficacy, and Tolerability of Sorafenib Combined With Therasphere in Subjects With Hepatocellular Carcinoma Awaiting Liver Transplantation	I	Enrolling by invitation	Evaluation of the safety, efficacy, and tolerability of Theraspheres <sup>®</sup> (also known as Y-90, or Y-90 Therasphere) combined with or without sorafenib (Nexavar <sup>®</sup> ), in patients with hepatocellular carcinoma (HCC, or liver cancer), awaiting liver transplantation
<i>NCT00712790</i> : Phase I/II Study of SIR-Spheres Plus Sorafenib as First-Line Treatment in Patients With Non-Resectable Primary Hepatocellular Carcinoma (SIRSA)	I/II	Unknown	Evaluation of the safety and activity of chemoradiotherapy comprising a regimen of Sorafenib chemotherapy plus SIR-Spheres yttrium-90 microspheres, for first-line treatment of patients with HCC in whom surgical resection is not feasible
<i>NCT01126645</i> : Evaluation of Sorafenib in Combination With Local Micro-therapy Guided by Gd-EOB-DTPA Enhanced MRI in Patients With Inoperable Hepatocellular Carcinoma (SORAMIC)	II	Recruiting	Evaluation of Sorafenib and local microtherapy guided by Primovist enhanced MRI in patients with inoperable liver cancer not suitable to TACE
<i>NCT01482442</i> : Sorafenib Versus RADIOEMBOLIZATION in Advanced Hepatocellular Carcinoma (Sarah)	III	Recruiting	Evaluation whether RE with Yttrium-90 microspheres is more effective on overall survival in advanced HCC with or without portal venous obstruction and no extrahepatic extension than sorafenib which is now the standard treatment of advanced HCC
<i>NCT01135056</i> : Phase III Multi-Centre Open-Label Randomized Controlled Trial of Selective Internal Radiation Therapy (SIRT) Versus Sorafenib in Locally Advanced Hepatocellular Carcinoma (SIRveNIB)Hepatocellular Carcinoma (HCC)	III	Recruiting	Determination of a difference, if any, in overall survival between SIRT and Sorafenib in Locally Advanced Hepatocellular Carcinoma without extrahepatic disease
<i>NCT01556490</i> : A Phase III Clinical Trial of Intra-arterial TheraSphere <sup>®</sup> in the Treatment of Patients With Unresectable Hepatocellular Carcinoma (HCC) (STOP-HCC)	III	Recruiting	Safety and effectiveness of Therasphere will be evaluated in patients with unresectable hepatocellular carcinoma in whom treatment with standard-of-care sorafenib is planned. All patients receive the standard-of-care sorafenib with or without the addition of Therasphere
<i>NCT01381211</i> : Transarterial Radioembolization Versus ChemoEmbolization for the Treatment of HCC: A Multicenter Randomized Controlled Trial (TRACE Trial)	II	Recruiting	Comparison of TACE-DEB and 90Y-RE, two novel treatments that both have theoretical and/or proven advantages compared to the use of conventional TACE, in patients with intermediate stage HCC
<i>NCT00956930</i> : An Investigator Initiated Multicenter Prospective Randomized Study of Chemoembolization Versus Radioembolization for the Treatment of Hepatocellular Carcinoma (PREMIERE Trial)	II	Recruiting	Studying radioembolization to see how well it works compared with chemoembolization in treating patients with liver cancer that cannot be treated with Radiofrequency Ablation or removed by surgery

monoclonal antibodies (e.g., bevacizumab, cetuximab) and tyrosine kinase inhibitors (e.g., sorafenib, sunitinib, erlotinib, gefitinib, lapatinib) could produce a moderate survival benefit over best supportive care in patients with advanced HCC as displayed in the SHARP trial (Llovet et al. 2008; Rimassa and Santoro 2009; Zhang et al. 2010).

Nevertheless, this result was and is encouraging numerous studies evaluating the potential advantageous effects of sorafenib on downsizing, improving time to progression,

reducing relapse, prolonging survival, improving life quality, etc., at various stages in HCC. Worldwide at present, 167 studies (92 still open) on the use of sorafenib in HCC, 26 studies (15 still open) on RE in HCC and 6 studies comparing RE and sorafenib alone or both in combination are registered, and only 2 studies comparing RE and TACE (status at 1/2013; <http://www.clinicaltrials.gov/>) (Table 2).

Chaudhury et al. presented already in 2010 a patient treated by RE plus sorafenib what resulted in an astounding

survival of 23 months—supporting the hypothesis that the different modes of action of both RE and sorafenib might be synergistically effective.

It will still take a while till first results from these studies will be available, however, important questions will—hopefully—then be answered: is RE enhancing the positive survival effect of sorafenib or vice versa; is there a “technical” impact by sorafenib on subsequent RE; how is the safety profile in a combination therapy; is sorafenib a valuable prerequisite before RE—as indicated by the study of Theyson et al. where a significant reduction of hepatopulmonary shunt could be achieved pre RE (Theysohn et al. 2012); is a combination therapy effective in downstaging before hepatic resection/ablation or transplantation?

## 5 Conclusion

There is a consistently growing data basis supporting the evidence for the therapeutic efficacy and safety of RE in HCC. However, this data are mainly not substantiated by randomized controlled trials. Several comparative, adequately designed trials are ongoing, though final data are lacking. Therefore, indications and recommendation for RE in HCC are still controversial discussed within the different national and international peer groups dealing with hepatic cancer.

The BCLC group and the European Association for the Study of the Liver (EASL) and European Organization for Research and Treatment of Cancer (EORTC) acknowledge the potential of RE in HCC, however, due to the missing study fundamental RE do not yet recommend RE within the recent consensus statements (Bruix and Sherman 2011; Forner et al. 2012). The European Society for Medical Oncology (ESMO) is a slightly more “progressive”, considering RE still as an investigational treatment but allow the clinical use in selected cases (i.e., “large solitary tumor with a few satellites and a sufficient amount of healthy liver to be spared”, branch or lobar portal-vein thrombosis) for bridging in hepatic resection or transplantation and as alternative therapy to TACE in diffuse HCC or in cases with contraindications to TACE (Jelic and Sotiropoulos 2010).

In contrast, the US National Comprehensive Cancer Network (NCCN) on clinical practice guidelines in oncology ([http://www.nccn.org/professionals/physician\\_gls/f\\_guidelines.asp](http://www.nccn.org/professionals/physician_gls/f_guidelines.asp)) and the US National Cancer Institute (NCI) bring RE (and also stereotactic beam radiation) and TACE in-line in patients compromised by unfavorable tumor location or extensive liver disease, reduced liver function, impaired performance status, and significant comorbidities who are in consequence not eligible for resection or transplantation (Thomas et al. 2010).

Surprisingly, the American Association for the Study of Liver Diseases (AASLD) recommends RE only under study conditions following the European reluctance (Bruix and Sherman 2011).

So far, one has to accept that for a number of relevant questions ample study evidence is still missing—but this evidence will be provided since several randomized controlled trials are initiated. Nevertheless, based on what is already known in the application of RE in different settings RE might be appropriate for downstaging in patients who just do not qualify for resection, ablation or transplantation, in patients with intermediate or advanced stage of disease, without or with portal-vein invasion, who are not amenable for TACE. In this latter stages, synergistic effects might be seen by the combination of RE and sorafenib or TACE.

## References

- Ahmadzadehfar H, Meyer C, Ezziddin S, Sabet A, Hoff-Meyer A, Muckle M, Logvinski T, Schild HH, Biersack HJ, Wilhelm K (2013) Hepatic volume changes induced by radioembolization with (90)Y resin microspheres. A single-centre study. *Eur J Nucl Med Mol Imaging* 40(1):80–90
- Anaya DA, Blazer DG, Abdalla EK (2008) Strategies for resection using portal vein embolization: hepatocellular carcinoma and hilar cholangiocarcinoma. *Semin Interv Radiol* 25(2):110–122
- Bruix J, Sherman M (2011) Management of hepatocellular carcinoma: an update. *Hepatology* 53(3):1020–1022
- Bruix J, Raoul JL, Sherman M, Mazzaferro V, Bolondi L, Craxi A, Galle PR, Santoro A, Beaugrand M, Sangiovanni A, Porta C, Gerken G, Marrero JA, Nadel A, Shan M, Moscovici M, Voliotis D, Llovet JM (2012) Efficacy and safety of sorafenib in patients with advanced hepatocellular carcinoma: subanalyses of a phase III trial. *J Hepatol* 57(4):821–829
- Burrel M, Reig M, Forner A, Barrufet M, de Lope CR, Tremosini S, Ayuso C, Llovet JM, Real MI, Bruix J (2012) Survival of patients with hepatocellular carcinoma treated by transarterial chemoembolisation (TACE) using Drug Eluting Beads. Implications for clinical practice and trial design. *J Hepatol* 56(6):1330–1335
- Carr BI, Kondragunta V, Buch SC, Branch RA (2010) Therapeutic equivalence in survival for hepatic arterial chemoembolization and yttrium 90 microsphere treatments in unresectable hepatocellular carcinoma: a two-cohort study. *Cancer* 116(5):1305–1314
- Chapman WC, Majella Doyle MB, Stuart JE, Vachharajani N, Crippin JS, Anderson CD, Lowell JA, Shenoy S, Darcy MD, Brown DB (2008) Outcomes of neoadjuvant transarterial chemoembolization to downstage hepatocellular carcinoma before liver transplantation. *Ann Surg* 248(4):617–625
- Chaudhury PK, Hassanain M, Bouteaud JM, Alcindor T, Nudo CG, Valenti D, Cabrera T, Kavan P, Feteih I, Metrakos P (2010) Complete response of hepatocellular carcinoma with sorafenib and Y radioembolization. *Curr Oncol* 17(5):67–69
- Chung GE, Lee JH, Kim HY, Hwang SY, Kim JS, Chung JW, Yoon JH, Lee HS, Kim YJ (2011) Transarterial chemoembolization can be safely performed in patients with hepatocellular carcinoma invading the main portalvein and may improve the overall survival. *Radiology* 258(2):627–634
- Clavien PA, Lesurtel M, Bossuyt PM, Gores GJ, Langer B, Perrier A (2012) Recommendations for liver transplantation for



- hepatocellular carcinoma: an international consensus conference report. *Lancet Oncol* 13(1):e11–e22
- Dancey JE, Shepherd FA, Paul K, Sniderman KW, Houle S, Gabrys J, Hendler AL, Goin JE (2000) Treatment of nonresectable hepatocellular carcinoma with intrahepatic 90Y-microspheres. *J Nucl Med* 41(10):1673–1681
- D'Avola D, Lnarrairaegui M, Bilbao JI, Martinez-Cuesta A, Alegre F, Herrero JI, Quiroga J, Prieto J, Sangro B (2009) A retrospective comparative analysis of the effect of Y90-radioembolization on the survival of patients with unresectable hepatocellular carcinoma. *Hepatogastroenterology* 56(96):1683–1688
- Denys A, Prior J, Bize P, Duran R, De Baere T, Halkic N, Demartines N (2012) Portal vein embolization: what do we know? *Cardiovasc Interv Radiol* 35(5):999–1008
- Di Sandro S, Giacomoni A, Slim A, Lauterio A, Mangoni I, Mihaylov P, Pirotta V, Aseni P, De Carlis L (2012) Living donor liver transplantation for hepatocellular carcinoma: the impact of neoadjuvant treatments on the long term results. *Hepatogastroenterology* 59(114):505–510
- EASL-EORTC clinical practice guidelines: management of hepatocellular carcinoma. (2012) *J Hepatol* 56(4): 908–943
- Forner A, Llovet JM, Bruix J (2012) Hepatocellular carcinoma. *Lancet* 379(9822):1245–1255
- Gaba RC, Lewandowski RJ, Kulik LM, Riaz A, Ibrahim SM, Mulcahy MF, Ryu RK, Sato KT, Gates V, Abecassis MM, Omary RA, Baker TB, Salem R (2009) Radiation lobectomy: preliminary findings of hepatic volumetric response to lobar yttrium-90 radioembolization. *Ann Surg Oncol* 16(6):1587–1596
- Garden OJ (2011) Pushing the limits of surgical management in patients with hepatocellular carcinoma. *Br J Surg* 98(9):1183–1184
- Gordon-Weeks AN, Snaith A, Petrinic T, Friend PJ, Burls A, Silva MA (2011) Systematic review of outcome of downstaging hepatocellular cancer before liver transplantation in patients outside the Milan criteria. *Br J Surg* 98(9):1201–1208
- Gulec SA, Pennington K, Hall M, Fong Y (2009) Preoperative Y-90 microsphere selective internal radiation treatment for tumor downsizing and future liver remnant recruitment: a novel approach to improving the safety of major hepatic resections. *World J Surg Oncol* 7:6. doi:10.1186/1477-7819-7-6
- Hilgard P, Hamami M, Fouly AE, Scherag A, Muller S, Ertle J, Heusner T, Cicinnati VR, Paul A, Bockisch A, Gerken G, Antoch G (2010) Radioembolization with yttrium-90 glass microspheres in hepatocellular carcinoma: European experience on safety and long-term survival. *Hepatology* 52(5):1741–1749
- Ibrahim SM, Kulik L, Baker T, Ryu RK, Mulcahy MF, Abecassis M, Salem R, Lewandowski RJ (2012) Treating and downstaging hepatocellular carcinoma in the caudate lobe with yttrium-90 radioembolization. *Cardiovasc Interv Radiol* 35(5):1094–1101
- Inarrairaegui M, Thurston KG, Bilbao JI, D'Avola D, Rodriguez M, Arbizu J, Martinez-Cuesta A, Sangro B (2010) Radioembolization with use of yttrium-90 resin microspheres in patients with hepatocellular carcinoma and portal vein thrombosis. *J Vasc Interv Radiol* 21(8):1205–1212
- Inarrairaegui M, Pardo F, Bilbao JI, Rotellar F, Benito A, D'Avola D, Herrero JI, Rodriguez M, Marti P, Zozaya G, Dominguez I, Quiroga J, Sangro B (2012) Response to radioembolization with yttrium-90 resin microspheres may allow surgical treatment with curative intent and prolonged survival in previously unresectable hepatocellular carcinoma. *Eur J Surg Oncol* 38(7):594–601
- Jakobs TF, Saleem S, Atassi B, Reda E, Lewandowski RJ, Yaghami V, Miller F, Ryu RK, Ibrahim S, Sato KT, Kulik LM, Mulcahy MF, Omary R, Murthy R, Reiser MF, Salem R (2008) Fibrosis, portal hypertension, and hepatic volume changes induced by intra-arterial radiotherapy with 90yttrium microspheres. *Dig Dis Sci* 53(9):2556–2563
- Jelic S and Sotiropoulos GC (2010) Hepatocellular carcinoma: ESMO Clinical Practice Guidelines for diagnosis, treatment and follow-up. *Ann Oncol* 21 (Suppl 5): v59-v64
- Kooby DA, Egnatashvili V, Srinivasan S, Chamsuddin A, Delman KA, Kauh J, Staley CA 3rd, Kim HS (2010) Comparison of yttrium-90 radioembolization and transcatheter arterial chemoembolization for the treatment of unresectable hepatocellular carcinoma. *J Vasc Interv Radiol* 21(2):224–230
- Kulik LM, Atassi B, van Holsbeeck L, Souman T, Lewandowski RJ, Mulcahy MF, Hunter RD, Nemcek AA Jr, Abecassis MM, Haines KG 3rd, Salem R (2006) Yttrium-90 microspheres (TheraSphere) treatment of unresectable hepatocellular carcinoma: downstaging to resection, RFA and bridge to transplantation. *J Surg Oncol* 94(7):572–586
- Lau WY, Ho S, Leung TW, Chan M, Ho R, Johnson PJ, Li AK (1998) Selective internal radiation therapy for nonresectable hepatocellular carcinoma with intraarterial infusion of 90yttrium microspheres. *Int J Radiat Oncol Biol Phys* 40(3):583–592
- Lewandowski RJ, Kulik LM, Riaz A, Senthilnathan S, Mulcahy MF, Ryu RK, Ibrahim SM, Sato KT, Baker T, Miller FH, Omary R, Abecassis M, Salem R (2009) A comparative analysis of transarterial downstaging for hepatocellular carcinoma: chemoembolization versus radioembolization. *Am J Transplant* 9(8):1920–1928
- Llovet JM, Ricci S, Mazzaferro V, Hilgard P, Gane E, Blanc JF, de Oliveira AC, Santoro A, Raoul JL, Forner A, Schwartz M, Porta C, Zeuzem S, Bolondi L, Greten TF, Galle PR, Seitz JF, Borbath I, Haussinger D, Giannaris T, Shan M, Moscovici M, Voliotis D, Bruix J (2008) Sorafenib in advanced hepatocellular carcinoma. *N Engl J Med* 359(4):378–390
- Luo J, Guo RP, Lai EC, Zhang YJ, Lau WY, Chen MS, Shi M (2011) Transarterial chemoembolization for unresectable hepatocellular carcinoma with portal vein tumor thrombosis: a prospective comparative study. *Ann Surg Oncol* 18(2):413–420
- Mazzaferro V, Sposito C, Bhoori S, Romito R, Chiesa C, Morosi C, Maccauro M, Marchiano A, Bongini M, Lanocita R, Civelli E, Bombardieri E, Camerini T, and Spreafico C (2012) Yttrium(90) radioembolization for intermediate-advanced hepatocarcinoma: A phase II study. *Hepatology*, Accepted Article. doi: 10.1002/hep.26014
- Memon K, Kulik L, Lewandowski RJ, Mulcahy MF, Benson AB, Ganger D, Riaz A, Gupta R, Vouche M, Gates VL, Miller FH, Omary RA, Salem R (2012) Radioembolization for hepatocellular carcinoma with portal vein thrombosis: Impact of liver function on systemic treatment options at disease progression. *J Hepatol*. doi: 10.1016/j.jhep.2012.09.003
- Otto G, Herber S, Heise M, Lohse AW, Monch C, Bittinger F, Hoppe-Lotichius M, Schuchmann M, Victor A, Pitton M (2006) Response to transarterial chemoembolization as a biological selection criterion for liver transplantation in hepatocellular carcinoma. *Liver Transpl* 12(8):1260–1267
- Raoul JL, Boucher E, Rolland Y, Garin E (2010) Treatment of hepatocellular carcinoma with intra-arterial injection of radionuclides. *Nat Rev Gastroenterol Hepatol* 7(1):41–49
- Riaz A, Kulik L, Lewandowski RJ, Ryu RK, Giakoumis Spear G, Mulcahy MF, Abecassis M, Baker T, Gates V, Nayar R, Miller FH, Sato KT, Omary RA, Salem R (2009) Radiologic-pathologic correlation of hepatocellular carcinoma treated with internal radiation using yttrium-90 microspheres. *Hepatology* 49(4):1185–1193
- Rimassa L, Santoro A (2009) Sorafenib therapy in advanced hepatocellular carcinoma: the SHARP trial. *Expert Rev Anticancer Ther* 9(6):739–745
- Salem R, Lewandowski RJ, Mulcahy MF, Riaz A, Ryu RK, Ibrahim S, Atassi B, Baker T, Gates V, Miller FH, Sato KT, Wang E, Gupta R, Benson AB, Newman SB, Omary RA, Abecassis M, Kulik L

- (2010) Radioembolization for hepatocellular carcinoma using Yttrium-90 microspheres: a comprehensive report of long-term outcomes. *Gastroenterology* 138(1):52–64
- Salem R, Lewandowski RJ, Kulik L, Wang E, Riaz A, Ryu RK, Sato KT, Gupta R, Nikolaidis P, Miller FH, Yaghami V, Ibrahim SM, Senthilnathan S, Baker T, Gates VL, Atassi B, Newman S, Memon K, Chen R, Vogelzang RL, Nemcek AA, Resnick SA, Chrisman HB, Carr J, Omary RA, Abecassis M, Benson AB, 3rd, and Mulcahy MF (2011) Radioembolization results in longer time-to-progression and reduced toxicity compared with chemoembolization in patients with hepatocellular carcinoma. *Gastroenterology* 140(2): 497–507 e2
- Sangro B, Bilbao JI, Boan J, Martinez-Cuesta A, Benito A, Rodriguez J, Panizo A, Gil B, Inarrairaegui M, Herrero I, Quiroga J, Prieto J (2006) Radioembolization using 90Y-resin microspheres for patients with advanced hepatocellular carcinoma. *Int J Radiat Oncol Biol Phys* 66(3):792–800
- Sangro B, Carpanese L, Cianni R, Golfieri R, Gasparini D, Ezziddin S, Paprottka PM, Fiore F, Van Buskirk M, Bilbao JI, Ettorre GM, Salvatori R, Giampalma E, Geatti O, Wilhelm K, Hoffmann RT, Izzo F, Inarrairaegui M, Maini CL, Urigo C, Cappelli A, Vit A, Ahmadzadehfar H, Jakobs TF, Lastoria S (2011) Survival after yttrium-90 resin microsphere radioembolization of hepatocellular carcinoma across Barcelona clinic liver cancer stages: a European evaluation. *Hepatology* 54(3):868–878
- Seidensticker R, Seidensticker M, Damm R, Mohnike K, Schutte K, Malfertheiner P, Van Buskirk M, Pech M, Amthauer H, Ricke J (2012) Hepatic toxicity after radioembolization of the liver using (90)Y-microspheres: sequential lobar versus whole liver approach. *Cardiovasc Interv Radiol* 35(5):1109–1118
- Strigari L, Sciuto R, Rea S, Carpanese L, Pizzi G, Soriani A, Iaccarino G, Benassi M, Ettorre GM, Maini CL (2010) Efficacy and toxicity related to treatment of hepatocellular carcinoma with 90Y-SIR spheres: radiobiologic considerations. *J Nucl Med* 51(9):1377–1385
- Theyssohn JM, Schlaak JF, Muller S, Ertle J, Schlosser TW, Bockisch A, Lauenstein TC (2012) Selective internal radiation therapy of hepatocellular carcinoma: potential hepatopulmonary shunt reduction after sorafenib administration. *J Vasc Interv Radiol* 23(7):949–952
- Thomas MB, Jaffe D, Choti MM, Belghiti J, Curley S, Fong Y, Gores G, Kerlan R, Merle P, O'Neil B, Poon R, Schwartz L, Tepper J, Yao F, Haller D, Mooney M, Venook A (2010) Hepatocellular carcinoma: consensus recommendations of the National Cancer Institute Clinical Trials Planning Meeting. *J Clin Oncol* 28(25):3994–4005
- Toso C, Mentha G, Kneteman NM, Majno P (2010) The place of downstaging for hepatocellular carcinoma. *J Hepatol* 52(6):930–936
- Vogl TJ, Nour-Eldin NE, Emad-Eldin S, Naguib NN, Trojan J, Ackermann H, Abdelaziz O (2011) Portal vein thrombosis and arteriportal shunts: effects on tumor response after chemoembolization of hepatocellular carcinoma. *World J Gastroenterol* 17(10):1267–1275
- Woodall CE, Scoggins CR, Ellis SF, Tatum CM, Hahl MJ, Ravindra KV, McMasters KM, Martin RC 2nd (2009) Is selective internal radioembolization safe and effective for patients with inoperable hepatocellular carcinoma and venous thrombosis? *J Am Coll Surg* 208(3):375–382
- Worns MA, Weinmann A, Schuchmann M, Galle PR (2009) Systemic therapies in hepatocellular carcinoma. *Dig Dis* 27(2):175–188
- Wu ZJ, Cai J, Xu AB, Su XQ, Wang XQ, Zhang YX, Shao BF, Li YJ, Chu KY (2011) Combined three-dimensional conformal radiotherapy plus transcatheter arterial chemoembolization and surgical intervention for portal vein tumor thrombus in patients with hepatocellular carcinoma. *Zhonghua Yi Xue Za Zhi* 91(40):2841–2844
- Yoo H, Kim JH, Ko GY, Kim KW, Gwon DI, Lee SG, Hwang S (2011) Sequential transcatheter arterial chemoembolization and portal vein embolization versus portal vein embolization only before major hepatectomy for patients with hepatocellular carcinoma. *Ann Surg Oncol* 18(5):1251–1257
- Yoon SM, Lim YS, Won HJ, Kim JH, Kim KM, Lee HC, Chung YH, Lee YS, Lee SG, Park JH, Suh DJ (2012) Radiotherapy plus transarterial chemoembolization for hepatocellular carcinoma invading the portal vein: long-term patient outcomes. *Int J Radiat Oncol Biol Phys* 82(5):2004–2011
- Yoshidome H, Takeuchi D, Kimura F, Shimizu H, Ohtsuka M, Kato A, Furukawa K, Yoshitomi H, Miyazaki M (2011) Treatment strategy for hepatocellular carcinoma with major portal vein or inferior vena cava invasion: a single institution experience. *J Am Coll Surg* 212(5):796–803
- Zhang XB, Wang JH, Yan ZP, Qian S, Du SS, Zeng ZC (2009) Hepatocellular carcinoma with main portal vein tumor thrombus: treatment with 3-dimensional conformal radiotherapy after portal vein stenting and transarterial chemoembolization. *Cancer* 115(6):1245–1252
- Zhang T, Ding X, Wei D, Cheng P, Su X, Liu H, Wang D, Gao H (2010) Sorafenib improves the survival of patients with advanced hepatocellular carcinoma: a meta-analysis of randomized trials. *Anticancer Drugs* 21(3):326–332

# Principles for Combining Radioembolisation with Systemic Chemotherapy for Metastatic Colorectal Cancer

Esme J. Hill, Ashley K. Clift, and Ricky A. Sharma

## Contents

<b>1</b>	<b>The Clinical Problem of Hepatic Metastases in Colorectal Carcinoma</b> .....	130
<b>2</b>	<b>Radioembolisation Therapy</b> .....	130
2.1	Technical Aspects and Licensing .....	130
2.2	Biomarkers of Response.....	131
<b>3</b>	<b>Scientific Rationale for Combining RE with Systemic Chemotherapy</b> .....	131
3.1	Spatial Co-operation.....	131
3.2	Intrinsic Radiosensitisation .....	132
3.3	Clinical Application.....	132
<b>4</b>	<b>Optimal Combinations of Systemic Chemotherapy with RE in Metastatic Colorectal Cancer: First-Line Therapy</b> .....	133
4.1	Combination with HAC .....	133
4.2	Combination with Systemic Fluorouracil .....	133
4.3	Combination with Systemic Oxaliplatin-Fluorouracil.....	134
4.4	Clinical Trials of RE with Systemic Oxaliplatin-Fluorouracil.....	134
<b>5</b>	<b>Clinical Rationale for Combining RE with Chemotherapy for Second and Subsequent Lines of Therapy</b> .....	134
5.1	Combination with Systemic Irinotecan .....	135
5.2	Combination with Systemic Infusional Fluorouracil .....	135
<b>6</b>	<b>Use and Limitations of RE Without Concomitant Systemic Chemotherapy</b> .....	135
<b>7</b>	<b>Guidelines for Combining RE with Systemic Chemotherapy</b> .....	136
7.1	Patient Selection .....	136
7.2	Line of Therapy .....	136
7.3	Choice of Radiosensitising Drug .....	136
7.4	Clinical Trials .....	136
7.5	Current Practice .....	137
<b>8</b>	<b>Conclusions</b> .....	137
	<b>References</b> .....	138

## Abstract

The commonest cause of death from advanced colorectal cancer is disease progression of hepatic metastases. Radiotherapy is an important treatment modality in locally advanced colorectal cancer. Radioembolisation (RE) is a technique for administering resin or glass microspheres that contain yttrium-90 to unresectable primary or secondary hepatic malignancies internally via the liver's arterial supply in a single procedure. It can be considered a form of selective internal radiotherapy (SIRT) or arterially-administered brachytherapy. Clinical trials of RE used with concomitant radiosensitising chemotherapy have shown promising results in patients with metastatic colorectal cancer. In this chapter, the scientific rationale for combining RE with chemotherapy is outlined and the evidence base for combining RE with systemic chemotherapy in the treatment of metastatic colorectal cancer is appraised.

## Abbreviations

RE	Radioembolisation
SIRT	Selective internal radiotherapy
HAC	Hepatic arterial chemotherapy
RECIST	Response evaluation criteria in solid tumours
5-FU	5-fluorouracil
LV	Leucovorin
FDG-PET/CT	18-fluorodeoxyglucose positron emission tomography/computed tomography
BSC	Best supportive care
ADC	Apparent diffusion coefficient

E. J. Hill · A. K. Clift · R. A. Sharma  
Department of Oncology, Cancer Research UK-Medical Research Council Gray Institute for Radiation Oncology and Biology, University of Oxford, Old Road Campus Research Building, Oxford, OX3 7DQ, UK

E. J. Hill · R. A. Sharma (✉)  
Oncology Department, Churchill Hospital, Oxford University Hospitals NHS Trust, Oxford, OX3 7LJ, UK  
e-mail: ricky.sharma@oncology.ox.ac.uk

(F)TV	(Functional) tumour volume
TLG	Total lesion glycolysis
CEA	Carcinoembryonic antigen
CRP	C-reactive protein
AST	Aspartate aminotransferase

## 1 The Clinical Problem of Hepatic Metastases in Colorectal Carcinoma

In the United Kingdom between 2007 and 2009, 60 % of all large bowel tumours were diagnosed in the descending colon, sigmoid colon, rectosigmoid junction, rectum and anus (Bowel cancer incidence statistics 2009). Distinctions between left- and right-sided colorectal tumours are not only observed in tumour incidence, but also in molecular profiles and predilection to metastasis. For example, hypermethylation and elevated mutation rates are more common in right-sided versus other colorectal cancers (Cancer Genome Atlas 2012). In another study of over 17,000 cases, although rates of synchronous distant metastases were comparable between left- and right-sided carcinomas, it was observed that hepatic and pulmonary metastasis was more common with left-sided tumours (Benedix et al. 2010).

Despite major advances in the systemic treatment of metastatic colorectal carcinoma, the 5-year survival rate remains disappointingly low at approximately 7 % (US SEER Data 2005). Currently, median survival for this patient group ranges from 1.5 to 2.5 years, and is dependent upon the continuation of systemic therapy for much of the patient's remaining life. Of all patients with metastatic colorectal cancer, 20–30 % have liver-only metastases and approximately 50 % of recurrences following resection of the primary tumour are confined to the liver alone. Surgical resection of hepatic metastases is the treatment of choice, but unfortunately this is only feasible for less than 15 % of patients at presentation (Delaunoy et al. 2005). For the subset of patients with metastatic colorectal cancer in whom surgical resection can be achieved, the 5-year overall survival probability is 30–40 %, with 20 % of patients achieving long-term cure (Nordlinger et al. 2007). Patients with unresectable liver-predominant metastases have increasingly become a focus of interest for improving the survival of patients with metastatic colorectal cancer. This prioritisation is underpinned by the outcomes from Phase II studies utilising downstaging neoadjuvant chemotherapy, in which 10–20 % of patients with originally inoperable liver disease have been converted to candidates for curative resection, and also due to the finding that there is a strong statistical correlation between tumour response and resection rates across clinical studies (Folprecht et al. 2005).

Multimodality treatment combining systemic agents with liver surgery have been proffered as a means of improving tumour response rates, and thus also improving the proportion of long-term survivors of metastatic colorectal cancer patients.

Despite much optimism that newly developed (albeit expensive) biologically targeted therapeutics combined with systemic chemotherapy may improve survival in this patient group, complete radiological responses or cures remain exceedingly rare. Preliminary data from Phase III trials of chemotherapy and biologically targeted agents have not consistently shown statistically significant increases in response rates, nor the frequency of downstaging to resectability, over chemotherapy alone. There are two limitations of delivering neoadjuvant chemotherapy prior to liver metastasectomy. First, the development of pathological liver steatosis and fibrosis may occur with oxaliplatin-based or irinotecan-based chemotherapy, and worsens with cumulative dosing. The second is the risk of disease relapse in the liver post-surgery, which is usually not at the resection site. Of those patients with liver-dominant or liver-only metastases, where the hepatic disease is unlikely to become resectable even with neoadjuvant systemic therapy, there is still a robust rationale for maximising efforts on local control of the liver disease, since up to 90 % of patients with metastatic colorectal cancer ultimately die of liver failure (Nagorney and Gigot 1996). Multiple locoregional strategies are therefore under investigation to improve the outcome for patients with unresectable colorectal liver metastases, including radiofrequency ablation, microwave ablation, hepatic arterial chemotherapy (HAC), cryotherapy and radioembolisation (RE), also known as selective internal radiotherapy (SIRT).

## 2 Radioembolisation Therapy

### 2.1 Technical Aspects and Licensing

RE with Yttrium-90 microspheres is a technique that has been developed to target multiple sites of disease within the liver as a form of arterially delivered brachytherapy. In contrast to surgical resection and radiofrequency ablation, its use is not limited by the number or sites of liver metastases. TheraSpheres<sup>®</sup> (MDS Nordion Inc., Kanata, Ontario, Canada) are glass microspheres and SIR-Spheres<sup>®</sup> (Sirtex Medical Ltd, Sydney, Australia) are resin microspheres, both of which contain the pure beta emitter, Yttrium-90, and have a mean diameter of 20–35 micrometres. SIR-spheres were first approved for use in Australia (1998) for the treatment of inoperable liver tumours and subsequently in the USA (2002) for the treatment of



unresectable primary or metastatic liver tumours when combined with hepatic arterial floxuridine, and in the European Union (2002) for the treatment of primary and metastatic liver cancer. Yttrium-90 glass microspheres are approved in Europe, India and Canada for the treatment of hepatic neoplasia. In the USA, yttrium-90 glass microspheres are cleared for Humanitarian Device use for unresectable hepatocellular carcinoma.

The technique of RE involves an outpatient procedure in which a trans-femoral catheterisation is performed, and in the case of resin microspheres, approximately 40–80 million microspheres are injected into the arterial supply of the liver under fluoroscopic guidance. This microsphere infusion is secondary to a pre-treatment ‘work-up’ procedure: hepatic angiography with application of Technetium-99 macro-aggregated albumin in conjunction with gamma scintigraphy is used to predict microsphere distribution and also ascertain the extent of hepatopulmonary shunting. Embolisation of other vessels supplying the gastroduodenal region may also be undertaken in order to avoid leakage of microspheres to other regions, which could cause iatrogenic radiation damage with deleterious effects. Whereas the normal liver receives the majority of its blood supply from the portal venous system, liver tumours obtain the majority of theirs from the hepatic artery. RE exploits this vascular phenomenon, and as a consequence ensures the deposition of the infused microspheres into the malignant microvasculature (Ho et al. 1997), delivering a high dose of radiation to tumour cells, whilst relatively sparing the normal liver parenchyma. The preferential lodging of microspheres within tumour microvessels derived from the hepatic artery predicates the targeting of multiple sites of liver disease within a single interventional procedure.

Many theoretical and clinical aspects of the utility of SIR-spheres for the treatment of metastatic colorectal cancer have been published, including reviews of the clinical response rate to treatment in the first-line, second-line and salvage settings (Kennedy et al. 2006; Stubbs et al. 2006; Gray et al. 2001; Van Hazel et al. 2004; Gray et al. 1992). Numerous factors influence the planning and effectiveness of this promising treatment, including calculation of the delivered tumouricidal radiation doses and therapeutic intent; it is therefore imperative that in planning the administration of RE, these factors be considered in order to deliver maximum benefit and also safety for each patient (Lau et al. 2012).

## 2.2 Biomarkers of Response

Two important studies have been published regarding biomarkers (imaging and serum biomarkers) which could ultimately be useful as early predictors of response to RE

and the need for further therapy. Such markers may be useful for the individualisation and optimisation of patient care. In a prospective study of 21 patients undergoing SIRT for hepatic metastases from colorectal cancer, Dudeck et al. (2010) used diffusion weighted (DW) MRI to measure tumour volume (TV) and the intratumoural apparent diffusion co-efficient (ADC) in 41 metastases within the patient cohort at baseline (prior to treatment), 2 days post-treatment and at a follow-up procedure 6 weeks post-treatment. After classification of the study metastases into responding and non-responding lesions according to TV changes observed at 6 weeks, their analysis showed an inverse correlation between changes in TV versus changes in ADC ( $p < 0.0001$ ) at the follow-up procedure. Furthermore, in responding lesions, ADC was observed to have reduced significantly ( $p < 0.0001$ ) at 2 days post-SIRT, demonstrating the potential ability of this imaging biomarker to predict the effects of RE therapy at a very early timepoint after the procedure.

Only one study, performed by Fahmueller and colleagues (Fahmueller et al. 2012), has prospectively explored serum biomarkers as a potential predictive test for the efficacy of RE as treatment of hepatic colorectal metastases. Blood samples were obtained from 49 patients pre-treatment, and 3, 6, 24 and 48 h post-treatment in order to examine a panel of biochemical markers, which included circulating nucleosomes, carcinoembryonic antigen (CEA), C-reactive protein (CRP) and aspartate-aminotransferase (AST), plus other liver-related parameters. Multivariate Cox regression analysis elucidated the most powerful prognostic model to be the combination of pre-therapeutic levels of CRP and AST; a model which was strengthened further by inclusion of the nucleosome levels at 24 h. Validation of these interesting results in a larger study group is merited in order to potentially develop this biomarker panel for clinical use.

---

## 3 Scientific Rationale for Combining RE with Systemic Chemotherapy

### 3.1 Spatial Co-operation

It could be argued that some of the greatest breakthroughs in the treatment of solid malignancies have been made by administering chemotherapy and radiotherapy concurrently in the first-line setting, thus sparing patients from mutilating surgery (Rose 2002; Pignon et al. 2000; Sebag-Montefiore 2006). Numerous mechanisms by which drugs interact with radiation can be exploited for therapeutic benefit (Bentzen et al. 2007). The administration of potent systemic chemotherapy against metastatic colorectal cancer alongside radiation therapy targeted to sites of liver disease exploits the mechanism of spatial co-operation, first described by

Steel in 1979 (Steel and Peckham 1979). Systemic chemotherapy targets macroscopic and microscopic disease outside the irradiated tissue, whilst radiation therapy targets both macroscopic and microscopic disease in the liver. In the case of Yttrium-90 microspheres, a very high dose of radiation is delivered preferentially to the tumour whilst sparing normal liver tissue. As RE and chemotherapy have mostly non-overlapping toxicities, the combination of the two therapies theoretically should result in therapeutic gain, improving overall disease control and time to disease progression, whilst minimising unacceptable toxicity. Whereas the principle of spatial co-operation can potentially operate in any line of therapy, the highest response rates to chemotherapy and radiation in metastatic colorectal cancer are generally observed in the first-line setting, with diminishing levels of response thereafter. Therefore, one might expect to see the best outcomes to be achieved from combining Yttrium-90 with systemic chemotherapy in the first-line therapy of metastatic colorectal cancer.

### 3.2 Intrinsic Radiosensitisation

Another mechanism by which chemotherapy drugs interact with radiation is by intrinsic radiosensitisation of tumour cells. At the cellular level, this means that the combined effect of administering chemotherapy and radiation concomitantly is greater than would be anticipated by merely adding together the independent anti-tumour effects expected from chemotherapy alone and radiation alone. In the case of metastatic colorectal cancer, all of the chemotherapy agents commonly used in the treatment of this disease have been demonstrated to be intrinsic radiosensitisers (Nicolay et al. 2009).

5-Fluorouracil (5-FU), the mainstay of colorectal cancer therapy, sensitises tumour cells to the effects of radiation by inhibiting the repair of radiation-induced DNA damage. It achieves this by producing double-stranded DNA breaks and killing cells in the relatively radioresistant S phase of the cell cycle, wherein DNA synthesis occurs (Lawrence et al. 1994; Yoshioka et al. 1987). Irinotecan is a chemotherapy drug that is approved for use in first line or subsequent therapy of metastatic colorectal cancer, either in combination with 5-FU or as a single agent. Also a radiosensitiser in colon cancer cell lines (Illum 2011), irinotecan is a pro-drug for the more lipophilic SN-38 which acts as an inhibitor of Topoisomerase I. Amongst its other roles in nucleic acid metabolism, this enzyme is involved in the production of the physiological single-stranded DNA breaks needed to relax supercoiled DNA during replication. One mechanism by which irinotecan is thought to act as a radiosensitising agent is via the stabilisation of a reversible topoisomerase 1-drug-DNA ternary 'cleavable' complex,

permitting the uncoiling of DNA but precluding the resealing phase. Subsequent processes such as attempted DNA replication followed by radiation-induced damages may then induce lethality (Illum 2011; Chen et al. 1997).

Oxaliplatin is a diaminocyclohexane compound which is a potent radiosensitiser in cells grown in vitro (Blackstock et al. 1999). It has also been evaluated in combination with 5-FU and radiation in vitro, where experiments revealed synergism in comparison to either radiation or the drugs alone (Kjellstrom et al. 2005). The majority of the DNA damage caused by oxaliplatin is in the form of intrastrand DNA cross-links and monofunctional adducts. It is believed that the cell can repair these lesions relatively easily as compared to *interstrand* DNA cross-links. Such lesions represent only a small proportion of the DNA lesions induced by oxaliplatin, but require repair of both DNA strands. It is thought that repair of the interstrand crosslink may overwhelm the cell's DNA damage repair capacity in the context of irradiation, causing cells to arrest and potentially resulting in cell death. Additionally, the more common bulky DNA adducts induced by oxaliplatin also distort the DNA duplex, potentially blocking replication and transcription. Not surprisingly, oxaliplatin causes cell cycle arrest, which tends to be in the G2/M phase of cell cycle, making the cell more radiosensitive.

### 3.3 Clinical Application

In summary, to capitalise on the potential enhancement of tumour response to Yttrium-90 radiation therapy by the mechanism of radiosensitisation, it seems logical to co-administer radiosensitising chemotherapy, regardless of whether the multi-modality treatment is being used as first-line therapy or a subsequent line of therapy.

It is important to consider imaging biomarker development in the context of the combination of chemotherapy with RE. A prospective study by Gulec et al. (2011) determined the prognostic value of parameters measured by FDG-PET/CT imaging in patients undergoing RE with chemotherapy. This study determined functional tumour volume (FTV) and total lesion glycolysis (TLG), two measures of tumour metabolic activity, in 20 patients within a phase II clinical trial setting. Patients were recruited on the basis of having multiple hepatic metastases secondary to colorectal cancer, and being either chemotherapy-naïve, or having experienced failure of 1 prior systemic chemotherapy regimen. All patients had liver-only or liver-predominant disease. Inherent to the study was an in vivo double arm control, i.e., differential treatment was administered to the left- and right-lobes as one received systemic chemotherapy only ('control lobe'), the other receiving RE with SIR-spheres in addition to systemic chemotherapy ('target lobe'). In addition to concluding

that combined chemotherapy and RE produced a significantly favourable objective tumour response, Gulec and colleagues also found pre-treatment measurements of FTV and TLG were predictive markers for survival, as were 4 week post-treatment measurements of the same parameters. Median survival for patients with pre-treatment FTV measurements above and below 200 cc were 11.2 and 26.9 months, respectively ( $p < 0.05$ ). When measured at the same time point, patients with TLG values above and below 600 g showed the same median survivals (also  $p < 0.05$ ). The Larson-Ginsberg index (LGI), defined as the percentage change in TLG between pre- and post-treatment scans was also found to be predictive of patient survival subsequent to chemotherapy plus RE. Incorporation of imaging biomarkers such as FDG-PET/CT and DW-MRI into larger scale studies of RE is now being performed in order to validate these imaging modalities as a means of patient selection and early indicators of response.

## 4 Optimal Combinations of Systemic Chemotherapy with RE in Metastatic Colorectal Cancer: First-Line Therapy

A number of published studies of yttrium-90 RE for metastatic colorectal cancer can be used to guide physicians in how to combine this treatment modality with systemic chemotherapy.

### 4.1 Combination with HAC

In 2001, Gray et al. (2001) published a randomised controlled trial comparing HAC with floxuridine plus RE versus HAC with floxuridine alone, in 74 patients with non-resectable colorectal liver metastases, 63 of whom had not received prior chemotherapy for metastatic disease. All patients were treated with floxuridine at 0.3 mg/kg body weight continuously for 12 days in 4-weekly cycles, for 18 cycles in total except in the case of discontinuation due to disease progression, unacceptable toxicity or patient choice. Patients receiving RE underwent a single treatment usually 4 weeks after insertion of the hepatic artery catheter. Analysis of the data collected from all 74 patients was reported and indicated a statistically significant improvement in radiological response rate from the addition of RE to HAC (17.6 % vs. 44 %  $p = 0.01$ ) and improvement in time to disease progression in the liver (9.7 months vs. 15.9 months,  $p = 0.01$ ). The trial was not powered to detect a statistically significant difference in survival between the two groups, but a trend was observed towards improved survival in the group receiving RE and HAC, with improved survival in those living more than

15 months. There was no statistically significant difference in grade 3 and 4 toxicities between the two groups, nor impairment of quality of life in the group treated with RE. This trial identified the failure of disease control outside the liver as a significant problem, underlining the importance of systemic chemotherapy in this patient group. On separate analysis of data from the 63 patients who received the treatment as first-line, for the purpose of a Cochrane systematic review (Townsend et al. 2009), the differences between the two groups were less pronounced, with response rates of 14 versus 37 % ( $p = 0.051$ ) in the HAC alone and HAC + RE groups, respectively. There was no statistically significant improvement in progression-free survival, nor overall survival observed as a result of the addition of RE to HAC in this patient group. It should be noted that 41 of the 63 patients had extrahepatic disease, which may account for the failure of the study to demonstrate a survival benefit, but even on analysis of those 22 patients with hepatic-only disease, there was no statistically significant difference in progression-free survival between the two groups.

### 4.2 Combination with Systemic Flurouracil

The second randomised trial comparing chemotherapy and RE against chemotherapy alone for patients with colorectal metastases in the first-line setting was published by Van Hazel et al. (2004) in 2004. A Phase II randomised trial of systemic 5-FU and Leucovorin (LV) plus SIRT versus 5-FU/LV alone was conducted in 21 patients, 5 of whom had extrahepatic metastases (2 in the combination group and 3 in the chemotherapy-only group). Consistent with the Mayo regime that was used widely at that time, all patients were allocated to receive 5-FU 425 mg/m<sup>2</sup>/day plus LV 20 mg/m<sup>2</sup> daily for 5 days, in 4 weekly cycles until the development of toxicity requiring cessation or disease progression; eleven of the patients were randomised to receive RE on the third or fourth day of the second cycle of chemotherapy.

The study found that the RECIST response rate was better in the combination treatment group than the chemotherapy alone group, with 10 out of 11 patients demonstrating a partial response in the former group compared to none of the 10 receiving chemotherapy alone. The median time to progression was significantly different between the two groups; 18.6 months in the combination group compared to 3.6 months in the chemotherapy group ( $p < 0.0005$ ) and median survival was 29.4 versus 12.8 months ( $p = 0.021$ ), respectively. Grade 3 or 4 toxicity was also greater in the combination group but no statistically significant difference in quality of life was detected. One criticism of this study is that the sample size

was small, with two patients in the chemotherapy-only arm not receiving any chemotherapy due to deterioration and patients in the combination group receiving more cycles of chemotherapy than those in the chemotherapy group (Townsend et al. 2009).

Analysis of the data from 15 patients with no extrahepatic disease in this trial by Townsend et al. (2009) revealed a radiological response rate of 78 % in the combination group and 0 % in the chemotherapy group, with a median progression-free survival of 19.1 months in the former group and 4.9 months in the latter group (CI: 0.06–0.91). The median survival of those with no extrahepatic disease was 31.9 versus 13.8 months (CI: 0.06–0.99). In summary, whilst the results of this trial are favourable towards the addition of RE to systemic chemotherapy, the small number of patients makes it difficult to draw definitive conclusions. Additionally, the systemic chemotherapy, used as first-line therapy in this trial is no longer in widespread use. Overall, this study was a key step forward to demonstrate safety and proof-of-principle for combining RE with radiosensitising chemotherapy, and paved the way for subsequent first-line studies using oxaliplatin or irinotecan in combination with 5-FU.

#### 4.3 Combination with Systemic Oxaliplatin-Fluorouracil

Oxaliplatin in combination with 5-FU/LV was adopted in the late 1990s as a significant new combination chemotherapy treatment for advanced or metastatic colorectal cancer. The FOLFOX4 regimen consists of bimonthly administration of Oxaliplatin 85 mg/m<sup>2</sup> with standard LV/5-FU, but a slightly different drug sequence (e.g., OxMDG) is often given in certain countries such as the UK. A number of large-scale studies using FOLFOX or its variants have consistently yielded RECIST response rates of 50–60 %, progression-free survival of 8–9 months and median survival of 16–18 months (Louvvet and de Gramont 2003). Sharma et al. (2007) reported promising results from a Phase I-II trial of FOLFOX chemotherapy in combination with RE for patients with unresectable colorectal liver metastases in the first-line setting. Twenty patients were treated with oxaliplatin at escalating doses of 30–85 mg/m<sup>2</sup> and full dose LV/5-FU for Cycle 1–3 and full dose FOLFOX 4 for cycles 4–12. The primary endpoint of the study was toxicity and the dose limiting toxicity was demonstrated to be grade 3/4 neutropenia (12 patients) with a maximum tolerated dose of oxaliplatin 60 mg/m<sup>2</sup> for cycles 1–3. The combination treatment was generally well tolerated and 18 of the 20 patients (90 %) demonstrated a partial RECIST response to treatment; two (10 %) had

stable disease. Two (10 %) of the patients responded to therapy sufficiently enough to enable them to undergo a partial hepatic resection. The median progression-free survival was 9.3 months overall, and 14.2 months in the seven patients with liver-only metastases, suggesting that the addition of RE might be most beneficial in this patient group. The overall median time to progression in the liver was 12.3 months.

#### 4.4 Clinical Trials of RE with Systemic Oxaliplatin-Fluorouracil

This phase I–II study has paved the way for larger scale randomised phase III trials of oxaliplatin and 5-FU with or without RE in the first-line therapy of patients with liver-dominant metastatic colorectal cancer. Two studies are currently open to recruitment: the international SIRFLOX study, which is a randomised comparison study of FOLFOX6 plus SIR-spheres versus FOLFOX6 alone as first-line treatment in patients with non-resectable liver metastases from primary colorectal cancer; and the UK National Cancer Research Network FOXFIRE trial, an open label randomised trial of 5-FU, Oxaliplatin and Folinic acid ± interventional RE as first-line treatment for patients with unresectable liver-only or liver-predominant metastatic colorectal cancer. In combination, these two trials aim to recruit 810 patients in total; data from the two trials will be pooled to analyse the primary endpoint of overall survival at 2 years of follow-up, as well as secondary endpoints including progression-free survival, response rate and quality of life. The FOXFIRE trial will also analyse health economics. It should be noted that these trials have attempted to define the concept of ‘liver-dominant’ disease, as there is currently no standard definition worldwide. Unless a significant amount of post-trial cross-over occurs in the subject group, it is hoped that the results of these large trials will definitively answer the question whether the addition of SIRT to first-line chemotherapy provides survival benefit over giving chemotherapy alone.

### 5 Clinical Rationale for Combining RE with Chemotherapy for Second and Subsequent Lines of Therapy

There is evidence to support the view that the combination of Yttrium-90 RE with chemotherapy provides clinical benefit to patients with colorectal liver metastases in the second or subsequent lines of therapy.



## 5.1 Combination with Systemic Irinotecan

In an important study of another radiosensitising drug used in routine clinical practice to treat metastatic colorectal cancer, Van Hazel et al. (2009) performed a Phase I dose escalation study using single agent Irinotecan and RE in 25 patients with liver-only or liver-dominant colorectal metastases who were refractory to 5-FU but had never previously received Irinotecan. Patients were treated with Irinotecan at escalating doses between 50 and 100 mg/m<sup>2</sup> on days 1 and 8 of a 21 day cycle for 2 cycles, with RE administered during cycle 1 and subsequently received full dose Irinotecan at 100 mg/m<sup>2</sup> on days 1 and 8 for cycles 3–9. The trial demonstrated that the combination of Irinotecan as second-line chemotherapy with RE was not only safe, but appeared to be efficacious. The maximum tolerated dose was not reached and therefore the recommended dose of Irinotecan for combination with RE was 100 mg/m<sup>2</sup> D1 and 8, 3 weekly. In the study, 48 % of patients were observed to have a partial radiological response to therapy with a median progression-free survival of 6 months and median survival of 12.2 months. Although not a randomised comparison, these statistics certainly compare favourably with those reported for other irinotecan-based regimes used in this clinical setting (Cunningham et al. 1998; Seymour et al. 2007; Schoemaker et al. 2004; Mabro et al. 2006).

## 5.2 Combination with Systemic Infusional Fluorouracil

RE plus chemotherapy has also been demonstrated to be a valuable treatment strategy for patients who have progressed on standard systemic anti-cancer chemotherapy. The most significant study in this setting is the recent report by Hendlisz et al. (2010). This was a Phase III study of 46 patients with chemorefractory liver-only colorectal metastases who were randomised to receive either infusional 5-FU or, infusional 5-FU with RE. Patients in the control arm received 5-FU 300 mg/m<sup>2</sup> days 1–14 every 3 weeks and patients in the RE arm received 5-FU 225 mg/m<sup>2</sup> days 1–14 for 1 cycle then 300 mg/m<sup>2</sup> days 1–14 in subsequent cycles. The primary endpoint of the trial was the time to progression within the liver (TTLP). Crossover was permitted for patients developing progressive disease. The trial reached its primary endpoint by showing that RE significantly extended TTLP by 3.4 months (from 2.1 to 5.5 months; hazard ratio 0.38, 95 % confidence interval [CI] 0.20 to 0.72;  $p = 0.003$ ). It also showed a statistically significant extension in time to progression (TTP) overall, from 2.1 to 4.6 months (hazard ratio 0.51, 95 % CI 0.28–0.94;  $p = 0.03$ ). The disease control rate (partial response and stable disease) was significantly better in the

RE arm compared with the control arm at 86 versus 35 % ( $p = 0.001$ ), respectively. Grade 3 and 4 toxicity rates were higher in the control arm, but this difference was not statistically significant. The median overall survival of the groups combined was 8.7 months, with no statistically significant difference between the two groups. This may partly be explained by the fact that 25 out of 44 patients whose data were analysed received further treatment for their cancer on progression of their disease, this included 10 out of 25 patients in the control arm who subsequently received RE.

## 6 Use and Limitations of RE Without Concomitant Systemic Chemotherapy

Although it may be optimal to combine RE with radiosensitising systemic therapy whenever possible and safe, there are also studies which suggest that Yttrium-90 RE *without* concurrent chemotherapy treatment is a beneficial treatment in the salvage setting. Seidensticker et al. (2012) performed a retrospective study of using RE alone as salvage therapy in 29 heavily pre-treated patients with extensive colorectal liver metastases, in comparison with a matched-pair control cohort of 29 patients who received best supportive care (BSC) only, defined as palliative care aiming to maximise patient quality of life. All patients had been heavily pre-treated with chemotherapy, with a median of 3 (range 2–6) lines of chemotherapy in each cohort. Median progression-free survival was significantly prolonged in patients receiving SIR-Spheres RE compared with those in the BSC only cohort (5.5 vs. 2.1 months;  $P < 0.001$ ). The median overall survival was significantly extended for the patients receiving RE compared with controls (8.3 vs. 3.5 months;  $P < 0.001$ ). This benefit was clearly evident at 3 months (97 % vs. 59 % survival) and was sustained through 12 months follow-up (24 % vs. 0 % survival). A multivariate Cox proportional hazard model analysis revealed that the only predictor for prolonged survival was treatment with SIR-Spheres ( $P < 0.001$ ), and that a significant association existed between extent of liver involvement and the increased risk of death ( $P = 0.028$ ). The conclusion drawn from this study was that addition of SIR-Spheres RE to BSC offers significant clinical benefit to treatment-refractory patients, who otherwise possess limited treatment options.

Similarly, Cosimelli et al. (2010) conducted a Phase II prospective trial of Yttrium-90 RE in 50 patients who had chemorefractory colorectal liver metastases, all having received more than three lines of chemotherapy, including one oxaliplatin-containing regime and one irinotecan-containing regime. The primary endpoint of this trial was objective response rate, determined to be 24 % (2 % complete responses and 22 % partial responses), with a further

24 % of patients demonstrating stable disease after therapy. Two of the responding patients were converted to candidates for a potentially curative liver resection. The median overall survival was 12.6 months, with a statistically significant difference between the survival of responders and non-responders (16 months vs. 8 months;  $p = 0.0006$ ). However, the median time to progression was only 3.7 months, much shorter than that observed in the first-line setting when combined with chemotherapy [18.6 months (Van Hazel et al. 2004)]. Collectively, these trials suggest that RE without chemotherapy is an appropriate treatment in the salvage setting in patients with liver-dominant colorectal metastases who have previously received multiple lines of chemotherapy.

Although RE can be used alone or in combination with systemic chemotherapy in the salvage setting, the view that Yttrium-90 RE combined with radiosensitising chemotherapy at an earlier stage in a patient's treatment may be preferable is reinforced by a meta-analysis of 18 trials involving Yttrium-90 RE (Vente et al. 2009). This determined that the response rate to RE and chemotherapy in the salvage setting was 79 %, but the researchers found it to be over 90 % in the first-line setting, irrespective of whether 5-FU was used alone or in combination with oxaliplatin or irinotecan.

## 7 Guidelines for Combining RE with Systemic Chemotherapy

Based on the current evidence base, rigid recommendations cannot be made regarding criteria to combine RE with systemic chemotherapy in metastatic colorectal cancer in different lines of treatment of metastatic disease. The following points are important considerations for guiding physicians towards optimal combination of these treatments.

### 7.1 Patient Selection

First, patient selection for RE should only be made subsequent to thorough radiological assessments of the extent of metastatic disease within and outside the liver. As analysis of the randomised trials published by Gray et al. (2001) and Van Hazel et al. (2004) suggested, the presence of a significant burden of extra-hepatic metastases may limit the potential benefit obtained from RE in some patients. Despite this, the trials described above demonstrate that RE may be very appropriate therapy in patients with unresectable liver metastases and limited extrahepatic metastases, as the hepatic disease is highly likely to be life-limiting for most patients.

### 7.2 Line of Therapy

Indeed, the case for RE is strongest for patients with liver-only disease or liver-dominant disease, where the combination of chemotherapy and radiotherapy has been shown to result in long-term disease control or down-sizing to surgery or ablative therapy in some patients. This case is exemplified by a series of 46 patients with liver-only metastases, derived from mostly colorectal and breast primary tumours, who received a single treatment with RE (Hoffmann et al. 2010). In five patients, the liver disease was sufficiently downsized for subsequent radiofrequency ablation (RFA) of the residual lesions to be performed. It is notable that all five of these patients had a complete radiological response to RFA. Since it is not currently clear which patients benefit most from RE therapy, it is desirable to deliver RE and chemotherapy in the context of a clinical trial, when available. Figure 1 shows how RE and chemotherapy are currently being integrated in different lines of therapy.

### 7.3 Choice of Radiosensitising Drug

A second consideration concerns which drug or combination of drugs should be given with RE for optimum radiosensitisation. It should be noted that, since the biological mechanism of radiosensitisation (as discussed above) may be independent of the mechanism of anti-cancer efficacy of the same drugs used without concomitant radiotherapy, there is a scientific rationale for using a radiosensitising chemotherapy drug that the patient has previously received and may even have previously shown "tumour resistance" too. Oxaliplatin, 5-FU and irinotecan are all radiosensitisers, and the selection of *radiosensitising* chemotherapy in clinical practice should be guided by the evidence-based dosing regimes which have been demonstrated to be safe with RE (Sharma et al. 2007; van Hazel et al. 2009; Hendlisz et al. 2010) rather than by the need to control microscopic or macroscopic disease outside the liver. Following the administration of radiosensitising chemotherapy with RE, the patient can subsequently receive a systemic regime which may offer further survival benefit.

### 7.4 Clinical Trials

Currently, insufficient evidence exists to recommend the routine addition of Yttrium-90 RE to systemic chemotherapy in the first-line setting. Patients who wish to receive RE as first-line therapy for their metastatic colorectal cancer, and who fulfil the inclusion criteria for the clinical trials, should participate in the SIRFLOX and FOXFIRE studies.

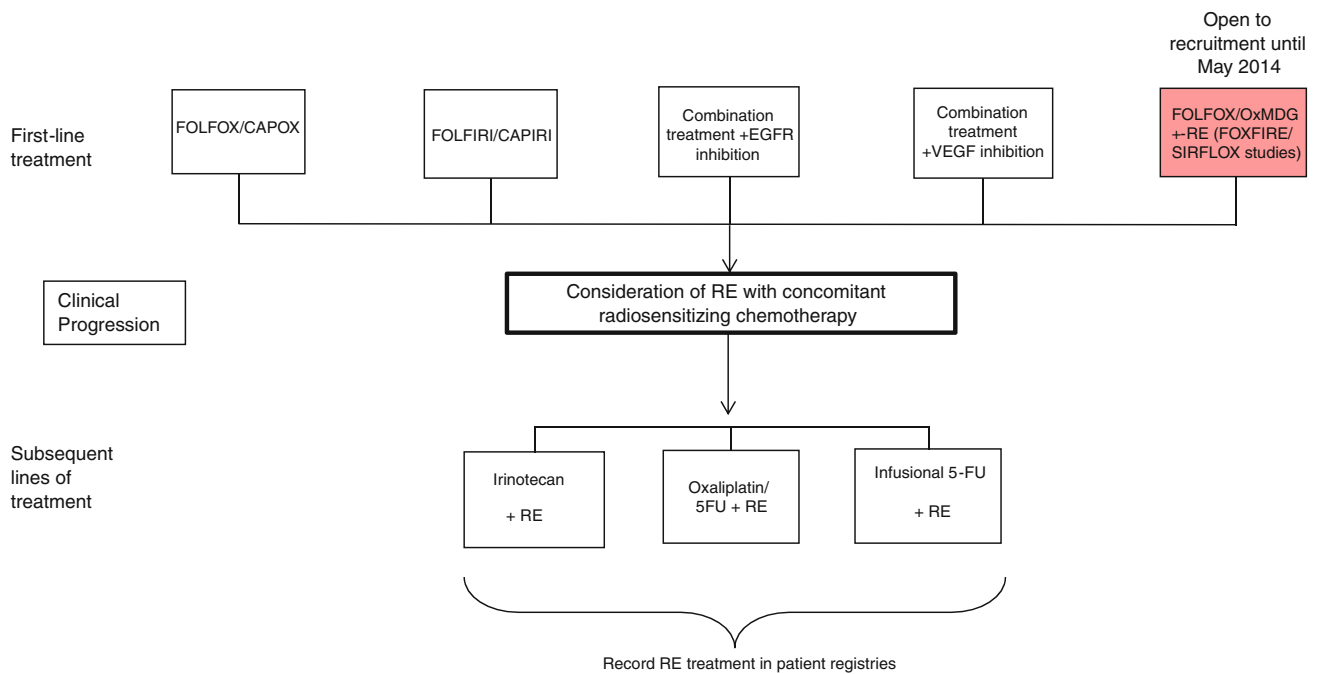


**Fig. 1** Potential points of integration of RE into the treatment pathway of patients with liver-only or liver-dominant unresectable colorectal liver metastases. The *shaded box* shows clinical trials testing RE with systemic therapy. *CAPIRI* capecitabine and irinotecan; *CAPOX* cetuximab, oxaliplatin and capecitabine; *5-FU* 5-fluorouracil;

*FOLFIRI* 5-fluorouracil, leucovorin and irinotecan; *FOLFOX* 5-fluorouracil, leucovorin and oxaliplatin; *RE* radioembolisation. An example of a patient registry in development is: <http://www.sirtex.com/content.cfm?sec=usa&MenuID=1120&ID=F4CCC1C2>

These clinical trials are currently recruiting patients in the UK, Europe, Australia, New Zealand and the USA. Since over 500 patients have already been recruited to these studies, it is anticipated that recruitment to both studies will be completed by 2014 and survival data should be available in 2017.

## 7.5 Current Practice

The practice at several institutions at present is to offer oxaliplatin and 5-FU chemotherapy [in the dosing regime shown to be safe in Sharma et al. (2007)] with RE as second-line or subsequent line therapy for patients with liver-dominant or liver-only metastases from colorectal cancer, regardless of their previous chemotherapy history. In patients who have experienced unacceptable toxicity with oxaliplatin (e.g., persistent peripheral neuropathy), RE can be combined with infusional 5-FU (Hendlisz et al. 2010) or with irinotecan (van Hazel et al. 2009), again using the dosing regimes of chemotherapy which have been shown to be safe. Consistent with current clinical trials, current practice at many centres is to administer RE on day 2, 3 or 4 of cycle 1 and to administer 6 weeks of chemotherapy in total for radiosensitisation. Following 6 weeks of therapy from the date of RE, chemotherapy can be switched to an

alternative systemic regime to optimally manage extrahepatic disease.

## 8 Conclusions

As the predominant cause of death in patients with advanced colorectal cancer, liver disease progression presents a major clinical challenge but also a therapeutic target. Within the context of limited extrahepatic disease, improved local control of liver metastases will offer survival benefit and therefore a better prognosis for such patients. Currently, the only potentially curative treatment modality for liver disease is surgical resection, which is only feasible in a minority of patients due to a number of constraints. However, combination of RE and systemic chemotherapy, which is not limited by the same constraints as surgery, has been shown to downstage a significant proportion of patients with initially unresectable disease, and thus convert them to candidates for potentially curative resection. The evidence base for combining RE and chemotherapy in the first-line treatment of metastatic colorectal cancer is robust enough for two large-scale phase III trials to be initiated to test the hypothesis that the greatest clinical benefit from RE may be achieved from this combination therapy at an early timepoint in a patient's disease course.

These randomised trials should provide high-quality evidence regarding whether this strategy improves the overall survival of patients with liver-dominant or liver-only unresectable liver metastases, and which subgroups of patients benefit most. In second-line and subsequent lines of therapy for metastatic colorectal cancer, we recommend that the combination of RE and systemic chemotherapy should be performed based on the principles of optimal intrinsic *radiosensitisation* of the liver metastases rather than by the concept of spatial cooperation, i.e. the need to control microscopic or macroscopic disease outside the liver. Following the administration of 6 weeks of radiosensitising chemotherapy with RE, patients can subsequently receive any systemic regime for further survival benefit.

**Acknowledgments** RAS is funded by the Bobby Moore Fund of Cancer Research UK, the Higher Education Funding Council for England and the NIHR Biomedical Research Centre Oxford.

## References

- Blackstock AW et al (1999) 202 Oxaliplatin: in vitro evidence of its radiation sensitizing activity—preclinical observations relevant to clinical trials. *Int J Radiat Oncol Biol Phys* 45(3, Supplement 1): 253–254
- Benedix F et al (2010) Comparison of 17,641 patients with right- and left-sided colon cancer: differences in epidemiology, perioperative course, histology, and survival. *Dis Colon Rectum* 53(1):57–64
- Bentzen SM, Harari PM, Bernier J (2007) Exploitable mechanisms for combining drugs with radiation: concepts, achievements and future directions. *Nat Clin Pract Oncol* 4(3):172–180
- Bowel cancer incidence statistics (2009) Available from: <http://www.cancerresearchuk.org/cancer-info/cancerstats/types/bowel/incidence/uk-bowel-cancer-incidence-statistics>
- Cancer Genome Atlas (2012) Comprehensive molecular characterization of human colon and rectal cancer. *Nature* 487(7407):330–337
- Chen AY et al (1997) Mammalian DNA topoisomerase I mediates the enhancement of radiation cytotoxicity by camptothecin derivatives. *Cancer Res* 57(8):1529–1536
- Cosimelli M et al (2010) Multi-centre phase II clinical trial of yttrium-90 resin microspheres alone in unresectable, chemotherapy refractory colorectal liver metastases. *Br J Cancer* 103(3):324–331
- Cunningham D et al (1998) Randomised trial of irinotecan plus supportive care versus supportive care alone after fluorouracil failure for patients with metastatic colorectal cancer. *Lancet* 352(9138):1413–1418
- Delaunoit T et al (2005) Chemotherapy permits resection of metastatic colorectal cancer: experience from Intergroup N. *Ann Oncol* 16(3):425–429
- Dudeck O et al (2010) Early prediction of anticancer effects with diffusion-weighted MR imaging in patients with colorectal liver metastases following selective internal radiotherapy. *Eur Radiol* 20(11):2699–2706
- Fahmueller YN et al (2012) Predictive and prognostic value of circulating nucleosomes and serum biomarkers in patients with metastasized colorectal cancer undergoing selective internal radiation therapy. *BMC Cancer* 12:5
- Folprecht G et al (2005) Neoadjuvant treatment of unresectable colorectal liver metastases: correlation between tumour response and resection rates. *Ann Oncol* 16(8):1311–1319
- Gray BN et al (1992) Regression of liver metastases following treatment with yttrium-microspheres. *Aust N Z J Surg* 62(2):105–110
- Gray B et al (2001) Randomised trial of SIR-Spheres plus chemotherapy vs. chemotherapy alone for treating patients with liver metastases from primary large bowel cancer. *Ann Oncol* 12(12):1711–1720
- Gulec SA et al (2011) The prognostic value of functional tumor volume and total lesion glycolysis in patients with colorectal cancer liver metastases undergoing 90Y selective internal radiation therapy plus chemotherapy. *Eur J Nucl Med Mol Imaging* 38(7):1289–1295
- Hendlisz A et al (2010) Phase III trial comparing protracted intravenous fluorouracil infusion alone or with Yttrium-90 resin microspheres radioembolization for liver-limited metastatic colorectal cancer refractory to standard chemotherapy. *J Clin Oncol* 28(23):3687–3694
- Ho S et al (1997) Tumour-to-normal uptake ratio of 90Y microspheres in hepatic cancer assessed with 99Tcm macroaggregated albumin. *Br J Radiol* 70(836):823–828
- Hoffmann RT et al (2010) Radiofrequency ablation after selective internal radiation therapy with Yttrium-90 microspheres in metastatic liver disease—Is it feasible? *Eur J Radiol* 74(1):199–205
- Illum H (2011) Irinotecan and radiosensitization in rectal cancer. *Anticancer Drugs* 22(4):324–329
- Kennedy AS et al (2006) Resin 90Y-microsphere brachytherapy for unresectable colorectal liver metastases: modern USA experience. *Int J Radiat Oncol Biol Phys* 65(2):412–425
- Kjellstrom J, Kjellen E, Johnsson A (2005) In vitro radiosensitization by oxaliplatin and 5-fluorouracil in a human colon cancer cell line. *Acta Oncol* 44:687–693
- Lau WY et al (2012) Patient selection and activity planning guide for selective internal radiotherapy with yttrium-90 resin microspheres. *Int J Radiat Oncol Biol Phys* 82(1):401–407
- Lawrence TS, Davis MA, Maybaum J (1994) Dependence of 5-fluorouracil-mediated radiosensitization on DNA-directed effects. *Int J Radiat Oncol Biol Phys* 29(3):519–523
- Louvet C, de Gramont A (2003) Colorectal cancer: integrating oxaliplatin. *Curr Treat Options Oncol* 4(5):405–411
- Mabro M et al (2006) A phase II study of FOLFIRI-3 (double infusion of irinotecan combined with LV5FU) after FOLFOX in advanced colorectal cancer patients. *Br J Cancer* 94(9):1287–1292
- Nagorney DM, Gigot JF (1996) Primary epithelial hepatic malignancies: etiology, epidemiology, and outcome after subtotal and total hepatic resection. *Surg Oncol Clin N Am* 5(2):283–300
- Nicolay NH, Berry DP, Sharma RA (2009) Liver metastases from colorectal cancer: radioembolization with systemic therapy. *Nat Rev Clin Oncol* 6(12):687–697
- Nordlinger B et al (2007) Does chemotherapy prior to liver resection increase the potential for cure in patients with metastatic colorectal cancer? A report from the European Colorectal Metastases Treatment Group. *Eur J Cancer* 43(14):2037–2045
- Pignon JP et al (2000) Chemotherapy added to locoregional treatment for head and neck squamous-cell carcinoma: three meta-analyses of updated individual data. MACH-NC Collaborative Group. *Meta-analysis of chemotherapy on head and neck cancer. Lancet* 355(9208):949–955
- Rose PG (2002) Chemoradiotherapy for cervical cancer. *Eur J Cancer* 38(2):270–278
- Schoemaker NE et al (2004) A randomised phase II multicentre trial of irinotecan (CPT-11) using four different schedules in patients with metastatic colorectal cancer. *Br J Cancer* 91(8):1434–1441



- Sebag-Montefiore D (2006) Developments in the use of chemoradiotherapy in rectal cancer. *Colorectal Dis* 8(Suppl 3):14–17
- Seymour MT et al (2007) Different strategies of sequential and combination chemotherapy for patients with poor prognosis advanced colorectal cancer (MRC FOCUS): a randomised controlled trial. *Lancet* 370(9582):143–152
- Seidensticker et al (2012) Matched-pair comparison of radioembolization plus best supportive care versus best supportive care alone for chemotherapy refractory liver-dominant colorectal metastases. *Cardiovasc Intervent Radiol* 35(5):1066–1073. Epub 2011 Jul 29
- Sharma RA et al (2007) Radioembolization of liver metastases from colorectal cancer using Yttrium-90 microspheres with concomitant systemic oxaliplatin, fluorouracil, and leucovorin chemotherapy. *J Clin Oncol* 25(9):1099–1106
- Steel GG, Peckham MJ (1979) Exploitable mechanisms in combined radiotherapy-chemotherapy: the concept of additivity. *Int J Radiat Oncol Biol Phys* 5(1):85–91
- Stubbs RS, O'Brien I, Correia MM (2006) Selective internal radiation therapy with 90y microspheres for colorectal liver metastases: single-centre experience with 100 patients. *ANZ J Surg* 76(8):696–703
- Townsend A, Price T, Karapetis C (2009) Selective internal radiation therapy for liver metastases from colorectal cancer. *Cochrane Database Syst Rev* (4). Art No. CD007045. DOI:10.1002/1465-1858.CD007045.pub2
- US SEER Data (2005) [www.seer.cancer.gov](http://www.seer.cancer.gov)
- Van Hazel G et al (2004) Randomised phase 2 trial of SIR-Spheres® plus fluorouracil/leucovorin chemotherapy versus fluorouracil/leucovorin chemotherapy alone in advanced colorectal cancer. *J Surg Oncol* 88(2):78–85
- van Hazel GA et al (2009) Treatment of fluorouracil-refractory patients with liver metastases from colorectal cancer by using Yttrium-90 resin microspheres plus concomitant systemic irinotecan chemotherapy. *J Clin Oncol* 27(25):4089–4095
- Vente M et al (2009) Yttrium-microsphere radioembolization for the treatment of liver malignancies: a structured meta-analysis. *Eur Radiol* 19(4):951–959
- Yoshioka A et al (1987) Deoxyribonucleoside triphosphate imbalance. 5-Fluorodeoxyuridine-induced DNA double strand breaks in mouse FM3A cells and the mechanism of cell death. *J Biol Chem* 262(17):8235–8241

---

# Results in Liver Metastatic Colorectal Cancer

Javier Rodríguez, Ana Chopitea, Bruno Sangro, and José Ignacio Bilbao

## Contents

<b>1</b>	<b>Introduction</b> .....	142
<b>2</b>	<b>Results of Radioembolization as Monotherapy in the Management of Liver Metastases from Colorectal Cancer Patients</b> .....	142
2.1	Phase II Trials.....	142
2.2	Prospective Cohort Studies.....	143
2.3	Retrospective Cohort Studies.....	143
2.4	Summary of <sup>90</sup> Y-RE as Monotherapy as Salvage Therapy.....	144
<b>3</b>	<b>Salvage Therapy Available Options in CRC Patients</b> ....	146
<b>4</b>	<b>Predictive Factors of Outcome After <sup>90</sup>Y-RE</b> .....	146
4.1	Imaging Predictive Factors.....	146
4.2	Molecular Predictive Factors.....	147
<b>5</b>	<b>Conclusions</b> .....	148
	<b>References</b> .....	148

---

## Abstract

Radioembolization (RE) is an increasingly used form of brachytherapy which consists of intraarterially injected microspheres loaded with <sup>90</sup>Y (a pure beta emitter with a 2.6-day half-life and an average 2.5-mm tissue penetration) as a source for internal radiation purposes. Its aim is to deliver tumoricidal doses of radiation to no matter how many liver tumors at a time while sparing the nontumoral liver from absorbing harmful doses of radiation. Colorectal cancer is one of the leading causes of cancer death worldwide, with the liver being the most common site of metastatic disease. Standard treatment for these patients with unresectable disease involves systemic therapy with either chemotherapy or targeted agents. In recent years, selective internal radiation therapy with embolization of branches of the hepatic artery with biocompatible resin-based <sup>90</sup>Y-labeled microspheres has emerged as a valuable tool for patients with this disease. Several phase I/II and randomized trials have proved the ability of SIR-Spheres to produce significant rates of tumor growth control among patients with liver metastases from colorectal cancer. Although the most promising data emerge from combinatorial approaches with systemic therapy, data supporting the use of <sup>90</sup>Y-RE as a stand-alone modality, especially in the salvage setting, are provided. Available clinical data with this therapeutic modality are discussed and compared to currently approved standard of care. In addition, this chapter highlights preliminary data regarding the discovery of potential predictive biomarkers of efficacy and efforts made in the field toward a personalized medicine.

---

J. Rodríguez (✉) · A. Chopitea  
Unit for the Research and Treatment of Gastrointestinal Malignancies, Department of Medical Oncology, Clínica Universidad de Navarra, University of Navarra, Pamplona, Spain  
e-mail: jrodriguez@unav.es

B. Sangro  
Liver Unit, Clínica Universidad de Navarra,  
University of Navarra, Pamplona, Spain

J. I. Bilbao  
Unit of Interventional Radiology, Clínica Universidad de Navarra, University of Navarra, Pamplona, Spain

## 1 Introduction

Over the past two decades, image-guided catheter-based or intraarterial techniques have emerged for locoregional treatment of the entire liver. The rationale for intraarterial treatment of liver tumors is that malignant intrahepatic lesions derive their blood supply almost entirely from the hepatic artery, as opposed to healthy liver tissue, which depends mainly on the portal vein for its blood supply (Breedis and Young 1954). Thus, agents that are delivered intraarterially to the liver are preferentially directed to malignant tissue, resulting in local tumor control and fewer systemic side effects compared to agents that are administered systemically (Alexander et al. 1996). Currently available liver-directed therapies for treating unresectable liver metastases include conformal radiation, radioembolization with yttrium-90 microspheres ( $^{90}\text{Y}$ -RE), hepatic arterial infusion chemotherapy, transarterial chemoembolization, or radiofrequency ablation (Robertson et al. 1995, 1997).

Yttrium-90 radioembolization is a liver-directed therapy that has become an increasingly applied treatment option for patients with unresectable primary or metastatic liver malignancies, including colorectal cancer (CRC). Therapy consists of intraarterial administration of microspheres with a diameter of 30–40  $\mu\text{m}$  tagged with or containing yttrium-90, a radioisotope that emits high-energy beta radiation with a mean tissue penetration depth of 2.5 mm.  $^{90}\text{Y}$ -RE most commonly involves the fluoroscopic-guided injection of millions of these radioactive microspheres within a lobar division of the hepatic artery. Once injected, these microspheres travel upstream and subsequently lodge within a vascular plexus that lies adjacent to a tumor. The anatomical “selectivity” allows these tumors to be selectively targeted by instillation of  $^{90}\text{Y}$  microspheres in the hepatic artery (de Baere and Deschamps 2011; Sigurdson et al. 1987).

Colorectal cancer is the most commonly diagnosed cancer in Europe and one of the leading causes of cancer death worldwide (Jemal et al. 2011). The liver is the most common site of metastatic disease, with 25 % of patients having detectable hepatic involvement at the time of first diagnosis. Liver failure secondary to hepatic tumor burden is responsible for more than 90 % of deaths in patients with this disease. When feasible, surgical resection remains the standard of care for patients with isolated hepatic metastases. However, even in selected cases, long-term survival is achieved in a minority of patients, and, in addition, only 10–15 % of them are candidates for up-front surgical resection. Standard treatment for these patients with unresectable disease involves chemotherapy based on fluoropyrimidines, oxaliplatin, irinotecan, and monoclonal antibodies targeting vascular endothelial growth factor

(VEGF) and epidermal growth factor receptor (EGFR) (Cunningham et al. 2010). In this setting,  $^{90}\text{Y}$ -RE has turned into another therapeutic alternative for the management of colorectal cancer liver metastases (CRCLM), with several phase I/II and randomized trials reported over the past years. Nevertheless, the exact role of  $^{90}\text{Y}$ -RE in the salvage setting of liver metastases from CRC patients remains to be determined. In fact, this approach has been performed either as monotherapy or in combination with standard systemic therapies, and as salvage therapy or early on in the course of the disease.

Although most of the recent literature on this topic is currently focusing on how to better combine  $^{90}\text{Y}$ -RE and systemic therapies in order to improve patients' outcome, these issues will be deeply discussed in Results of Radioembolization in the Management of Liver Metastases from Colorectal Cancer. In this chapter, we present a comprehensive overview of published studies of RE as a stand-alone modality in CRCLM, including phase II trials, prospective and retrospective cohort studies.

---

## 2 Results of Radioembolization as Monotherapy in the Management of Liver Metastases from Colorectal Cancer Patients

### 2.1 Phase II Trials

Sato et al. (2008) prospectively evaluated the safety, efficacy, and survival achieved with yttrium 90 glass microspheres in chemorefractory patients with CRCLM. Between 2002 and 2006, 137 patients with chemorefractory liver-dominant metastases from various primary malignancies were prospectively enrolled in this open-label phase II study. The trial included a heterogeneous population, which limits the ability to generalize the findings. Primary sites included 51 patients with CRC. All patients were considered to have unresectable disease, and none had responded to standard-of-care polychemotherapy. A complete response was demonstrated in 2.1 % of lesions, and 40.7 % of lesions had a partial response, for an overall response rate of 42.8 %. A subset analysis of patients with colorectal tumors demonstrated a median survival of 15.2 months.

Differences in survival were seen according to the tumor type, ECOG performance status, tumor burden, imaging findings (hypovascular or hypervascular tumors at angiography and cross-sectional imaging), and number of liver metastases. Patients with an ECOG performance status (PS) of 0 had a median survival time of 731 days, compared to 137 days in those with a PS of more than 0. This trend was maintained across all tumor types and reached statistical significance, supporting the notion of poor prognosis once

cancer-related symptoms appear. The median survival rate for those younger than 65 was 255 days, compared to 591 days for those older than 65 years old. Patients with hypervascular tumors at angiography and those with four or fewer liver lesions also had a longer median survival.

On the other hand, Cosimelli et al. (2010) reported a multicenter phase II clinical trial that, for the first time, prospectively evaluated the use of radioembolization in patients with colorectal liver metastases who had failed previous oxaliplatin- and irinotecan-based systemic chemotherapy regimens. Among the 50 eligible patients, 38 (76 %) had received more than 4 lines of chemotherapy and most of them presented with synchronous disease (72 %), 25–50 % replacement of total liver volume (60 %) and bilateral spread (70 %). By intention-to-treat analysis using Response Evaluation Criteria in Solid Tumors (RECIST), 1 patient (2 %) had a complete response, 11 (22 %) partial responses, and 12 (24 %) stable disease. The median time to progression and progression-free survival was 3.7 months (95 % CI, 2.6–4.9). Median overall survival was 12.6 months (95 % CI; 7.0–18.3) with 1- and 2-year survival rates of 50.4 and 19.6 %, respectively. There was a significant difference in survival between patients showing a response to radioembolization (CR/PR/SD) and those who did not respond (PD) (16 vs. 8 months,  $p < 0.001$ ), with a 2-year survival rate of 40.3 and 0 %, respectively. Two deaths were classified as possibly related to treatment. One patient died 40 days after treatment from acute renal failure and another responding patient died 60 days after treatment due to liver failure. All other adverse events were classified as WHO grade 1/2. Interestingly, the authors prospectively recorded a measurement of quality-of-life parameters through cancer- and site-specific questionnaires (EORTC QLQ C30 and EORTC QLQ CR38), showing that quality of life was not adversely affected by radioembolization.

## 2.2 Prospective Cohort Studies

Mulcahy et al. (2009) analyzed 72 patients with unresectable hepatic colorectal metastases treated at a targeted absorbed dose of 120 Gy. Anatomic imaging and positron emission tomography (PET) were used to assess response. At the time of  $^{90}\text{Y}$ -RE treatment, the majority of patients had liver-only disease (60 %). Of the 29 patients (40 %) who had minimal extrahepatic metastases, the sites of disease included lung (18 %), the lymph nodes (21 %), and the peritoneal lining (11 %). Sixty-seven patients (93 %) had received 5-Fluorouracil, 51 patients (72 %) had received oxaliplatin, and 35 patients (49 %) had received irinotecan. Bevacizumab and cetuximab had been administered to 33 (46 %) and 12 patients (17 %), respectively. The median dose delivered was 118 Gy. One hundred twenty-eight

target lesions were used to determine response, time to hepatic progression, and duration of response. A partial response according to WHO criteria was noted in 29 of 72 patients (40.3 %). At the lesional level, the response rate was 40.6 % (partial response rate, 37.5 %; complete response rate, 3.1 %), stable disease was observed in 44.5 % of patients, and disease progression was observed in 14.8 % of patients. The PET response rate was 77 %.

Treatment-related toxicities included fatigue (61 %), nausea (21 %), and abdominal pain (25 %). Grade 3 and 4 bilirubin toxicities were observed in 9 of 72 patients (12.6 %).

The median time to hepatic progression was 15.4 months, and the median response duration was 15 months. Overall survival from the first  $^{90}\text{Y}$ -RE treatment was 14.5 months. Subset analysis identified PS, tumor burden  $<25$  %, and the absence of extrahepatic disease as favorable predictors of survival from the time of  $^{90}\text{Y}$ -RE treatment. Distribution of metastases (unilobar vs. bilobar) did not predict outcome. Patients who had an ECOG PS of 0, a liver tumor burden  $<25$  %, and no extrahepatic disease had a median survival of 25.8 months (95 % CI, 16.9–64.3 months) from the time of  $^{90}\text{Y}$ -RE therapy. Radiographic response to therapy did predict an improved overall survival (23.5 vs. 8.5 months). The authors concluded that  $^{90}\text{Y}$ -RE liver therapy appears to provide sustained disease stabilization with acceptable toxicity. Asymptomatic patients with preserved liver function at the time of  $^{90}\text{Y}$ -RE appeared to benefit most from this therapy.

## 2.3 Retrospective Cohort Studies

Hong et al. (2009) reported a dose escalation study in 43 colorectal cancer patients. No life-threatening or fatal toxicities were observed. The reported median survival was 408 days, with 81 % of patients achieving stable disease. Higher doses were associated with a greater tumor response and an increased survival. In addition, tumor hypervascularity, higher baseline performance status, and less liver involvement were associated with better outcomes.

Seidensticker et al. (2012) performed a matched-pair comparison of 29 patients with mCRC refractory to a median of 3 lines of chemotherapy treated with RE. These patients were retrospectively matched with a contemporary cohort of  $>500$  patients who received best supportive care (BSC). Matching pairs were identified in a two-stage design. Initially, matching criteria included prior treatment history and tumor burden and subsequently, the following: liver involvement, synchronous versus metachronous metastases, increased versus normal alkaline phosphatase (ALP) levels; and carcinoembryonic antigen levels. The first 29 consecutive matching patients identified were included in this analysis.



Of 29 patients in each study arm, 16 pairs (55.2 %) matched for all four criteria, and 11 pairs (37.9 %) matched three criteria. Patients in both groups had a similar performance status. Median OS was significantly longer in patients who received RE plus BSC (8.3 vs. 3.5 months). This benefit was clearly evident at 3 months (97 vs. 59 % survival) and sustained through the 12-month follow-up (24 vs. 0 %). In the multivariate analysis, radioembolization was the only significant predictor for prolonged survival (HR = 0.3; 95 % CI; 0.16–0.55;  $p < 0.001$ ).

Bester et al. (2012) retrospectively evaluated the efficiency, in particular in terms of survival benefits, of radioembolization in the treatment of liver metastases in their institution. Out of the 417 patients who were assessed for eligibility to receive this therapy, a total of 339 patients with chemotherapy-refractory liver metastases were considered suitable candidates, and underwent  $^{90}\text{Y}$ -RE. The cohort included 224 mCRC patients. Seventy-eight patients did not satisfy the inclusion criteria and were referred back to their treating clinicians for continuing BSC treatment. However, only 51 patients were included in the statistical analysis as a standard-of-care control group, since the additional 27 patients likely indicated a group with more advanced disease. There was no statistically significant difference between the two cohorts in all analyzed baseline parameters. For patients with metastatic CRC who were treated with  $^{90}\text{Y}$ -RE, the median OS was 11.9 months (95 % CI 10.1–14.9 months), compared to a median OS of 6.6 months in the BSC cohort (log-rank test,  $P = 0.001$ ). There was a statistically significant reduction of 43 % in the hazard of death for patients receiving radioembolization in the multivariate analysis.

Martin et al. (2012) reported their experience in a subset of 24 patients with CRCLM. Their median age was 63 years, 54 % of the patients had extrahepatic disease and 67 % of them had bilobar involvement. The median of previous lines of therapy was 3. No objective responses were observed by the authors, although five patients had a CEA tumor marker decrease. Median PFS and OS were 3.9 months (95 % CI, 2.4–4.8 months) and 8.9 months (95 % CI, 4.2–16.7 months), respectively. Patients older than 65 years had an improved PFS (4.6 vs. 2.4 months) and OS (14 vs. 5.5 months) compared to younger patients. This finding is likely due to the receipt of  $^{90}\text{Y}$ -RE treatment earlier in their disease course. The presence of extrahepatic disease and the absence of CEA response appeared negatively predictive of efficacy. Toxicities were expected and manageable.

Gulec et al. (2007) analyzed the treatment records and follow-up data of 40 patients with primary and metastatic liver malignancies who underwent a single whole-liver treatment with  $^{90}\text{Y}$  resin microspheres, including 15 metastatic colorectal cancer patients. In this study, tumor

response correlated with a higher tumor flow ratio as measured by Tc-99m MAA imaging. Administered activities for the  $^{90}\text{Y}$  resin microspheres ranged from 0.4 to 2.4 GBq (mean:  $1.2 \pm 0.5$  GBq). The mean absorbed doses for the tumor, liver, and lungs were  $121.5 \pm 85.6$ ,  $17.2 \pm 18.6$ , and  $2.1 \pm 2.3$  Gy, respectively. The absorbed doses delivered to the tumors ranged from 40.1 to 494.8 Gy (mean:  $121.5 \pm 85.6$  Gy). Partial response or disease stabilization was observed in 27 (67.5 %) patients. Interestingly, median tumor absorbed doses for responders and nonresponders were 107.8 and 76.9 Gy, respectively, with the lowest tumor absorbed dose producing a detectable response being 40 Gy. The tumor response rate for patients with CRC was 47 %.

Kennedy et al. (2006) reported the outcome of 208 patients who had failed irinotecan- and oxaliplatin-based chemotherapy and were subsequently treated with  $^{90}\text{Y}$ -RE in a lobar and whole-liver basis. Imaging response was 35 % and PET response was 91 %. Median overall survival was 10.5 and 4.5 months for responders and nonresponders, respectively.

Jakobs et al. (2008) reported results on 41 salvage patients with unresectable hepatic colorectal metastasis. The mean CEA decrease was 32 % for the entire cohort. By RECIST criteria, partial response, stable disease, and progressive disease were observed in 7, 25, and 4 patients, respectively. Median overall survival was 10.5 months. Improved survival was observed for patients with CEA and imaging response (19.1 vs. 5.4 months and 29.3 vs. 4.3 months, respectively  $p < 0.001$ ).

Finally, in the most recently published trial to date, Smits et al. (2013) have reported the outcome of 59 patients with liver metastasis for CRC ( $n = 30$ ), NET ( $n = 6$ ) and other primary tumors ( $n = 23$ ). No grade 3–4 clinical toxicity was observed, whereas laboratory toxicity grade 3–4 was observed in 38 % of patients. Whole-liver treatment in one session was not associated with increased laboratory toxicity. Three-month disease control rates for target lesions, whole liver, and overall responses were 35, 21, and 19 %, respectively. Median TTP was 6.2 months for target lesions, 3.3 months for the whole liver, and 3.0 months overall. Median overall survival was 8.9 months (95 % CI: 6.9–10.9) for colorectal cancer liver metastases.

## 2.4 Summary of $^{90}\text{Y}$ -RE as Monotherapy as Salvage Therapy

A summary of the most relevant studies with the use of  $^{90}\text{Y}$ -RE monotherapy as salvage treatment in CRCLM is provided in Tables 1 and 2. Disease control rate (complete response, partial response, and stable disease) in this setting ranged from 29 to 90 %, and overall response rate

**Table 1** Summary of studies with radioembolization as monotherapy in CRCLM

Author	N	Setting	Response	PET response	TTP	OS	Comments
Bester	224	Refractory	NA	NA	NA	11.9 m	Comparative retrospective cohort study with BSC. Reduction of 43 % in the hazard of death for patients receiving RE. Overall incidence of RILD; 34 %
Martin	24	After a median of 3 prior lines of therapy	0 %	NA	3.9 m	8.9 m	54 % extrahepatic disease 67 % bilobar liver involvement
Gulec	15	Refractory	47 %	NA	NA	NA	Tumor response correlated with higher tumor flow ratio as measured by Tc-99m MAA imaging
Kennedy	208	87 % had received 3 lines of systemic therapy	35.5 % (SD; 55 %)	85 %	NA	10.5 m (vs. 4.5 m in nonresponders)	

TTP time to progression; OS overall survival; L-OHP oxaliplatin; CPT-11 irinotecan; m months; NA not available; BSC best supportive care

**Table 2** Summary of studies with radioembolization as monotherapy in CRCLM

Author	N	Setting	Response	PET response	TTP	OS	Comments
Mulcahy	72	Salvage	40.3 % (SD; 44.5 %)	77 %	15 m	14.5 m	Median dose delivered; 118 Gy. Liver replacement, ECOG, and extrahepatic disease correlated with outcome
Sato	51	Salvage	42.8 % (SD; 47 %)	90 %	NA	457 days	<sup>90</sup> Y-glass microspheres. ECOG, tumor burden, number of liver metastases, and hypervascularity correlated with OS. Heterogeneous population
Seidensticker	29	Refractory to L-OHP and CPT-11	41.4 % (SD; 17.2 %)	NA	5.5 m	8.3 m	Matched-pair comparison. RE increases median survival compared to BSC (8.3 vs. 3.5 months)
Cosimelli	50	Refractory to L-OHP and CPT-11. 22 % prior bevacizumab	24 % (SD; 24 %)	NA	3.7 m	12.6 m (2-year OS; 19.6 %)	76 % > 4 lines of therapy, 58 % > 4 liver mets, 60 % >25–50 % of liver replacement. QoL not adversely affected by RE

TTP time to progression; OS overall survival; L-OHP oxaliplatin; CPT-11 irinotecan; m months; NA not available

(complete response and partial response) ranged from 18 to 46 %. Fahmueller et al. (2012) reported the lowest response rate with <sup>90</sup>Y-RE as monotherapy (disease control rate of 29 %), whereas Kennedy et al. (2006) reported a disease control rate as high as 90 %. Response was measured with PET/CT in the former study and with CT and RECIST criteria in the latter, potentially explaining part of the above-mentioned differences in response.

The proportion of patients alive at 12 months also varied from one study to another, ranging from 37 to 59 %. Progression-free survival also ranged from 3.9 to 9.2 months. These results suggest that up to 50 % of patients with CRCLM treated with <sup>90</sup>Y-RE in the salvage setting are alive

at 12 months after therapy. When survival data are compared for <sup>90</sup>Y-RE as monotherapy, the shortest overall survival was reported by Seidensticker et al. (8.3 months), and the longest overall survival was reported by Sato et al. (15.2 months). However, comparison of these two trials is hard since one used resin-based spheres and the other glass-based spheres. There is also a lack of information regarding the median administered activity and the inclusion of a relatively large percentage of patients with extrahepatic disease (Cianni et al. 2009; Townsend et al. 2009; Nace et al. 2011).

From the previously outlined trials, it seems clear that great heterogeneity between different studies exist. Thus,

the amount of extrahepatic disease and the acceptable tumor burden allowed to entry into the trials do not seem to be clearly outlined. The patients' performance status (only reported in 50 % of the published articles) and the prognostic impact of previous systemic treatments (most studies on  $^{90}\text{Y}$ -RE as monotherapy include patients with a median of 3 or more prior lines) should also be further detailed. Finally, tumor response rate varies widely in these trials. This may be explained in part by differences in methodology for response assessment. Several trials do not specify whether RECIST criteria have been followed. Tumor response should be differentiated in target lesions, liver, and overall response. Moreover, in order to improve interpretability of overall response rates, studies should indicate whether patients have baseline evidence of extrahepatic disease (Rosenbaum et al. 2013).

### 3 Salvage Therapy Available Options in CRC Patients

Currently, a broad variety of trials and retrospective analysis in metastatic colorectal cancer patients have provided insight into the selection and duration of treatment, the role of targeted agents, and the best way to tailor therapy according to clinical and molecular parameters. Nevertheless, there remains a high medical need for effective treatments for patients with unresectable CRC liver metastases who have failed conventional chemotherapy regimens.

At present,  $^{90}\text{Y}$  radioembolization as monotherapy is provided mainly to patients with progressive disease after first- or second-line chemotherapy. In this setting of refractory disease other therapeutic alternatives have been tested. More specifically, three-targeted agents have provided a survival advantage over BSC.

Van Cutsem et al. (2007) compared the activity of panitumumab (a fully human monoclonal antibody directed against the epidermal growth factor receptor (EGFR) plus best supportive care (BSC) to that of BSC alone in 463 patients with metastatic colorectal cancer who had progressed after standard chemotherapy. Panitumumab significantly prolonged PFS. Objective response rates also favored panitumumab over BSC (10 % for panitumumab and 0 % for BSC). No difference was observed in OS, although cross-over was allowed.

Junker et al. (2007) randomized 572 patients who had colorectal cancer expressing immunohistochemically detectable EGFR and who had been previously treated with a fluoropyrimidine, irinotecan, and oxaliplatin to Cetuximab, an IgG1 chimeric monoclonal antibody against EGFR plus best supportive care (287 patients) or best supportive care alone (285 patients). Cetuximab treatment was associated with a significant improvement in overall

survival (hazard ratio for death, 0.77) and in progression-free survival (hazard ratio for disease progression or death, 0.68). The median overall survival was 6.1 months in the cetuximab group and 4.6 months in the group assigned to supportive care alone. Partial responses for the cetuximab and BSC groups were 8.0 and 0 %, respectively. Quality of life was also better preserved in the cetuximab group, with less deterioration in physical function and global health status.

Finally, Grothey et al. (2013) randomized 760 CRC patients to receive placebo or regorafenib, an oral multi-kinase inhibitor that blocks the activity of several protein kinases such as VEGFR 1-3, Raf, Kit, and Ret. Median overall survival was 6.4 months in the regorafenib arm versus 5.0 months in the placebo group ( $p = 0.005$ ), with an overall survival rate at 9 months of 38.2 and 30.8 %, respectively. Included patients in these trials were similar to those deemed eligible for  $^{90}\text{Y}$  radioembolization, withstanding their potential extrahepatic disease load. This suggests that in the appropriately selected patients (liver-dominant disease, acceptable disease burden, preserved hepatic function, and performance status) a longer overall survival may be expected from RE compared to current standard third-line treatment options. Nevertheless, prospective comparative studies evaluating survival, tumor response, and quality of life after  $^{90}\text{Y}$ -RE are warranted.

### 4 Predictive Factors of Outcome After $^{90}\text{Y}$ -RE

Given the wide variety in tumor response rates and survival times, great effort is put into optimal patient selection through the identification of prognostic and predictive factors for  $^{90}\text{Y}$ -RE. Further on, availability of early information on the efficacy of the therapy during the first days after RE application would be highly appreciated as therapy may be intensified by means of further systemic therapy or combined locoregional approaches. This is particularly appealing since the regular staging of the patients by imaging is usually performed about 3 months after RE application. Unfortunately, so far, data on predictive factors for RE outcome are scarce.

#### 4.1 Imaging Predictive Factors

Dunfee et al. (2010) reported that the degree of radiological response, based on World Health Organization criteria, 1 month after radioembolization was a favorable prognostic marker. More recently, diffusion-weighted imaging was found to predict therapy response as soon as 2 days after RE application in a small study on 21 patients.

Whereas changes in tumor volumes can be assessed with morphologic MR imaging or CT, metabolic response can be measured with PET-FDG. Several studies have suggested a high prognostic value of (Jakobs et al. 2008) F-FDG PET in the prediction of survival after  $^{90}\text{Y}$ -RE. To evaluate the prognostic value of metabolic parameters, most PET trials have endeavored to correlate tracer uptake in the tumor with CT or MR imaging volumes. The maximum (Jakobs et al. 2008) F-FDG SUV within the tumor (SUVmax) has been traditionally taken as an indicator of tumor vitality. More recently, PET response criteria in solid tumors (PERCIST) led to the adoption of SUV peak, defined as the mean FDG uptake within a spheric 1-cm<sup>3</sup> region around the tumor voxel with the highest SUV. Fendler et al. (2013) have recently evaluated the prognostic value of Jakobs et al. (2008) F-FDG PET/CT metabolic parameters for predicting survival after  $^{90}\text{Y}$ -RE in 80 pts with CRCLM. PET/CT was performed at baseline and 3 months after treatment. Metabolic volumes, total lesion glycolysis, SUVmax, and SUV peak were obtained in 3-liver lesions in each patient. Overall median survival was 60 weeks. Responders who had a change in metabolic volume or total lesion glycolysis had a significantly longer survival. However, neither RECIST 1-1 criteria nor SUVmax or SUV peak after treatment predicted outcome.

## 4.2 Molecular Predictive Factors

As previously mentioned, in a multicenter phase 2 trial conducted in 50 chemorefractory liver-dominant metastatic CRC, Cosimelli et al. (2010) reported an overall response rate of 48 % and a median OS of 12.6 months after RE with  $^{90}\text{Y}$  radiolabeled resin microspheres. As an extension of this trial, the authors evaluated a panel of biomarkers related to apoptosis as potential predictive factors. To this end, liver metastases biopsies were taken 8–21 días prior to  $^{90}\text{Y}$ -RE and 2 months thereafter. Tissue specimens were pre and posttherapy available from 29 to 15 patients, respectively. Thirteen patients had concomitantly available pre- and post- $^{90}\text{Y}$ -RE samples. The biomarker analysis included IHC analysis of apoptosis and cell proliferation protein regulators, such as p53, bcl-2, survivin, and ki-67. The IHC analysis showed a reduction in the expression of survivin (from 92 to 54 %), p53 (from 100 to 69 %), bcl-2 (from 46 to 31 %), and a nonsignificant disease in Ki-67 positivity (from 77 to 61 %) in the post-therapy biopsies. Among the 13 matched patients, 75 % of those with no biomarker variation presented progressive disease, whereas all patients showing changes in biomarkers expression achieved partial response or stable disease (Melucci et al. 2013). Although the number of patients is limited, this is the first study that has evaluated the predictive value of molecular markers

related to radiosensitivity. A major drawback of these findings comes from the fact that, in resected liver tumors, altered expression of survivin, p53, ki67, and k-ras have also been correlated with a higher likelihood of relapse, so a prognostic role for these biomarkers cannot be ruled out.

Alternatively to tumor tissue analysis, serum biomarkers may potentially be valuable as predictors of therapy response, since they are measured noninvasively and cost-efficiently, facilitating serial determinations and kinetic interpretations.

In a first study by the group of Fahmueller et al. (2012) the authors had investigated several tumor-related, liver-related, and cell death-related biomarkers in liver metastases from 49 colorectal cancer patients treated with RE. Blood samples were collected prospectively before therapy and at 3, 6, 24, and 48 h after SIRT Measurements of CEA, CA 19-9, CYFRA 21-1, nucleosomes, lactate dehydrogenase (LDH), C-reactive protein (CRP), aspartate aminotransferase (AST), alanine aminotransferase (ALT), bilirubin, gamma-glutamyl-transferase (GGT), alkaline phosphatase (AP), amylase, lipase, and choline esterase were included. They found that C-reactive protein and baseline levels of CA 19-9, CEA, CYFRA 21-1, LDH, and AST correlated with response. Most notably, increased nucleosome levels 24 h after  $^{90}\text{Y}$ -RE indicated significantly poor therapy response and reduced survival time. One may speculate that nonresponding tumors have a high cell turnover and a better blood supply leading to more effective release of nucleosomes into the blood or a less effective elimination of nucleosomes from the circulating due to an impaired immune system. Nucleosomes had already been proven useful for the early estimation of chemotherapy response in several solid tumors (Stoetzer et al. 2012), but no reports were available with RE.

There is also a growing body of evidence that links patient immune response and therapeutic outcome. For these reasons, serum levels of high mobility group box 1 (HMGB1), receptor of glycation end products (RAGE), and activity of desoxyribonuclease (involved in the hydrolysis of nucleosomal DNA and in the elimination of circulating nucleosomes) were correlated with response to therapy (regularly determined radiologically 3 months after therapy) and with overall survival (Fahmueller et al. 2013). Blood samples were taken from 49 consecutive CRC patients with extensive hepatic metastases before, 24 and 48 h after  $^{90}\text{Y}$ -RE. Serum levels of HMGB1 increased 24 h after RE, RAGE levels decreased, and DNase remained unchanged. Interestingly, serum HMGB1 levels determined 24 h after  $^{90}\text{Y}$ -RE were significantly higher in patients with progressive disease compared to responding patients, while no difference was observed for RAGE and DNase according to radiological response. In addition, high baseline and 24 h levels of HMGB1 correlated with a worse



survival. In the multivariate analysis, the combination of HMGB1 (24 h) and CRP (24 h) yielded the highest prognostic power.

High mobility group box 1 (HMGB1) is a nuclear protein with close association to the chromatin that plays an essential role in the regulation of transcription processes. In the blood circulation, HMGB1, once released during cell death, acts as danger associated molecular pattern (DAMP) protein that binds to specific immune cells, promotes phagocytation, antigenic cross-priming, presentation of pathogenic cell death products, and stimulation of immune responses. HMGB1 binds to specific receptors on dendritic cells such as the multiligand receptor RAGE and the toll-like receptors 4 (TLR4). Subsequently, phagocytized (tumor-related) particles are processed intracellularly and cross-presented at the cellular surface leading to promotion of tumor-specific cytotoxic T-cell response. The release of DAMPs during this so-called “immunogenic cell death,” is essential for a sustained therapy response after chemotherapy. Indeed, neutralization or knockdown of HMGB1 or TLR4 correlated with a reduced anticancer immune response both in vitro and in vivo and with shortened survival times. At the same time, HMGB1 can also promote neoangiogenesis and tumor invasiveness, and its overexpression seems essential for tumor progression and invasiveness in colorectal cancer. This may likely be the reason why the authors find that pretherapeutic and 24 h levels of HMGB1 were significantly higher in nonresponding patients and correlated with a poor overall survival (Van Beijnum et al. 2013; Lin et al. 2012; Yao et al. 2010).

These exploratory and hypotheses-generating approaches aimed to identify potential predictive biomarkers of therapy response represent valuable efforts that should be reinforced. The discovery and validation of new biomarkers hold promise and will definitively allow for a more rational selection of those patients more likely to benefit from  $^{90}\text{Y}$ -RE. These preliminary findings should be validated in larger and prospectively designed trials.

## 5 Conclusions

$^{90}\text{Y}$  microspheres RE offer an attractive alternative in the available therapies for patients with metastatic colorectal cancer. Given careful patient selection and proper angiographic techniques, this approach offers patients a minimally invasive, low-toxicity treatment with very favorable tumor response and potential survival benefit, even in the context of refractory disease after the previous use of standard systemic therapies. A growing body of evidence supports its use as a stand-alone modality in the salvage setting or earlier on in the course of the disease in combination with chemotherapy or targeted agents. In this sense, major advances in

patient outcome would probably depend on the development of better strategies aimed to combine systemic therapies with RE within a multidisciplinary approach. Moreover, because mCRC patients have different underlying biological behavior in terms of therapy sensitivity, patterns of dissemination, or risk of relapse, future trials should concentrate on specific clinical scenarios (salvage setting, consolidative procedure, combined therapy...).

Finally, patient selection remains a critical point, as a subgroup of patients with huge metastases or preexisting extrahepatic manifestations seem to benefit less from this therapeutic modality. Future studies should routinely incorporate molecular determinants of response or predictive gene signatures to more precisely define the subsets of patients most likely to benefit from this therapeutic modality.

## References

- Alexander HR, Bartlett DL, Fraker DL, Libutti SK (1996) Regional treatment strategies for unresectable primary or metastatic cancer confined to the liver. *Princ Pract Oncol* 10:1–19
- Bester L, Meteling B, Pocock N et al (2012) Radioembolization versus standard care of hepatic metastases: comparative retrospective cohort study of survival outcomes and adverse events in salvage patients. *J Vasc Interv Radiol* 23:96–105
- Breedis C, Young G (1954) Blood supply of neoplasms of the liver. *Am J Pathol* 30:969–972
- Cianni R, Urigo C, Notarianni E et al (2009) Selective internal radiation therapy with SIR-Spheres for the treatment of unresectable colorectal hepatic metastases. *Cardiovasc Interv Radiol* 32:1179–1186
- Cosimelli M, Golfieri R, Cagol PP et al (2010) Multi-centre phase II clinical trial of yttrium-90 resin microspheres alone in unresectable, chemotherapy refractory colorectal liver metastases. *Br J Cancer* 103:324–331
- Cunningham D, Atkin W, Lenz HJ et al (2010) Colorectal cancer. *Lancet* 375:1030–1047
- de Baere T, Deschamps F (2011) Arterial therapies of colorectal cancer metastases to the liver. *Abdom Imaging* 36:661–670
- Dunfee BL, Riaz A, Lewandowski RJ et al (2010) Yttrium-90 radioembolization for liver malignancies: prognostic factors associated with survival. *J Vasc Interv Radiol* 21:90–95
- Fahmueller YN, Nagel D, Hoffmann RT et al (2012) Predictive and prognostic value of circulating nucleosomes and serum biomarkers in patients with metastasized colorectal cancer undergoing selective internal radiation therapy. *BMC Cancer* 12:5
- Fahmueller YN, Nagel D, Hoffmann RT et al (2013) Immunogenic cell death biomarkers HMGB1, RAGE, and DNase indicate response to radioembolization therapy and prognosis in colorectal cancer patients. *Int J Cancer* 132(10):2349–2358
- Fendler WP, Philippe Tiega DB, Ilhan H et al (2013) Validation of several SUV-based parameters derived from  $^{18}\text{F}$ -FDG PET for prediction of survival after SIRT of hepatic metastases from colorectal cancer. *J Nucl Med* 54:1202–1208
- Grothey A, Van Cutsem E, Sobrero A et al. CORRECT Study Group (2013) Regorafenib monotherapy for previously treated metastatic colorectal cancer (CORRECT): an international, multicentre, randomised, placebo-controlled, phase 3 trial. *Lancet* 381:303–312
- Gulec SA, Mesoloras G, Dezarn WA, McNeillie P, Kennedy AS (2007) Safety and efficacy of Y-90 microsphere treatment in

- patients with primary and metastatic liver cancer: the tumor selectivity of the treatment as a function of tumor to liver flow ratio. *J Transl Med* 5:15
- Hong K, McBride JD, Georgiades CS et al (2009) Salvage therapy for liver-dominant colorectal metastatic adenocarcinoma: comparison between transcatheter arterial chemoembolization versus yttrium-90 radioembolization. *J Vasc Interv Radiol* 20:360–367
- Jakobs TF, Hoffmann R-T, Dehm K et al (2008) Hepatic yttrium-90 radioembolization of chemotherapy-refractory colorectal cancer liver metastases. *J Vasc Interv Radiol* 19:1187–1195
- Jemal A, Bray F, Center MM, Ferlay J, Ward E, Forman D (2011) Global cancer statistics. *CA Cancer J Clin* 61:69–90
- Jonker DJ, O'Callaghan CJ, Karapetis CS et al (2007) Cetuximab for the treatment of colorectal cancer. *N Engl J Med* 357:2040–2048
- Kennedy AS, Coldwell D, Nutting C et al (2006) Resin <sup>90</sup>Y-microsphere brachytherapy for unresectable colorectal liver metastases: modern USA experience. *Int J Radiat Oncol Biol Phys* 65:412–425
- Lin L, Zhong K, Sun Z, Wu G, Ding G (2012) Receptor for advanced glycation end products (RAGE) partially mediates HMGB1-ERKs activation in clear cell renal cell carcinoma. *J Cancer Res Clin Oncol* 138:11–22
- Martin LK, Cucci A, Wei L et al (2012) Yttrium-90 radioembolization as salvage therapy for colorectal cancer with liver metastases. *Clin Colorectal Cancer* 11:195–199
- Melucci E, Cosimelli M, Carpanese L et al. Italian Society of Locoregional Therapies in Oncology (S.I.T.I.L.O.) (2013) Decrease of survivin, p53 and Bcl-2 expression in chemorefractory colorectal liver metastases may be predictive of radiosensitivity after radioembolization with yttrium-90 resin microspheres. *J Exp Clin Cancer Res* 32:13
- Mulcahy MF, Lewandowski RJ, Ibrahim SM et al (2009) Radioembolization of colorectal hepatic metastases using yttrium-90 microspheres. *Cancer* 115:1849–1858
- Nace GW, Steel JL, Amesur N et al (2011) Yttrium-90 radioembolization for colorectal cancer liver metastases: a single institution experience. *Int J Surg Oncol* 2011:571261
- Robertson JM, Lawrence TS, Walker S et al (1995) The treatment of colorectal liver metastases with conformal radiation therapy and regional chemotherapy. *Int J Radiat Oncol Biol Phys* 32:445–450
- Robertson JM, McGinn CJ, Walker S et al (1997) A phase I trial of hepatic arterial bromodeoxyuridine and conformal radiation therapy for patients with primary hepatobiliary cancers or colorectal liver metastases. *Int J Radiat Oncol Biol Phys* 39:1087–1092
- Rosenbaum CE, Verkooijen HM, Lam MG et al (2013) Radioembolization for treatment of salvage patients with colorectal cancer liver metastases: a systematic review. *J Nucl Med*. [Epub ahead of print] PubMed PMID: 24071510
- Sato KT, Lewandowski RJ, Mulcahy MF et al (2008) Unresectable chemorefractory liver metastases: radioembolization with <sup>90</sup>Y microspheres—safety, efficacy, and survival. *Radiology* 247:507–515
- Seidensticker R, Denecke T, Kraus P et al (2012) Matched-pair comparison of radioembolization plus best supportive care versus best supportive care alone for chemotherapy refractory liver-dominant colorectal metastases. *Cardiovasc Interv Radiol* 35:1066–1073
- Sigurdson ER, Ridge JA, Kemeny N et al (1987) Tumor and liver drug uptake following hepatic artery and portal vein infusion. *J Clin Oncol* 5:1836
- Smits ML, van den Hoven AF, Rosenbaum CE et al (2013) Clinical and laboratory toxicity after intra-arterial radioembolization with <sup>90</sup>Y-microspheres for unresectable liver metastases. *PLoS One* 8(7):e69448
- Stoetzer OJ, Wittwer C, Lehner J et al (2012) Circulating nucleosomes and biomarkers of immunogenic cell death as predictive and prognostic markers in cancer patients undergoing cytotoxic therapy. *Expert Opin Biol Ther* 12(Suppl 1):S217–S224
- Townsend A, Price T, Karapetis C (2009) Selective internal radiation therapy for liver metastases from colorectal cancer. *Cochrane Database Syst Rev* 4:CD007045
- Van Beijnum JR, Nowak-Sliwinska P, van den Boezem E et al (2013) Tumor angiogenesis is enforced by autocrine regulation of high-mobility group box 1. *Oncogene* 32:363–374
- Van Cutsem E, Peeters M, Siena S et al (2007) Open-label phase III trial of panitumumab plus best supportive care compared with best supportive care alone in patients with chemotherapy-refractory metastatic colorectal cancer. *J Clin Oncol* 25:1658–1664
- Yao X, Zhao G, Yang H, Hong X, Bie L, Liu G (2010) Overexpression of high-mobility group box 1 correlates with tumor progression and poor prognosis in human colorectal carcinoma. *J Cancer Res Clin Oncol* 136:677–684

---

# Treatment of Neuroendocrine Tumors with Selective Internal Radiation Therapy

Douglas M. Coldwell, Martin Vyleta, and Mahmood Samman

## Contents

<b>1</b>	<b>Neuroendocrine Tumors</b> .....	151
1.1	Epidemiology.....	152
<b>2</b>	<b>Imaging</b> .....	152
<b>3</b>	<b>Therapy</b> .....	152
3.1	Practical Aspects of SIRT for mNETs.....	154
	<b>References</b> .....	155

---

## Abstract

The pathophysiology of neuroendocrine tumors (NET) is discussed and the differences in types of tumors within this broad category are highlighted. While carcinoid is the most common of the NETs, the general principles of treatment can be extrapolated to the NETs in general. The chemotherapy treatments have not been historically very effective and the major treatment is surgery with removal of the primary as well as debulking metastases. This regimen only occurs in a small minority of patients since the disease has metastasized to the liver in 90 % of cases. Unresectable disease can be treated with modern chemotherapy for small cell cancer with reasonable results but loco-regional treatment of the liver disease is the primary treatment utilized. While ablative therapies can treat one lesion at a time, most patients benefit from having a regional approach to their treatment. Use of <sup>90</sup>Yttrium beads has been demonstrated to not only be safe and effective but also to permit significant quality of life since the treatments are performed on an outpatient basis.

---

## 1 Neuroendocrine Tumors

Neuroendocrine tumors (NET) are rare tumors originating from the neuroendocrine system and produce both peptide and amines that are produced its particular cell of origin. The most common, the carcinoid tumor, is a vasoactive tumor that produces 5-hydroxytryptamine (5-HT) and a host of other vasoactive hormones and proteins (such as adrenocorticotrophic hormone, 5-hydroxytryptophan, gastrin, chromogranins A and C, growth hormone), that are excreted in the kidney as 5-hydroxyindoleacetic acid (5-HIAA) (Doherty 2011). These hormones are responsible for the systemic effects of the tumor, which usually occur when the tumor metastasizes to the liver, since the products can be directly secreted into the hepatic veins and from there to the

---

D. M. Coldwell (✉) · M. Vyleta · M. Samman  
Department of Radiology, University of Louisville,  
530 South Jackson St, Louisville, KY, USA  
e-mail: dmcold01@louisville.edu

heart. They are responsible for the “carcinoid syndrome,” a set of physiological symptoms that are characteristic of carcinoid tumor: episodic flushing, hypertension, and diarrhea (Soga et al. 1999). The flushing lasts only a few minutes but may be prolonged for hours especially in patients with bronchial carcinoid. Cardiac effects include a fibrosis that is found in the ventricles, particularly the right ventricle and affects the chordae leading tricuspid regurgitation and heart failure (Robiolio et al. 1995). The secretion of these hormones also permit the diagnosis of carcinoid to be conclusively made and the effects of treatment followed by urine levels of 5-HIAA or serum levels of chromogranin A (Singh and Law 2012).

But not all carcinoid tumors consistently produce this syndrome. It has more to do with the embryologic origin of the cells than the histology of the tumor. This tumor may arise from the foregut, midgut, or hindgut and each has a set of associated signs and symptoms that are slightly different.

Usually the foregut carcinoids:

1. Produce low levels of 5-HT and a variety of hormones,
2. Rarely produce the carcinoid syndrome but the flushing of the carcinoid syndrome may last for hours rather minutes as in the midgut carcinoids,
3. Commonly metastasize to bone.

The midgut carcinoids are the usual culprits when one thinks of the stereotypical carcinoid tumors. These tumors:

1. Produce high levels of 5-HT,
2. May produce multiple hormones,
3. Frequently is the cause of the carcinoid syndrome when the tumor metastasizes to the liver,
4. Rarely metastasizes to bone.

Finally, the hindgut carcinoids:

1. Rarely produces 5-HT
2. Rarely produces the carcinoid syndrome
3. Commonly metastasizes to bone.

Practically, the most common sites of origin of carcinoid and, indeed, most NETs are the bronchus, small bowel, and colon/rectum (Kulke et al. 2012).

## 1.1 Epidemiology

Overall, the incidence of carcinoids and NETs is increasing. From 1973 until 2004, the incidence increased by almost fivefold from 1.09/100,000 to 5.25/100,000. The reason for this rapid increase is unclear since the disease is so rare that the risk factors are not known. Smoking, alcohol consumption, and occupational exposure have not been found to be a significant contributor to the origin of NETs. However, nutrition has been implicated in the formation of small bowel carcinoids in patients who consume a high fat diet increasing 3.72 times above the mean for each 10 g increase in fat intake per 1000 kcal. However, a definitive

explanation for this increase has yet to be made (Hassan and Yao 2011).

The only genetic association with NETs is in the occurrence of familial multiple endocrine neoplasia (MEN) syndromes. MEN1 is an autosomal dominant syndrome characterized by endocrine tumors of the parathyroid gland, the gastroenteropancreatic tract (usually a pancreatic neuroendocrine tumor), and the anterior pituitary. Any of these tumors are rare unto themselves and any occurrence of two of them should suggest the presence of the syndrome. Since the tumors in MEN1, especially a pancreatic NET, may metastasize to the liver, it is the syndrome that may be present when liver metastases are treated. MEN2 includes pheochromocytoma and medullary thyroid carcinoma with MEN2A also has a parathyroid hyperplasia or tumor present. MEN2B also has mucocutaneous neuromas and gastrointestinal motility disorders and muscular hypotonia. Marfanoid habitus may also be a part of MEN2B (Landry et al. 2011).

## 2 Imaging

Routine enhanced computed tomographic scans (CTs) obtained will demonstrate a brightly enhancing mass that little different from any other seen in the context of tumor diagnosis. However, the differential diagnosis of an extremely enhancing mass in the areas of origin of carcinoid tumors, as noted above, must include carcinoid tumors particularly when the patient presents with a history suggesting the carcinoid syndrome.

Use of peptide receptor scintigraphy with <sup>111</sup>In-DTPA octreotide (the so-called “octreo-scan”) has been reported to be 80–100 % effective in the detection of carcinoids and NETs (Laverman et al. 2012). Since the tumors that are avid for this imaging agent will also preferentially bind octreotide, a somatostatin receptor blocker, this test is also an indicator of the ability to suppress the carcinoid syndrome with octreotide. This imaging method may also demonstrate unrecognized sites of disease, guide surgery for those patients able to undergo definitive therapy, and follow treatment. Positron emission tomography (PET) scans utilizing <sup>18</sup>Fluorodeoxyglucose is not usually picked up by this tumor unless it is highly malignant.

## 3 Therapy

Surgery is the definitive treatment for this disease. If all the tumor is able to be removed, disease free survival ranges from 42 to 46 months (Yao et al. 2001). Although current consensus guidelines recommend the surgical removal of as much tumor as possible, it is only possible in less than 10 %



of the patients (Madoff et al. 2006). Palliative debulking of the metastatic NET in the liver is of assistance in providing symptomatic relief for 6–24 months but the complication rates and the mortality of the surgery are both high at 33 and 9 %, respectively (Chamberlain et al. 2000).

The development of the somatostatin analogues, such as octreotide, provided symptomatic relief as well as in some antiproliferative effects, but the effects of this drug eventually diminishes due to tachyphylaxis and disease progression (Kolby et al. 2003; Biku and Davidson 2012). After surgery, or in a patient in whom surgery is not an option, octreotide has been the best available systemic treatment. Until recently, chemotherapeutic options have been limited in number as well as in response with the streptozocin/doxorubicin protocols achieving a response rate of 16 % (Ref. Kennedy et al. 2011). More modern chemotherapy regimens that treat these tumors similarly to small cell lung cancer with cisplatin/etoposide or temozolamide/capecitabine have seen response rates around 50 % in the more aggressive mNETs (Mitry et al. 1999). But, these will also not provide a long-term solution to inoperable lesions as the tumors will eventually become unresectable or the side effects of the agents will not permit the treatment to continue.

Targeted therapy to individual tumors in the liver is an attractive option if they are few in number and easily accessible. The use of Radiofrequency Ablation (RFA), cryoablation, Irreversible Electroporation, or microwave destruction of tumor has been reported as successful treatments. However, they all suffer from the difficulty of placement of a fairly good-sized (14–19 gauge) probe into the tumor, the ability to treat only a single tumor at a time, and the tumors need to be less than 3 cm in diameter in order to obtain a complete treatment. When patients present with more than a handful of tumors, it is simply too extensive process to treat each tumor with these techniques. Even when a few of the existing tumors are treated, the hormonal activity of the tumor may not be stopped since it is usually necessary to ablate at least 90 % of the visible tumors (O'Toole and Ruzsniwski 2005).

Consequently, lobar or regional therapies have been the mainstay of treatment for unresectable disease in patients having these tumors. Over the past 20 years, cytoreductive therapies with arterially based approaches have been developed. This approach is based upon the tumors receiving their blood supply from the hepatic artery and the normal hepatic parenchyma receiving its supply from the portal vein. Since these tumors are extremely hypervascular when compared with the background liver parenchyma, the agents utilized are even more preferentially flow directed to the tumors when compared with the relatively hypovascular lesions such as colorectal cancer metastases. Arterially approaches using particles cause ischemia of the tumor by

applying them to the tumors individually if there are few enough or to the hepatic lobe have achieved a response in symptom control, growth retardation, and biochemical marker decrease (Gupta et al. 2005). When chemotherapy is added to the embolic particles (chemoembolization), there may be some additional benefit but no significant increase in either time to progression, overall response rate, or survival over use of the particles alone (bland embolization). Furthermore, there is no consensus as to either the chemotherapeutic agent to utilize or even if the addition of the agent is worthwhile (Ruutinen et al. 2007). Both bland and chemoembolization produce significant side effects, notably the post-embolization syndrome (nausea, vomiting, fever, right upper quadrant pain, leukocytosis, increased liver function tests) usually requiring hospitalization for both pain control and hydration (Dhand and Gupta 2011). Recently, a higher incidence of biliary ductal injury and abscess formation has been noted in NET patients who have undergone both a pancreaticoduodenectomy and chemoembolization (Jones et al. 2012).

Selective internal radiation therapy (SIRT) for these patients has become an attractive option. This therapy utilizes the properties of <sup>90</sup>Yttrium on an arterially delivered bead measuring 35–40 micrometers in diameter. The half-life of this isotope is 64.2 h and the beta particle that is emitted has a mean depth of penetration into tissue of 4 mm. This allows the treating physician to apply a significant dose of radiation to the tumor while sparing the normal hepatic parenchyma. The dose to the tumors is calculated to be at least 120 Gy but it has been demonstrated that the tumors receive at least 500–1000 Gy (Kennedy et al. 2004). While this study utilized explanted livers in the treatment of hepatocellular carcinoma, the NETs should receive a similar amount as both are extremely vascular resulting in preferential hepatic arterial flow to the tumors over any cross-over flow to the normal parenchyma (Fig. 1).

The effectiveness of this treatment has been demonstrated in both retrospective and prospective studies. A prospective trial of SIRT using systemic 5-fluorouracil (5-FU) therapy as a radiation sensitizer was conducted and resulted in a 65 % response rate (18 % complete response, 32 % partial response, and 15 % stable disease) (King et al. 2008). The decrease in the amount of disease present, as measured by RECIST criteria, parallels the drop in the systemic biochemical markers with 41 % showing a decrease in Chromogranin A at 3 months and 46 % showing a drop at 30 months with responders showing a greater decrease than the nonresponders. While three-quarters of the patients had carcinoid syndrome, half of these patients reported symptomatic improvement but as important, no new cases of carcinoid syndrome were reported. A survival improvement is expected since at the time of publication,

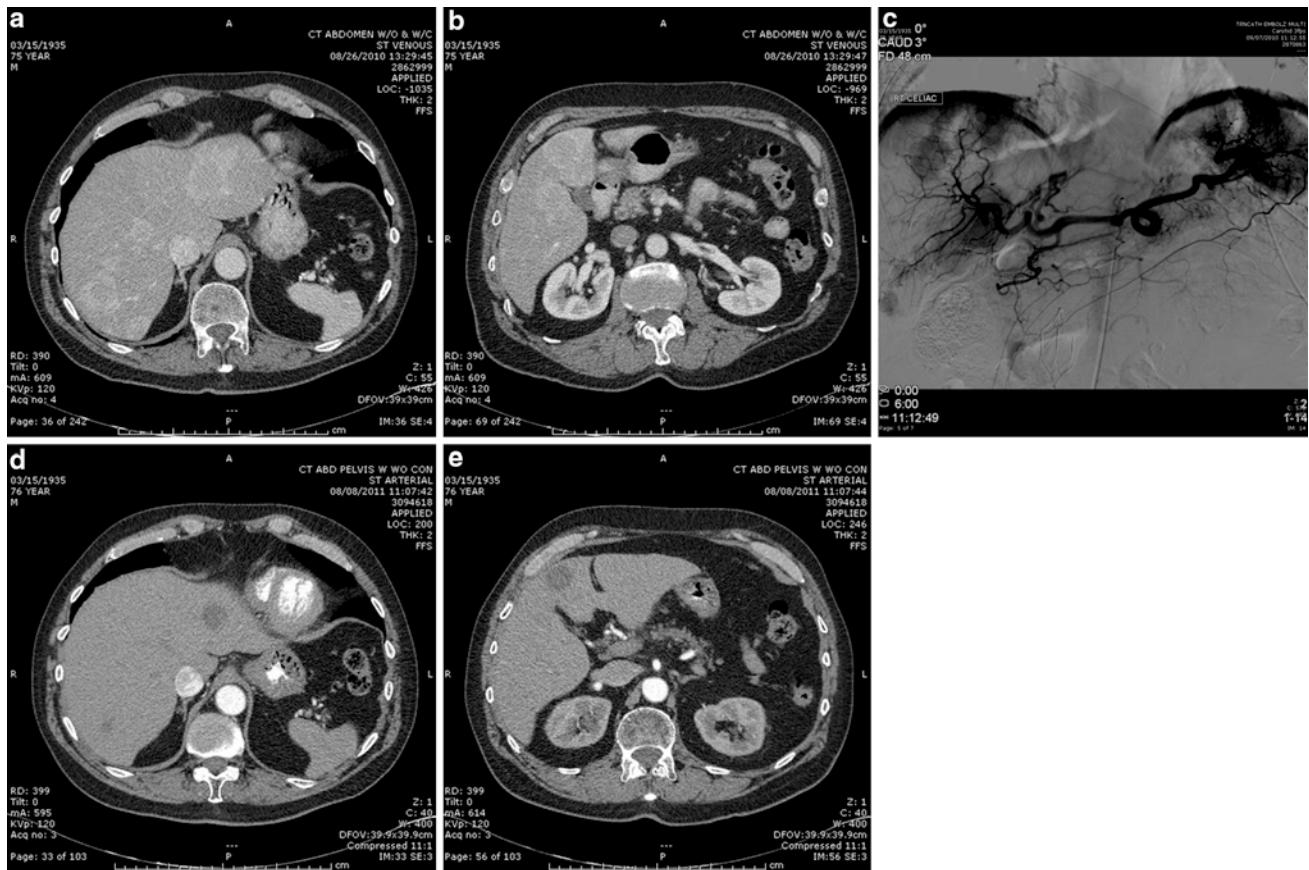


**Fig. 1** 76yr male with metastatic carcinoid to his liver. He has had the carcinoid syndrome daily for the last 3 years and was treated with long acting octreotide injections. However, the octreotide was starting to become ineffective and he was referred for SIRT. **a** and **b** These are representative images from his pretreatment scan demonstrating multiple highly enhancing metastases within his liver. **c** This is a

celiac arteriogram demonstrating the extreme vascularity of the lesions, **d** and **e** 4 months after treatment of both lobes of his liver with yttrium-90 microspheres, the previously noted enhancing metastases no longer enhance and have a sharp border. No new lesions were present. His carcinoid syndrome was completely relieved within 1 week after treatment. He remains disease free in his liver 1 year later

the mean survival had not reached the median. Complications are usually mild with abdominal pain, nausea, fever, and lethargy reported beginning 4–7 days after treatment and lasting between 1 week and 1 month. Gastritis or ulcers were seen in 3/34 patients and there was one death from radiation-induced liver disease. This therapy appears to be a significant improvement over bland or chemoembolization where no complete responders have been reported and the observed survival is shorter than in SIRT. Additionally, most patients did not require hospitalization and the quality of life is much better.

A multi-institutional retrospective review of patients undergoing SIRT for salvage therapy after prior chemotherapy, surgery, and bland or chemoembolization, demonstrated that there was a 86 % response rate with 60 % showing partial response, 3 % complete response, and stable disease in 23 % (Kennedy et al. 2008). Extra-hepatic tumors were responsible for most deaths as has been noted previously (Saxena et al. 2010). The toxicity was also noted

to be very low with two-thirds of the patients not having a Grade 3 or 4 event. Safety was again demonstrated with no radiation-induced liver disease appearing.

While there has been no “magic bullet” developed to cure metastatic NETs, a number of studies, both prospective and retrospective, have shown that SIRT is a safe and very effective therapy.

### 3.1 Practical Aspects of SIRT for mNETs

The basic principles and details of this treatment have been detailed in earlier chapters. However, there are several additional consideration when this treatment is performed that are specific to mNETs:

1. Pretreatment medications should include the basic anti-emetic and steroid but also octreotide to prevent a carcinoid crisis during the procedure. Two hundred micrograms of octreotide should be administered

intravenously immediately before the treatment as well as before the screening arteriograms (Vyleta and Coldwell 2011).

2. Dosimetry for the best effect in these tumors should take into account the very high vascular volume contained in the tumor. For SirSpheres, the Body Surface Area calculation equation gives a dose that is likely to be appropriate for the tumor. It has been previously noted that a reduction in dose is appropriate in most tumors due to extensive prior therapy; however, the increased vascular volume in these tumors make it more likely than not that such a decrease in dose is not required.
3. After the SIRT is completed, the patient should be kept on their octreotide therapy for several weeks since the tumors are necrosing and spilling their contents into the systemic circulation.

## References

- Biku JJ, Davidson BR (2012) Treatment options for unresectable neuroendocrine liver metastases. *Expert Rev Gastroenterol Hepatol* 6:357–369
- Chamberlain RS, Brown KT, Canes D et al (2000) Hepatic neuroendocrine metastases: does intervention alter outcomes? *J Am Coll Surg* 190:432–445
- Dhand S, Gupta R (2011) Hepatic transcatheter arterial chemoembolization complicated by postembolization syndrome. *Semin Intervent Radiol* 28:207–2011
- Doherty G (2011) Neuroendocrine tumors and the Carcinoid syndrome. In: DeVita V, Lawrence T, Rosenberg S (eds) *Cancer principles and practice of oncology*, 9th edn. Lippincott, Williams and Wilkins, Philadelphia
- Gupta S, Johnson MM, Murthy R et al (2005) Hepatic arterial embolization and chemoembolization for the treatment of patients with metastatic neuroendocrine tumors. *Cancer* 104:1590–1602
- Hassan MM, Yao JC (2011) Global epidemiology of neuroendocrine tumors. In: Yao JO, Hoff PM, Hoff AO (eds) *Neuroendocrine tumors*. Humana Press, Springer, New York
- Jones NB, Shah MH, Bloomston M (2012) Liver-Directed therapies in patients with advanced neuroendocrine tumors. *J Natl Compr Canc Netw* 10:765–774
- Kennedy AS, Nutting C, Coldwell DM et al (2004) Pathologic response and microdosimetry of 90Y-microspheres in man: review of four explanted whole livers. *Int J Radiat Oncol Biol Phys* 60:1552–1563
- Kennedy AS, Dezarn WA, McNeillie P, Coldwell D et al (2008) Radioembolization for unresectable neuroendocrine hepatic metastases using resin 90Y-microspheres: early results in 148 patients. *Am J Clin Oncol* 31:271–279
- Kennedy A, Coldwell D, Sangro B, Wasan H, Salem R (2011) Integrating radioembolization into the treatment paradigm for metastatic neuroendocrine tumors in the liver. *Am J Clin Oncol* (Epub ahead of print)
- King J, Quinn R, Glenn D et al (2008) Radioembolization with selective internal radiation microspheres for neuroendocrine liver metastases. *Cancer* 113:921–929
- Kolby L, Persson G, Franzen S et al (2003) Randomized clinical trial of the effect of interferon alpha on survival in patients with disseminated midgut carcinoid tumours. *Br J Surg* 90:687–693
- Kulke M, Benson A, Bergsland E et al (2012) Neuroendocrine tumors. *J Natl Compr Canc Netw* 10:724–764
- Landry CS, Rich T, Jimenez C, Grubbs EG, Lee JE, Perrier ND (2011) Multiple endocrine Neoplasia. In: Yao JO, Hoff PM, Hoff AO (eds) *Neuroendocrine tumors*. Humana Press, New York, New York
- Laverman P, Sosabowski JK, Boerman OC, Oyen WJG (2012) Radiolabelled peptides for oncological diagnosis. *Eur J Nucl Med Mol Imaging* 39(Suppl 1):78–92
- Madoff D, Gupta S, Ahrar K et al (2006) Update on the management of neuroendocrine hepatic metastases. *J Vasc Interv Radiol* 17:1235–1250
- Mitry E, Baudin E, Ducreux M et al (1999) Treatment of poorly differentiated neuroendocrine tumours with etoposide and cisplatin. *Br J Cancer* 81:1351–1355
- O'Toole D, Ruzsiewicz P (2005) Chemoembolization and other ablative therapies for liver metastases of gastrointestinal endocrine tumours. *Best Pract Res Clin Gastroenterol* 19:585–594
- Robiolio PA, Rigolin VH, Wilson JS et al (1995) Carcinoid heart disease correlation of high serotonin levels with valvular abnormalities detected by cardiac catheterization and echocardiography. *Circulation* 92:790–795
- Ruutinen AT, Soulen MC, Tuite CM et al (2007) Chemoembolization and bland embolization of neuroendocrine tumor metastases to the liver. *J Vasc Interv Radiol* 18:847–855
- Saxena A, Chua TC, Bester L et al (2010) Factors predicting response and survival after yttrium-90 radioembolization of unresectable neuroendocrine tumor liver metastases: a critical appraisal of 48 cases. *Ann Surg* 251:910–916
- Singh S, Law C (2012) Chromogranin A: a sensitive biomarker for the detection and post-treatment monitoring of gastroenteropancreatic neuroendocrine tumors. *Expert Rev Gastroenterol Hepatol* 6:313–334
- Soga J, Yakuwa Y, Osaka M (1999) Carcinoid syndrome: a statistical evaluation of 748 reported cases. *J Exp Clin Cancer Res* 18:133–141
- Vyleta M, Coldwell D (2011) Radioembolization in the treatment of neuroendocrine tumor metastases to the liver. *Int J Hepatol* 2011: 785315, Epub Dec 22
- Yao KA, Talamonti MS, Nemcek A et al (2001) Indications and results of liver resection and hepatic chemoembolization for metastatic gastrointestinal neuroendocrine tumors. *Surgery* 130:677–682

---

# Yttrium-90 Microspheres for Other Liver Metastases

J. Rodriguez, A. Chopitea, B. Sangro, and J. I. Bilbao

## Contents

1	Introduction.....	157
2	Breast Cancer.....	159
3	Lung Cancer.....	160
4	Noncolorectal Gastrointestinal Cancer.....	160
4.1	Pancreatic Cancer.....	160
4.2	Gastric Cancer.....	161
4.3	Cancer of the Biliary Tract.....	161
5	Melanoma.....	162
6	Renal Cell Carcinoma.....	162
7	Mixed Neoplasia.....	162
8	Conclusions.....	163
	References.....	163

---

## Abstract

Radioembolization (RE) is a form of brachytherapy in which intraarterially injected microspheres loaded with  $^{90}\text{Y}$  (a pure beta emitter with a 2.6-day half-life and an average 2.5-mm tissue penetration) serve as sources for internal radiation purposes. Its aim is to deliver tumoricidal doses of radiation to no matter how many liver tumors at a time while sparing the non-tumoral liver from absorbing harmful doses of radiation. In recent years, selective internal radiation therapy with embolization of branches of the hepatic artery with biocompatible resin-based  $^{90}\text{Y}$ -labeled microspheres has emerged as a valuable tool for patients with extended liver disease. Several large, prospectively designed phase 2 and 3 trials have proved the ability of SIR-Spheres to produce significant rates of tumor growth control among patients with either hepatocarcinoma or liver metastases from colorectal cancer and neuroendocrine tumors. In the present chapter current data regarding the role of this approach in the management of liver metastases from other tumor types are provided.

---

J. Rodriguez (✉) · A. Chopitea  
Unit for the Research and Treatment  
of Gastrointestinal Malignancies,  
Departments of Medical Oncology,  
Clinica Universidad de Navarra,  
University of Navarra, Pamplona, Spain  
e-mail: jrodriguez@unav.es

B. Sangro  
Liver Unit, Clinica Universidad de Navarra,  
University of Navarra, Pamplona, Spain

J. I. Bilbao  
Interventional Radiology, Clinica Universidad de Navarra,  
University of Navarra, Pamplona, Spain

---

## 1 Introduction

Primary or secondary liver cancer is a major cause of cancer-related mortality worldwide and local tumor growth within the liver determines survival in a great number of patients (Okuda et al. 1985). Although surgical resection is considered to be the only curative approach for patients with hepatocellular carcinoma (HCC) or metastatic disease confined to the liver, in most cases, hepatic resection is not a therapeutic option owing to the size, number, or location of the lesions. Therefore, a number of palliative local treatment modalities have gained importance in recent years. These methods, however, are only applicable to patients with a limited tumor burden within the liver.



Liver metastases (LM) have been shown to heavily depend on the hepatic artery for most of their blood supply, whereas the majority of the blood supply of the normal liver parenchyma is provided by the portal vein (Breedis and Young 1954). Exploitation of the differential dependence on the hepatic artery between tumor and normal parenchyma has allowed the development of regional treatment strategies, including direct intraarterial chemotherapy, transarterial chemoembolization and various methods of reversible or irreversible vascular occlusion. The historical development and optimization of these regional techniques have been reviewed elsewhere (Alexander et al. 1996).

Radiotherapy was originally thought to have a limited role in the treatment of intrahepatic malignancies. The key limitation of external beam radiotherapy (EBRT) was the tolerance of normal liver parenchyma to radiation. The dose required to destroy a solid tumor, estimated in the range of 70 Gy, is far greater than the normal liver tolerance dose (Ingold et al. 1965; Wharton et al. 1973). However, the use of three-dimensional conformal radiotherapy treatment planning has permitted the delivery of higher doses of radiation to localized intrahepatic disease, which has led to significantly higher response rates than would be anticipated from whole-liver RT alone (Robertson et al. 1995, 1997).

On this basis, selective internal radiation therapy (SIRT) with embolization of branches of the hepatic artery with biocompatible resin-based  $^{90}\text{Y}$ -labeled microspheres (SIR-Spheres<sup>®</sup>, SIRTex Medical; North Ryde, New South Wales, Australia) has emerged as a valuable tool for patients with extended liver disease. Following injection into the hepatic artery, these  $^{90}\text{Y}$ -resin microspheres become embolized in the microvasculature where the beta radiation emitted by  $^{90}\text{Y}$  provides a local radiotherapeutic effect (Breedis and Young 1954; Sigurdson et al. 1987).

Several large, prospectively designed phase 2 and 3 trials have proved the ability of SIR-Spheres to produce significant rates of tumor growth control among patients with either HCC or LM from colorectal cancer (CRC) and neuroendocrine tumors (NET) (Sangro et al. 2006; Kennedy et al. 2006; Van Hazel et al. 2004; Coldwell et al. 2005; Gray et al. 2001; Stubbs et al. 2001). However, to date, few data have been reported regarding the role of this approach in the management of LM from other tumor types. This subgroup of noncolorectal, nonneuroendocrine cancers metastatic to the liver are often referred to as mixed neoplasia and include liver-dominant metastatic disease from various primary tumors. Although some evidence of activity has been reported, controlled phase 2 studies aimed to analyze time to progression, tumor response, or progression-free survival outcomes with the use of SIR-Spheres in this subset of patients are still scarce.

The 11 most prevalent malignancies listed by The American Cancer Society included, in order of incident, prostate cancer, breast cancer, lung cancer, colorectal cancer, non-Hodgkin's lymphoma, bladder cancer, malignant melanoma, uterine/cervical cancer, ovarian cancer, pancreatic adenocarcinoma, and kidney cancer. The liver is an uncommon site for metastases for several of these malignancies, including prostate, bladder, uterine/cervical, and kidney cancers. In addition, the treatment for non-Hodgkin's lymphoma is primarily medical, rather than surgical, and is not commonly associated with hepatic lesions. The remaining common malignancies that may meet criteria for liver-directed therapies are breast cancer, melanoma, and ovarian cancer. Other uncommon malignancies with a propensity to metastasize to the liver include specific subtypes of sarcoma and gastric cancer.

Unlike colorectal LM, which can be considered as a stage of localized regional disease reaching the liver by the portal route (Leather et al. 1993), the presence of LM from other primaries are usually the only visible part of a systemic tumor spread (Papachritou and Fortner 1981; Glaves et al. 1988; Komeda et al. 1995). Moreover, anatomic factors are different from those seen in CRC, and the presence of isolated (unique or multiple) liver involvement is rare, reflecting an initial selection of patients with metastatic disease (Pickren et al. 1982; Merion-Thomas et al. 1978).

Several groups have analysed the outcome of hepatic metastasectomy in patients with a noncolorectal primary. Yedibela et al. (2005) reported on the results of 203 hepatic resections performed for noncolorectal liver metastases in 185 patients. The overall observed survival rates were 49 % after 2 years and 26 % after 5 years, with a median survival of 23 months. This approach seemed particularly beneficial in LM from breast cancer, leiomyosarcoma, and renal carcinoma, with 5-year survival rates as high as 50 %. Similarly, Elias et al. (1998) performed an analysis of 147 patients submitted to hepatectomy for LM from a noncolorectal primary. The crude 5-year survival was 36 %, and survival without progressive disease was 28 %. Survival times were similar between synchronous and metachronous LM, and the outcome was not related to the number of them. According to the primary, 5-year survival rates were 20 % for breast cancers, 74 % for NET, 46 % for testicular tumors, 18 % for sarcomas, and slightly less than 20 % for gastric carcinomas, melanomas, and tumors of the gallbladder. Survival exceeded 20 % for gynecologic tumors but was disappointing for head and neck cancers, when the primary was unknown, or when the tumor was truly undifferentiated, suggesting that selection criteria for surgery remain of outstanding importance.

Impossibility to achieve an R<sub>0</sub> resection or the presence of unfavorable surrogate markers for tumor biology may represent the ideal scenario where alternative options such

as radioembolization (RE) should be tested. Indeed, a recently reported retrospective work suggested that RE is an effective and safe approach for patients with chemotherapy-refractory LM likely to achieve survival improvements compared to best supportive care alone. This survival benefit was seen in both CRC and nonCRC LM patients, suggesting that the RE therapeutic effect is independent from the tumor origin (Bester et al. 2012).

## 2 Breast Cancer

Although significant progress has been made in the management of breast cancer (BC), mainly owing to the incorporation of highly effective systemic therapies, the development of distant metastases portends a poor prognosis. Breast cancer LM are present in 15 % of newly diagnosed patients and are the only site of distant disease in one-third of them (Insa et al. 1999; Clark et al. 1987). Ultimately, as many as 50 % of patients with stage IV disease will develop LM. For patients with advanced liver-dominant breast cancer, median survival ranges from 3 to 15 months (Goldhirsch et al. 1988; O'Reilly et al. 1990). BC patients with LM are rarely referred for surgery mostly due to the high prevalence of extrahepatic disease (Lee 1984). However, prognosis is significantly improved for patients who receive liver-directed strategies compared to those who only receive systemic therapy (Eichbaum et al. 2006), and the role of hepatic resection within a multidisciplinary approach has shown promising results in a subset of patients with this disease. In a report by Adam et al. (2006) including 85 consecutive patients, median and 5-year overall survival were 32 months and 37 %, respectively, whereas median and 5-year disease-free survivals were 20 months and 21 %. Study variables independently associated with poor survival included failure to respond to preoperative chemotherapy, an R2 resection, and the absence of repeat hepatectomy. Other studies have also shown, in a highly selected subgroup of patients, the benefit in terms of increased survival of local approaches, such as surgery (Bathe et al. 1999; Raab et al. 1998) or thermal ablation (Livraghi et al. 2001; Mack et al. 2004).

Regarding the use of RE using  $^{90}\text{Y}$  resin-microspheres, Jakobs et al. (2007) included seven metastatic BC patients among 39 patients with nonresponding liver cancer. The assessment of cross-sectional imaging showed that all of the seven patients presented with stable disease or partial response 3 months after the procedure. The median time to progression was 8.5 months (range 5–12 months) and the median overall survival was 3.7 months. Rubin et al. (2004) presented a case report of a patient with metastatic BC to the liver treated with SIR-Spheres. The authors concluded that the use of an integrative approach to cancer treatment

including SIR-Spheres was successful in the performance of a palliative therapy in this setting. Bangash et al. (2007) analyzed the outcome of 27 metastatic BC patients progressed after standard polychemotherapy. The mean radiation dose to the left and right lobe was 119 and 109 Gy, respectively. At 3 months, overall response rate was 39.1 % by CT-scan and 63 % by PET. A longer median survival was observed in patients with ECOG = 0 and in those with a tumor burden less than 25 %. In a similar study, 30 patients refractory to standard systemic therapy underwent RE with  $^{90}\text{Y}$  labeled resin-microspheres as a whole-liver treatment. Overall response rate was 61 %, with a median OS of 11.7 months (23.6 months in responding patients). There was 1 toxic death attributed to hepatic toxicity (Jakobs et al. 2008).

Coldwell and colleagues (Coldwell et al. 2007) evaluated the feasibility, side effects, and complications of RE in the treatment of LM from BC in 44 patients with an Eastern Cooperative Group (ECOG) performance score of 0 or 1 and an expected survival of at least 3 months. All patients have been previously treated with systemic chemotherapy and/or trastuzumab. Patients were excluded if brain metastases were present or total bilirubin exceeded 2 mg/dl. Patients were followed with CT and PET scans every 3 months. Bilateral LM and bone metastases were present in 100 and 63 % of the patients, respectively. The average dose of radiation administered was 2.1 GBq (56 mCi). Eight patients required hospitalization for more than one night for pain control or dehydration. Grade 3 toxicities of nausea and vomiting were present in seven patients. Two patients had documented gastric ulcers. Partial responses were found on CT scans in 47 % of the patients, with another 47 % presenting with stable disease or minor response. The maximal response occurred at 12 weeks post-treatment. The PET scans showed response in up to 95 % of the patients. After a median follow-up of 14 months, 86 % of the patients are still alive. Deaths were due to brain metastases ( $n = 5$ ) and recurrent hepatic disease ( $n = 3$ ). All patients reported palliation of liver-related symptoms. These results clearly encourage further research of  $^{90}\text{Y}$ -microspheres as an adjunct to chemotherapy and other therapeutic modalities in metastatic BC (Table 1).

The high variability in terms of efficacy with the use of RE in BC patients may be partly explained by differences in histologic tumor grading, hormone or Her-2/neu receptor status, tumor burden, performance status or treatment response to RE as assessed by CT or MRI. More recently, the change in  $\text{SUV}_{\text{max}}$  as assessed by  $^{18}\text{F}$ -FDG PET/CT before and 3 months after RE has been identified as the main independent predictor of survival (Haug 2012). A decrease of more than 30 % in the follow-up scan, compared with the baseline examination, indicated therapy response. The response definition was based on the summed

**Table 1** Radioembolization in refractory metastatic breast cancer

Author	n	Activity	ORR (MRI/CT) %	ORR (PET) %	OS	Comments
Haug	58	1.8 GBq	25.6	51	47 wks	Changes in SUV <sub>max</sub> at 3 months were the only predictor of survival
Paprottka	27	2.08 GBq	59.3	–	–	
Bangash	27	109–110 Gy	39.1	63	2.0–9.4 months	Longer OS if ECOG = 0 and tumor burden <25 %
Jakobs	30	1.9 GBq	61	–	11.7 months	1 toxic death
Coldwell	44	2.1 GBq	47	95	1 year OS; 86 %	

ORR Overall response rate, OS Overall survival, Wks Weeks

percentage change in SUV<sub>max</sub> in up to 5 of the most prominent LM, although further studies are warranted to more precisely identify the optimal method for metabolic response assessment. Finally, some authors have suggested that RE was associated with a significant mean decrease in the whole liver volume and an increase in both the diameters of the main portal vein and the splenic volume (Paprottka et al. 2011). Although these changes did not seem to correlate with clinically meaningful sequelae, longer follow-up seems advisable.

### 3 Lung Cancer

LM from lung cancer represent advanced and incurable disease and thus local therapies are usually contraindicated, because it is without any shown benefit in survival or quality of life. Murthy et al. (2008) described a cohort of six patients with unresectable LM from lung cancer treated with <sup>90</sup>Y resin-microspheres after having failed systemic chemotherapy, RF ablation, or arterial embolization. RE was administered as second- to sixth-line therapy. A median dose of 36.1 mCi (range, 12.9–54 mCi) was delivered. A decrease in the size of LM (one patient) and stable disease (two patients) were reported. One patient had a mixed response, and two patients had progression of disease. One grade 3 and one grade 4 liver toxicity occurred. All patients experienced grade 1/2 fatigue. Time to progression of liver disease ranged from 3 to 9 months. The authors concluded that, when the treatment was deemed effective, the duration of local disease control after one treatment seem to equal or exceed what would be expected with chemotherapy.

### 4 Noncolorectal Gastrointestinal Cancer

Over 200,000 gastrointestinal malignancies are diagnosed annually in the United States, and the liver is the predominant site of metastasis in most of them. Although there have been significant advances in systemic chemotherapy,

most patients will eventually succumb to their disease. As a result, much effort has been put forward to develop methods of local liver tumor ablation aimed to achieve improved outcomes.

With the exception of gastric cancer, surgical results for other gastrointestinal primaries remain highly disappointing. The distinctive natural histories and the lower chemoresponsiveness of these tumors turn into a shorter projected survival for advanced disease than for CRC. Therefore, alternative approaches are eagerly awaited in order to bring some hope of long-term survival. For this reason, RE is being increasingly incorporated into treatment strategies, since its effectiveness may rely more on the dependence of a given tumor on its vascular supply than strictly on its chemosensitivity. Moreover, it may be possible to overcome steep dose-response curves for chemotherapy effect by attaining more protracted and locally concentrated levels of radiation near the tumor.

#### 4.1 Pancreatic Cancer

Although pancreatic adenocarcinoma frequently metastasizes to the liver, until now hepatic resection for this disease has never been shown to result in a survival benefit (Takada et al. 1997). Indeed, patients with LM from pancreatic adenocarcinoma usually have a dismal prognosis. Cao et al. reported the results of RE with <sup>90</sup>Y resin-microspheres in seven patients with histologically proven pancreatic cancer. Two patients achieved a partial response, whereas stable disease was observed in one patient. Interestingly, one of the responding patients survived for nearly 15 months after RE (Cao et al. 2010). Gibbs et al. (2010) investigated the utility of <sup>90</sup>Y resin-microspheres in combination with weekly 5-Fluorouracil (600 mg/m<sup>2</sup>) in 15 patients with LM from pancreatic adenocarcinoma. Overall response rate was 23 %, with a median progression-free survival of 5.6 months and a median OS of 6.2 months. Extra-hepatic progression was the main cause of death. Further studies of

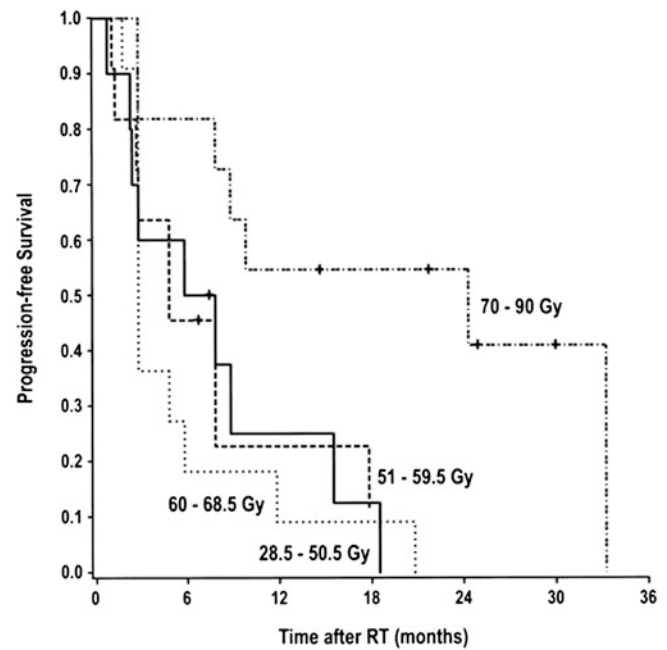
RE in this setting should help to clarify the role of this approach in terms of safety and efficacy.

## 4.2 Gastric Cancer

Liver metastasis is one of the most common failure patterns of this disease after surgery along with peritoneal dissemination and extensive lymph node metastases. Although isolated LM can be found in 5–9 % of patients with gastric cancer (Koga et al. 1980; Sakamoto et al. 2003; Okuyama et al. 1985), metastatic liver tumors are frequently accompanied by peritoneal dissemination and multiple metastases in both lobes of the liver (Hiratsuka et al. 2003), resulting in a curative resection rate of only 10–15 % (Ochiai et al. 1994). Several authors have reported on limited experiences of liver metastasectomy in selected patients with gastric cancer, with 5 years survival rates ranging from 0 to 38 % (Miyazaki et al. 1997; Ambiru et al. 2001). Intrahepatic recurrence following hepatectomy is found in up to 60 % of the patients. Some variables independently associated with poor survival include bilobar metastasis and a maximum tumor diameter of 4 cm (Ochiai et al. 1994). To date there have been no reports of RE specifically designed for patients with gastric cancer. Cianni et al. (2006) reported on 29 patients with liver metastases that had shown progression despite multiple chemotherapy lines treated with SIR-Spheres. Primaries included pancreas, oesophagus, and gastric cancers. Patients with bilirubin levels greater than 1.8 mg/dL and greater than 20 % lung shunting were excluded. The investigators obtained a response in all cases by imaging or tumor markers. The authors concluded that RE was safe and effective for this pretreated population.

## 4.3 Cancer of the Biliary Tract

Intrahepatic cholangiocarcinoma (ICC) is a rapidly fatal epithelial cancer originating from the intrahepatic bile ducts whose incidence has increased in developed countries worldwide. The great majority of patients have unresectable disease at the time of diagnosis and most of them ultimately relapse in the liver. Several palliative treatment options are available, including systemic chemotherapy, TACE, radio-frequency ablation, liver transplantation or external-beam radiotherapy. Radiation dose remains a key factor in the local control of this type of tumors. Increased rates and lengths of palliation as well as improved survival have been reported in patients treated with a boost of RT to the tumor as compared with those treated with whole-liver RT alone (Mohiuddin et al. 1996). Moreover, the median survival of patients who received RT doses higher than 70 Gy resembles that seen in surgical series (Dawson 2000).



Progression-free survival is also improved in patients who were treated with higher doses of RT. The improved outcome with increasing RT dose does not seem to depend entirely on the fact that smaller tumors received higher doses, because there was not a significant association between dose and tumor volume.

In view of this clinical background,  $^{90}\text{Y}$  microspheres RE is emerging as a promising tool in the management of ICC, primarily vascularized by the hepatic artery, given its ability to deliver radiation doses as high as 1,000 Gy to the tumor while sparing the normal tissue. Besides some preliminary case reports suggesting that both, inoperable gallbladder carcinoma and ICC could be safely treated with this procedure (Wijlemans et al. 2011), several groups have reported on the outcome of  $^{90}\text{Y}$  RE for the treatment of this disease. Saxena et al. (2010) treated 25 unresectable ICC patients with a partial response being observed in 6 (24 %), stable disease in 11 (48 %), and progressive disease in five patients (20 %). The median survival was 8.1 months, although patients with peripheral tumor type and ECOG score of 0 had the best outcome, with survival times reaching 18 months. Ibrahim et al. treated 24 ICC patients during a 4 years period. On imaging follow-up, 27 % of the patients achieved a partial response. By using EASL guidelines, 77 % of the patients showed a >50 % tumor necrosis. The median survival for patients with an ECOG performance status of 0, 1, and 2 was 31.8, 6.1, and 1 month, respectively, whereas it was 31.8 and 5.7 months for patients with peripheral versus peri ductal-infiltrative tumors (Ibrahim et al. 2008). Coldwell et al. described 23 patients with nodular cholangiocarcinoma treated with SIR-Spheres. All patients had



**Table 2** Clinical outcome of RE in ICC patients

Author	n	Activity	Response	PFS	OS
Saxena	25	1.76 GBq	24 % (48 % SD)	–	9.3 months 2 years OS; 27 %
Hoffman	33	1.54 GBq	36.4 %	9.8 months	22 months
Haug	26	–	22 % (MRI) 78 % (PET)		51 wks
Ibrahim	24	105 Gy	27 %		14.9 months

PFS Progression-free survival, OS Overall survival, Wks Weeks

previously received two chemotherapy regimens. The mean activity infused was 1.5 GBq, with a mean tumor dose of 150 Gy. After a median follow-up time of 14 months, median survival was not reached, with 19 of 23 patients being alive at the time of the analysis (Coldwell and Kennedy 2006).

More recently, Hoffmann et al. aimed to retrospectively determine prognostic factors in 33 patients with unresectable ICC treated with RE. Most of them had been pre-treated with chemotherapy. Response was assessed at 3 months intervals according to RECIST criteria. Overall, 12 patients achieved a partial response, 17 had stable disease and 5 had progressive disease. Median time to progression and overall survival were 9.8 and 22 months, respectively. Survival times were significantly longer in patients with an ECOG status of 0, tumor burden <25 %, and tumor response to RE (Hoffmann et al. 2012). Other prognostic factors include the presence of portal vein thrombosis (Ibrahim et al. 2008), extensive tumor vascularization in the MAA-SPECT and metabolic response by FDG-PET (Haug et al. 2011).

The results of these trials warrant further prospective investigation. A summary of currently available clinical results with the use of <sup>90</sup>Y microspheres RE in ICC is provided in Table 2.

## 5 Melanoma

Ocular melanoma is an aggressive disease that usually metastasizes to the liver. Overall survival rates have been reported to decrease to less than 1 year after the development of metastases. Although some rare long-term survivors have been reported after hepatectomy, most patients present with unresectable liver disease (Lejeune et al. 1992). Kennedy et al. (2009) reported their experience on 11 patients treated with RE with a mean activity of 1.55 GBq. PET-CT at 3 months showed a response in all patients. More recently, Klingenstein et al. (2012) retrospectively evaluated the outcome of 13 metastatic uveal melanoma patients after RE as salvage therapy. Most patients had already undergone dacarbazine-based

chemotherapy. The mean activity administered was 1.7 MBq. Eight patients achieved a partial response, and the median survival time after RE was 7 months.

## 6 Renal Cell Carcinoma

For renal tumors (Wilms' or adenocarcinoma), the survival times after hepatectomy are close to those achieved for colorectal primaries (Schwartz 1995). Surgical resection of LM in this disease remains a component of total oncologic treatment in carefully selected patients. Factors significant for positive outcome benefit usually include complete resection and a large interval from primary resection to the development of subsequent hepatic metastases. Since these factors are only found in a minority of patients, the role of alternative liver-directed therapies is being actively investigated. A recent report investigated the safety and efficacy of yttrium-90 RE in six patients with liver-dominant renal cell carcinoma refractory to immunotherapy and targeted agents. The median dose delivered was 1.89 GBq. Three patients achieved a complete response, and one additional patient had a partial response. These patients are alive at 64, 55, 17, and 7 months after treatment, respectively, (Abdelmaksoud et al. 2012).

## 7 Mixed Neoplasia

Jakobs et al. (2007) reported results on 39 treated patients that included metastatic pancreatic cancer, carcinoma of unknown primary, ICC, thymus carcinoma, malignant melanoma, and choroid melanoma. Some evidence of activity was noted, with a median time to progression of 8 months (range 3–11 months). Lim et al. (2005) prospectively evaluated the efficacy and safety of <sup>90</sup>Y microspheres in 46 patients with unresectable primary or secondary hepatic malignancies. Tumor types included patients with adenocarcinoma of unknown primary and single cases of hepatic angiosarcoma, gastrointestinal stromal tumor (GIST), ocular melanoma, gastric cancer, pulmonary carcinoid, cholangiocarcinoma, and prostate cancer. With the

exception of the single patient with a GIST, activity was not seen in any other tumor type. Popperl et al. (2005) reported on 23 patients with unresectable hepatic malignancies who were not suitable for resection and were no longer responding to polychemotherapy and/or other local forms of treatment. Primary tumors in the mixed group included thymic carcinoma and choroidal melanoma. The mean activity of treatment was 2,270 MBq. Follow-up data showed a marked decrease of FDG uptake, a decrease in tumor marker levels, and unchanged or slightly decreasing lesion size (on CT) in 10 of 13 patients. Wong et al. (2005) described 19 patients with unresectable chemotherapy-refractory hepatic metastatic disease of various origins treated with SIR-Spheres. The median absorbed dose for the tumor was 76 Gy. By PET criteria, 15 of patients (79 %) showed response to therapy, whereas four (21 %) showed no response. Yu et al. (2006) reported on 49 patients with CRC, pancreatic, breast, carcinoid, lung, thyroid, squamous cell, renal-cell, gastrointestinal stromal tumor, and endometrial cancer who underwent 78 administrations of SIR-Spheres. All patients had undergone previous multiple-agent chemotherapy, which had failed. The mean dose of resin-microspheres administered was 0.83 GBq, which translates to 42 Gy absorbed dose. A RECIST response rate of 29 % and a PET response rate of 79 % were noted. Mean and median survival times were 305 and 175 days, respectively. Jakobs et al. (2006) presented midterm results on 88 patients who received 118 administrations of SIR-Spheres. Forty-five of them had CRC, whereas the remaining cases comprised pancreatic, breast, NET, lung thyroid, squamous-cell, GIST, thymus, melanoma, and endometrial cancers, and HCC. All patients had undergone prior chemotherapy. The mean dose infused was 0.83 GBq for lobar and whole-liver treatments. The mean absorbed dose was 42 Gy. The response rate according to RECIST criteria was 18 %, whereas the functional response rate according to PET was 62 %. Mean and median survival times were 285 days and 180 days, respectively. Unfortunately, the inclusion of such a heterogeneous tumor types in these studies adds little to the data on efficacy and reinforce the need for specific disease directed-trials.

## 8 Conclusions

<sup>90</sup>Y microspheres RE offer an attractive alternative in the available therapies for extended liver disease. Given careful patient selection and proper angiographic technique, this approach offers patients a minimally invasive, low-toxicity treatment with very favorable tumor response and potential survival benefit, even in the context of extrahepatic disease. A growing body of evidence supports its use as a component of the overall treatment strategy in breast cancer and

intrahepatic cholangiocarcinoma. Promising data are also available for patients with metastatic melanoma and renal cell carcinoma, although more mature data are required. Although any liver tumor may be a potential target for this therapy, there is some histology that is probably more sensitive to this therapy than others. Moreover, because different tumor types have different underlying biological behavior in terms of therapy sensitivity, patterns of dissemination or risk of relapse, future trials should concentrate on just a specific tumor type to allow meaningful conclusions.

Major advances in patient outcome would probably depend on the development of better systemic therapies to use in combination with RE, considering the growing evidence from the literature suggesting that <sup>90</sup>Y-microspheres might be less appropriate as a stand-alone modality but should rather be considered within a multidisciplinary approach.

Only large and prospectively designed trials based on specific histologies may answer the question of whether long-term survival can be improved by <sup>90</sup>Y-microspheres RE. Patient selection remains a critical point, as a subgroup of patients with huge metastases or pre-existing extrahepatic manifestations seem to benefit less of this therapeutic modality. Future studies will hopefully shed light into the integration of this procedure within the global oncological management of cancer patients.

## References

- Abdelmaksoud MH, Louie JD, Kothary N et al (2012) Yttrium-90 radioembolization of renal cell carcinoma metastatic to the liver. *J Vasc Interv Radiol* 23:323–330
- Adam R, Aloia T, Krissat J et al (2006) Is liver resection justified for patients with hepatic metastases from breast cancer? *Ann Surg* 244:897–908
- Alexander HR, Bartlett DL, Fraker DL, Libutti SK (1996) Regional treatment strategies for unresectable primary or metastatic cancer confined to the liver. *Princ Pract Oncol Updates* 10:1–19
- Ambiru S, Miyazaki M, Ito H et al (2001) Benefits and limits of hepatic resection for gastric metastasis. *Am J Surg* 181:279–283
- Bangash AK, Atassi B, Kaklamani V et al (2007) <sup>90</sup>Y radioembolization of metastatic breast cancer to the liver: toxicity, imaging response, survival. *J Vasc Interv Radiol* 18:621–628
- Bathe OF, Kaklamanos IG, Moffat FL et al (1999) Metastasectomy as a cytoreductive strategy for treatment of isolated pulmonary and hepatic metastases from breast cancer. *Surg Oncol* 8:35–42
- Bester L, Meteling B, Pavlakis N et al (2012) Radioembolization versus standard care of hepatic metastases: comparative retrospective cohort study of survival outcomes and adverse events in salvage patients. *J Vasc Interv Radiol* 23:96–105
- Breedis C, Young G (1954) Blood supply of neoplasms of the liver. *Am J Pathol* 30:969–972
- Cao C, Yan TD, Morris DL et al (2010) Radioembolization with yttrium-90 microspheres for pancreatic cancer liver metastases: results from a pilot study. *Tumori* 96:955–958

- Cianni R, Saltarelli A, Notarianni E et al (2006) Radioembolism (yttrium 90) of hepatic liver metastases: preliminary experience. Paper presented at the world conference on interventional oncology, Cemobbio, Italy
- Clark GM, Sledge GW Jr, Osborne CK et al (1987) Survival from first recurrence: relative importance of prognostic factors in 1,015 breast cancer patients. *J Clin Oncol* 5:55–61
- Coldwell D, Nutting C, Kennedy AK (2005) Use of yttrium-90 SIR-Spheres to treat metastatic unresectable neuroendocrine tumors to the liver. Paper presented at the world congress of gastrointestinal cancer, Barcelona, Spain, 27–30 June 2005
- Coldwell DM, Kennedy AS, Nutting CW (2007) Use of Yttrium-90 microspheres in the treatment of unresectable hepatic metastases from breast cancer. *Int J Radiation Oncology Biol Phys* 69:800–804
- Dawson LA, McGinn CJ, Normolle D et al (2000) Escorted focal liver radiation and concurrent hepatic artery fluoro deoxyuridine for unresectable intrahepatic malignancies. *J Clin Oncol* 18:2210–2218
- Eichbaum MH, Kaltwasser M, Bruckner T et al (2006) Prognostic factors for patients with liver metastases from breast cancer. *Breast Cancer Res Treat* 96:53–62
- Elias D, de Cavalcanti AA, Eggenpieler P et al (1998) Resection of liver metastases from a noncolorectal primary: indications and results based on 147 monocentric patients. *J Am Coll Surg* 187:487–493
- Gibbs P, Lipton L, Price D et al (2010) A phase II trial of radioembolization and systemic chemotherapy in patients with liver metastases from primary cancer of the pancreas. *Ann Oncol* 21(8):845
- Glaves D, Huben RP, Weiss L (1988) Haematogenous dissemination of cells from human renal carcinomas. *Br J Cancer* 57:32–35
- Goldhirsch A, Gelber RD, Castiglione M (1988) Relapse of breast cancer after adjuvant treatment in premenopausal and perimenopausal women: patterns and prognoses. *J Clin Oncol* 6:89–97
- Gray B, Van Hazel G, Hope M et al (2001) Randomized trial of SIR-Spheres plus chemotherapy versus chemotherapy alone for treating patients with liver metastases from primary large bowel cancer. *Ann Oncol* 12:1711
- Haug A, Heinemann V, Bruns CJ et al (2011) <sup>18</sup>F-FDG PET independently predicts survival in patients with cholangiocellular carcinoma treated with <sup>90</sup>Y microspheres. *Eur J Nucl Med Mol Imaging* 38:1037–1045
- Haug AR, Tiega Donfack BP, Trumm C et al (2012) <sup>18</sup>F-FDG PET/CT predicts survival after radioembolization of hepatic metastases from breast cancer. *J Nucl Med* 53:371–377
- Hiratsuka M, Yano T, Yamamoto M et al (2003) Management of patients with hepatic metastases from gastric carcinoma. *Nippon Geka Gakkai Zasshi* 104:711–716
- Hoffmann RT, Paprottka PM, Schön A et al (2012) Transarterial hepatic yttrium-90 radioembolization in patients with unresectable intrahepatic cholangiocarcinoma: factors associated with prolonged survival. *Cardiovasc Intervent Radiol* 35:105–116
- Ibrahim SA, Mulcahy M, Lewandowski RJ et al (2008) Treatment of unresectable cholangiocarcinoma using yttrium-90 microspheres. *Cancer* 113:2119–2128
- Ingold J, Reed G, Kaplan H (1965) Radiation hepatitis. *Am J Roentgenol* 93:200–208
- Insa A, Lluch A, Prosper F et al (1999) Prognostic factors predicting survival from first recurrence in patients with metastatic breast cancer: analysis of 439 patients. *Breast Cancer Res Treat* 56:67–78
- Jakobs T, Hoffman RT, Yu M et al (2006) Yttrium-90 SIR-Spheres treatment for metastatic cancer to the liver: midterm results. Paper presented at the world conference on interventional oncology, Cemobbio, Italy
- Jakobs TF, Hoffmann RT, Poepferl G, Schmitz A, Lutz J, Koch W, Tatsch K, Lubiensky A, Reiser MF, Helmberger T (2007) Mid-term results in otherwise treatmentrefractory primary or secondary liver confined tumours treated with selective internal radiation therapy (SIRT) using (90)Yttrium resin-microspheres. *Eur Radiol* 17(5):1320–1330 [Epub 2006 Dec 6. PubMed PMID: 17149621]
- Jakobs TF, Hoffmann RT, Fischer T et al (2008) Radioembolization in patients with hepatic metastases from breast cancer. *J Vasc Interv Radiol* 19:683–690
- Coldwell D, Kennedy AK (2006) Treatment of nodular cholangiocarcinoma with yttrium-90 microspheres. Paper presented at the world congress on gastrointestinal cancer, Barcelona, Spain
- Kennedy A, Coldwell D, Nutting C et al (2006) Resin <sup>90</sup>Y microspheres brachytherapy for unresectable colorectal liver metastases: modern USA experience. *Int J Radiat Oncol Biol Phys* 65:412–425
- Kennedy AS, Nutting C, Jakobs T et al (2009) A first report on radioembolization for hepatic metastases from ocular melanoma. *Cancer Invest* 27:682–690
- Klingenstein A, Haug AR, Zech CJ et al (2012) Radioembolization as loco regional therapy of hepatic metastases in uveal melanoma patients. *Cardiovascular Intervention Radiology* (in press)
- Koga S, Kawaguchi H, Kishimoto H et al (1980) Therapeutic significance of noncurative gastrectomy for gastric cancer with liver metastasis. *Am J Surg* 140:356–359
- Komeda T, Fukuda Y, Sando T et al (1995) Sensitive detection of circulating hepatocellular carcinoma cells in peripheral venous blood. *Cancer* 75:2214–2219
- Leather AJ, Gallegos NC, Kocjan C et al (1993) Detection and enumeration of circulating tumour cells in colorectal cancer. *Br J Surg* 80:777–780
- Lee YT (1984) Breast carcinoma: pattern of recurrence and metastasis after mastectomy. *Am J Clin Oncol* 7:443–449
- Lejeune FJ, Lienard D, Sales F et al (1992) Surgical management of distant melanoma metastases. *Semin Surg Oncol* 8:381–391
- Lim L, Gibbs P, Yip D et al (2005) Prospective study of treatment with selective internal radiation therapy spheres in patients with unresectable primary or secondary hepatic malignancies. *Intern Med J* 35:222–227
- Livraghi T, Goldberg SN, Solbiati L et al (2001) Percutaneous radiofrequency ablation of liver metastases from breast cancer: initial experience in 24 patients. *Radiology* 220:145–149
- Mack MG, Straub R, Eichler K et al (2004) Breast cancer metastases in liver: laser-induced interstitial thermotherapy-local tumour control rate and survival data. *Radiology* 233(2):400–409
- Merion-Thomas J, Redding WH, Coombes RC et al (1978) Failure to detect intra-abdominal metastases from breast cancer: a case for staging laparotomy. *BMJ* 2:157–159
- Miyazaki M, Itho H, Nakagawa K et al (1997) Hepatic resection of liver metastases from gastric carcinoma. *Am J Gastroenterol* 92:490–493
- Mohiuddin M, Chen E, Ahmad N (1996) Combined liver radiation and chemotherapy for palliation of hepatic metastases from colorectal cancer. *J Clin Oncol* 14:722–728
- Murthy R, Oh Y, Tam A et al (2008) Yttrium-90 labeled microsphere radioembolotherapy of liver dominant metastases from thoracic malignancies. *J Vasc Interv Radiol* 19:299–300
- Ochiai T, Sasako M, Mizuno S et al (1994) Hepatic resection for metastatic tumours from gastric cancer: analysis of prognostic factors. *Br J Surg* 81:1175–1178
- Okuda K, Ohtsuki T, Obata H et al (1985) Natural history of hepatocellular carcinoma and prognosis in relation to treatment; study of 850 patients. *Cancer* 56:918
- Okuyama K, Isono K, Juan IK et al (1985) Evaluation of treatment for gastric cancer with liver metastasis. *Cancer* 55:2498–2505

- O'Reilly SM, Richards MA, Rubens RD (1990) Liver metastases from breast cancer: the relationship between clinical, biochemical and pathological features and survival. *Eur J Cancer* 26:574–577
- Papachritou DN, Fortner JG (1981) Is gastric cancer generalized at the time of surgery? *Surg Oncol* 18:27–29
- Paprottka PM, Schmidt GP, Trumm CG et al (2011) Changes in normal liver and spleen volume after radioembolization with 90Y-resin microspheres in metastatic breast cancer patients: findings and clinical significance. *Cardiovasc Intervent Radiol* 34:964–972
- Pickren JW, Tsukada Y, Lane WW (1982) Liver metastases: analysis of autopsy data. In: Weiss L (ed) *Liver metastases*. Gilbert-Hall Publishing, Boston, pp 2–19
- Popperl G, HeImberger T, Munzing W et al (2005) Selective internal radiation therapy with SIR-Spheres in patients with nonresectable liver tumors. *Cancer Biother Radiopharm* 20:200–208
- Raab R, Nussbaum KT, Behrend M et al (1998) Liver metastases of breast cancer: results of liver resection. *Anticancer Res* 18:2231–2233
- Robertson JM, Lawrence TS, Walker S et al (1995) The treatment of colorectal liver metastases with conformal radiation therapy and regional chemotherapy. *Int J Radiat Oncol Biol Phys* 32:445–450
- Robertson JM, McGinn CJ, Walker S et al (1997) A phase I trial of hepatic arterial bromodeoxyuridine and conformal radiation therapy for patients with primary hepatobiliary cancers or colorectal liver metastases. *Int J Radiat Oncol Biol Phys* 39:1087–1092
- Rubin D, Nutting C, Jones B (2004) Metastatic breast cancer in a 54-year-old woman: integrative treatment with yttrium-90 radioembolization. *Integr Cancer Ther* 3:262–267
- Sakamoto Y, Ohyama S, Yamamoto J et al (2003) Surgical resection of liver metastases of gastric cancer: an analysis of a 17 years experience with 22 patients. *Surgery* 133:507–511
- Sangro B, Bilbao JI, Boan J et al (2006) Radioembolization using 90Y-resin microspheres for patients with advanced hepatocellular carcinoma. *Int J Radiat Oncol Biol Phys* 66:792–800
- Saxena A, Bester L, Chua T et al (2010) Yttrium-90 radiotherapy for unresectable intrahepatic cholangiocarcinoma: a preliminary assessment of this novel treatment option. *Ann Surg Oncol* 17:484–491
- Schwartz SI (1995) Hepatic resection for noncolorectal nonneuroendocrine metastases. *World J Surg* 19:72–75
- Sigurdson ER, Ridge JA, Kemeny N et al (1987) Tumor and liver drug uptake following hepatic artery and portal vein infusion. *J Clin Oncol* 5:1836
- Stubbs RS, Cannan RJ, Mitchell AW (2001) Selective internal radiation therapy (SIRT) with 90Yttrium microspheres for extensive colorectal liver metastases. *Hepatogastroenterology* 48:333
- Takada T, Yasuda H, Amano H et al (1997) Simultaneous hepatic resection with pancreato-duodenectomy for metastatic pancreatic head carcinoma: does it improve survival? *Hepatogastroenterology* 44:567–573
- Van Hazel G, Blackwell A, Anderson J et al (2004) Randomised phase 2 trial of SIR-Spheres plus fluorouracil/leucovorin chemotherapy versus fluorouracil/leucovorin chemotherapy alone in advanced colorectal cancer. *J Surg Oncol* 88:78–85
- Wharton JT, Delclos L, Gallager S et al (1973) Radiation hepatitis induced by abdominal irradiation with the cobalt 60 moving strip technique. *Am J Roentgenol Radium Ther Nucl Med* 117:73–80
- Wijlemans JW, Van Erpecum KJ, Lam M et al (2011) Trans-arterial 90yttrium radioembolization for patients with unresectable tumors originating from the biliary tree. *Ann Hepatol* 10:349–354
- Wong CY, Qing F, Savin M et al (2005) Reduction of metastatic load to liver after intraarterial hepatic yttrium-90 radioembolization as evaluated by [18F] fluorodeoxyglucose positron emission tomographic imaging. *J Vasc Interv Radiol* 16:1101–1106
- Yedibela S, Gohl J, Graz V et al (2005) Changes in indication and results after resection of hepatic metastases from noncolorectal primary tumors: a single institutional review. *Ann Surg Oncol* 12:778–785
- Yu M, Lewandowski RJ, Wong C et al (2006) Yttrium-90 (SIR-Spheres) treatment for metastatic cancer to the liver: midterm results. Paper presented at the society of interventional radiology annual meeting, Toronto



---

# Surgical Treatment and Radioembolization

Patricia Martínez-Ortega, Fernando Pardo, and Bruno Sangro

## Contents

<b>1</b>	<b>Introduction</b> .....	167
<b>2</b>	<b>Radioembolization Prior to Surgery in Hepatocellular Carcinoma</b> .....	167
2.1	Contralateral Hypertrophy.....	168
<b>3</b>	<b>Radioembolization Prior to Surgery in Liver Metastases from Distant Tumors</b> .....	169
	<b>References</b> .....	169

---

## Abstract

<sup>90</sup>Y radioembolization supposes a useful downstaging strategy to reduce tumor burden and increase the proportion of patients eligible for radical treatments in the hepatocellular carcinoma management. Moreover, contralateral hypertrophy is one of the most important advantages of this tactic with compared to other transarterial treatments, and it could be effective not only in hepatocellular carcinoma but also in selected patients with liver metastases. Since these metastases are usually unresectable at initial diagnosis, this treatment has been increasingly used in salvage setting for these patients.

---

## 1 Introduction

Over the last 10 years, there has been significant scientific advancement in the field of Yttrium 90 (<sup>90</sup>Y) radioembolization. Standardization of practice and indications has made this procedure routine in experienced centers. And in the recent years, several groups have reported the outcome of patients receiving liver surgery after <sup>90</sup>Y radioembolization. Great interest has emerged from these results in the use of radioembolization as a tool to drive patients to surgery. Although most of it is preliminary, we will briefly review the available evidence. First, in primary liver cancer where most of the data have been generated, and finally in liver metastases.

---

## 2 Radioembolization Prior to Surgery in Hepatocellular Carcinoma

Hepatocellular carcinoma (HCC) is the third most common cause of cancer-related mortality and the leading cause of death among patients with cirrhosis (El-Serag 2011). Thus, it is difficult to prognosticate the outcome of patients with

---

P. Martínez-Ortega · F. Pardo (✉) · B. Sangro  
Clínica Universidad de Navarra, Pamplona, Spain  
e-mail: fpardo@unav.es

HCC due to the coexistence of two life-threatening conditions: cirrhosis and cancer (Mazzaferro et al. 2013). It is generally known that between 50 and 70 % of cases of HCC are diagnosed at a stage when they are not able to undergo radical treatments (surgical resection or transplantation) (Llovet et al. 2008). Liver transplantation is considered the best option since it removes not only the tumor but also the underlying liver cirrhosis. However, its benefits are mostly restricted to those patients that fulfill the Milan criteria consisting in one tumor not larger than 5 cm or up to 3 tumors none of them larger than 3 cm (Mazzaferro et al. 1996). Although some experienced centers have reported comparable outcomes using expanded criteria (Herrero et al. 2008; Yao et al. 2007), this approach has not been prospectively validated and is not recommended by guidelines.

Interventional (endovascular and transcatheter) therapies such as transarterial embolization (TAE), chemoembolization (TACE), radiofrequency ablation (RFA), and radioembolization, can be used as downstaging strategies to reduce tumor burden and increase the proportion of patients eligible for radical treatments (Lau and Lai 2007; Ravaioli et al. 2008). Prior to transplantation, the goal of downstaging is to diminish the tumor load within valid limits. Before surgical resection, its aim is to turn nonresectable patients into resectable, or just simplify the surgical procedure (decreasing tumor size and enabling a larger remnant liver) (Iñárraegui et al. 2012). Increasing the number of patients eligible for radical therapy is an important goal provided overall and recurrence-free survival is similar to that achieved at an earlier stage.

TACE is the standard of care for patients with intermediate-stage HCC according to the Barcelona Clinic Liver Cancer (BCLC) staging system and treatment algorithm that has been endorsed by European and American guidelines. First used for patients unfit for TACE or having progressed after TACE,  $^{90}\text{Y}$  radioembolization has been increasingly used for the treatment of less advanced cases.

Tumor shrinkage of varying degrees usually follows  $^{90}\text{Y}$  radioembolization. Several case reports were published earlier, but it was not until 2006 that Kulik et al. reported on a series of 35 patients with UNOS T3 stage HCC treated by radioembolization, among which 19 (56 %) were downstaged to T2 and 11 (32 %) were downstaged to lesions measuring 3 cm or less amenable for RFA (Kulik et al. 2006). In 2009, the same group first compared the ability of  $^{90}\text{Y}$  radioembolization and TACE to allow downstaging HCC patients to radical therapies (Lewandowski et al. 2009). They compared the rate at which downstaging from UNOS T3 to T2 stage was achieved after  $^{90}\text{Y}$ -radioembolization and TACE. Downstaging was achieved in 58 % of cases post-radioembolization and 31 % of cases post-TACE among patients with a median tumor diameter of 5.6 and 5.7 cm, respectively ( $p = 0.023$ ). Furthermore, overall survival

when patients were not censored at the time of transplantation or resection significantly favored radioembolization (Kulik et al. 2006).

Furthermore, Riaz et al. (2009) conducted an extensive review of the pathologic findings following to  $^{90}\text{Y}$  radioembolization among 35 patients bridged to resection or transplantation. They showed a high (89 %) rate of complete pathologic necrosis in smaller lesions (1–3 cm) and an acceptable rate up to 65 % in larger lesions (3–5 cm). After comparing these data with an identical pathology review after TACE, radioembolization achieved better antitumoral effect. Successful downstaging to liver transplantation has also been reported by other authors (Iñárraegui et al. 2012; Khalaf et al. 2010).

Our group has also analyzed patient outcomes after downstaging of HCC patients treated with a palliative intent with resin microspheres (Iñárraegui et al. 2012). In a group in which patients usually had a high tumor load (median tumor diameter of 11.2 cm), 29 % of patients at UNOS T3 stage were treated by surgical resection or liver transplantation after responding to  $^{90}\text{Y}$  radioembolization. And what is more important, survival rate was 75 % at 3 years, an outcome that compares well with that observed in patients with early stage disease who are treated radically at the time of diagnosis (N'Kontchou et al. 2009; Chen et al. 2004).

Despite the relatively small sample, an important lesson from this study is that successful downstaging can be achieved also in large tumors. This finding has two different implications in terms of patient selection and successful treatment. On the one hand, patients can be considered as potential candidates for downstaging regardless of their initial tumor volume. On the other, excellent long-term outcomes might be observed in naturally selected, less aggressive tumors such as large tumors without vascular invasion or extrahepatic spread.

More recently, Tohme et al. have published a retrospective review of 20 consecutive patients with HCC who were listed to receive a liver transplant and underwent  $^{90}\text{Y}$  radioembolization as a bridge (Tohme et al. 2013). All cases that originally met Milan criteria remained within them at the time of transplantation, and 33 % of those originally outside Milan criteria subsequently fulfilled them. Complete pathologic response with no evidence of viable tumor on pathologic assessment was found in 36 % of patients who were within Milan criteria, further substantiating the ability of radioembolization to produce complete ablation of small tumors.

## 2.1 Contralateral Hypertrophy

In our own experience, most patients downstaged to radical therapies were treated by liver resection after  $^{90}\text{Y}$  radioembolization (Iñárraegui et al. 2012). And this was made

**Table 1** Research targets for  $^{90}\text{Y}$  radioembolization and liver resection

Radiation-induced segmentectomy for patients unfit for ablation or embolization
Radiation-induced hepatectomy associated with tumor treatment, for patients unfit for surgery because of comorbidities or insufficient remnant liver
Downstaging procedure for patients with intermediate and advanced hepatocellular carcinoma
Downstaging procedure for patients with liver metastases from colorectal cancer (in combination with chemotherapy for treatment naïve or as salvage procedure for chemorefractory)

possible by an increase in the liver remnant induced by single lobe radioembolization (Fernandez-Ros et al. 2013). Contralateral lobe hypertrophy is one of the most important advantages of  $^{90}\text{Y}$  radioembolization when compared to other transarterial treatments, including TACE. Portal vein embolization is commonly used to induce contralateral hypertrophy. However, hypertrophy rates are suboptimal in cirrhotic patients. Treating the right-lobe disease with  $^{90}\text{Y}$  radioembolization could uniquely allow to, simultaneously, provide tumor therapy and induce contralateral hypertrophy. Probably related to the more progressive diversion of portal venous flow due to the right-lobe atrophy, contralateral hypertrophy may have rates up to 40 %. The 6–12 weeks' waiting period serves as a test of time that provides better biological information to identify those patients who are optimal candidates for resection. Although much research is yet needed to predict the extension of segmental or lobar atrophy/hypertrophy after  $^{90}\text{Y}$  radioembolization, this is certainly an appealing use of radioembolization not only in HCC but also in selected patients with liver metastases.

### 3 Radioembolization Prior to Surgery in Liver Metastases from Distant Tumors

Aside from primary malignancies, the liver is a relevant site of metastasis from a wide variety of neoplasms such as colorectal cancer, pancreatic adenocarcinoma, neuroendocrine tumors, melanoma, and breast cancer and 60–80 % of these patients will develop liver metastases (Salem and Thurston 2006; Ahmadzadehfar et al. 2010). It is well known that morbidity and mortality in patients with primary and metastatic liver cancer are directly related to the presence of hepatic disease, as it is a crucial organ of metabolism and homeostasis regulation. Thereby, due to its essential role for survival and quality of life, therapeutic strategies intended to achieve hepatic tumor control are clinically meaningful. Including  $^{90}\text{Y}$  into a multidisciplinary approach gives us a powerful tool to achieve regional tumor response and disease control in hepatic malignancy of various origins.

The most effective method for enhancing survival in patients with metastatic liver cancer without disseminated disease is surgical resection. Nevertheless, the main problem is that hepatic metastases are usually unresectable at initial diagnosis as well as at recurrence (Abdalla et al. 2004). Surgery is particularly important in patients with colorectal cancer in which approximately 50 % of patients develop liver metastases at diagnosis or during follow-up.  $^{90}\text{Y}$  radioembolization has been commonly used in the salvage setting for these patients. According to a recent review, approximately 50 % of salvage patients with liver metastases from colorectal cancer survived more than 12 months after radioembolization (Rosenbaum et al. 2013). Downstaging to resection has been reported in some clinical trials and cohorts studied of patients with liver metastases from colorectal cancer, but the information is too scarce to allow an identification of good candidates or attribute a significant impact on long-term outcome.

In conclusion,  $^{90}\text{Y}$  radioembolization represents a promising treatment challenging the current paradigm of malignant liver disease and the next few years will yield relevant information about its usefulness. Table 1 describes some of the future developments that are currently being studied.

### References

- Abdalla EK, Vauthey JN, Ellis LM, Ellis V, Pollock R, Broglio KR, et al (2004) Recurrence and outcomes following hepatic resection, radiofrequency ablation, and combined resection/ablation for colorectal liver metastases. *Ann Surg* 239(6):818, 25 (discussion 825–827)
- Ahmadzadehfar H, Biersack HJ, Ezziddin S (2010) Radioembolization of liver tumors with yttrium-90 microspheres. *Semin Nucl Med* 40(2):105–121
- Chen WT, Chau GY, Lui WY, Tsay SH, King KL, Loong CC et al (2004) Recurrent hepatocellular carcinoma after hepatic resection: prognostic factors and long-term outcome. *Eur J Surg Oncol* 30(4):414–420
- El-Serag HB (2011) Hepatocellular carcinoma. *N Engl J Med* 365(12):1118–1127
- Fernandez-Ros N, Silva N, Bilbao JI, Iñarrairaegui M, Benito A, D'Avola D, et al (2013) Partial liver volume radioembolization induces hypertrophy in the spared hemiliver and no major signs of portal hypertension. *HPB (Oxford)*. doi: 10.1111/hpb.12095

- Herrero JI, Sangro B, Pardo F, Quiroga J, Iñarrairaegui M, Rotellar F et al (2008) Liver transplantation in patients with hepatocellular carcinoma across Milan criteria. *Liver Transpl* 14(3):272–278
- Iñarrairaegui M, Pardo F, Bilbao JI, Rotellar F, Benito A, D'Avola D et al (2012) Response to radioembolization with yttrium-90 resin microspheres may allow surgical treatment with curative intent and prolonged survival in previously unresectable hepatocellular carcinoma. *Eur J Surg Oncol* 38(7):594–601
- Khalaf H, Alsuhaibani H, Al-Sugair A, Al-Mana H, Al-Mutawa A, Al-Khadi Y, Al-Sebayel M (2010) Use of Yttrium-90 Microsphere radioembolization of hepatocellular carcinoma as downstaging and bridge before liver transplantation: a case report. *Transpl Proc* 42:994–998
- Kulik LM, Atassi B, van Holsbeeck L, Souman T, Lewandowski RJ, Mulcahy MF et al (2006) Yttrium-90 microspheres (TheraSphere) treatment of unresectable hepatocellular carcinoma: downstaging to resection, RFA and bridge to transplantation. *J Surg Oncol* 94(7):572–586
- Lau WY, Lai EC (2007) Salvage surgery following downstaging of unresectable hepatocellular carcinoma—a strategy to increase resectability. *Ann Surg Oncol* 14(12):3301–3309
- Lewandowski RJ, Kulik LM, Riaz A, Senthilnathan S, Mulcahy MF, Ryu RK et al (2009) A comparative analysis of transarterial downstaging for hepatocellular carcinoma: chemoembolization versus radioembolization. *Am J Transplant* 9(8):1920–1928
- Llovet JM, Di Bisceglie AM, Bruix J, Kramer BS, Lencioni R, Zhu AX et al (2008) Design and endpoints of clinical trials in hepatocellular carcinoma. *J Natl Cancer Inst* 100(10):698–711
- Mazzaferro V, Regalia E, Doci R, Andreola S, Pulvirenti A, Bozzetti F et al (1996) Liver transplantation for the treatment of small hepatocellular carcinomas in patients with cirrhosis. *N Engl J Med* 334(11):693–699
- Mazzaferro V, Sposito C, Bhoori S, Romito R, Chiesa C, Morosi C et al (2013) Yttrium-90 radioembolization for intermediate-advanced hepatocellular carcinoma: a phase 2 study. *Hepatology* 57(5):1826–1837
- N'Kontchou G, Mahamoudi A, Aout M, Ganne-Carrie N, Grando V, Coderc E et al (2009) Radiofrequency ablation of hepatocellular carcinoma: long-term results and prognostic factors in 235 western patients with cirrhosis. *Hepatology* 50(5):1475–1483
- Ravaioli M, Grazi GL, Piscaglia F, Trevisani F, Cescon M, Ercolani G et al (2008) Liver transplantation for hepatocellular carcinoma: results of down-staging in patients initially outside the Milan selection criteria. *Am J Transplant* 8(12):2547–2557
- Riaz A, Kulik L, Lewandowski RJ, Ryu RK, Giakoumis Spear G, Mulcahy MF et al (2009) Radiologic-pathologic correlation of hepatocellular carcinoma treated with internal radiation using yttrium-90 microspheres. *Hepatology* 49(4):1185–1193
- Rosenbaum CE, Verkooijen HM, Lam MG, Smits ML, Koopman M, van Seeters T et al (2013) Radioembolization for treatment of salvage patients with colorectal cancer liver metastases: a systematic review. *J Nucl Med* 54:1890–1895
- Salem R, Thurston KG (2006) Radioembolization with 90Yttrium microspheres: a state-of-the-art brachytherapy treatment for primary and secondary liver malignancies. part 1: technical and methodologic considerations. *J Vasc Interv Radiol* 17(8):1251–1278
- Tohme S, Sukato D, Chen HW, Amesur N, Zajko AB, Humar A et al (2013) Yttrium-90 radioembolization as a bridge to liver transplantation: a single-institution experience. *J Vasc Interv Radiol* 24:1632–1638
- Yao FY, Xiao L, Bass NM, Kerlan R, Ascher NL, Roberts JP (2007) Liver transplantation for hepatocellular carcinoma: validation of the UCSF-expanded criteria based on preoperative imaging. *Am J Transplant* 7(11):2587–2596



---

# Complications and Side Effects

R. T. Hoffmann, Lourdes Diaz-Dorrnsoro, and José I. Bilbao

## Contents

<b>1</b>	<b>Extrahepatic Complications</b> .....	171
1.1	Radiation-Induced Pancytopenia and Lymphopenia .....	171
1.2	Radiation-Induced Pneumonitis .....	172
1.3	Gastrointestinal and Pancreatic Complications .....	172
<b>2</b>	<b>Intrahepatic Complications</b> .....	172
2.1	Radiation-Induced Cholecystitis .....	172
<b>3</b>	<b>Bile Duct Complications</b> .....	173
<b>4</b>	<b>Conclusion</b> .....	174
	<b>References</b> .....	174

---

## Abstract

Radioembolization represents an effective tool for the treatment of primary and secondary liver tumors. Adequate use of this therapy requires knowledge and a multidisciplinary effort in order to obtain optimal results and avoid therapy-specific complications. A great deal of research has been undertaken in order to understand the angiographic, technical, and safety aspects concerning liver radioembolization. The most common complications of radioembolization include non-target radiation (pancreatitis, GI ulcers, cholecystitis), radiation pneumonitis, radiation-induced liver disease (radiation hepatitis), and biliary complications.

---

## 1 Extrahepatic Complications

In addition to well-known mild postembolization symptoms occurring after various types of liver embolization (e.g., transarterial chemoembolization–TACE), complications specific for radioembolizations including not only intrahepatic, but also different extrahepatic complications have to be considered. Most often, the extrahepatic complications are due to accidentally administered non-target radiation (especially gastrointestinal, esophageal, and pancreatic complications) (Lau et al. 1998; Yip et al. 2004) as well as shunts resulting in an increased radiation dose to the lungs (radiation-induced pneumonitis) (Salem and Thurston 2006).

### 1.1 Radiation-Induced Pancytopenia and Lymphopenia

Pancytopenia or lymphopenia as a result of bone marrow suppression from leaching Yttrium90 was published after the use of the earliest microsphere device (Mantravadi et al. 1982). This is not surprising, because bone marrow and lymphocytes are highly sensitive to irradiation. However,

---

R. T. Hoffmann (✉) · L. Diaz-Dorrnsoro · J. I. Bilbao  
University Hospital Dresden, Dresden, Germany  
e-mail: ralf-thorsten.hoffmann@uniklinikum-dresden.de

after multiple improvements of the device since then, this kind of side effect was not reported anymore.

## 1.2 Radiation-Induced Pneumonitis

Lung tissue is very sensitive to radiation. Most cases of radiation-induced pneumonitis described in the literature occurred after external beam radiation (Leung et al. 1995) affecting large parts of the lung. After intraarterial injection of Yttrium 90 microspheres into the liver, a substantial part of the radioactive substances is shunted into the lung via intrametastatic arteriovenous shunts (Leung et al. 1994). If a large proportion of the injected radionuclide microspheres (more than 15 %) is shunted into the lung, the risk of radiation-induced pneumonitis is greatly increased (Leung et al. 1995). The symptoms indicating radiation pneumonitis include dry cough, progressive dyspnea, restrictive ventilatory deficits resulting in deteriorating lung function, and even death 1 month after radioembolization. The authors, Leung et al. (1995) were able to show a significant correlation of the percentage of shunted Tc-MAA and the probability for a pneumonitis to occur. Therefore, reliable <sup>99m</sup>Tc-labelled macroaggregated albumin (Tc-MAA) studies for the assessment of arterial–pulmonary shunting have been introduced and are employed for dose calculation in order to minimize severe pulmonary side effects.

## 1.3 Gastrointestinal and Pancreatic Complications

The most feared complications of radioembolization are those caused by accidental spread of radioactive spheres into extrahepatic organs. The reason for this misdistribution is most often collaterals arising from the hepatic artery with extrahepatic communication. These collaterals should be identified at angiography prior to the radioembolization procedure and if present, they should be embolized prior to radioembolization. Otherwise the spheres may spread into the vascular territory of the gastrointestinal organs resulting in a severe damage of the gastrointestinal organs. Radiation as well as diminished blood supply due to embolization with the spheres and subsequent hypoxia may result in ulceration and even perforation of the stomach and duodenum (Lau et al. 1998; Yip et al. 2004). Yttrium 90-induced ulceration to the stomach or duodenum may not respond to medical therapy so that surgery may be required (Carretero et al. 2007).

If microspheres spread into the vessels supplying the pancreas, radiation-induced pancreatitis may be found which most frequently affects the pancreatic head. This kind of adverse effect can be very painful for the patient leading

to a prolonged hospitalization, food restriction, and further i.v. treatment. Therefore, meticulous angiographic analysis is indispensable in order to identify all extrahepatic arterial communications possibly leading to a misdistribution of the particles. In case such extrahepatic communications are detected, aggressive prophylactic embolization has to be performed to avoid those severe complications. Another—more theoretical—concern is the possibility to cause radiation-induced damage to organs adjacent to the liver via attenuated radiation. Especially segments 5–7 of the liver are adjacent to the colon and the left lobe of the liver is in close proximity to the stomach and may be at risk for increased radiation dose. It is not clear whether this can really result in radiation-induced gastritis or enteritis in rare cases. Another possible effect of attenuated radiation can be the occurrence of right pleural effusion.

Overall, the incidence of complications rate after radioembolization is low, if patients' selection and preparing examinations are performed thoroughly, if aberrant vessels are embolized, and if the dose administration is performed very carefully.

## 2 Intrahepatic Complications

### 2.1 Radiation-Induced Cholecystitis

**Background.** Cholecystitis is caused by 90Y microspheres that enter the cystic artery and irradiate the gallbladder (Szyszko et al. 2007). Although the most common origin of this vessel is the right hepatic artery, it may also arise from the left hepatic, middle hepatic, gastroduodenal, or replaced (accessory) right hepatic arteries (Covey et al. 2002). The blood supply to the gall bladder comes not only from the cystic artery but also from perforators to the body of the gall bladder from the hepatic parenchyma and the gastroduodenal artery (Liu et al. 2005). The gall bladder may therefore be assumed to have redundant blood supply and may receive microspheres from surrounding perforators. The cystic artery may also supply liver tumors that protrude into the gall bladder fossa and large hepatocellular carcinomas (Kim et al. 2005). In these cases, infusion distal to the cystic artery in order to prevent radiation-induced cholecystitis may result in suboptimal microsphere distribution. As has been mentioned, infusion of 90Y microspheres distal to the cystic artery is ideal but it is often not feasible. This is because the microspheres should be infused at a location that will allow admixture of microspheres with flowing blood, resulting in even and flow-dependent distribution. The cystic artery often arises deep within the right hepatic artery near its bifurcation into anterior (segments 5/8) and posterior (6/7) sectorial vessels. When this is the case and when the cystic artery arises distal to the ideal location for

90Y infusion, avoiding microsphere flow into the gall bladder becomes impossible (Lewandosky et al. 2007). At all times during 90Y embolization the treating physician should balance the risks of: (1) infusion proximal to the cystic artery with potential radiation cholecystitis; (2) infusion distal to the cystic artery but with suboptimal microsphere distribution; and (3) infusion proximal to the cystic artery following its prophylactic embolization, resulting in optimal microsphere distribution but with a risk of ischemic cholecystitis (Lewandosky et al. 2007).

**Histopathological basis.** Radiation-induced cholecystitis or gall bladder infarction is a rare complication of radioembolization and is due to the radiation effect of the microspheres. Unlike transarterial chemoembolization, 90Y treatment does not produce a significant embolic effect (Salem et al. 2005). Animal studies performed in dogs to examine the tolerance to radioembolization with 90Y labelled resin microspheres have shown that cholecystitis is encountered to some extent in almost all of the animals that received radioactive microspheres, but was absent in the animals infused with nonradioactive microspheres (Wollner et al. 1987). Similar studies performed in pigs that received Sirtex particles demonstrated the presence of particles in the gall bladder without inflammatory wall changes (De Luis et al. 2008). It is also possible that attenuated radiation from 90yttrium microspheres in liver metastases adjacent to the gallbladder also contribute to this complication; however, this is thought less likely because it implies that radiation-induced gastritis and colitis would occur more often (Salem et al. 2005). When radiation-induced cholecystitis occurs, a characteristic thick walled appearance of the gall bladder may be observed on cross-sectional images.

**Clinical presentation.** The clinical signs and symptoms of radiation-induced cholecystitis are those of acalculous cholecystitis. The most frequent physical and laboratory findings include fever, right upper quadrant (RUQ) pain, nausea, leukocytosis, and elevation of liver associated enzymes and bilirubin. All of these clinical parameters are nonspecific. In almost all instances in which it can be evaluated, abdominal pain is present; however, it is often not localized to the RUQ. Fever is present in two-thirds of patients, and leukocytosis and liver function abnormalities are present in approximately 80 %. Ultrasound evaluation should be the initial imaging test performed. Abdominal CT is preferred if other differential possibilities are more likely or if CT needs to be performed for another indication. On US, the diagnosis of radiation-induced cholecystitis requires two major criteria or one major plus two minor criteria as follows to be fulfilled, as well as a previous history of radioembolization. Major criteria are: gallbladder wall thickening greater than 3 mm, striated gallbladder (i.e., gallbladder wall edema), sonographic Murphy sign (i.e., localized gallbladder tenderness), pericholecystic fluid

(without ascites or hypoalbuminemia), mucosal sloughing, and intramural gas. Minor criteria are: gallbladder distention (>5 cm transverse) and echogenic bile (sludge).

**Treatment.** Treatment is conservative in the majority of cases. However, surgical cholecystectomy or percutaneous cholecystostomy may be necessary in patients with gall bladder perforation or emphysematous cholecystitis (Salem et al. 2005; Nakamura and Kondoh 1986).

---

### 3 Bile Duct Complications

**Background.** Biliary complications both intra and extrahepatic following 90Y administration are due to the embolic and radiation-induced necrosis of the biliary ducts (Northover and Terblanche 1979). In contrast to the normal liver parenchyma, the intrahepatic bile ducts do not have a dual blood supply and are fed exclusively from the hepatic arterial branches that give off a vascular plexus (peribiliary capillary plexus) around the bile ducts. This microscopic peribiliary arterial plexus has a similar diameter to that of the microspheres (10–60  $\mu\text{m}$ , mean 35  $\mu\text{m}$ ). Therefore, ischemia of the intrahepatic bile ducts can occur after radioembolization (Salem et al. 2005).

The blood supply to the bile duct system was studied by Northover and Terblanche in 1979 (Northover and Terblanche 1979). They found that the right and left hepatic ducts were supplied by numerous small vessels from the right and left hepatic arteries. The upper common bile duct is supplied by axial vessels from the retroduodenal or gastroduodenal arteries (Kim et al. 2001). Therefore, necrosis of the right and left hepatic ducts may occur after radioembolization when the catheter is placed at the proximal part of the right or left hepatic artery, but rarely of the supraduodenal common bile duct (Kim et al. 2001).

**Histopathological basis.** Biliary injury may take the form of biloma formation, diffuse mild dilatation of the intrahepatic ducts or focal strictures of the common bile duct (Makuchi et al. 1985). The possible mechanism of biloma formation is the development of peripheral bile duct necrosis with bile leakage caused by microvascular damage of the peribiliary plexus (Makuchi et al. 1985; Ashizawa et al. 1991; Kabayashi et al. 1993). This mechanism is supported by the pathologic findings: intrahepatic bile duct necrosis, bile leakage through Glisson's sheath, coagulation necrosis of the liver parenchyma adjacent to bile leakage, and thrombosis and coagulation necrosis of the small arterial branches adjacent to the necrotic bile duct (Sakamoto et al. 2003).

Cholangitis occurs in the presence of partial or complete obstruction of the common bile duct (CBD), with increased intraluminal pressures, bacterial infection of the bile with multiplication of the organisms within the duct, and seeding

of the bloodstream with bacteria or endotoxin. Cholangitis can rapidly become a life-threatening condition.

**Clinical presentation.** Bile duct complications develop within 2 months of chemoembolization but some may develop at a later stage (De Luis et al. 2008). Most patients with biliary strictures remain asymptomatic until the lumen of the bile duct is sufficiently narrowed to cause resistance to the flow of bile. Occasionally, patients may have intermittent episodes of RUQ (biliary colic), with or without laboratory features of biliary obstruction. Patients may present with the Charcot triad of fever and chills, jaundice, and RUQ abdominal pain, and even altered mental status and hypotension (i.e., Reynold pentad) due to ascending cholangitis. Patients with partial obstruction have elevated serum alkaline phosphatase and gamma-glutamyl transpeptidase. The serum of patients with clinically apparent jaundice shows increases in total and conjugated bilirubin. Alkaline phosphatase levels are increased to more than three times the normal. Elevated alkaline phosphatase levels are accompanied by increases in gamma-glutamyl transpeptidase and 5'-nucleotidase, usually disproportionate to serum transaminase levels. Serum aminotransferase levels usually are less than 300 IU/ml.

When radiation-induced bile duct injury is suspected, the initial imaging study should be an abdominal ultrasound (US). Sonography can accurately detect dilatation of intra- and extrahepatic bile ducts, thus providing indirect evidence for the presence of bile duct strictures. If the US examination findings show dilated bile ducts, magnetic resonance cholangiopancreatography (MRCP) or abdominal CT scan should be performed in order to determine the level and extent of the stricture. CT scanning is highly sensitive for the diagnosis of biliary obstruction. Intrahepatic biloma and bile duct injury are seen on CT as round, solitary, or multiple cystic lesions with or without segmental bile duct dilatation; a branching appearance of hypoattenuating area along Glisson's sheath simulating dilatation of the intrahepatic bile duct; or a subcapsular fluid collection of low density similar to the bile duct (Sakamoto et al. 2003).

**Treatment.** Conservative treatment is recommended if there are no signs of infection (Park et al. 2002). Patients with cholangitis or who fail to improve with conservative treatment require decompression of the biliary system as well as antibiotics. Treatment options for bile duct strictures include: (1) endoscopic or percutaneous balloon dilatation and insertion of an endoprosthesis, or (2) surgery.

**Predisposing factors.** Sakamoto et al. (2003) observed that biloma formation was more prevalent in patients with metastatic tumors than in the hepatocellular carcinoma group. In patients with hepatocellular carcinoma, the arteries that fed the tumor and the intratumoral arteries are dilated. On the other hand, in metastatic liver tumors the feeding arteries and the intratumoral arteries are not usually dilated.

This may result in pooling of the radioembolic agent in the surrounding liver parenchyma and initiation of biliary epithelial damage. These differences in tumor vasculature may be the cause of the difference in the incidence of intrahepatic biloma formation between the two groups (Sakamoto et al. 2003). Predisposing factors for bile duct injury have been described: non-cirrhotic livers and intact liver function may further intrahepatic biliary lesions, the bile ducts in the advanced cirrhotic livers are more resistant to ischemic injury. Biliary stents and previous biliaryenteric surgery which can damage the peribiliary vascular network may predispose to extrahepatic biliary lesions (Yu et al. 2002).

## 4 Conclusion

Liver radioembolization is a well-tolerated therapeutic procedure that has been proven to be as effective as other treatments currently available.

Complication rates are low but potentially life-threatening. Toxicity profile can be kept to a minimum by applying an adequate and meticulous technique.

## References

- Ashizawa K, Matsunaga N, Aso N et al (1991) Bile lake: a complication of transcatheter hepatic arterial infusion and embolization therapy. *Nippon Iagaku Hoshasen Gakkai Zasshi* 51:121–126
- Carretero C, Munoz-Navas M, Betes M et al (2007) Gastrointestinal injury after radioembolization of hepatic tumors. *Am J Gastroenterol* 102:1–5
- Covey AM, Brody LA, Maluccio MA, Getradjman GJ, Brown KT (2002) Variant hepatic arterial anatomy revisited: digital subtraction angiography performed in 600 patients. *Radiology* 224:542–547
- De Luis E, Bilbao JI, Garcia-Jalon de Ciercoles JA et al (2008) In vivo evaluation of a new embolic spherical particle "Hepasphe" in a kidney animal model. *Cardiovasc Intervent Radiol* 31(2):367–376
- Kabayashi S, Nakamura Y, Terada T et al (1993) Postmortem survey of bile duct necrosis and biloma in hepatocellular carcinoma after transcatheter arterial chemoembolization therapy: relevant to microvascular damages of peribiliary capillary plexus. *Am J Gastroenterol* 88:1410–1415
- Kim HK, Cheng YH, Song BC et al (2001) Ischemic bile duct injury as a serious complication after transarterial chemoembolization in patients with hepatocellular carcinoma. *J Clin Gastroenterol* 32:423–427
- Kim HC, Cheng JW, Lee W, Jae HJ, Park JH (2005) Recognizing extrahepatic collateral vessels that supply hepatocellular carcinoma to avoid complications of transcatheter arterial chemoembolization. *Radiographics* 25:S25–S39
- Lau WY, Ho S, Leung TW et al (1998) Selective internal radiation therapy for nonresectable hepatocellular carcinoma with intraarterial infusion of 90yttrium microspheres. *Int J Radiat Oncol Biol Phys* 40:583–592
- Leung WT, Lau WY, Ho SK et al (1994) Measuring lung shunting in hepatocellular carcinoma with intrahepatic-arterial technetium-99 m macroaggregated albumin. *J Nucl Med* 35:70–73



- Leung TW, Lau WY, Ho SK et al (1995) Radiation pneumonitis after selective internal radiation treatment with intraarterial <sup>90</sup>yttrium-microspheres for inoperable hepatic tumors. *Int J Radiat Oncol Biol Phys* 33:919–924
- Lewandosky RJ, Sato KT, Atassi B et al (2007) Radioembolization with <sup>90</sup>Y microspheres: angiographic and technical considerations. *Cardiovasc Intervent Radiol* 30:571–592
- Liu DM, Salem R, Bui JT et al (2005) Angiographic considerations in patients undergoing liver-directed therapy. *J Vasc Interv Radiol* 16:911–935
- Makuchi M, Sukigara M, Mori T et al (1985) Bile duct necrosis: complication of transcatheter hepatic arterial embolization. *Radiology* 156:331–334
- Mantravadi RV, Spigos DG, Tan WS et al (1982) Intraarterial yttrium 90 in the treatment of hepatic malignancy. *Radiology* 142:783–786
- Nakamura H, Kondoh H (1986) Emphysematous cholecystitis: complications of hepatic arterial embolization. *Cardiovasc Intervent Radiol* 9:152–153
- Northover JMA, Terblanche J (1979) A new look at the arterial supply of the bile duct in man and its surgical implications. *Br J Surg* 66:379–384
- Park WK, Chang JC, Lee HZ, Kim HJ, Choi JH, Gu MJ (2002) A case of resection of biloma with hepatocellular carcinoma after embolization. *TaehanKan Hakhoe Chi* 8:331–335
- Sakamoto I, Iwanaga S, Nagaoki K et al (2003) Intrahepatic biloma formation (bile duct necrosis) after transcatheter arterial chemoembolization. *AJR Am J Roentgenol* 181:79–87
- Salem R, Thurston KG (2006) Radioembolization with <sup>90</sup>Yttrium microspheres: a state-of-the-art brachytherapy treatment for primary and secondary liver malignancies. Part 1: technical and methodologic considerations. *J Vasc Interv Radiol* 17:1251–1278
- Salem R, Lewandosky RJ, Atassi B et al (2005) Treatment of unresectable hepatocellular carcinoma with intrahepatic yttrium 90 microspheres: factors associated with liver toxicities. *J Vasc Interv Radiol* 16:1627–1639
- Szyszkowski T, Al-Nahhas A, Tait P et al (2007) Management and prevention of adverse effects related to treatment of liver tumours with <sup>90</sup>Y microspheres. *Nucl Med Commun* 28:21–24
- Wollner IS, Knutsen CA, Ullrich KA et al (1987) Effects of hepatic arterial yttrium-90 microsphere administration alone and combined with regional bromodeoxyuridine infusion in dogs. *Cancer Res* 47:3285–3290
- Yip D, Allen R, Ashton C et al (2004) Radiation-induced ulceration of the stomach secondary to hepatic embolization with radioactive yttrium microspheres in the treatment of metastatic colon cancer. *J Gastroenterol Hepatol* 19:347–349
- Yu JS, Kim KW, Jeong MG et al (2002) Predisposing factors of bile duct injury after transcatheter arterial chemoembolization for hepatic malignancy. *Cardiovasc Intervent Radiol* 25:270–274

---

# Radioembolization-Induced Liver Disease

Bruno Sangro, Mercedes Iñárraegui, and Andrew S. Kennedy

## Contents

<b>1 Basic Concepts on Radiobiology After External Irradiation</b> .....	177
1.1 Types of Radiation Damage .....	177
1.2 Cellular and Molecular Responses to Radiation .....	178
1.3 Subacute and Late Effects of External Irradiation of the Liver .....	178
<b>2 Liver Damage Induced by Radioembolization</b> .....	179
2.1 Incidence and Course .....	179
2.2 Predisposing Factors .....	179
2.3 An Approach to Prophylaxis and Treatment .....	181
<b>References</b> .....	183

---

## Abstract

The aim of liver radioembolization is to deliver an effective dose of radiation to liver tumors while the nontumoral liver is only exposed to much lower, nonharmful dose. However, irradiation of the nontumoral compartment of the liver may produce cell damage that can translate into changes in laboratory tests or clinical signs of liver dysfunction. Radioembolization-induced liver disease has been recently described as a syndrome consisting in jaundice and ascites that appears 1–2 months after treatment in the absence of tumor progression or bile duct occlusion. This complication is extremely rare in the absence of cirrhosis or intense prior exposure to chemotherapeutic agents particularly if chemotherapy is continued immediately after radioembolization. Its incidence is likely to be lower than 10 % and it has a transient or stable course in most cases, but it may unusually lead to overt liver failure. A conservative dose prescription and the use of low-dose steroids or ursodeoxycholic acid have been suggested as prophylactic measures.

---

## 1 Basic Concepts on Radiobiology After External Irradiation

### 1.1 Types of Radiation Damage

Radiation used in the treatment of malignant cells can be directed into the body from an external source via a mechanical process. Electrons are accelerated (in a linear accelerator) and strike a target releasing electromagnetic energy (photons). This form of energy is without charge or mass and thus can penetrate deeply into the body and easily reach liver tumors. Energetic waves in the distant past can also be directed from a treatment machine containing  $^{60}\text{Co}$  which as it decays releases high-energy photons. Internal radiation, termed brachytherapy, also uses radioactive

---

B. Sangro (✉) · M. Iñárraegui  
Clínica Universidad de Navarra, Avda. Pio XII 36,  
31008, Pamplona, Spain  
e-mail: bsangro@unav.es

B. Sangro · M. Iñárraegui  
Centro de Investigación Biomedica en Red de Enfermedades  
Hepáticas y Digestivas (CIBEREHD), Pamplona, Spain

A. S. Kennedy  
Radiation Oncology Research, Sarah Cannon Research Institute,  
3322 West End Avenue, Suite 800, Nashville, Tennessee,  
37203, USA

A. S. Kennedy  
Department of Biomedical Engineering, Department of  
Mechanical and Aerospace Engineering, North Carolina State  
University Raleigh, Raleigh, NC, USA

decay as the source of ionizing radiation. However in the case of Yttrium-90 ( $^{90}\text{Y}$ ), which delivers beta decay energy, the particle released has both mass and a charge, thus significantly limiting the distance traversed in tissue.

The seminal event in the tumor cell targeted by radiation is ionization of the DNA in the nucleus. Although there are many potential targets in the malignant cell in which radiation can cause damage, it is the cessation of reproductive capacity that is the true goal of radiation therapy. The direct effect on DNA, which is the photon or beta particle striking one of the two DNA strands, causing irreversible damage, occurs in only 25 % of lethal interactions. The indirect radiation effect on DNA, which leads to cell death in 75 % of encounters, involves a water molecule absorbing radiation energy, ejection of a Compton electron from the outer shell of the oxygen atom, creating a free radical. It is the highly unstable and reactive free radical that develops within 4 nm of the DNA strand, which leads to either a single strand or double-strand DNA break. If unrepaired, the cell will lose reproductive integrity, and die either via apoptosis, or after a few additional cell divisions. The presence of oxygen is critical for the successful creation of free radical damage near to the DNA (Hall 2006).

## 1.2 Cellular and Molecular Responses to Radiation

Continuous low-dose radiotherapy is the type of brachytherapy delivered by  $^{90}\text{Y}$  microspheres. Compared to external beam (via modern linear accelerators) which is high dose (500 cGy/minute), pulsatile (once/24 h), five days/week; radioembolization (RE) delivers low dose (50 cGy/minute), continuous (every second), seven days/week for 14 days of effective dose rate radiation. The malignant cell has checkpoints in the cell cycle in which the damage is recognized and repair attempted before proceeding to the next phase of reproduction (cell cycle checkpoints). If cells are blocked in a radiation sensitive portion of the cycle, i.e., G2/M or G1, they are especially vulnerable to radiation cell killing, compared to the relatively insensitive S-phase. Having continuous radiation can take advantage of this type of cellular and molecular response to radiation.

## 1.3 Subacute and Late Effects of External Irradiation of the Liver

Despite more than 80 years of research in liver tolerance to ionizing radiation, there is not yet an acceptable animal model to study radiation-induced liver disease (RILD). Studies using dogs, swine, mice, rats, and rabbits have been

unfit for RILD studies because despite extremely high doses of external and internal radiation, histopathological injuries of the liver do not occur in a similar fashion or frequency as RILD in human livers at much lower absorbed doses of radiation (Kennedy et al. 2004).

It was first reported in the mid-1960s that radiation therapy to the abdomen could produce clinical complications in the liver. Within 3 months of therapy, a significant number of patients developed weight gain, ascites, liver enlargement, and occasionally, jaundice (Ingold et al. 1965). Most patients recovered but some of them died because of this RILD and histopathological findings in these livers resembled veno-occlusive disease (Reed and Cox 1966). The threshold, 30–35 Gy in conventional fractionations, was too low to produce significant tumor responses and external beam radiation therapy (EBRT) was neglected for the treatment of liver cancer. Thirty years later, the University of Michigan developed a Lyman normal tissue complication probability (NTCP) model based on 79 patients treated with partial liver EBRT that were prospectively followed for RILD (Lawrence et al. 1992). The NTCP model assumes a sigmoid relationship between dose of uniform radiation given to a volume of an organ and the chance of a complication occurring. It is based on three parameters, namely the whole-liver dose associated with a 50 % probability of toxicity, the steepness of the dose response at TD50, and a volume effect parameter that indicates a larger volume effect as it increases. The high volume effect observed in liver EBRT indicates a strong correlation between NTCP and mean liver dose. For patients with liver metastasis and primary liver cancer, the mean liver doses associated with a 5 % probability of liver toxicity are 37 and 32 Gy, respectively (Dawson and Ten Haken 2005). However, dosing is not the only safety concern in EBRT. A multivariate analysis performed in more than 200 patients disclosed that in addition to mean liver dose, primary liver tumor, concurrent chemotherapy, and male sex were also independent factors contributing to RILD (Dawson et al. 2002). Unfortunately, the use of these models has not totally prevented the occurrence of RILD. Following EBRT of primary liver tumors, RILD occurs in 5–33 % of patients (Cheng et al. 2004; Furuse and Ishii 2005; Park et al. 2005), and may result in significant mortality rates particularly among cirrhotic patients (Cheng et al. 2002).

A Consensus Conference held in 1995 (Lawrence et al. 1995), differentiated RILD from combined modality-induced liver disease (CMILD) that appears after allogeneic bone marrow transplantation when high-dose chemotherapy and total body irradiation are used as preparative procedures. Although both syndromes share the pathological hallmark of veno-occlusive disease they also have unique features. RILD typically emerges 4–8 weeks after the

completion of treatment with fatigue, rapid weight gain, and ascites. Patients are rarely jaundiced at presentation, and elevation in alkaline phosphatase is out of proportion with that of the other liver enzymes. CMILD usually appears 1–4 weeks after transplantation as jaundice and weight gain, with or without right upper quadrant pain, ascites, and encephalopathy. Total bilirubin is remarkably elevated, with only mildly elevated transaminases and alkaline phosphatase (almost the mirror image of those in RILD). Interestingly, CMILD has also been described after chemoradiation of primary liver tumors. In a large cohort of patients with hepatocellular carcinoma receiving EBRT concurrently with chemotherapy delivered either by transarterial chemoembolization (lower systemic exposure) or hepatic arterial infusion (higher systemic exposure), the incidence of RILD was similar in both groups (5.6 vs. 3.7 %) but CMILD occurred only in the latter (0 vs. 8.8 %) (Shim et al. 2007).

---

## 2 Liver Damage Induced by Radioembolization

### 2.1 Incidence and Course

With early series not reporting significant liver-related toxicities and lacking relevant animal models, liver damage after RE was not thoroughly studied in parallel with clinical development. From a clinical standpoint, many of the retrospective series and even prospective clinical trials published before 2005 do not provide specific information about changes in liver function tests. Thereafter, most cohort series and clinical trials have reported on changes in liver function tests using NCI Common Toxicity Criteria or similar scores.

Tables 1, 2, and 3 provide a summary of liver-related toxicities reported after RE for different patient populations. Mild elevations in transaminases or alkaline phosphatase have been described after RE (Nosher et al. 2011) although less consistently than increased bilirubin. In 2006, we identified among patients without prior cirrhosis treated by RE, a distinctive syndrome that shared features with both RILD and CMILD. It typically emerged 4–8 weeks after initiation of treatment when patients became jaundiced and ascites was observed at physical examination. Tumor progression and bile duct dilatation were discarded by imaging, and laboratory tests revealed an increase in bilirubin, GGTP, and alkaline phosphatase, with mild or absent changes in transaminases. In most cases the course of the disease was stable or transient but some patients had a more aggressive pattern and in this group pathological changes were consistent with veno-occlusive disease (VOD). Because of the differences with classic RILD, we proposed

the term RE-induced liver disease (REILD) to describe this entity that was likely to be a form of sinusoidal obstruction syndrome occurring mainly in patients previously exposed to anticancer chemotherapy and receiving RE in a whole-liver fashion. As illustrated in Fig. 1, REILD is not the only form of liver damage after RE but is probably the most significant due to its potentially serious outcomes.

The incidence of REILD in other series cannot be established because they usually report separately those individual parameters such as increased bilirubin or ascites. And they do it along different periods of time, from 30 days to the entire follow-up period. Patients with liver tumors, particularly if they are cirrhotics, may develop hyperbilirubinemia or ascites as a consequence of tumor or cirrhosis progression. A causal relationship between RE and these findings may thus be confirmed only in controlled clinical trials in which adverse events are recorded prospectively and compared to those occurring in a control arm. However, it is very likely that the increased bilirubin levels reflect REILD in a significant fraction of these patients with early hyperbilirubinemia. This opinion is further supported by the fact that the early increase in bilirubin is not associated with other changes that may reflect abating liver function such as decreased albumin levels or prothrombin activity, even in cirrhotic patients (Sangro et al. 2011).

In most cases, REILD is transient or has a stable course (Piana et al. 2011; Sangro et al. 2008) but it may also lead to overt liver insufficiency and be a cause of treatment-related death. However, with a conservative approach in activity calculation for the high risk candidates and the empiric prophylactic use of ursodeoxycholic acid and low-dose steroids, life-threatening REILD occurred in only 3 of 185 (1.6 %) RE treated patients (Gil-Alzugaray et al. 2012). Globally, Tables 1, 2, and 3 show that RE as it is currently performed worldwide is by and large well tolerated by the liver.

### 2.2 Predisposing Factors

A multinational review of 680 RE treatments with resin microspheres in more than 500 patients found three significant contributors to liver toxicity: lower safety margins at the treating center; treatment of the whole liver in preference to lobar approaches; and greater delivered  $^{90}\text{Y}$  activity (Kennedy et al. 2009). The correlation of REILD with high administered activity and bilobar treatment was reiterated in our first report (Sangro et al. 2008). More recently we have analyzed the incidence of REILD in a much larger cohort of 250 patients and studied the factors involved in its appearance (Gil-Alzugaray et al. 2012). REILD did not appear in the absence of cirrhosis or prior exposure to chemotherapeutic agents. In the cirrhotic liver,



**Table 1** Liver-related adverse events among patients with hepatocellular carcinoma treated by radioembolization

Reference, year	Device	Lobar	FUP interval	No. patients	Cirrhosis	Child B	Grade > 3 Bilirubin <sup>a</sup>	Ascites	Findings
(Dancey et al. 2000)	Glass	0 %	nr	22	nr	nr	22 %*	nr	2 potential REILD-related deaths
(Geschwind et al. 2004)	Glass	65 %	Any time	80	nr	10 %	28 %*	7 %	1 treatment-related death
(Carr et al. 2004)	Glass	100 %	0–180	65	75 %	nr	38 %*	12 %	1 definite and 2 probable treatment-related deaths
(Salem et al. 2005)	Glass	51 %	0–90	43	60 % <sup>b</sup>	nr	14 %	7 %	
(Sangro et al. 2006)	Resin	46 %	0–90	24	71 %	0 %	12 %		2 treatment-related deaths
(Kulik et al. 2008)	Glass	nr	0–180	82	100 %	33 %	40 %*	18 %	
(Kulik et al. 2008)	Glass	nr	0–180	26	0 %	–	4 %*	4 %	
(Hilgard et al. 2010)	Glass	most	0–90	108	76 %	22 %	23 %	0 %	
(Salem et al. 2010)	Glass	nr	Any time	291	87 %	55 % <sup>c</sup>	19 %	nr	
(Sangro et al. 2011)	Resin	55 %	0–90	325	78 %	17 %	5 %	nr	
(Mazzaferro et al. 2012)	Glass	94 %	0–90	52	100 %	17 %	13 %	8 %	23 % of patients developed liver decompensation <sup>d</sup>

FUP interval days after radioembolization. TRD treatment-related death. nr not reported

<sup>a</sup> CTC grade 3 (>3 x ULN increase) unless otherwise specified. \*SWOG grade 3 (>200 % increase from baseline)

<sup>b</sup> portal hypertension

<sup>c</sup> includes 3 % of patients with Child C

<sup>d</sup> liver decompensation was defined as the occurrence of any of the following features during follow-up: clinically detectable ascites, bleeding from esophageal varices, hepatic encephalopathy, total bilirubin >3 mg/dL, or prothrombin time INR >2.2

microsphere distribution can be altered by the intrinsic vascular changes that include the absence of portal triads (substituted for fibrotic tracts surrounding the regenerative nodules), and the presence of arterioportal and arteriovenous shunts. All these factors may modify the radiation dose absorbed by the nontumoral liver and have an impact on treatment tolerance and effectiveness. Besides, the reduced functional reserve of the cirrhotic liver results in an increased risk of liver failure after extensive resection, or liver insults including toxic or viral acute hepatitis, or external irradiation (Sangro et al. 2012).

The device used for RE seems to play no particular role in the occurrence of REILD. In the two largest series published on HCC patients that are mostly cirrhotics (Sangro et al. 2011; Salem et al. 2010), grade 3 or higher CTCAE bilirubin levels (a hallmark of REILD) were observed within 3 months after therapy in 14 % of patients treated with glass spheres mostly in a lobar fashion, and in nearly 6 % of patients treated with resin spheres almost half of them treated in a bilobar fashion.

Regarding chemotherapy, its ability to produce liver toxicity is well known and the occurrence of liver damage

may affect surgical outcomes (Khan et al. 2009). The use of 5-Fluorouracil plus Leucovorin is linked to the development of hepatic steatosis and to increased postoperative infection rates. Irinotecan produces a form of nonalcoholic steatohepatitis that is associated with inferior outcomes following hepatic surgery mainly due to hepatic insufficiency and poor regeneration. Oxaliplatin combinations may produce a sinusoidal obstruction syndrome that may translate into an increased risk for intraoperative bleeding and decreased hepatic reserve. Finally, intraarterial Floxuridine therapy damages the extrahepatic biliary tree in addition to causing parenchymal liver damage, and has been shown to be associated with increased morbidity after hepatic resection. In prospective studies, the concurrent use of RE in combination with either FOLFOX or Irinotecan as first- and second-line therapy, respectively, has produced little liver toxicity in patients with liver metastasis from colorectal cancer (Sharma et al. 2007; Van Hazel et al. 2004). Yet, a higher rate of liver toxicity was observed when RE was combined with infusional 5-Fluorouracil as rescue therapy in heavily pretreated patients (Hendlisz et al. 2010). In a similar way, retrospective studies have shown that extensive

**Table 2** Liver-related adverse events among patients with liver metastases from colorectal carcinoma treated by radioembolization

Ref, year	Device	Lobar	FUP Interval	No. patients	Prior chemo	Concurrent chemo	Grade > 3 bilirubin <sup>a</sup>	Ascites	Findings
(Sharma et al. 2007)	Resin	25 %	Any time	20	1st line	FOLFOX6	10 %	–	
(Van Hazel et al. 2004)	Resin	–	Any time	11	1st line	5FU/LV (Mayo)	0 %**		No difference with 5FU/LV alone
(Gray et al. 2001)	Resin	–	Any time	35	1st line (86 %)	IA FUDR	3 %**		RCT nonsignificant difference with FUDR alone
(van Hazel et al. 2009)	Resin	nr	Any time	25	2nd line (68 %)	Irinotecan	4 %**	–	
(Seidensticker et al. 2011)	Resin	14 %	Any time	29	Salvage	No	–	–	3 % REILD
(Hendlisz et al. 2010)	Resin	0 %	Any time	21	Salvage	Protracted Iv 5FU	–	–	RCT No liver-related toxicities
(Mulcahy et al. 2009)	Glass	17 %	Any time	72	Salvage	No	13 %		
(Jakobs et al. 2008)	Resin	–	Any time	41	Salvage	No	–	–	
(Kennedy et al. 2006)	Resin	27 %	Any time	208	Salvage	No	1.5 %	–	No VOD
(Lim et al. 2005)	Resin	–	Any time	30	Salvage	5FU <sup>b</sup>	nr	nr	1 RILD

FUP interval days after radioembolization. nr not reported. FU fluorouracil. LV leucovorin. RCT randomized controlled trial. REILD radioembolization-induced liver disease. VOD veno-occlusive disease. RILD radiation-induced liver disease

<sup>a</sup> CTC grade 3 (>3 xULN increase) unless otherwise specified. \*UICC grade 3 (not defined)

<sup>b</sup> as radiosensitizer

**Table 3** Liver-related adverse events among patients with liver metastases from neuroendocrine tumors treated by radioembolization

Reference, year	Device	Lobar	FUP Interval	No. patients	Prior Treat	Concurrent chemo	Grade > 3 Bilirubin <sup>a</sup>	Ascites	Findings
(Ezziddin et al. 2012)	Resin/ Glass	22 %	0–180	23	PRRT	No	9 %	–	
(King et al. 2008)	Resin	–	Any time	32	SSA 15 % Chemo	5FU	nr	–	1 jaundiced patient
(Kennedy et al. 2008)	Resin	59 %	0–90	148	nr	nr	nr	0.5 %	

PRRT: Peptide Receptor Radionuclide Therapy. SSA: somatostatin analogs 5FU as radiosensitizer (x7 days). nr: not reported

<sup>a</sup> CTC grade 3 (> 3 xULN increase)

exposure to chemotherapy prior to RE render the liver susceptible to REILD, particularly if chemotherapy is also delivered following RE (Piana et al. 2011; Gil-Alzugaray et al. 2012).

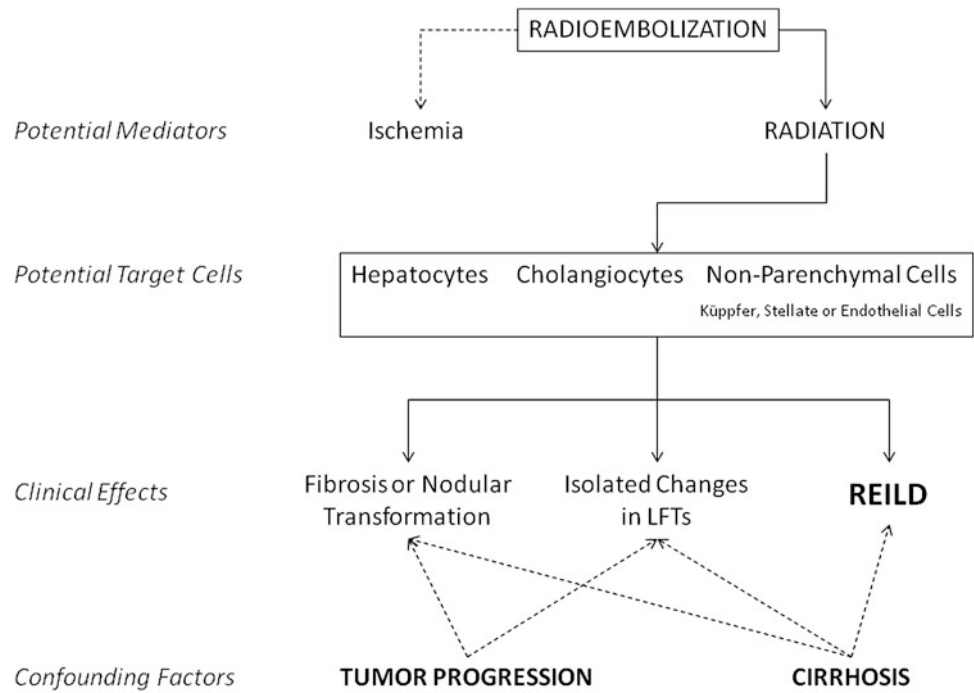
### 2.3 An Approach to Prophylaxis and Treatment

The pathophysiology of RILD is far from being understood. It has been postulated that injury to endothelial or stellate cells rather than hepatocytes may play a key role and inflammation-related molecules such as tumor growth factor-beta and

tumor necrosis factor-alpha have been implicated. A number of studies have suggested that a hypercoagulable state is important in the pathogenesis of CMILD (Scrobohaci et al. 1991) and that recombinant tPA may be effective in the treatment of established severe CMILD (Bearman et al. 1992). The situation is even worse for REILD since we know virtually nothing about its pathophysiology. In animal models, resin microspheres had little or no embolic effect on medium to small arteries and an ischemic effect on liver tissue was not observed (Bilbao et al. 2009) so REILD is most likely a consequence of radiation alone.

As mentioned before, treatment intensity matters in REILD. For glass microspheres, the prescribed activity is

**Fig. 1** Potentially relevant factors in the development of liver toxicities after radioembolization of liver tumors



calculated from a 2-compartment dosimetry model (lung and liver) with the aim of delivering a radiation dose of 120 Gy to the targeted liver irrespective of tumor burden. For resin microspheres, users have to choose between two different methods. The most commonly used is a formula in which the activity is basically proportional to the liver volume (derived from the body surface area) but slightly modified depending on tumor burden. A 3-compartment dosimetry model (lung, tumor, and nontumoral liver) in which the aim is to deliver a radiation dose of 70–80 Gy to the targeted nontumoral liver may also be used. These methods for activity calculation are nevertheless highly empirical.

In RE, millions of sources of radiation are liberated in the bloodstream. A simulation of the actual treatment is performed prior to RE by the injection of technetium-99 m labeled macroaggregated albumin (99 mTc-MAA) particles followed by planar and/or SPECT gamma camera imaging. A number of 3D software packages may take the distribution of  $^{99m}\text{Tc}$ -MAA or  $^{90}\text{Y}$  microspheres for a given patient and combine it with anatomic information (from CT or MRI) to yield absorbed dose estimates that are specific to that particular patient (Flamen et al. 2008). However, the absorbed dose to the liver or other organs cannot be directly measured *in vivo* after RE as it also happens for other nuclear medicine procedures. It can be estimated from the data obtained during the simulation. With the medical internal radiation dose (MIRD) method of calculation, the dose absorbed by an organ from isotopes distributed homogeneously throughout that particular organ can be

estimated. Using this method, much higher absorbed doses of radiation are tolerated after RE in comparison to EBRT. This may be explained in part by the short penetration of beta radiation emitted by  $^{90}\text{Y}$  and the heterogeneous distribution of microspheres. However, in the 3D model these considerations are based upon the assumption that microspheres are always positioned in the distal arterial branches and are uniformly scattered throughout the entire liver parenchyma in a nonclustered distribution. Quite differently, microspheres can be actually found in portal and hepatic veins in the normal liver and in the fibrotic septa in the cirrhotic liver, where they not infrequently form clusters, and may be distributed in a very heterogeneous way.

There are differences between the simulation and the actual treatment procedure in the size and specific gravity of  $^{99m}\text{Tc}$ -MAA and  $^{90}\text{Y}$  microspheres, in the precise site, volume, and velocity of injection, and quite importantly in the hemodynamic conditions inside the liver under which particle injection is performed, that often vary during the procedure. When the correlation between the distribution of MAA and resin  $^{90}\text{Y}$ -microspheres has been analyzed (Knesaurek et al. 2010) it varied from high to very poor, and the average correlation was not the ideal one, most likely because of differences in the position of the catheter between the diagnostic and the therapeutic angiography (Jiang et al. 2012). No data are available for glass microspheres but there is no reason to think they will behave differently.

Despite the inaccuracy of the available dosimetry tools, the MAA scan may be used to anticipate the average dose of

radiation that can be delivered to tumor and nontumoral areas for both resin and glass microspheres. With this approach, a clear and consistent dose–event relationship in liver tolerance has not been proved. Not surprisingly, the estimated absorbed radiation dose tends to be higher among patients that develop some signs of liver dysfunction (Strigari et al. 2010). However, a consistent cut-off point has not been established although REILD is extremely rare when patients receive less than 0.8 GBq of resin <sup>90</sup>Y-microspheres per liter of liver volume, which corresponds to 40 Gy in a 2-compartment model (Gil-Alzugaray et al. 2012). An expert agreement is that the dose absorbed by the nontumoral liver tissue should be kept below 50 Gy for all patients and maybe below 40 Gy for patients with an impaired nontumoral liver (Lau et al. 2012).

Experienced centers have described different attempts to use dosimetry models to improve the efficacy of RE with both resin (Kao 2012) and glass microspheres (Chiesa et al. 2011). The early experience reported with these dosimetry models is encouraging but only prospective studies in large series of patients will tell us if this approach succeed in preserving safety while they increase efficacy.

A sequential approach to RE has been reported to result in a reduced rate of liver toxicities including a wide range of laboratory and clinical parameters (Seidensticker et al. 2011). The rationale behind this idea is that by waiting 4–6 weeks, the potential of the first-targeted liver volume to regenerate is increased thus compensating the potential damage to the second-targeted volume. However, there is no evidence that this is actually the case. The now well-known effect of contralateral hypertrophy after lobar RE results in the second lobe being undertreated if the prescribed activity is calculated before this hypertrophy occurs, as it happened in the above-mentioned study. Since sequential treatment increases significantly the cost of RE, we feel that a prospective controlled trial is needed before this approach is widely recommended.

It has been recently shown that a conservative approach to activity calculation when the entire liver volume needs to be targeted by RE, together with the use of ursodeoxycholic acid or prolonged low-dose steroids, or any combination of these factors, resulted in a reduced incidence of all grades and severe forms of REILD (Gil-Alzugaray et al. 2012). However, only prospective comparative studies may help elucidate the individual contribution of both agents, although its use is safe even in cirrhotic patients.

Treatment for REILD is supportive, generally consisting of diuretics and symptomatic care. Steroids are sometimes used although supporting evidence is lacking. For severe cases with impending liver failure, the placing of a transjugular intrahepatic stent shunt may be lifesaving (Sangro et al. 2008).

**Acknowledgments** CIBEREHD is funded by Instituto de Salud Carlos III. The authors wish to thank Paloma Sangro for her valuable work in the review of the literature and the preparation of the manuscript.

## References

- Bearman SI, Shuhart MC, Hinds MS, McDonald GB (1992) Recombinant human tissue plasminogen activator for the treatment of established severe venocclusive disease of the liver after bone marrow transplantation. *Blood* 80(10):2458–2462
- Bilbao JI, Martino A, Luis E, Díaz-Dorransoro L, Alonso-Burgos A, de la Martínez A, Cuesta A et al (2009) Biocompatibility, inflammatory response, and recanalization characteristics of nonradioactive resin microspheres: histological findings. *Cardiovasc Intervent Radiol* 32(4):727–736
- Carr BI (2004) Hepatic arterial<sup>90</sup>Yttrium glass microspheres (Therasphere) for unresectable hepatocellular carcinoma: interim safety and survival data on 65 patients. *Liver Transpl* 10(S2):S107–S110
- Cheng JC-H, Wu J-K, Huang C-M, Liu H-S, Huang DY, Cheng SH et al (2002) Radiation-induced liver disease after three-dimensional conformal radiotherapy for patients with hepatocellular carcinoma: dosimetric analysis and implication. *Int J Radiat Oncol Biol Phys* 54(1):156–162
- Cheng JC-H, Wu J-K, Lee PC-T, Liu H-S, Jian JJ-M, Lin Y-M et al (2004) Biologic susceptibility of hepatocellular carcinoma patients treated with radiotherapy to radiation-induced liver disease. *Int J Radiat Oncol Biol Phys* 60(5):1502–1509
- Chiesa C, Maccauro M, Romito R, Spreafico C, Pellizzari S, Negri A et al (2011) Need, feasibility and convenience of dosimetric treatment planning in liver selective internal radiation therapy with (<sup>90</sup>Y) microspheres: the experience of the National Tumor Institute of Milan. *Q J Nucl Med Mol Imaging* 55(2):168–197
- Dancey JE, Shepherd FA, Paul K, Sniderman KW, Houle S, Gabrys J et al (2000) Treatment of nonresectable hepatocellular carcinoma with intrahepatic <sup>90</sup>Y-microspheres. *J Nucl Med* 41(10):1673–1681
- Dawson LA, Ten Haken RK (2005) Partial volume tolerance of the liver to radiation. *Semin Radiat Oncol* 15(4):279–283
- Dawson LA, Normolle D, Balter JM, McGinn CJ, Lawrence TS, Haken Ten RK (2002) Analysis of radiation-induced liver disease using the Lyman NTCP model. *Int J Radiat Oncol Biol Phys* 53(4):810–821
- Ezziddin S, Meyer C, Kahancova S, Haslerud T, Willinek W, Wilhelm K et al (2012) <sup>90</sup>Y radioembolization after radiation exposure from peptide receptor radionuclide therapy. *J Nucl Med* 53(11):1663–1669
- Flamen P, Vanderlinden B, Delatte P, Ghanem G, Ameye L, Van Den Eynde M et al (2008) Multimodality imaging can predict the metabolic response of unresectable colorectal liver metastases to radioembolization therapy with Yttrium-90 labeled resin microspheres. *Phys Med Biol* 53(22):6591–6603
- Furuse J, Ishii H, Nagase M, Kawashima M, Ogino T, Yoshino M (2005) Adverse hepatic events caused by radiotherapy for advanced hepatocellular carcinoma. *J Gastroenterol Hepatol* 20(10):1512–1518
- Geschwind J-FH, Salem R, Carr BI, Soulen MC, Thurston KG, Goin KA et al (2004) Yttrium-90 microspheres for the treatment of hepatocellular carcinoma. *Gastroenterology* 127(5):S194–S205
- Gil-Alzugaray B, Chopitea A, Iñárraiaegui M, Bilbao JI, Rodríguez-Fraile M, Rodríguez J et al. (2012) Prognostic factors and prevention of radioembolization-induced liver disease. *Hepatology*. doi: 10.1002/hep.26191. [Epub ahead of print]



- Gray B, van Hazel G, Hope M, Burton M, Moroz P, Anderson J et al (2001) Randomised trial of SIR-Spheres plus chemotherapy vs. chemotherapy alone for treating patients with liver metastases from primary large bowel cancer. *Ann Oncol* 12(12):1711–1720
- Hall E (2006) Physics and chemistry of radiation absorption. In: *Radiobiology for the Radiologist*. Lippincott Williams & Wilkins, Philadelphia, pp 5–16
- Hendlisz A, Eynde MVD, Peeters M, Maleux G, Lambert B, Vannote J et al (2010) Phase III trial comparing protracted intravenous fluorouracil infusion alone or with Yttrium-90 resin microspheres radioembolization for liver-limited metastatic colorectal cancer refractory to standard chemotherapy. *J Clin Oncol* 28(23):3687–3694
- Hilgard P, Hamami M, Fouly AE, Scherag A, Müller S, Ertle J et al (2010) Radioembolization with yttrium-90 glass microspheres in hepatocellular carcinoma: European experience on safety and long-term survival. *Hepatology* 52(5):1741–1749
- Ingold JA, Reed GB, Kaplan HS, Bagshaw MA (1965) Radiation hepatitis. *Am J Roentgenol Radium Ther Nucl Med* 93:200–208
- Jakobs TF, Hoffmann RT, Dehm K, Trumm C, Stemmler H-J, Tatsch K et al (2008) Hepatic Yttrium-90 radioembolization of chemotherapy-refractory colorectal cancer liver metastases. *JVIR*. 19(8):1187–1195
- Jiang M, Fischman A, Nowakowski FS et al (2012) Segmental perfusion differences on paired Tc-99m macroaggregated albumin (MAA) hepatic perfusion imaging and Yttrium-90 (Y-90) bremsstrahlung imaging studies in SIR-Sphere radioembolization: associations with angiography. *J Nucl Med Radiat Ther* 3:122. doi: [10.4172/2155-9619.1000122](https://doi.org/10.4172/2155-9619.1000122)
- Kao YH, Hock Tan AE, Burgmans MC, Irani FG, Khoo LS, Gong Lo RH et al (2012) Image-guided personalized predictive dosimetry by artery-specific SPECT/CT partition modeling for safe and effective 90Y radioembolization. *J Nucl Med* 53(4):559–566
- Kennedy AS, Nutting C, Coldwell D, Gaiser J, Drachenberg C (2004) Pathologic response and microdosimetry of 90Y microspheres in man: Review of four explanted whole livers. *Int J Radiat Oncol Biol Phys* 60(5):1552–1563
- Kennedy AS, Coldwell D, Nutting C, Murthy R, Wertman DE Jr, Loehr SP et al (2006) Resin 90Y-microsphere brachytherapy for unresectable colorectal liver metastases: modern USA experience. *Int J Radiat Oncol Biol Phys* 65(2):412–425
- Kennedy AS, Dezarn WA, McNeillie P, Coldwell D, Nutting C, Carter D et al (2008) Radioembolization for unresectable neuroendocrine hepatic metastases using resin 90Y-microspheres: early results in 148 patients. *Am J Clin Oncol* 31(3):271–279
- Kennedy AS, McNeillie P, Dezarn WA, Nutting C, Sangro B, Wertman D et al (2009) Treatment parameters and outcome in 680 treatments of internal radiation with resin 90Y-microspheres for unresectable hepatic tumors. *Int J Radiat Oncol Biol Phys* 74(5):1494–1500
- Khan AZ, Morris-Stiff G, Makuuchi M (2009) Patterns of chemotherapy-induced hepatic injury and their implications for patients undergoing liver resection for colorectal liver metastases. *J Hepatobiliary Pancreat Surg* 16(2):137–144
- King J, Quinn R, Glenn DM, Janssen J, Tong D, Liaw W et al (2008) Radioembolization with selective internal radiation microspheres for neuroendocrine liver metastases. *Cancer* 113(5):921–929
- Knesaurek K, Machac J, Muzinic M, DaCosta M, Zhang Z, Heiba S (2010) Quantitative comparison of yttrium-90 (90Y)-microspheres and technetium-99 m (99 mTc)-macroaggregated albumin SPECT images for planning 90Y therapy of liver cancer. *Technol Cancer Res Treat* 9(3):253–262
- Kulik LM, Carr BI, Mulcahy MF, Lewandowski RJ, Atassi B, Ryu RK et al (2008) Safety and efficacy of 90Y radiotherapy for hepatocellular carcinoma with and without portal vein thrombosis. *Hepatology* 47(1):71–81
- Lau W-Y, Kennedy AS, Kim YH, Lai HK, Lee R-C, Leung TWT et al (2012) Patient selection and activity planning guide for selective internal radiotherapy with Yttrium-90 resin microspheres. *Int J Radiat Oncol Biol Phys* 82(1):401–407
- Lawrence TS, Ten Haken RK, Kessler ML, Robertson JM, Lyman JT, Lavigne ML et al (1992) The use of 3-D dose volume analysis to predict radiation hepatitis. *Int J Radiat Oncol Biol Phys* 23(4):781–788
- Lawrence TS, Robertson JM, Anscher MS, Jirtle RL, Ensminger WD, Fajardo LF (1995) Hepatic toxicity resulting from cancer treatment. *Int J Radiat Oncol Biol Phys* 31(5):1237–1248
- Lim L, Gibbs P, Yip D, Shapiro JD, Dowling R, Smith D et al (2005) Prospective study of treatment with selective internal radiation therapy spheres in patients with unresectable primary or secondary hepatic malignancies. *Intern Med J* 35(4):222–227
- Mazzaferro V, Sposito C, Bhoori S, Romito R, Chiesa C, Morosi C et al (2012) Yttrium-90 radioembolization for intermediate-advanced hepatocarcinoma: a phase II study. *Hepatology* n/a–n/a
- Mulcahy MF, Lewandowski RJ, Ibrahim SM, Sato KT, Ryu RK, Atassi B et al (2009) Radioembolization of colorectal hepatic metastases using Yttrium-90 microspheres. *Cancer* 115(9):1849–1858
- Nosher JL, Ohman-Strickland PA, Jabbour S, Narra V, Nosher B (2011) Changes in liver and spleen volumes and liver function after radioembolization with Yttrium-90 resin microspheres vol 22(12). *JVIR*. Elsevier Inc, pp 1706–1713
- Park W, Lim DH, Paik SW, Koh KC, Choi MS, Park CK et al (2005) Local radiotherapy for patients with unresectable hepatocellular carcinoma. *Int J Radiat Oncol Biol Phys* 61(4):1143–1150
- Piana PM, Gonsalves CF, Sato T, Anne PR, McCann JW, Ad VB et al (2011) Toxicities after radioembolization with Yttrium-90 SIR-Spheres: incidence and contributing risk factors at a single center vol 22(10). *JVIR*. Elsevier Inc, pp 1373–1379
- Reed GB, Cox AJ (1966) The human liver after radiation injury. A form of veno-occlusive disease. *Am J Pathol* 48(4):597–611
- Salem R, Lewandowski RJ, Atassi B, Gordon SC, Gates VL, Barakat O et al (2005) Treatment of unresectable hepatocellular carcinoma with use of 90Y microspheres (therasphere): safety, tumor response, and survival. *J Vasc Interv Radiol* 16(12):1627–1639
- Salem R, Lewandowski RJ, Mulcahy MF, Riaz A, Ryu RK, Ibrahim S, et al (2010) Radioembolization for hepatocellular carcinoma using Yttrium-90 microspheres: a comprehensive report of long-term outcomes. *Gastroenterology*, vol 138(1). Elsevier Inc, pp 52–64
- Sangro B, Bilbao JI, Boan J, Martinez-Cuesta A, Benito A, Rodriguez J et al (2006) Radioembolization using 90Y-resin microspheres for patients with advanced hepatocellular carcinoma. *Int J Radiat Oncol Biol Phys* 66(3):792–800
- Sangro B, Gil-Alzugaray B, Rodriguez J, Sola I, Martinez-Cuesta A, Viudez A et al (2008) Liver disease induced by radioembolization of liver tumors. *Cancer* 112(7):1538–1546
- Sangro B, Carpanese L, Cianni R, Golfieri R, Gasparini D, Ezziddin S et al (2011) Survival after yttrium-90 resin microsphere radioembolization of hepatocellular carcinoma across Barcelona clinic liver cancer stages: a European evaluation. *Hepatology* 54(3):868–878
- Sangro B, Iñárraegui M, Bilbao JI (2012) Radioembolization for hepatocellular carcinoma. *J Hepatol*. European Association for the Study of the Liver 56(2):464–473
- Scrobohaci ML, Drouet L, Monem-Mansi A, Devergie A, Baudin B, D'Agay MF et al (1991) Liver veno-occlusive disease after bone

- marrow transplantation changes in coagulation parameters and endothelial markers. *Thromb Res* 63(5):509–519
- Seidensticker R, Seidensticker M, Damm R, Mohnike K, Schütte K, Malfertheiner P et al (2011a) Hepatic toxicity after radioembolization of the liver using <sup>90</sup>Y-microspheres: sequential lobar versus whole liver approach. *Cardiovasc Intervent Radiol* 35(5):1109–1118
- Seidensticker R, Denecke T, Kraus P, Seidensticker M, Mohnike K, Fahlke J et al (2011b) Matched-pair comparison of radioembolization plus best supportive care versus best supportive care alone for chemotherapy refractory liver-dominant colorectal metastases. *Cardiovasc Intervent Radiol* 35(5):1066–1073
- Sharma RA, van Hazel GA, Morgan B, Berry DP, Blanshard K, Price D et al (2007) Radioembolization of liver metastases from colorectal cancer using Yttrium-90 microspheres with concomitant systemic oxaliplatin, fluorouracil, and leucovorin chemotherapy. *J Clin Oncol* 25(9):1099–1106
- Shim SJ, Seong J, Lee JJ, Han KH, Chon CY, Ahn SH (2007) Radiation-induced hepatic toxicity after radiotherapy combined with chemotherapy for hepatocellular carcinoma. *Hepatol Res* 37(11):906–913
- Strigari L, Sciuto R, Rea S, Carpanese L, Pizzi G, Soriani A et al (2010) Efficacy and toxicity related to treatment of hepatocellular carcinoma with <sup>90</sup>Y-SIR Spheres: radiobiologic considerations. *J Nucl Med* 51(9):1377–1385
- Van Hazel G, Blackwell A, Anderson J, Price D, Moroz P, Bower G et al (2004) Randomised phase 2 trial of SIR-Spheres plus fluorouracil/leucovorin chemotherapy versus fluorouracil/leucovorin chemotherapy alone in advanced colorectal cancer. *J Surg Oncol* 88(2):78–85
- van Hazel GA, Pavlakis N, Goldstein D, Olver IN, Tapner MJ, Price D et al (2009) Treatment of fluorouracil-refractory patients with liver metastases from colorectal cancer by using Yttrium-90 resin microspheres plus concomitant systemic Irinotecan chemotherapy. *J Clin Oncol* 27(25):4089–4095

# Index

## A

AASLD guidelines, 110  
Accidental contamination, 70  
Activity measurements, 71  
Advanced stage, 113  
Alpha-fetoprotein, 109

## B

Barcelona clinic liver cancer (BCLC), 120, 125  
BCLC, 168  
BCLC stage, 107, 110  
Benign liver lesions, 15  
B-mode gray scale, 93  
Breast cancer management, 159

## C

Carcinoid, 151–154  
Carcinoid syndrome, 152–154  
Celiac trunk, 28, 29, 31, 33, 38  
Chemoembolization, 153, 154  
Chemorefractory patients, 142  
Chemotherapy, 129–138  
Colorectal cancer, 129–138  
Combined modality induced liver disease, 178  
Common hepatic artery, 28–32, 38  
Complications, 154  
Consolidation, 45  
Contrast enhanced ultrasound, 94  
Cystic artery, 37, 38

## D

Diagnostic imaging equipment, 13  
Diffusion-weighted MRI, 22, 97  
DNA strand, 178  
Downsizing, 122–124  
Downstaging, 113, 121, 122, 125, 168  
Dyna-CT, 24

## E

Early stage, 111  
EASL criteria, 81

ENRY trial, 122  
Extrahepatic uptake, 67

## F

Falciform artery, 35, 36  
FDG PET/CT, 98  
Focal Nodular Hyperplasia, 18  
Free radical, 178

## G

Gadobenate-dimeglumine, 21  
Gadolinium, 96  
Gadoxetic-acid, 21  
Gamma photons, 65  
Gastroduodenal artery, 28–32, 37, 38  
Gigabecquerel (GBq), 53, 55–57  
Gray (Gy), 54, 55, 58

## H

Hemangiomas, 22  
Hepatopulmonary shunting, 65  
HMGB1, 147  
Hypertrophy, 122, 169

## I

Immune response, 147  
Inferior Phrenic, 43  
Intercostal arteries, 43  
Intermediate stage, 112  
Internal mammary, 43  
Irinotecan, 144

## L

Left gastric artery, 28–32, 35–39  
Legal regulations, 12  
Liver atrophy, 110  
Liver damage, 179  
Liver metastases, 19, 22  
Liver-specific contrast agents, 22  
Liver-specific MRI, 16

Liver transplantation, 168  
 Liver tumors, 15  
 Lobectomy, 110  
 Lung shunt, 66

## M

99m Tc-MAA, 64  
 Magnetic resonance imaging, 20  
 Malignant liver lesions, 15  
 Mangafodipir trisodium, 21  
 Medical internal radiation dose (MIRD), 53, 55, 56, 59  
 Michels classification, 29–31, 42  
 Microbubbles, 16  
 Milan criteria, 121, 122  
 MIRD, 67  
 Multidisciplinary approach, 11  
 Multiple endocrine neoplasia, 152

## N

NET, 151–154  
 Neuroendocrine, 151, 152

## O

Octreo-scan, 152  
 Octreotide, 152–155  
 Omental artery, 38, 39, 43  
 Oxaliplatin, 144

## P

Pancreaticoduodenal arcade, 30, 31, 33, 34  
 Parallel imaging, 20  
 Pathologic findings, 168  
 Patient-specific dosimetry, 71  
 PERCIST, 147  
 Perihilar plexus, 43  
 PET/CT, 16, 81, 82  
 Phase II, 143  
 Phase 3 trials, 158  
 Portal vein invasion, 113  
 Post-embolization syndrome, 153  
 Prastitized extrahepatic arteries, 48  
 PREMIERE, 114  
 Primary index lesion, 108  
 Proper hepatic artery, 28–30, 32, 33, 35, 36, 39

## R

Radiofrequency, 168  
 Radiolabelling process, 72  
 Radiation induced liver disease (RILD), 54, 58, 59, 178  
 Radiation safety issues, 13  
 Radioembolisation, 129, 137  
 Radioembolization and pancreatic cancer, 160  
 Radioembolisation in refractory metastatic breast cancer, 160

Radioembolization induced liver disease (REILD), 58, 59  
 Radioembolization in gastric cancer, 161  
 Radioembolization in melanoma, 162  
 Radioembolization team, 11  
 Radiosensitisation, 132, 136–138  
 Radiotherapy, 158  
 RECIST, 79  
 Redistribution, 44  
 REILD, 109, 179  
 RE-induced liver disease, 179  
 Resection, 120–123, 125  
 Right gastric artery, 37  
 RILD, 178

## S

Salvage therapy, 146  
 SARAH, 115  
 Segmentectomy, 110  
 Selective internal radiation therapy (SIRT), 153–155  
 Selective internal radioembolization and ICC, 162  
 Sequential, 183  
 SIR-spheres, 130–132, 134, 135  
 SonoVue®, 16  
 Sorafenib, 120, 122–125  
 SORAMIC, 115  
 SPECT/CT scan, 65  
 Superparamagnetic iron oxide (SPIO), 21, 96  
 Stereotactic body radiotherapy (SBRT), 1  
 Superior mesenteric artery, 28–32, 38

## T

Thermal ablation, 120  
 Training of interventional radiologist, 13  
 Transarterial chemoembolization (TACE), 54, 56, 120, 122–125  
 Transarterial embolization (TAE), 54  
 Transplantation, 120–123, 125

## U

Ultrasound, 16

## V

Vascular redistribution, 70  
 Venous-occlusive disease, 178, 179

## W

WHO, 79  
 Whole-body imaging, 99  
 Whole-body MRI, 82, 83

## Y

Y-resin microspheres and lung cancer, 160  
 Yttrium, 151, 153, 154